Università
Ca'Foscari
Venezia

Master's Degree

in Sustainable Chemistry and Technologies

Final Thesis

Supramolecular catalysis by the resorcin[4]arene hexameric capsule: intra- and intermolecular aromatic allylations and a new aldehyde-isocyanide condensation reaction

Supervisor
Ch. Prof. Alessandro Scarso

Co-supervisor
Ch. Prof. Fabrizio Fabris

Graduand
Luca Fiorini
Matriculation number
869876

Academic Year
2021/2022

“Sic parvis magna”
- Sir Francis Drake

Compounds of interest

Table of synthesized and purified compounds

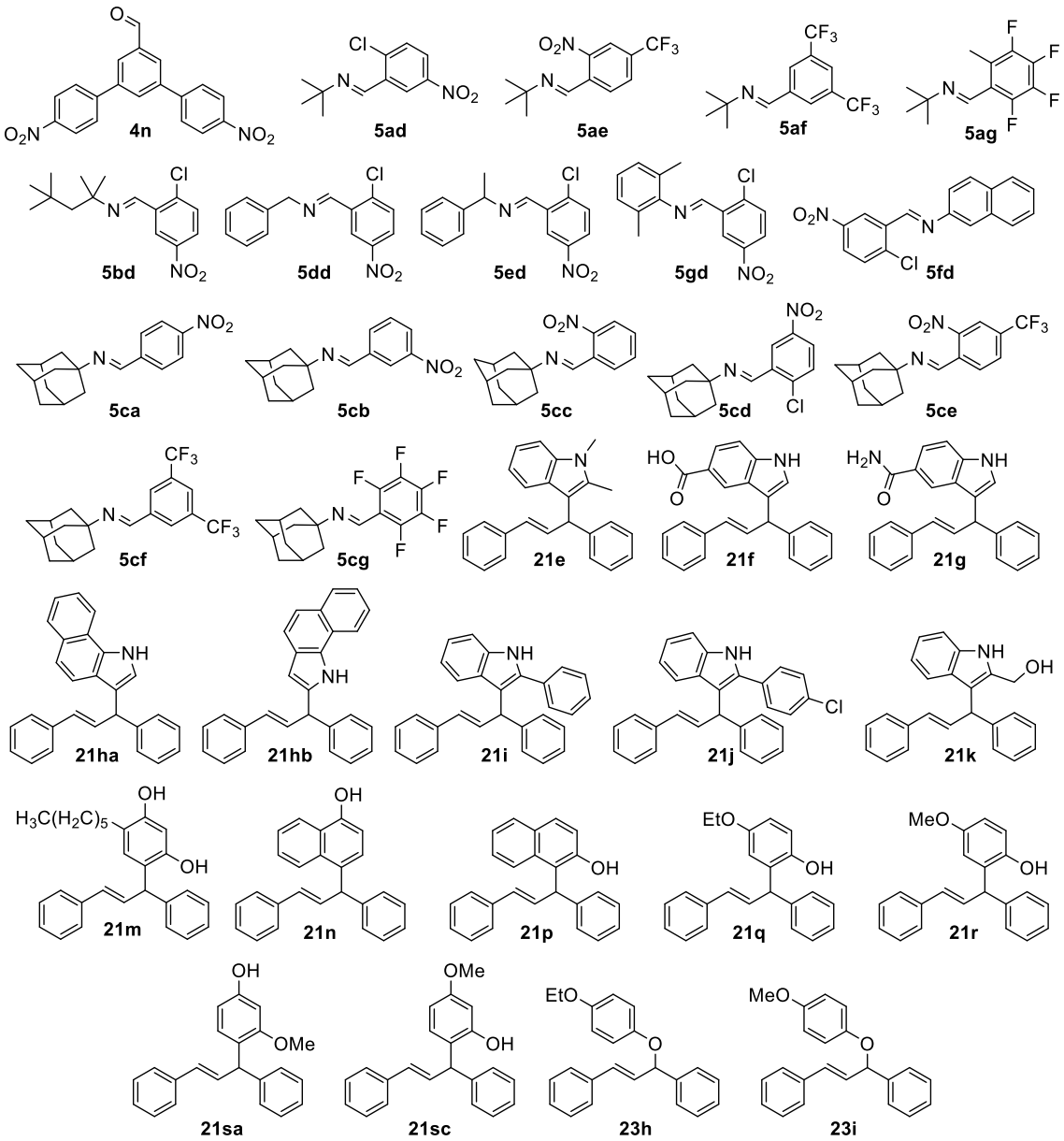

Other compounds of interest

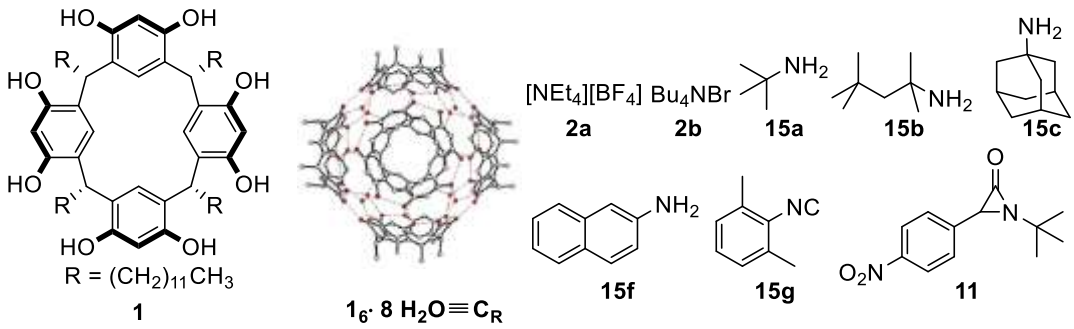

3a

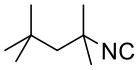

3b

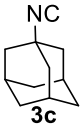

3c

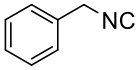

3d

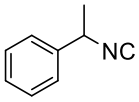

3e

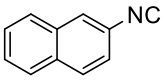

3f

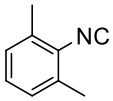

3g

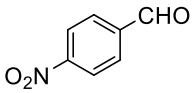

4a

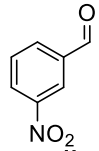

4b

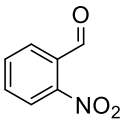

4c

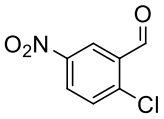

4d

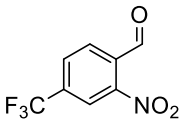

4e

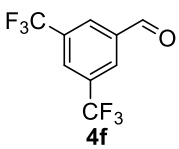

4f

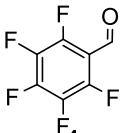

4g

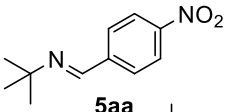

5aa

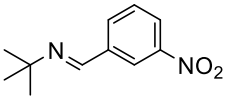

5ab

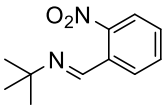

5ac

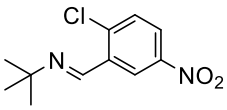

5ad

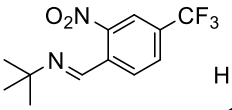

5ae

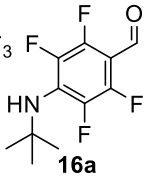

16a

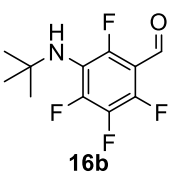

16b

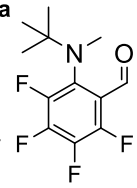

16c

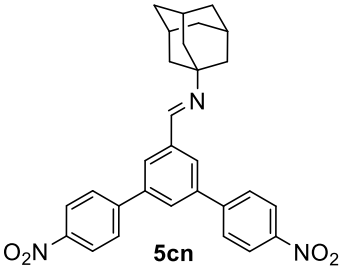

5cn

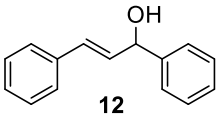

12

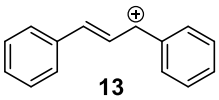

13

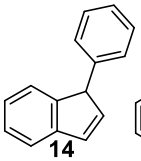

14

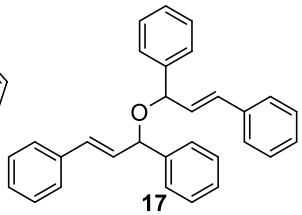

17

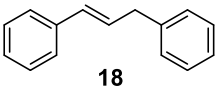

18

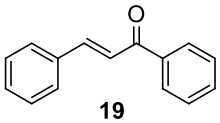

19

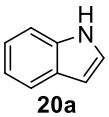

20a

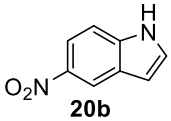

20b

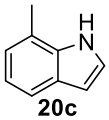

20c

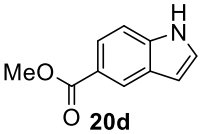

20d

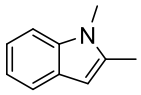

20e

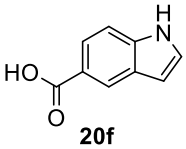

20f

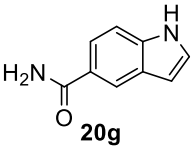

20g

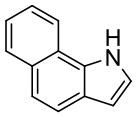

20h

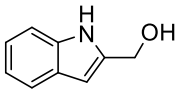

20k

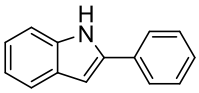

20i

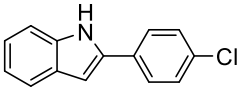

20j

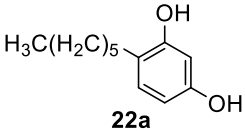

22a

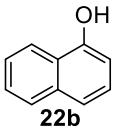

22b

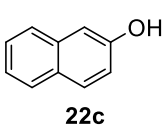

22c

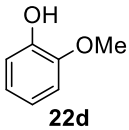

22d

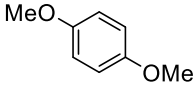

22e

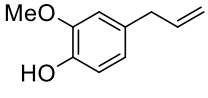

22f

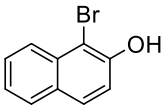

22g

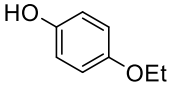

22h

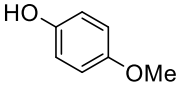

22i

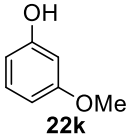

22k

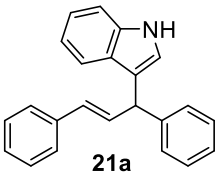

21a

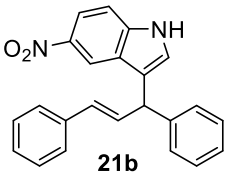

21b

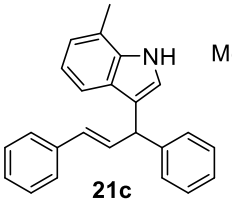

21c

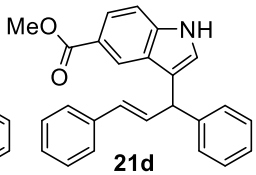

21d

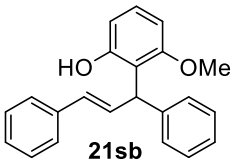

21sb

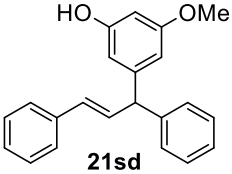

21sd

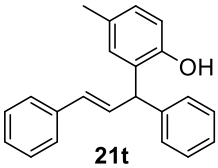

21t

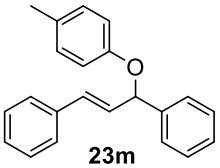

23m

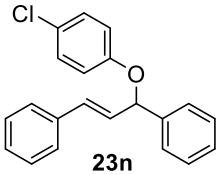

23n

Contents

Introduction

1. Supramolecular Chemistry

One of the main proponents of supramolecular chemistry, Jean-Marie Lehn, defined it in his Nobel Lecture in 1988 as "'chemistry beyond the molecule', bearing on the organized entities of higher complexity that result from the association of two or more chemical species held together by intermolecular forces."[1] This field of chemistry arose in the 1960s from research into macrocyclic ligands for metal cations, having its initial breakthrough with Charles J. Pedersen's discovery of crown ethers.[2] From its origins as host-guest chemistry, supramolecular chemistry went on to include concepts such as self-assembly, molecular recognition and folding and supramolecular catalysis.[3]

In host-guest chemistry, the "host" is a large molecule or aggregate with a central cavity which can accommodate a chemical species, known as "guest", by means of non-covalent interactions. Guests can be of various nature, ranging from small ions or ion pairs to more complex organic molecules or metal complexes. The inclusion of a guest into a host can be mediated by a plethora of types of non-covalent interaction: ion-ion, ion-dipole, ion-π or π-π interactions, hydrogen bonding, solvation and hydrophobic effects are all crucial concepts in understanding supramolecular inclusion and self-assembly phenomena.[4]

When host systems completely surround the guest, they could be either fully covalent structures like cages (**Scheme I.1 left**) or containers obtained by the spontaneous self-assembly between homologous or different subunits, typically through H-bonding or metal-ligand coordination (**Scheme I.1 right**). A general rule states that the binding between a capsule and its guest is optimal when the latter occupies (55 ± 9)% of the host cavity.[5]

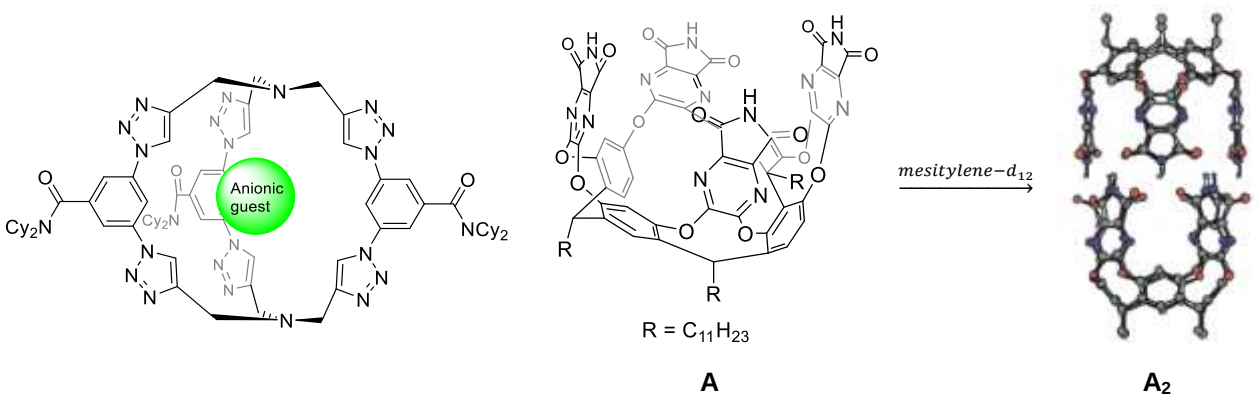

Scheme I.1 *Liu et al.'s triazolo cage (**left**);[6] Rebek and Chen's self-assembled cylindrical dimeric capsule* ***A₂*** *(**right**, image taken from Rebek et al.[7])*

Considering the reversible inclusion of guest *G* into host *H* to form the inclusion compound *HG* (**Equation I.1**), the thermodynamic stability of the latter can be quantified as the binding constant *K*. While *K* should be dimensionless – as it is ideally supposed to be calculated as a ratio of chemical activity measurements (**Equation I.2**) – it is often calculated using concentrations, under the approximation that concentrations be approximately equal to activities at sufficiently high levels of dilution (**Equation I.3**).

$$H + G \rightleftharpoons HG$$

Equation I.1 *Chemical equation of the reversible formation of inclusion compound HG.*

$$K = \frac{a_{HG}}{a_H \cdot a_G}$$

Equation I.2 *Formal equation for K, where a_X is the equilibrium activity of species X.*

$$K \approx \frac{[HG]}{[H] \cdot [G]}$$

Equation I.3 *Approximate equation for K, where [X] is the equilibrium molar concentration of X.*

Various methods can be employed in order to evaluate the binding constant of a host-guest pair. One notable technique – which was used in this thesis work – is nuclear magnetic resonance titration.[8] This method consists in adding small aliquots of guest to a solution of host in a deuterated solvent: since the electronic properties of the host cavity are different than those of the bulk solution, the NMR resonances of the guest often change upon inclusion. Depending on whether the recognition phenomenon is in slow or fast exchange on the chemical shift timescale, separate signals for free and encapsulated guest and host are visible (enabling direct quantification) or the weighted average chemical shift is observed, requiring proper fitting with a binding model for the determination of *K*.

2. Supramolecular catalysts as enzyme mimics

Through billions of years of evolution, nature has developed the most effective catalysts known to man: enzymes. These polypeptidic molecules can accelerate biochemical reactions by many orders of magnitude, achieving levels of specificity and of chemo-, regio- and enantioselectivity which are unrivalled by artificial catalysts to this day.[9] Chemists have long since tried to understand the reasons behind these wondrous properties, starting with Emil Fischer's 1894 *lock-and-key* theory, according to which the specificity of enzymes is due to the presence of an active site whose geometry is perfectly complementary to the corresponding substrates.[10] Fischer's model was later integrated by Daniel Koshland's *induced fit* model, which theorized that the active site of an enzyme is continuously reshaped to accommodate the substrates as they react; this theory explains the stabilisation of transition states achieved by enzymes.[11,12] An example of this behaviour is shown in **Scheme I.2**.

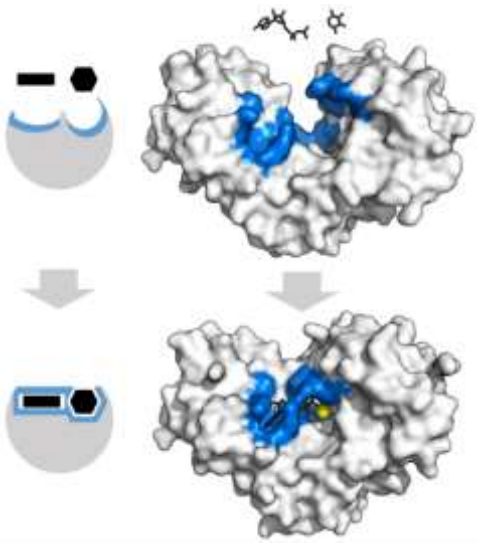

Scheme I.2 *Hexokinase binds adenosine triphosphate and xylose through a notable induced fit motion. Image by T. Shafee.*[13]

Non-covalent interactions are at the root of many of the enviable catalytic properties of enzymes. Therefore, chemists have been putting ever greater efforts into designing supramolecular compounds capable of acting as enzyme mimics through tailored non-covalent interactions. The idea which initially led to the development of host-guest enzyme mimics was that increasing the concentration of reactants in a reactive centre would lead to an increase of the reaction rate. It has since been found that catalytic effects are not attributable merely to overconcentration phenomena, but also to desolvation of the reactants, stabilization of proper substrate conformations, stabilisation of intermediate species and related transition states, and favourable conformation of the product within the catalytic pocket.[14]

Initial efforts were focused on small supramolecular catalysts consisting of a reactive centre included within a binding site; cyclodextrin derivatives combined with organic or metal-ligand catalytic centres are a prime example of this.[15] More recently, the possibility of exploiting the peculiar characteristics of the internal cavities of non-covalent hosts – such as self-assembled capsules (see **Introduction §3**) – for catalytic purposes has gained traction. The first example of this kind of catalysis was reported in 1997 by Rebek and Kang, who observed significant acceleration of a Diels-Alder reaction within the "softball" capsule formed through the H-bond mediated self-assembly of two subunits (**Scheme I.3**).[16]

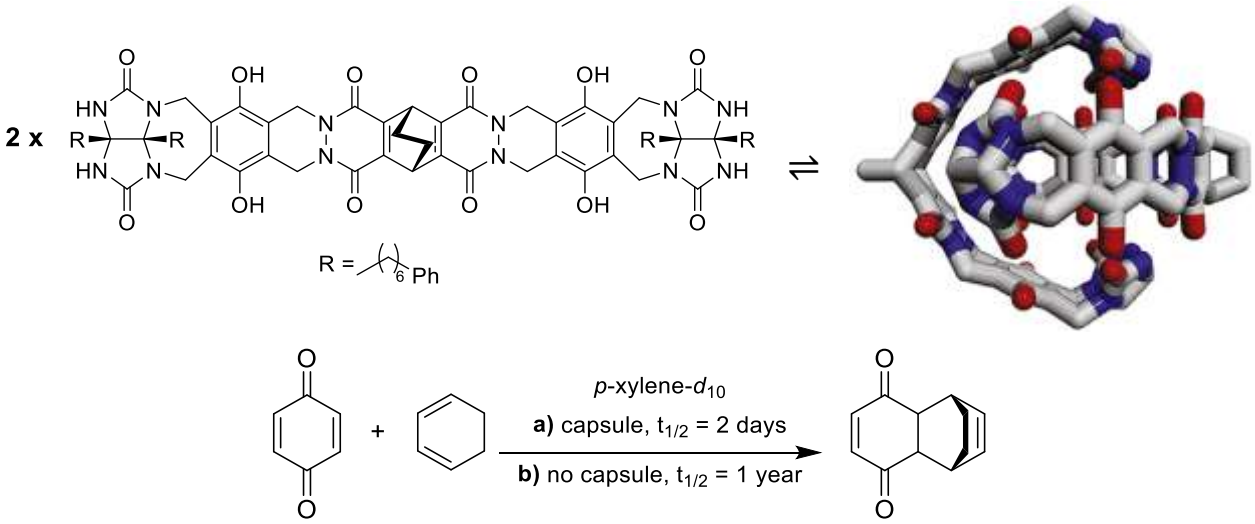

Scheme I.3 *Structure of Rebek and Kang's softball capsule and of its subunits (**top**, image taken from Scarso and Borsato[9]) and scheme of the Diels-Alder reaction accelerated by said capsule (**bottom**; reference: see text).*

Another example of catalysis within a self-assembled capsule was reported by Rebek and Chen, who found that $\mathbf{A_2}$ (**Scheme I.1**) promotes 1,3-dipolar cycloaddition between phenylacetylene and phenyl azide, yielding exclusively the 1,4-regioisomer due to spatial constraints (**Scheme I.4**).[7] More recently, Toste *et al.* altered the mechanism of an aza-Prins cyclization by using a tetrahedral metal-ligand based supramolecular cage, whose physical constraints stabilized the more compact transition state (**Scheme I.5**, pathway **a**) rather than the all-equatorial transition state which is favoured in the bulk solution (**Scheme I.5**, pathway **b**).[17]

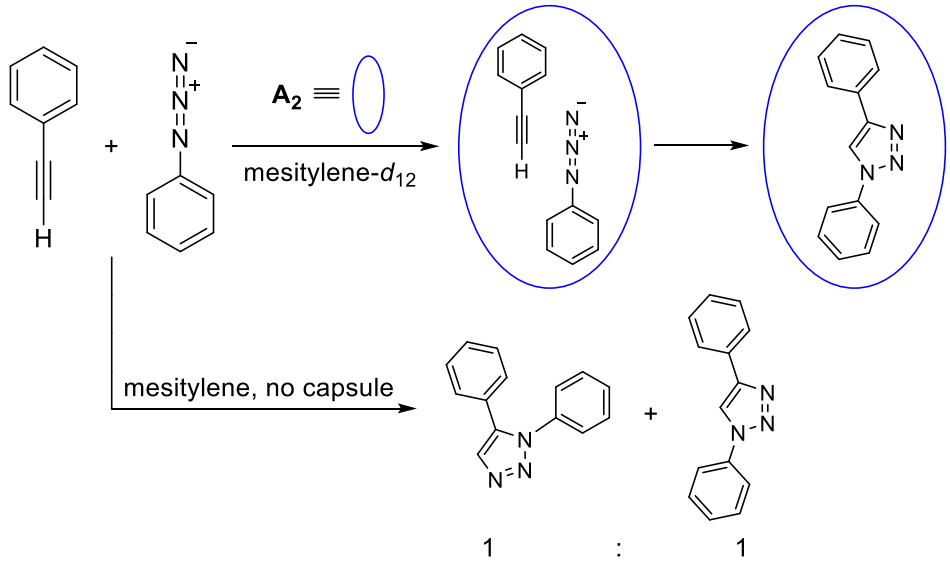

Scheme I.4 *1,3-dipolar cycloaddition catalysed regioselectively by Rebek and Chen's capsule* ***A₂*** *(reference: see text).*

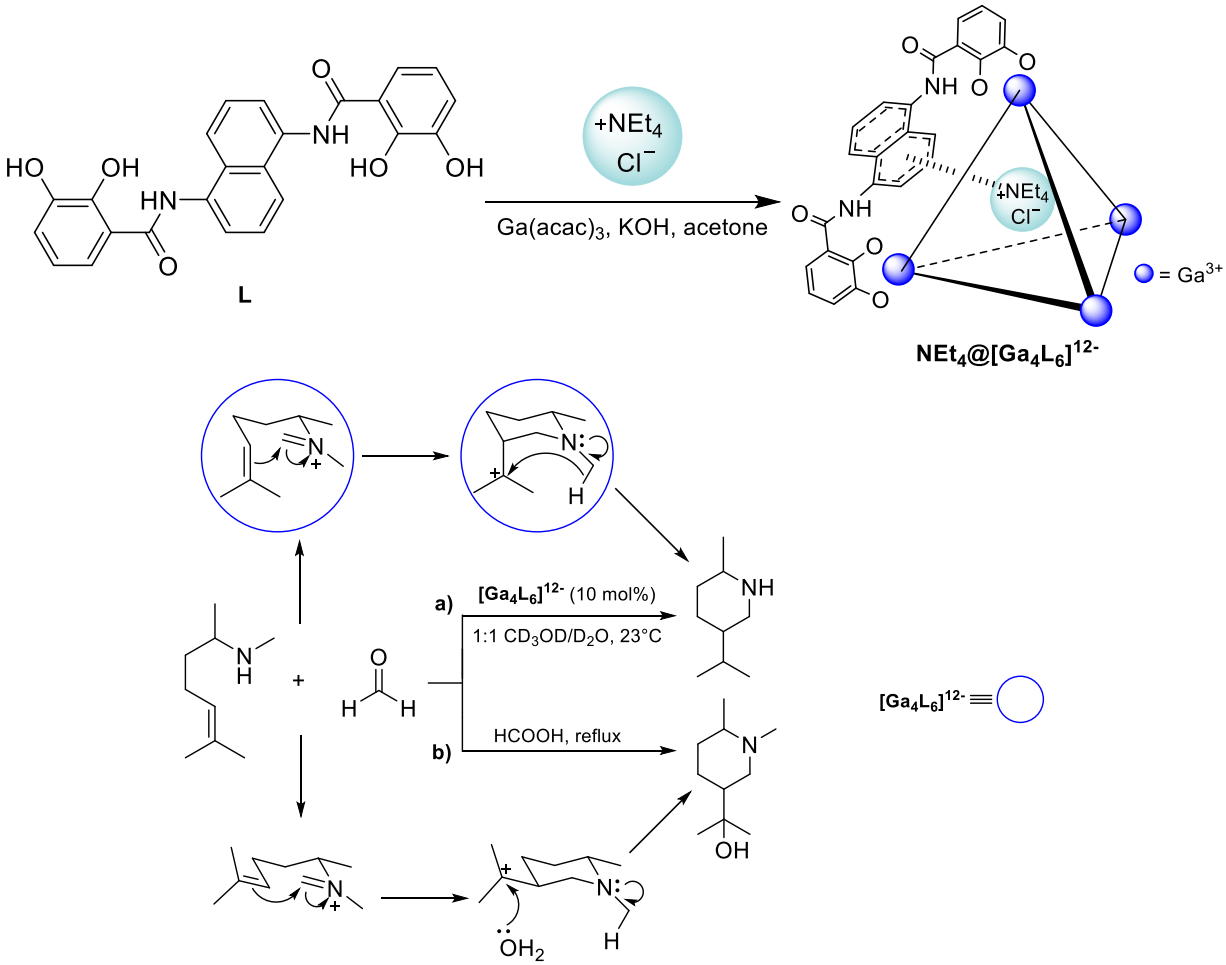

Scheme I.5 *Structure of Toste et al.'s metal-ligand based cage, which requires a small cationic guest such as* Et_4N^+ *to thermodynamically drive its own self-assembly (**top**, the symbol **@** is used to signal inclusion), and proposed mechanism of the aza-Prins reaction catalysed by the cage (**bottom**; reference: see text).*

3. Self-assembled hosts

There is one clear issue with host design: the required large and complex molecular structures can be difficult to synthesize. A convenient solution is offered by self-assembled hosts, which are supramolecular compounds that form through spontaneous assembly of a limited number of subunits in solution. Self-assembled hosts can present much desired enzyme-mimicking behaviours, without the inconvenience of synthesizing complex molecular framework. Two main subclasses of self-assembled hosts can be identified: metal-ligand based cages and non-covalent bonded capsules, mainly hydrogen bonded, ion pairing and hydrophobic capsules.[18]

The assembly of metal-ligand based capsules is driven by coordination bonding between ligands and metal centres, such as in Toste *et al.*'s Gd-based capsule (see **Introduction §2**, **Scheme I.4**) and in Fujita *et al.*'s octahedral Pd(II)-based capsule (**Scheme I.6**).[19]

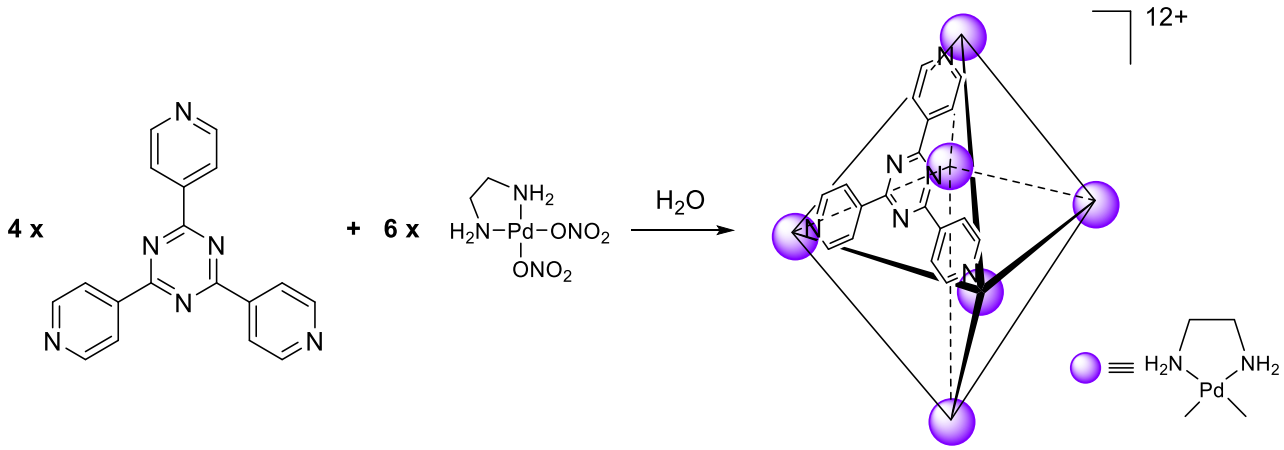

Scheme I.6 *Structure of Fujita et al.'s self-assembled metal-ligand based cage (reference: see text).*

On the other hand, non-covalent bonded capsules have been defined by Conn and Rebek as "receptors with enclosed cavities that are formed by the reversible noncovalent interaction of two or more, not necessarily identical, subunits."[20] The same authors cited the hydrogen bond's merits of being directional, specific and of biological relevance as the main reasons that make it the favourite intermolecular force in these supramolecular systems. Some examples of non-covalent bonded capsules are Rebek and Chen's cylindrical dimer (**Scheme I.1**),[7] Rebek and Kang's softball capsule (**Scheme I.3**),[16] and the resorcin[4]arene hexamer which will be the focus of this thesis.

4. The resorcin[4]arene hexameric capsule as a catalyst

Resorcin[4]arenes are well known macrocyclic compounds, easily synthesized by means of acid-catalysed condensation of an equimolar mixture of resorcinol and an aldehyde in solution,[21] though solvent-free synthesis options have also been reported.[22] In 1997, MacGillivray and Atwood were able to demonstrate that, in the crystal state, six molecules of resorcin[4]arene assemble into a hexamer by combining with eight water molecules via spontaneous formation of 60 O–H···O hydrogen bonds, with each water molecule establishing three bonds with the OH groups of three adjacent resorcin[4]arene monomers, and each monomer bonding with four adjacent monomers (**Scheme I.7**).[23] It was later proven that *C*-undecyl-resorcin[4]arene **1** preserves the same supramolecular structure (**$1_6 \cdot 8H_2O \equiv C_R$**) when dissolved in wet apolar solvents such as chloroform and benzene, with six to eight solvent molecules filling its cavity.[24]

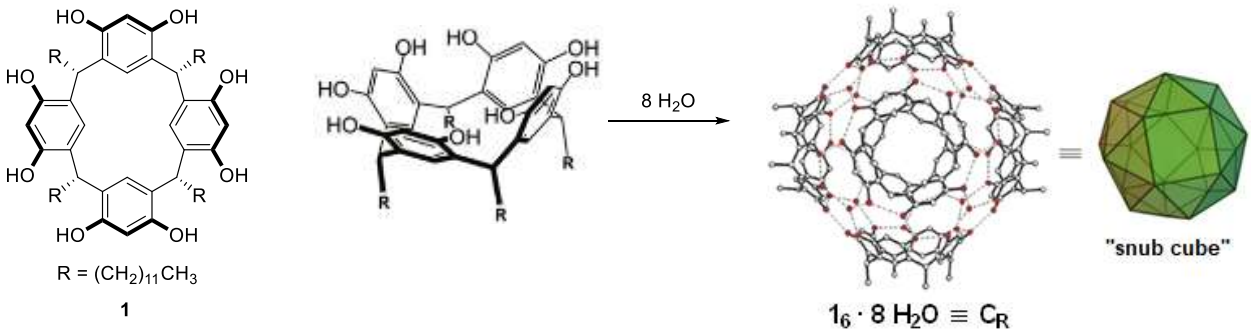

Scheme I.7 *3D structure of the self-assembled C-undecyl-resorcin[4]arene capsule (references of the images: [25]).*

Some important properties of capsule **C_R** are:

- its relatively large size: **C_R**'s roughly spherical internal cavity has a maximum diameter of 17.7 Å and a volume of ~1375 Å^3, allowing it to encapsulate several small- or medium-sized guests;
- the reversible nature of its assembly, which allows for easy entrance and egress of guests, probably by way of a "portal" mechanism consisting in the temporary dissociation of one monomer, which exposes the internal cavity to the bulk solution;[26]
- its capability of losing H^+ from one of its OH moieties and of delocalising the resulting negative charge over the entire hexamer, which makes **C_R** much more acidic than its individual monomers **1**, with a pK_a of roughly 5.5–6 compared to a pK_a of about 9.3 for resorcinol;
- the presence of 24 aromatic rings that give rise to an inward-directed electronic density distribution, which makes the environment of the cavity very electron-rich and therefore particularly suitable to host cationic species, such as ammonium ions or transition metal catalysts, and electron-poor guests like isocyanides and aromatic compounds with electron-withdrawing groups.[9]

Due to its spatially constrained, acidic, and electron-rich interior, the resorcin[4]arene capsule has a great catalytic potential, permitting stabilisation of cationic and/or electron-poor substrates, transition states and intermediates and possibly unlocking reaction pathways which would not be favoured or possible in the bulk solution.

The catalytic behaviour of capsule **C_R** has long been a subject of research in the laboratory where this thesis work was carried out, both as a stoichiometric nano-reactor and as a proper catalyst itself. For example, Scarso and co-workers found that **C_R** can strongly alter the product distribution in alkyne hydration reactions

catalysed by a cation NHC-Au(I) complex[27] and of the amide formation reaction mediated by a carbodiimide cationic coupling agent (**Scheme I.8**).[28] Scarso and co-workers also reported that **C_R** can efficiently catalyse isocyanide hydration,[29] 1,3-dipolar cycloaddition between diazoacetate esters and electron-poor alkenes,[30] and cycloaddition between an azide and an isocyanide;[31] it is noteworthy that these reactions progress better with smaller substrates – which are more easily encapsulated – and are greatly hindered by the competitive encapsulation of cationic guest Et_4N^+ (**Scheme I.9**). Several research groups also investigated other reactions catalysed by the resorcin[4]arene capsule, enriching the corresponding literature with numerous examples.[32,33,34,35,36]

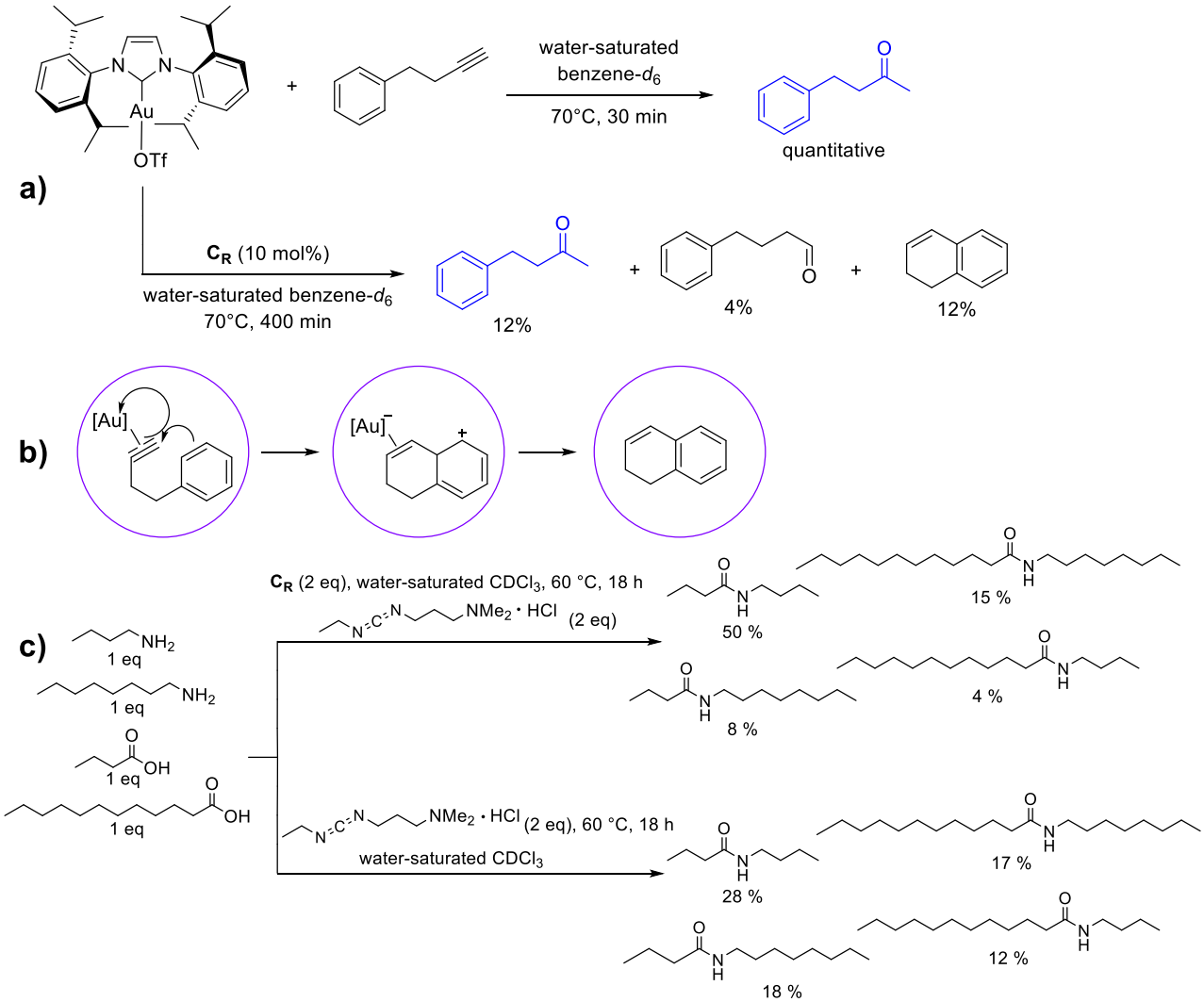

Scheme I.8 *NHC-Au(I) complex-catalysed hydration of 4-phenyl-1-butyne with and without encapsulation within* ***C_R*** *(**a**) and mechanism explaining the formation of the unusual 1,2-dihydronapthalene product due to folding of the substrate (**b**). Competitive coupling of carboxylic acids with aliphatic amines mediated by a cationic carbodiimide coupling agent in presence and absence of* ***C_R*** *(**c**); notice how the presence of* ***C_R*** *favours the conversion of smaller substrates, which are more readily encapsulated (references: see text).*

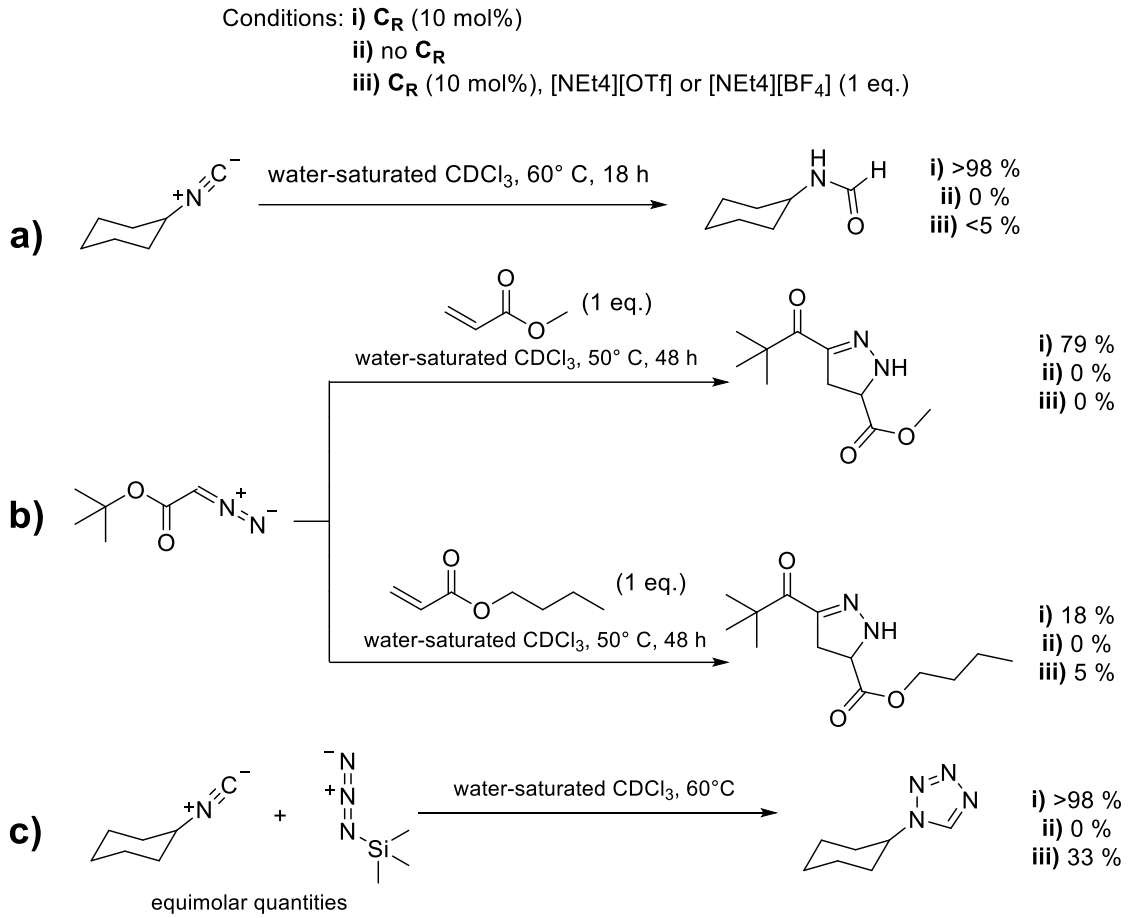

Scheme I.9 *Isocyanide hydration (**a**), 1,3-dipolar cycloaddition between a diazoacetate ester and an electron-poor alkene (**b**), and cycloaddition between an isocyanide and trimethylsilyl azide catalysed by capsule* C_R *(**c**); notice how the presence of* C_R *favours the conversion of smaller substrates, which are more readily encapsulated, and how the reactions are hindered by the competitive encapsulation of* Et_4N^+ *(references: see text).*

5. New reactions catalysed by the resorcin[4]arene capsule

5.1 Imine formation via condensation of an electron-poor aromatic aldehyde and an isocyanide

5.1.1 Overview

As stated above, isocyanides are excellent guests for capsule C_R which also promotes their attack by nucleophiles like water and azides (**Introduction §4**). The former compounds are generally considered of great synthetic interest because of the unique characteristics of the carbon atom in the isocyanide moiety, which can function as either an electrophile or a nucleophile depending on the chemical scenario.[37,38] In the famous Passerini and Ugi multicomponent reactions,[39] an isocyanide moiety acts as both a nucleophile and an electrophile, and is completely incorporated into the final product.

Recently, Scarso's and Tiefenbacher's research groups collaborated on an imine formation reaction which has no precedent in the literature. The reaction consists in a coupling between an electron-poor aromatic aldehyde and an isocyanide in the presence of a catalytic amount of capsule C_R, with the irreversible expulsion of a molecule of carbon monoxide as the thermodynamic driving force (**Scheme I.10**).

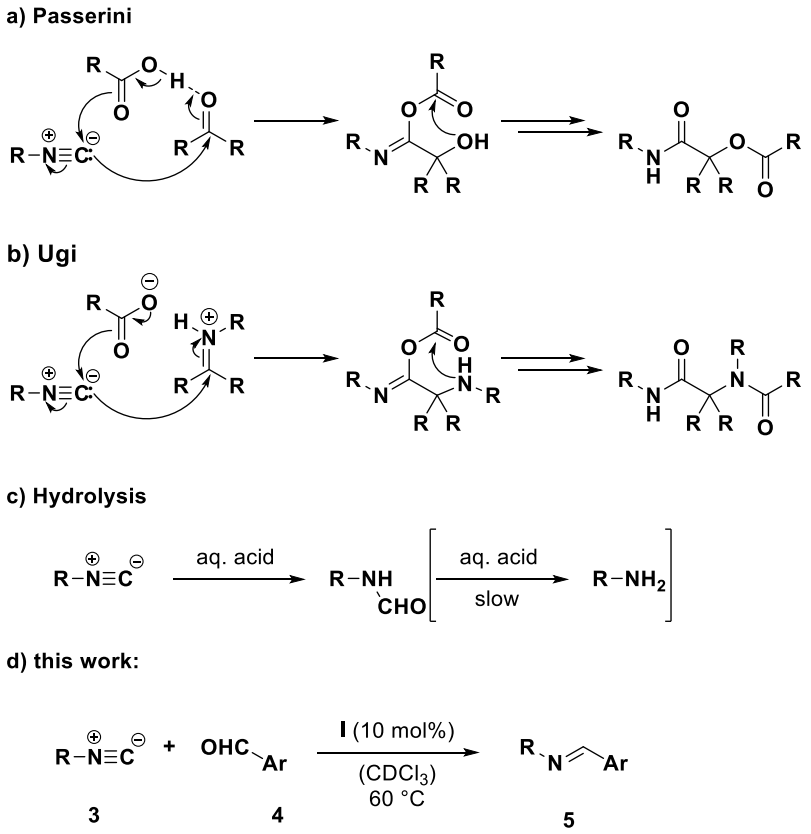

Scheme I.10 Overview of some reactions of interest involving isocyanides.

Initially, it was observed that heating to 50 °C a solution of *tert*-butyl isocyanide **3a**, 4-nitrobenzaldehyde **4a** and resorcin[4]arene **1** in de-acidified chloroform-*d* (filtered through basic Al_2O_3) yielded an unexpected product: imine **5aa**, with one fewer carbon atom with respect to the initial reactants. The identity of the product was confirmed by comparison with NMR spectra of **5aa** present in the literature. The reaction conditions were optimised as follows: 60 °C, isocyanide:aldehyde ratio of 2:1 and 60 mol% of **1** with respect to the aldehyde (equivalent to 10 mol% of $\mathbf{C_R}$). Several control experiments were conducted (**Table I.1**) to confirm the catalytic role of the capsule in the reaction:

- substituting $\mathbf{C_R}$ with an equal amount of acetic acid, a Brønsted acid with a pK_a comparable to that of $\mathbf{C_R}$ (see **Introduction §4**), yielded no product;
- substituting $\mathbf{C_R}$ with 24 eq. of n-hexyl-resorcinol with respect to **4a**, a number of capsule subunits equivalent to 10 mol% of $\mathbf{C_R}$, yielded no product;
- running the reaction without $\mathbf{C_R}$ yielded no product;
- running the reaction with an added 1 eq. of high-affinity guest Et_4N^+ (in the form of $[NEt_4][BF_4]$ **2a**) resulted in a much lower yield compared to the reaction conducted without Et_4N^+.

The former two results indicated that the reaction is not promoted either by the acidic nature of $\mathbf{C_R}$ nor by its capability of establishing H-bonds, whereas the latter two results validate the hypothesis that the inner cavity of $\mathbf{C_R}$ be in fact responsible for the catalytic effect.

*Table I.1 Control experiments for the reaction between 4-Nitrobenzaldehyde (**4a**) and t-butyl isocyanide **3a**.*

Entry #	I	Additive	Yield [%][a]
1	+	-	39
2	-	-	no conversion
3	-	HOAc (13.3 mM)	no conversion
4	-	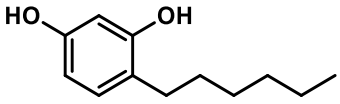 (320 mM)	decomposition
5	+	$[NEt_4][BF_4]$ (**2**, 133mM)	7

[**4a**] = 133 mM, [**3a**] = 266 mM, [**1**] = 80 mM, 0.5 mL $CDCl_3$, 50 °C, 24 h; +: presence, -: absence; [a)] determined by ^{1}H NMR spectroscopy.

5.1.2 Reaction scope

The aldehyde scope of the reaction was explored by attempting the reaction between *tert*-butyl isocyanide **3a** and several aromatic and aliphatic aldehydes (**4b**-**m**). Electron-withdrawing groups were found to be crucial for reactivity – possibly due to them being a requirement for encapsulation – as electron-rich and aliphatic aldehydes **4h**-**m** showed no conversion. The isocyanide scope was also investigated using 2-chloro-5-nitrobenzaldehyde **4g** and a series of isocyanides **3b**-**h**: several primary, secondary, tertiary and even aromatic isocyanides reacted successfully; remarkably, only the isocyanides **3g** and **3h**, which contain an ester moiety, displayed no conversion (**Scheme I.11**, **Table I.2**, **Table I.3**).

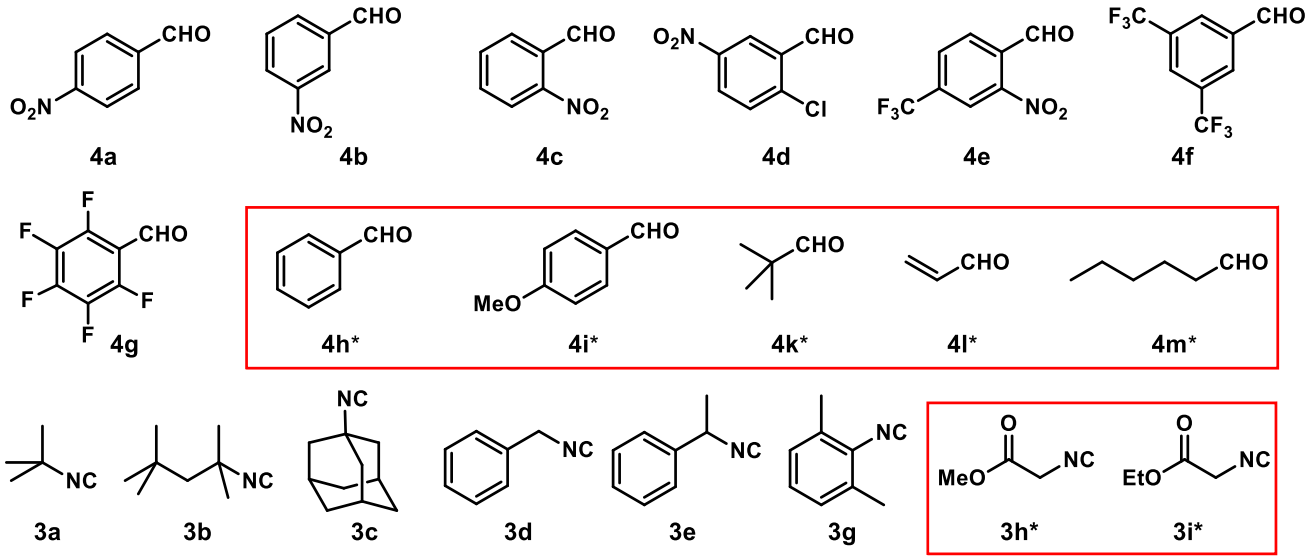

Scheme I.11 Aldehydes and isocyanides on which the reaction was tested. The substrates in the red boxes did not show the desired reactivity.

*Table I.2 Aldehyde scope of the reaction between isocyanide **3a** and aldehydes **4a-f** in the presence of C_R.*

Entry #	Aldehyde	Product	Yield (%)[a]	Entry #	Aldehyde	Product	Yield (%)[a]
1	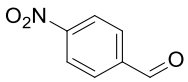 **4a**	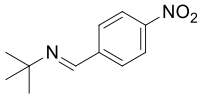 **5aa**	60 0[b] 8[c]	4	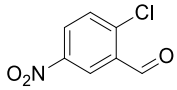 **4d**	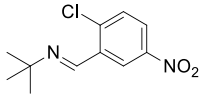 **5ad**	77 0[b] 8[c]
2	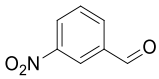 **4b**	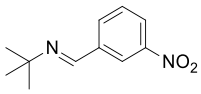 **5ab**	41 0[b] 2[c]	5	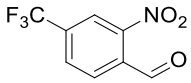 **4e**	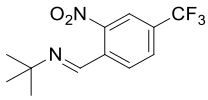 **5ae**	85 0[b] 25[c]
3	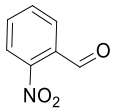 **4c**	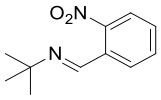 **5ac**	55 0[b] 5[c]	6	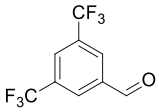 **4f**	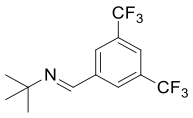 **5af**	33 0[b] <1[c]

[**4**] = 90 mM, [**3a**] = 180 mM, [**1**] = 54 mM, 0.5 mL water-saturated $CDCl_3$, 60 °C, 24 h. [a] Determined by ^1H NMR. [b] no **1** added; [c] [**2a**] = 90 mM (10 eq. with respect to the capsule)

*Table I.2 Isocyanide scope of the reaction between aldehyde **4d** and isocyanides **3b-l** in the presence of C_R.*

Entry #	Isonitrile	Product	Yield (%)[a]	Entry #	Isonitrile	Product	Yield (%)[a]
1	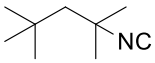 **3b**	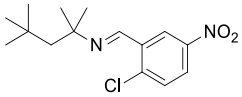 **5bd**	94 0[b] 28[c]	4	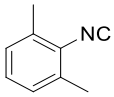 **3g**	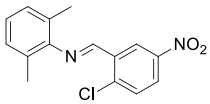 **5gd**	13 0[b] <1[c]
2	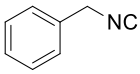 **3d**	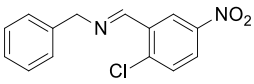 **5dd**	86 0[b] 19[c]	5	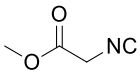 **3h**	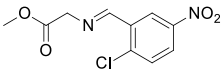 **5hd**	0 0[b] 0[c]
3	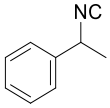 **3e**	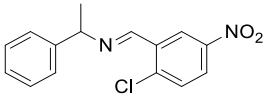 **5ed**	90 0[b] 9[c]	6	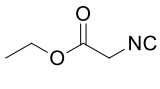 **3i**	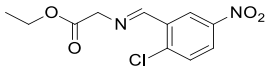 **5id**	0 0[b] 0[c]

[**4d**] = 90 mM, [**3**] = 180 mM, [**1**] = 54 mM, 0.5 mL water-saturated $CDCl_3$, 60 °C, 24 h. [a] Determined by ^1H NMR. [b] no **1** added; [c] [**2a**] = 90 mM (10 eq. with respect to the capsule)

5.1.3 Mechanistic study

The first step taken to investigate the mechanism of the imine formation reaction was to prepare ^{13}C-labelled 1-adamantyl isocyanide **3c*** and have it react with 2-chloro-5-nitrobenzaldehyde **4d** and 2-nitro-4-trifluoromethylbenzaldehyde **4e**, leading to the formation of unlabelled imines **5cd** and **5ce**, respectively; the identities of **5cd** and **5ce** were confirmed by ^1H NMR spectroscopy and GC/MS (**Scheme I.12**). This indicates that the N-C bond of the isocyanide moiety is cleaved during the reaction, presumably releasing the corresponding carbon atom as carbon monoxide, which was indeed detected in the atmosphere over the reaction mixture.

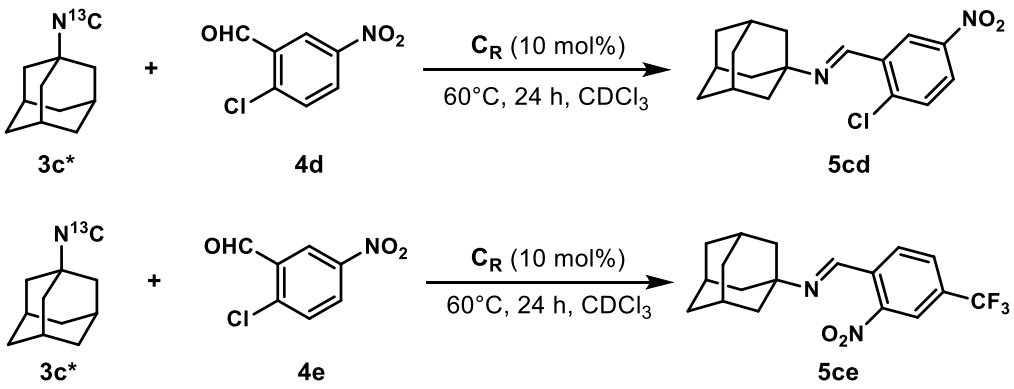

*Scheme I.12 Reactions between ^{13}C-labelled isocyanide **3c*** and aldehydes **4d** and **4e**.*

Almost no literature was found regarding the cleavage of the N-C bond of isocyanides, with the exception of a BF_3-mediated reaction between isocyanides and ketones which was studied by Zeeh *et al.*, Fujii *et al.*, and Kabbe (**Scheme I.13**).[40,41,42] However, Scarso and Tiefenbacher concluded that the mechanism of their reaction had to be different from those proposed by the former authors, as neither amide **6** nor oxetane **8** were detected in the reaction mixture.

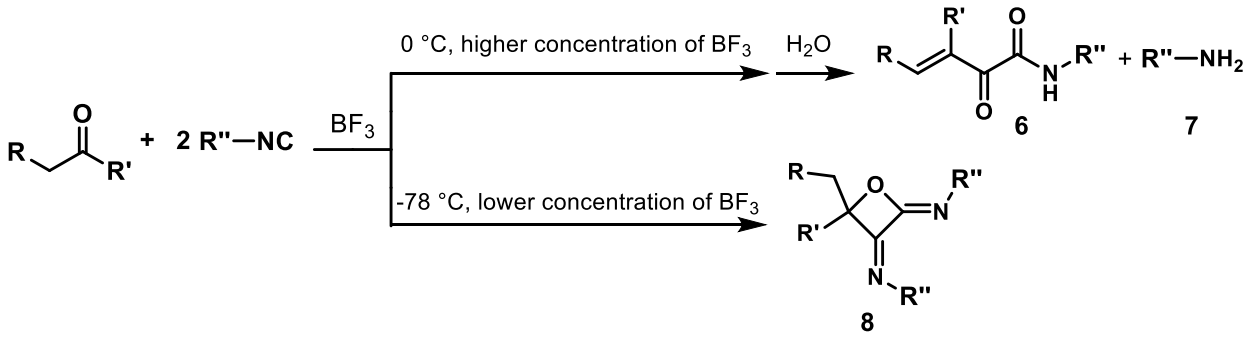

Scheme I.13 Products obtainable through the BF_3-mediated reaction between an isocyanide and an aldehyde (references: see text).

Since some further experiments indicated that there was a positive order for all components (isocyanide, aldehyde and capsule), a pathway based on a cycloaddition/cycloreversion metathesis-like mechanism including the formation of an oxazetidine intermediate **9** was hypothesized (red profile in **Scheme I.14**). Due to the very high activation energy that was computed for the formation of **9**, however, this mechanism seemed unlikely. Therefore, molecular dynamics simulations revealed a possible alternative pathway characterised by much lower gas-phase energy barriers, including the formation of iminooxirane **10**, which would isomerise to aziridinone **11** before decomposing into imine **5aa** and carbon monoxide (blue profile in **Scheme I.14**).

Literature research revealed that a differently substituted iminooxirane was found to quickly isomerise to the corresponding aziridinone.[43] Moreover, aziridinones were reported to decompose upon heating above 75 °C into the corresponding isocyanide and ketone or into a mixture of unsaturated amides through an iminooxirane intermediate (**Scheme I.15**).[44] This, together with the lower activation energy barriers involved, led to the conclusion that the blue pathway (**Scheme I.14**) is the most likely to represent the actual mechanism. This idea was further tested by independently synthesizing aziridinone **11**, whose structure was confirmed by X-ray crystallography, and heating it to 60 °C in water-saturated chloroform-*d* in the presence and absence of capsule $\mathbf{C_R}$. In the presence of $\mathbf{C_R}$, a mixture of aldehyde **4a** (24% yield) and imine **5aa** (16%

yield) was formed; in the absence of C_R, however, only imine **5aa** was produced (92 % yield). This may be due to the Brønsted acidity of C_R, which could promote the hydrolysis of imine **5aa** into the corresponding aldehyde and amine. No other decomposition products were detected, and therefore the blue pathway is considered plausible.

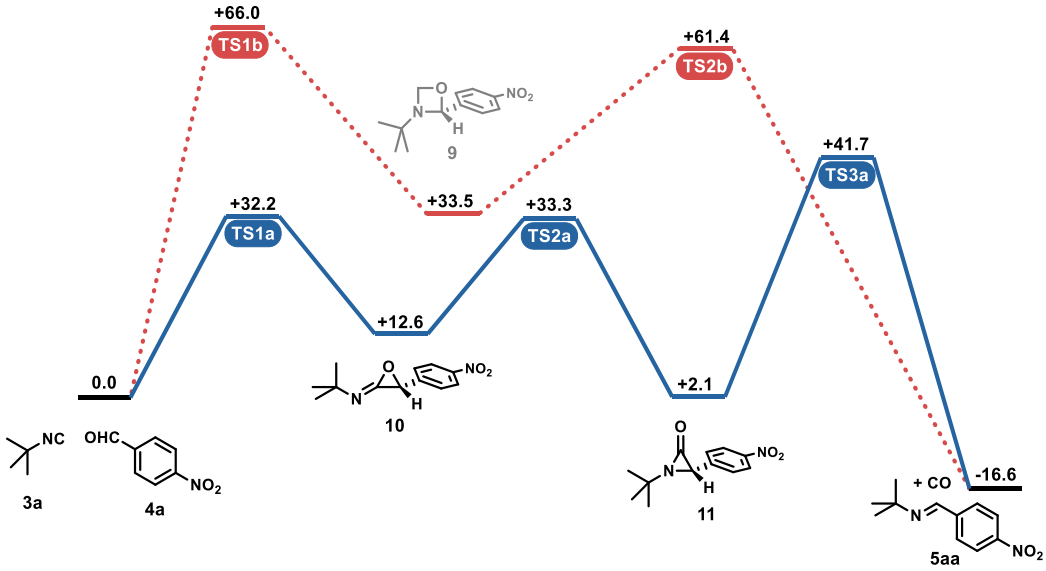

*Scheme I.14 Gas-phase energy profiles for the proposed mechanisms via formation of oxazetidine **11** (red pathway) or iminooxirane **12** (blue pathway); relative energies given in kcal/mol, calculated for T = 323 K.*

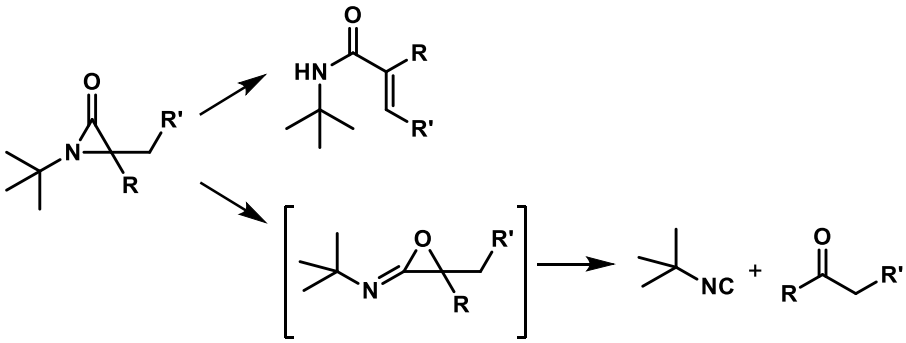

Scheme I.15 Pathways for the thermal decomposition of aziridinones (reference: see text).

5.2 Unusual reactivity of 1,3-diphenylallyl cation promoted by the resorcin[4]arene capsule

Recently, preliminary experiments led by Scarso's research group gave an unexpected result: heating *trans*-1,3-diphenylprop-2-en-1-ol **12** to 60 °C in the presence of capsule $\mathbf{C_R}$ in a solution of $CDCl_3$ led to the formation of a species with a characteristic slightly broad ^{1}H NMR peak at 4.67 ppm (**Figure I.1**). Literature research led to the conclusion that the observed species was 1-phenyl-1*H*-indene **14**.

It has already been shown that capsule $\mathbf{C_R}$ can have an effect on several reactions involving alcohol substrates which eliminate water and form carbocationic intermediates. For example, capsule $\mathbf{C_R}$ was shown to efficiently promote dehydration of an alcohol to the corresponding alkene[45] and dehydrative cyclization and subsequent rearrangement of unsaturated tertiary alcohols to form substituted cyclopentenes (**Scheme I.16**).[46] It was thus hypothesized that the capsule's acidity may be responsible for the protonation and subsequent dehydration of **12**, leading to 1,3-diphenylallyl carbocation **13** which can be stabilised by the capsule's electron-rich inner cavity, where it can rearrange to its cisoid form and undergo intramolecular allylation with an electrophilic aromatic substitution-type (S_EAr) mechanism (**Scheme I.17**).

This result prompted the idea to fully investigate the potential of capsule $\mathbf{C_R}$ to stabilise carbocation **13**, for instance to achieve intermolecular S_EAr allylation of other aromatic substrates. This possibility was then assigned as second aim of this thesis work.

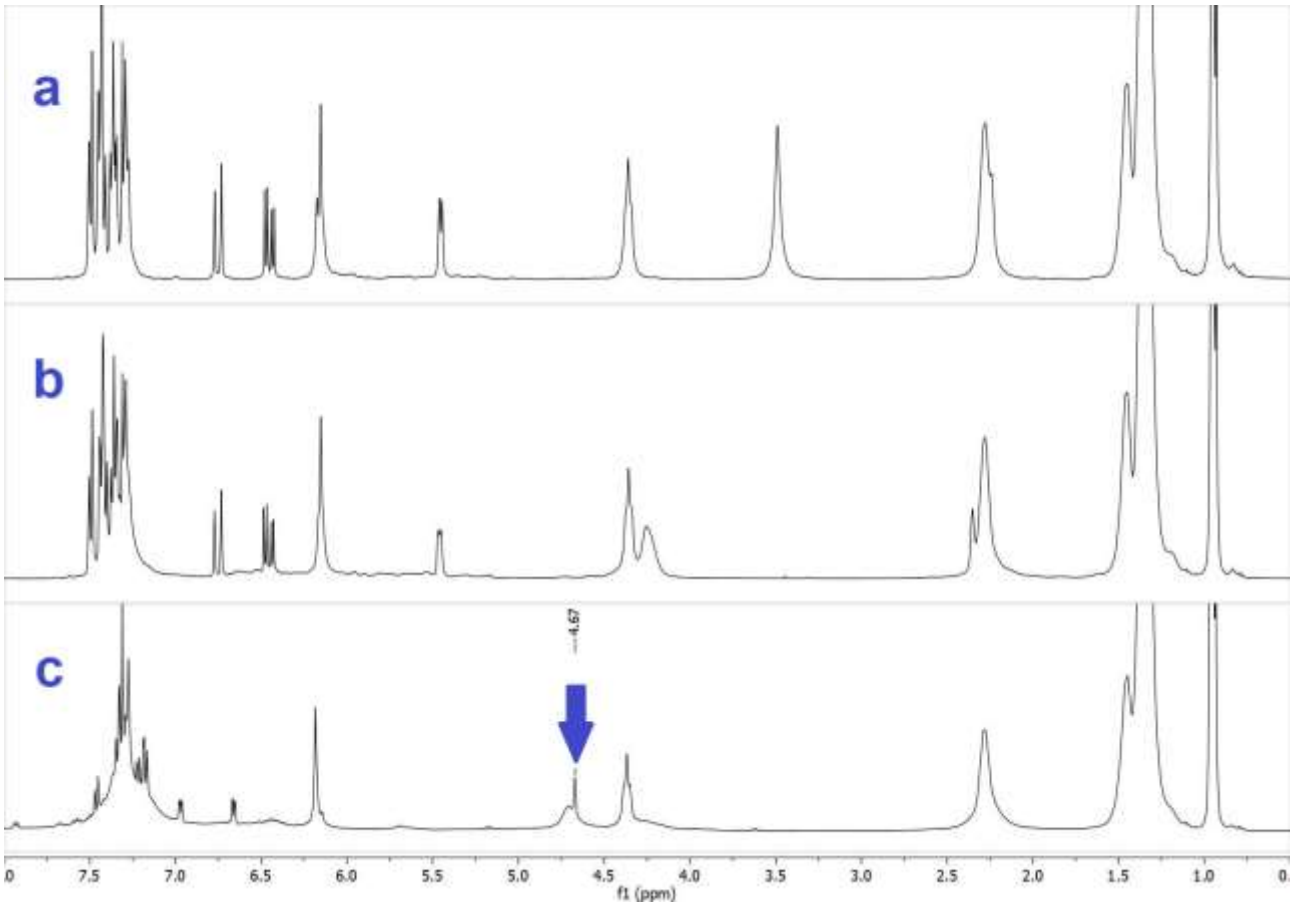

Figure I.1 *^{1}H NMR spectra of a solution of 75 mM **12** and 45 mM of **1** in $CDCl_3$ after 0 (**a**), 1 (**b**) and 17.5 h (**c**) of heating at 60°C; ↓: peak of product **14**.*

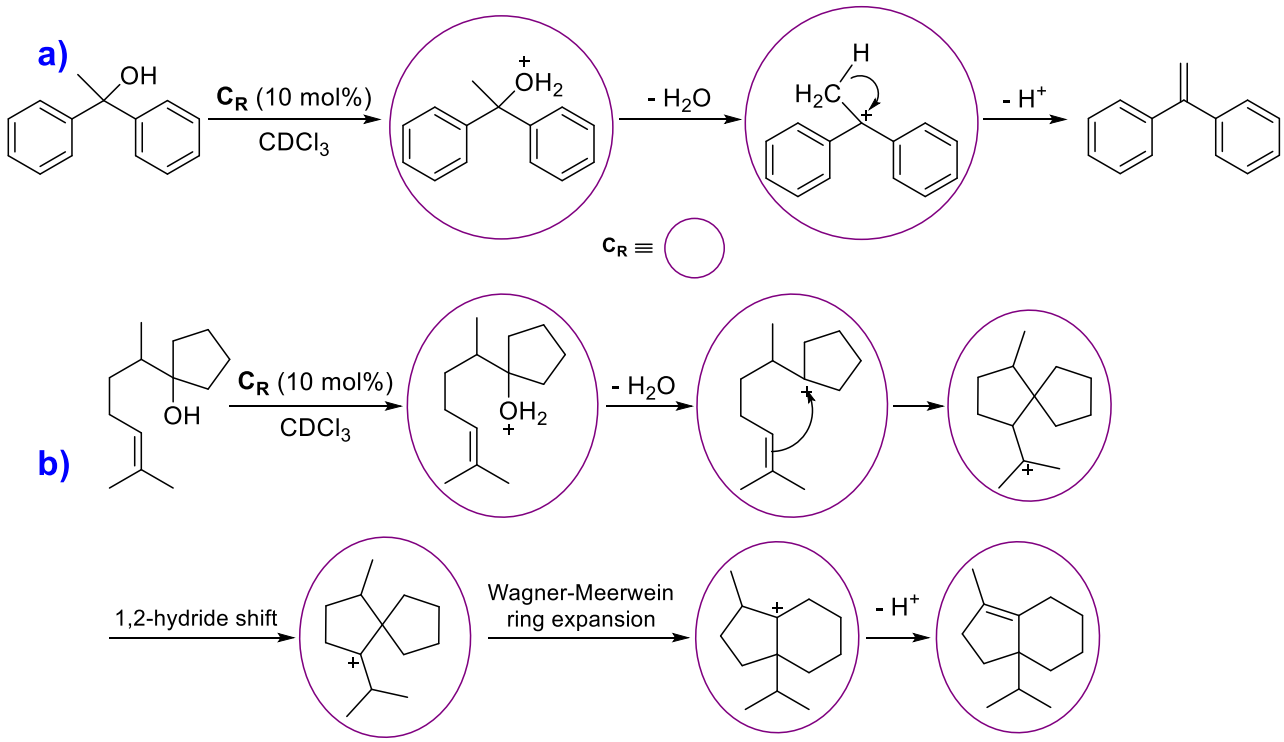

Scheme I.16 *Proposed mechanism for the dehydration of 1,1-diphenylethanol to 1,1-diphenylethylene (**a**) and for the dehydrative cyclization and rearrangement of an unsaturated tertiary alcohol to a substituted cyclopentene promoted by the resorcin[4]arene capsule (references: see text).*

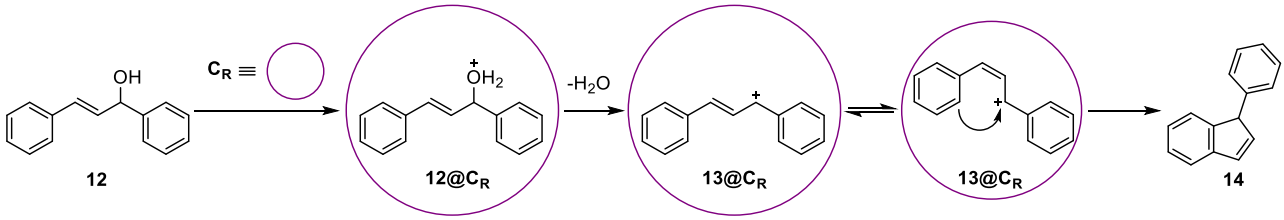

Scheme I.17 *Proposed mechanism for the dehydration and subsequent intramolecular S_EAr allylation of **12** to yield product **14** promoted by the resorcin[4]arene capsule.*

Aim of the thesis

1. General

The focus of this thesis work was twofold: on one hand we sought to finalise the research on the imine formation reaction (**Introduction §5.1**) so that it be ready for publication, and on the other we studied the reactivity of 1,3-diphenylpropenol **12** in the presence of the resorcin[4]arene capsule, investigating whether the 1,3-diphenylallyl cation **13** could be used as an electrophile for intermolecular electrophilic aromatic substitution reactions with several aromatic substrates.

2. Imine formation reaction via condensation of an electron-poor aromatic aldehyde and an isocyanide

The first matter at hand was to replicate the control experiments for the model reaction between 4-nitrobenzaldehyde **4a** and *tert*-butyl isocyanide **3a** (see **Table I.1**) under the optimised conditions that were used for the testing of the reaction scope. Said conditions are as follows: T = 60 °C, reaction time t = 24 h, [**3a**] = 180 mM, [**4a**] = 90 mM, [**1**] = 54 mM (corresponding to 9 mM of $\mathbf{C_R}$) in 0.6 mL of deacidified $CDCl_3$. One further control experiment was carried out, which consisted in performing the same model reaction in the presence of DMSO-d_6, which is able to interact through hydrogen-bonding with **1**, thereby preventing it from self-assembling into $\mathbf{C_R}$.

In order to further demonstrate that the reaction takes place within the cavity of the resorcin[4]arene capsule, we set ourselves the goal of synthesizing a particularly sterically encumbered electron-poor aromatic aldehyde and of having it react with an isocyanide in the presence of the capsule. It is expected that the larger the size of the substrate, the lower the expected yield would be. This would serve as extra validation of the hypothesis that the inner cavity of $\mathbf{C_R}$ is indeed responsible for the observed catalytic effect.

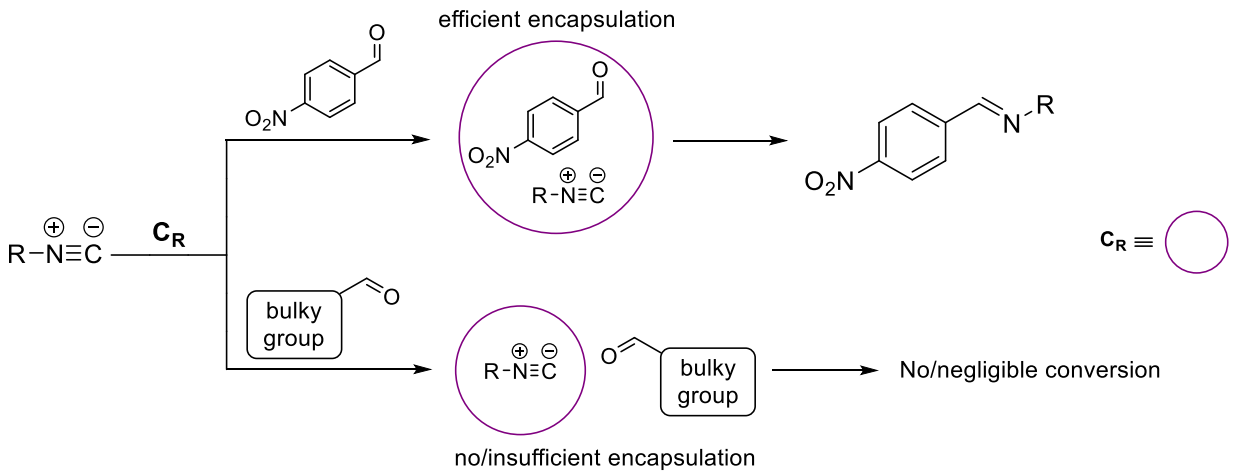

Scheme A.1 *Principle of the control test of the reaction between a sterically encumbered aldehyde and an isocyanide.*

We then moved further, expanding the reaction scope by reacting a series of aldehydes with 1-adamantyl isocyanide **3c**. We also sought to synthesize, purify and characterise all the imine products which had not been previously reported in the literature (**Scheme A.1**, see also **Scheme R.2**).

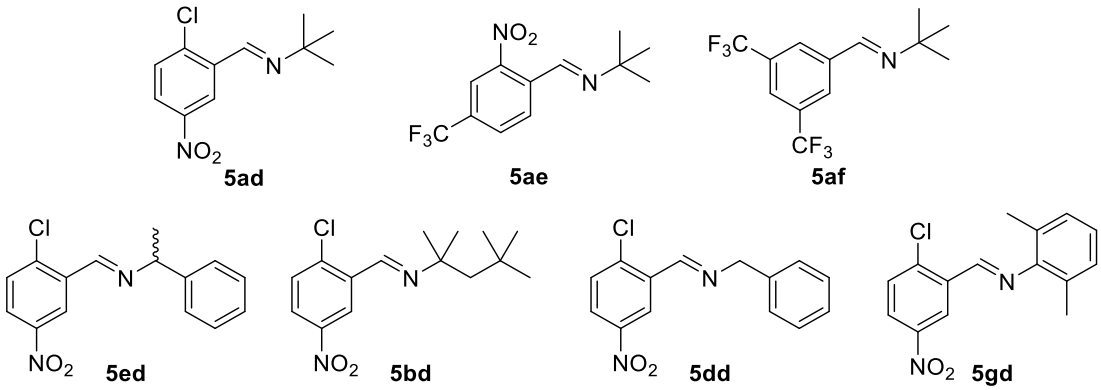

Scheme A.2 *Imines produced by Scarso and Tiefenbacher during the initial investigation of the imine formation reaction scope whose characterisation data was not present in the literature.*

Lastly, in order to further validate the mechanism proposed in **Scheme I.14**, we decided to attempt to observe the aziridinone intermediate **11** over the course of the reaction between aldehyde **4a** and isocyanide **3a**. Aziridinone **11** was synthesized and isolated and its characterisation data were made available by Tiefenbacher's group (see **Results and discussion §1.5**, **Figure R.8** and **Figure R.9**).

3. Reactions of the 1,3-diphenylallyl cation promoted by the resorcin[4]arene capsule

Differently from the imine formation reaction, the research on the reactivity of *trans*-1,3-diphenylprop-2-en-1-ol **12** was in its initial stages: optimization and scope of the reaction. Hence we set out to investigate the behaviour of **12** in the absence and in the presence of capsule $\mathbf{C_R}$ as well as in combination with other substrates.

At first, several control tests were executed to confirm that the catalysis of the dehydration and intramolecular S_EAr allylation of **12** is indeed attributable to the inner cavity of $\mathbf{C_R}$. This led us to discover that **12** displays an interesting, multifaceted behaviour in its interaction with Brønsted acids, which we examined.

Consequently, we tested the reactivity of the 1,3-diphenyl allyl cation **13** in electrophilic aromatic substitutions (S_EAr) with a variety of electron-rich aromatic compounds, attempting to provide proof of a wide reaction scope. A regioselectivity question arose when reactions between **12** and alkoxyphenols were performed: examining this phenomenon, we found that using capsule $\mathbf{C_R}$ as catalyst instead of a generic Brønsted acid significantly changes the distribution of the regioisomers. In order to prove the exclusive characteristics of the catalytic activity of capsule $\mathbf{C_R}$ in these S_EAr reactions, control tests were carried out.

Results and discussion

1. Imine formation by capsule-catalysed condensation of an isocyanide and an electron-poor aldehyde

1.1 Control tests: reaction between *p*-nitrobenzaldehyde **4a** and *tert*-butyl isocyanide **3a** under optimised conditions

Previously, control tests for the capsule-catalysed imine formation reaction had been carried out under non-optimised conditions (see **Introduction §5.1.1** and **Table I.1**). It was therefore decided to repeat such experiment to consolidate the results under optimised conditions consisting in running the reaction at 60 °C, with an isocyanide:aldehyde ratio equal to 2:1 and 60 mol% of resorcin[4]arene **1** (equivalent to 10 mol% of capsule $\mathbf{C_R}$) with respect to the aldehyde. An explanation of the conditions of the control experiments can be found in **Table R.1**, whereas the results are displayed in **Table R.2**. As mentioned in **Aim of the thesis §2**, one further control experiment was added, consisting in conducting the reaction in the presence of DMSO-d_6, which is able to bind **1** through H-bonding, hindering its self-assembly into $\mathbf{C_R}$. As expected, all the control tests confirmed the crucial role of the assembled capsule $\mathbf{C_R}$ in the specific catalyzed reaction.

Table R.1 *Conditions of the control tests for the reaction between 4-Nitrobenzaldehyde (**4a**) and t-butyl isocyanide **3a**.*

Test #	Conditions	Principle	Expected result
1	60 mol%[a] of **1** (equivalent to 10 mol%[a] of capsule $\mathbf{C_R}$), no other additives	Reaction conducted normally	Normal yield
2	No **1**, no other additives	Without catalyst, the reaction is not expected to occur	No yield
3	No **1**, 10 mol%[a] of acetic acid	Acetic acid has a pK_a similar to that of $\mathbf{C_R}$; this aims to prove that the reaction is not catalysed by the Brønsted acidity of the capsule	No yield
4	No **1**, 2.4 eq[a]. of *n*-hexylresorcinol (a quantity of capsule subunits equivalent to 10 mol%[a] of capsule)	This aims to prove that the reaction is not catalysed by the property of the resorcinol units to interact with the substrates via H-bonding	No yield
5	60 mol%[a] of **1**, 1 eq.[a] of $[NEt_4][BF_4]$ **2a**	NEt_4 is a very competitive guest for $\mathbf{C_R}$, making the inner cavity of the capsule inaccessible to the substrates	Low yield
6	60 mol%[a] of **1**, 10 eq.[a] of DMSO-d_6	DMSO-d_6 binds **1** through H-bonding, preventing it from self-assembling into $\mathbf{C_R}$	No/low yield

[a)] with respect to the aldehyde.

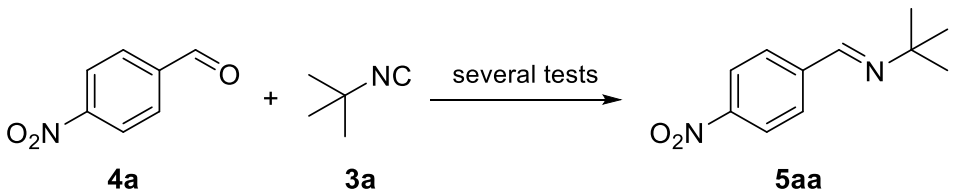

Scheme R.1 *Model reaction adopted for the control experiments*

*Table R.2 Results of the control tests for the reaction between 4-Nitrobenzaldehyde **4a** and t-butyl isocyanide **3a**.*

Test #	C_R	Additive	Yield [%][a]
1	+	-	49
2	-	-	no conversion
3	-	HOAc (10 mol%[b])	no conversion
4	-	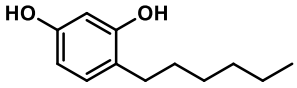 (2.4 eq.[b])	decomposition
5	+	$TEABF_4$ (**2**, 1 eq.[b])	7
6	+	DMSO-d_6 (10 eq.[b])	no conversion

T = 60 °C, t = 24 h, [3a] = 180 mM, [1] = 54 mM, [4a] = 90 mM, 0.6 mL de-acidified $CDCl_3$. +: presence; -: absence; [a)] determined by ^{1}H NMR spectroscopy; [b)] with respect to the aldehyde.

1.2 Expansion of the reaction scope

Feeling that the scientific validity of this work could benefit from the expansion of the reaction scope (see **Introduction §5.1.2**), we attempted the reaction between 1-adamantyl isocyanide **3c** and a series of aldehydes **4a**-**g**. Yields greater than 60% were observed in all cases, specifically >80% in more than half of the reactions. Almost always, the yields were higher than those obtained for the reactions between the same aldehydes and *tert*-butyl isocyanide **3a**, except in the case of 4-trifluoromethyl-2-nitrobenzaldehyde **4e** (see **Table I.2**). We also attempted the reaction between *tert*-butyl isocyanide **3a** and pentafluorobenzaldehyde **4g** (a new electron poor aldehyde never tested before) and between 2-naphtyl isocyanide **3f** and 2-chloro-5-nitrobenzaldehyde **4d** (see **Scheme I.11**). The results are presented in **Table R.3** and **Table R.4**.

*Table R.3 Results of the reactions between isocyanide **3a** and aldehyde **4g** and between **3f** and **4d**.*

Entry #	Isocyanide	Aldehyde	Product	Yield (%)[a]
1	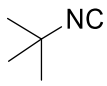 **3a**	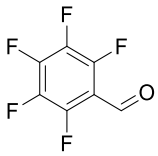 **4g**	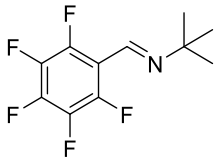 **5ag**	89
2	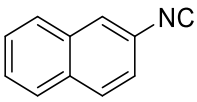 **3f**	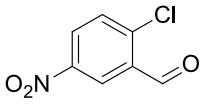 **4d**	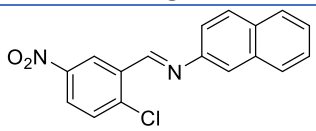 **5fd**	36

[**4**] = 90 mM, [**3**] = 180 mM, [**1**] = 54 mM, 0.6 mL de-acidified $CDCl_3$, 60 °C, 24 h. [a)] Determined by ^{1}H NMR.

Table R.4 *Results of the reactions between 1-adamantyl isocyanide **3c** and aldehydes **4a-g** in the presence of C_R.*

Entry #	Aldehyde	Product	Yield (%)[a]	Entry #	Aldehyde	Product	Yield (%)[a]
1	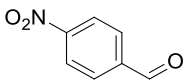 **4a**	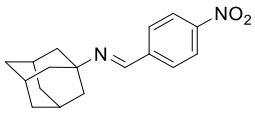 **5ca**	91	5	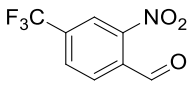 **4e**	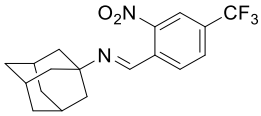 **5ce**	83
2	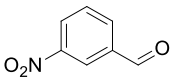 **4b**	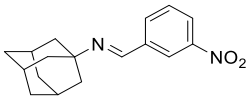 **5cb**	90	6	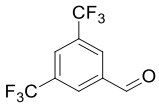 **4f**	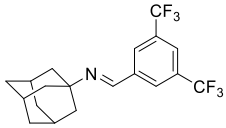 **5cf**	62
3	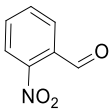 **4c**	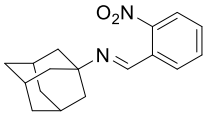 **5cc**	66	7	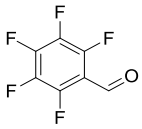 **4g**	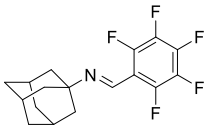 **5cg**	90
4	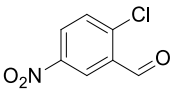 **4d**	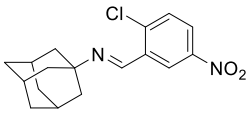 **5cd**	96				

[**4**] = 90 mM, [**3**] = 180 mM, [**1**] = 54 mM, 0.6 mL de-acidified $CDCl_3$, 60 °C, 24 h. [a)] Determined by ^{1}H NMR.

1.3 Synthesis and characterisation of unknown imine products

Several imine products obtained throughout the examination of the reaction scope are not reported in the literature (**Scheme R.2**), so it was necessary to synthesize and purify them and obtain their characterisation data.

Since *tert*-butylamine **15a**, *tert*-octylamine **15b**, benzylamine **15d** and 1-phenylethylamine **15e** were available in the laboratory, imines **5dd**, **5ed** and **5ad-ag** were synthesized via condensation of the corresponding aldehyde-amine pair. Since *tert*-butylamine **15a** is a very volatile liquid (boiling point ~ 45 °C), **5ad-af** could be produced by neat reaction of a 5:1 amine-aldehyde solution in a sealed vial under heating at 100 °C. Complete conversion was confirmed by ^{1}H NMR spectroscopy after 3-3.5 h of reaction, at which point it was sufficient to remove the excess amine by distillation under reduced pressure, affording the product in near-quantitative yields (**Scheme R.3**). The reactions were conducted in an inert atmosphere to prevent oxidation of the aldehydes into the corresponding carboxylic acids.

When the same method was employed with pentafluorobenzaldehyde **4g**, a ^{1}H NMR spectrum of an aliquot of the reaction mixture indicated that the reaction had not progressed appreciably even after a day. Believing that this was due to having reached the equilibrium between the condensation reaction and the hydrolysis of **5ag**, molecular sieves were added to remove water from the mixture and push the equilibrium towards the imine product. After an additional day of reaction, the sieves were removed and the volatiles were removed by rotary evaporation, affording a yellow oil which was found to contain at least three different

compounds upon TLC analysis. Preparative TLC was employed to attempt to purify the components of the oil, leading to the collection of two yellow oily fractions which were analysed by ^{1}H- and ^{19}F NMR spectroscopy (**Figure R.1**). The resulting spectra showed only a weak resonance compatible with the desired imine product, and the presence of many resonances both in the ^{19}F spectrum and in the aliphatic zone of the ^{1}H spectrum led us to hypothesize that nucleophilic aromatic substitution (S_NAr) had occurred (**Scheme R.4**); this hypothesis was validated by literature research showing that pentafluorobenzaldehyde is in fact susceptible to S_NAr with aliphatic amines.[47]

Believing that the S_NAr reaction could be limited under less harsh conditions, synthesis of **5ag** was re-attempted by having aldehyde **4g** react with a 50 % excess of amine **3a** in chloroform-*d* at 60 °C; the progress of the reaction was monitored frequently by ^{1}H NMR spectroscopy in order to ascertain that no S_NAr occurred and complete conversion was achieved after 4 h. The excess of amine was then removed by employing rotary evaporation for the shortest time necessary, in order to limit the evaporation of **5ag**, which is also volatile. This afforded the pure product. Similar methods were used to successfully synthesize and purify **5dd** and **5ed** (**Scheme R.5**).

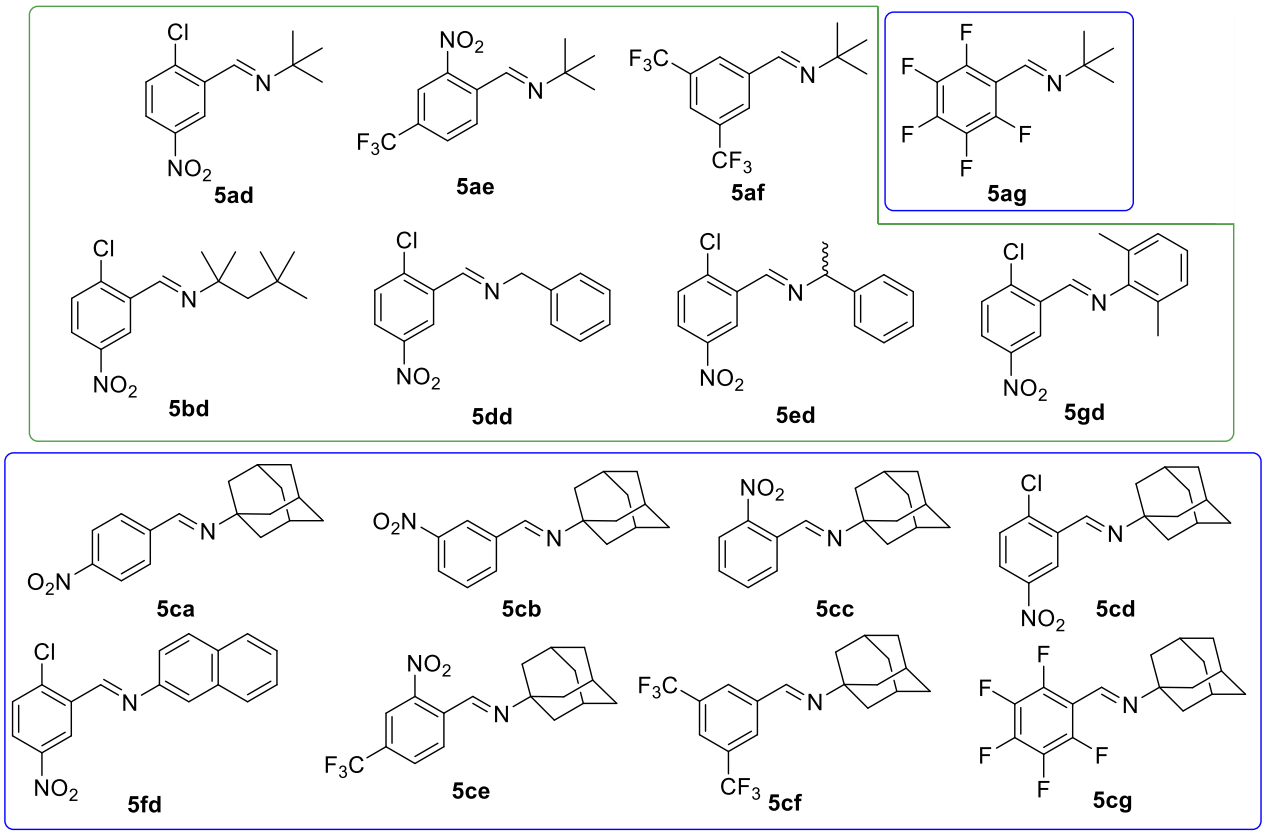

Scheme R.2 *Imine products whose characterisation data was not present in the literature. The imines highlighted in green and blue are, respectively, from Scarso and Tiefenbacher's initial research and from the expansion of the reaction scope carried out for this thesis.*

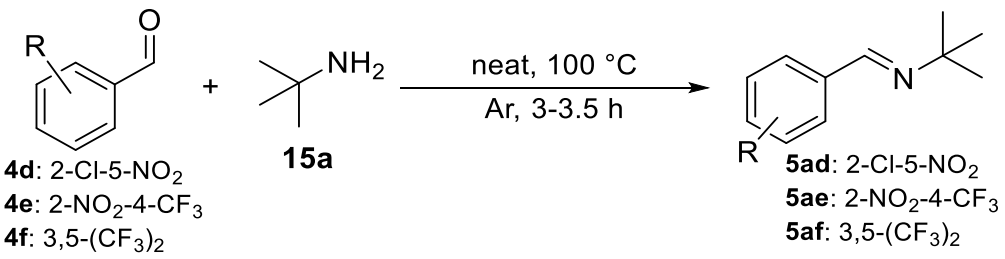

Scheme R.3 *General method for the synthesis of imines* ***5ad-af****.*

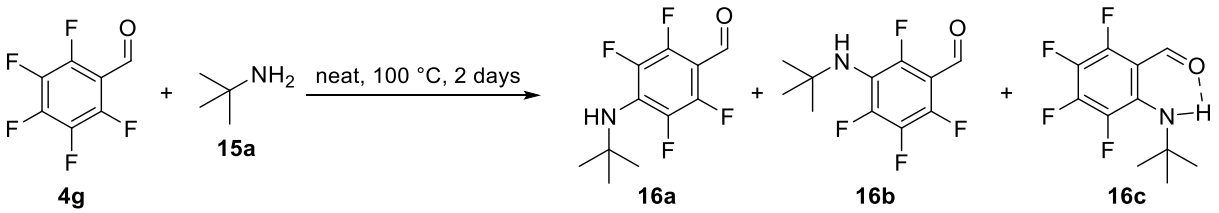

Scheme R.4 *Possible* S_NAr *reaction between aldehyde* ***4g*** *and amine* ***3a*** *to form* tert*-butylaminosubstituted products* ***16a-c****.*

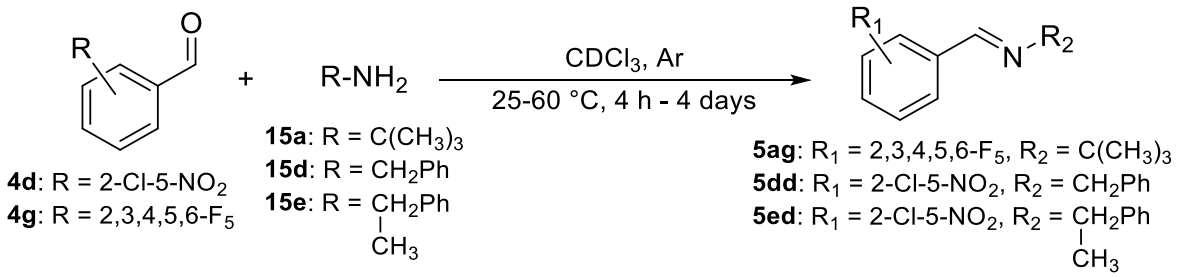

Scheme R.5 *General method for the synthesis of imines* ***5ag, 5dd*** *and* ***5ed****.*

Seeing as *tert*-octylamine **15b**, 1-adamantylamine **15c**, 2-naphtylamine **15f** and 1,6-dimethylaniline **15g** were not immediately available for the direct synthesis with the aldehyde, it was decided to attempt to synthesize the imines from the corresponding isocyanides by means of the capsule-catalysed reaction (**Scheme R.6**) in 0.2-0.7 mmol scale, with the added purpose of proving the validity of the reaction as a chemical synthesis tool. This was first investigated on the reaction between pentafluorobenzaldehyde **4g** and *tert*-butyl isocyanide **3a**, in order to optimise the method. Purification by preparative TLC failed, presumably due to the presence of a relatively large amount of resorcin[4]arene **1**, which saturated the initial portion of the TLC plate and caused co-elution of the other species present in the mixture (**Figure R.2**). Therefore, it became apparent that, in order to achieve good chromatographic separation, resorcin[4]arene would have to be at least partially removed from the reaction mixture beforehand.

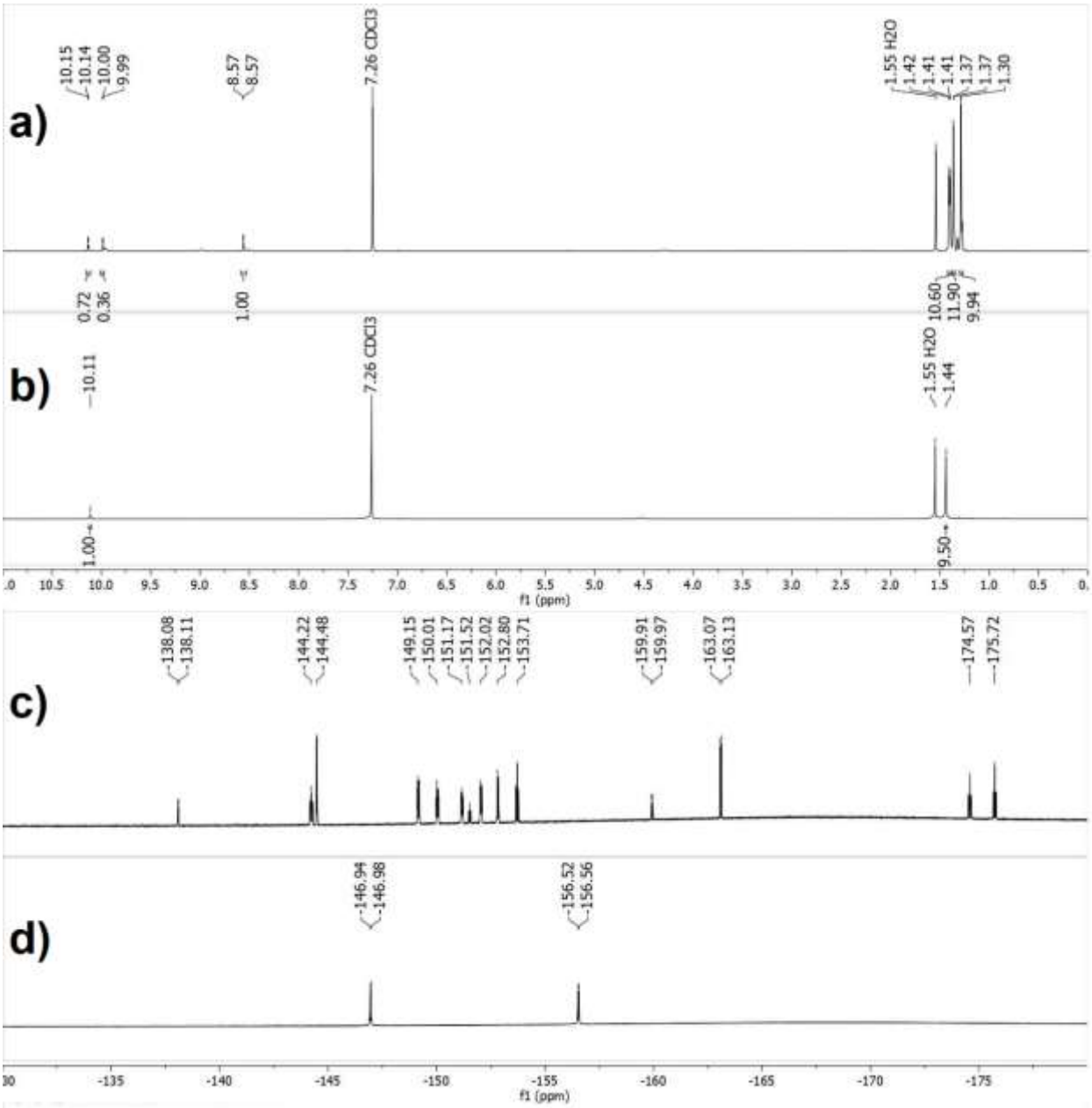

Figure R.1 [1]*- (a) and* [19]*F NMR (c) spectra of the first fraction and* [1]*H (b) and* [19]*F NMR (d) spectra of the second fraction obtained from the preparative TLC separation of the mixture of the reaction between* ***4g*** *and* ***15a****. Given that the second fraction shows only one and two resonances in the* [1]*H and* [19]*F NMR spectra respectively, it is plausible that it contains pure 4-(*tert*-butylamino)-2,3,5,6-tetrafluorobenzaldehyde* ***16a****, whereas the first fraction likely contains a mixture of the* ortho- *and* meta*-isomers as well as other by-products.*

Over the course of the laboratory work, it was observed that resorcin[4]arene was scarcely eluted in TLC analyses by cyclohexane-ethyl acetate eluent mixtures with ethyl acetate in 10-40% range. It was thus decided to attempt to try to simply "filter away" the resorcin[4]arene from the reaction mixture with silica gel: successful removal was achieved by solvent evaporation by rotary evaporation, re-dissolution of the resulting solid in an appropriate cyclohexane-ethyl acetate mixture and filtration through silica gel in a funnel (**Figure R.3**). It was found empirically that about 15-20 cm^3 of packed silica gel were needed to successfully remove 100 mg of resorcin[4]arene. Unfortunately, though, silica gel proved to be able to promote acid hydrolysis of the imine products upon filtration of the mixture. This problem was solved by adding ~1% triethylamine to the eluent solution. Once resorcin[4]arene was removed, it was then possible to successfully

purify the imine products via column chromatography on silica gel with an appropriate cyclohexane-ethyl acetate eluent mixture basified with ~1% triethylamine.

In summary, imines **5bd**, **5gd**, **5fd** and **5ca-cg** were obtained via condensation of the corresponding isocyanide-aldehyde pair in 2:1 ratio catalysed by 10 mol% $\mathbf{C_R}$ in $CDCl_3$ in a 0.2-0.7 mmol scale, which is 4-13 times larger than the reaction conditions previously used for the common tests. The volatiles were then removed by rotary evaporation and the remaining solid was purified of resorcin[4]arene by filtration on a silica gel plug, as described above. The resulting solution was treated by rotary evaporation to remove the solvent. This afforded the final product in the case of **5bd**, as isocyanide **3b** was volatile; in the other cases, it afforded a solid from which the imine product was isolated by column chromatography, as described above. The details regarding the experimental procedures are available in **Experimental section §2.3** and the spectra of the products are reported in **Characterisation data §1**.

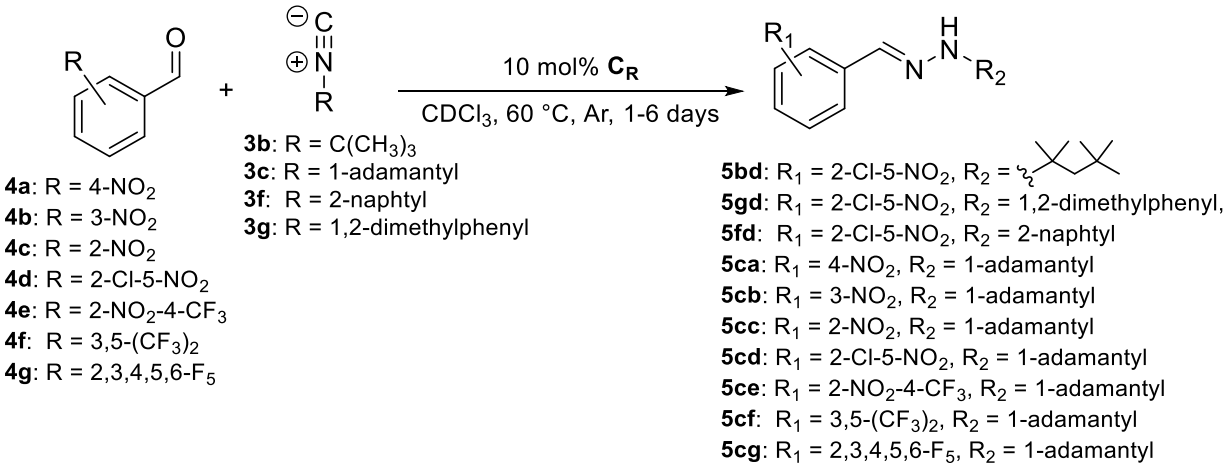

Scheme R.6 *General method for the synthesis of imines **5bd, 5gd, 5fd** and **5ca-cg**.*

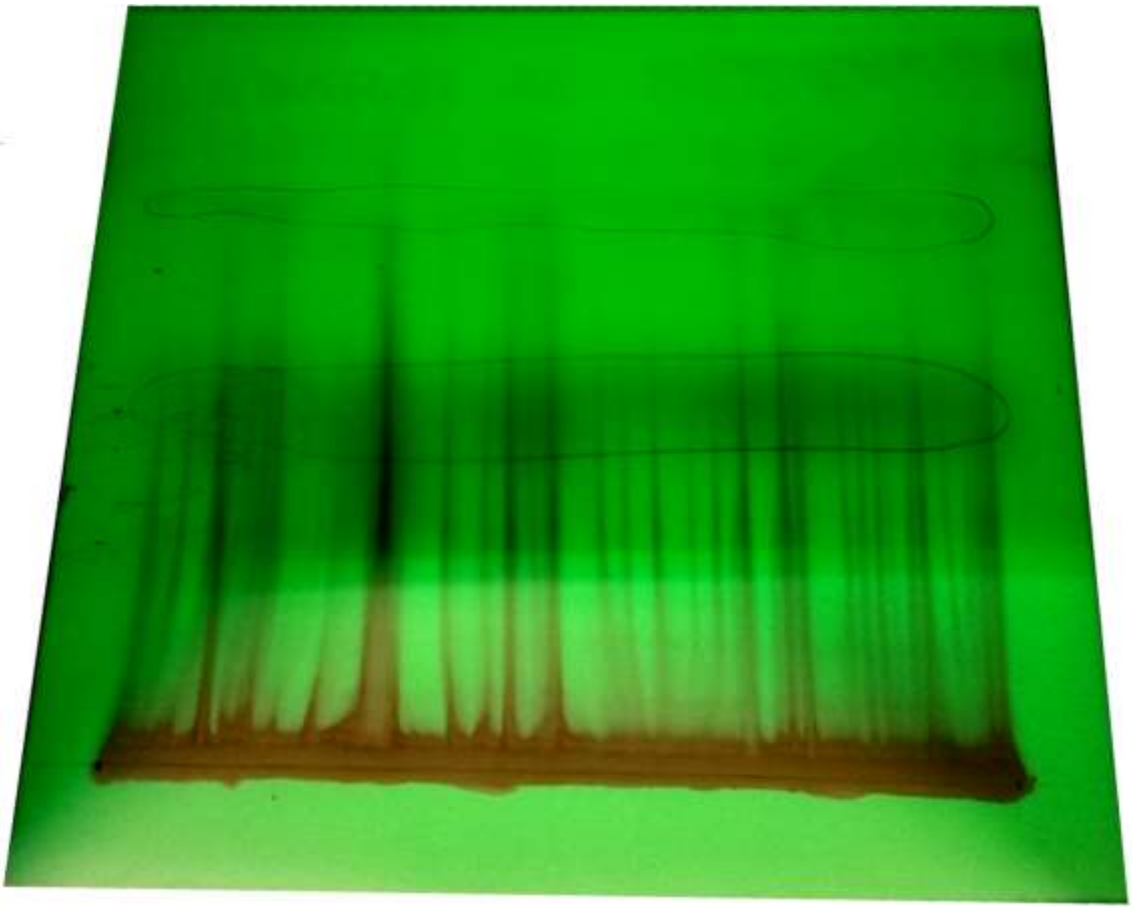

Figure R.2 *Photograph of the TLC plate used for the preparative TLC with which it was initially attempted to purify an imine product under a UV lamp. Notice how resorcin[4]arene has saturated the lower part of the plate, compromising the separation.*

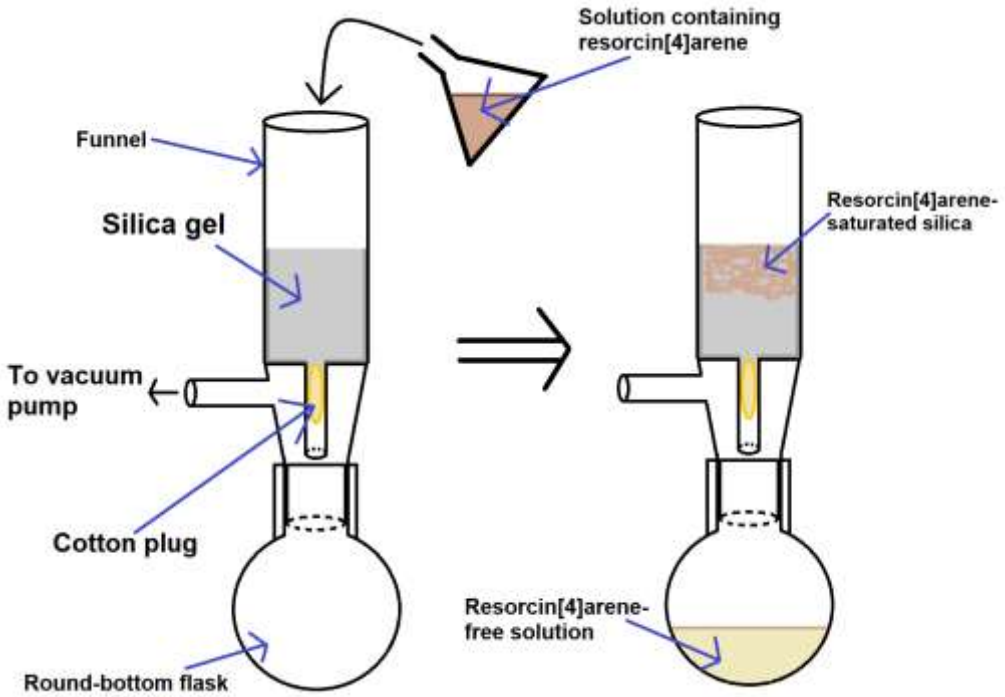

Figure R.3 *Schematic representation of the apparatus used to remove resorcin[4]arene from a solution by filtration on silica gel.*

1.4 Comparison of the encapsulation affinity of *tert*-butyl isocyanide **3a** and 1-adamantyl isocyanide **3c**

As mentioned in **Results and discussion §1.2**, the yield of the reaction between an aldehyde and 1-adamantyl isocyanide **3c** was often higher than that of the reaction between the same aldehyde and *tert*-butyl isocyanide **3a** (**Figure R.4**). It was thus hypothesized that **3c** could display a greater affinity than **3a** for the inner cavity of capsule $\mathbf{C_R}$, thereby being more readily encapsulated and reacting more quickly. To investigate the extent of the encapsulation of **3a** and **3c**, NMR titrations were carried out. For each isocyanide, four solutions in chloroform-*d* were prepared, containing 1 equivalent of capsule $\mathbf{C_R}$ and 1, 5, 10 and 20 equivalents of isocyanide, respectively. ^{1}H NMR spectra of each sample were recorded, showing resonances at low, background-free chemical shifts which are neither attributable to the free isocyanide nor to capsule $\mathbf{C_R}$, and are thus assigned to the encapsulated isocyanide (1.45 ppm for free **3a**, -0.53– -0.68 ppm for **3a@C$_R$**; 2.12–1.61 ppm for free **3c**, 0.62– -0.12 ppm for **3c@C$_R$**, "@" indicates encapsulation; **Figure R.7**); the low values of the chemical shift are due to the very electron-rich nature of the cavity. Since changes in the concentration of the isocyanide did not affect the chemical shifts of these resonances, but rather only their intensities, it was concluded that the encapsulation-exchange phenomenon operates on a timescale longer than that of the NMR chemical shift (see **Introduction §1**). Thus, it was considered possible to calculate the concentration of encapsulated isocyanide through the ratios of the intensities of the resonances, as shown in **Equation R.1**.

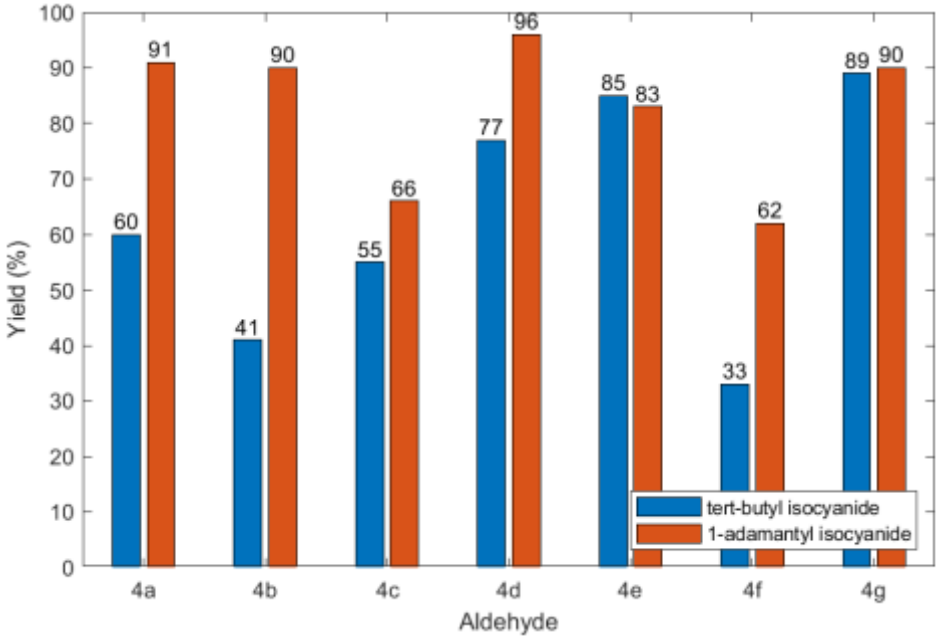

Figure R.4 *Comparison of the yields of the capsule-catalysed reactions between aldehydes* ***4a-g*** *and* tert-*butyl isocyanide* ***3a*** *(**blue**) or 1-adamantyl isocyanide* ***3c*** *(**orange**).*

$$[\mathbf{3@C_R}] = \frac{I_{\mathbf{3@C_R}}}{I_{\mathbf{3@C_R}} + I_{free\ \mathbf{3}}} \cdot [\mathbf{3}]_{tot},$$

Equation R.1 *[**X**]: molar concentration of **X**, I_Y: intensity of the resonance of **Y**.*

Unfortunately, the resonances of the free isocyanides were covered by those of capsule $\mathbf{C_R}$, so another method for calculating the concentration of the encapsulated isocyanides **3a@C$_R$** and **3c@C$_R$** had to be devised. In the end, with the reasonable assumption that the intensity of an NMR signal be directly proportional to the concentration of the corresponding chemical species with *n·f* as proportionality constant, where *n* is the number of H nuclei corresponding to the resonance and *f* is a response factor expressed as

mmol^{-1}, we worked out the encapsulated isocyanide-to-capsule ratios (**[3@C$_R$]/[C$_R$]**) as shown in **Equation R.2**.

$$I_{C_R} = 24 \cdot f \cdot [\boldsymbol{C_R}]_{tot}, \quad I_{3a@C_R} = 9 \cdot f \cdot [\boldsymbol{3a@C_R}], \quad I_{3c@C_R} = 15 \cdot f \cdot [\boldsymbol{3c@C_R}]$$

$$\Rightarrow \frac{[\boldsymbol{3a@C_R}]}{[\boldsymbol{C_R}]_{tot}} = \frac{24 \cdot I_{3a@C_R}}{9 \cdot I_{C_R}}, \quad \frac{[\boldsymbol{3c@C_R}]}{[\boldsymbol{C_R}]_{tot}} = \frac{24 \cdot I_{3c@C_R}}{15 \cdot I_{C_R}}$$

Equation R.2 *Equations used to calculate [**3@C$_R$**]/[**C$_R$**] ratios. The numerical factors 24, 9 and 15 are due to the fact that the resonances of **C$_R$**, **3a** and **3c** are assigned to 24, 9 and 15 protons of the corresponding chemical species, respectively.*

Since different nuclei have different relaxation times, new ^{1}H NMR spectra of the samples were recorded with a longer delay time between successive scans (15 seconds instead of 1 second), in order to ensure that the value of *f* be the same for all ^{1}H nuclei. The ^{1}H NMR analyses were then repeated after having left the sample sitting at room temperature for 16 and 24 h, to account for the possibility that equilibrium between encapsulation and egress might not be achieved immediately. The results are plotted in **Figure R.5**, and details about the calculations are available in **Experimental section §2.4**.

The plots clearly indicate that each supermolecule **C$_R$** tends to include several isocyanide molecules **3**, with the exact number of **3@C$_R$/C$_R$** stabilising between 1 and 1.5 at high concentrations in the case of 1-adamantyl isocyanide **3c**, whereas well over 2.5 molecules of *tert*-butyl isocyanide **3a** seem to be included by each supermolecule **C$_R$** at the same conditions (which most closely represent the conditions at which the reactions are carried out). In general, the ratio [**3@C$_R$**]/[**C$_R$**] is higher for **3a** than for **3c**, indicating that **C$_R$** tends to encapsulate a higher number of molecules of the former. This, however, could be simply due to the smaller size of **3a**, not necessarily implying a lower affinity of **3c** for the inner cavity of **C$_R$**.

In order to better judge the relative of affinity of **3a** and **3c** for the cavity of the capsule, we then calculated the binding constants K_{3a} *and* K_{3c} as shown in **Equation R.3**. This calculation was carried out only on the dataset extracted from the samples with $[\mathbf{3}]_{tot}$ = 1 eq., as the plots in **Figure R.5** indicate that only in these conditions can the equilibria of encapsulation of higher numbers of isocyanide molecules be neglected. The results are displayed in **Figure R.6**. Due to the very approximate nature of this calculation, the numerical values of *K* should not be considered in absolute terms, but rather be used for comparison. Indeed, the estimated values of *K* are almost always greater for **3a** than for **3c**, being in accordance with the above reported results in suggesting that **3a** has a higher affinity than **3c** for the inner cavity of capsule **C$_R$**.

<u>In conclusion</u>, since *tert*-butyl isocyanide **3a** shows a superior tendency for encapsulation than 1-adamantyl isocyanide **3c**, the greater reactivity of the latter substrate cannot be explained simply in terms of its propensity to reside in the inner cavity of the catalytic capsule.

$$f = \frac{I_{C_R}/24}{[\boldsymbol{C_R}]_{tot}}, \quad [\boldsymbol{3@C_R}] = \frac{I_{3@C_R}/n}{f}, \quad [\mathbf{3}]_{free} = [\mathbf{3}]_{tot} - [\boldsymbol{3@C_R}], \quad [\boldsymbol{C_R}]_{free} = [\boldsymbol{C_R}]_{tot} - [\boldsymbol{3@C_R}]$$

$$\Rightarrow K \approx \frac{[\boldsymbol{3@C_R}]}{[\mathbf{3}]_{free} \cdot [\boldsymbol{C_R}]_{free}}$$

Equation R.3 *Mathematical procedure employed to calculate the binding constants K of* tert-*butyl isocyanide **3a** and 1-adamantyl isocyanide **3c**. n is equal to 9 for the former and to 15 for the latter species (see caption of **Equation R.2**).*

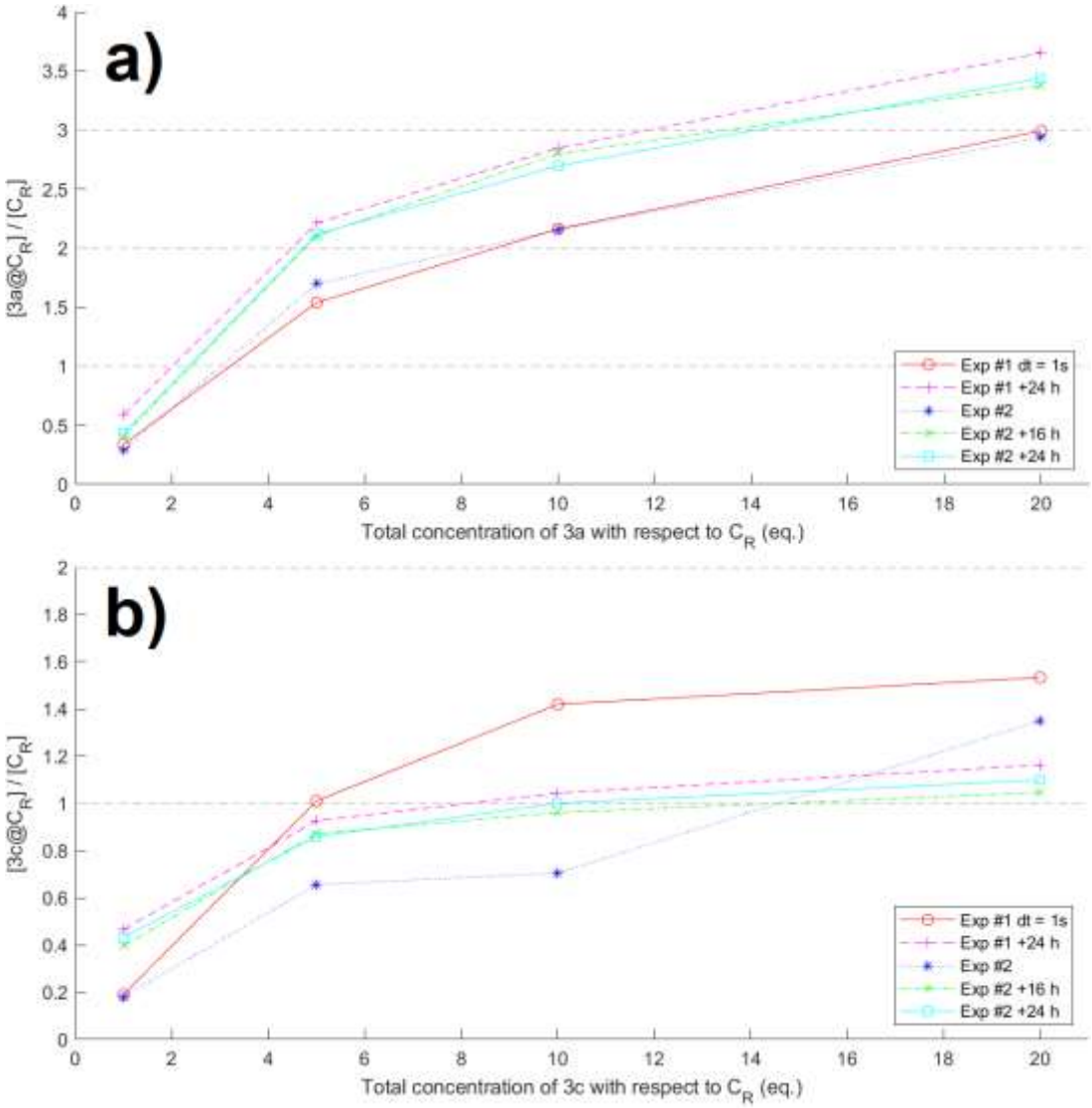

Figure R.5 *Plot of the ratio of encapsulated* tert-*butyl isocyanide to capsule [**3a@C$_R$**] / [**C$_R$**] (**a**) and of the ratio of encapsulated 1-adamantyl isocyanide to capsule [**3c@C$_R$**] / [**C$_R$**] (**b**) as a function of the total concentration of isocyanide. "dt = 1s" signals that the spectra from which the dataset was extracted were recorded with a delay time between successive scans equal to 1 second instead of 15 seconds. "+XX h" indicates the time for which the sample was left to sit before the spectrum was recorded; the absence of this label means that the spectrum was recorded immediately after the preparation of the sample.*

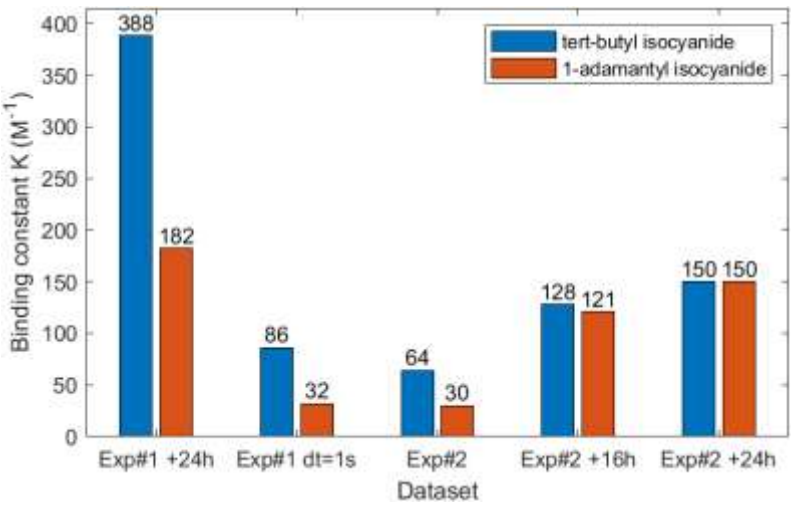

Figure R.6 *Bar plot of the binding constants of* tert-*butyl isocyanide **3a** and 1-adamantyl isocyanide **3c**.*

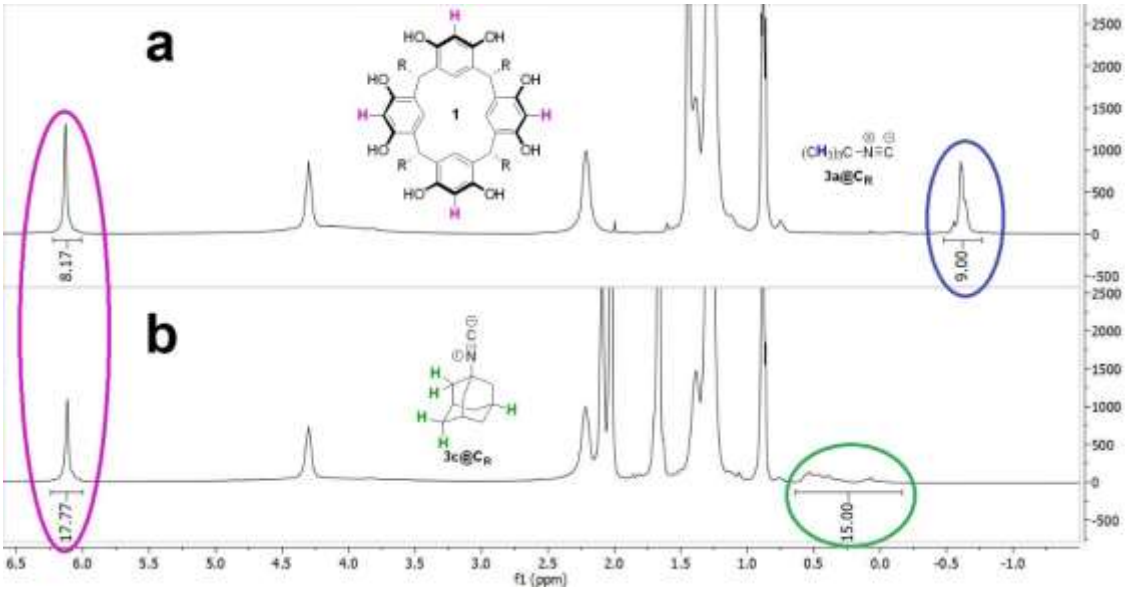

*Figure R.7 ^{1}H NMR spectra of a solution of 55 mM **1** and 1.1 M **3a** (a) or **3b** (b) in de-acidified $CDCl_3$.*

1.5 Observation of the aziridinone intermediate **11** in the reaction mixture

With the goal of providing further validation to the reaction mechanism proposed by Tiefenbacher's group (**Scheme I.14**), it was decided to attempt to detect the presence of aziridinone **11** in the mixture of the reaction between aldehyde **4a** and isocyanide **3a** catalysed by capsule $\mathbf{C_R}$. Aziridinone **11** was synthesized and purified by Tiefenbacher's group, and its characterisation data are as follows (see also **Figure R.8** and **Figure R.9**):

^{1}H NMR (600 MHz, $CDCl_3$): δ [ppm] = 8.22 (d, ^3J = 8.8 Hz, 2H), 7.51 (d, ^3J = 8.8 Hz, 2H), 3.92 (s, 1H), 1.40 (s, 9H).
^{13}C NMR (151 MHz, $CDCl_3$): δ [ppm] = 152.0, 147.6, 143.5, 126.8, 124.0, 58.6, 44.9, 27.7.
HRMS (ESI) = calc.: 229.0947 [M-CO+Na], found: 229.0945.

As a first experiment, a **4a**-**3a**-**1** solution in a 1:2:0.6 ratio in chloroform-*d* was heated to 60 °C in an NMR tube. ^{1}H NMR spectra were recorded after 1, 2 and 3 h of heating, until it became apparent that the intensity of the small resonances attributable to trace components of the mixture were not increasing, meaning that the reaction had reached a steady state of advancement. No resonances attributable to **11** were detected in any of the ^{1}H NMR spectra.

The reaction was repeated and, in order to eliminate the interference of the resonances of resorcin[4]arene **1**, the latter was removed by filtration on silica gel (see **Results and discussion §1.3**) after observing with ^{1}H NMR spectra that the reaction proceeded in the same way as in the previous iteration of the test. Once, again, no ^{1}H NMR resonances compatible with the presence of any detectable amount of **11** were visible. COSY and DOSY analyses similarly gave no clear indication as to the presence or absence of **11** in the mixture.

Concluding that aziridinone **11** be present in a concentration too low to be detected by NMR spectroscopy, we analysed the mixture by GC/MS, observing no signals compatible with the presence of **11**. Since aziridinones tend to decompose above 75 °C (see **Introduction §5.1.3**), it was hypothesized that **11** could decompose in the GC column, preventing its detection. We thus analysed the mixture by low-resolution MS

with an ESI source, finding no mass peaks corresponding to **11** either in its M^+ nor in its $[M+Na]^+$ form. Just like Tiefenbacher's group, we observed only a signal compatible with **11** in its $[M - CO + Na]^+$ form (exact mass = 229.0947; detected mass = 229.18); unfortunately, said signal is absolutely indistinguishable from that of the imine product **5aa** in its $[M+Na]^+$ form (**Scheme R.7**). Therefore, it became apparent that **11** cannot be detected by mass spectrometry analysis of the reaction mixture.

In conclusion, the detection of the aziridinone intermediate **11** was not successful. The results we obtained, however, are in no way incompatible with its presence in the reaction mixture, thus not subtracting validity from the hypothesized mechanistic pathway.

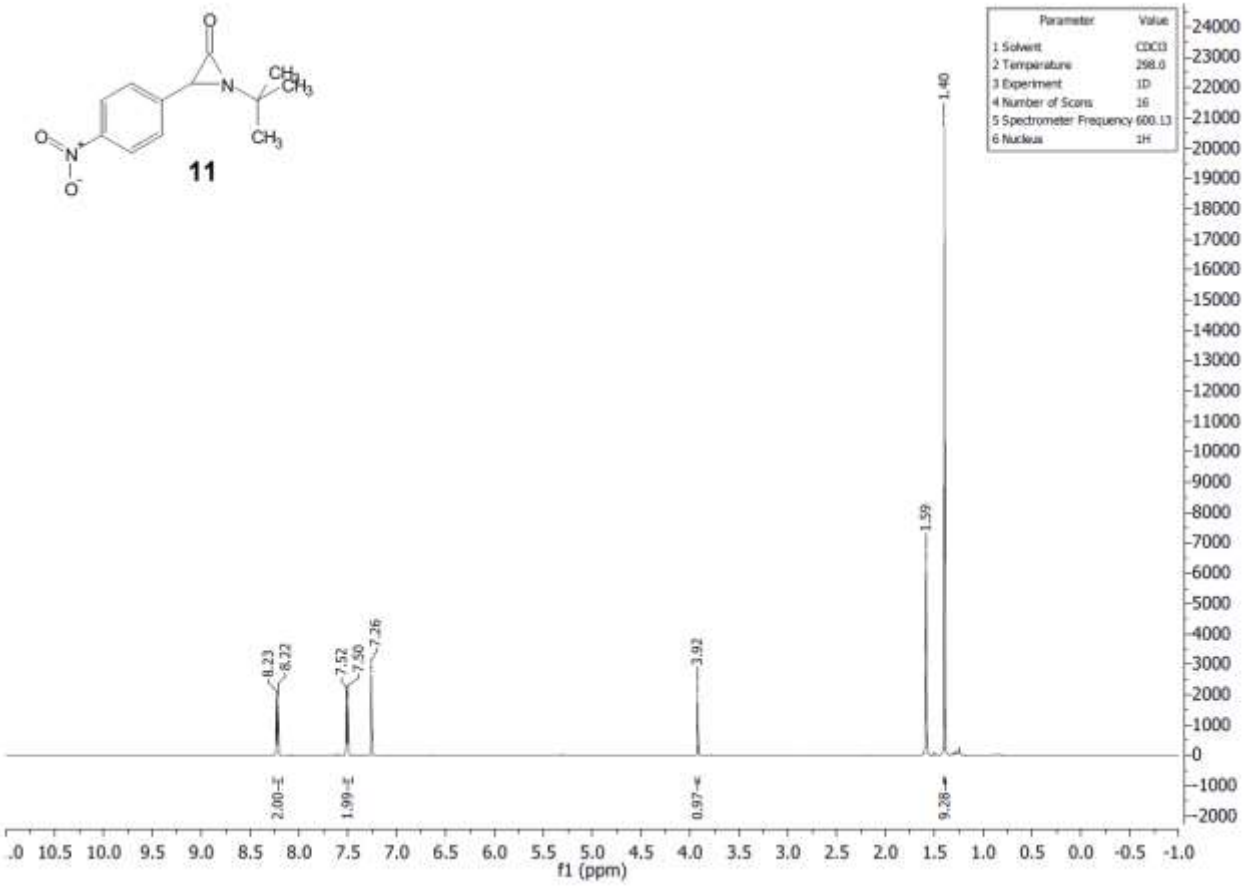

Figure R.8 *^{1}H NMR spectrum of 1-*tert*-butyl-3-(4-nitrophenyl)aziridin-2-one **11** in $CDCl_3$.*

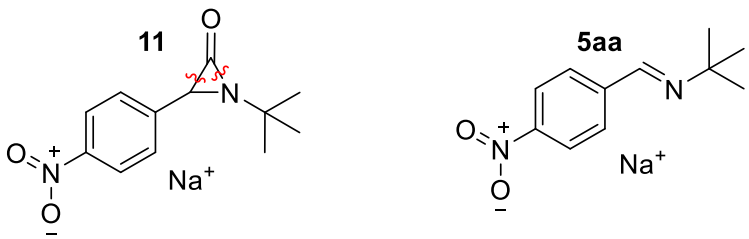

Exact Mass [**11** - CO + Na^+]: 229.0947 Exact Mass [**5aa** + Na^+]: 229.0947

Exact Mass [**11**$^+$]: 234.0999

Exact Mass [**11** + Na^+]: 257.0897

Scheme R.7 *Exact masses of the chemical species relevant to the mass spectrometry detection attempt of the aziridinone intermediate **11**.*

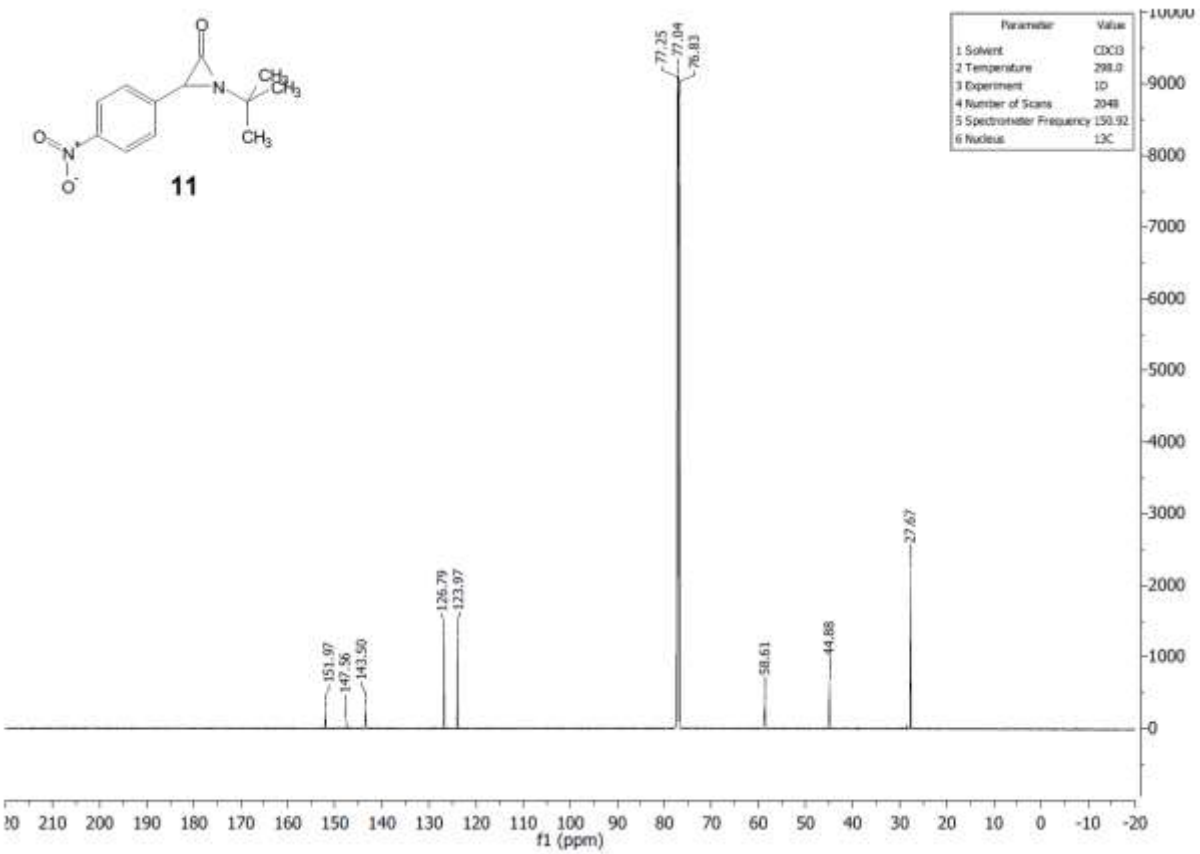

Figure R.9 ^{13}C *NMR spectrum of 1-*tert*-butyl-3-(4-nitrophenyl)aziridin-2-one* ***11*** *in* $CDCl_3$.

1.6 Test of the aldehyde-isocyanide condensation reaction with a sterically encumbered electron-poor aromatic aldehyde

In order to further demonstrate the crucial role of the cavity of capsule $\mathbf{C_R}$ in catalysing the imine formation reaction, we sought to synthesize a sterically encumbered electron-poor aromatic aldehyde. This aldehyde would then be used as a substrate in the capsule catalysed reaction with an isocyanide with the expectation that it would not react, thus proving that substrates too bulky to be efficiently encapsulated cannot undergo the particular mechanistic pathway illustrated in **Scheme I.14**.

For this role, 3,5-bis(4-nitrophenyl)benzaldehyde **4n** was designed and synthesized by converting 1,3,5-tribromobenzene into 3,5-dibromophenyllithium which was then carbonylated with DMF, affording 3,5-dibromobenzaldehyde. The latter product was converted into **4n** via Suzuki coupling with 2 eq. of 4-nitrophenylboronic acid (**Scheme R.8**).

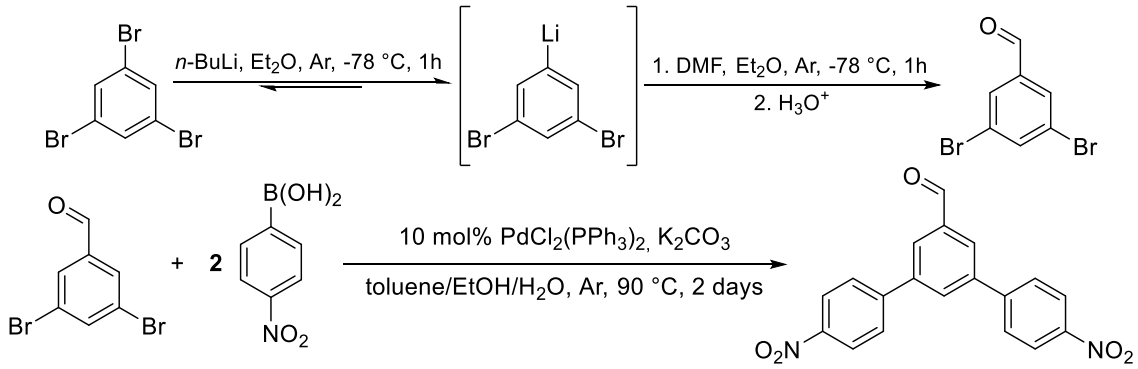

Scheme R.8 Synthetic route employed to obtain 3,5-bis(4-nitrophenyl)benzaldehyde ***4n***.

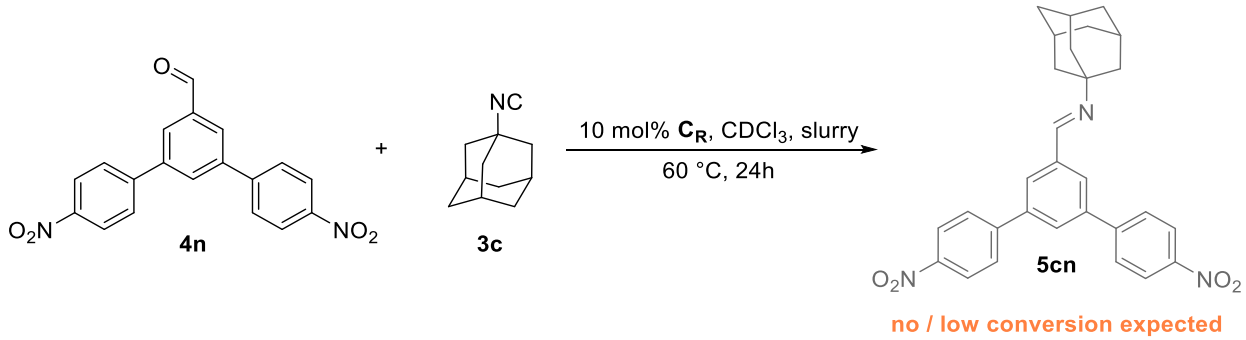

*Scheme R.9 Reaction between aldehyde **4n** and isocyanide **3c** catalysed by capsule **C$_R$**.*

Unfortunately, **4n** proved to be poorly soluble in most common organic solvents, including chloroform, DMSO, diethyl ether and benzene. Nevertheless, we reacted **4n** with **3c** to see if the reaction would take place through progressive dissolution of the aldehyde (Scheme R.9).

To our surprise, ^{1}H NMR spectra of the heterogeneous reaction mixture (Figure R.10) suggested that aldehyde **4n** actually did react with isocyanide **3c** to form the corresponding imine **5cn**: though the ^{1}H NMR resonances of the latter compound are not reported in the literature, the resonances in the spectrum of the reaction mixture subjected to 24 h of heating to 60 °C were compatible with those that would be expected for imine **5cn**. The high intensity of these NMR signals, however, could be due to a higher solubility of product **5cn** with respect to substrate **4n**, which is probably caused by the bulky adamantly group hindering π-stacking phenomena, which most likely contribute to the scarce solubility of **4n**.

The solvent was removed from two aliquots of the reaction mixture by rotary evaporation and substituted with benzene-d_6 and DMSO-d_6 with the aim of obtaining a completely homogeneous mixture whose NMR spectra could be used to estimate a yield; however, all attempts to make a homogeneous sample at a concentration compatible with NMR analysis were unsuccessful. A homogeneous sample was finally obtained in DMSO-d_6 at temperatures above 80 °C, which was analysed by ^{1}H NMR spectroscopy; unfortunately, the spectrum hinted that decomposition phenomena had occurred. A spectrum of another sample in DMSO-d_6 was recorded at 60 °C under the hypothesis that, at that temperature, product **5cn** would be completely dissolved even though **4n** was not: this would allow for estimation of the yield from the integrals of the former compound and of isocyanide **3c**; an estimated yield of ~40% was thus worked out (details in Experimental section §2.6). Although the complexity of the spectrum in the region of the resonances of **3c** could easily have resulted in a non-negligible error, such a large figure likely indicates that **4n** does indeed react successfully with **3c**. This led us to hypothesize that **4n** is simply not sufficiently bulky to prevent its encapsulation. This hypothesis is corroborated by a recently published article, where Neri *et al.* employed a much more sterically encumbered substrate than our aldehyde **4n** in order to prevent it from reacting within capsule **C$_R$** (Scheme R.10).[48]

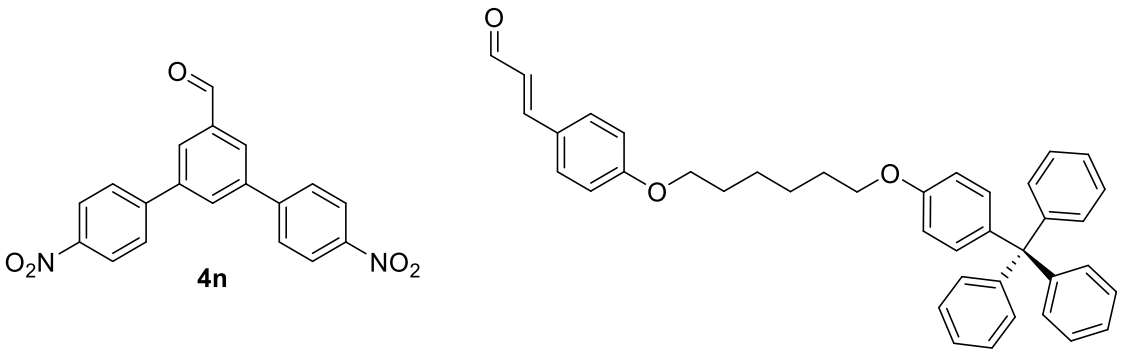

*Scheme R.10 Comparison of our bulky aldehyde **4n** (left) and the sterically encumbered substrate used by Neri et al. (right) which was too bulky to be converted in a Diels-Alder reaction in capsule **C_R** (reference: see text).*

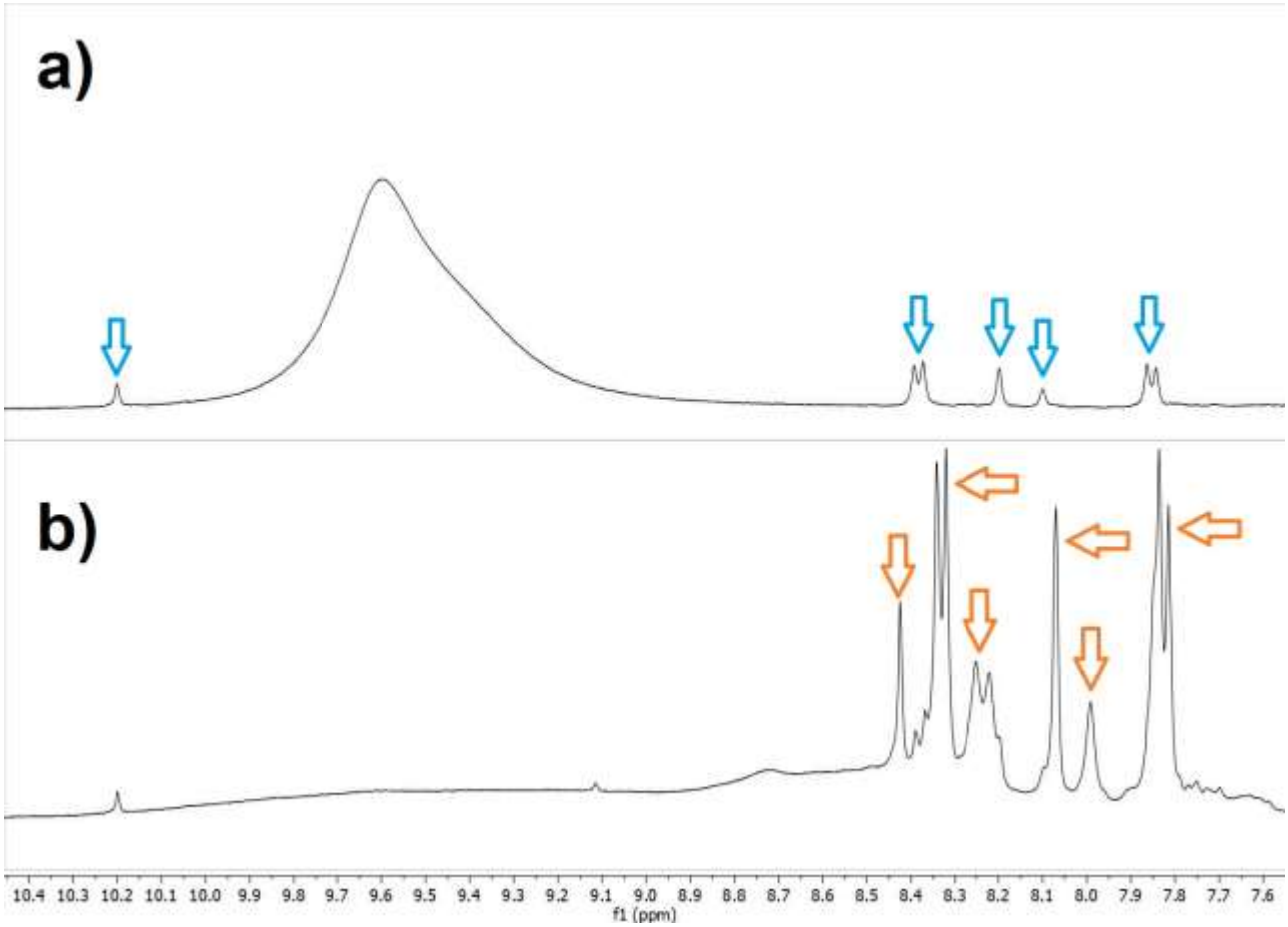

*Figure R.10 Detail of the ^{1}H NMR spectra of the mixture of the reaction in Scheme R.9 before the start of the reaction (a) and after 24 h of heating (b). The blue and orange arrows indicate, respectively, the resonances of aldehyde **4n** and those of a reaction product, likely imine **5cn**.*

2. Reactivity of 1,3-diphenylpropenol catalysed by the resorcin[4]arene capsule

2.1 Intramolecular S_EAr allylation and acid-catalysed decomposition of 1,3-diphenylpropenol

As mentioned in **Aim of the thesis §3**, the first matter at hand was to ascertain the crucial role of capsule $\mathbf{C_R}$ in catalysing the intramolecular S_EAr allylation of *trans*-1,3-diphenylprop-2-en-1-ol **12** to form 1-phenyl-1*H*-indene **14**. To this end, control tests were carried out with the same conditions illustrated in **Table R.1**, with the difference that tetrabutylammonium bromide **2b** was used as competitive guest instead of tetraethylammonium tetrafluoroborate **2a**. The results reported in **Table R.5** confirm that the cyclization reaction is not promoted exclusively either by Brønsted acidity or by the H-bonding properties of $\mathbf{C_R}$, but rather by a combination of effects including the stabilization of cationic intermediate **13** within the electron rich cavity of the host.

We noticed that an apparent triplet was visible at 5.14 ppm in the ^{1}H NMR spectra (**Figure R.1**) of the reaction mixtures of all the control tests, even when capsule $\mathbf{C_R}$ was not present or when no **14** was formed. This resonance was attributed to an unknown compound which we hypothesized to be ether **17**. In order to obtain this compound in a higher yield and better compare its resonances with those reported in the literature, **12** was reacted with 10 mol% of 4-toluenesulphonic acid. Surprisingly, the ^{1}H NMR spectrum of the resulting reaction mixture showed even different resonances, which were found to be representative of a 1:1 mixture of *trans*-1,3-diphenylpropene **18** and chalcone **19**, as confirmed by comparison with literature spectra. The other unknown compound was later obtained via reaction of **12** with 10 mol% of trifluoroacetic acid and purification by flash chromatography on silica gel; its identity as ether **17** was confirmed by comparison of its ^{1}H NMR spectrum with spectra reported in the literature. This led to the conclusion that Brønsted acids protonate the OH group of **12**, promoting its subsequent substitution via nucleophilic attack of another molecule of **12** to form **17**, which can then disproportionate into **18** and **19**; the mechanism illustrated in **Scheme R.11** is proposed for these reactions. This explanation was validated further by the observation that weaker acids, shorter reaction times and lower temperatures lead to higher yields of **17**, whereas more severe conditions push the reaction towards **18** and **19** (**Table R.6**).

It is important to stress that catalysis with simple Brønsted acids never yielded the cyclic intramolecular product **14**, which forms only in the presence of capsule $\mathbf{C_R}$. This implies that the nature of the inner cavity of the capsule plays a crucial role in driving cation **13** towards the intramolecular allylation product **14** instead of products **17**-**19**, probably thanks to the steric constriction caused by the encapsulation.

(*E*)-3-Phenylprop-2-en-1-ol (cinnamyl alcohol) and 1,3-diphenylprop-2-yn-1-ol were also tested at 60 °C in the presence of 10 mol% of $\mathbf{C_R}$. No significant changes were observed in the ^{1}H NMR spectra recorded after 2 and 20 h of heating, indicating no reactivity comparable to that of **12**.

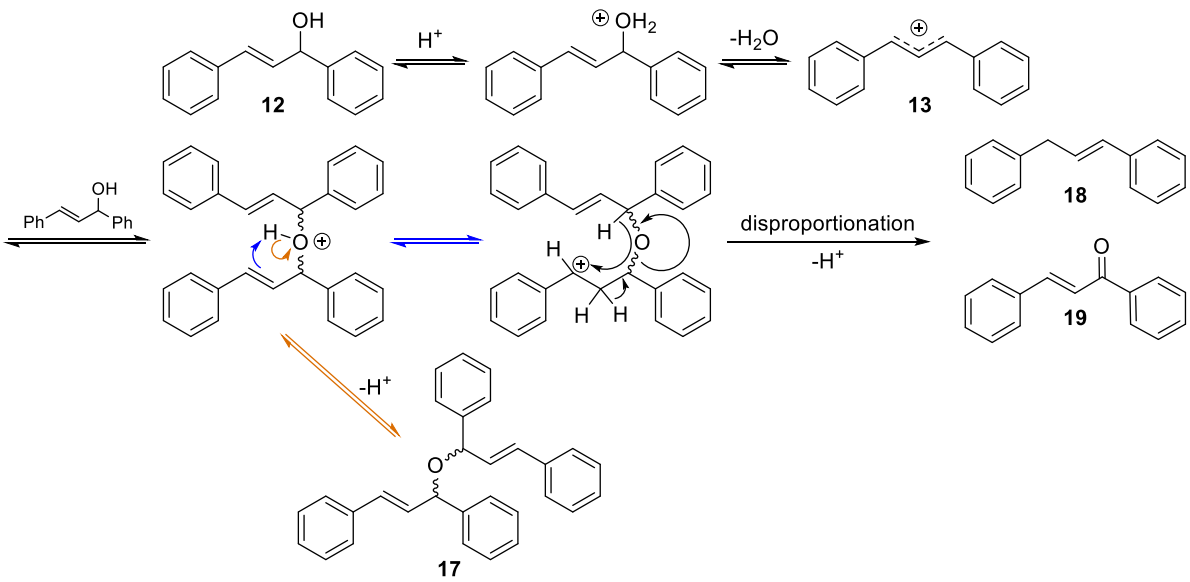

*Scheme R.11 Mechanism proposed for the acid-catalysed conversion of **12** into ether derivative **17** or into disproportionation products **18** and **19**.*

*Table R.5 Results of the control tests for the capsule-catalysed intramolecular S_EAr allylation of **12**.*

Test #	C_R	Additive	12 Yield [%][a]	17 Yield [%][a]
1	+	-	36	25
2	-	-	no conversion	3
3	-	HOAc (40 mol%[b])	no conversion	3
4	-	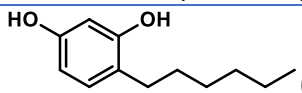 (2.4 eq.[b])	no conversion	no conversion
5	+	Bu_4NBr (**2b**, 1 eq.[b])	no conversion	9
6	+	DMSO-d_6 (10 eq.[b])	no conversion	4

T = 60 °C, t = 8 h, [**12**] = 75 mM, [**1**] = 45 mM, 0.6 mL de-acidified $CDCl_3$. +: presence; -: absence; [a)] determined by ^{1}H NMR spectroscopy; [b)] with respect to **12**.

*Table R.6 Tests of the effects of different reaction conditions on the acid-catalysed decomposition of **12**.*

Acid catalyst[a]	pK_a[49]	Temperature (°C)	Reaction time	Yield 17 (%)[b]	Yield 18 (%)[b]	Yield 19 (%)[b]
HOAc (8 eq.)	4.76	60	2.5 days	48	0	0
			7 days	90	0	0
TFA (0.1 eq.)	-0.25	RT	1 h	90	0	traces
			3 h	91	traces	traces
TFA (12 eq.)	-0.25	RT	2.5 days		decomposition	
		60	20 h	46	24	25
MSA (0.1 eq.)	-1.9	60	20 h	0	50	50
PTSA (0.1 eq.)	-2 – -6	60	20 h	0	50	50

[**12**] = 175–277 mM, 0.6 mL de-acidified $CDCl_3$; [a)] concentrations with respect to **12**, [b)] determined by ^{1}H NMR spectroscopy; "TFA": trifluoroacetic acid, "MSA": methanesulphonic acid, "PTSA": *p*-toluenesulphonic acid, "RT": room temperature.

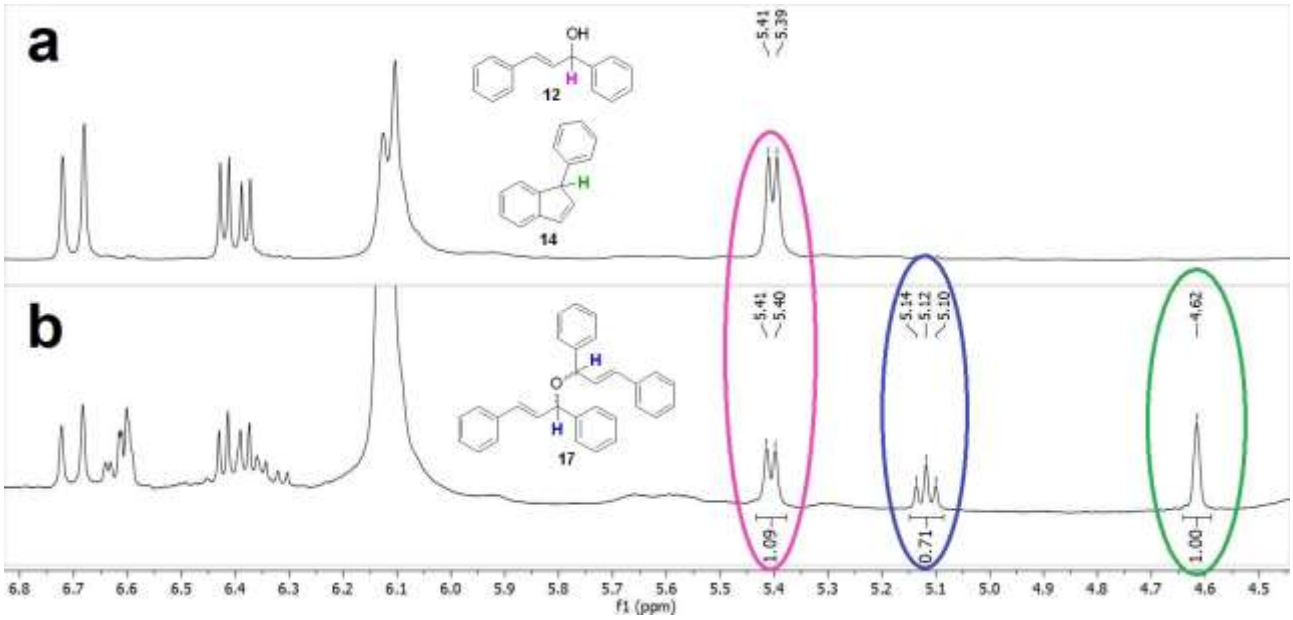

Figure R.11 ^{1}H NMR spectra of a solution of 75 mM **12** and 45mM **1** in 0.6 mL of de-acidified $CDCl_3$ before heating (**a**) and after 8 h of heating at 60 °C (**b**).

2.2 Intermolecular S_EAr reactivity of the 1,3-diphenyallyl cation

Having observed that the 1,3-diphenyallyl cation **13** undergoes intramolecular S_EAr allylation inside the capsule, a question arose whether **13** could act as electrophile in intermolecular S_EAr reactions as well. In order to test this, indole **20a** was selected for its very electron-rich nature. Heating equimolar amounts of **12** and **20a** in $CDCl_3$ in the presence of 10 mol% of capsule $\mathbf{C_R}$ yielded substituted derivative **21a** in nearly quantitative yield (**Scheme R.12**, **Figure R.11**), whose identity was confirmed by comparison with spectra reported in the literature. Control tests equivalent to those reported in **Results and discussion §2.1** and **§1.1** were carried out to confirm that the catalytic effect was completely attributable to the accessible cavity of capsule $\mathbf{C_R}$ (see **Table R.1** for an explanation of the conditions of the control tests, bearing in mind that Bu_4NBr **2b** was used as competitive guest instead of $[Et_4N][BF_4]$ **2a**). The results are displayed in **Table R.7**.

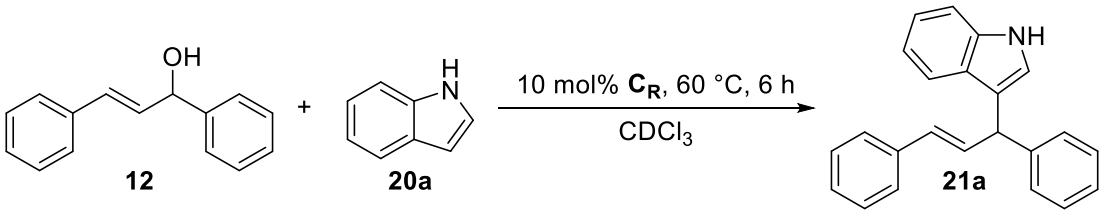

Scheme R.12 Capsule-catalysed S_EAr allylation reaction between **12** and indole **20a** leading to the substituted derivative **21a**.

*Table R.7 Results of the control tests for the capsule-catalysed intermolecular S_EAr reaction between **20a** and the allyl cation generated by **12**.*

Test #	C_R	Additive	20a Yield [%][a]	17 Yield [%][a]
1	+	-	99	0
2	-	-	0	2
3	-	HOAc (40 mol%[b])	0	2
4	-	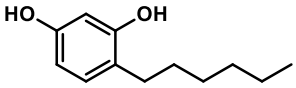 (2.4 eq.[b])	0	low[c]
5	+	Bu_4NBr (**2b**, 1 eq.[b])	18	0
6	+	DMSO-d_6 (10 eq.[b])	<4[d]	<4[d]

[**12**] = [**20a**] = 75 mM, [**1**] = 45 mM, T = 60 °C, t = 6 h; [a] determined by ^{1}H NMR; [b] with respect to **12**; [c] resonance covered by signals of the additive; [d] resonances of **17** and **20a** partially overlap, rendering the determination of the exact yield difficult.

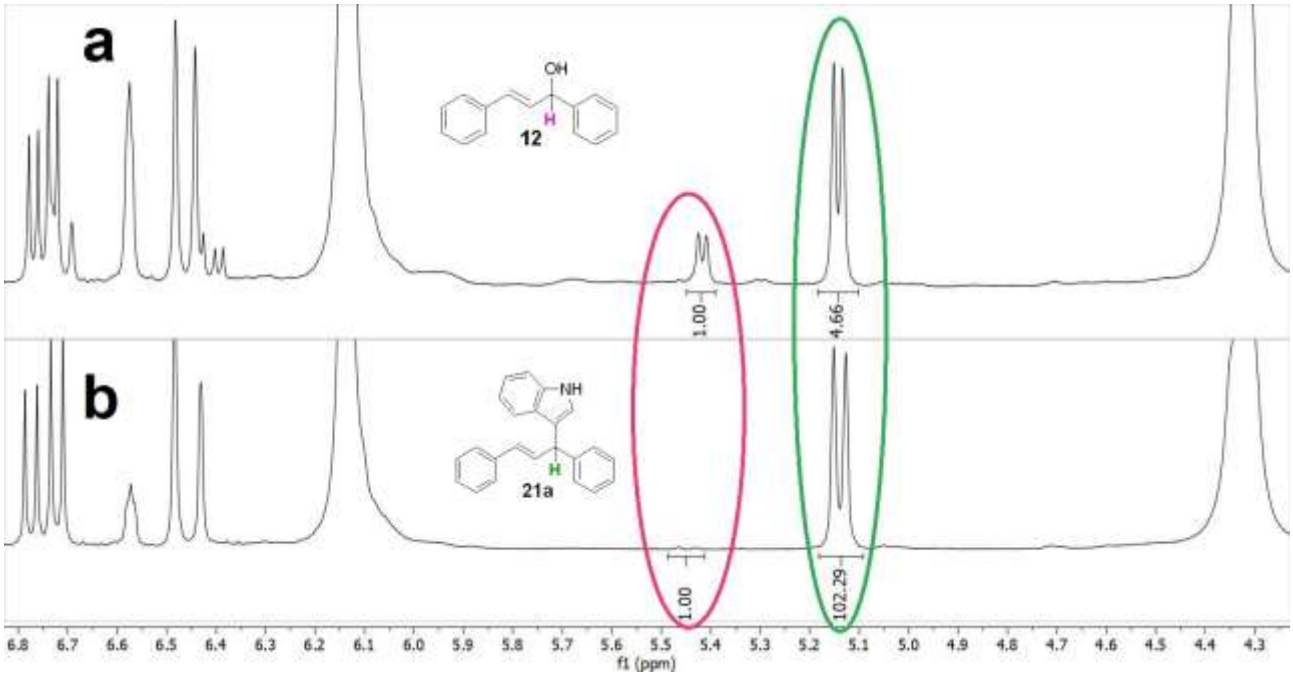

*Figure R.11 ^{1}H NMR spectra of a solution of 75 mM **12**, 75 mM **20a** and 45 mM **1** in 0.6 mL de-acidified $CDCl_3$ after 2 h (**a**) and 6 h (**b**) of heating at 60 °C.*

In order to expand the reaction scope, the capsule-catalysed intermolecular S_EAr allylation was attempted between **12** and a series of substituted indoles (**Table R.8**). It was observed that the reaction proceeded successfully with all indoles, albeit with lower yields when the aromatic nucleophile was endowed with strongly electron-withdrawing groups (see indole-5-carboxamide **21g**).

The reaction was also attempted with alkoxyphenols and other substituted aromatic compounds as nucleophiles (**Table R.9**). The results indicate that the reactivity of these substrates is more complex than that of indoles: very electron-rich *n*-hexylresorcinol **22a** and naphtols **22b-c** showed excellent yields and selectivity, whereas less electron-rich compounds did not react. The behaviour of alkoxyphenols is even

different: 3-methoxyphenol **22k** successfully underwent S_EAr allylation, yielding all four possible *C*-substituted regioisomers; we found that capsule $\mathbf{C_R}$ strongly altered the regioselectivity of this reaction compared to the use of a strong Brønsted acid (see **Results and discussion §2.4**). Contrastingly, guaiacol **22d** did not react at all, possibly because the *ortho-para* activating effects of the OH and OMe groups do not activate the same the positions, unlike in **22k**. *Para*-alkoxyphenols **22h-i** instead reacted with allyl cation **13** by nucleophilic attack, yielding *O*-substituted products **23h-i** which then isomerised into the *ortho C*-substituted products **21q-r** via Claisen rearrangement with total regioselectivity (see **Results and discussion §2.3**).

With the aim of examining two other possible carbocation precursors, we also tested the reactivity of indole **20a** with cinnamyl alcohol or 1,3-diphenylprop-2-yn-1-ol in the presence of 10 mol% of $\mathbf{C_R}$ at 60 °C. ^{1}H NMR spectra recorded after 2 and 6 h of heating, however, showed no evidence of the formation of the expected S_EAr products.

In conclusion, it was demonstrated that capsule $\mathbf{C_R}$ can efficiently catalyse S_EAr allylation between **12** and numerous electron-rich aromatic compounds; in particular, all indoles proved excellent substrates.

Table R.8 *Scope of the capsule-catalysed intermolecular S_EAr allylation between **12** and a series of indoles and other aromatic compounds.*

Entry #	Substrate	Product	2b	Yields[a] (%) 21	17	14
1	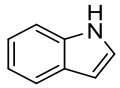 **20a**	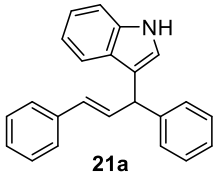 **21a**	-	99	0	0
			+	18	0	0
2	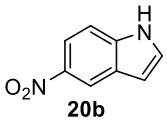 **20b**	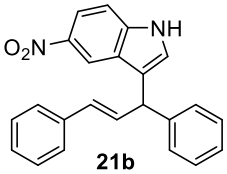 **21b**	-	90	0	0
			+	6	0	0
3	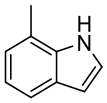 **20c**	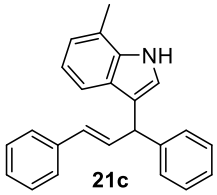 **21c**	-	94	0	0
			+	8	0	0
4	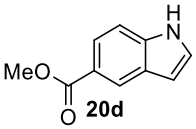 **20d**	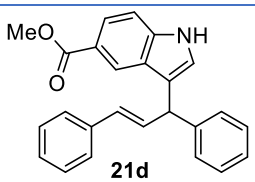 **21d**	-	92	0	0
			+	7	0	0
5	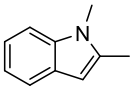 **20e**	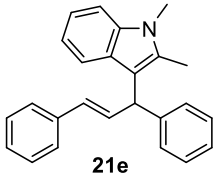 **21e**	-	86	1	0
			+	10	2	0

6	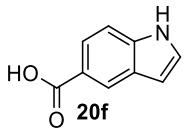 **20f**	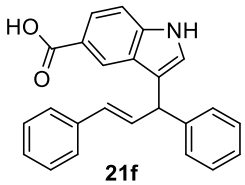 **21f**	-	97	0	2
			+	22	0	0
7	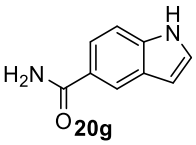 **20g**	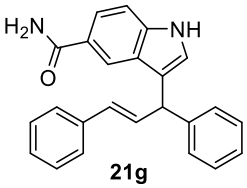 **21g**	-	52	0	0
			+	0.5	2	0
9	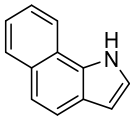 **20h**	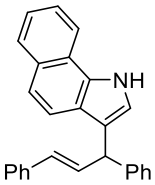 **21ha** 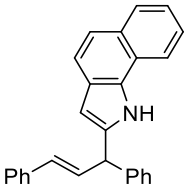 **21hb**	-	57 (**a**) 37 (**b**)	0	0
			+	8 (**a**) 4 (**b**)	1	0
10	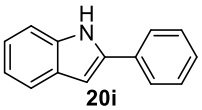 **20i**	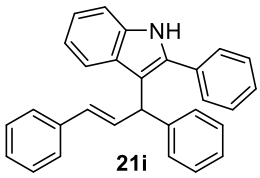 **21i**	-	92	2	0
			+	9	1	0
11	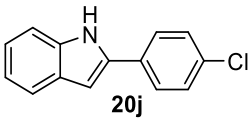 **20j**	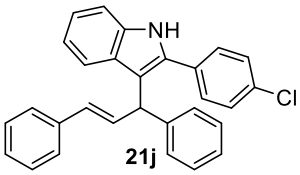 **21j**	-	80	4	11
			+	26	2	0
12	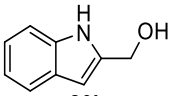 **20k**	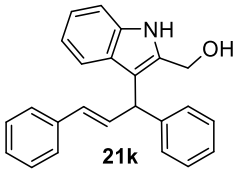 **21k**	-	99	1	0
			+	41	1	0

[**12**] = 75 mM, [**20**] or [**22**] = 75 mM, [**1**] = 45 mM, [**2b**] = 75 mM, 0.6 mL de-acidified $CDCl_3$, 60 °C, 6 h.
[a] Determined by ^{1}H NMR.

Table R.9 *Scope of the capsule-catalysed intermolecular S_EAr allylation between **12** and a series of phenols and other aromatic compounds.*

Entry #	Substrate	Product	2b	Yields[a] (%) 21	17	14
1	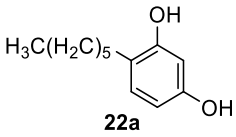 **22a**	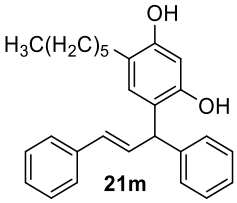 **21m**	-	96	2	0
			+	0	4	0
2	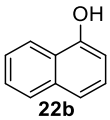 **22b**	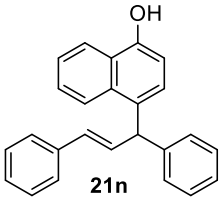 **21n**	-	97	3	traces
			+	20	4	0
3	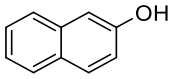 **22c**	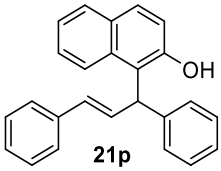 **21p**	-	>99	traces	0
			+	10	4	0
4	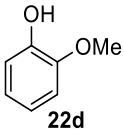 **22d**	No conversion				
5	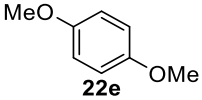 **22e**	No conversion				
6	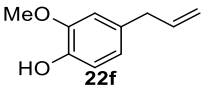 **22f**	No conversion				
7	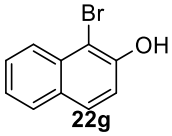 **22g**	No conversion				
8	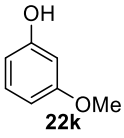 **22k**	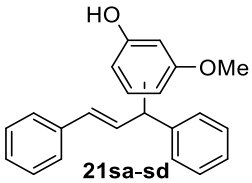 **21sa-sd**	See **Results and discussion §2.4**			
9	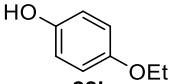 **22h**	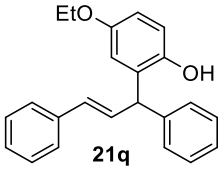 **21q**	See **Results and discussion §2.3**			
10	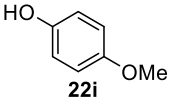 **22i**	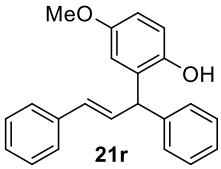 **21r**				

[**12**] = 75 mM, [**20**] or [**22**] = 75 mM, [**1**] = 45 mM, [**2b**] = 75 mM, 0.6 mL de-acidified $CDCl_3$, 60 °C, 6 h.
[a)] Determined by ^1H NMR.

2.3 Formation of unexpected *O*-substituted nucleophilic attack products and subsequent Claisen rearrangement

When 1,3-diphenylpropenol **12** was reacted with *p*-alkoxyphenols in the presence of 10 mol% of $\mathbf{C_R}$, an unexpected result was obtained: the appearance of a ^{1}H NMR doublet at chemical shifts higher than the doublet of the reagent **12**. Literature spectra (see **Experimental section §1.3**) show that S_EAr products **21** exhibit a characteristic ^{1}H NMR doublet in the 4.9-5.2 ppm range, lower than the doublet of **12**.[50] The corresponding ^{1}H of *O*-substituted products **23** instead resonates in the 5.65-5.85 ppm range.[51,52] The spectra in **Figure R.12** thus indicate that the capsule-catalysed reaction between **12** and 4-ethoxyphenol **22h** yields firstly *O*-substituted compound **23h** as major product after 6 h, which then isomerises into **21q** if the reaction is left to proceed; equivalent results were obtained by reacting **12** with 4-methoxyphenol **22i**.

At first, we hypothesized the existence of a competition between a reversible S_N1 mechanism, leading to kinetically favoured product **23**, and a non-reversible S_EAr mechanism which yields thermodynamically favoured product **21** (**Scheme R.13**). If this hypothesis were accurate, however, two S_EAr products **21** would be expected, whereas ^{1}H NMR resonances indicate the formation of a single product **21**. This led us to propose that *O*-substituted intermediates **23** undergo Claisen rearrangement, yielding exclusively the corresponding *C*-substituted products with the substitution in the *ortho* position with respect to the phenolic OH group (**Scheme R.14**).

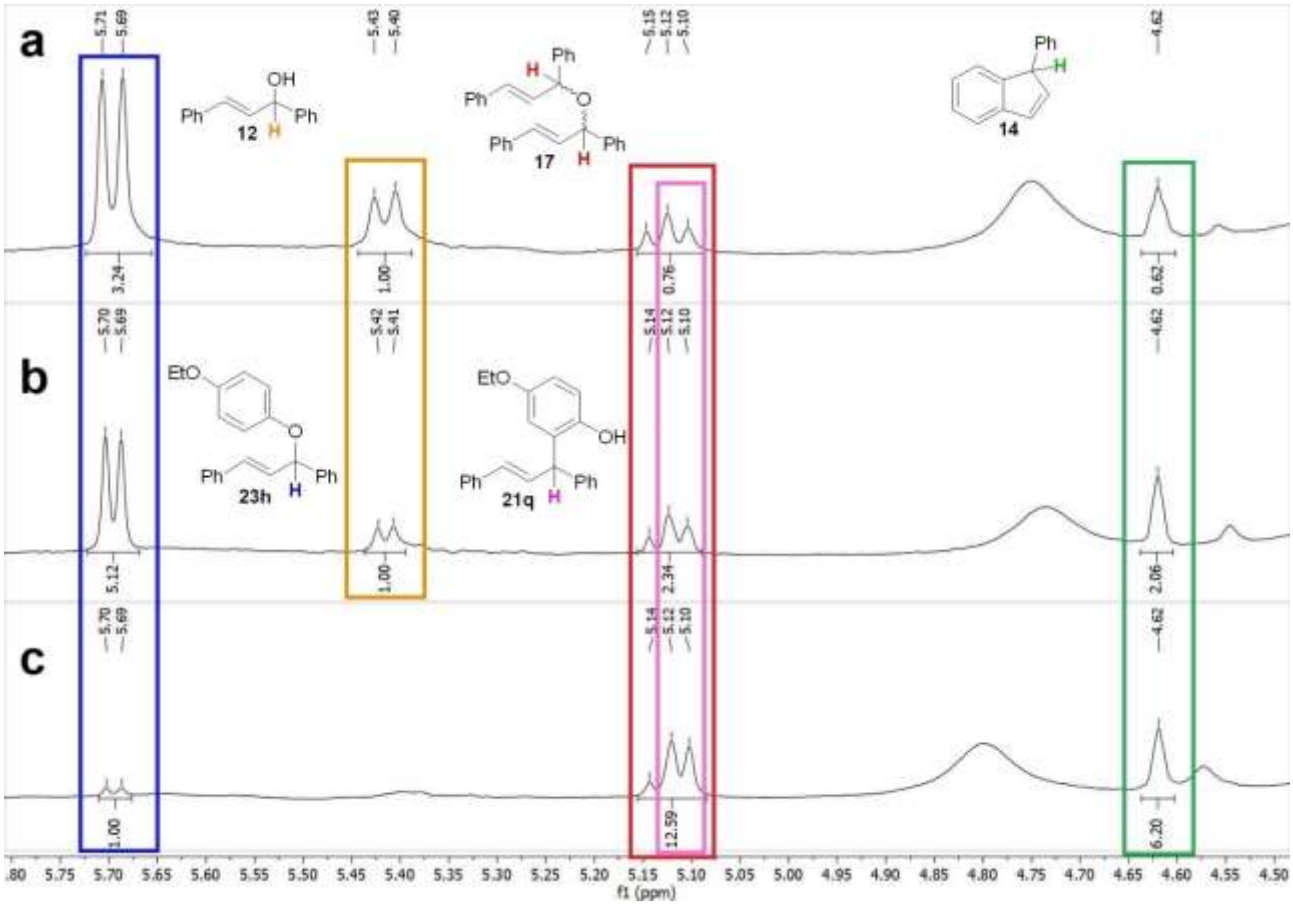

Figure R.12 *^{1}H NMR spectra of a solution of 75 mM of **12**, 75 mM of 4-ethoxyphenol **22h** and 45 mM of resorcin[4]arene **1** in 0.6 mL of de-acidified $CDCl_3$ after 2 (**a**), 6 (**b**) and 24 h (**c**) of heating at 60 °C.*

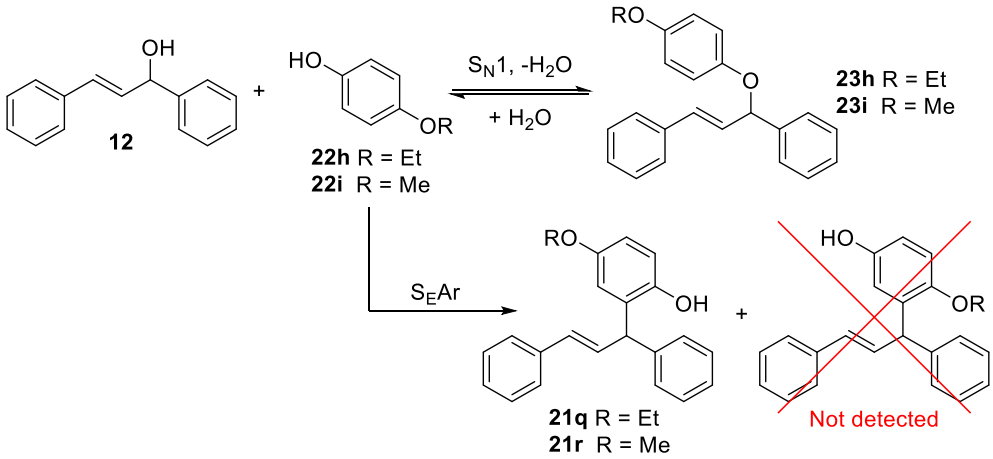

Scheme R.13 *Initially proposed mechanism for the capsule-catalysed formation of* C*-substituted products* ***21*** *by competition of a reversible S_N1 pathway and a non-reversible S_EAr pathway. This mechanism was later deemed unlikely since the product where the* ortho *position with respect to the alkoxy group is substituted was not detected.*

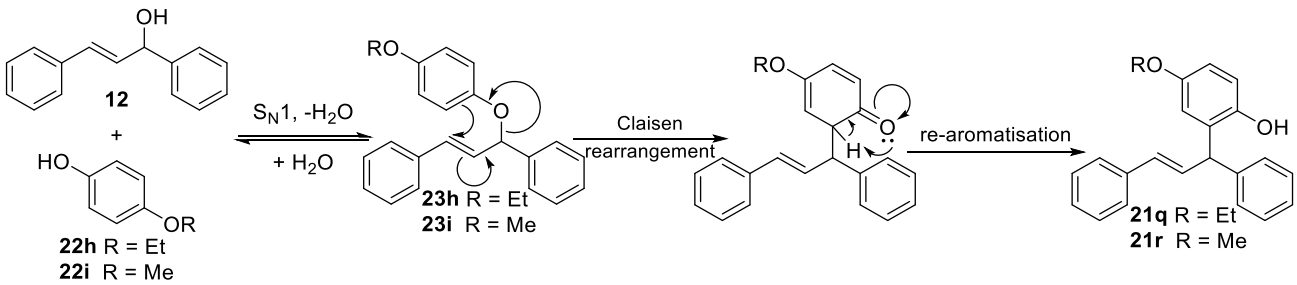

Scheme R.14 *Proposed mechanism for the capsule-catalysed formation of* C*-substituted products* ***21*** *by formation of* O*-substituted product* ***23*** *and subsequent Claisen rearrangement and re-aromatisation. This mechanism explains why the product where the* ortho *position with respect to the alkoxy group is substituted was not detected.*

Eager to discover whether this reactivity was typical of alkoxyphenols, we attempted to react **12** with 2-methoxyphenol **22j** and 3-methoxyphenol **22k**. Interestingly – as mentioned in **Results and discussion §2.2** – the former showed no reactivity: ^{1}H NMR spectra of the reaction mixture showed no resonances compatible either with *O*- or *C*-substituted products. Conversely, ^{1}H NMR spectra recorded over the course of the reaction with 3-methoxyphenol **22k** showed the emergence of four resonances in the chemical shift range typical of *C*-substituted products and no resonances compatible with *O*-substituted products. This indicates that **22k** reacts solely and directly via the S_EAr pathway, yielding all four possible regioisomers **21sa-sd**. It is also possible that the *O*-allylation could be much slower compared to the Claisen rearrangement, thereby preventing the accumulation of the *O*-substituted intermediate. Nevertheless, this is deemed unlikely since Claisen rearrangement would not lead to the formation of all four possible *C*-substituted regioisomers. Therefore, it seems that the formation of an *O*-substituted derivative and subsequent Claisen rearrangement is exclusive to *para*-substituted phenols. To confirm this, the reaction was repeated with *p*-cresol **22m** and 4-chlorophenol **22n** (**Scheme R.15**): ^{1}H NMR spectra of the reaction mixtures showed that the *O*-substituted product formed in both cases, but only the derivative of **22m** progresses to the *C*-substituted product. The *O*-substituted derivative of **22n** instead accumulated without reacting further, likely due to the de-activating effect of the chloro substituent, which disfavours Claisen rearrangement.

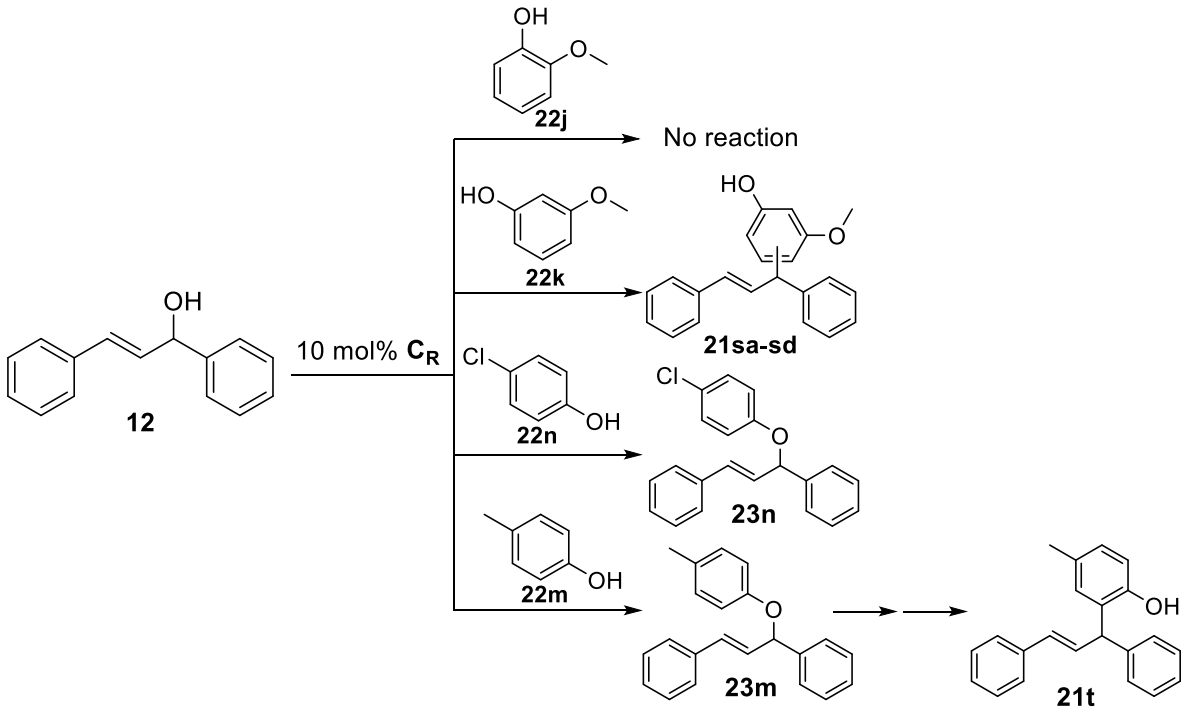

*Scheme R.15 Capsule catalysed reactivity of substituted phenols **22j-k** and **22m-n** with **12**.*

Control tests equivalent to those reported in **Results and discussion §2.2**, **§2.1** and **§1.1** were carried out to confirm that the accessible cavity of capsule $\mathbf{C_R}$ is responsible for catalysing the formation of *O*-substituted products **23h-i** and **23m-n** (see **Table R.1** for an explanation of the conditions of the control tests, bearing in mind that Bu_4NBr **2b** was used as competitive guest instead of $[Et_4N][BF_4]$ **2a**). The reaction between 1,3-diphenylpropenol **12** and 4-methoxyphenol **22i** was employed for these tests. The results are displayed in **Table R.10** and indicate that, although the reaction proceeds even with Brønsted acids or in the absence of any catalyst, the presence of $\mathbf{C_R}$ significantly accelerates it.

*Table R.10 Results of the control tests of the reaction between **12** and **22i**.*

Test #	C_R	Additive	t = 6 h		t = 24 h	
			23i Yield [%][a]	21r Yield [%][a]	23i Yield [%][a]	21r Yield [%][a]
1	+	-	62	9	0	33
2	-	-	3	0	3	3
3	-	HOAc (40 mol%[b])	3	3	2	11
4	-	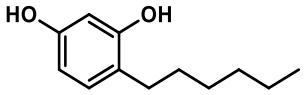 (2.4 eq.[b])	0	low[c]	0	low[c]
5	+	Bu_4NBr (**2b**, 1 eq.[b])	12	4	4	26
6	+	DMSO-d_6 (10 eq.[b])	0	0	0	0

[**12**] = 75 mM, [**22i**] = 75 mM, [**1**] = 45 mM, 0.6 mL de-acidified $CDCl_3$, 60 °C. [a)] determined by ^{1}H NMR spectroscopy; [b)] with respect to **12**; [c)] the yield cannot be determined exactly because the resonance is covered by the resonance of *n*-hexylresorcinol.

2.4 Regioselectivity differences between acid-catalysed and capsule-catalysed S_EAr allylation between 1,3-diphenylpropenol **12** and 3-methoxyphenol **22k**

As mentioned in **Results and discussion §2.3**, the capsule-catalysed S_EAr allylation between 1,3-diphenylpropenol **12** and 3-methoxyphenol **22k** yields all four possible *C*-substituted regioisomers **21sa-sd**, each of which is characterised by a doublet in the 5.00-5.30 ppm range. The same result was obtained in the presence of 10 mol% of trifluoroacetic acid (TFA). In the latter case, however, the four regioisomers were obtained in much different relative ratios (see **Scheme R.16** and **Figure R.13**).

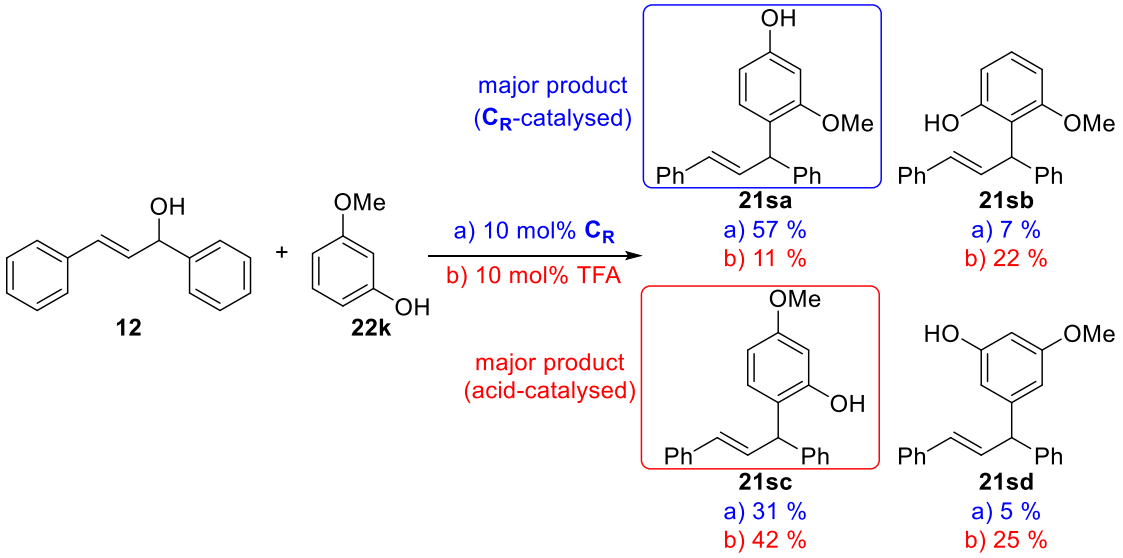

Scheme R.16 *S_EAr allylation between **12** and **22k** catalysed by capsule **C_R** and by TFA. The yields were determined by integration of the corresponding ^{1}H NMR resonances. For the assignments of the resonances, see text.*

In order to describe this drastic change in regioselectivity, it was necessary to assign each doublet to the corresponding regioisomer. The doublets were named "A", "B", "C", and "D" in order of decreasing chemical shift. One drop of triethylamine was added to the reaction mixture containing TFA in order to neutralise the acidity, then COSY, ^{13}C NMR, HSQC and HMBC spectra of the mixture were recorded (see **Experimental section §3.4**). The HMBC spectrum allowed for identification of the ^{13}C resonances of the carbon atoms linked to the OH groups, which have high chemical shifts and show no coupling with the ^{1}H nuclei of the OMe groups, and of the carbon atoms linked to the OMe groups, which show coupling with said ^{1}H nuclei. ^{1}H doublets C and D show no coupling with ^{13}C-OMe, and can thus be assigned to either **21sc** or **21sd**. Since in **21sd** the substitution is on the most de-activated carbon of the aromatic ring, the less intense doublet D was assigned to this regioisomer, and C was therefore assigned to **21sc**. This result is in accordance with the literature spectrum of **21sc**, which is the only isomer whose characterisation data is available in the literature (see **Experimental section §1.3**). Doublets A and B, on the other hand, show coupling with ^{13}C-OMe in the HMBC spectrum, but only B is coupled with a ^{13}C-OH; B was therefore assigned to **21sb** and A was assigned to **21sa**. This is corroborated by the observation that the most intense doublet (C) was assigned to the product in which the substitution is on the most activated carbon atom of the aromatic ring (**21sc**).

It is clearly noticeable that, when the reaction was carried out in the presence of a Brønsted acid such as TFA, the major product is **21sc** and the minor product is **21sa**, whereas in the presence of **C_R** the regioselectivity is inverted. Moreover, using **C_R** as catalyst significantly limits the formation of **21sb** and **21sd**. The explanation of this much greater preference for product **21sa** is beyond the aim of this thesis work, but it can be

hypothesized that H-bonding between the OH group of **22k** and an OH group of a resorcin[4]arene unit may favour the orientation of **22k** optimal for electrophilic attack in its *para* position, as shown in **Scheme R.17**.

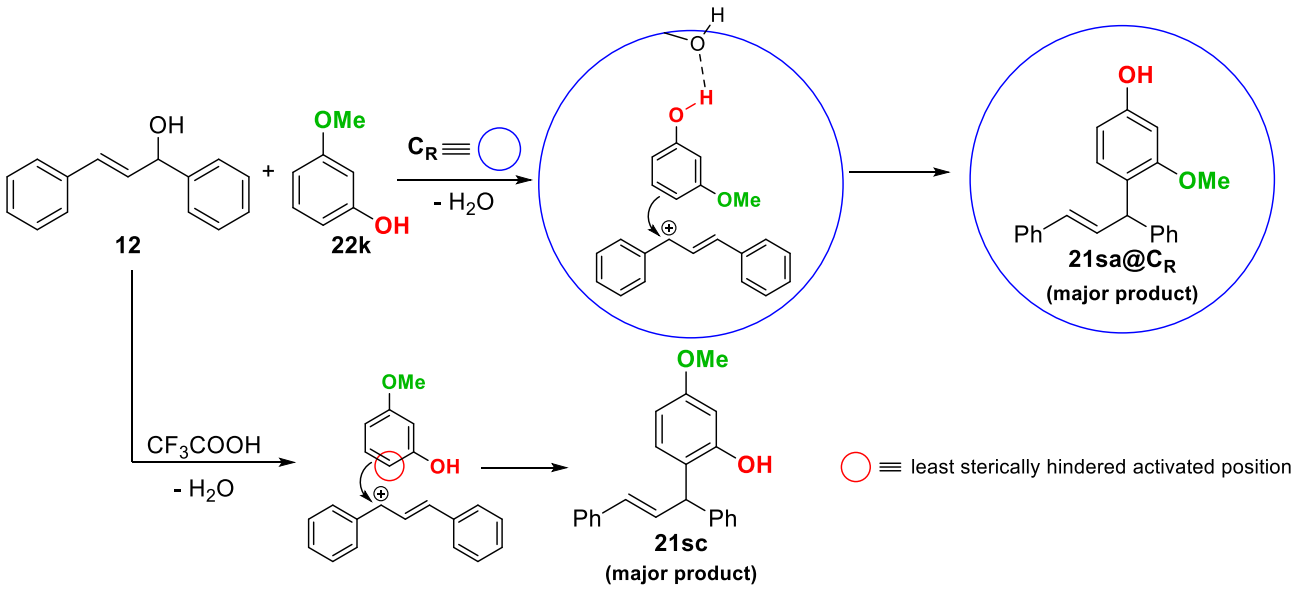

Scheme R.17 *Hypothetical orientation of **22k** thanks to H-bonding with the OH group of a resorcin[4]arene unit which would explain the preferential formation of regioisomer **21sa** in the presence of capsule **C_R** (**above**) compared with the absence of preferential orientation of **22k** in the acid-catalysed S_EAr allylation, which leads to regioisomer **21sc** (**below**).*

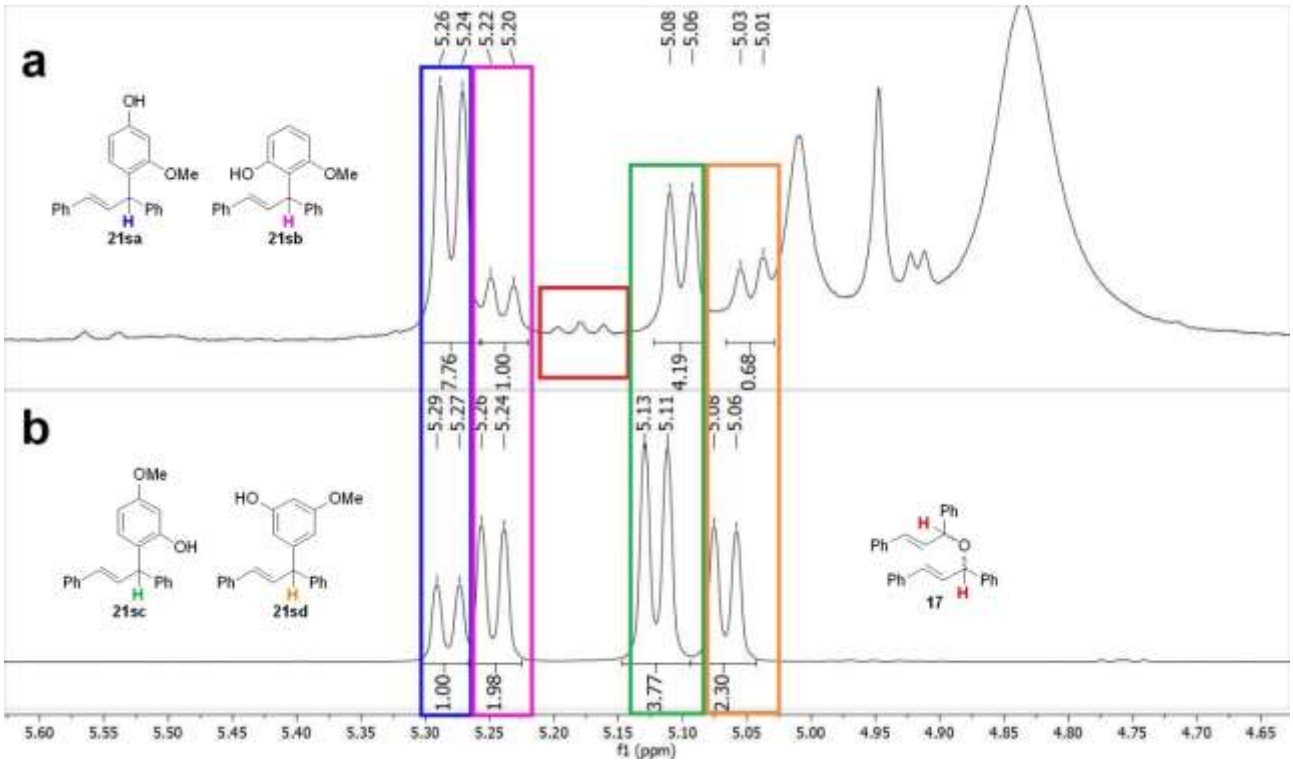

Figure R.13 *^{1}H NMR spectra of a solution of 75 mM of **12**, 75 mM of **22k** and 45 mM in $CDCl_3$ of **1** after 6 h of heating at 60 °C (**a**) and of a solution of 317 mM of **12**, 317 mM of **22k** and 32 mM of TFA in $CDCl_3$ after 2 h at room temperature (**b**).*

2.5 Synthesis and characterisation of unknown *C*-substituted S_EAr products and *O*-substituted nucleophilic substitution products

Several products obtained throughout the examination of the scope of the capsule-catalysed S_EAr allylation are not available in the literature; *O*-substituted products **23h** and **23i** are also not reported (**Scheme R.18**). It was thus necessary to synthesize and purify them to obtain their full characterisation data.

C-substituted products **21e**, **21g-f**, **21ha-hb**, **21i-k**, **21m** and **21p-q** were synthesized via the capsule-catalysed S_EAr allylation by reacting 0.23 mmol of **12** and an equimolar quantity of the corresponding substituted aromatic compound **20** with 60 mol% of **1** (corresponding to 10 mol% of capsule $\mathbf{C_R}$) in 3 mL of de-acidified chloroform-*d* at 60 °C for 18-24 h. The solvent was then removed by rotary evaporation and the resulting solid was dissolved in an appropriate cyclohexane-ethyl acetate mixture, obtaining a solution which was then passed through a silica gel plug to remove **1**, as described in **Results and discussion §1.3**. The solvent was then removed by rotary evaporation and the desired product was purified from the resulting solid mixture by preparative TLC.

O-substituted products **23h-i** were synthesized by reacting 0.36 mmol of **12** with an equimolar quantity of the corresponding phenol in the presence of 10 mol% of TFA in 3.5 mL of chloroform-*d* at room temperature for one hour. The solvent was then removed by rotary evaporation and the resulting viscous oil was treated by flash chromatography on a silica gel column with a 95:5 cyclohexane-ethyl acetate eluent mixture. ~1% triethylamine was added to the eluent mixture, because **23h-i** are susceptible to acid-catalysed decomposition on silica gel. This afforded the products as viscous oils in 11-13% yield.

The details regarding the experimental procedures are available in **Experimental section §3.5** and the spectra of the product are reported in **Characterisation data §2**.

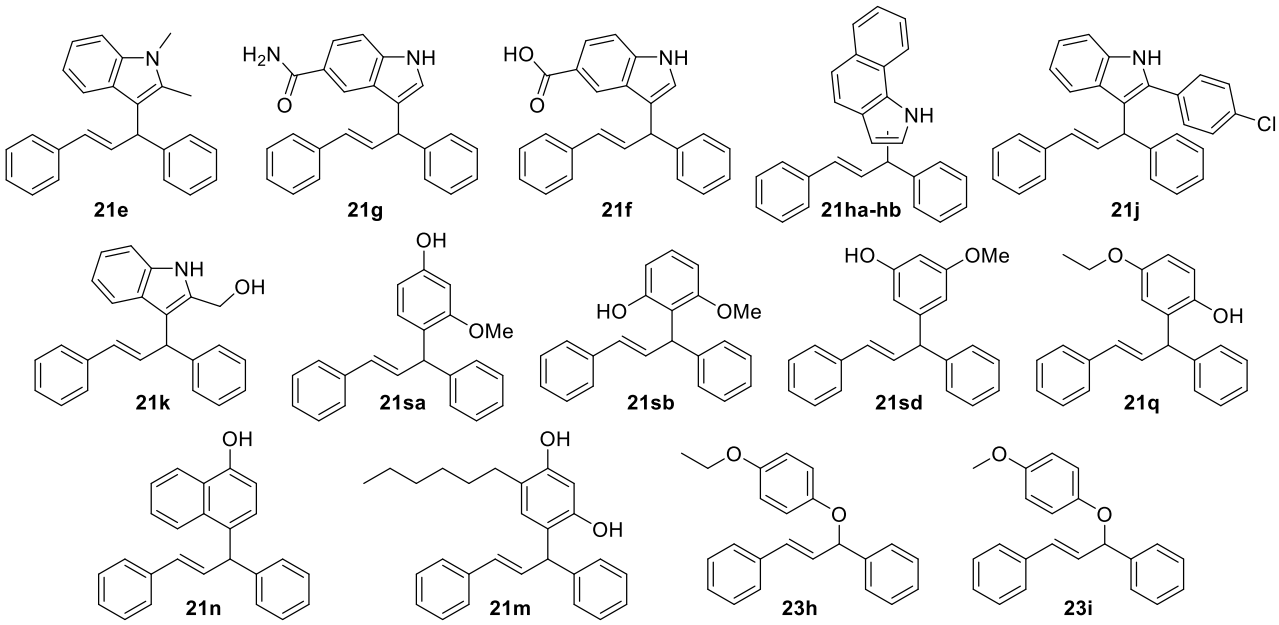

Scheme R.18 *C- and O-substituted derivatives of 1,3-diphenylpropenol* ***12*** *whose characterisation data was not available in the literature.*

Conclusions

The focus of this thesis work was two-fold: the first objective was the completion of the exploration of the capsule-catalysed aldehyde-isocyanide condensation reaction discovered through the joint effort of Scarso's and Tiefenbacher's research groups. For this purpose, control tests of the reaction were carried out under optimised conditions and the reaction scope was expanded considerably. Unfortunately, the test with the *ad hoc* synthesized sterically encumbered aldehyde gave inconclusive results. It is likely that a much larger aldehyde will be synthesized and tested in the future. In order to demonstrate the validity of the proposed reaction mechanism, it was also attempted to observe the formation of the aziridinone intermediate *in situ*; the unstable nature of this compound, however, made it impossible to detect by mass spectrometry, whereas ^{1}H NMR spectroscopy proved insufficiently sensitive.

Subsequently, following the observation that 1-adamantyl isocyanide tended to react more readily than *tert*-butyl isocyanide, the relative affinity of these substrates for the inner cavity of the resorcin[4]arene hexameric capsule was investigated by NMR titration. This led to the conclusion that the greater reactivity of 1-adamantyl isocyanide is caused by effects different from its tendency towards encapsulation, which is lower than that of *tert*-butyl isocyanide.

Finally, 16 previously unreported imine products were successfully synthesized, purified, and characterised by NMR spectroscopy and GC-MS; it is worth stressing that over half of the imines were synthesized via the capsule-catalysed condensation of the corresponding aldehyde and isocyanide. In order to remove the resorcin[4]arene from the reaction mixture, a method of filtration over a silica gel plug was specially devised.

As second focus of this thesis work, the reactivity of the 1,3-diphenylallyl cation formed by dehydration of *trans*-1,3-diphenylprop-2-en-1-ol was investigated. Control experiments were carried out to confirm the crucial role of the resorcin[4]arene hexameric capsule in catalysing intramolecular S_EAr allylation of 1,3-diphenylpropenol. Subsequently, intermolecular S_EAr allylation was explored, uncovering a vast array of indoles and other electron-rich aromatic compounds which efficiently reacted with the 1,3-diphenylallyl cation in the presence of the capsule.

Over the course of this examination, alkoxyphenols were found to display an intriguing behaviour: while 2-methoxyphenol showed no reactivity, 3-methoxyphenol reacted with 1,3-diphenylpropenol to yield all four possible S_EAr products. Interestingly, the resorcin[4]arene capsule was found to induce a markedly different regioselectivity with respect to catalysis by a Brønsted acid. 4-methoxy- and 4-ethoxyphenol, on the other hand, reacted with 1,3-diphenylpropenol by nucleophilic substitution, yielding the corresponding *O*-allylated derivative which then rearranged to the *ortho C*-substituted product with absolute regioselectivity via Claisen rearrangement.

Overall 15 *C*- and *O*-substituted products whose characterisation data was not available in the literature were synthesized, purified, and characterised by NMR spectroscopy and GC-MS. Once again, many of these compounds were afforded by the capsule-catalysed reaction, with the added purpose of proving the potential of resorcin[4]arene as a chemical synthesis tool.

Experimental section

1. General

1.1 General information

NMR spectra were recorded either on a Bruker Advance 300 spectrometer operating at 300 MHz at 298 K or on a Bruker Advance 400 spectrometer operating at 400 MHz at 298 K. Chemical shifts δ are reported in ppm relative to $Si(CH_3)_4$. The proton signal of the deuterated solvent was used as reference: $CDCl_3$ $\delta(^1H)$ = 7.26 ppm, $\delta(^{13}C)$ = 77.16 ppm; methanol-d_4 $\delta(^1H)$ = 3.34 ppm, $\delta(^{13}C)$ = 49.00 ppm; DMSO-d_6 $\delta(^1H)$ = 2.05 ppm. Coupling constants (*J*) are reported in Hertz (Hz). Standard abbreviations indicating multiplicity were used as follows: s (singlet), d (doublet), t (triplet), q (quadruplet), dd (doublet of doublets), dt (doublet of triplets), m (multiplet).

GC-MS analyses were performed on a GC Trace GC 2000 coupled with a quadrupole MS Thermo Finnigan Trace MS with *Full Scan* method. Experimental conditions are reported in the following table.

Experimental conditions for GC-MS analyses	
Capillary column:	HP5-MS 30 m, 0.25 mm x 0.25 µm
Initial T, °C:	80°C for 5 min
Rate, °C/min:	30°C/min
Final T, °C:	280°C for 30 min
Injector T (split), °C:	280°C
Gas carrier flow, mL/min.	0.8 mL/min
Injected volume, µL	0.8-1 µL
Solvent delay, min.	4 min.
Mass range, amu:	35-500 amu
Detector voltage, V:	350 V
Interface T, °C	280°C
Source T, °C:	200°C

Low-resolution MS analyses were performed on a Waters ZQ spectrometer in positive polarity mode. The analytes were dissolved in methanol and injected directly into the ESI source via an integrated syringe pump.

Column chromatography was performed on 230-400 mesh silica, thin layer chromatography (TLC) was carried out on 20 cm x 20 cm ALUGRAM® Xtra SIL G/UV_{254} MACHEREY-NAGEL.

All reagents and solvents, including deuterated solvents, were purchased from Merck or Alfa Caesar and used without further purification. De-acidified chloroform-*d* was obtained by shaking chloroform-*d* in a sealed bottle containing activated basic alumina. Although alumina dries chloroform considerably, de-acidified chloroform-*d* was found to have sufficient water content to ensure the self-assembly of capsule $\mathbf{C_R}$.

Transfer of liquids with a volume in the 5-100 µL range was performed with Hamilton Microliter syringes. Weighting of solid substrates, catalysts and other materials was carried out with a Ohaus® Pioneer™ analytical balance model PA214C.

1.2 Synthesis of *C*-undecylcalix[4]resorcinarene **1**

To a stirred solution of 99.9% ethanol (270 mL) and 37% aqueous HCl (90 mL), resorcinol (70.9 g, 644 mmol, 1.0 eq.) was added. After complete dissolution and cooling to 0 °C, a solution of dodecanal (143 mL, 119 g, 644 mmol, 1.0 eq.) in 99.9% ethanol (180 mL) was added dropwise into the reaction mixture over the course of 40 min. The resulting solution was allowed to warm to r.t. and subsequently refluxed at 100 °C for 18 h. Upon cooling to r.t. a yellow precipitate formed from the dark red solution. The precipitate was dispersed in cold methanol, filtered, and subsequently washed with cold methanol until the washings were light yellow. The solid was recrystallized from methanol (150 mL). To remove remaining yellow impurities, the solid was washed extensively with a mixture of methanol/water (50/50, 8 × 100 mL). The crystalline material was dried under reduced pressure (15 mbar) at 55 °C using a rotary evaporator. The drying process was continued until the residual methanol was completely removed. In order to obtain a satisfying water content, the material was moistened with cold methanol, washed with water (8 × 100 mL), and dried under reduced pressure at 55 °C. Compound **1** (109 g, 98.5 mmol, 61%) was obtained as a slightly yellowish powder.

1.3 References of literature spectra

Name and reference	Skeletal formula
C-undecyl resorcin[4]arene **1**[53]	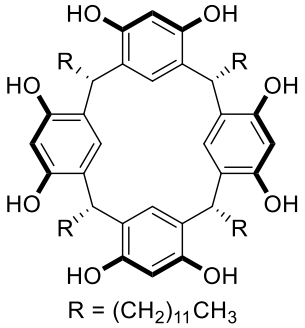
N-tert-butyl-1-(4-nitrophenyl)methanimine **5aa** *N-tert*-butyl-1-(3-nitrophenyl)methanimine **5ab** *N-tert*-butyl-1-(2-nitrophenyl)methanimine **5ac**[54]	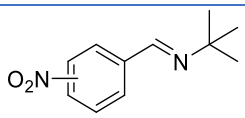
3,5-dibromobenzaldehyde[55]	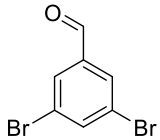
3,5-bis(4-nitrophenyl)benzaldehyde **4n**[56]	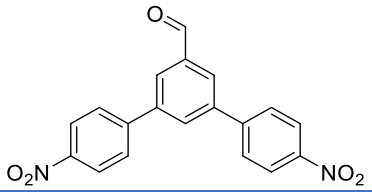
1-phenyl-1*H*-indene **14**[57]	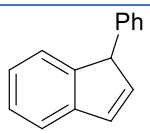
bis(1,3-diphenylallyl) ether **17**[58]	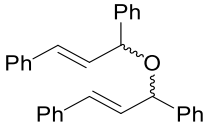

1,3-diphenylpropene **18**[59]	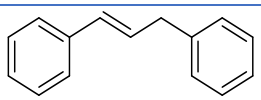
(*E*)-Chalcone **19**[60]	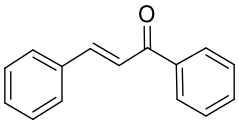
(*E*)-3-(1,3-diphenylallyl)indole **21a**[61]	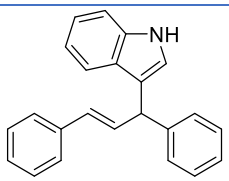
(*E*)-3-(1,3-diphenylallyl)-5-nitroindole **21b**[61]	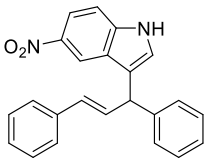
(*E*)-3-(1,3-diphenylallyl)-7-methylindole **21c**[62]	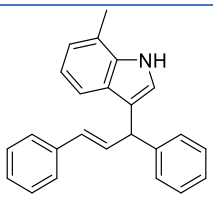
Methyl 3-((*E*)-1,3-diphenylallyl)indole-5-carboxylate **21d**[63]	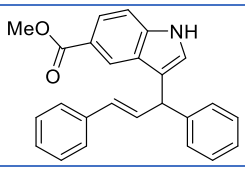
(*E*)-3-(1,3-diphenylallyl)-2-phenylindole **21i**[64]	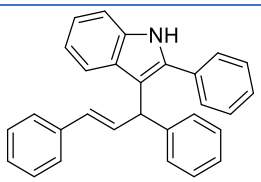
(*E*)-1-(1,3-difenilallyl)-2-naphtol **21p**[65]	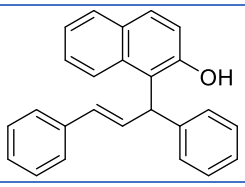
5-methoxy-2-((*E*)-1,3-diphenylallyl)phenol **21sc**[66]	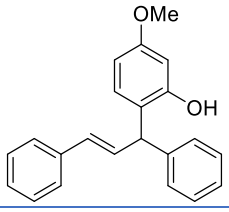
4-methoxy-2-((*E*)-1,3-diphenylallyl)phenol **21r**[50]	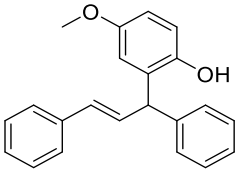
(*E*)-3-(4-methylphenyloxy)-1,3-diphenylprop-1-ene **23m**[67]	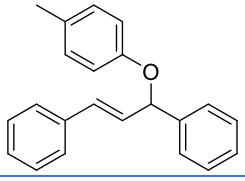

4-methyl-2-((*E*)-1,3-diphenylallyl)phenol **21t**[50]	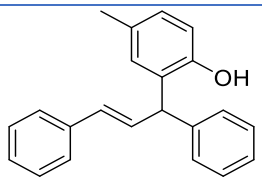
(*E*)-3-(4-chlorophenyloxy)-1,3-diphenylprop-1-ene **23n**[52]	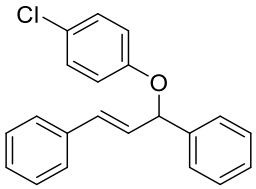

2. Imine formation by capsule-catalysed condensation of an isocyanide and an electron-poor aldehyde

2.1 Control experiments: condensation of *tert*-butyl isocyanide **3a** and 4-nitrobenzaldehyde **4a**

8.2 mg (0.054 mmol) of **4a**, 9.0 mg (0.108 mmol) of **3a** and 600 µL of de-acidified chloroform-*d* were loaded in six NMR tubes; additional components were added as illustrated in **Table E.1**. The tubes were closed and left in a water bath at 60 °C for 24 h. Then, ^{1}H NMR spectra were taken (**Figure E.1**) and the yields were determined by integration of the corresponding resonances.

Table E.1 *Additives used for the control tests of the condensation reaction between **3a** and **4a**.*

Tube #	Additives [in mg and in (mmol)]
1	36 mg (0.033 mmol) resorcin[4]arene **1**
2	No additives
3	10 µL of a 0.54 M solution of acetic acid in $CDCl_3$
4	25 mg (0.130 mmol) 4-n-hexylresorcinol
5	36 mg (0.033 mmol) of **1** and 11.7 mg (0.054 mmol) of $[NEt_4][BF_4]$ **2a**
6	36 mg (0.033 mmol) of **1** and 38 µL (0.54 mmol) of DMSO-d_6

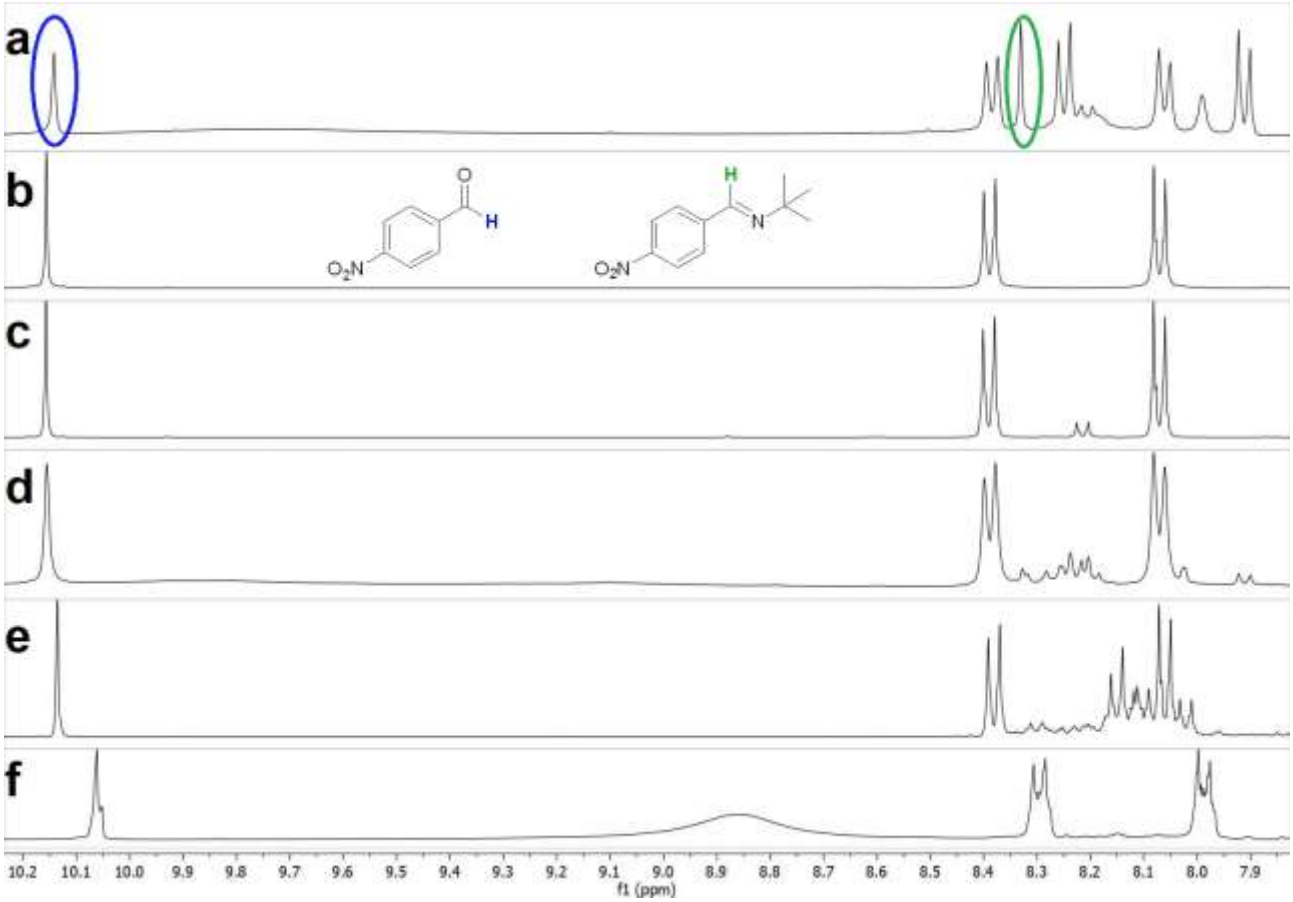

Figure E.1 *^{1}H NMR spectra of solutions of **3a** (180 mM) and **4a** (90 mM) in 0.6 mL of $CDCl_3$ after 24 h at 60 °C with the following additional components: 54 mM of **1** (**a**), no additives (**b**), 9 mM of acetic acid (**c**), 216 mM of 4-n-hexylresorcinol (**d**), 54 mM of **1** and 90 mM of $[Et_4N][BF_4]$ (**e**), 54 mM of **1** and 900 mM of DMSO-d_6 (**f**).*

2.2 Expansion of the reaction scope

The condensation reactions were carried out as follows: 36 mg (0.032 mmol) of **1** were dissolved in 0.6 mL of de-acidified $CDCl_3$ in an NMR tube, obtaining a light brown-pale red solution to which 0.054 mmol of aldehyde and 0.108 mmol of isocyanide were added. The tube was then closed and put in a water bath at 60 °C for 24 h, after which a ^{1}H NMR spectrum was recorded (**Figure E.2** and **Figure E.3**). The yields were determined by integration of the resonances corresponding to the aldehyde and to the imine.

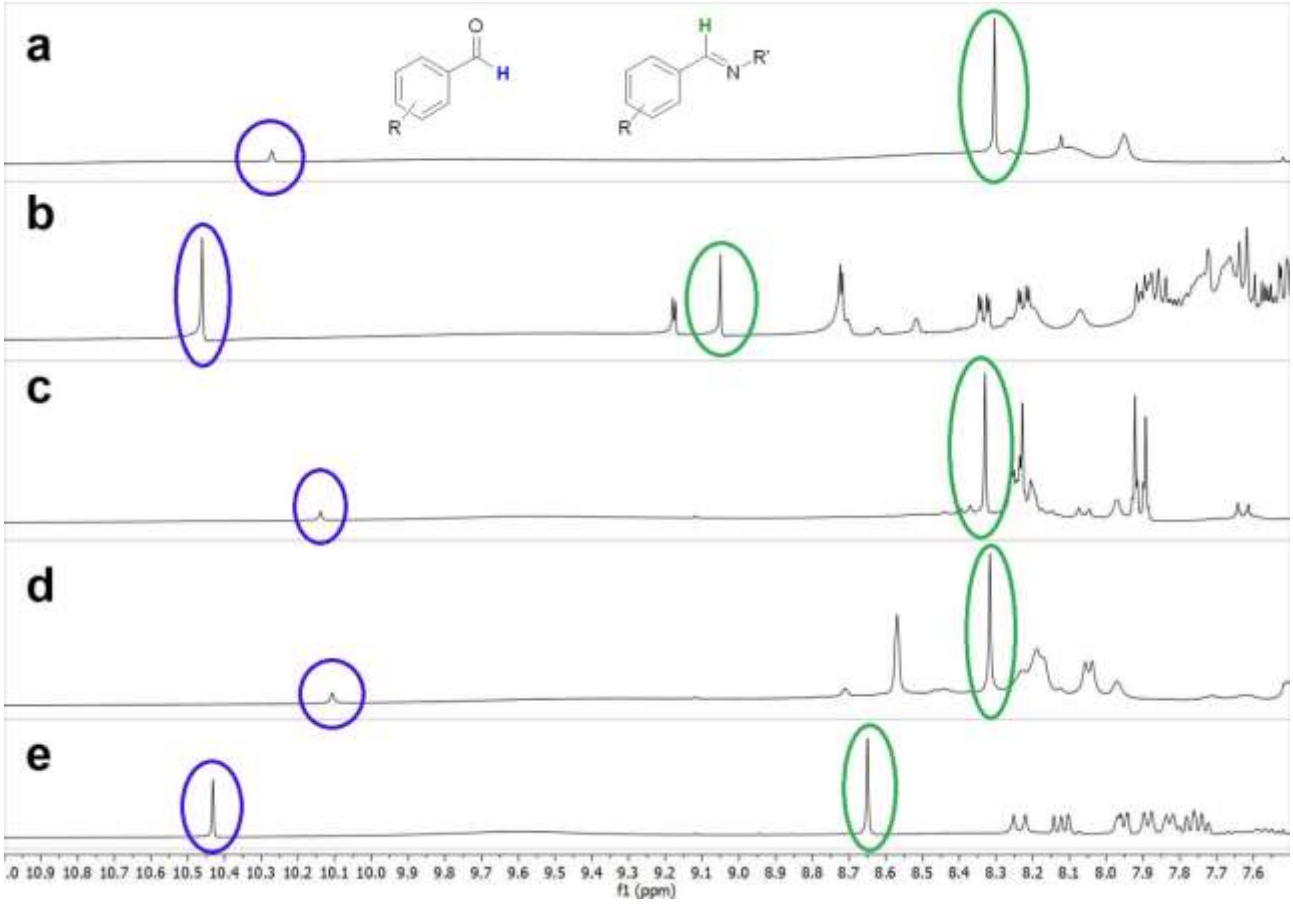

Figure E.2 *^{1}H NMR spectra of solutions of aldehyde (90 mM), isocyanide (180 mM) and **1** (54 mM) in 0.6 mL of de-acidified $CDCl_3$ after 24 h at 60 °C. The aldehyde-isocyanide pairs are: **4g**-**3a** (a), **4d**-**3f** (b), **4a**-**3c** (c), **4b**-**3c** (d), **4c**-**3c** (e).*

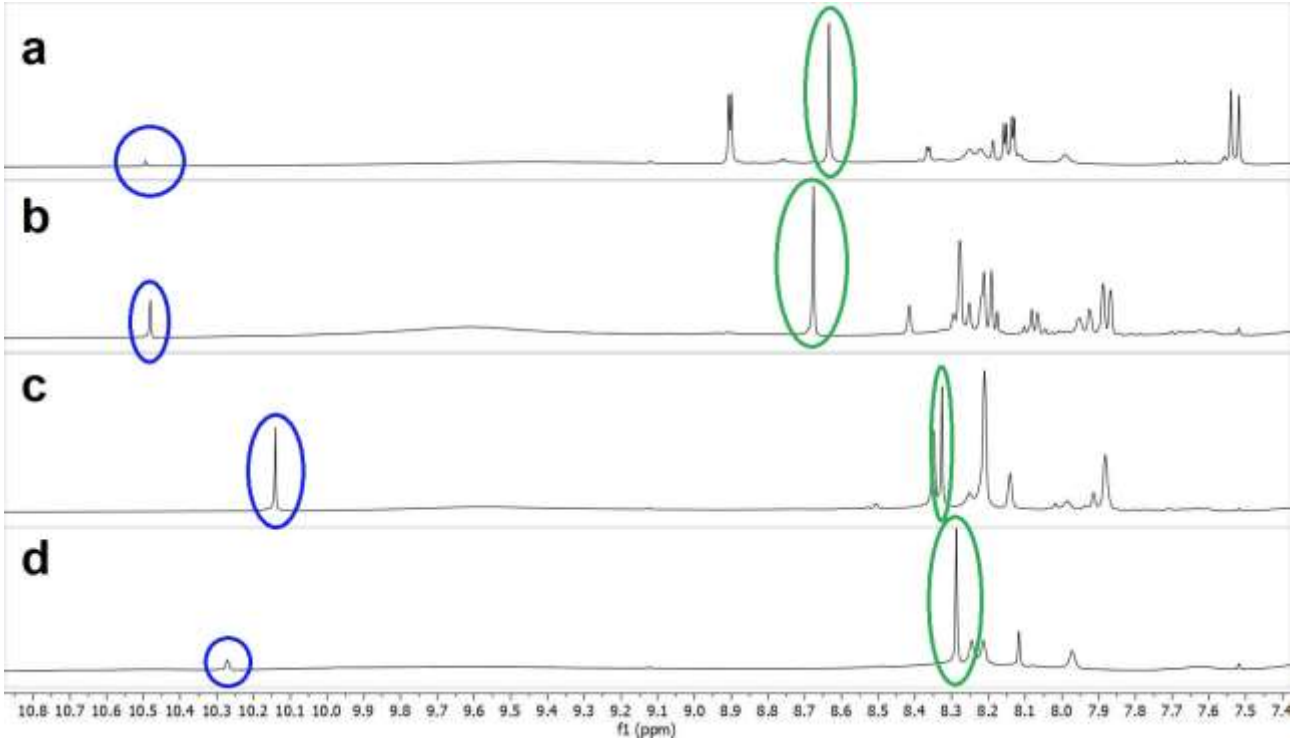

Figure E.3 *^{1}H NMR spectra of solutions of aldehyde (90 mM), isocyanide (180 mM) and **1** (54 mM) in 0.6 mL of de-acidified $CDCl_3$ after 24 h at 60 °C. The aldehyde-isocyanide pairs are: **4d-3c** (a), **4e-3c** (b), **4f-3c** (c), **4g-3c** (d).*

2.3 Synthesis and characterisation of unknown imine products

***N-tert*-butyl-1-(2-chloro-5-nitrophenyl)methanimine (5ad)**: 579 mg (3.12 mmol) of 2-chloro-5-nitrobenzaldehyde **4d** and 1.6 mL (15.2 mmol) of *tert*-butylamine **15a** were inserted in a screw-capped vial with a magnetic stirring bar. The vial was sealed and put in a silicone oil bath at 100 °C for 3.5 h with vigorous magnetic stirring. The mixture was diluted with a few mL of diethyl ether and transferred into a round-bottomed flask. The excess of amine was removed by rotary evaporation and then evaporation under reduced pressure, affording imine **5ad** in near quantitative yield (750 mg).

***N-tert*-butyl-1-(2-nitro-4-(trifluoromethyl)phenyl)methanimine (5ae)**: 326 mg (1.49 mmol) of 2-nitro-4-(trifluoromethyl)benzaldehyde **4e** and 0.8 mL (7.57 mmol) of *tert*-butylamine **15a** were inserted in a screw-capped vial with a magnetic stirring bar. The vial was sealed and put in a silicone oil bath at 100 °C for 3 h with vigorous magnetic stirring. The mixture was diluted with a few mL of diethyl ether and transferred into a round-bottomed flask. The excess of amine was removed by rotary evaporation and then evaporation under reduced pressure, affording imine **5ae** in near quantitative yield (405 mg).

***N-tert*-butyl-1-(3,5-bis(trifluoromethyl)phenyl)methanimine (5af)**: 734 mg (3.03 mmol) of 3,5-bis(trifluoromethyl)benzaldehyde **4f** and 1.6 mL (15.2 mmol) of *tert*-butylamine **15a** were inserted in a screw-capped vial with a magnetic stirring bar. The vial was sealed and put in a silicone oil bath at 100 °C for 3 h with vigorous magnetic stirring. The mixture was diluted with a few mL of diethyl ether and transferred into a round-bottomed flask. The excess of amine was removed by rotary evaporation and then evaporation under reduced pressure, affording imine **5af** in near quantitative yield (909 mg).

***N-tert*-butyl-1-(pentafluorophenyl)methanimine (5ag)**: 98 mg (0.5 mmol) of pentafluorobenzaldehyde **4g** and 79 µL (0.75 mmol) of *tert*-butylamine **15a** were inserted in a screw-capped vial with a magnetic stirring

bar and dissolved in 2.5 mL of de-acidified $CDCl_3$. The atmosphere inside the vial was replaced with argon, the vial was sealed and put in a silicone oil bath at 100 °C for 4 h with vigorous magnetic stirring. The mixture was diluted with a few mL of diethyl ether and transferred into a round-bottomed flask. The excess of amine was removed by rotary evaporation for the shortest time necessary. The resulting yellow oil was further purified by evaporation under reduced pressure for one minute, affording imine **5ag** in 72% yield (91 mg).

***N-tert*-octyl-2-chloro-5-nitrobenzaldehyde (5bd)**: 143 mg (0.13 mmol) of resorcin[4]arene **1** were dissolved in 2.5 mL of de-acidified $CDCl_3$ in a screw-capped vial. 40 mg (0.22 mmol) of 2-chloro-5-nitrobenzaldehyde **4d** and 120 µL (0.65 mmol) of *tert*-octyl isocyanide **3b** were added to the mixture. The atmosphere inside the vial was replaced with argon, the vial was sealed and put in a silicone oil bath at 60 °C for 5.5 days (131 h) with vigorous magnetic stirring. The reaction mixture was then diluted with a few mL of diethyl ether and transferred to a round-bottomed flask. The solvent was removed by rotary evaporation and the resulting solid was dissolved in a small aliquot of 9:1 cyclohexane-ethyl acetate solution to which ~1% triethylamine was added. The resulting mixture was deposited on a silica gel plug (see **Results and discussion §1.3**) and then ~80 mL of the same cyclohexane-ethyl acetate eluent mixture was passed through the plug, and the filtered solution was collected in a round-bottomed flask. The solvent was removed by rotary evaporation and then by evaporation under reduced pressure (~400 mTorr). This afforded imine **5bd** as a viscous yellow oil in 65% yield (42 mg).

***N*-benzyl-1-(2-chloro-5-nitrophenyl)methanimine (5dd)**: 100 mg (0.54 mmol) of 2-chloro-5-nitrobenzaldehyde **4d** and 125 µL (1.08 mmol) of benzylamine **15d** were dissolved 4 mL of de-acidified $CDCl_3$ in a screw-capped vial with a magnetic stirring bar. The atmosphere inside the vial was replaced with argon, the vial was sealed and put in a silicone oil bath at 60 °C for 17 h with vigorous magnetic stirring. The reaction mixture was then diluted with a few mL of diethyl ether and transferred to a round-bottomed flask. The solvent was removed by rotary evaporation and the resulting yellow oil was further purified by evaporation under reduced pressure (vacuum pump). This afforded **5dd** as a viscous yellow oil in 94% yield (140 mg).

***N*-(1-phenylethyl)-1-(2-chloro-5-nitrophenyl)methanimine (5ed)**: 40 mg (0.22 mmol) of 2-chloro-5-nitrobenzaldehyde **4d** and 56 µL of racemic 1-phenylethylamine were dissolved in 2 mL of de-acidified $CDCl_3$ in a screw-capped vial with a magnetic stirring bar. The atmosphere inside the vial was replaced with argon, the vial was sealed and put in a silicone oil bath at 60 °C for 20 h with vigorous magnetic stirring. The reaction mixture was then diluted with a few mL of diethyl ether and transferred to a round-bottomed flask. The solvent was removed by rotary evaporation and the resulting solid was further purified by evaporation under reduced pressure (vacuum pump). This afforded **5ed** as a pale yellow solid in near quantitative yield (63 mg).

General method for the synthesis and purification of imines from solid isocyanides: 0.2-0.8 mmol of aldehyde, 0.8-3 equivalents of isocyanide and ~0.6 equivalents of resorcin[4]arene **1** were dissolved in 2.4-7.4 mL of de-acidified $CDCl_3$ in a screw-capped vial with a magnetic stirring bar. The atmosphere inside the vial was replaced with argon, the vial was sealed and put in a silicone oil bath at 60 °C for 1-6 days with vigorous magnetic stirring. The reaction mixture was then diluted with a few mL of diethyl ether and transferred to a round-bottomed flask. The solvent was removed by rotary evaporation and the resulting solid was dissolved in a small aliquot of a suitable cyclohexane-ethyl acetate solution to which ~1% triethylamine was added. The resulting mixture was deposited on a silica gel plug (see **Results and discussion §1.3**) and then 80-200 mL of the same cyclohexane-ethyl acetate eluent mixture were passed through the

plug, and the filtered solution was collected in a round-bottomed flask. The solvent was removed by rotary evaporation and the resulting solid was treated by flash chromatography on a silica gel column, affording the product as pale yellow or pale orange solid in 7-30% yield. Specific details are listed below:

***N*-(2,6-dimethylphenyl)-1-(2-chloro-5-nitrophenyl)methanimine (5gd)**: 103 mg (0.56 mmol) of 2-chloro-5-nitrobenzaldehyde **4d**, 185 mg (1.41 mmol) of 2,6-dimethylphenyl isocyanide **3g** and 305 mg (0.28 mmol) of resorcin[4]arene **1** in 3 mL of de-acidified $CDCl_3$; reaction time: 4.5 days; yield: 10% (17 mg).

***N*-(2-napthyl)-1-(2-chloro-5-nitrophenyl)methanimine (5gd)**: 150 mg (0.81 mmol) of 2-chloro-5-nitrobenzaldehyde **4d**, 254 mg (1.66 mmol) of 2-napthyl isocyanide **3f** and 540 mg (0.49 mmol) of resorcin[4]arene **1** in 5 mL of de-acidified $CDCl_3$; reaction time: 5.5 days. All chromatography fractions were impure, so the least contaminated fractions were collected and the solvent was removed by rotary evaporation. A mixture of 6:4 cyclohexane-ethyl acetate (3 mL) was added to the resulting solid, obtaining a heterogeneous mixture which was filtered through a cotton plug. The filtered solid was the pure product. Yield: 8% (20 mg).

***N*-(1-adamantyl)-1-(4-nitrophenyl)methanimine (5ca)**: 100 mg (0.66 mmol) of 4-nitrobenzaldehyde **4a**, 106 mg of 1-adamantyl isocyanide **3c** (0.66 mmol) and 439 mg (0.40 mmol) of resorcin[4]arene **1** in 7.4 mL of de-acidified $CDCl_3$; reaction time: 5.5 days; yield: 10% (18 mg).

***N*-(1-adamantyl)-1-(3-nitrophenyl)methanimine (5cb)**: 33 mg (0.22 mmol) of 3-nitrobenzaldehyde **4b**, 90 mg of 1-adamantyl isocyanide **3c** (0.56 mmol) and 143 mg (0.13 mmol) of resorcin[4]arene **1** in 2.4 mL of de-acidified $CDCl_3$; reaction time: 2 days; yield: 22% (14 mg).

***N*-(1-adamantyl)-1-(4-nitrophenyl)methanimine (5cc)**: 33 mg (0.22 mmol) of 2-nitrobenzaldehyde **4a**, 57 mg of 1-adamantyl isocyanide **3c** (0.35 mmol) and 143 mg (0.13 mmol) of resorcin[4]arene **1** in 2.4 mL of de-acidified $CDCl_3$; reaction time: 2 days; yield: 27% (17 mg).

***N*-(1-adamantyl)-1-(4-nitrophenyl)methanimine (5cd)**: 40 mg (0.22 mmol) of 2-chloro-5-nitrobenzaldehyde **4d**, 51 mg of 1-adamantyl isocyanide **3c** (0.32 mmol) and 143 mg (0.13 mmol) of resorcin[4]arene **1** in 2.4 mL of de-acidified $CDCl_3$; reaction time: 2 days; yield: 42% (29 mg).

***N*-(1-adamantyl)-1-(4-nitrophenyl)methanimine (5ce)**: 47 mg (0.22 mmol) of 4-(trifluoromethyl)-2-nitrobenzaldehyde **4e**, 56 mg of 1-adamantyl isocyanide **3c** (0.35 mmol) and 143 mg (0.13 mmol) of resorcin[4]arene **1** in 2.4 mL of de-acidified $CDCl_3$; reaction time: 2 days; yield: 19% (15 mg).

***N*-(1-adamantyl)-1-(4-nitrophenyl)methanimine (5cf)**: 52 mg (0.22 mmol) of 3,5-bis(trifluoromethyl)benzaldehyde **4f**, 77 mg of 1-adamantyl isocyanide **3c** (0.48 mmol) and 143 mg (0.13 mmol) of resorcin[4]arene **1** in 2.4 mL of de-acidified $CDCl_3$; reaction time: 3 days; yield: 35% (29 mg).

***N*-(1-adamantyl)-1-(4-nitrophenyl)methanimine (5cg)**: 48 mg (0.24 mmol) of pentafluorobenzaldehyde **4g**, 67 mg of 1-adamantyl isocyanide **3c** (0.41 mmol) and 159 mg (0.14 mmol) of resorcin[4]arene **1** in 2.7 mL of de-acidified $CDCl_3$; reaction time: 2 days; yield: 18% (14 mg).

2.4 Comparison of the encapsulation affinity of *tert*-butyl isocyanide **3a** and 1-adamantyl isocyanide **3c**

The samples were prepared by dissolving 36 mg (0.033 mmol) of resorcin[4]arene **1** and either *tert*-butyl isocyanide **3a** or 1-adamantyl isocyanide **3c** in 600 µL of $CDCl_3$ in an NMR tube. The tubes were then heated to 60 °C in a water bath for one minute, in order to ensure encapsulation. The specific quantities of isocyanide are reported in **Table E.2**. ^{1}H NMR spectra were recorded of all samples; an exemplary set of stacked spectra is displayed in **Figure E.4**. The encapsulated isocyanide-to-capsule ratios (**[3@C_R]/[C_R]**) were calculated by integrating the corresponding signals (see **Figure E.4**) with a spreadsheet as shown in **Table E.3**.

Table E.2 *Quantities of isocyanide used for the preparation of the samples for ^{1}H NMR titration.*

Equivalents of isocyanide with respect to **1**	Quantity of isocyanide		
	3a (µL)	**3c** (mg)	(mmol)
1	0.6	0.9	0.033
5	3.1	4.4	0.16
10	6.2	8.7	0.33
20	12	17	0.66

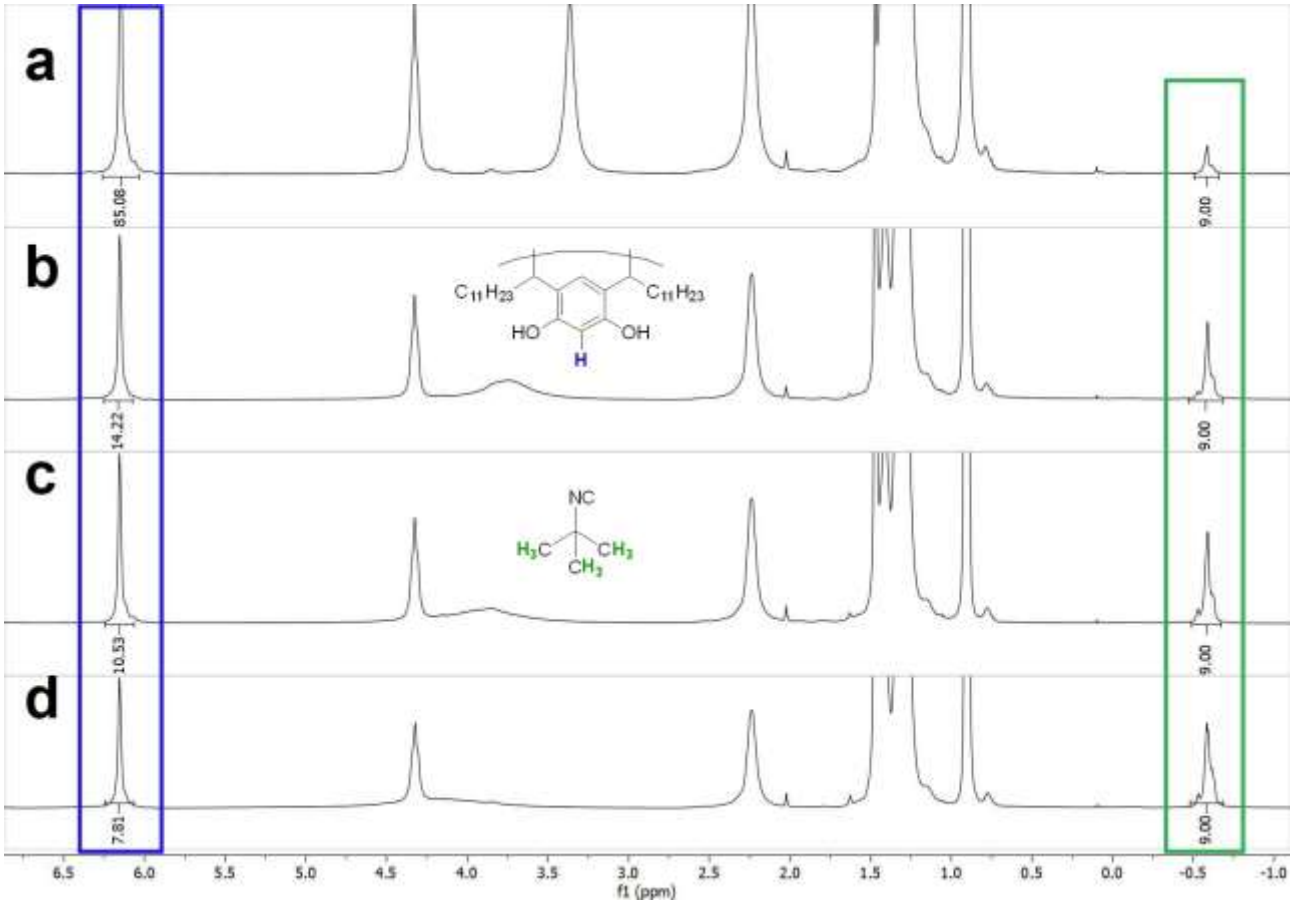

Figure E.4 *^{1}H NMR spectra of a solution of 55 mM resorcin[4]arene **1** and either 55 mM (**a**), 275 mM (**b**), 550 Mm (**c**) or 1.1 M (**d**) of* tert-*butyl isocyanide **3a**. The resonances highlighted in green correspond to the ^{1}H nuclei of the encapsulated isocyanide **3a@C_R**.*

*Table E.3 Example of the spreadsheet used to calculate the encapsulated isocyanide-to-capsule ratios ([**3a@C$_R$**]/[**C$_R$**]). n is the number of ^{1}H-nuclei corresponding to each resonance (24 for **C$_R$** and 9 for **3a**). The last column is obtained by dividing the fifth column by the third column.*

([3@C$_R$]/[C$_R$]) Equivalents of **3a**	Integral of the resonance of **C$_R$**	Second column divided by *n*	Integral of the resonance of **3a@C$_R$**	Fourth column divided by *n*	[3a@C$_R$]/[C$_R$]
1	82.60	3.44	9.00	1.00	0.29
5	14.13	0.59	9.00	1.00	1.70
10	11.14	0.46	9.00	1.00	2.15
20	8.17	0.34	9.00	1.00	2.94

2.5 Observation of the aziridinone intermediate **11** in the reaction mixture

72 mg (0.065 mmol) of resorcin[4]arene **1** were dissolved in 0.6 mL of de-acidified chloroform-*d* in an NMR tube. 16.4 mg (0.11 mmol) of 4-nitrobenzaldehyde **4a** and 24 µL (0.22 mmol) of *tert*-butyl isocyanide **3a** were added to the mixture. The tube was closed and put in a water bath at 60 °C. ^{1}H NMR spectra were recorded after 1, 2 and 3 h, and are displayed in **Figure E.5**.

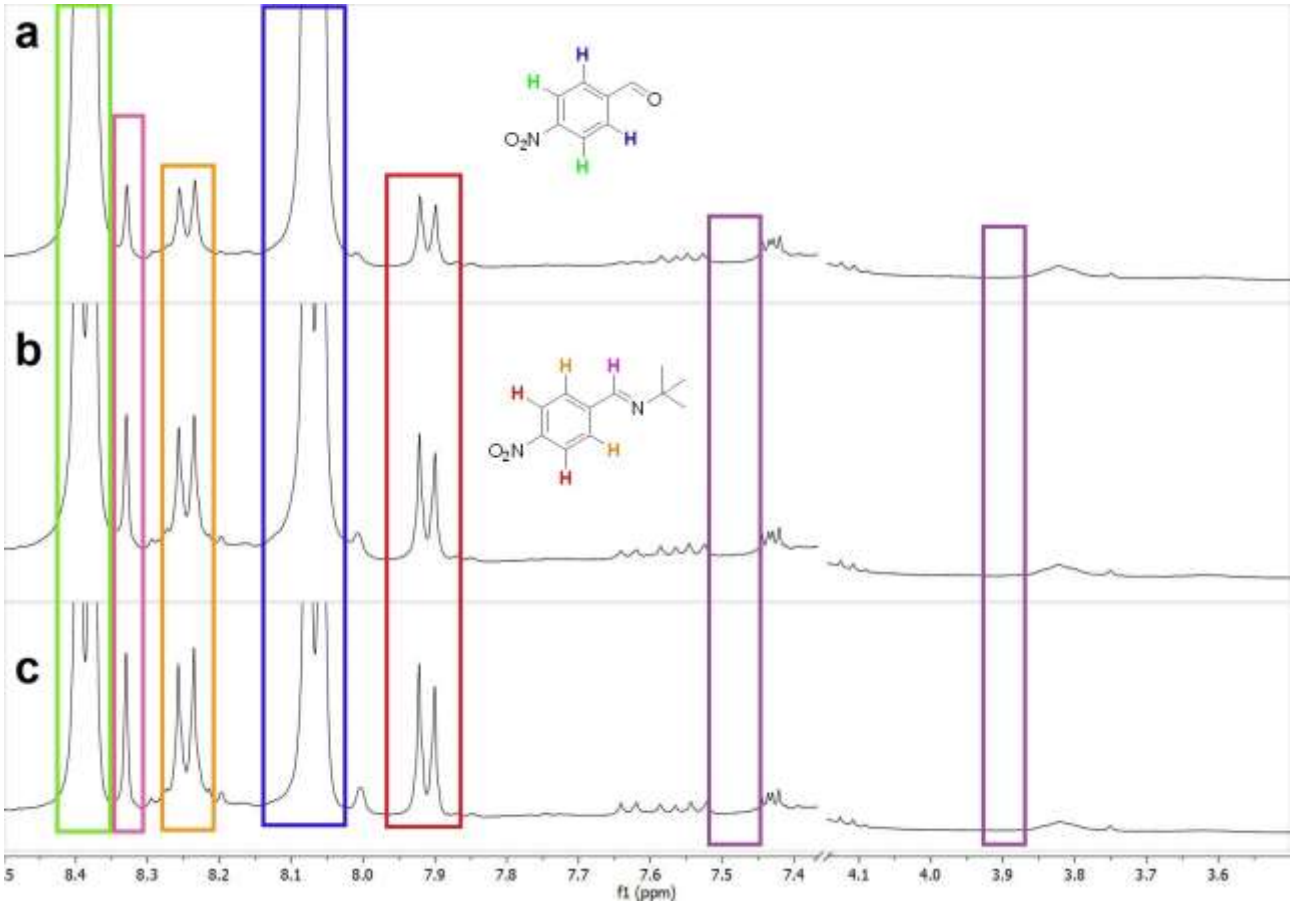

*Figure E.5 ^{1}H NMR spectra of a solution of 180 mM 4-nitrobenzaldehyde **4a**, 360 mM* tert-*butyl isocyanide **3a** and 11 mM of resorcin[4]arene **1** in 0.6 mL of de-acidified $CDCl_3$ after 1 (**a**), 2 (**b**) and 3 h (**c**) of heating at 60 °C. The two purple rectangles indicate where the resonances of aziridinone **11** were expected to appear.*

2.6 Test of the aldehyde-isocyanide condensation reaction with a sterically encumbered electron-poor aromatic aldehyde

3,5-dibromobenzaldehyde: A magnetically stirred solution of 1,3,5-tribromobenzene (2.00 g, 6.35 mmol) in dry diethyl ether (33 mL) was cooled at -78 °C (acetone/liquid nitrogen bath) in a two-necked round-bottomed flask equipped with an argon inlet and a rubber septum. A solution of *n*-butyllithium in hexanes (2.5 M, 2.5 mL, 6.35 mmol) was added dropwise via syringe over the course of 15 minutes under vigorous magnetic stirring. *N*,*N*-Dimethylformamide (1 mL, 12.8 mmol) was added to the mixture via syringe. The mixture was maintained at the same temperature for 1 hour, then the reaction was quenched by the addition of a 1 M aqueous solution of HCl (20 mL). The two phases were separated and the aqueous phase was extracted with 30 mL of diethyl ether. The combined organic phases were washed with 20 mL of water and the volatile materials were removed by rotary evaporation. The resulting white solid was recrystallized from cyclohexane (15-20 mL), affording pure 3,5-dibromobenzaldehyde as a white solid in 53% yield (893 mg). The identity of the product was confirmed by comparison of its ^{1}H NMR spectrum to literature spectra.

3,5-bis(4-nitrophenyl)benzaldehyde (4n): 264 mg (1 mmol) of 3,5-dibromobenzaldehyde, 400 mg (2.4 mmol) of 4-nitrophenylboronic acid, 70 mg (0.1 mmol) of bis(triphenylphosphine)palladium(II) dichloride and 2.02 g (14.6 mmol) of potassium carbonate were loaded in a Schlenck tube equipped with a rubber septum under an argon atmosphere. 10 mL of toluene, 10 mL of 96% ethanol and 5.5 mL of water were added via syringe through the septum. The tube, which contained a bright yellow heterogeneous mixture, was heated to 90 °C in an oil bath under vigorous magnetic stirring. Upon heating, the colour of mixture quickly changed to orange and then to dark brown. After 40 h, the tube was removed from the oil bath and the reaction mixture was filtered on a Gooch funnel affording 3,5-bis(4-nitrophenyl)benzaldehyde **4n** as a grey solid in 98% yield (341 mg).

Aldehyde-isocyanide condensation test: 18 mg (0.016 mmol) of resorcin[4]arene **1** were dissolved in 0.3 mL of de-acidified $CDCl_3$ in an NMR tube. Then, 9.5 mg (0.027 mmol) of 3,5-bis(4-nitrophenyl)benzaldehyde **4n** and 8.7 mg (0.054 mmol) of 1-adamantyl isocyanide **3c** were added to the tube, which was then sealed and put in a water bath at 60 °C for 24 h. The solvent was removed by evaporation under reduced pressure and then 0.6 mL of DMSO-d_6 were added to the tube. The tube was shaken thoroughly, until a very fine suspension was obtained. Then, a ^{1}H NMR spectrum was recorded at 60 °C (**Figure E.6**). To ensure reproducibility, this experiment was carried out four times. The yield was determined by integration of the resonances of the imine product and of **3c**, highlighted in blue and green, respectively.

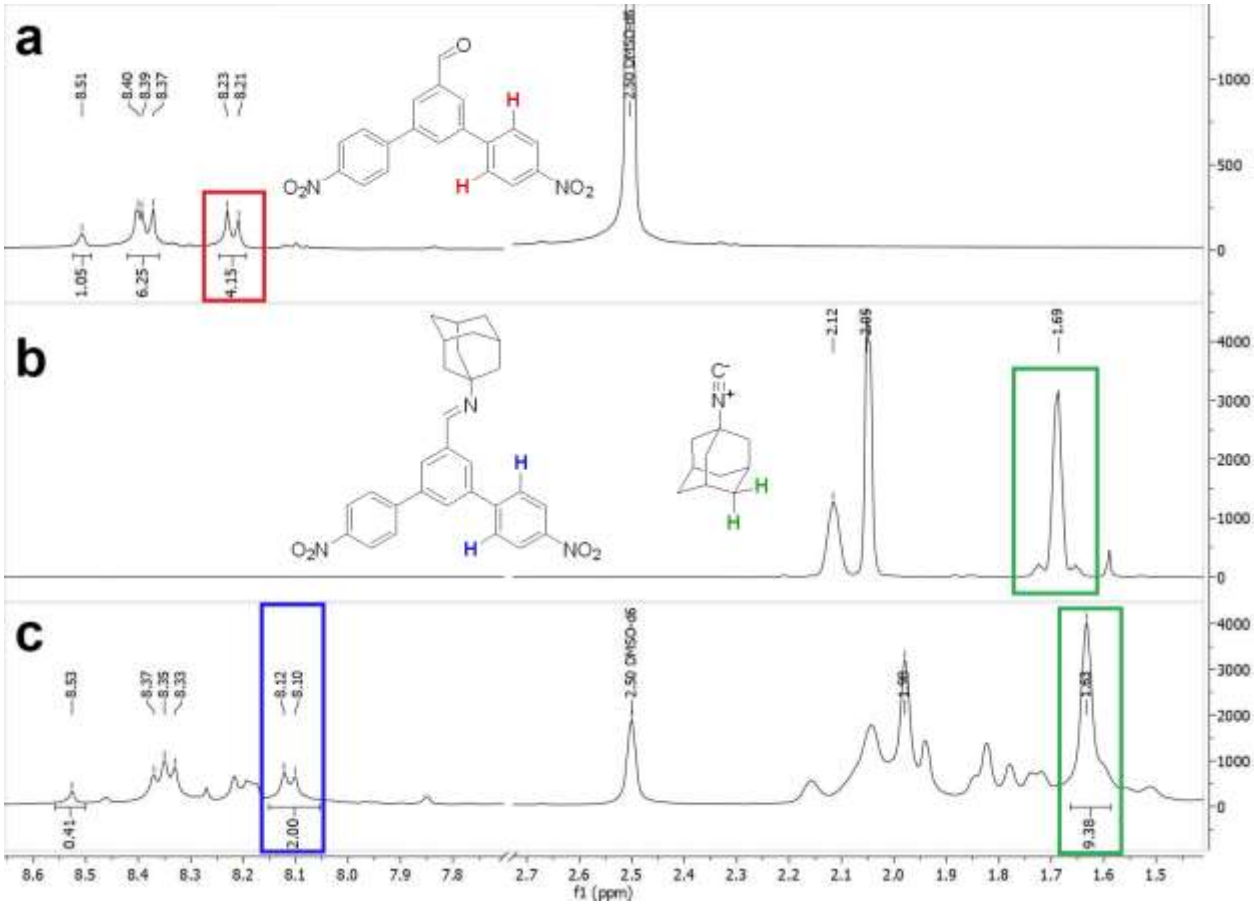

Figure E.6 ^{1}H NMR spectra of 3,5-bis(4-nitrophenyl)benzaldehyde **4n** in DMSO-d_6 (**a**) and of ^{1}H NMR spectrum of 1-adamantyl isocyanide **3c** in $CDCl_3$ (**b**); ^{1}H NMR spectrum in DMSO-d_6 recorded at 60 °C of the reaction mixture of the capsule-catalysed condensation test between **4n** and **3c** after 24 h of heating at 60 °C in $CDCl_3$ and replacement of the solvent with DMSO-d_6 (**c**).

3. Reactivity of 1,3-diphenylpropenol catalysed by the resorcin[4]arene capsule

3.1 Intramolecular S_EAr allylation and acid-catalysed decomposition of 1,3-diphenylpropenol

Control tests of the dehydration and subsequent intramolecular S_EAr allylation of 1,3-diphenylpropenol: 9.5 mg (0.045 mmol) of *trans*-1,3-diphenylprop-2-en-1-ol **12** and 0.6 mL of de-acidified chloroform-*d* were put in six NMR tubes; additional components were added as illustrated in **Table E.4**. The tubes were closed and left in a water bath at 60 °C for 8 h. Then, ^{1}H NMR spectra were taken (**Figure E.7**) and the yields were determined by integration of the corresponding resonances.

Table E.4 *Additives used for the control tests of the intramolecular S_EAr allylation of **12**.*

Tube #	Additives
1	30 mg (0.027 mmol) of resorcin[4]arene **1**
2	No additives
3	100 µL of a 0.175 M solution of acetic acid in $CDCl_3$[a]
4	21 mg (0.108 mmol) 4-*n*-hexylresorcinol
5	30 mg (0.027 mmol) of **1** and 15 mg (0.047 mmol) of Bu_4NBr **2b**
6	30 mg (0.027 mmol) of **1** and 32 µL (0.45 mmol) of DMSO-d_6

[a)] in this case, 0.5 mL of $CDCl_3$ were used as solvent instead of 0.6 mL, so that the cumulative volume would be 0.6 mL.

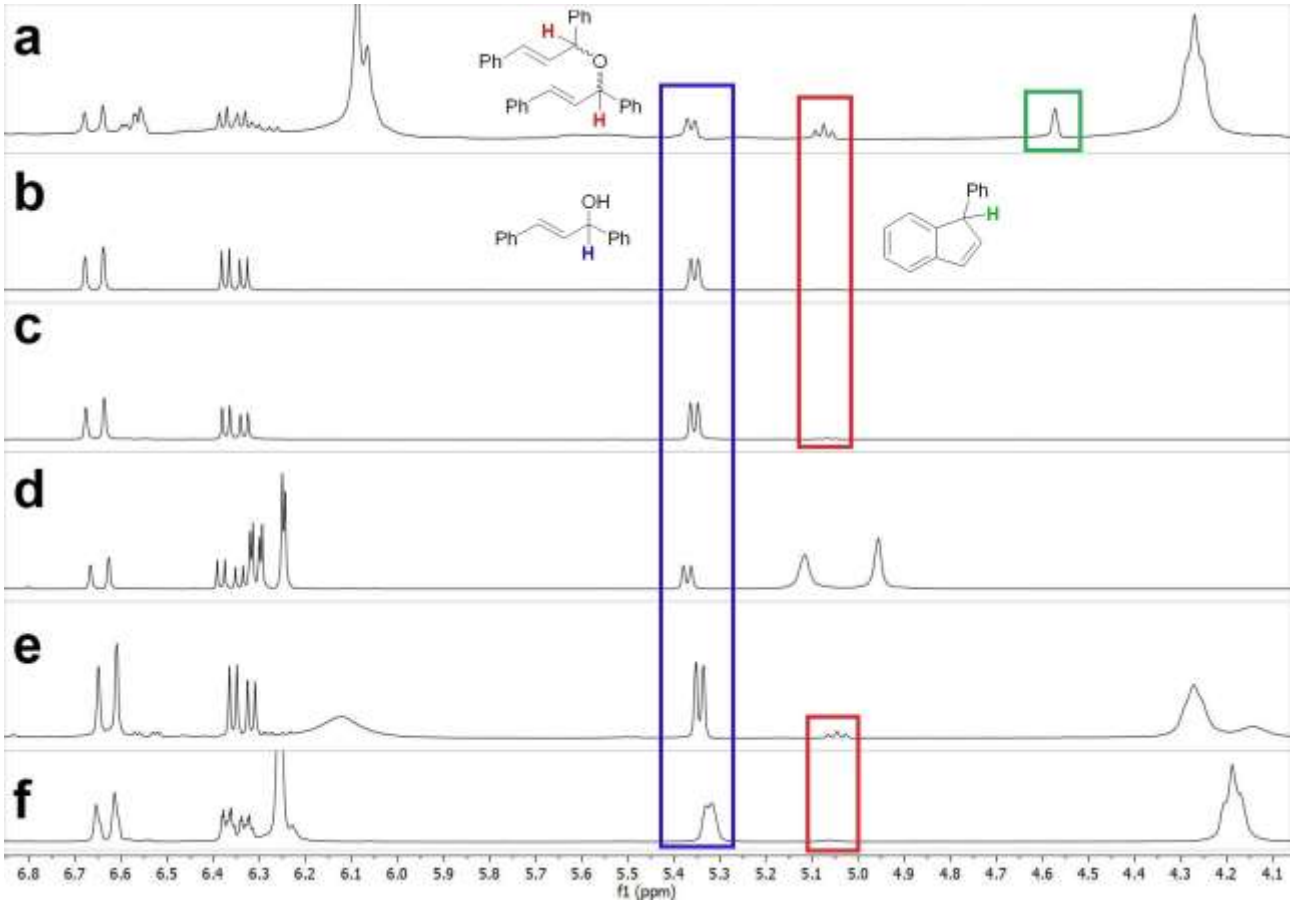

Figure E.7 *^{1}H NMR spectra of solutions of **12** (75 mM) in 0.6 mL of $CDCl_3$ after 8 h at 60 °C with the following additional components: 45 mM of **1** (a), no additives (b), 29 mM of acetic acid (c), 180 mM of 4-n-hexylresorcinol (d), 45 mM of **1** and 75 mM of **2b** (e), 45 mM of **1** and 750 mM of DMSO-d_6 (f).*

Tests of the acid-catalysed decomposition of 1,3-diphenylpropenol: The test reactions were carried out in 6 vials. See **Table E.5** for details about the contents of the vials, the specific reaction conditions and the times at which the reaction mixtures were analysed by ^{1}H NMR spectroscopy.

Table E.5 *Quantities of the reagents and catalysts used for the tests of the acid-catalysed decomposition of* ***12****.*

Vial #	Quantity of 12	Acid catalyst	Temperature (°C)	Time of ^{1}H NMR analysis
1	22 mg (0.105 mmol)	AcOH 50 µL (0.83 mmol)	60	2.5 days, 7 days
2	22 mg (0.105 mmol)	TFA 1 µL (0.01 mmol)	RT	1 h, 3 h
3	22 mg (0.105 mmol)	TFA 0.1 mL (1.3 mmol)	RT	2.5 days
4	22 mg (0.105 mmol)	TFA 0.1 mL (1.3 mmol)	60	20 h
5	35 mg (0.166 mmol)	MSA 1 µL (0.017 mmol)	60	20 h
6	35 mg (0.166 mmol)	PTSA·H_2O 3.2 mg (0.017 mmol)	60	20 h

Solvent: 0.6 mL of de-acidified $CDCl_3$, "TFA": trifluoroacetic acid, "MSA": methanesulphonic acid, "PTSA": *p*-toluenesulphonic acid, "RT": room temperature.

Synthesis and purification of ether 17: 132 mg (0.63 mmol) of *trans*-1,3-diphenylprop-2-en-1-ol **12** and 5 µL (0.065 mmol) of trifluoroacetic acid were dissolved in 3 mL of de-acidified $CDCl_3$ in a screw-capped vial containing a magnetic stirring bar. The reaction mixture was left at room temperature for 1.5 h under vigorous magnetic stirring, then 4 drops of triethylamine were added to quench the reaction. The solvent was removed by rotary evaporation and the resulting solid was treated by flash column chromatography on silica gel using a 1:1 cyclohexane-dichloromethane solution as eluent. This afforded ether **17** as a colourless oil in 21% yield (26 mg).

3.2 Intermolecular S_EAr reactivity of the 1,3-diphenyallyl cation

Control tests of the intermolecular S_EAr allylation between indole 20a and the allyl cation generated by 1,3-diphenylpropenol: Six NMR tubes were prepared by dissolving 9.5 mg (0.045 mmol) of *trans*-1,3-diphenylprop-2-en-1-ol **12** and 5.3 mg (0.045 mmol) of indole **20a** in 0.6 mL of de-acidified $CDCl_3$. Additional components were added as shown in **Table E.6**. The tubes were closed and put in a water bath at 60 °C for 6 h. Then, ^{1}H NMR spectra were recorded (see **Figure E.8**).

Table E.6 *Additives used for the control tests of the intermolecular S_EAr allylation between* ***12*** *and* ***20a****.*

Tube #	Additives
1	30 mg (0.027 mmol) of resorcin[4]arene **1**
2	No additives
3	100 µL of a 0.175 M solution of acetic acid in $CDCl_3$[a]
4	21 mg (0.108 mmol) 4-*n*-hexylresorcinol
5	30 mg (0.027 mmol) of **1** and 15 mg (0.047 mmol) of Bu_4NBr **2b**
6	30 mg (0.027 mmol) of **1** and 32 µL (0.45 mmol) of DMSO-d_6

[a)] in this case, 0.5 mL of $CDCl_3$ were used as solvent instead of 0.6 mL, so that the cumulative volume would be 0.6 mL.

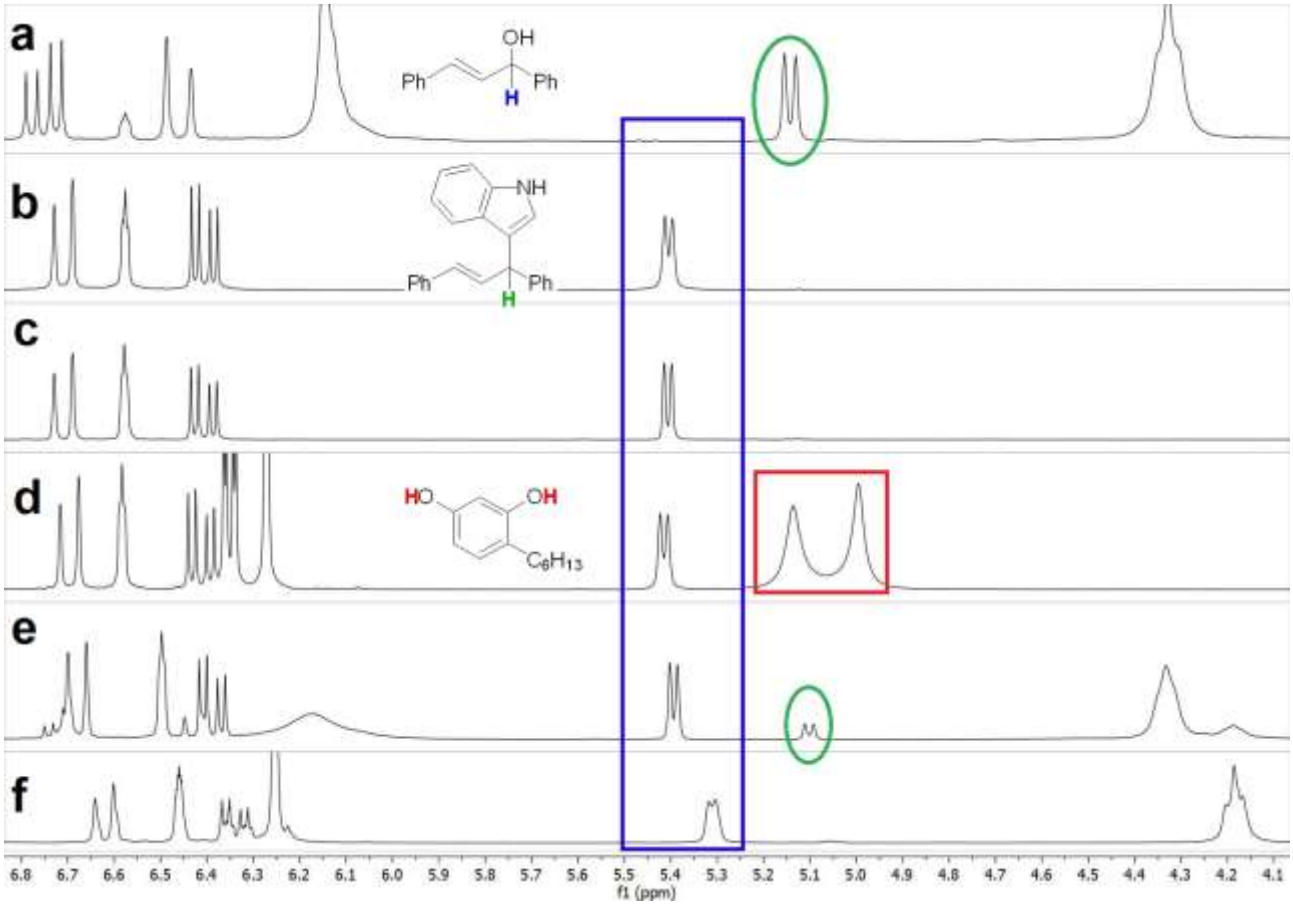

Figure E.8 *^{1}H NMR spectra of solutions of **12** (75 mM) and **20a** (75 mM) in 0.6 mL of $CDCl_3$ after 6 h at 60 °C with the following additional components: 45 mM of **1** (**a**), no additives (**b**), 29 mM of acetic acid (**c**), 180 mM of 4-n-hexylresorcinol (**d**), 45 mM of **1** and 75 mM of **2b** (**e**), 45 mM of **1** and 750 mM of DMSO-d_6 (**f**).*

Investigation of the scope of the reaction: 30 mg (0.027 mmol) of resorcin[4]arene **1** were dissolved in 0.6 mL of de-acidified $CDCl_3$ in an NMR tube. Then, 9.5 mg (0.045 mmol) of *trans*-1,3-diphenylprop-2-en-1-ol **12** and 0.045 mmol of an electron-rich aromatic substrate were added. Another NMR tube was prepared in the same way, but with addition of 15 mg (0.047 mmol) of Bu_4NBr **2b**. The tubes were closed and put in a water bath at 60 °C for 6 h, then ^{1}H NMR spectra were recorded.

3.3 Formation of unexpected *O*-substituted nucleophilic attack products and subsequent Claisen rearrangement

Tests of the reactions between 1,3 diphenylpropenol and phenols 22m-n: 30 mg (0.027 mmol) of resorcin[4]arene **1** were dissolved in 0.6 mL of de-acidified $CDCl_3$ in an NMR tube. 9.5 mg (0.045 mmol) of *trans*-1,3-diphenylpropenol **12** and 0.045 mmol of phenol **22m** or **22n** were then added. The tubes were closed and put in a water bath at 60 °C. ^{1}H NMR spectra were recorded after 2, 6 and 24 h of heating (**Figure E.9** and **Figure E.10**)

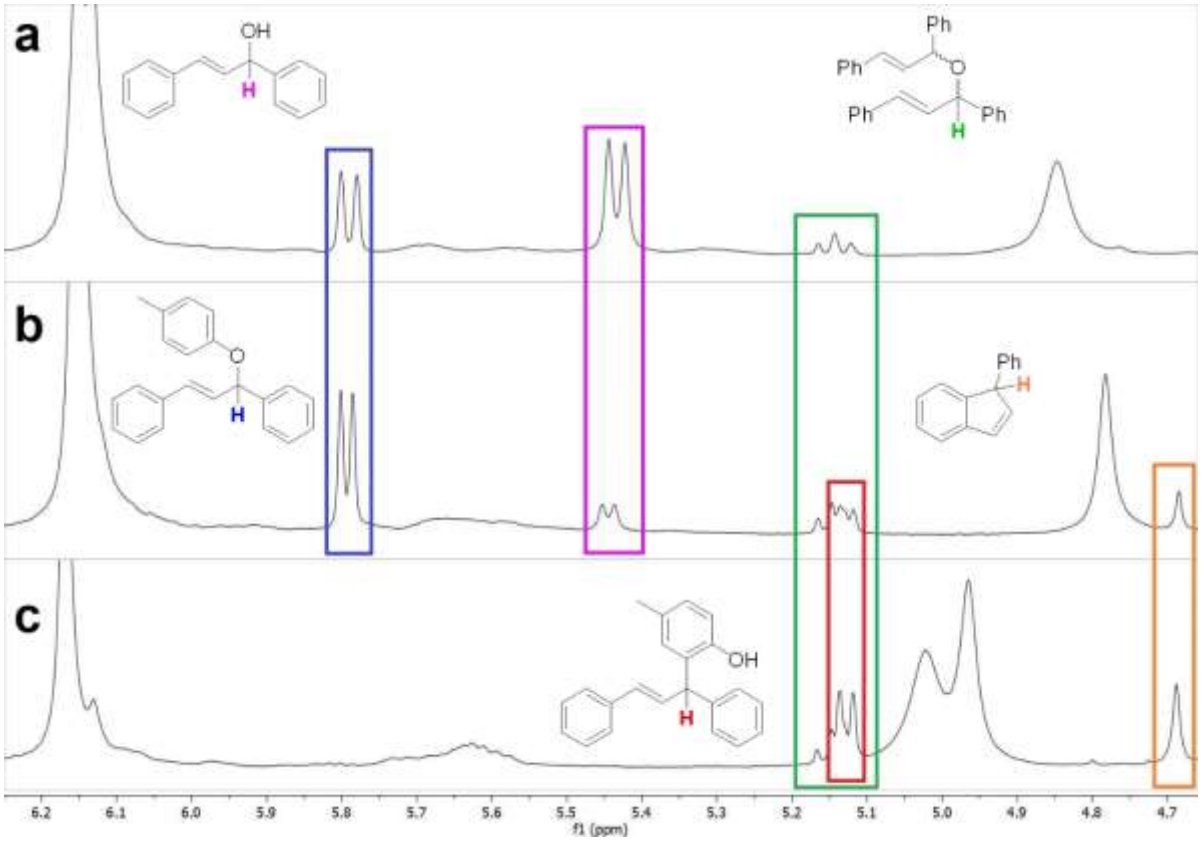

Figure E.9 *^{1}H NMR spectra of a solution of 75 mM* trans*-1,3-diphenylprop-2-en-1-ol* ***12****, 75 mM* p*-cresol* ***22m*** *and 45 mM resorcin[4]arene* ***1*** *in 0.6 mL of de-acidified $CDCl_3$ after 2 (**a**), 6 (**b**) and 24 (**c**) h of heating at 60 °C.*

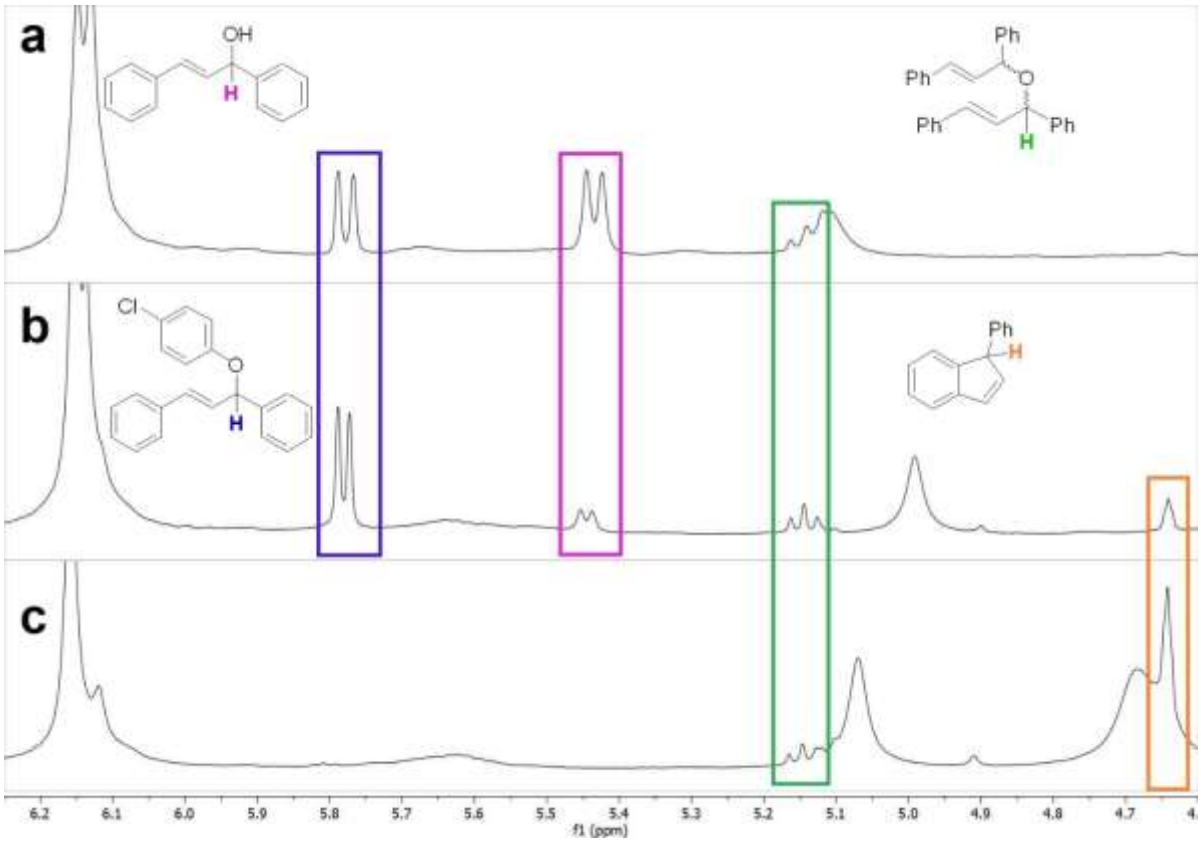

Figure E.10 *^{1}H NMR spectra of a solution of 75 mM* trans*-1,3-diphenylprop-2-en-1-ol* ***12****, 75 mM 4-chlorophenol* ***22n*** *and 45 mM resorcin[4]arene* ***1*** *in 0.6 mL of de-acidified $CDCl_3$ after 2 (**a**), 6 (**b**) and 24 (**c**) h of heating at 60 °C.*

Control tests of the reaction between 1,3-diphenylpropenol and 4-methoxyphenol: Six NMR tubes were prepared by dissolving 9.5 mg (0.045 mmol) of *trans*-1,3-diphenylprop-2-en-1-ol **12** and 5.6 mg (0.045 mmol) of 4-methoxyphenol **22i** in 0.6 mL of de-acidified $CDCl_3$. Additional components were added as shown in **Table E.7**. The tubes were closed and put in a water bath at 60 °C. ^{1}H NMR spectra were recorded after 6 and 24 h of heating (**Figure E.11**).

*Table E.7 Additives used for the control tests of the intermolecular S_EAr allylation between **12** and **20a**.*

Tube #	Additives
1	30 mg (0.027 mmol) of resorcin[4]arene **1**
2	No additives
3	72 µL of a 0.25 M solution of acetic acid in $CDCl_3$
4	21 mg (0.108 mmol) 4-*n*-hexylresorcinol
5	30 mg (0.027 mmol) of **1** and 15 mg (0.047 mmol) of Bu_4NBr **2b**
6	30 mg (0.027 mmol) of **1** and 32 µL (0.45 mmol) of DMSO-d_6

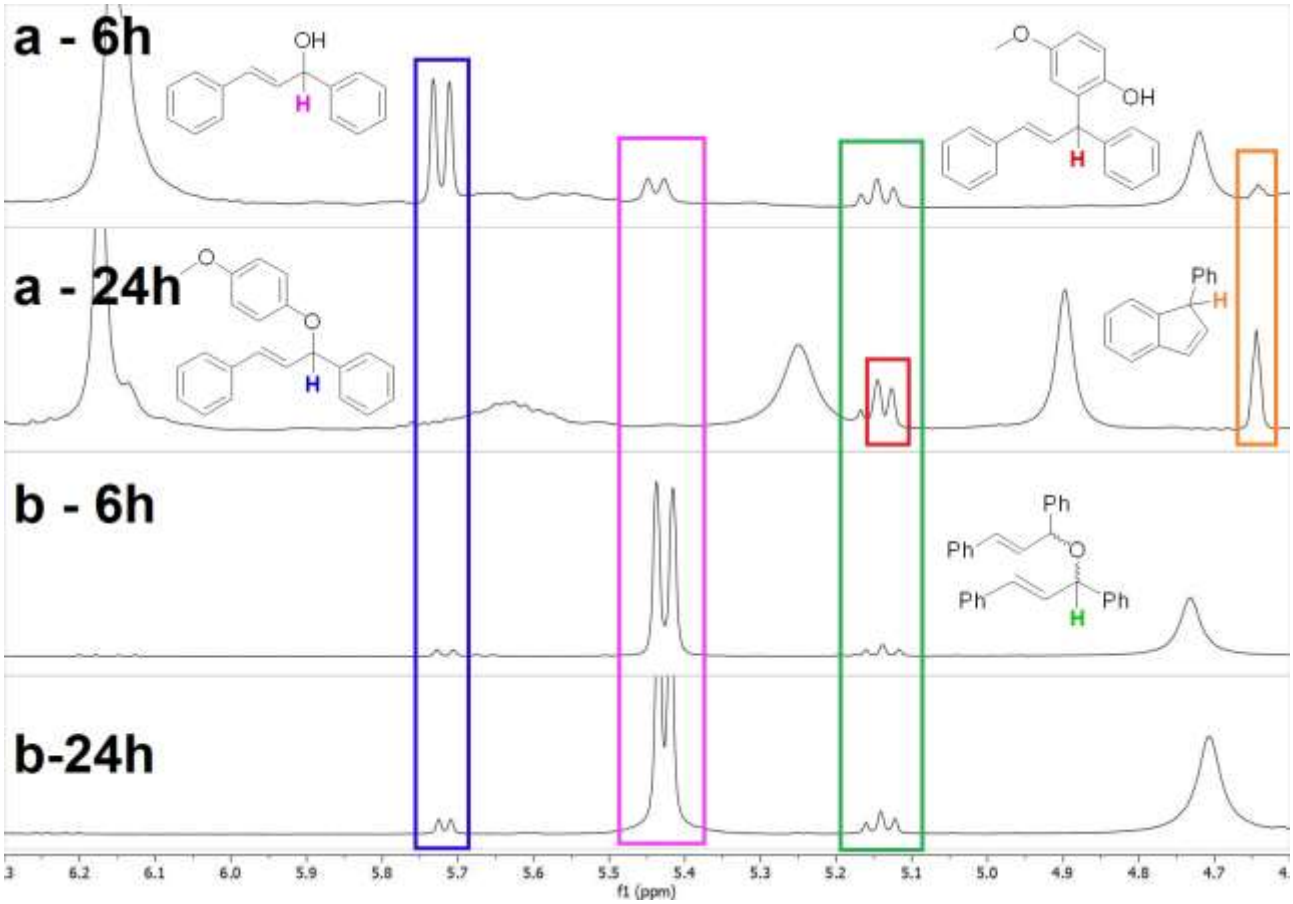

*Figure E.11 ^{1}H NMR spectra of solutions of **12** (75 mM) and **22i** (75 mM) in 0.6 mL of $CDCl_3$ after 6 h (**6h**) and 24 h (**24h**) of heating at 60 °C with the following additional components: 45 mM of **1** (**a**), no additives (**b**).*

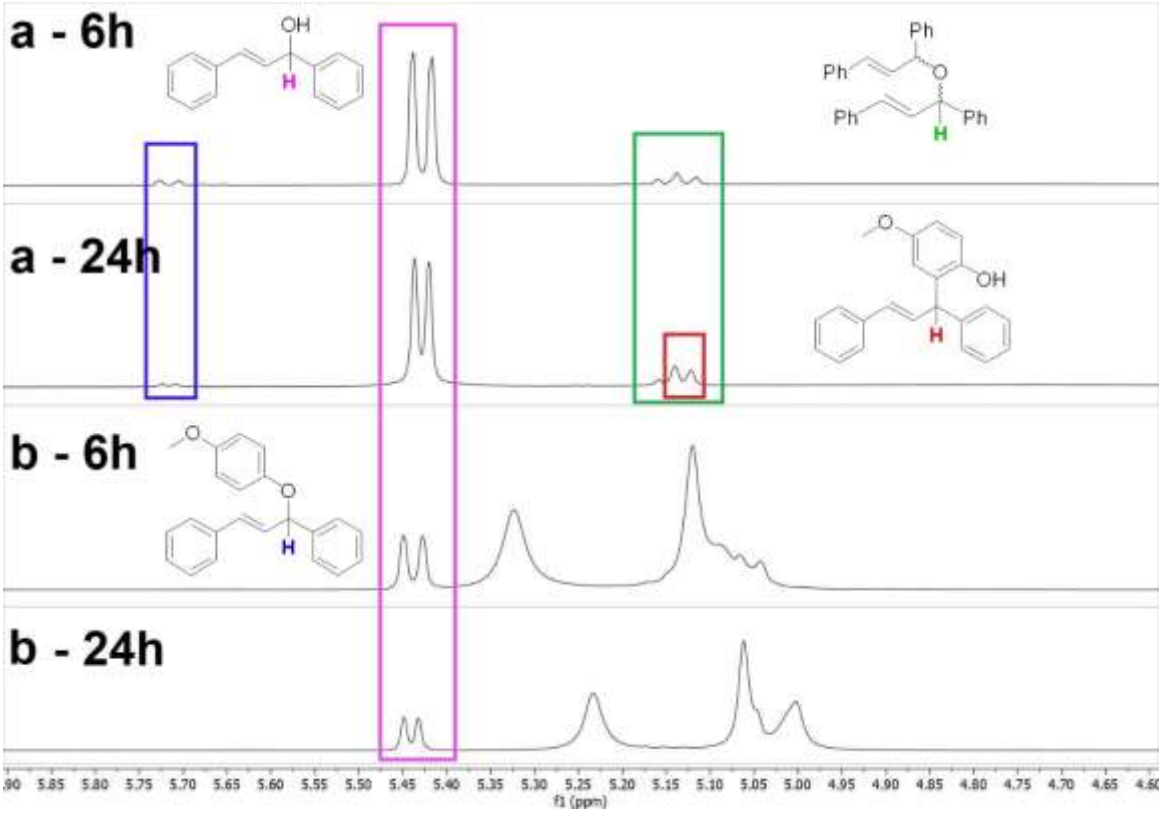

Figure E.11 ^{1}H NMR spectra of solutions of **12** (75 mM) and **22i** (75 mM) in 0.6 mL of $CDCl_3$ after 6 h (6h) and 24 h (24h) of heating at 60 °C with the following additional components: 29 mM of acetic acid (a), 180 mM of 4-n-hexylresorcinol (b).

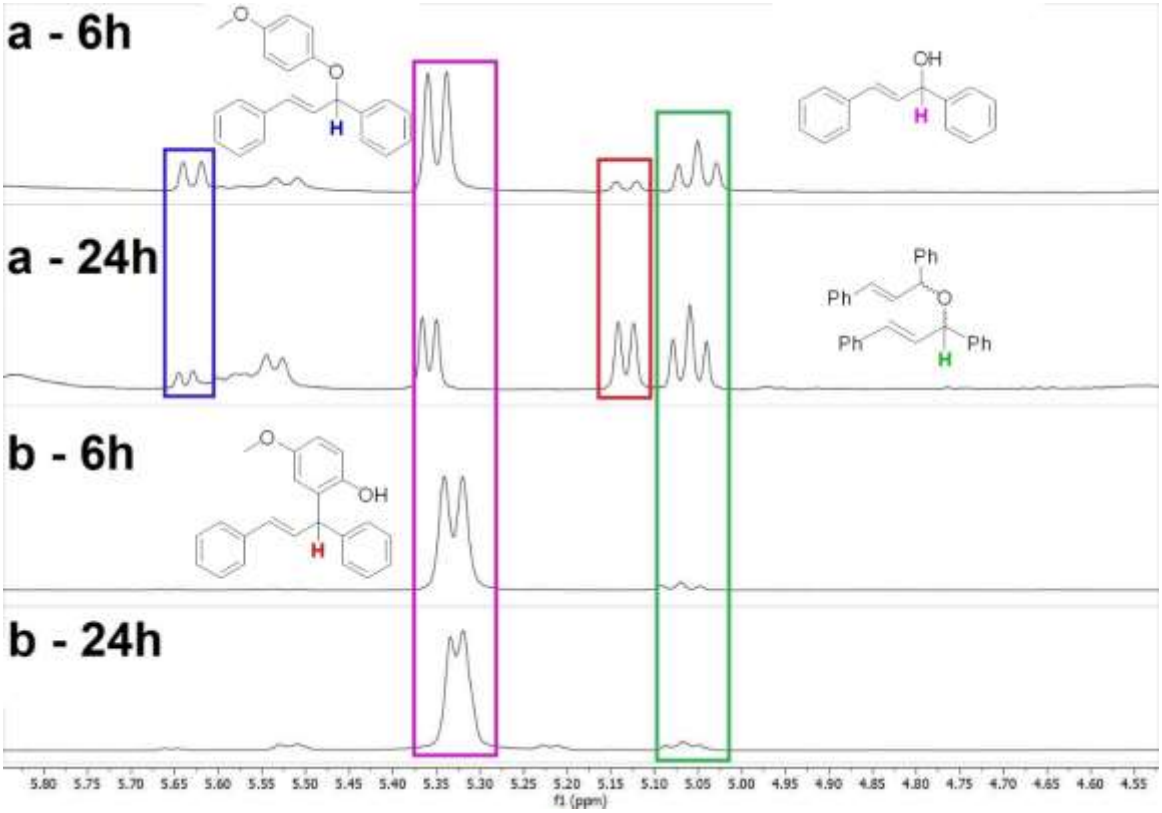

Figure E.11 ^{1}H NMR spectra of solutions of **12** (75 mM) and **22i** (75 mM) in 0.6 mL of $CDCl_3$ after 6 h (6h) and 24 h (24h) of heating at 60 °C with the following additional components: 45 mM of **1** and 75 mM of **2b** (a), 45 mM of **1** and 750 mM of DMSO-d_6 (b).

3.4 Regioselectivity differences between acid-catalysed and capsule-catalysed S_EAr allylation between 1,3-diphenylpropenol **12** and 3-methoxyphenol **22k**

40 mg (0.19 mmol) of *trans*-1,3-diphenylprop-2-en-1-ol **12**, 20 µL (0.19 mmol) of 3-methoxyphenol **22k** and 40 µL (0.02 mmol) of a 0.47 M solution of trifluoroacetic acid TFA in $CDCl_3$ were dissolved in 0.6 mL of $CDCl_3$ in an NMR tube. The tube was sealed and heated to 60 °C in a water bath for 2 h. A drop of triethylamine was then added to the reaction mixture. ^{1}H NMR, ^{13}C NMR, COSY, HSQC and HMBC spectra were recorded (see **Figures E.12-E.15**).

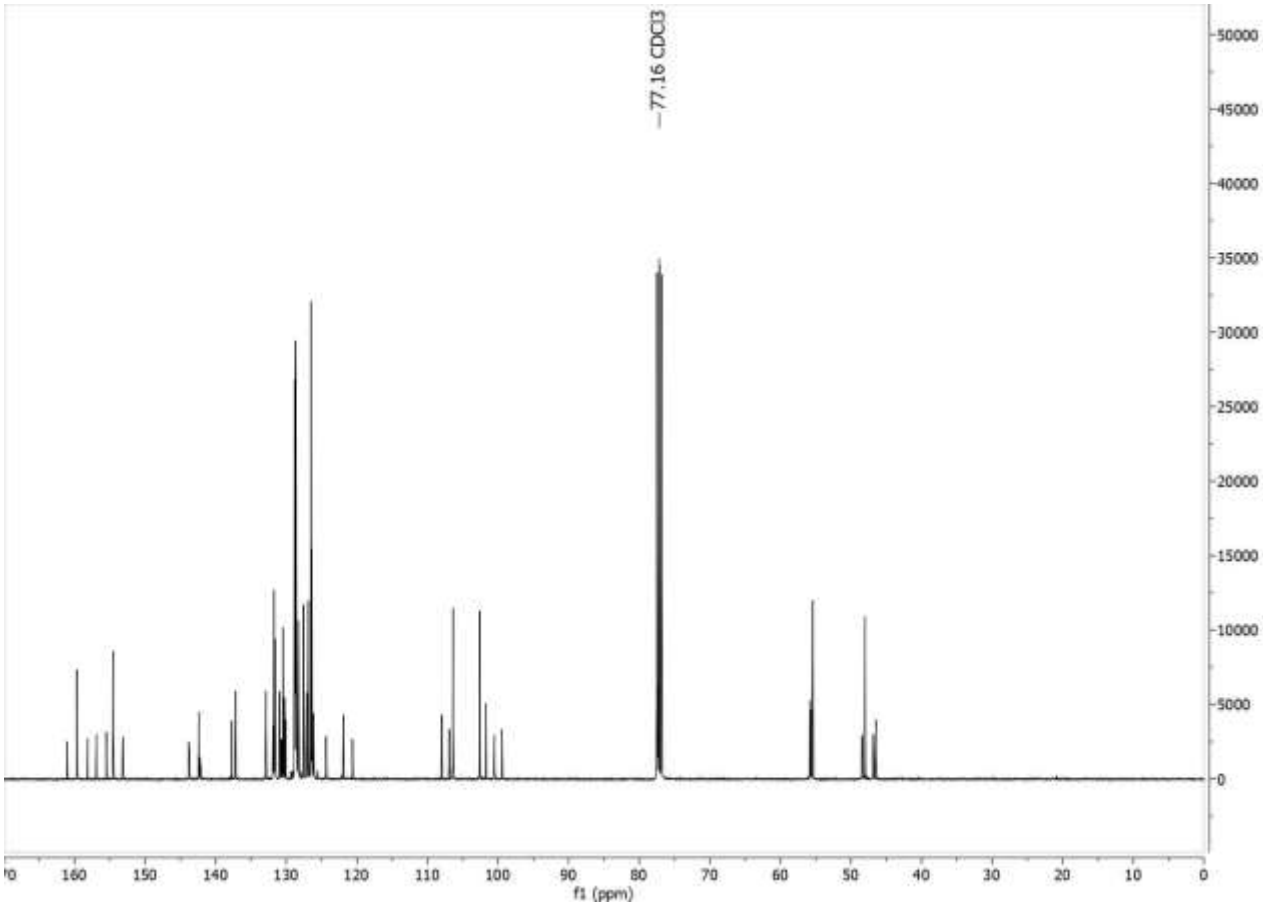

Figure E.12 *^{13}C NMR spectrum of a solution of 317 mM of **12**, 317 mM of **22k** and 32 mM of TFA in $CDCl_3$ after 2 h of heating at 60 °C.*

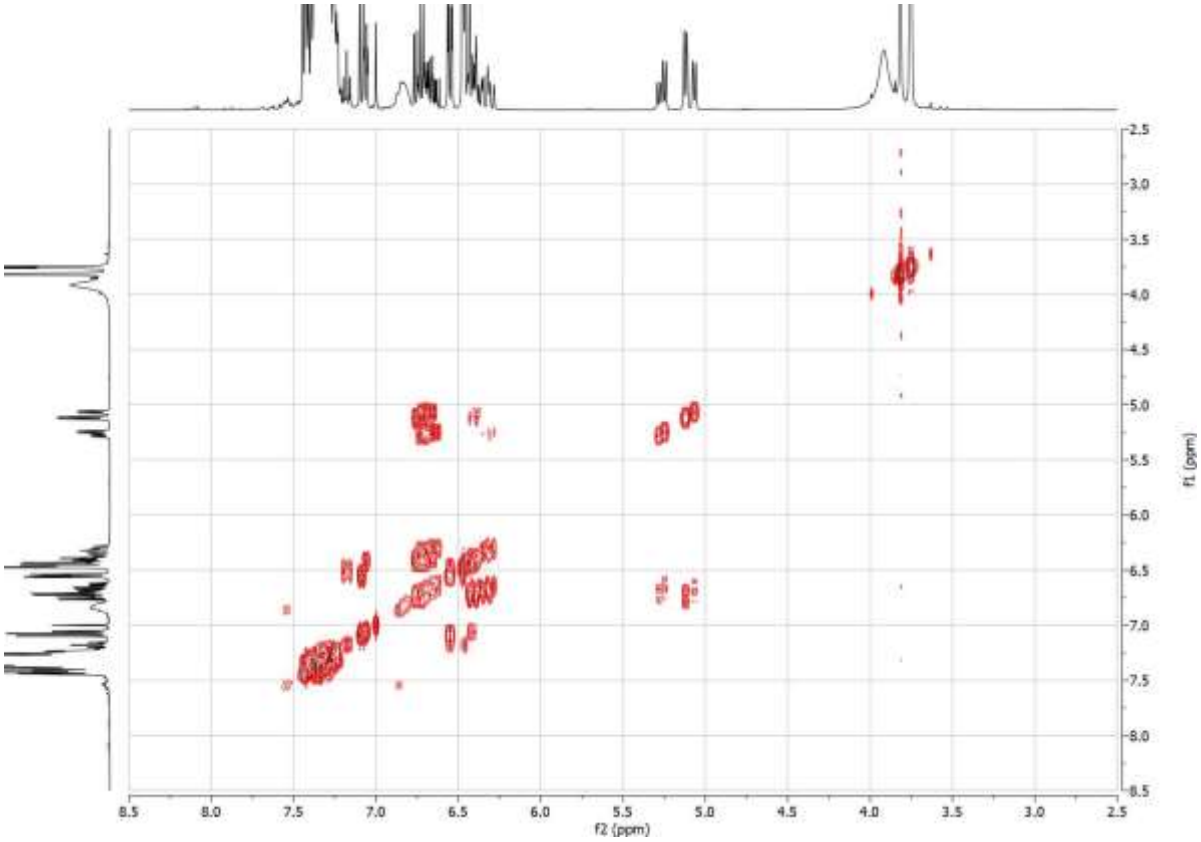

Figure E.13 *COSY spectrum of a solution of 317 mM of* ***12****, 317 mM of* ***22k*** *and 32 mM of TFA in $CDCl_3$ after 2 h of heating at 60 °C.*

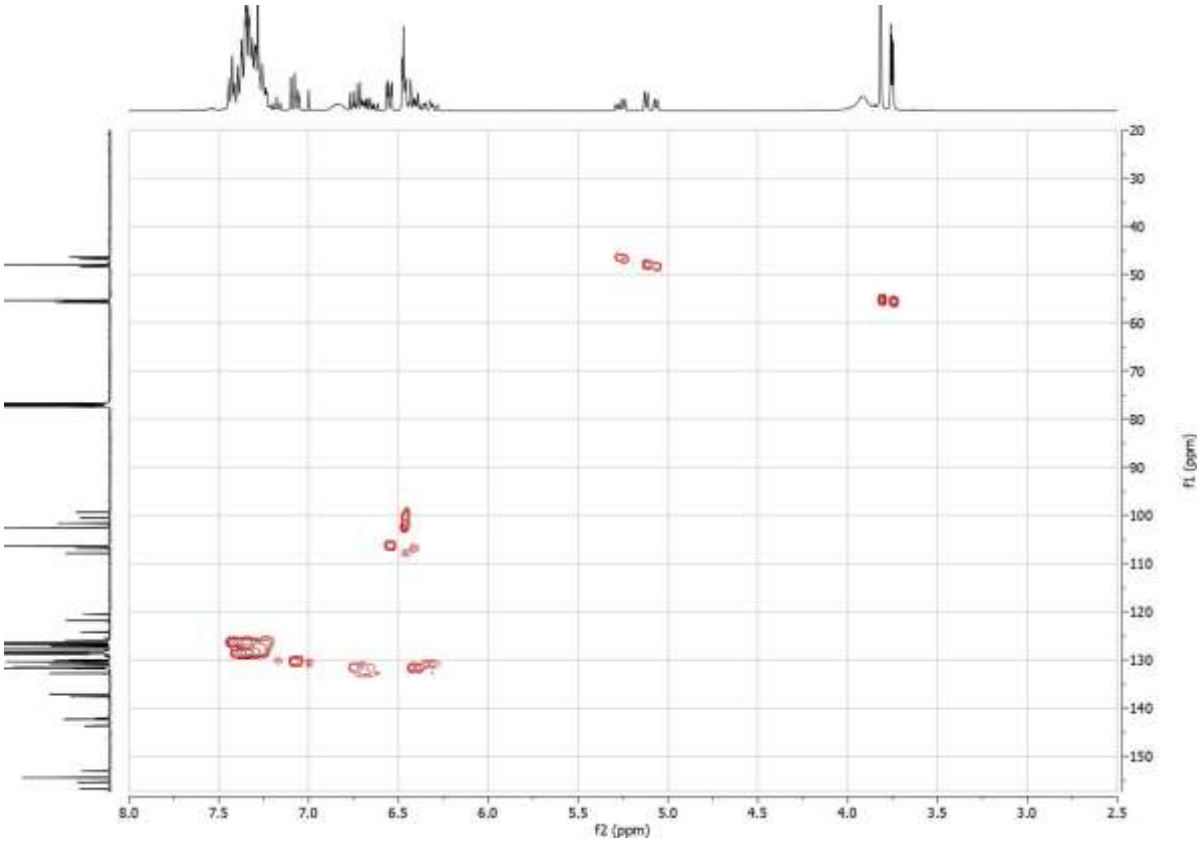

Figure E.14 *HSQC spectrum of a solution of 317 mM of* ***12****, 317 mM of* ***22k*** *and 32 mM of TFA in $CDCl_3$ after 2 h of heating at 60 °C.*

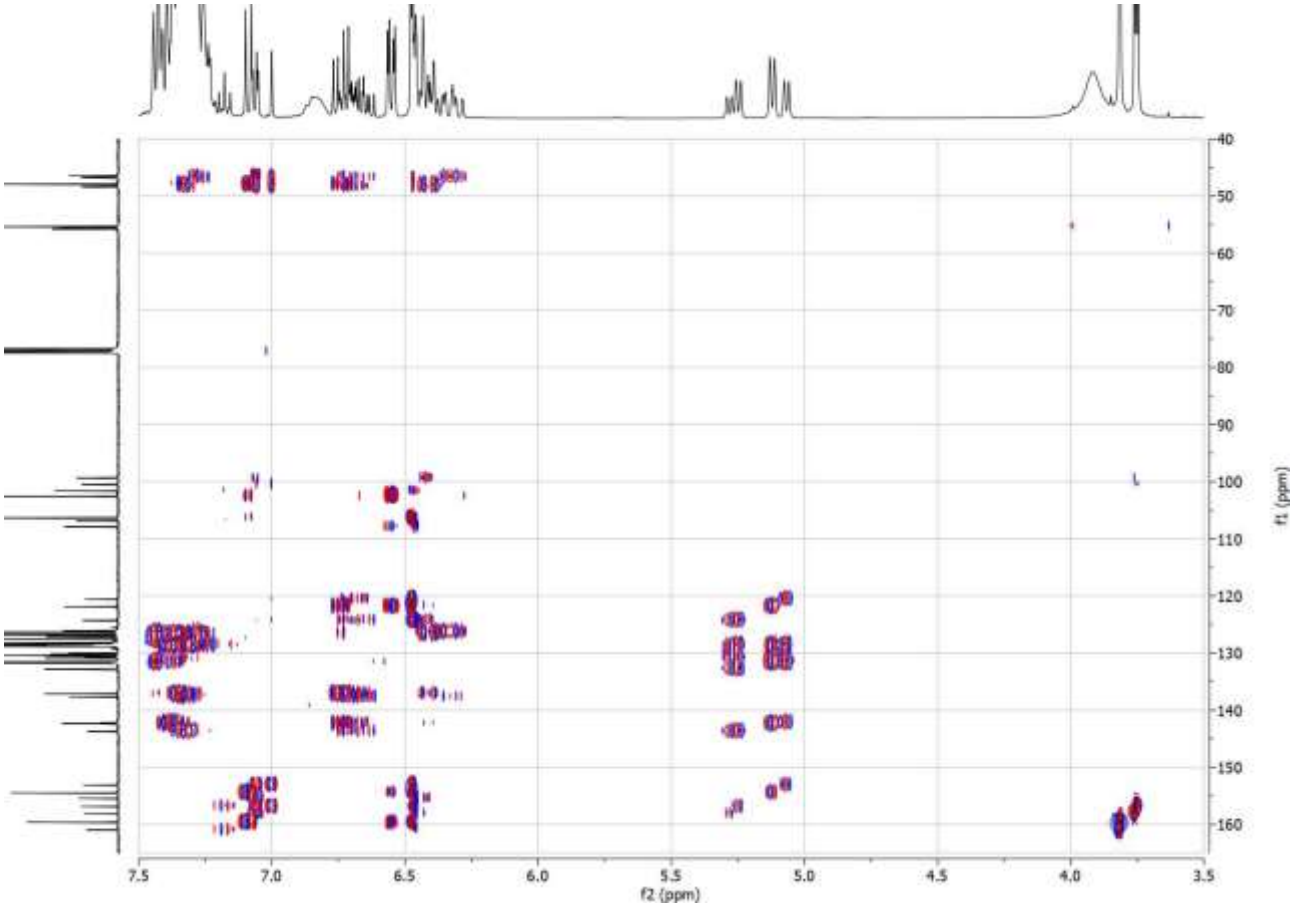

*Figure E.15 HMBC spectrum of a solution of 317 mM of **12**, 317 mM of **22k** and 32 mM of TFA in $CDCl_3$ after 2 h of heating at 60 °C.*

3.5 Synthesis and characterisation of unknown *C*-substituted S_EAr products and *O*-substituted nucleophilic substitution products

Procedure for the synthesis and purification of products 21e, 21f, 21g, 21h, 21i, 21j, 21k, 21m, 21n, 21p, 21q 47.5 mg (0.23 mmol) of *trans*-1,3-diphenylprop-2-en-1-ol **12**, 150 mg (0.14 mmol) of resorcin[4]arene **1** and 0.23 mmol of an electron-rich aromatic substrate were dissolved in 3 mL of de-acidified $CDCl_3$ in a screw-capped vial with a magnetic stirring bar. The vial was put in a temperature-controlled aluminium heating block at 60 °C for a day under vigorous magnetic stirring. The reaction mixture was then diluted with a few mL of diethyl ether and transferred to a round-bottomed flask. The solvent was removed by rotary evaporation and the resulting solid was dissolved in a small aliquot of a suitable cyclohexane-ethyl acetate solution to which ~1% triethylamine was added. The resulting mixture was deposited on a silica gel plug (see **Results and discussion §1.3**) and then 80 mL of the same cyclohexane-ethyl acetate eluent mixture were passed through the plug, and the filtered solution was collected in a round-bottomed flask. The solvent was removed by rotary evaporation and the resulting solid was treated by preparative TLC on a silica plate, affording the product as a white, pale yellow or light brown solid in 10-30% yield.

General procedure for the synthesis and purification of ether derivatives 23h and 23i: 75 mg (0.36 mmol) of *trans*-1,3-diphenylprop-2-en-1-ol **12**, 0.36 mmol of 4-alkoxyphenol and 70 µL (0.035 mmol) of a 0.5 M

solution of trifluoroacetic acid in $CDCl_3$ were dissolved in 3.5 mL of $CDCl_3$ in a screw-capped vial equipped with a magnetic stirring bar. The vial was sealed and left to sit at room temperature under vigorous magnetic stirring for one hour. The reaction mixture was then transferred into a round-bottomed flask and the solvent was removed by rotary evaporation. The resulting pale yellow oil was treated by flash column chromatography on silica gel with a 95:5 cyclohexane-ethyl acetate mixture to which ~1% triethylamine was added. This afforded the product as a colourless oil in 11-13% yield. Specific details are listed below:

(*E*)-3-(4-ethoxyphenyloxy)-1,3-diphenylprop-1-ene (23h): 48 mg (0.36 mmol) of 4-ethoxyphenol **22h**; yield: 13% (16 mg);
(*E*)-3-(4-methoxyphenyloxy)-1,3-diphenylprop-1-ene (23i): 44 mg (0.36 mmol) of 4-methoxyphenol **22i**; yield: 11% (12 mg).

Characterisation data

1. Imine products

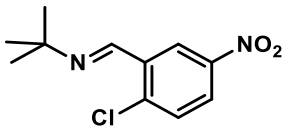

5ad

Chemical Formula: $C_{11}H_{13}ClN_2O_2$
Molecular Weight: 240,68700

^{1}H NMR (400 MHz, Chloroform-d) δ [ppm] = 8.89 (d, J = 2.8 Hz, 1H), 8.64 (s, 1H), 8.15 (dd, J = 8.8, 2.8 Hz, 1H), 7.54 (d, J = 8.7 Hz, 1H), 1.33 (s, 10H).

^{13}C NMR (101 MHz, Chloroform-d) δ [ppm] = 150.14, 147.14, 141.19, 135.80, 130.86, 125.14, 123.64, 58.85, 29.68.

GC/MS (EI): calc. for $C_{11}H_{13}ClN_2O_2$ $[M]^+$: 240.067; found: 240.032, $C_{10}H_{10}ClN_2O_2$ $[M-CH_3^{\cdot}]$ 225.026, C_4H_9 57.073.

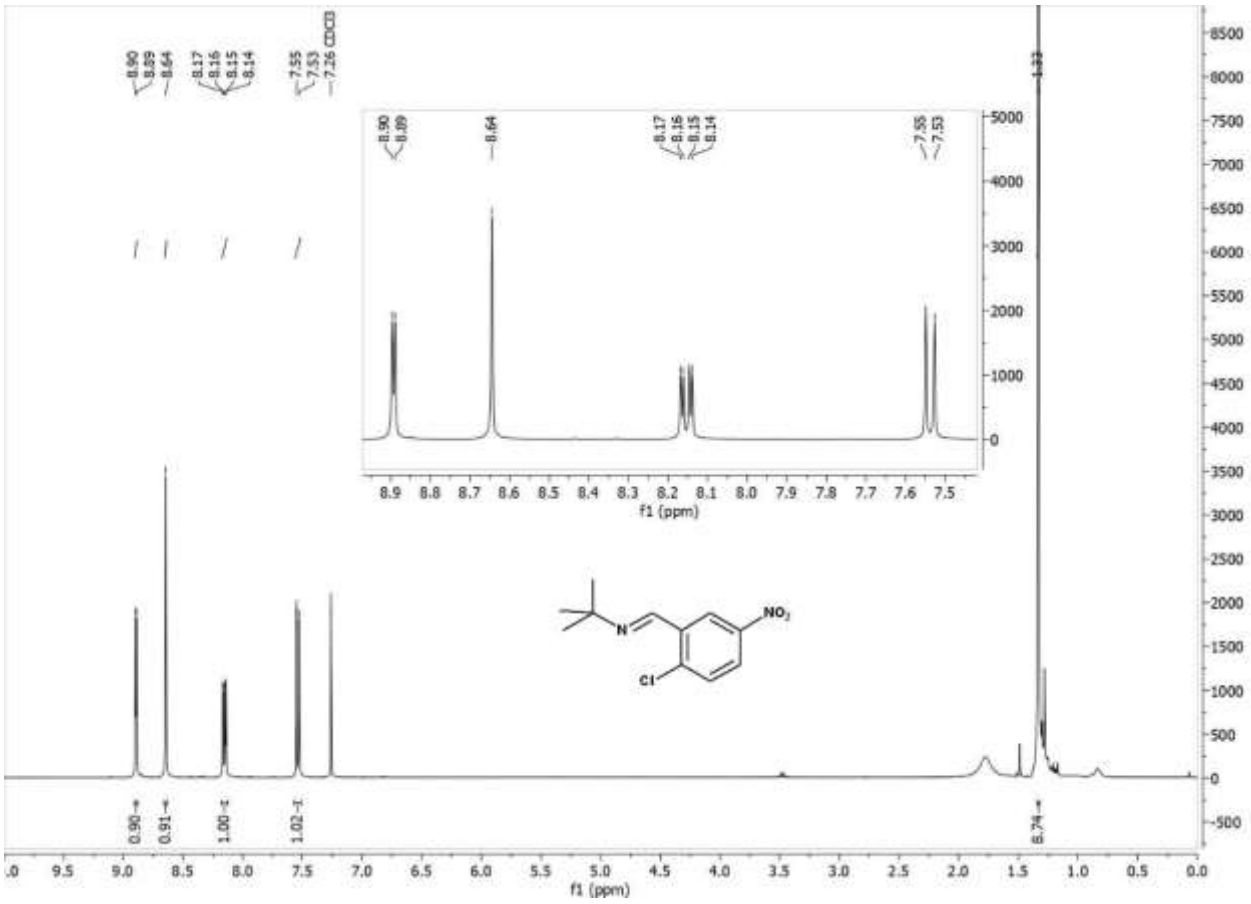

*Figure C.1 ^{1}H NMR spectrum of **5ad** in $CDCl_3$.*

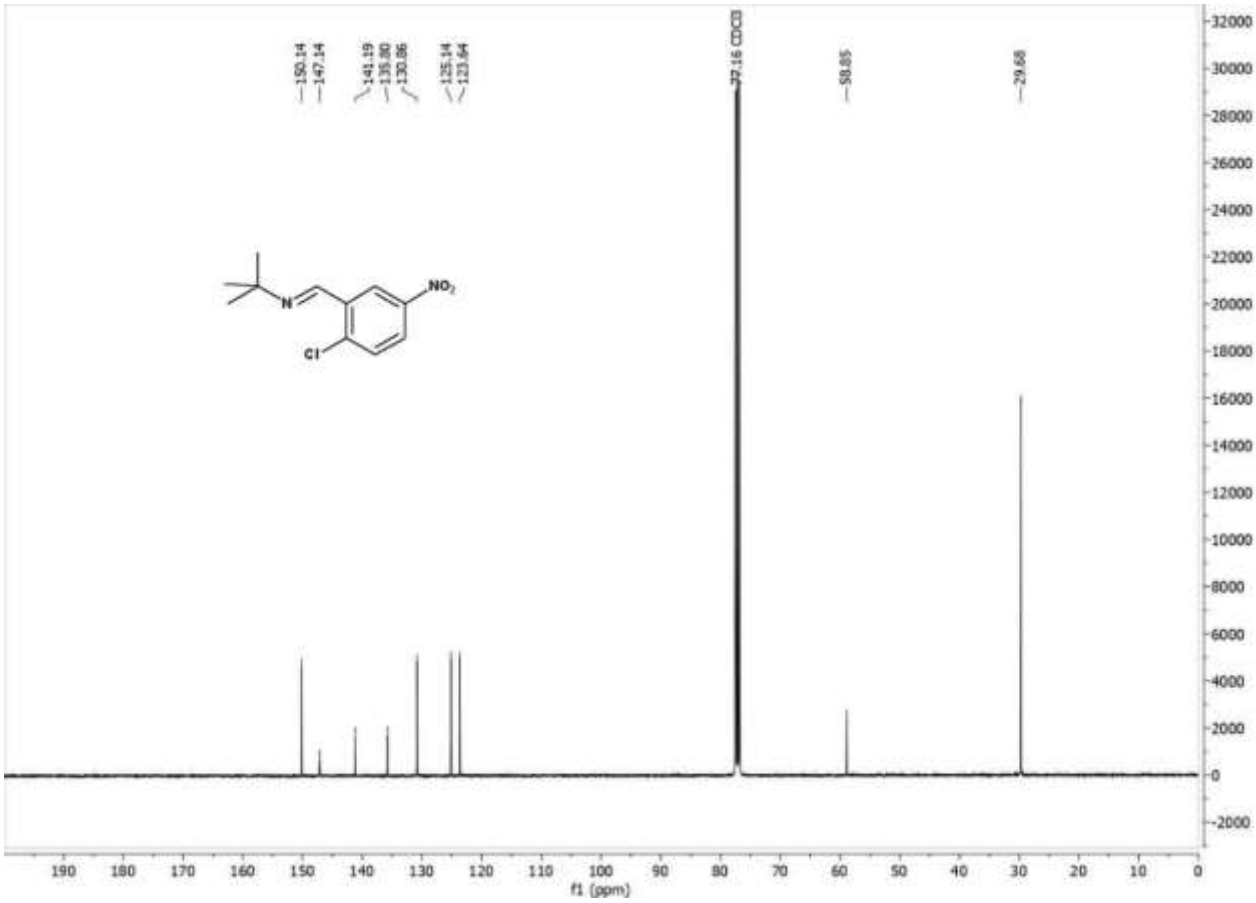

Figure C.2 $^{13}C(^{1}H)$ *NMR spectrum of* ***5ad*** *in* $CDCl_3$.

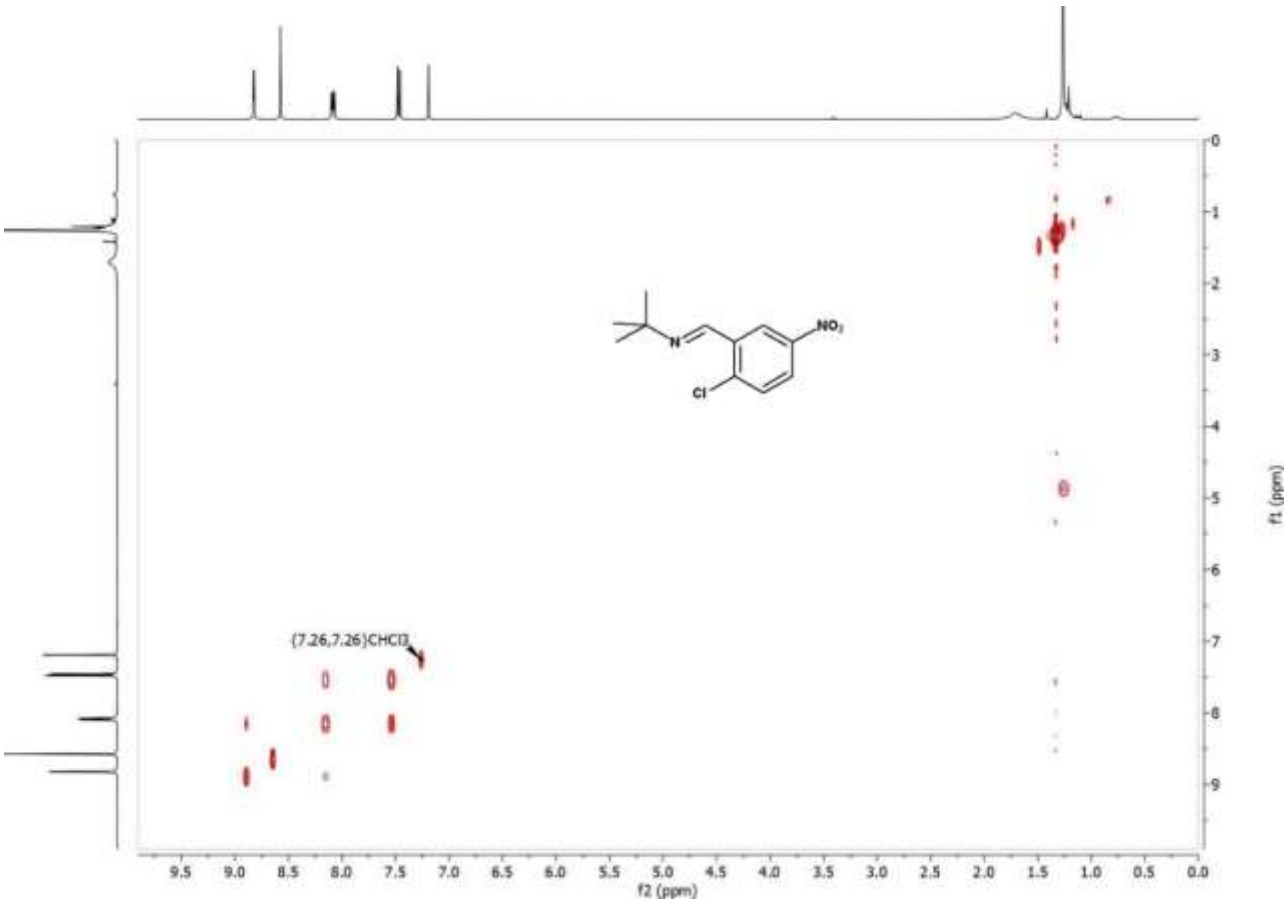

Figure C.3 COSY spectrum of ***5ad*** *in* $CDCl_3$.

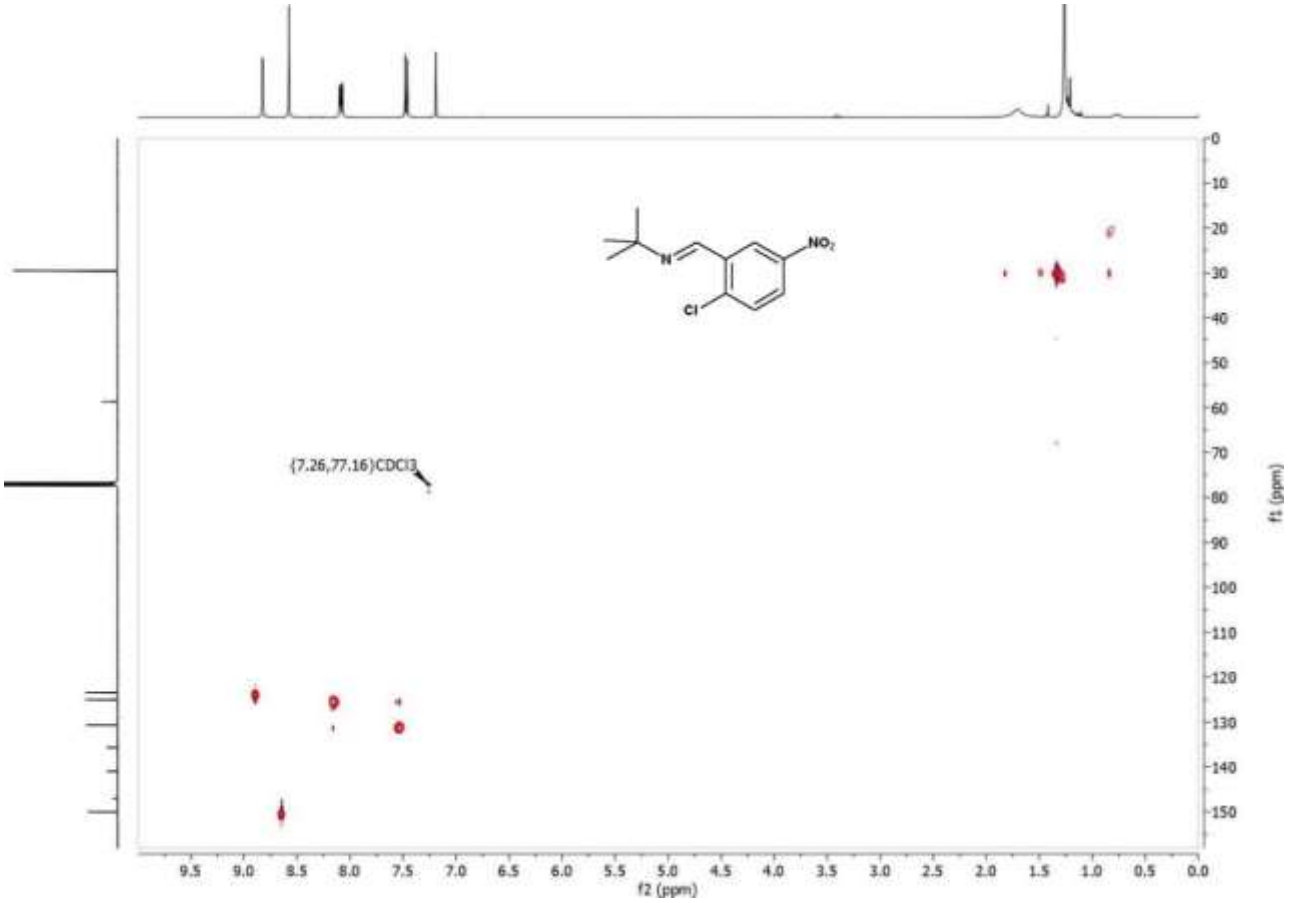

Figure C.4 HSQC spectrum of **5ad** in $CDCl_3$.

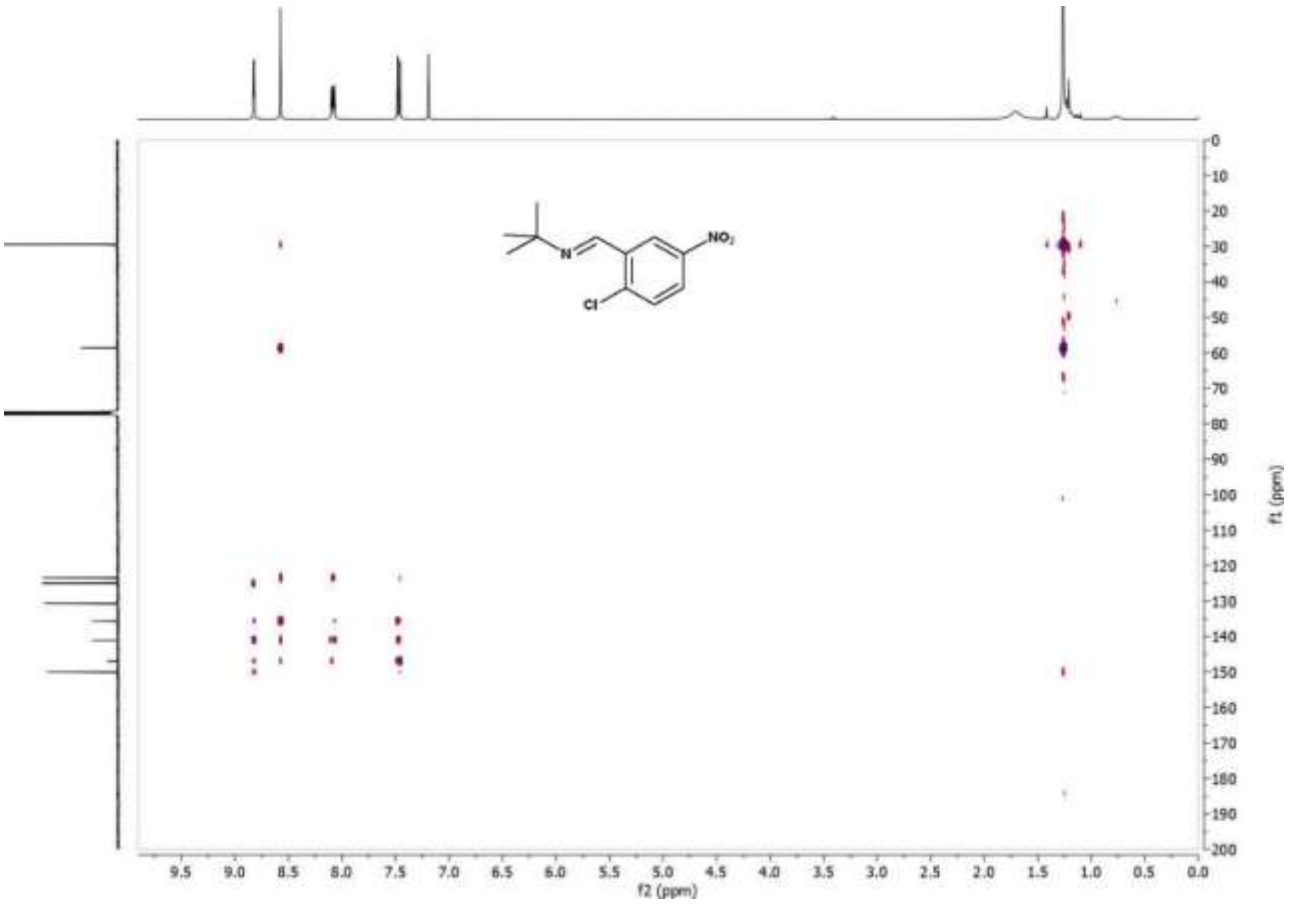

Figure C.5 HMBC spectrum of **5ad** in $CDCl_3$.

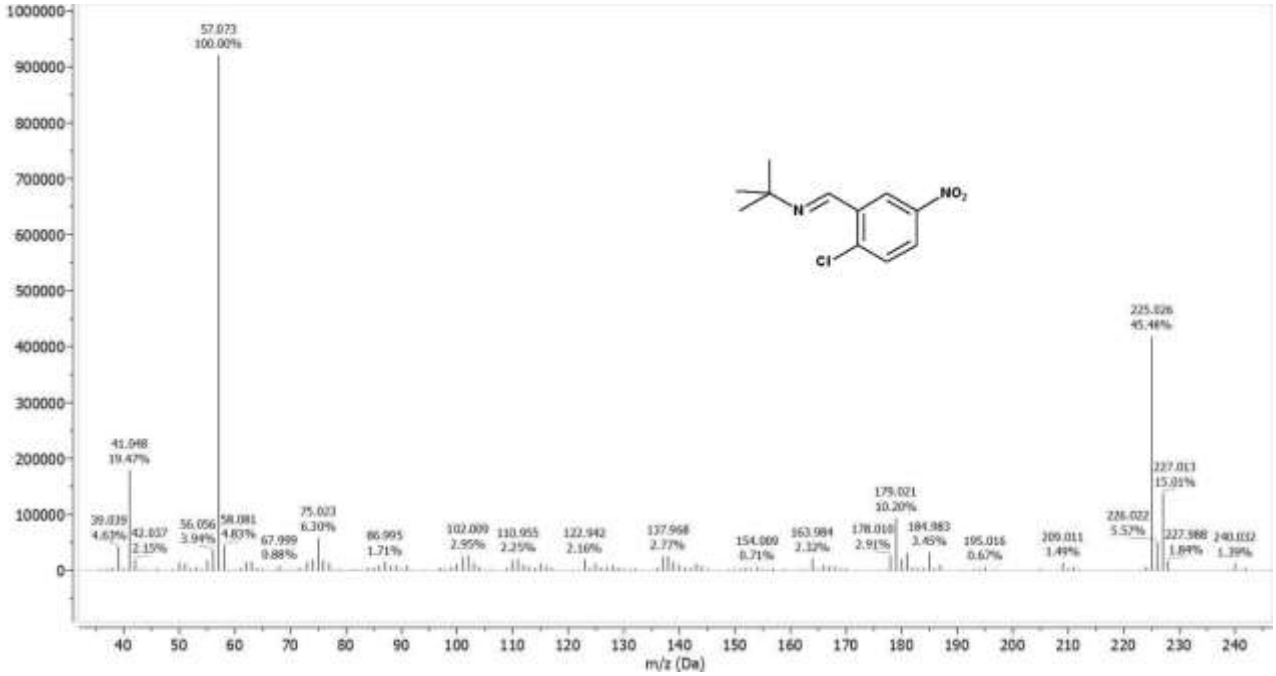

Figure C.6 *GC-MS spectrum of imine* ***5ad****.*

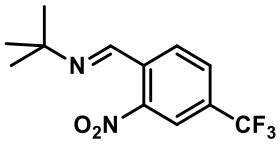

Chemical Formula: $C_{12}H_{13}F_3N_2O_2$
Molecular Weight: 274,24321

5ae

^{1}H NMR (400 MHz, Chloroform-d) δ [ppm] = 8.68 (s, 1H), 8.28 (s, 1H), 8.20 (d, J = 7.8 Hz, 1H), 7.89 (d, J = 8.1 Hz, 1H), 1.33 (s, 9H).

^{13}C NMR (101 MHz, Chloroform-d) δ [ppm] = 150.71, 148.79, 135.58, 133.14, 132.80, 130.97, 130.02, 129.99, 129.95, 129.92, 124.23, 121.87, 121.83, 121.79, 121.75, 59.02, 29.48.

GC/MS (EI): calc. for $C_{12}H_{13}F_3N_2O_2$ $[M\text{-}CH_3^{\cdot}]^+$: 259.069; found: 259.051, C_4H_9 57.072.

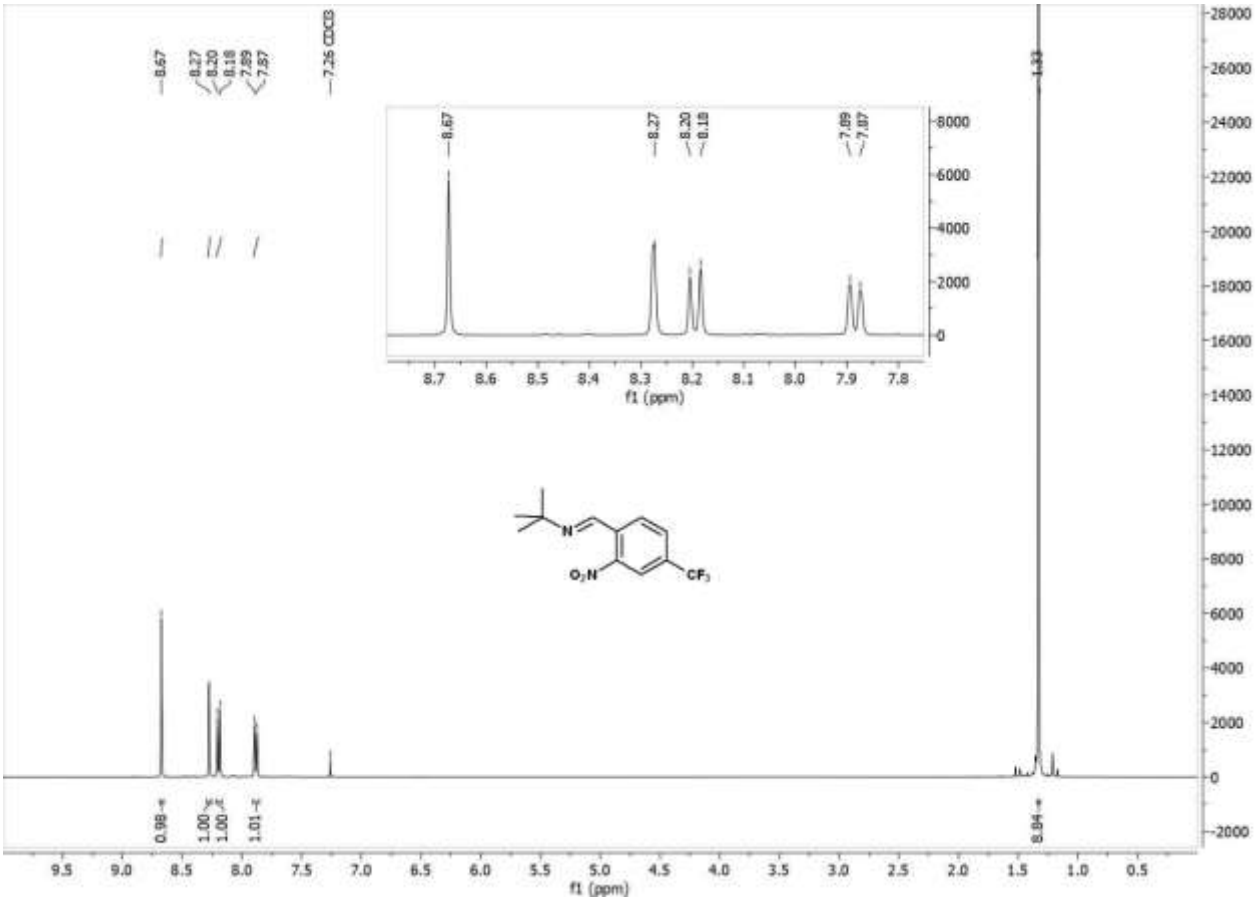

*Figure C.7 ^{1}H NMR spectrum of **5ae** in $CDCl_3$.*

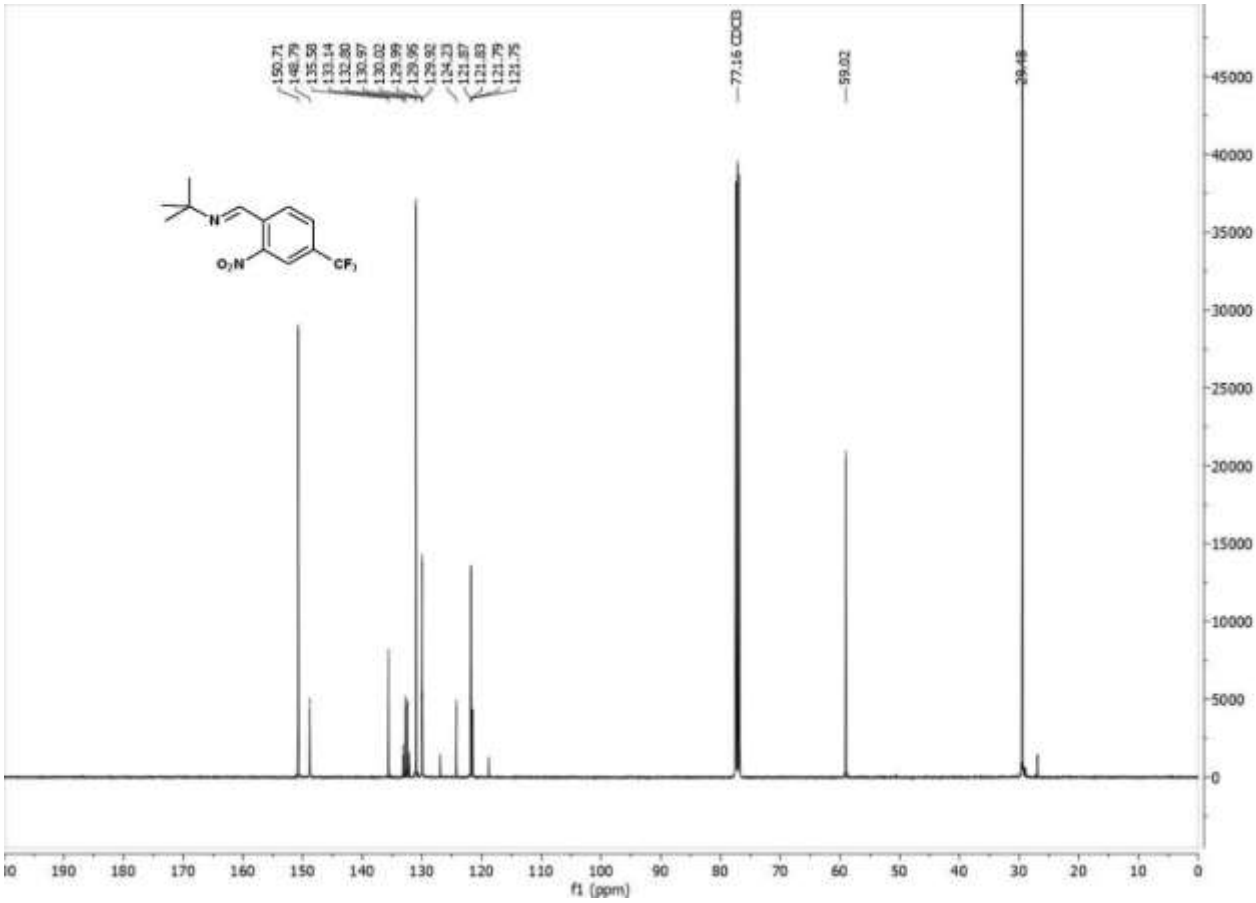

Figure C.8 $^{13}C(^{1}H)$ *NMR spectrum of* ***5ae*** *in* $CDCl_3$.

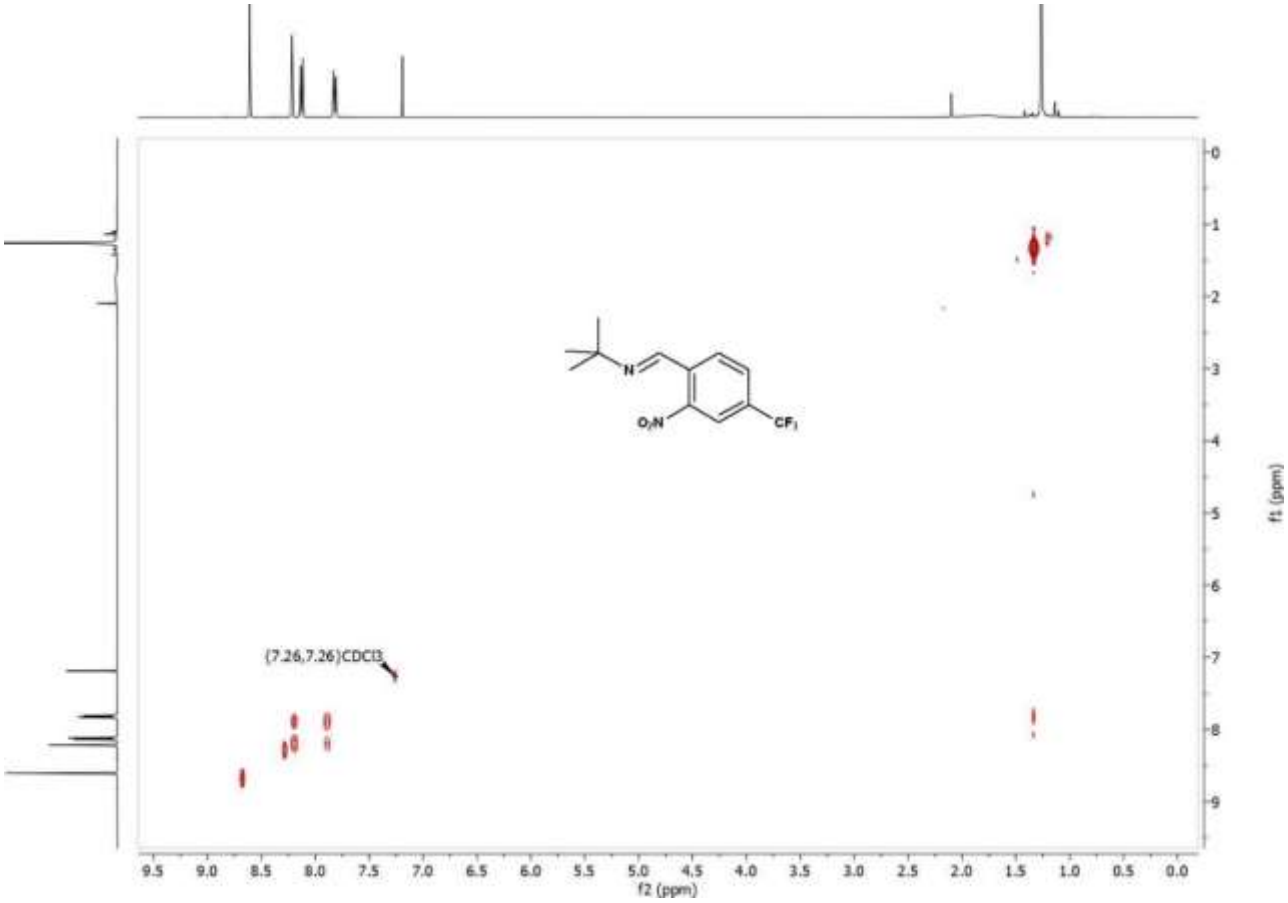

Figure C.9 COSY spectrum of ***5ae*** *in* $CDCl_3$.

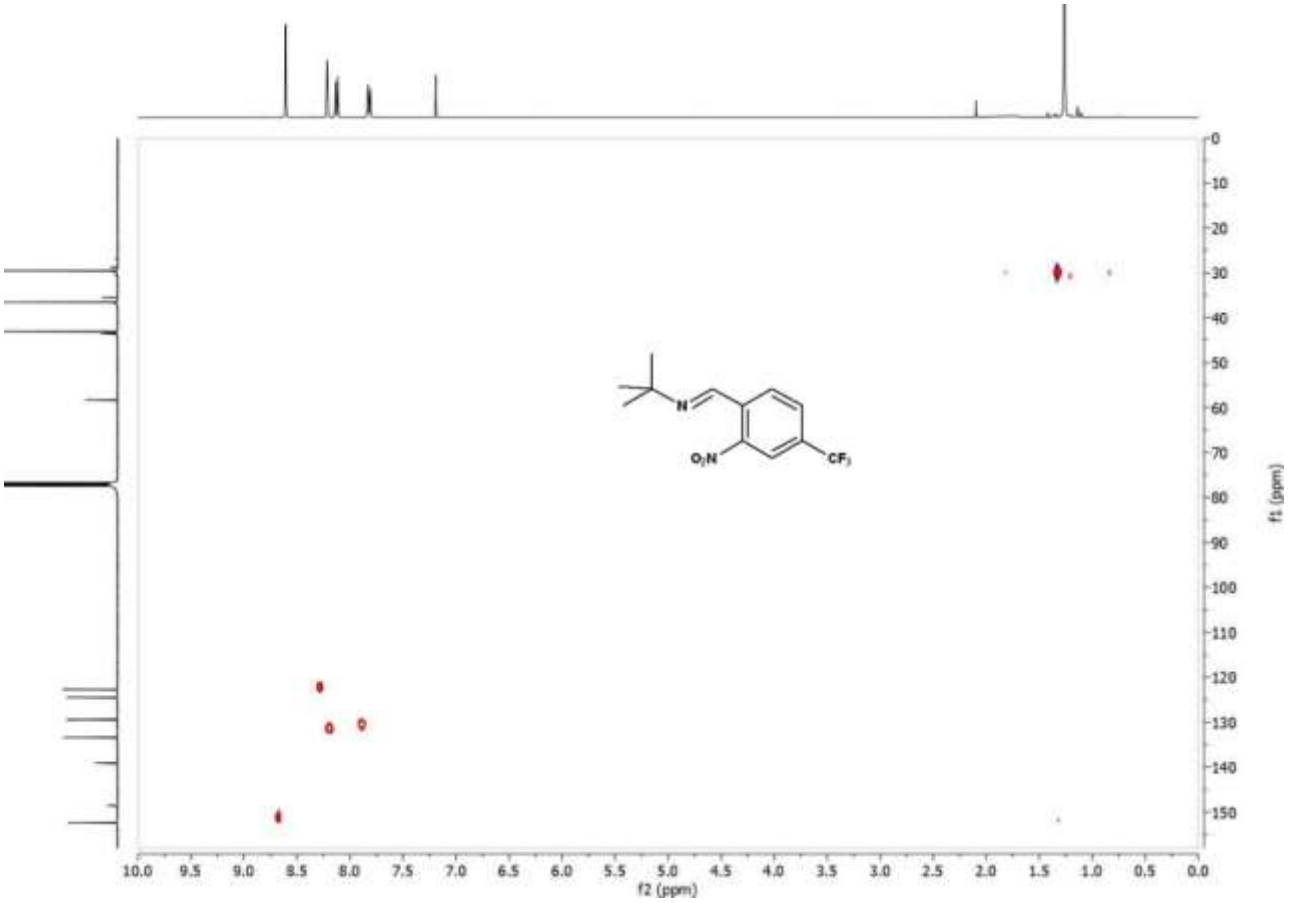

Figure C.10 HSQC spectrum of **5ae** in $CDCl_3$.

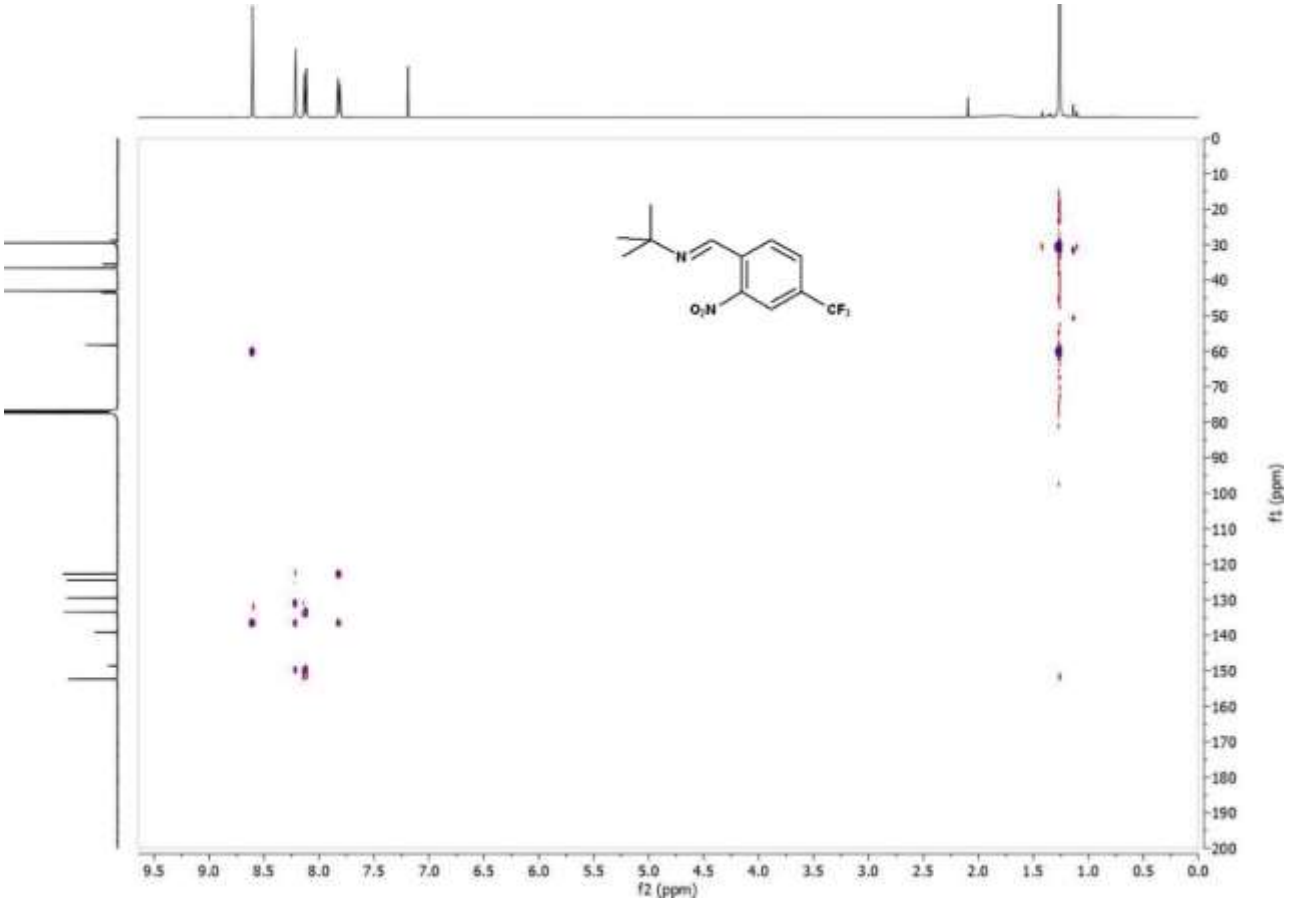

Figure C.11 HMBC spectrum of **5ae** in $CDCl_3$.

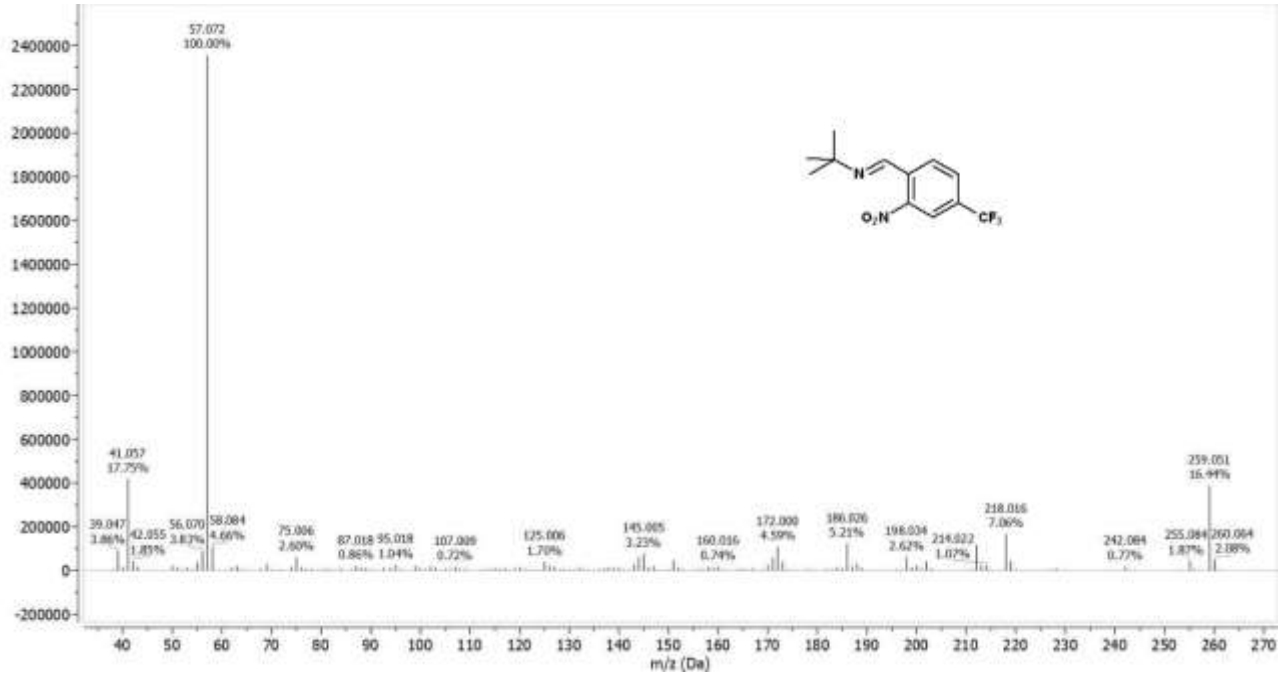

Figure C.12 *GC-MS spectrum of imine* ***5ae****.*

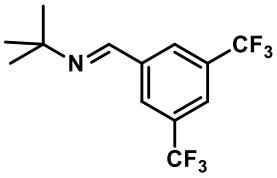

Chemical Formula: $C_{13}H_{13}F_6N$
Molecular Weight: 297,24442

5af

^{1}H NMR (400 MHz, Chloroform-d) δ [ppm] = 8.34 (s, 1H), 8.22 (s, 2H), 7.89 (s, 1H), 1.33 (s, 9H).

^{13}C NMR (101 MHz, Chloroform-d) δ[ppm] = 152.14, 139.35, 132.63, 132.30, 131.96, 131.63, 128.03, 128.00, 124.82, 123.64, 123.61, 123.57, 123.53, 123.49, 122.11, 58.28, 29.61.

GC/MS (EI): calc. for $C_{13}H_{13}F_6N$ $[M]^+$: 297.095; found: 297.060, $C_{12}H_{10}F_6N$ $[M\text{-}CH_3^{\cdot}]^+$ 282.070, C_4H_9 57.080.

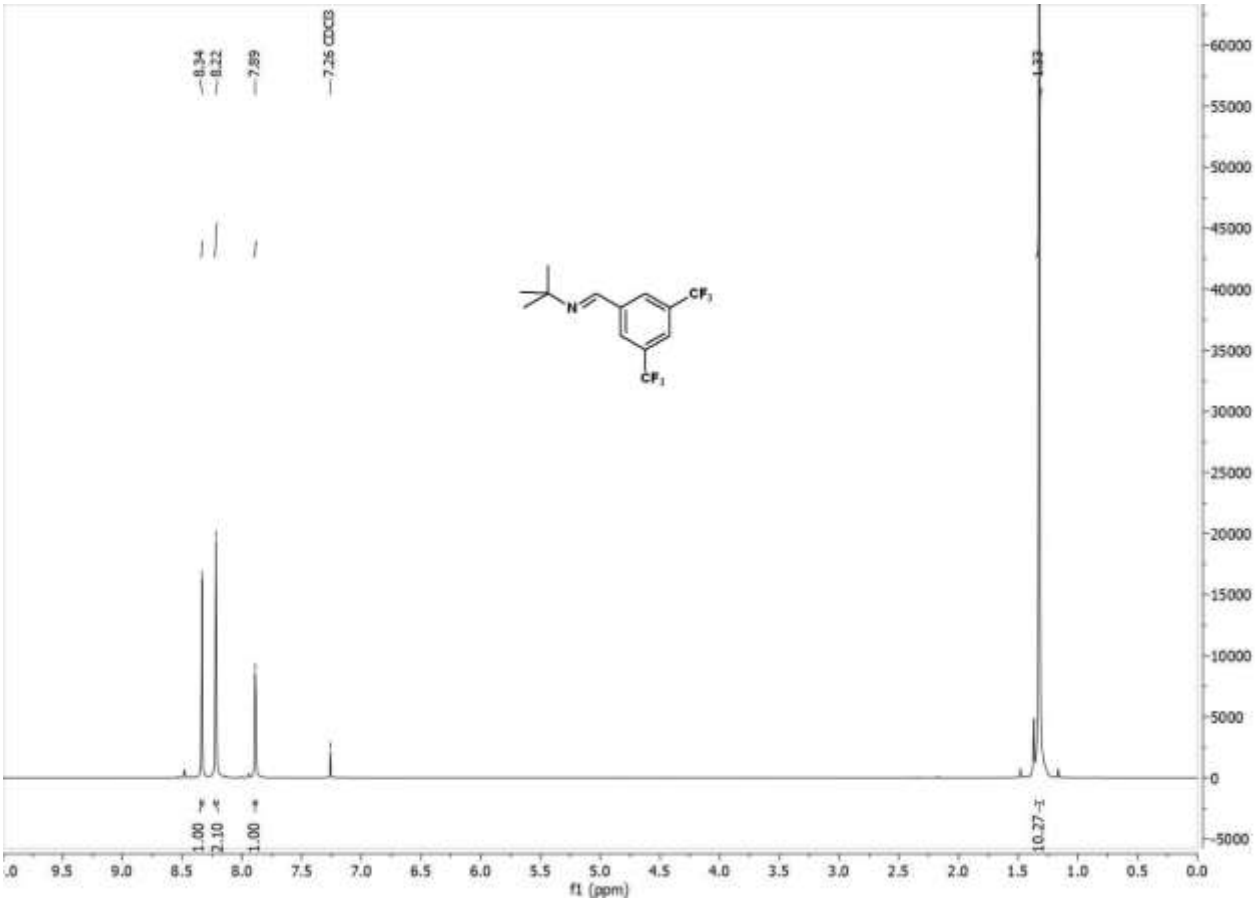

*Figure C.13 ^{1}H NMR spectrum of **5af** in $CDCl_3$.*

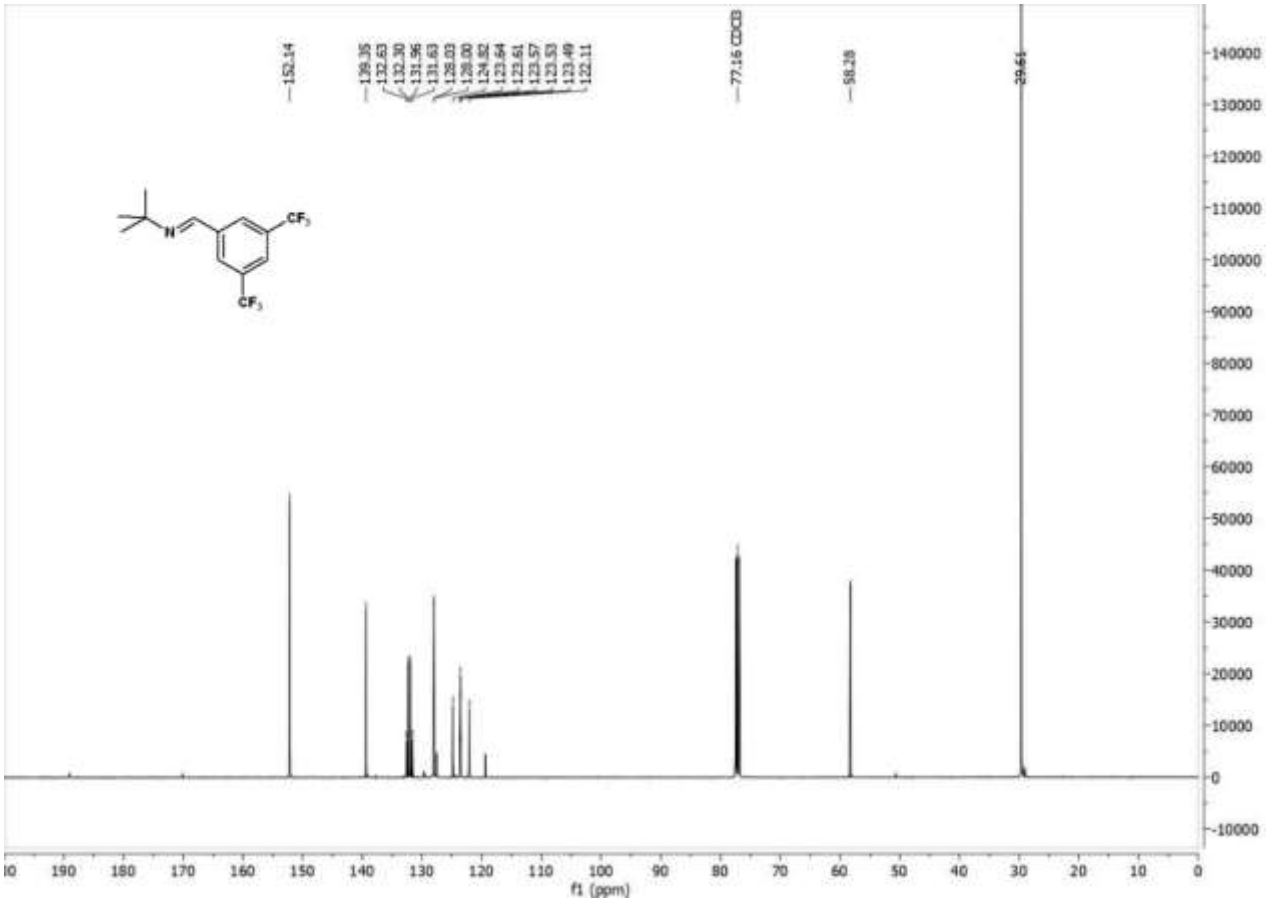

Figure C.14 $^{13}C(^{1}H)$ *NMR spectrum of* ***5af*** *in* $CDCl_3$.

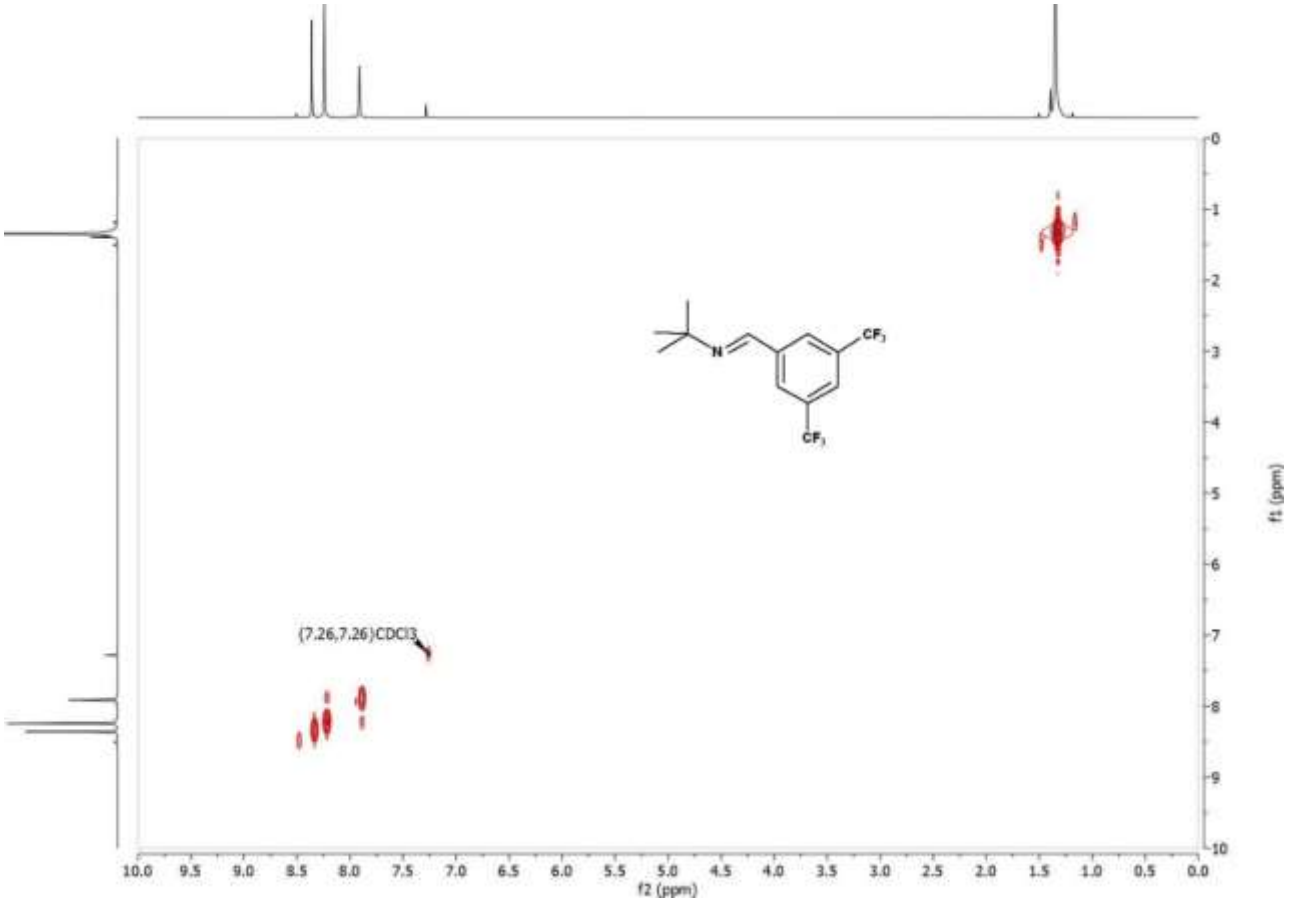

Figure C.15 COSY spectrum of ***5af*** *in* $CDCl_3$.

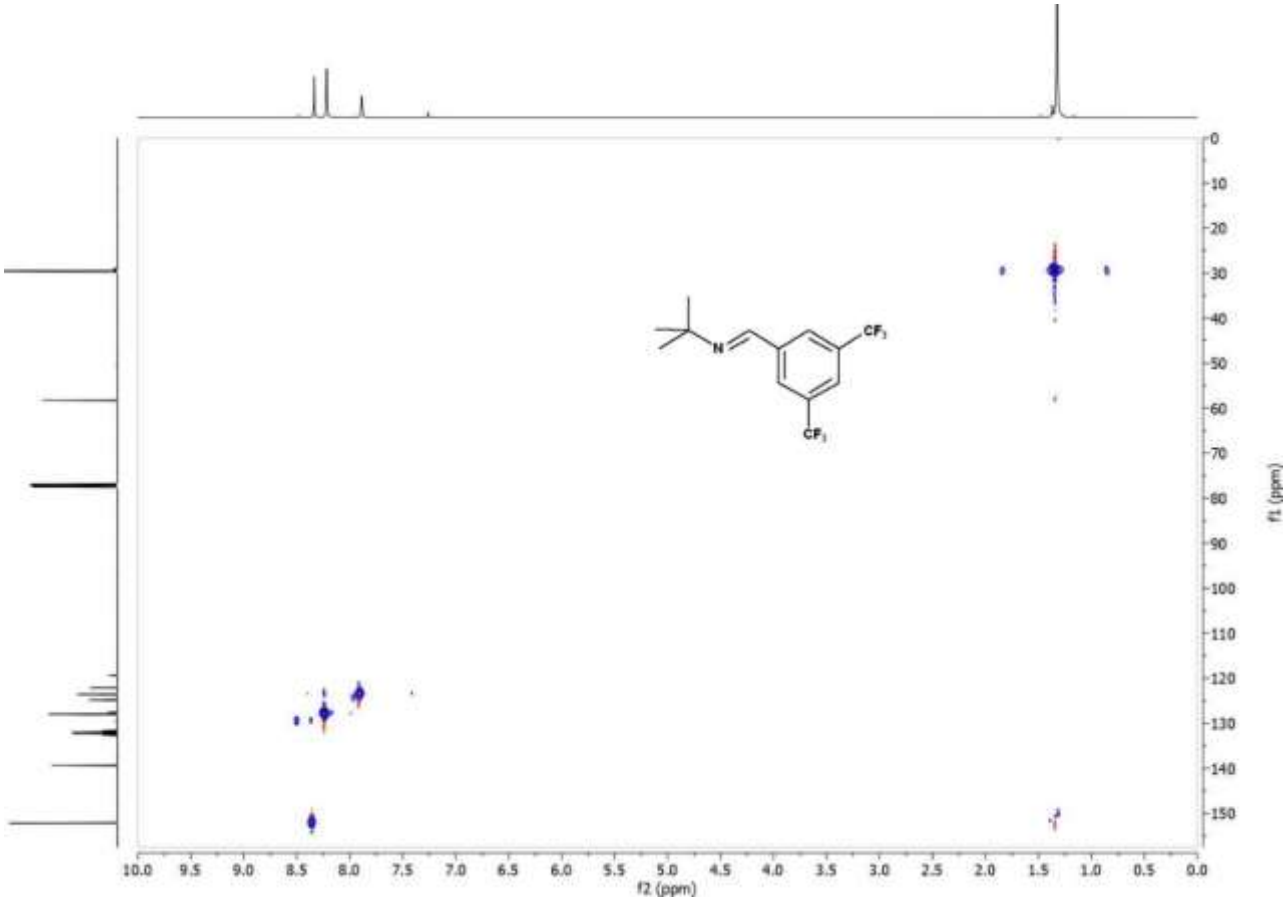

*Figure C.16 HSQC spectrum of **5af** in $CDCl_3$.*

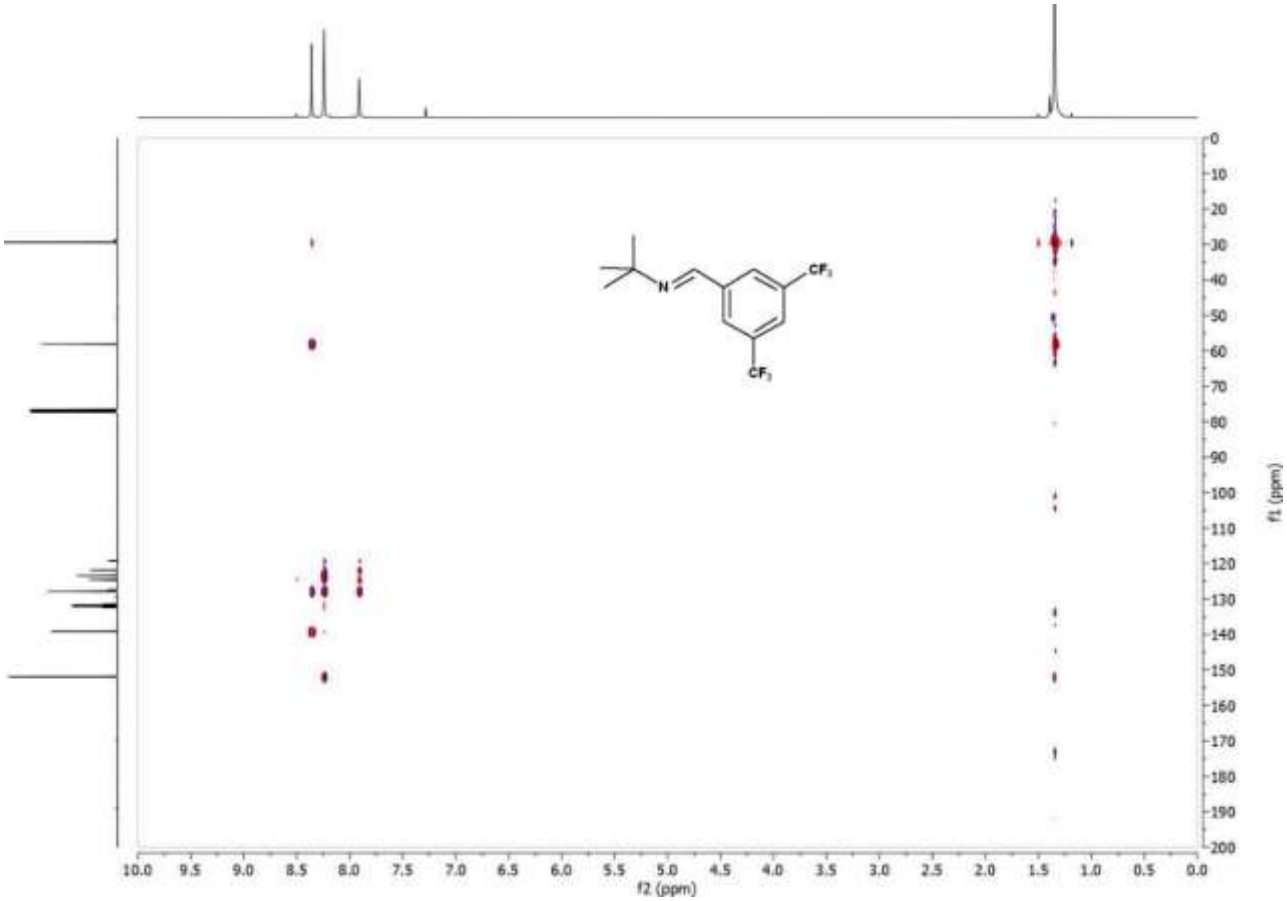

*Figure C.17 HMBC spectrum of **5af** in $CDCl_3$.*

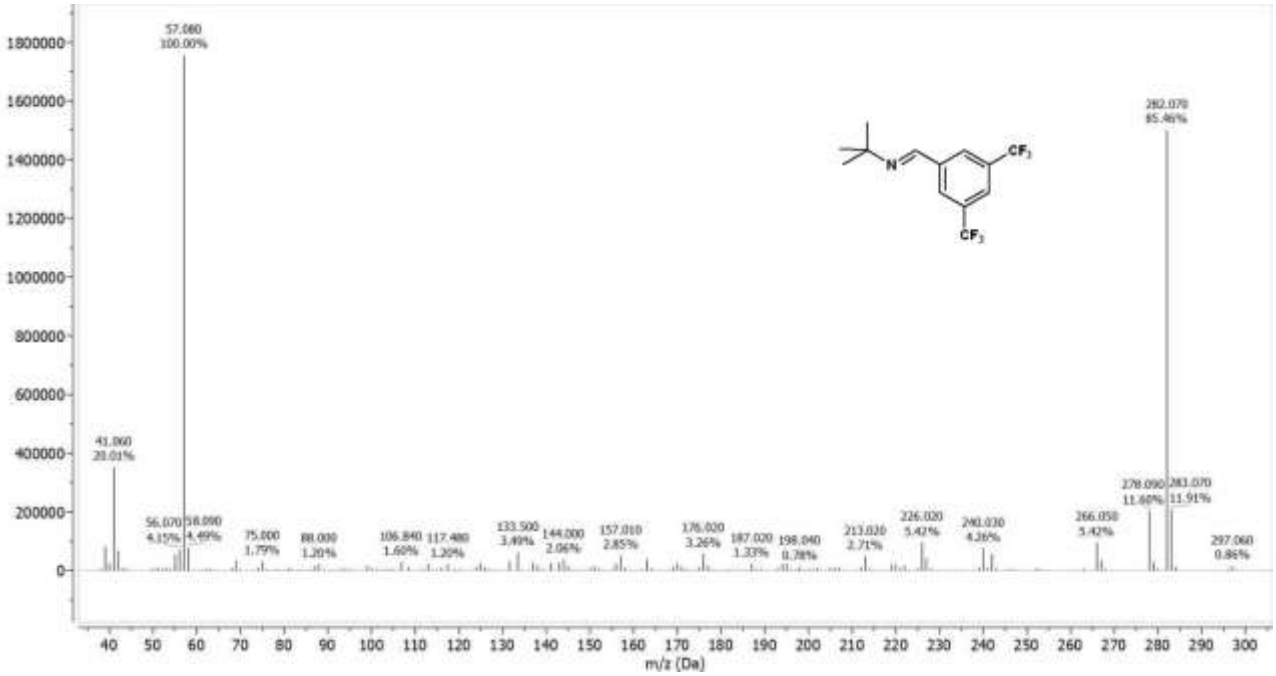

Figure C.18 *GC-MS spectrum of imine* ***5af****.*

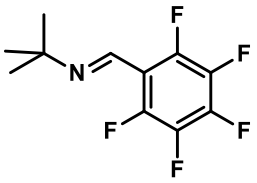

Chemical Formula: $C_{11}H_{10}F_5N$
Molecular Weight: 251,20002

5ag

^{1}H NMR (400 MHz, Chloroform-d) δ [ppm] = 8.29 (s, 1H), 1.30 (s, 9H).

^{19}F NMR (376 MHz, Chloroform-d) δ [ppm] = -143.56 – -143.78 (m), -152.56 – -153.00 (m), -162.37 – -162.67 (m).

^{13}C NMR (101 MHz, Chloroform-d) δ [ppm] = 147.23 – 144.25 (m), 144.20 – 143.87 (m), 143.32 – 140.22 (m), 139.38 – 136.22 (m), 112.47 (td, J = 12.3, 4.1 Hz), 59.73, 29.31.

GC/MS (EI): calc. for $C_{11}H_{10}F_5N$ $[M]^+$: 251.073; found: 251.030, $C_{10}H_7F_5N$ $[M\text{-}CH_3^{\cdot}]^+$ 236.040, C_7HF_5 179.970, C_4H_9 57.070.

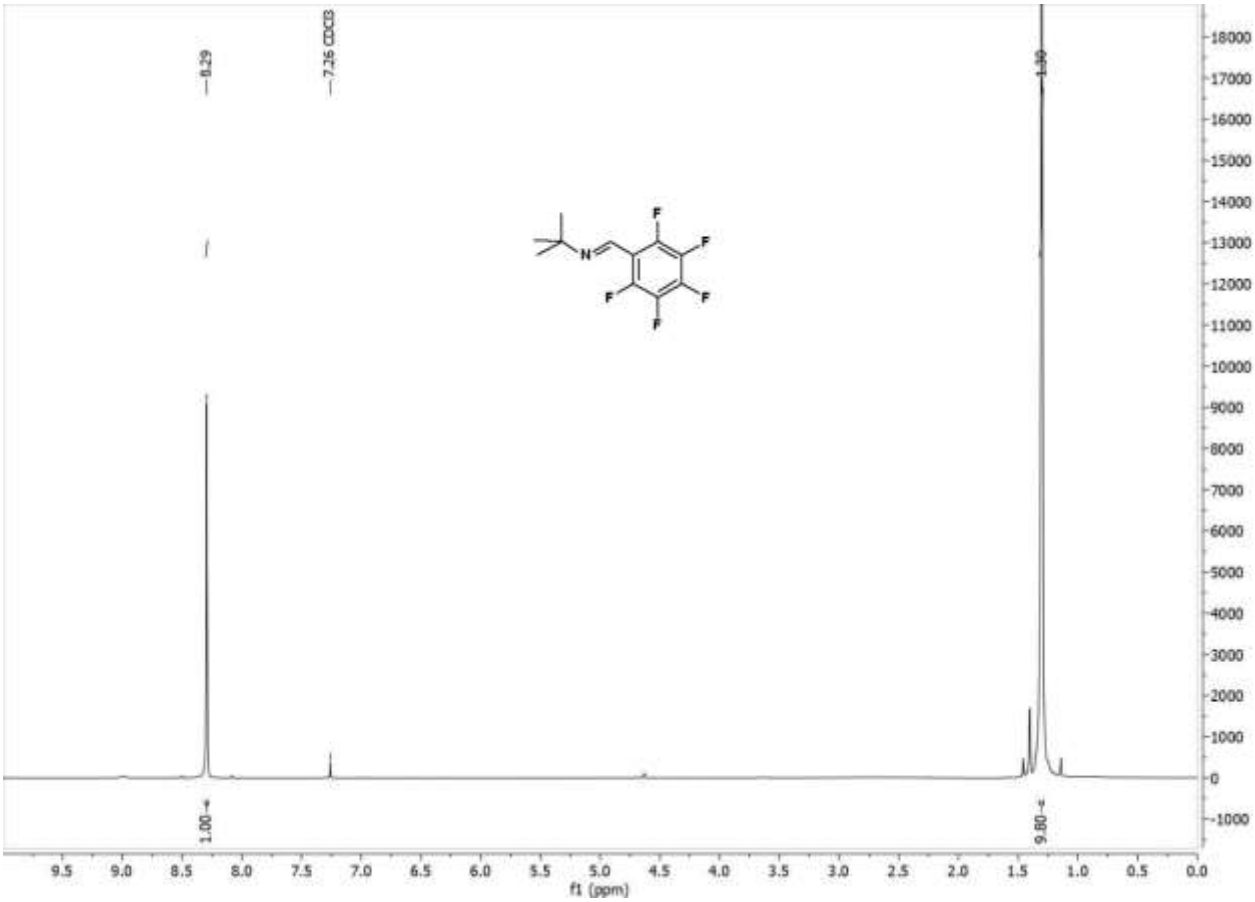

*Figure C.19 ^{1}H NMR spectrum of **5ag** in $CDCl_3$.*

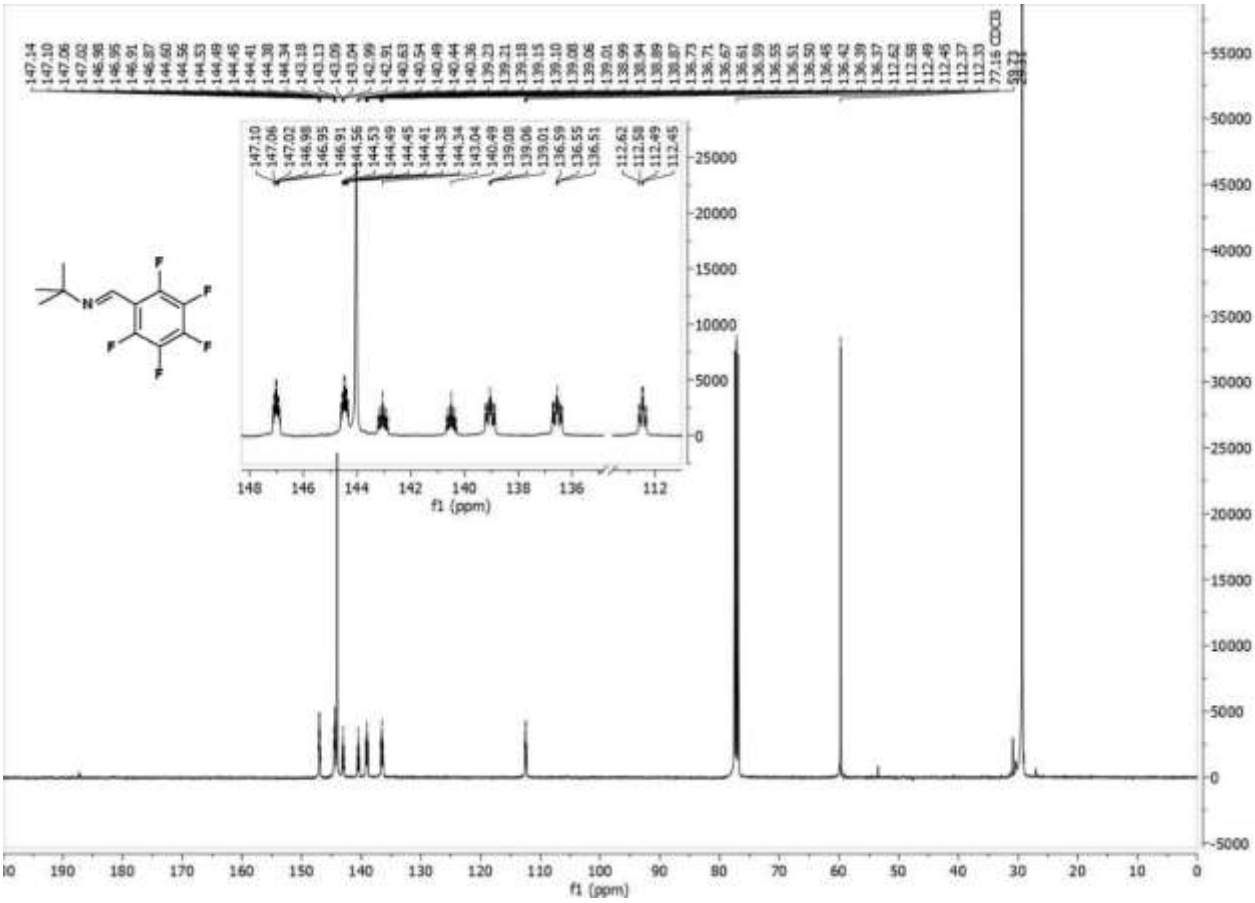

Figure C.20 $^{13}C(^{1}H)$ *NMR spectrum of* ***5ag*** *in* $CDCl_3$.

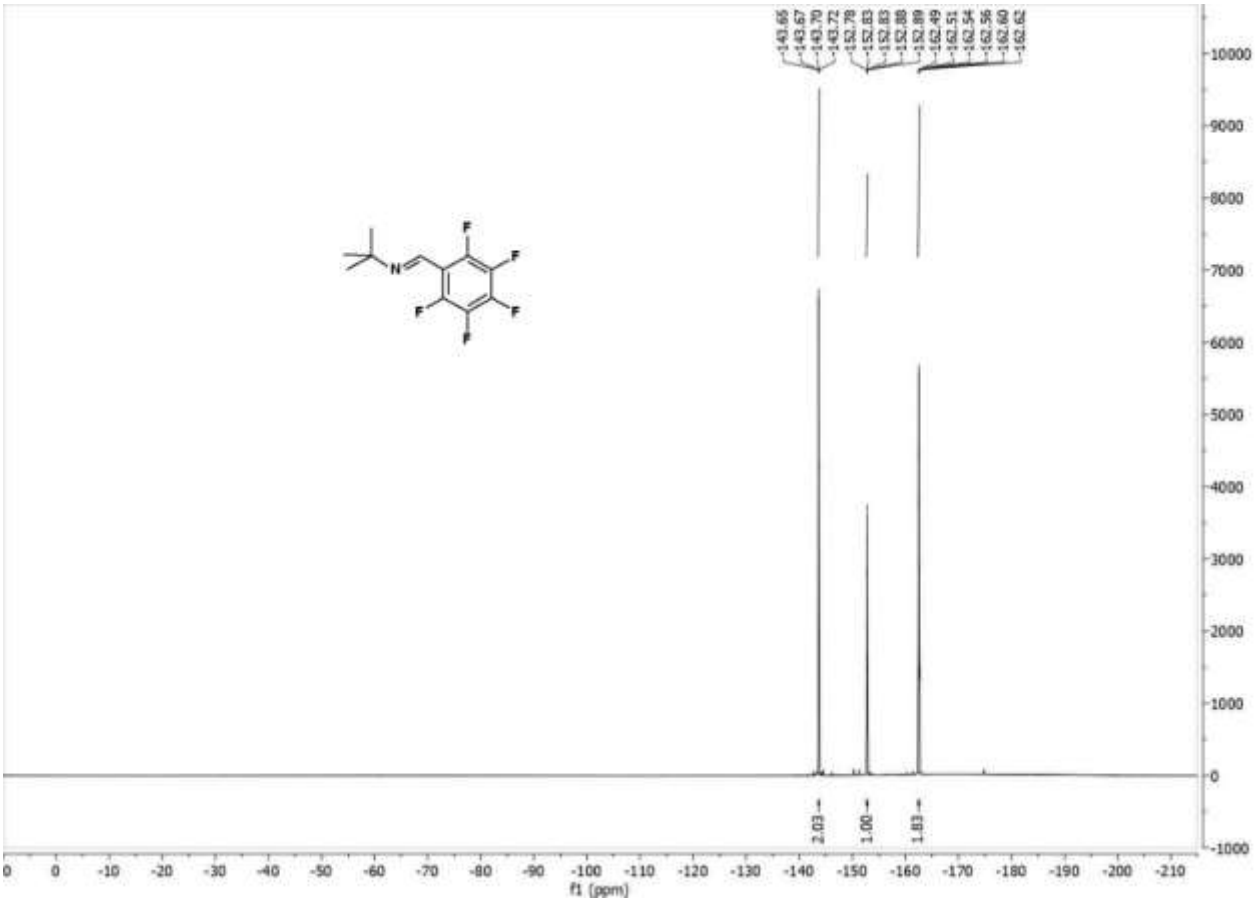

Figure C.21 ^{19}F *NMR spectrum of* ***5ag*** *in* $CDCl_3$.

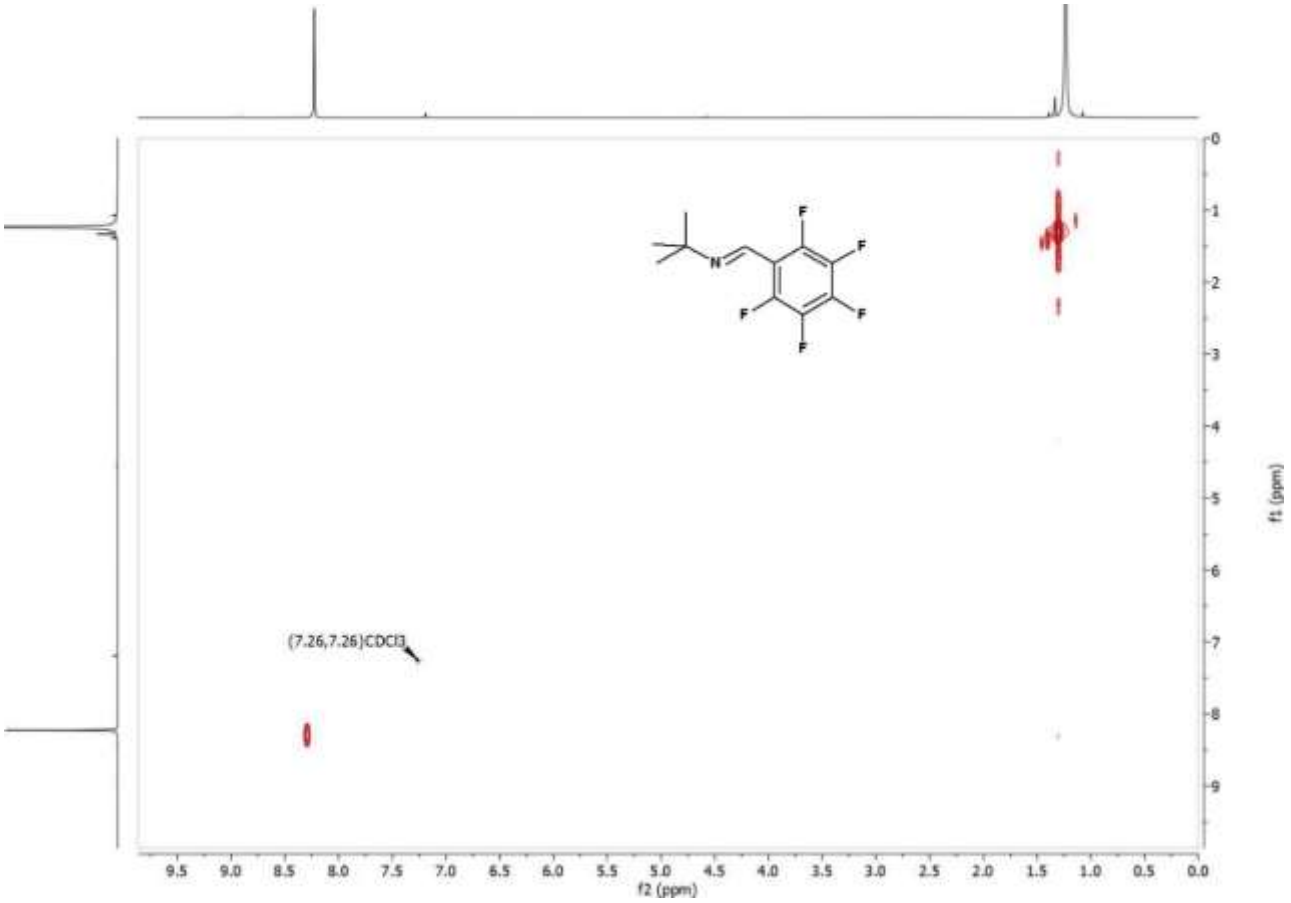

Figure C.22 *COSY spectrum of* ***5ag*** *in* $CDCl_3$.

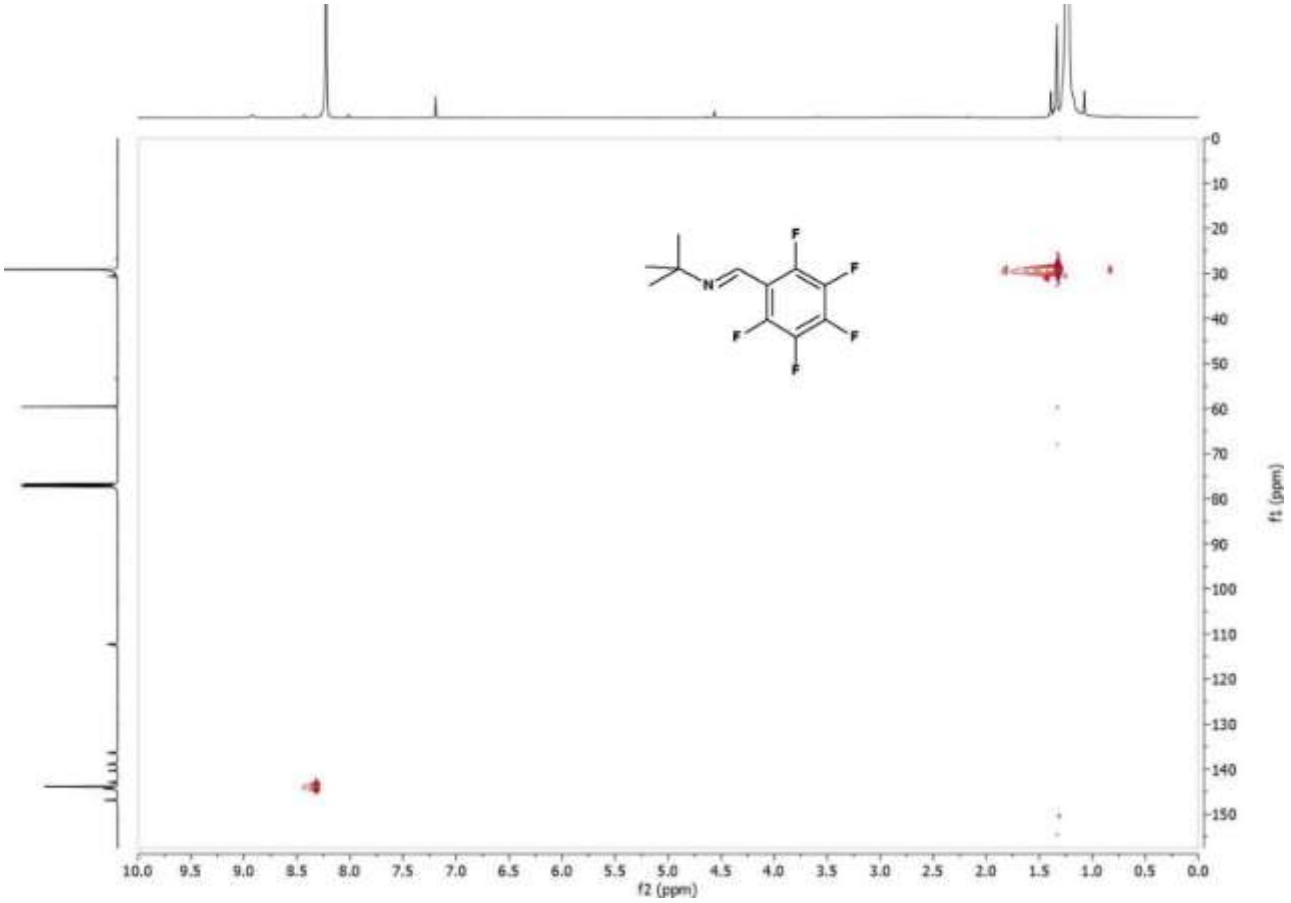

Figure C.23 *HSQC spectrum of* ***5ag*** *in* $CDCl_3$.

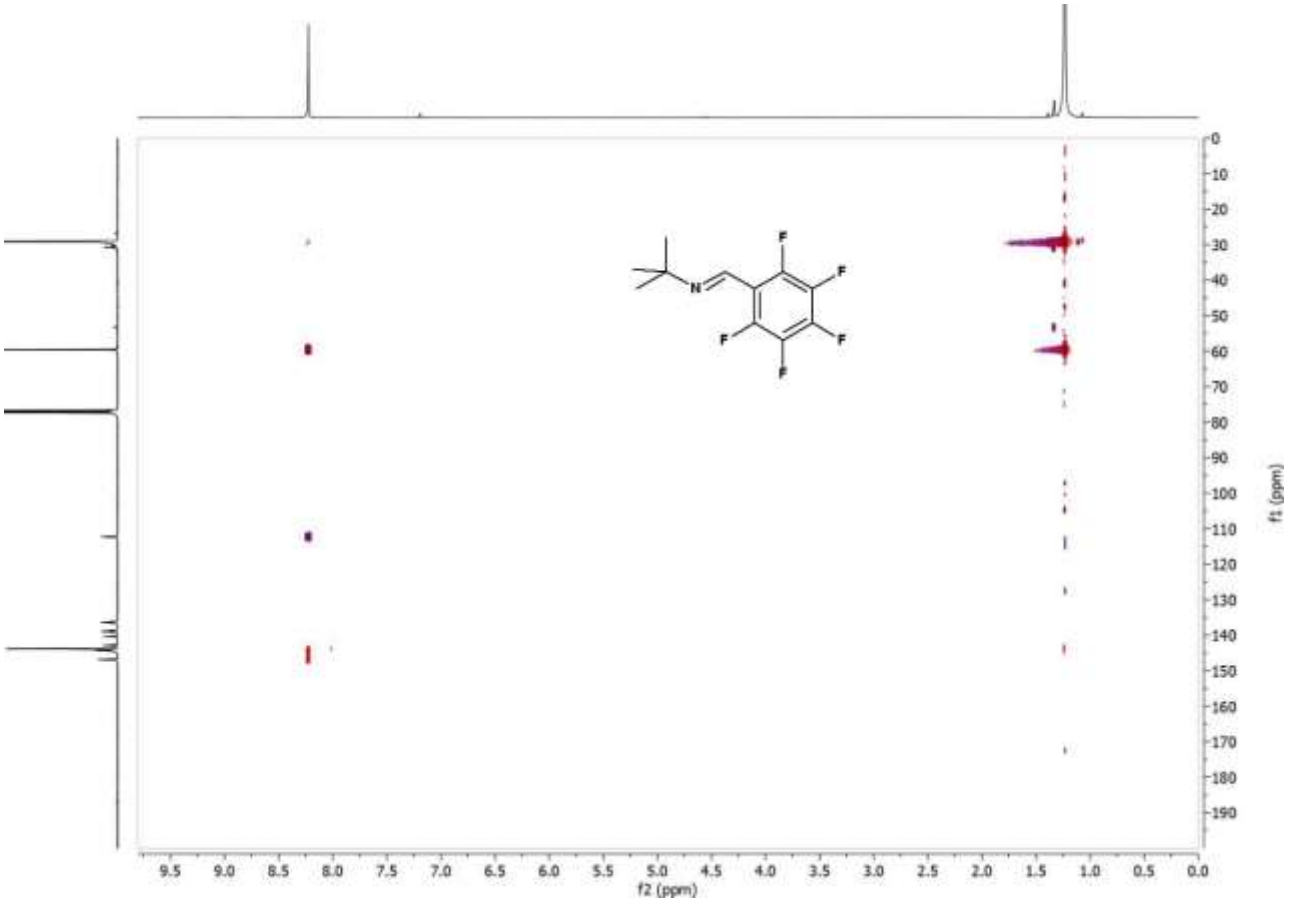

Figure C.24 HMBC spectrum of **5ag** in $CDCl_3$.

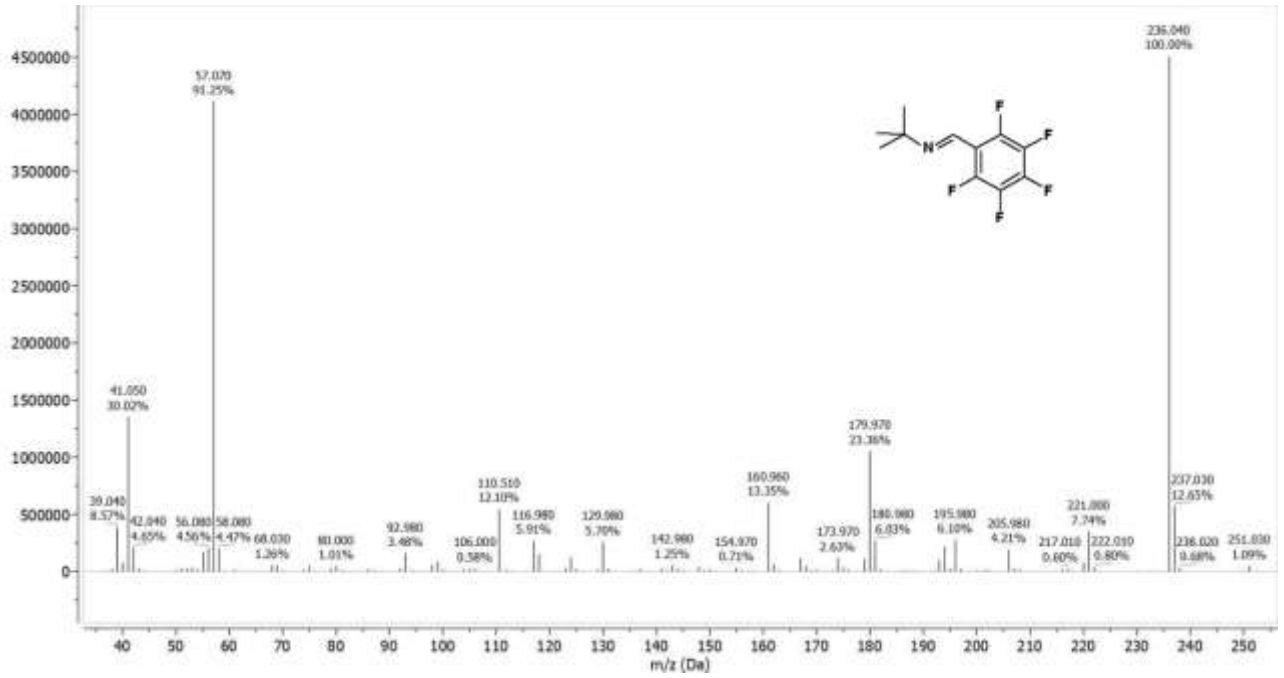

Figure C.25 GC-MS spectrum of imine **5ag**.

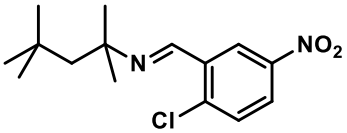

Chemical Formula: $C_{15}H_{21}ClN_2O_2$
Molecular Weight: 296,79500

5bd

^{1}H NMR (400 MHz, Chloroform-d) δ [ppm] = 8.89 (d, J = 2.8 Hz, 1H), 8.63 (s, 1H), 8.15 (dd, J = 8.8, 2.8 Hz, 1H), 7.54 (d, J = 8.7 Hz, 1H), 1.74 (s, 2H), 1.36 (s, 6H), 0.96 (s, 9H).

^{13}C NMR (101 MHz, Chloroform-d) δ [ppm] = 149.59, 147.19, 141.11, 135.82, 130.87, 124.99, 123.48, 62.57, 56.54, 32.20, 31.89, 29.70.

GC/MS (EI): calc. for $C_{14}H_{18}ClN_2O_2$ $[M\text{-}CH_3^{\cdot}]^+$: 281.106; found: $[M\text{-}CH_3^{\cdot}]^+$ 281.106, $C_{10}H_{10}ClN_2O_2$ 225.037, $C_7H_6ClN_2O_2$ 184.983, C_4H_9 57.094.

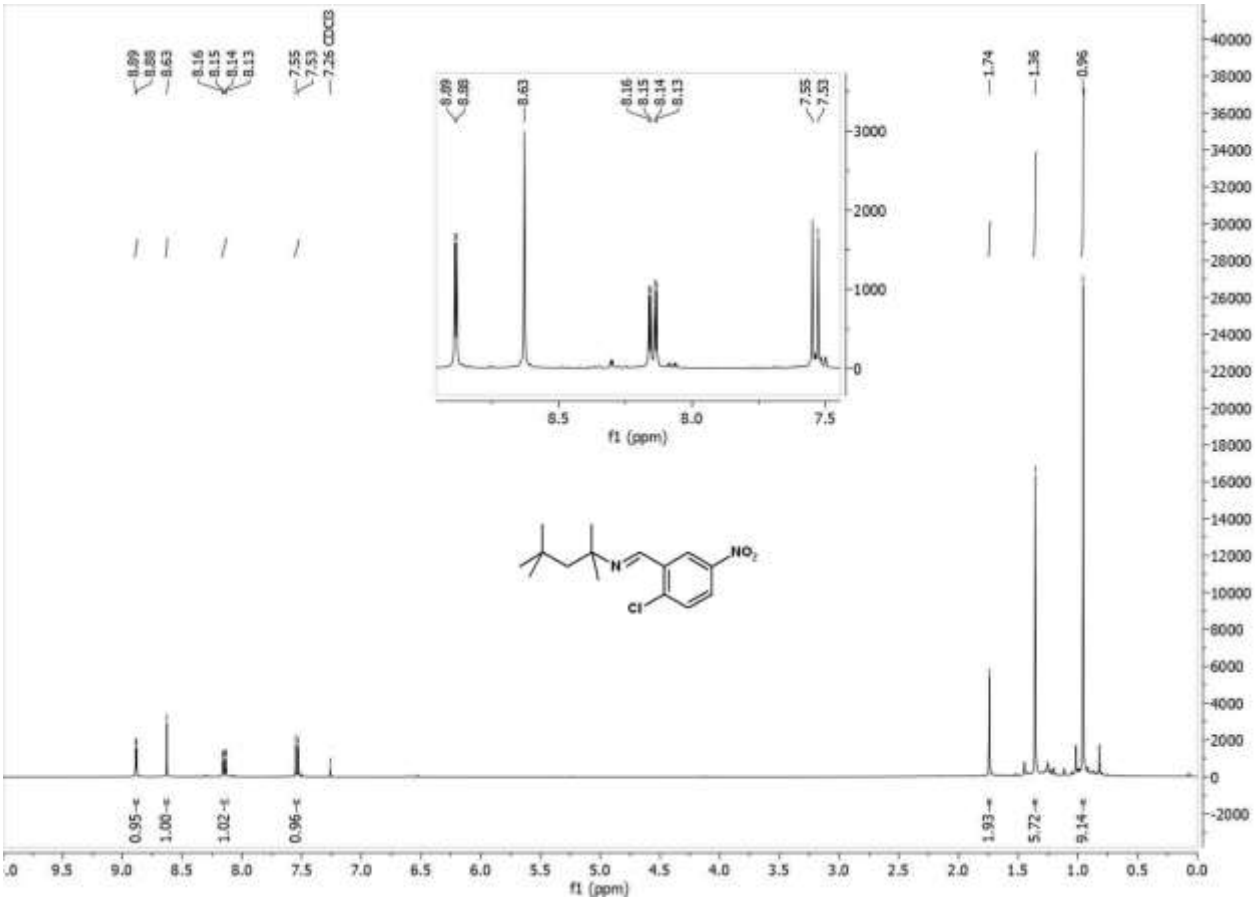

*Figure C.26 ^{1}H NMR spectrum of **5bd** in $CDCl_3$.*

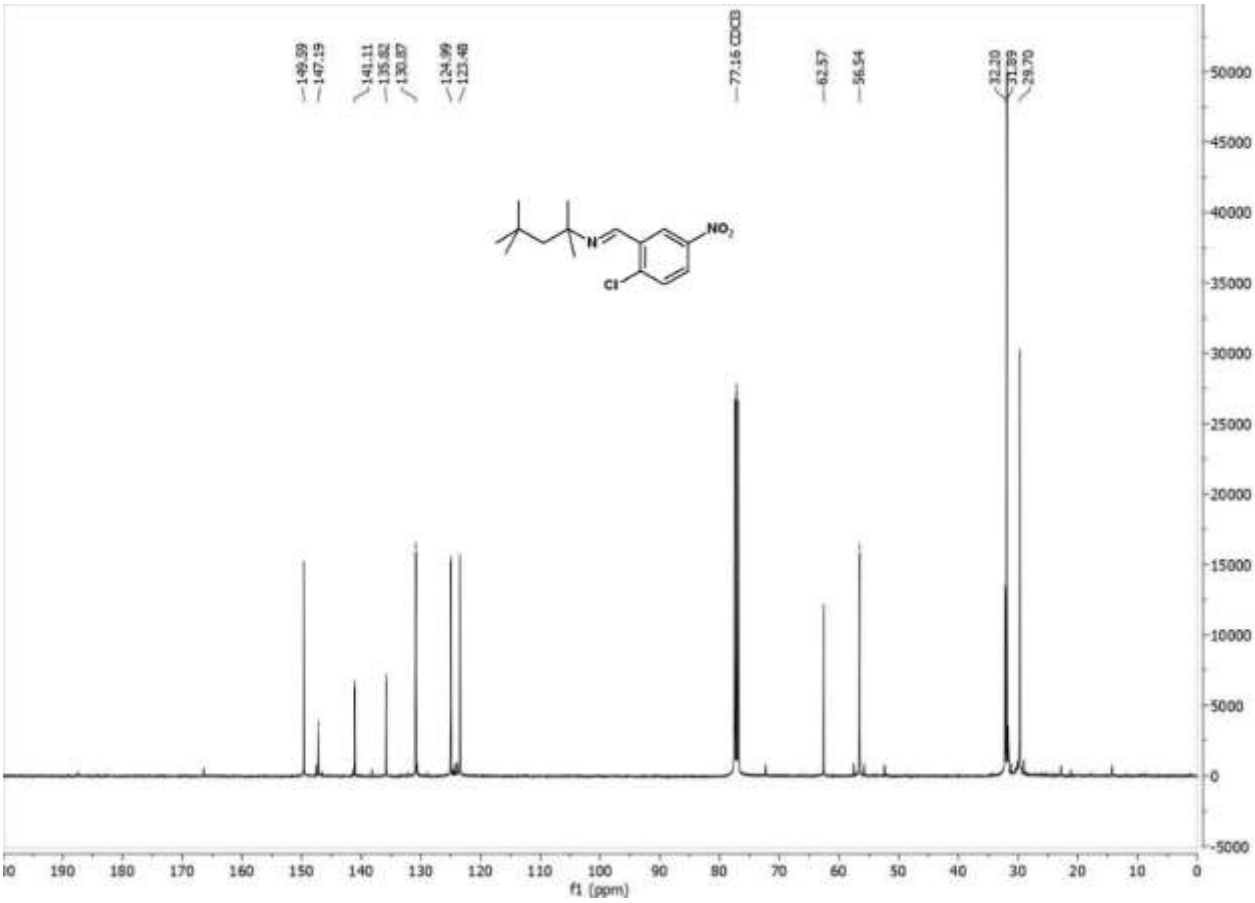

Figure C.27 $^{13}C(^{1}H)$ *NMR spectrum of* ***5bd*** *in* $CDCl_3$.

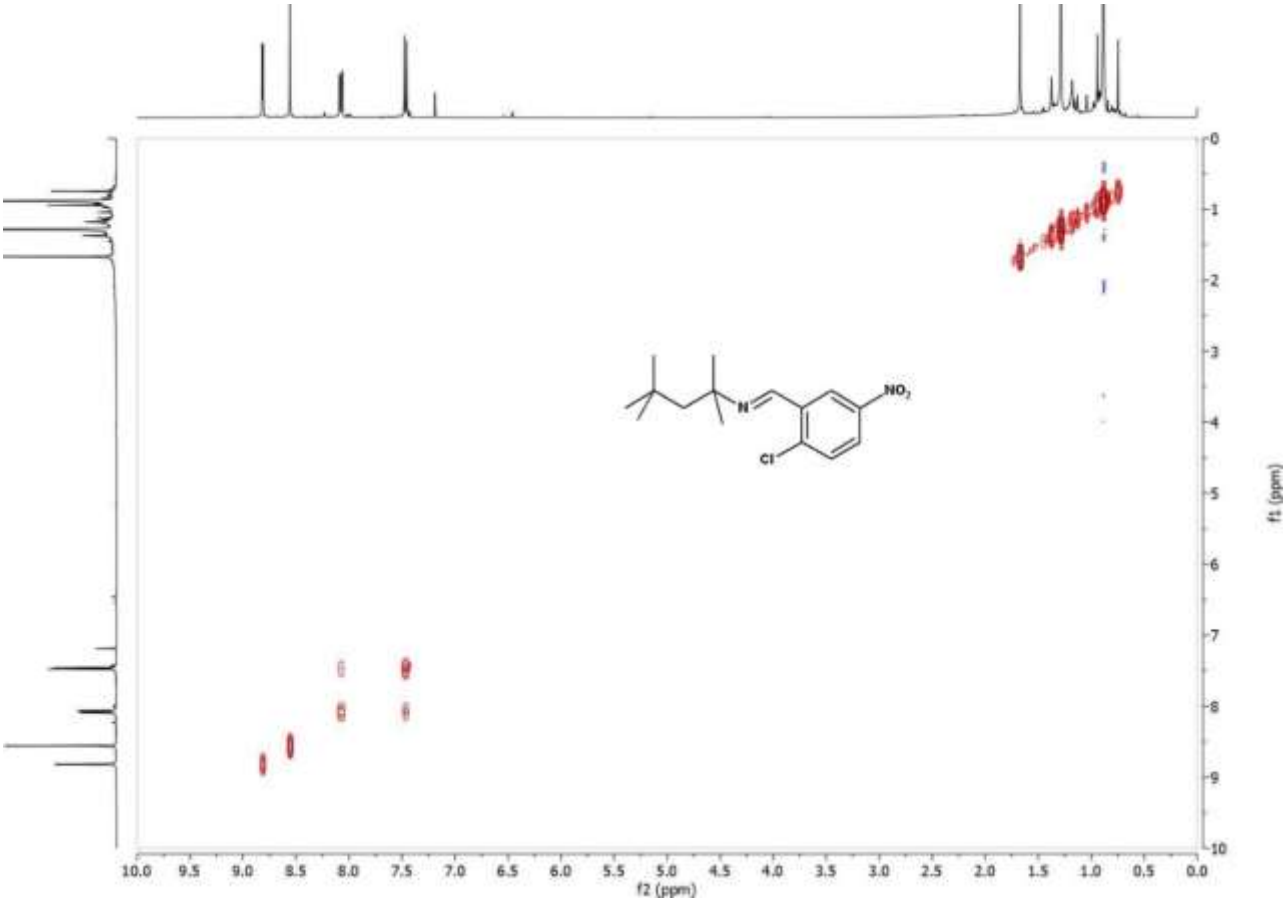

Figure C.28 COSY spectrum of ***5bd*** *in* $CDCl_3$.

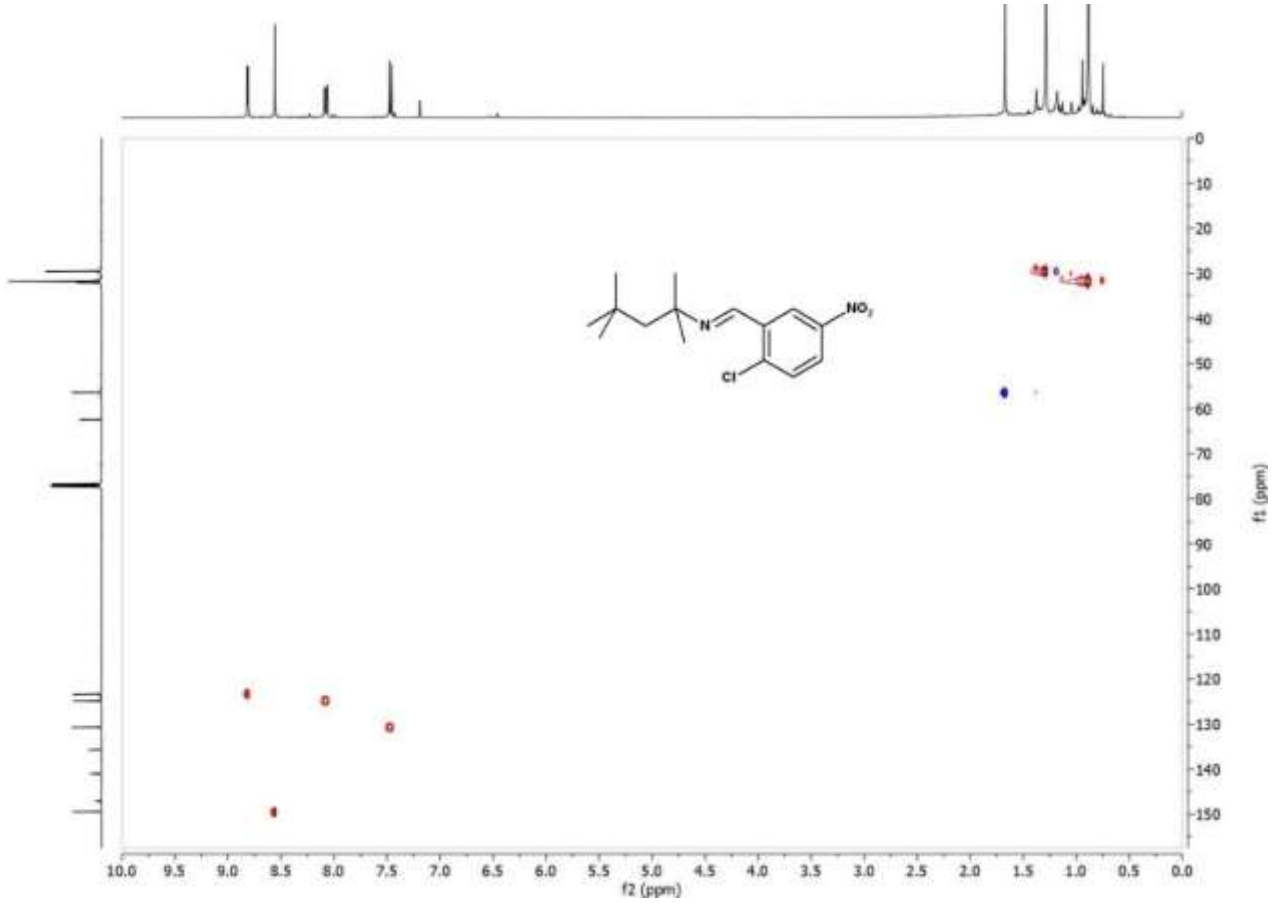

Figure C.29 HSQC spectrum of **5bd** in $CDCl_3$.

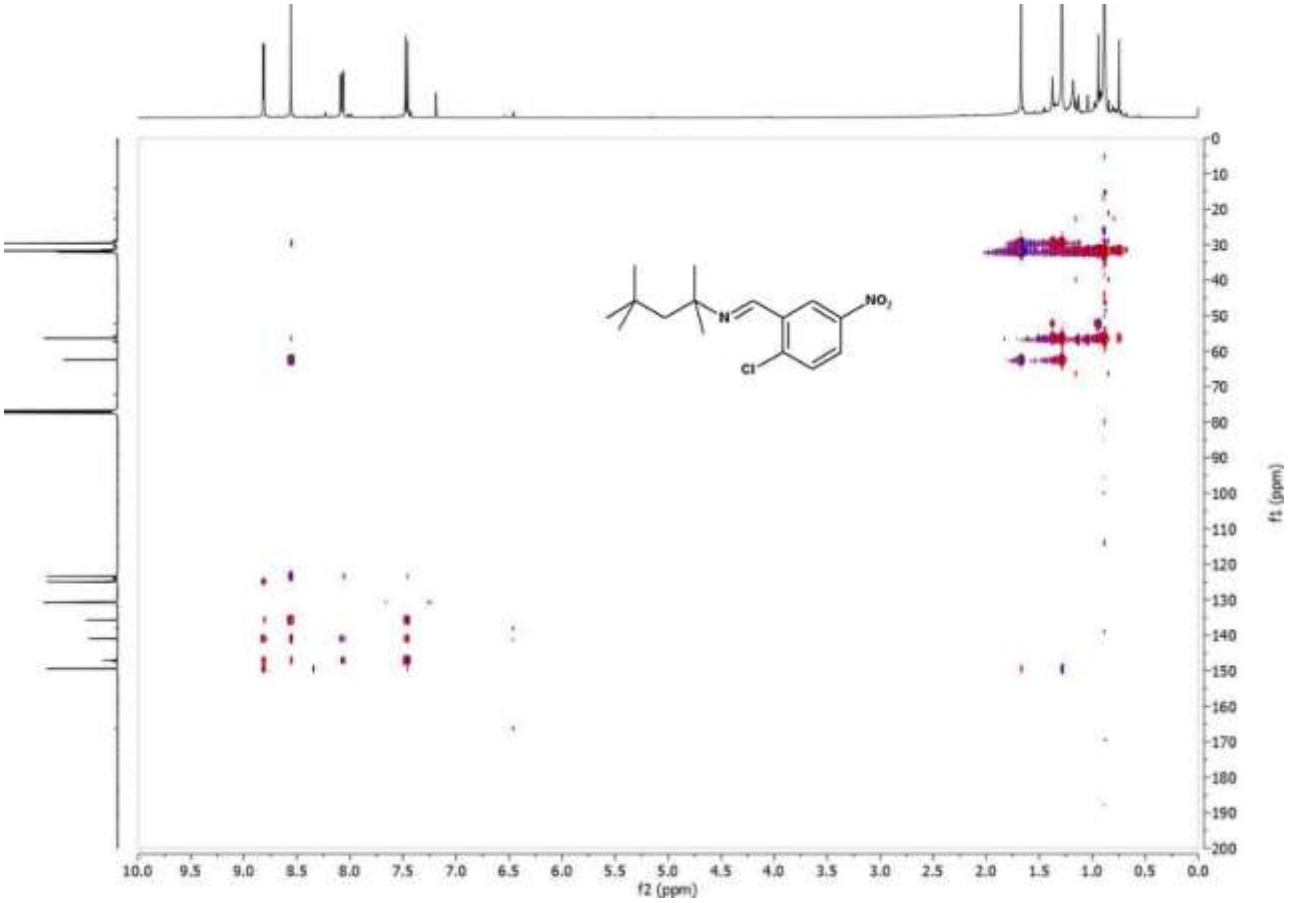

Figure C.30 HMBC spectrum of **5bd** in $CDCl_3$.

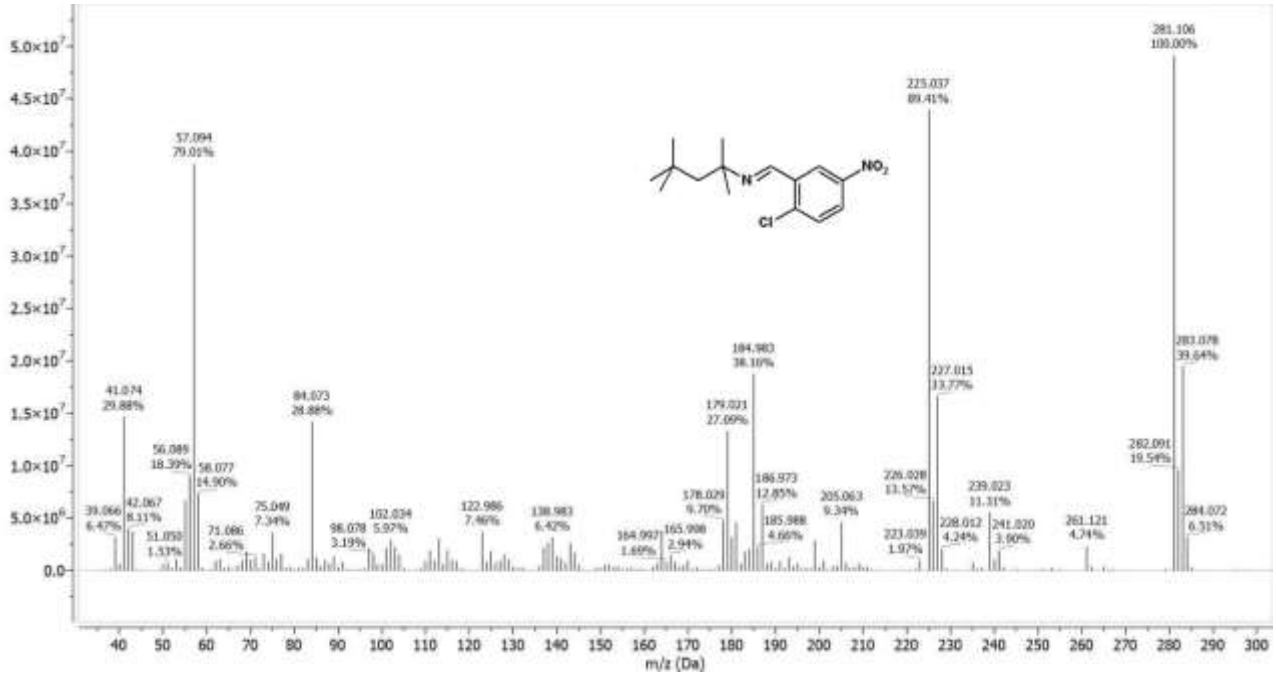

Figure C.31 *GC-MS spectrum of imine* ***5bd****.*

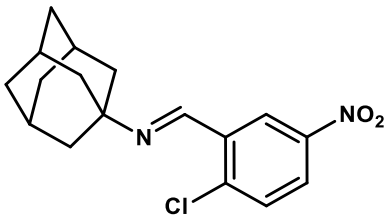

Chemical Formula: $C_{17}H_{19}ClN_2O_2$
Molecular Weight: 318,80

5cd

^{1}H NMR (400 MHz, Chloroform-d) δ [ppm] = 8.90 (d, J = 2.8 Hz, 1H), 8.63 (s, 1H), 8.15 (dd, J = 8.8, 2.8 Hz, 1H), 7.53 (d, J = 8.7 Hz, 1H), 2.20 (s, 3H), 1.83 (d, J = 2.9 Hz, 6H), 1.75 (q, J = 12.2 Hz, 6H).

^{13}C NMR (101 MHz, Chloroform-d) δ [ppm] = 149.99, 147.13, 141.22, 135.97, 130.83, 125.07, 123.54, 59.21, 43.16, 36.62, 29.63.

GC/MS (EI): calc. for $C_{17}H_{19}ClN_2O_2$ $[M]^+$: 318.114; found: $[M]^+$ 318.097, $C_{10}H_{15}$ 135.156.

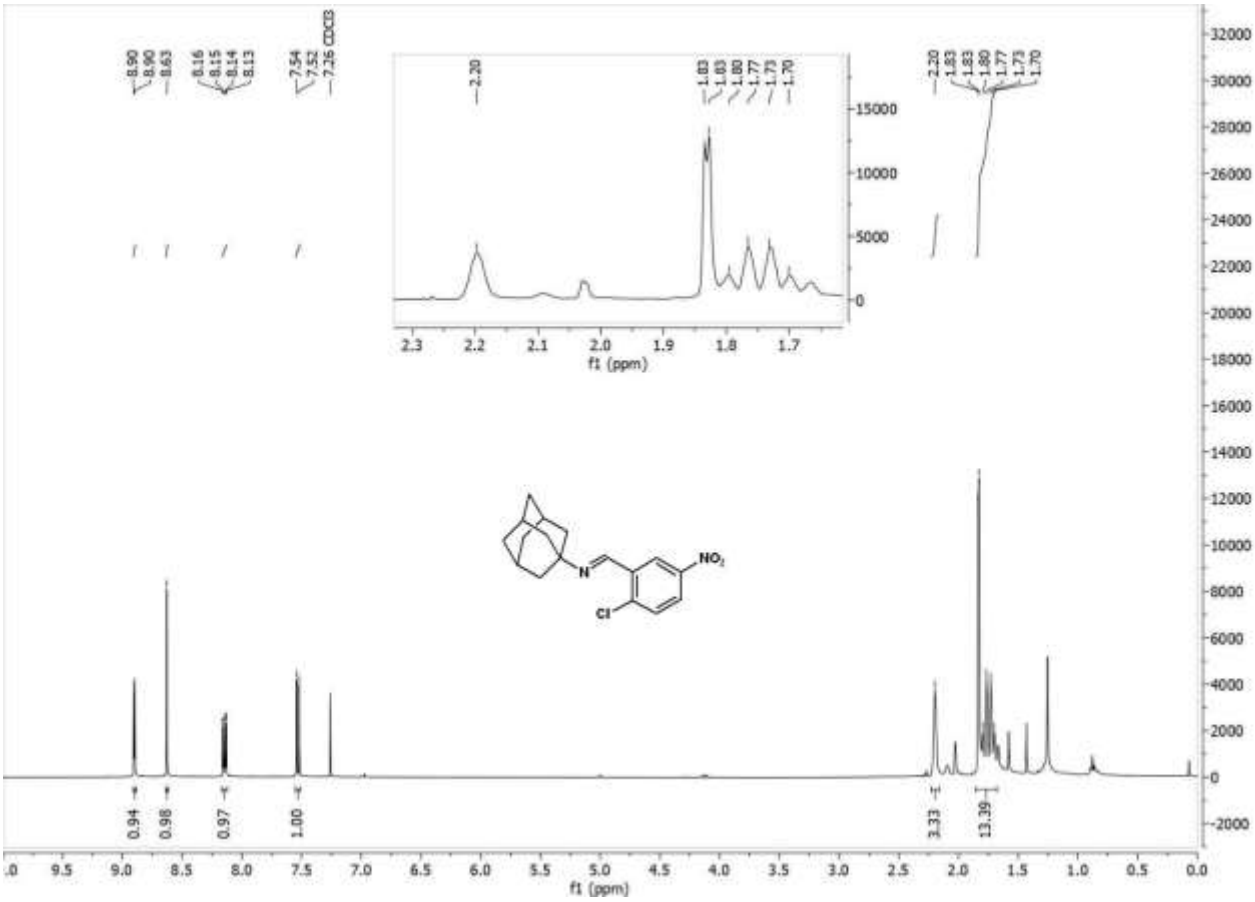

*Figure C.32 ^{1}H NMR spectrum of **5cd** in $CDCl_3$.*

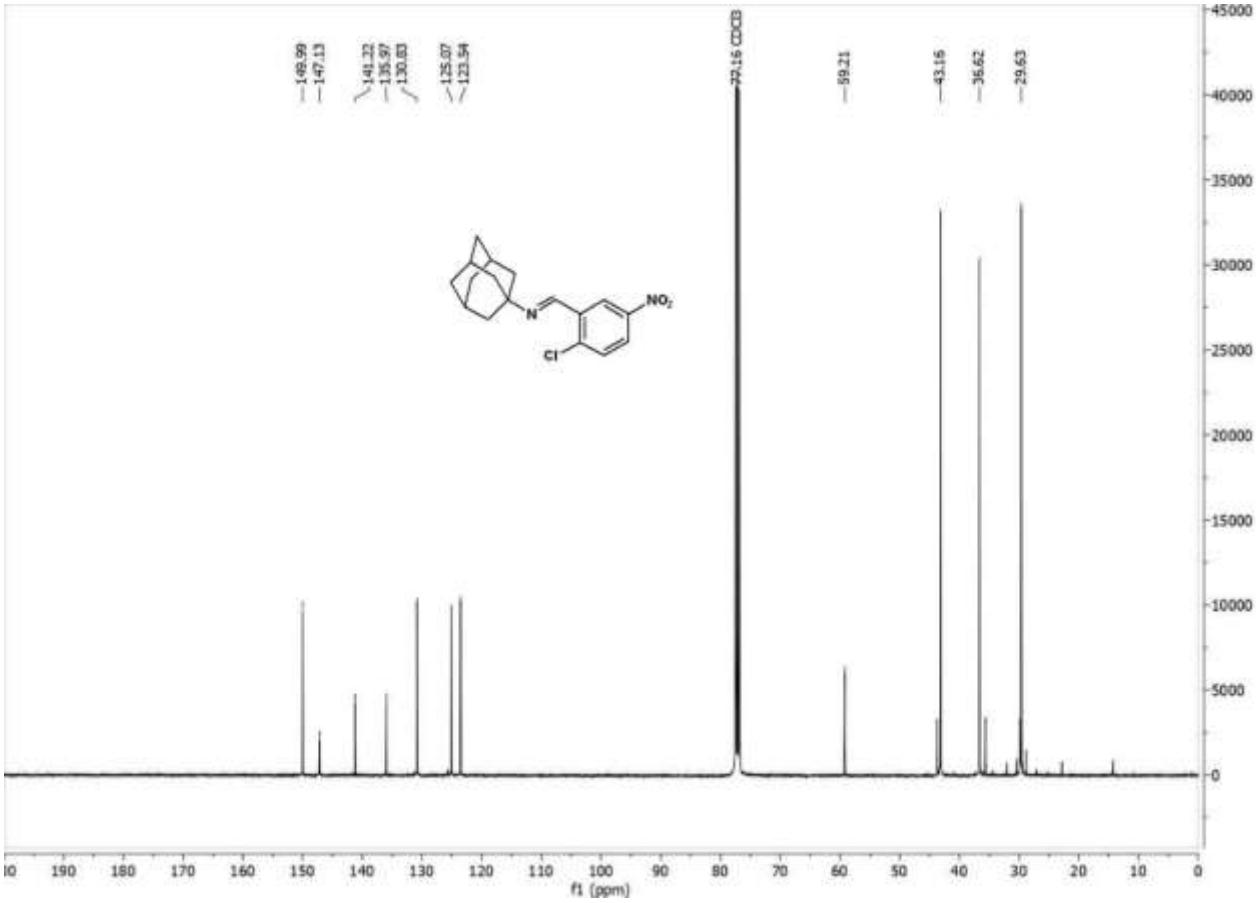

Figure C.33 $^{13}C(^{1}H)$ *NMR spectrum of* ***5cd*** *in* $CDCl_3$.

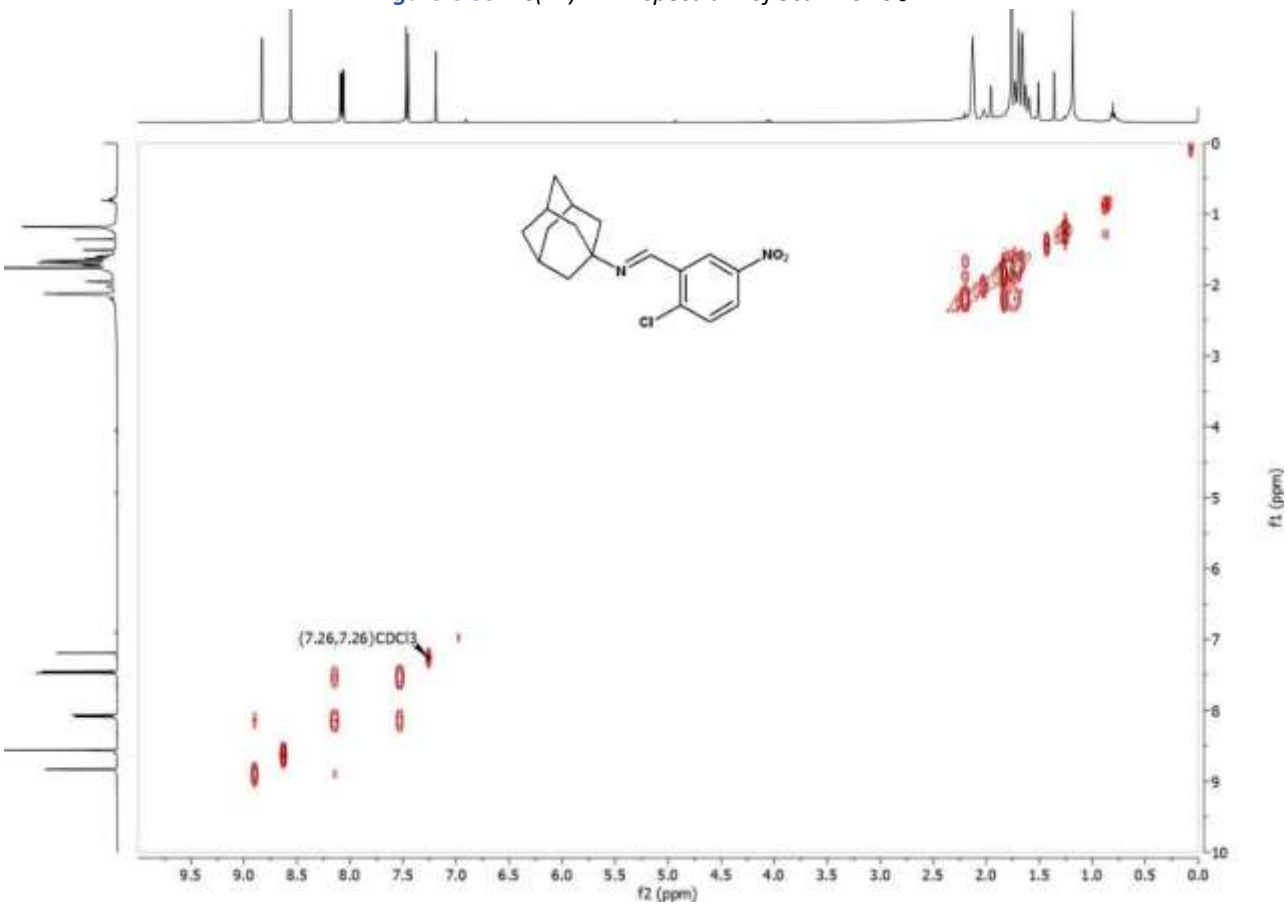

Figure C.34 COSY spectrum of ***5cd*** *in* $CDCl_3$.

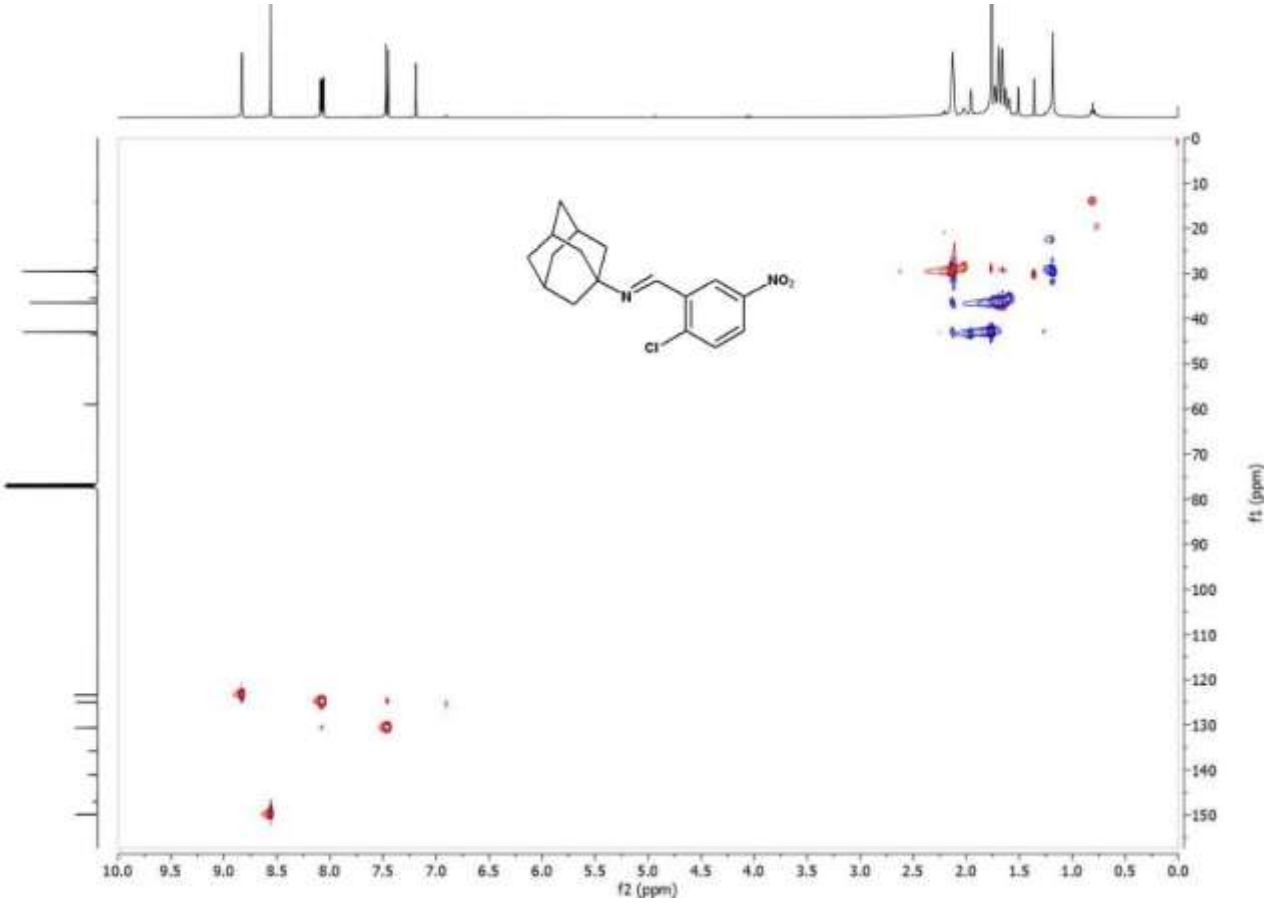

Figure C.35 HSQC spectrum of **5cd** in $CDCl_3$.

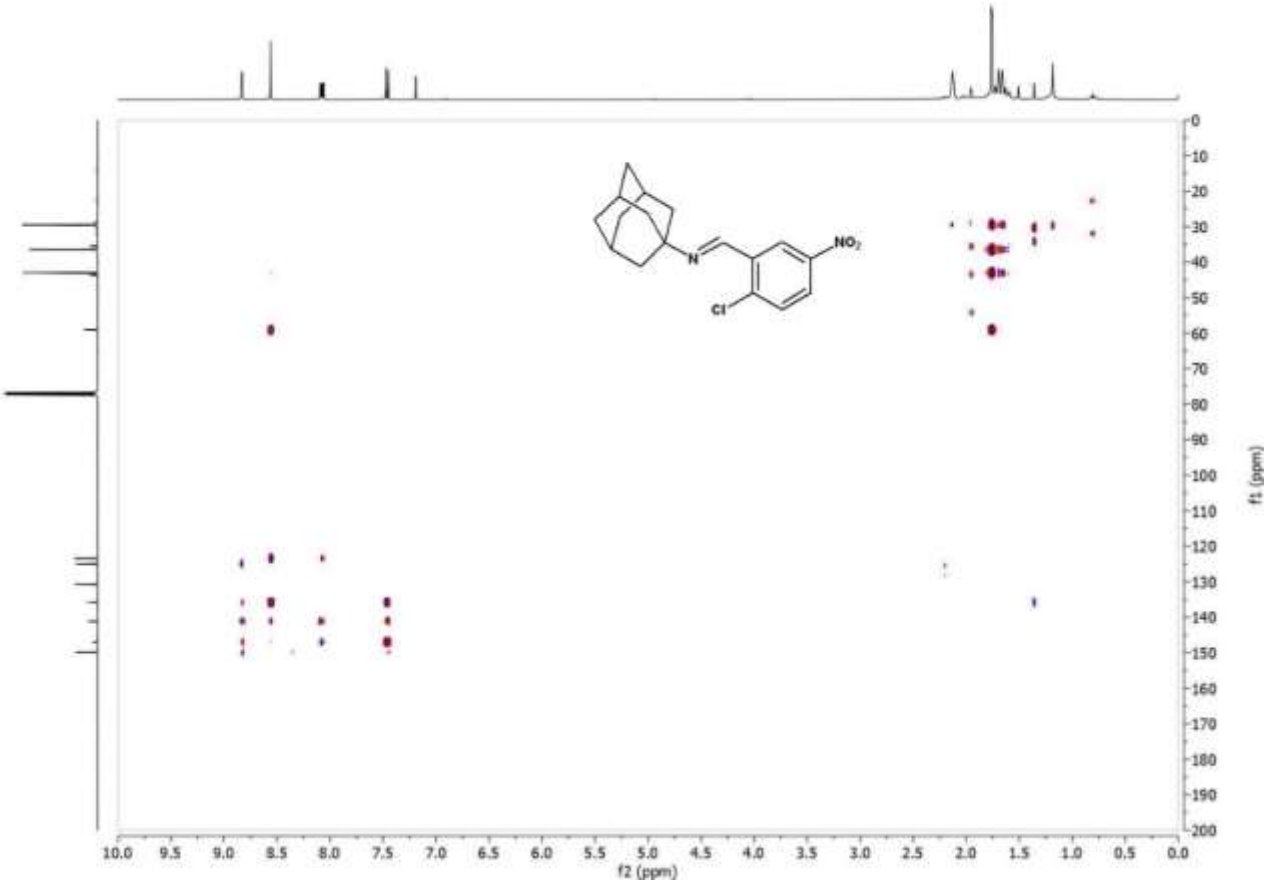

Figure C.36 HMBC spectrum of **5cd** in $CDCl_3$.

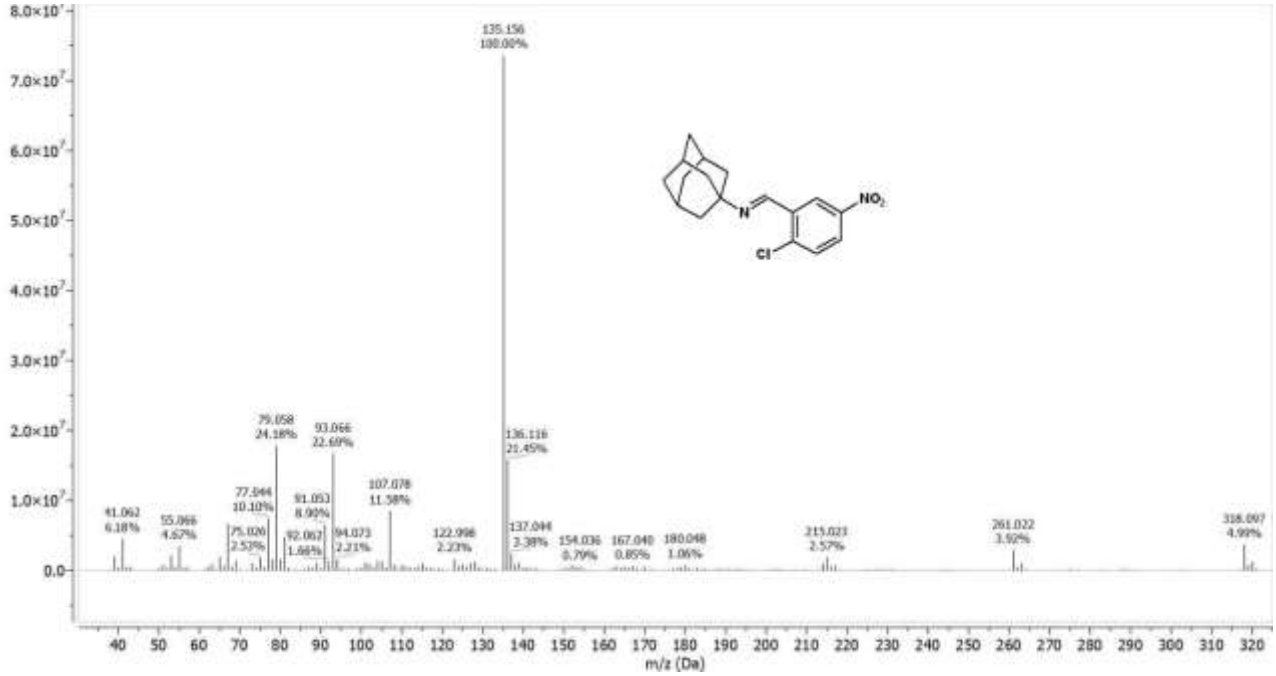

Figure C.37 GC-MS spectrum of imine ***5cd***.

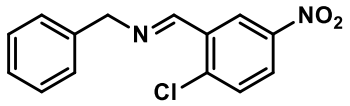

Chemical Formula: $C_{14}H_{11}ClN_2O_2$
Molecular Weight: 274,70400

5dd

^{1}H NMR (400 MHz, Chloroform-d) δ [ppm] = 8.83 (d, J = 2.9 Hz, 1H), 8.71 (t, J = 1.6 Hz, 1H), 8.07 (dd, J = 8.8, 2.8 Hz, 1H), 7.45 (d, J = 8.8 Hz, 1H), 7.32 – 7.14 (m, 5H), 4.81 (d, J = 1.5 Hz, 2H).

^{13}C NMR (101 MHz, Chloroform-d) δ [ppm] = 156.40, 147.07, 141.18, 138.44, 134.74, 131.02, 128.80, 128.20, 127.49, 125.66, 123.83, 65.42.

GC/MS (EI): calc. for $C_{14}H_{11}ClN_2O_2$ $[M]^+$: 274.051; found: $[M]^+$ 274.038, C_7H_7 91.047.

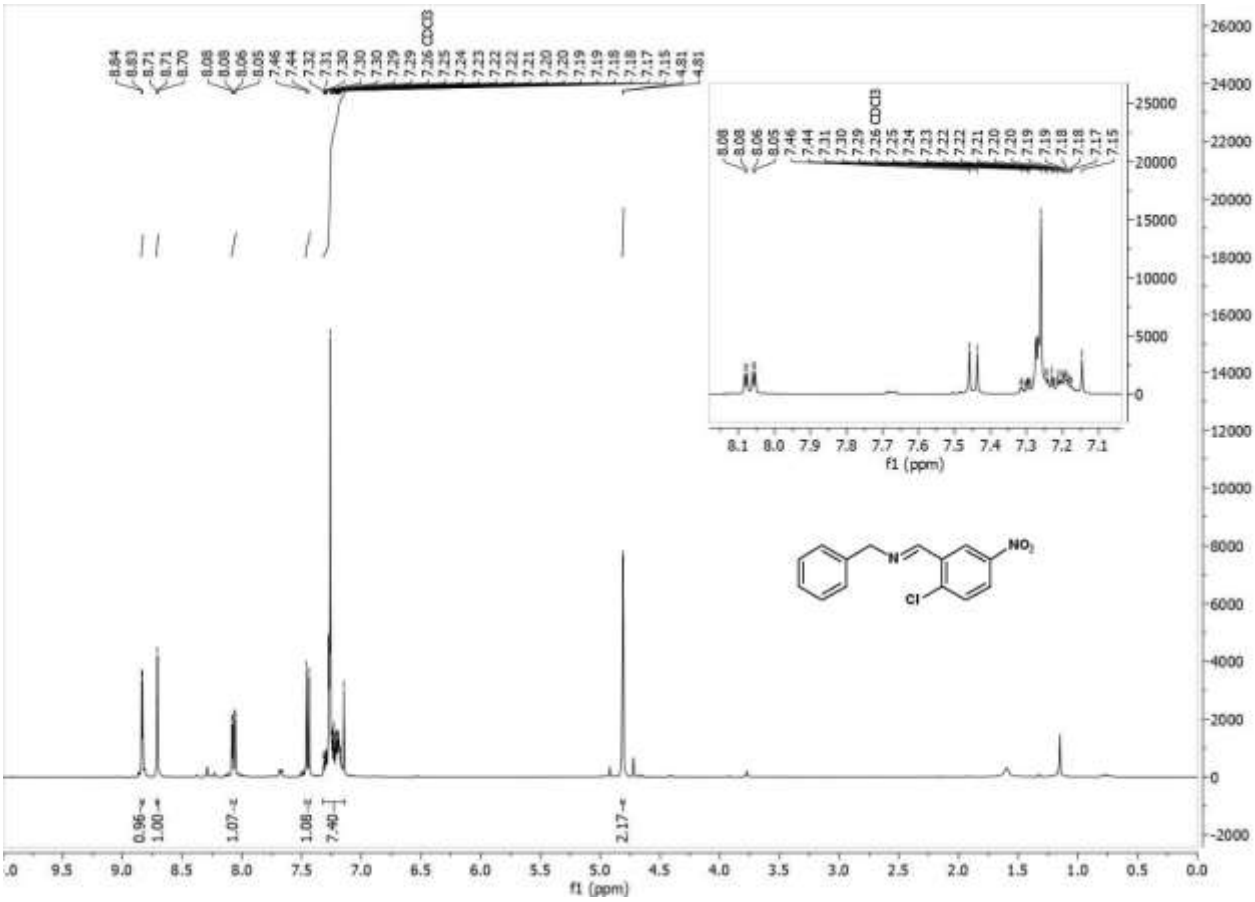

*Figure C.38 ^{1}H NMR spectrum of **5dd** in $CDCl_3$.*

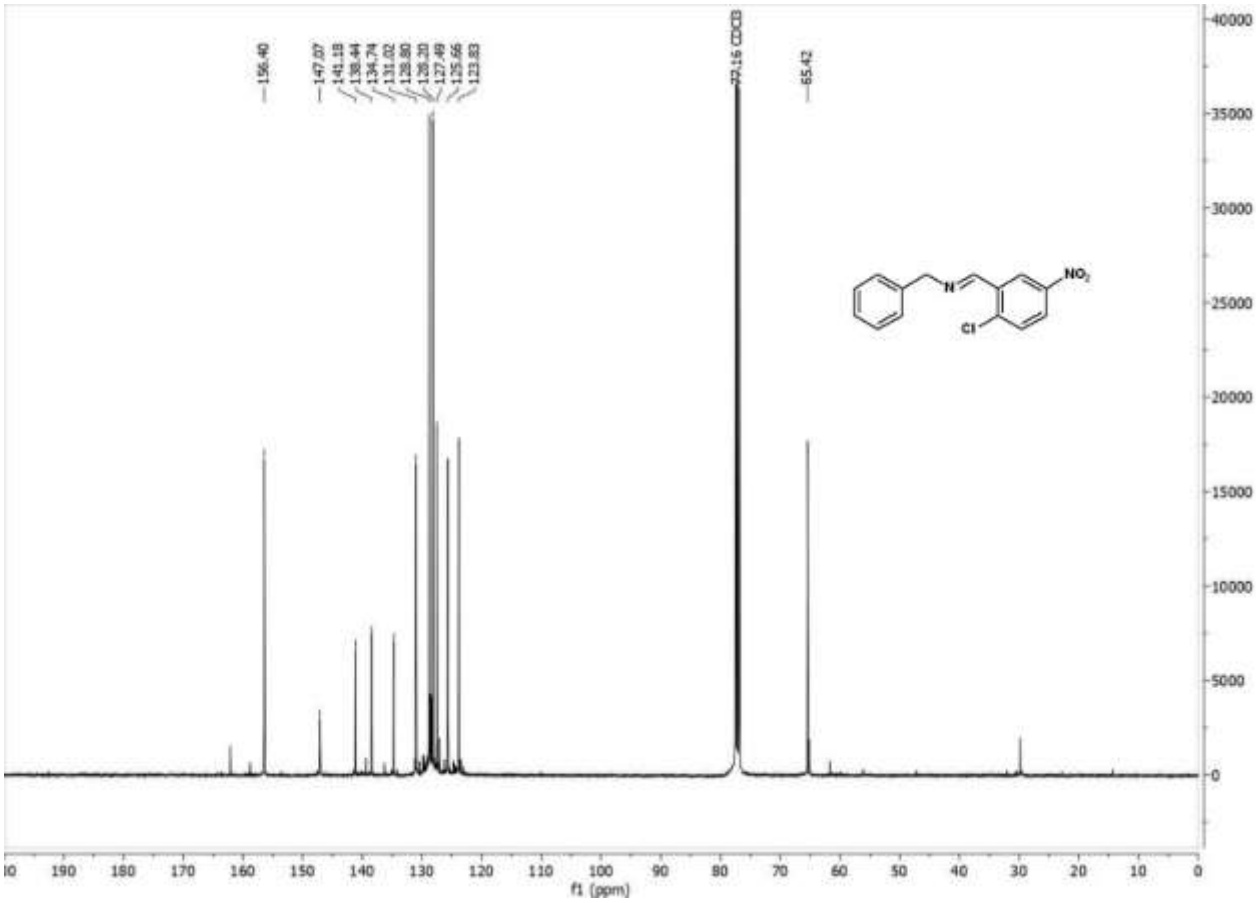

Figure C.39 $^{13}C(^{1}H)$ *NMR spectrum of* ***5dd*** *in* $CDCl_3$.

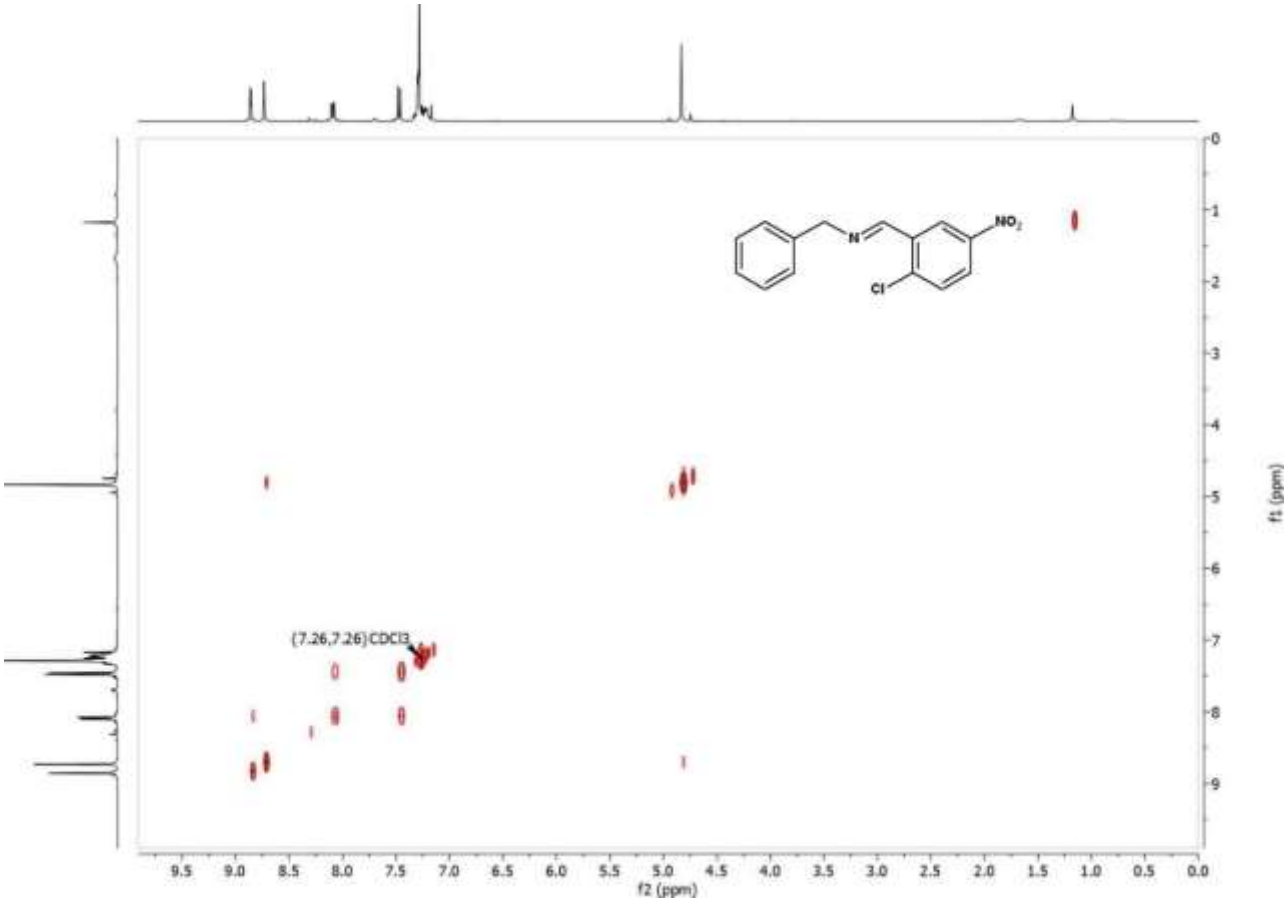

Figure C.40 COSY spectrum of ***5dd*** *in* $CDCl_3$.

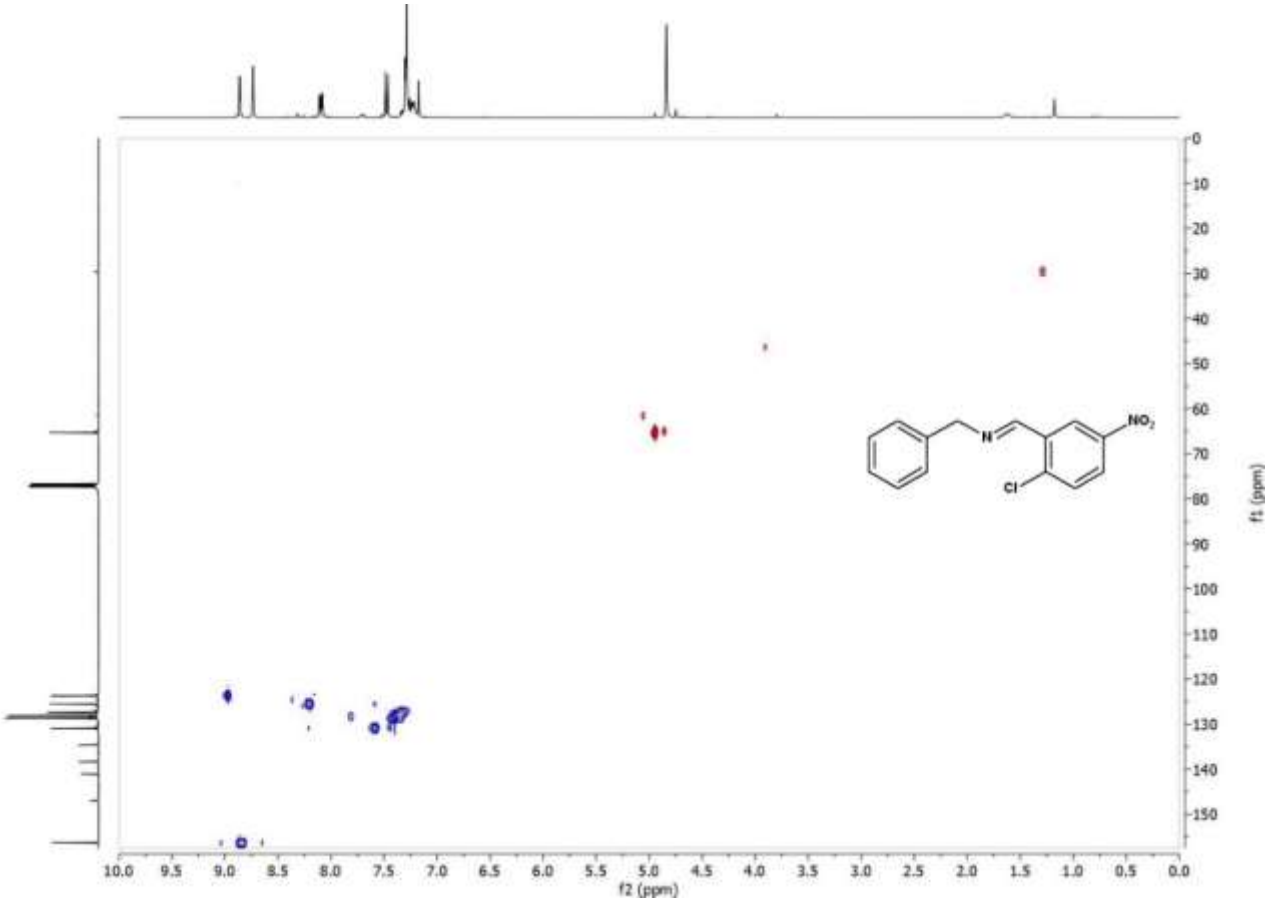

Figure C.41 HSQC spectrum of **5dd** in $CDCl_3$.

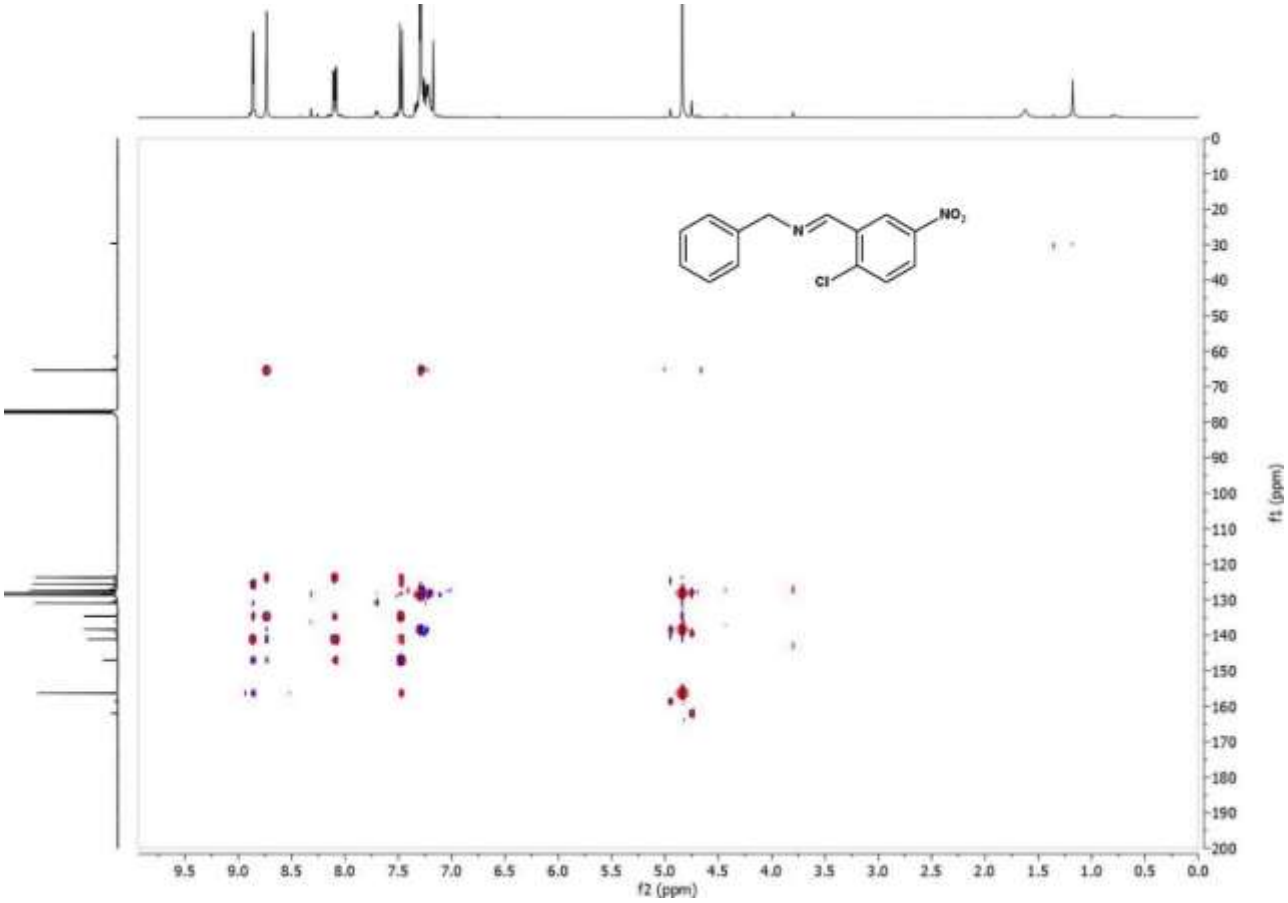

Figure C.42 HMBC spectrum of **5dd** in $CDCl_3$.

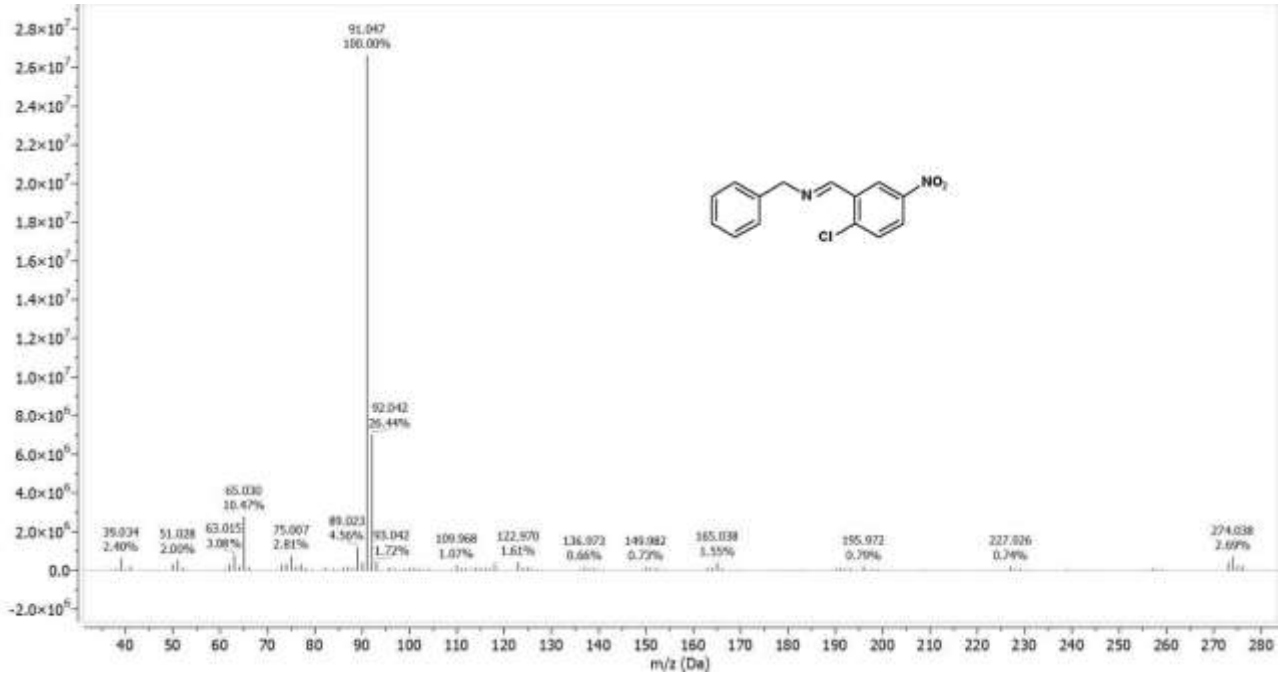

Figure C.43 *GC-MS spectrum of imine* ***5dd****.*

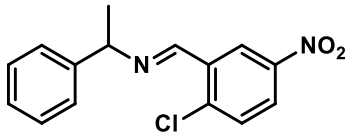

Chemical Formula: $C_{15}H_{13}ClN_2O_2$
Molecular Weight: 288,73100

5ed

^{1}H NMR (400 MHz, Chloroform-d) δ [ppm] = 8.99 (d, J = 2.9 Hz, 1H), 8.81 (s, 1H), 8.16 (dd, J = 8.8, 2.9 Hz, 1H), 7.56 – 7.26 (m, 6H), 4.70 (q, J = 6.6 Hz, 1H), 1.66 (d, J = 6.6 Hz, 3H).

^{13}C NMR (101 MHz, Chloroform-d) δ [ppm] = 153.98, 146.98, 144.35, 141.10, 134.85, 130.92, 128.69, 127.30, 126.70, 125.47, 123.81, 70.34, 25.04.

GC/MS (EI): calc. for $C_{15}H_{13}ClN_2O_2$ $[M]^+$: 288.067; found: $[M]^+$ 288.063, $[M\text{-}CH_3^{\cdot}]^+$ 273.040, C_8H_9 105.149, C_6H_5 77.072.

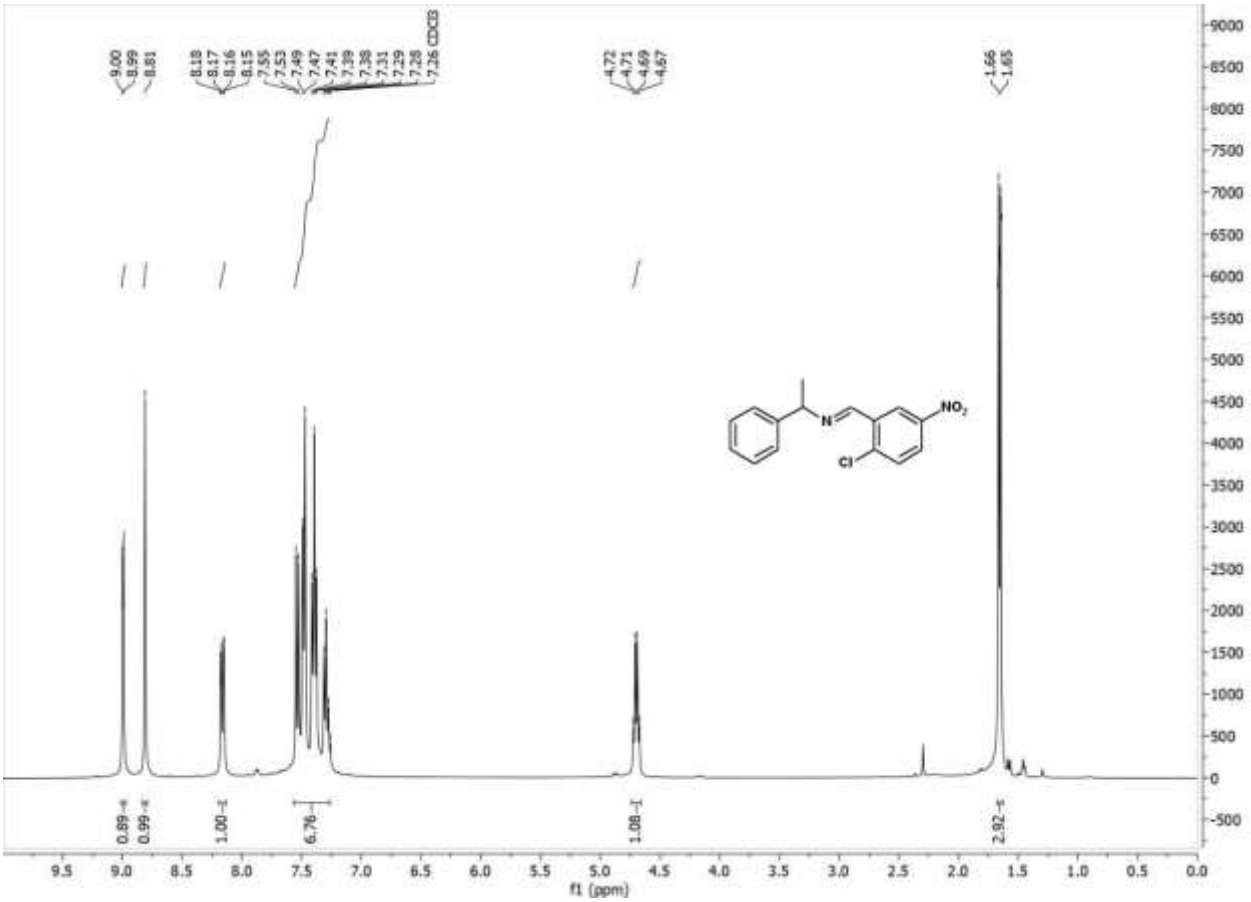

*Figure C.44 ^{1}H NMR spectrum of **5ed** in $CDCl_3$.*

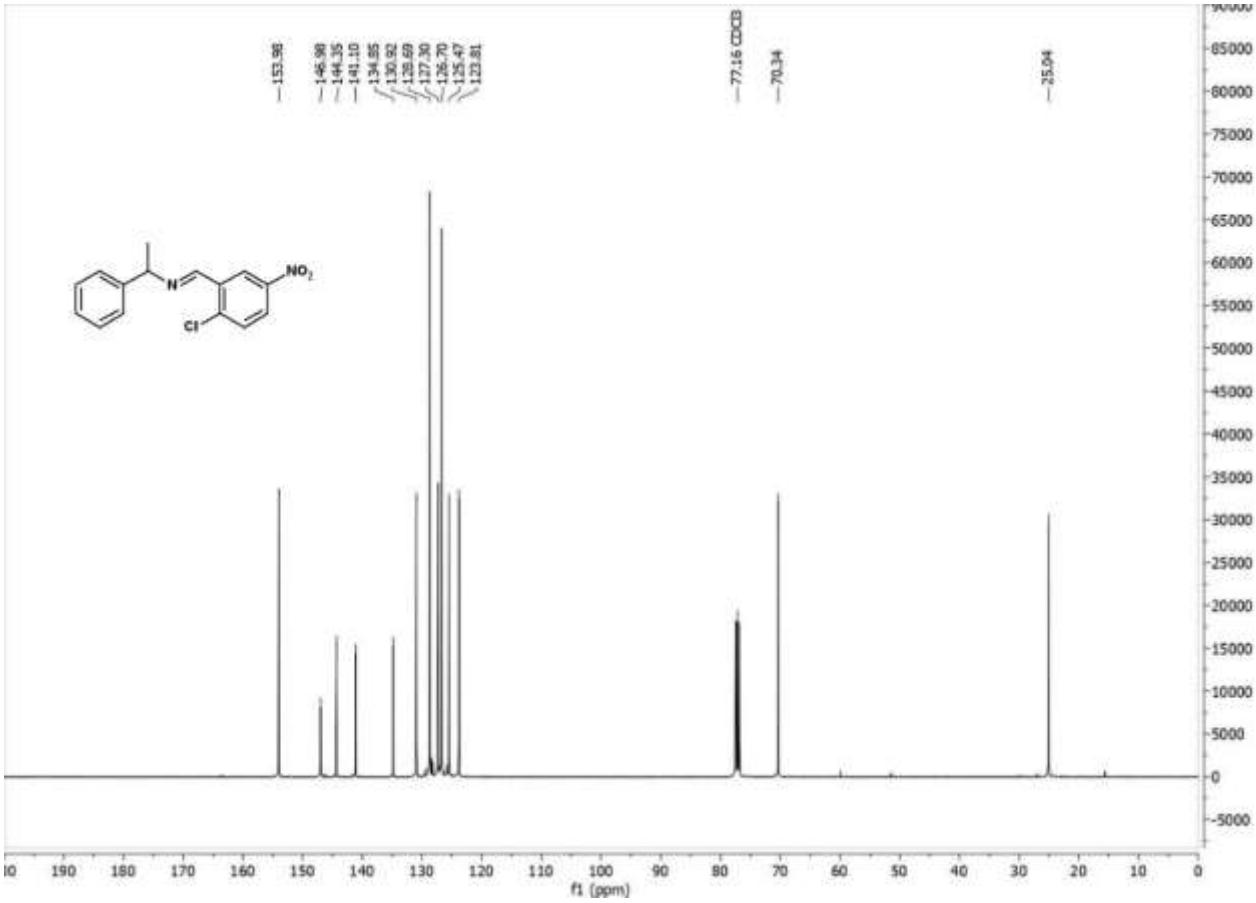

Figure C.45 $^{13}C(^{1}H)$ *NMR spectrum of* ***5ed*** *in* $CDCl_3$.

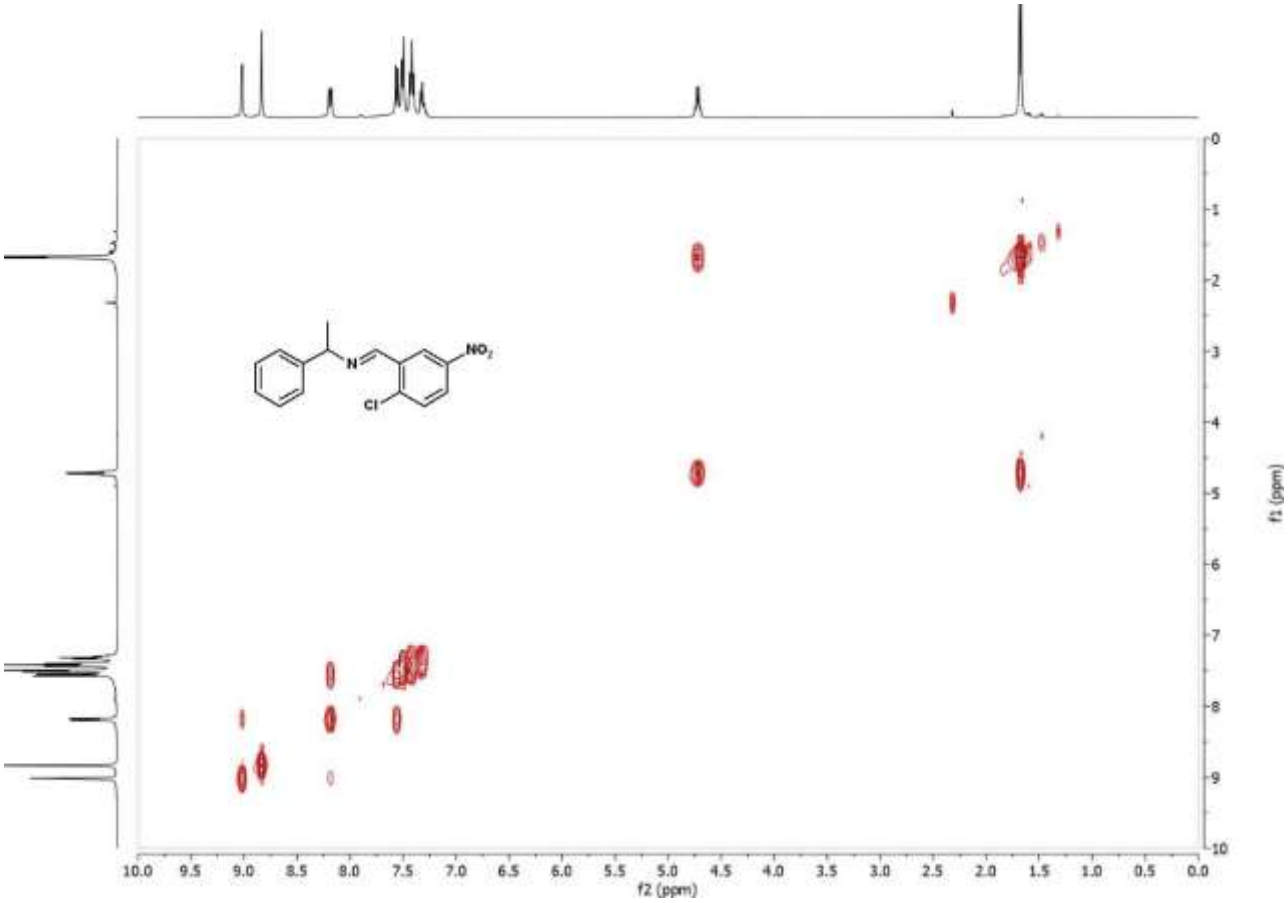

Figure C.46 COSY spectrum of ***5ed*** *in* $CDCl_3$.

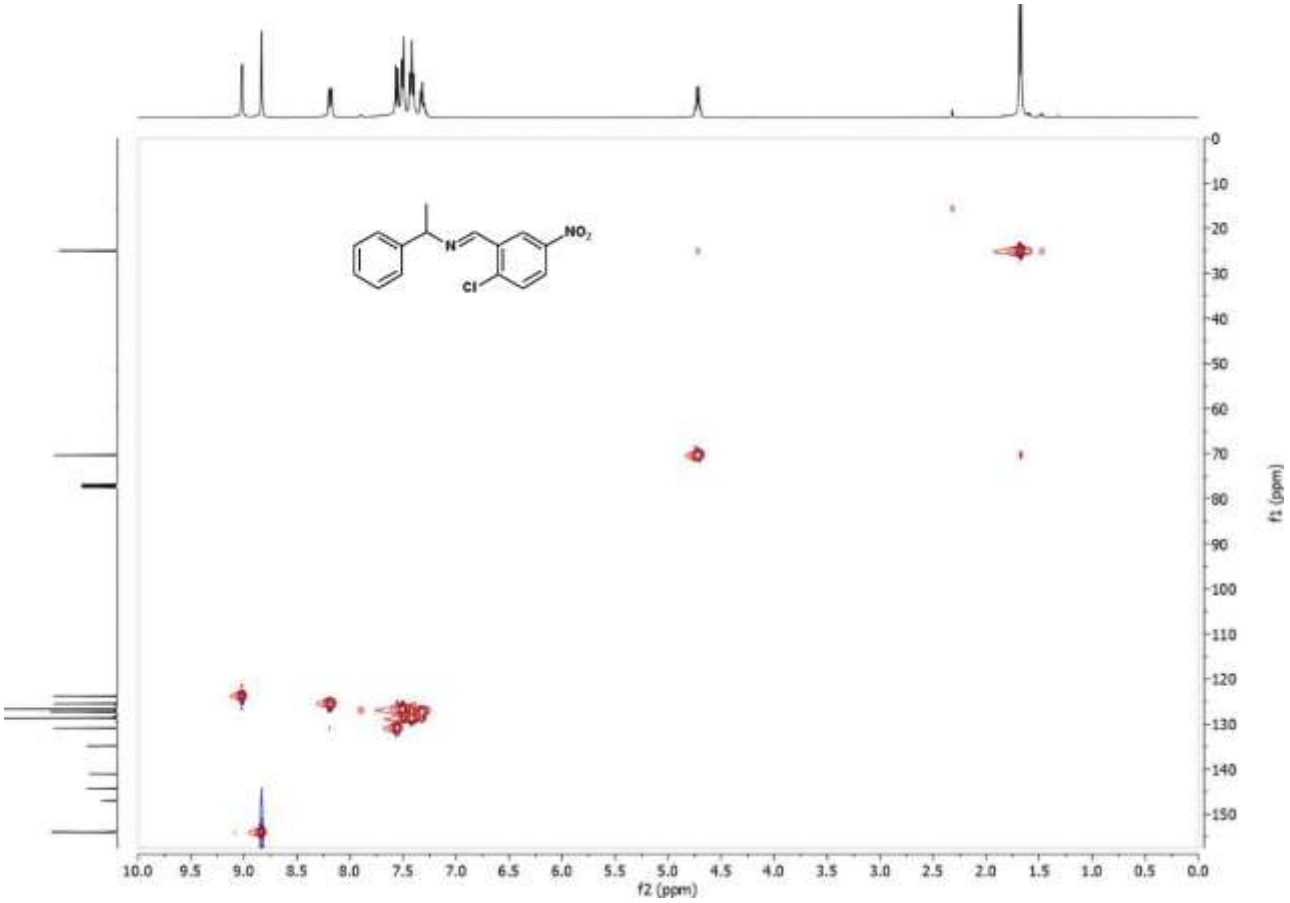

Figure C.47 HSQC spectrum of **5ed** in $CDCl_3$.

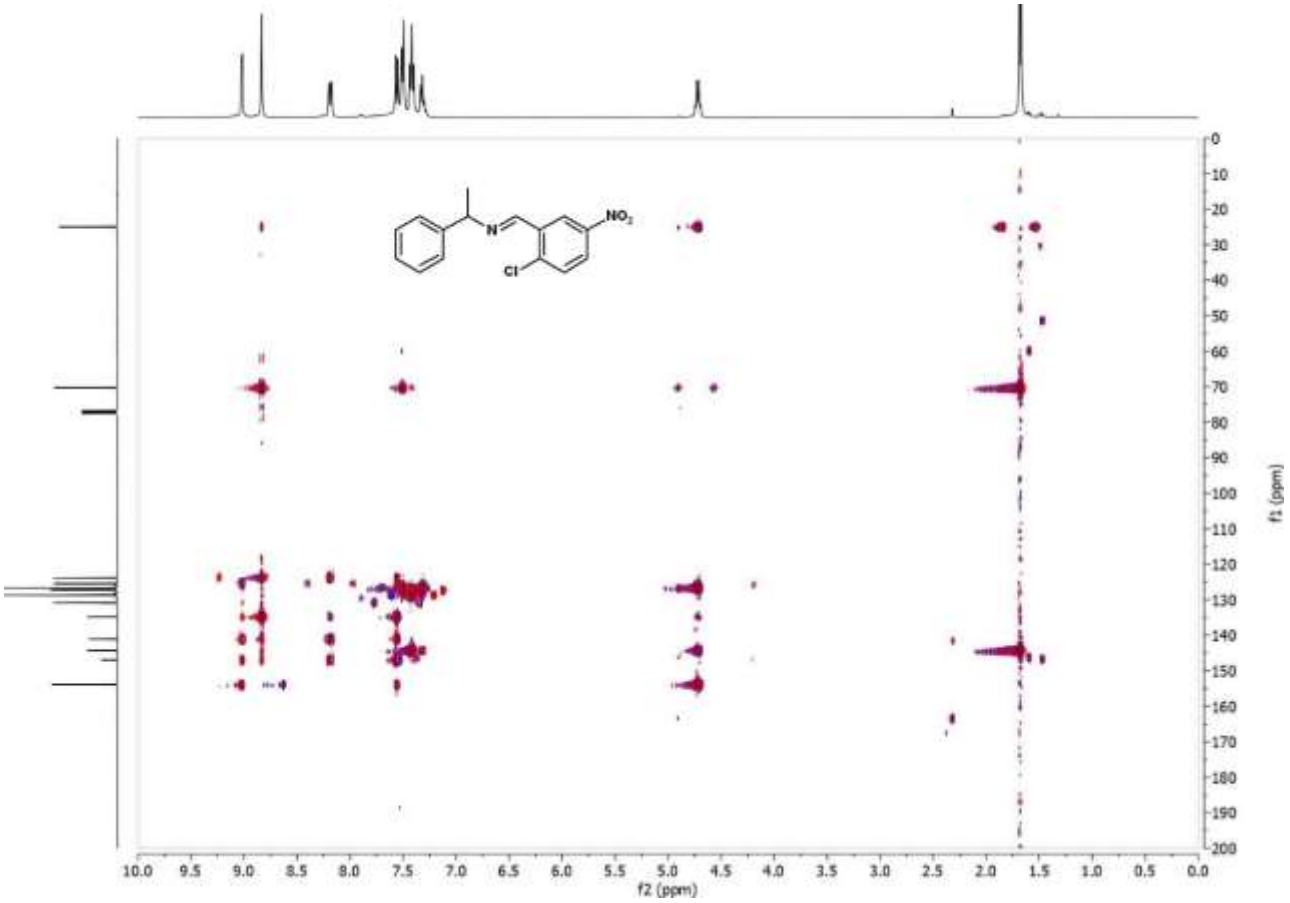

Figure C.48 HMBC spectrum of **5ed** in $CDCl_3$.

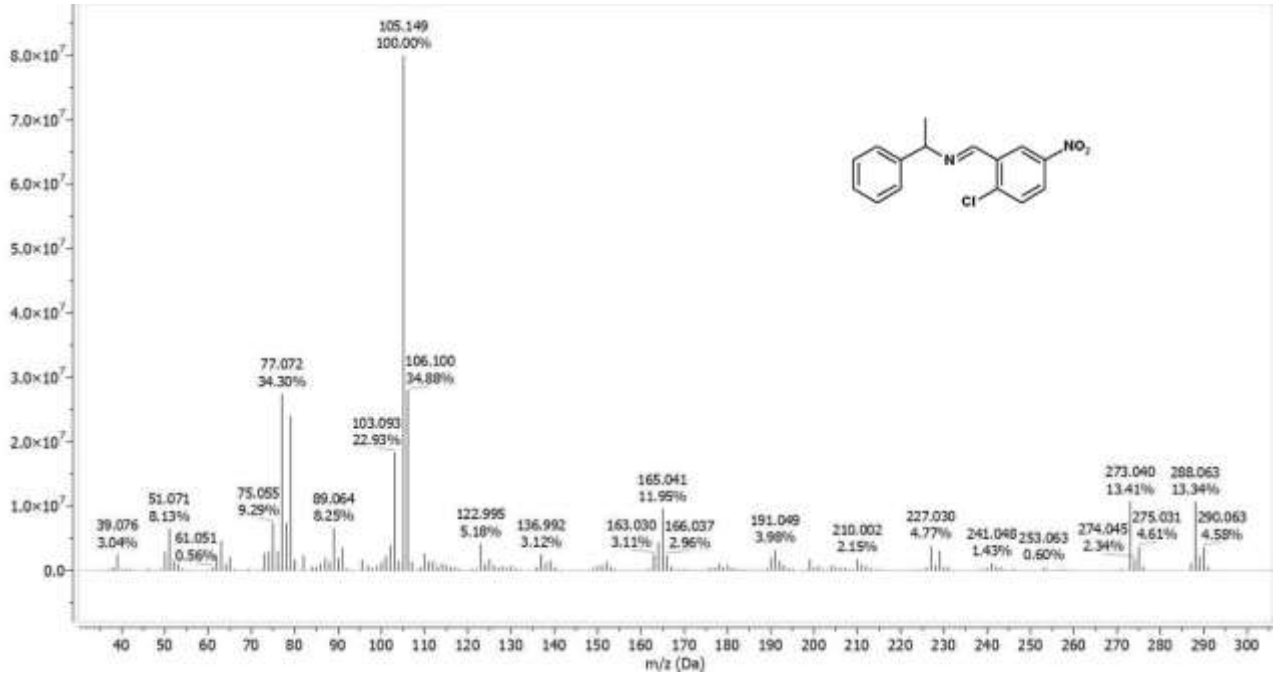

Figure C.49 *GC-MS spectrum of imine* ***5ed****.*

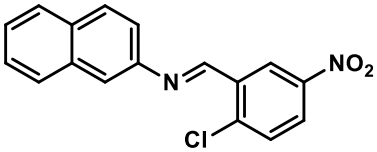

5fd

Chemical Formula: $C_{17}H_{11}ClN_2O_2$
Molecular Weight: 310,73700

^{1}H NMR (400 MHz, Chloroform-d) δ [ppm] = 9.17 (d, J = 2.8 Hz, 1H), 9.05 (s, 1H), 8.23 (dd, J = 8.8, 2.9 Hz, 1H), 7.93 – 7.84 (m, 4H), 7.72 (s, 1H), 7.62 (d, J = 8.8 Hz, 1H), 7.55 – 7.45 (m, 3H).

^{13}C NMR (101 MHz, Chloroform-d) δ [ppm] = 154.11, 148.19, 147.19, 141.87, 134.87, 134.05, 132.79, 131.23, 129.42, 128.39, 127.93, 126.85, 126.24, 125.99, 123.92, 120.54, 119.51.

GC/MS (EI): calc. for $C_{17}H_{11}ClN_2O_2$ $[M]^+$: 310.051; found: $[M]^+$ 310.016, $C_{17}H_{11}N$ 229.044, $C_{10}H_7$ 127.014.

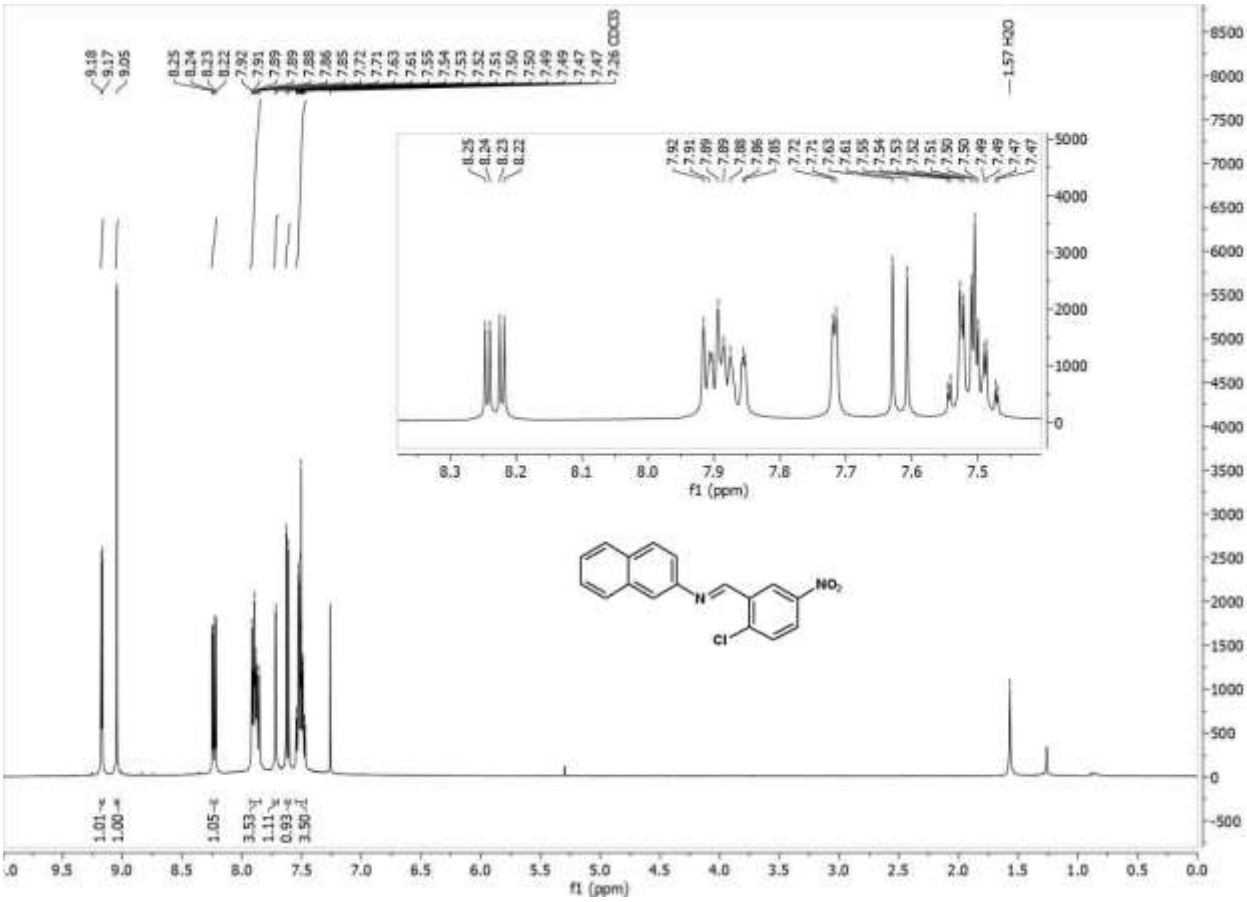

Figure C.50 ^{1}H NMR spectrum of 5fd in $CDCl_3$.

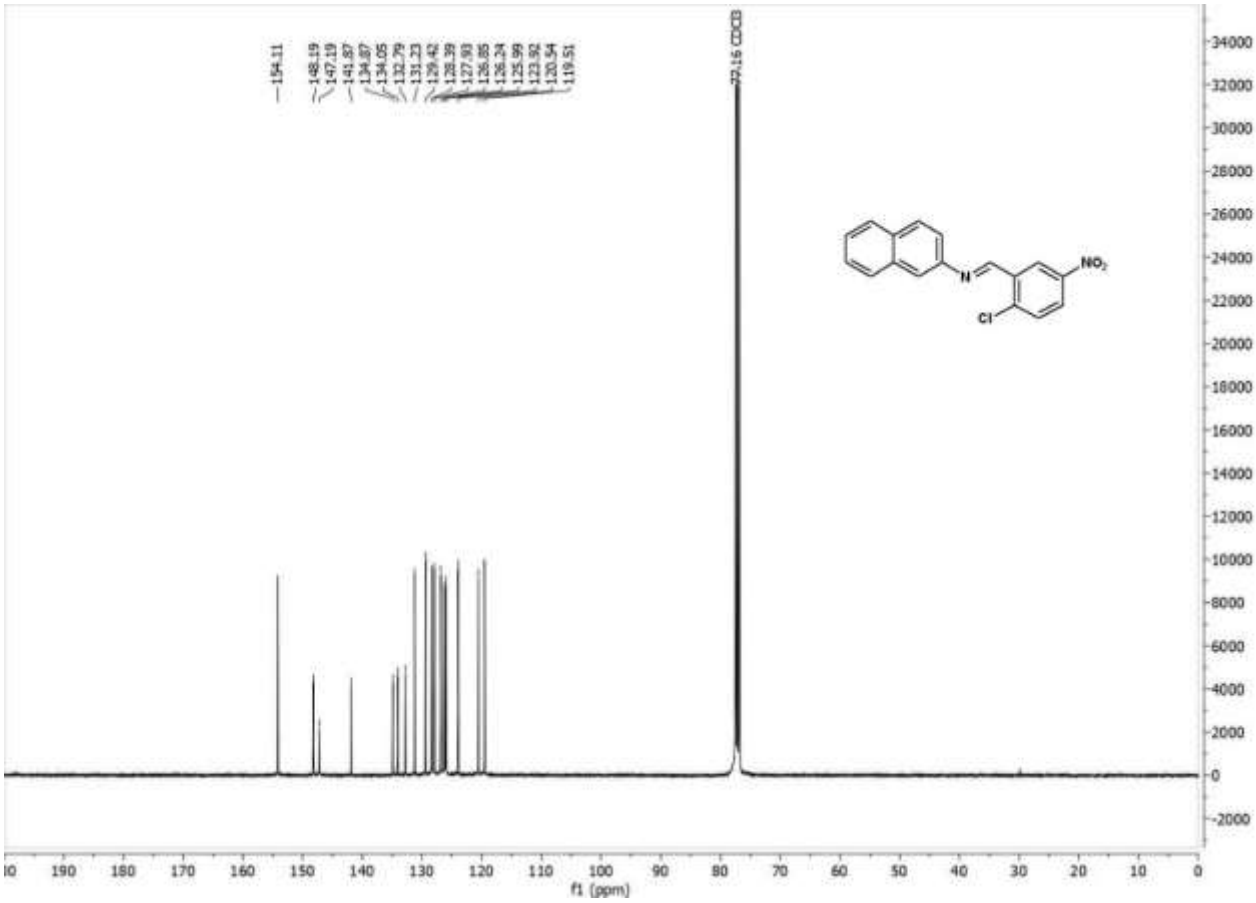

Figure C.51 $^{13}C(^{1}H)$ *NMR spectrum of* ***5fd*** *in* $CDCl_3$.

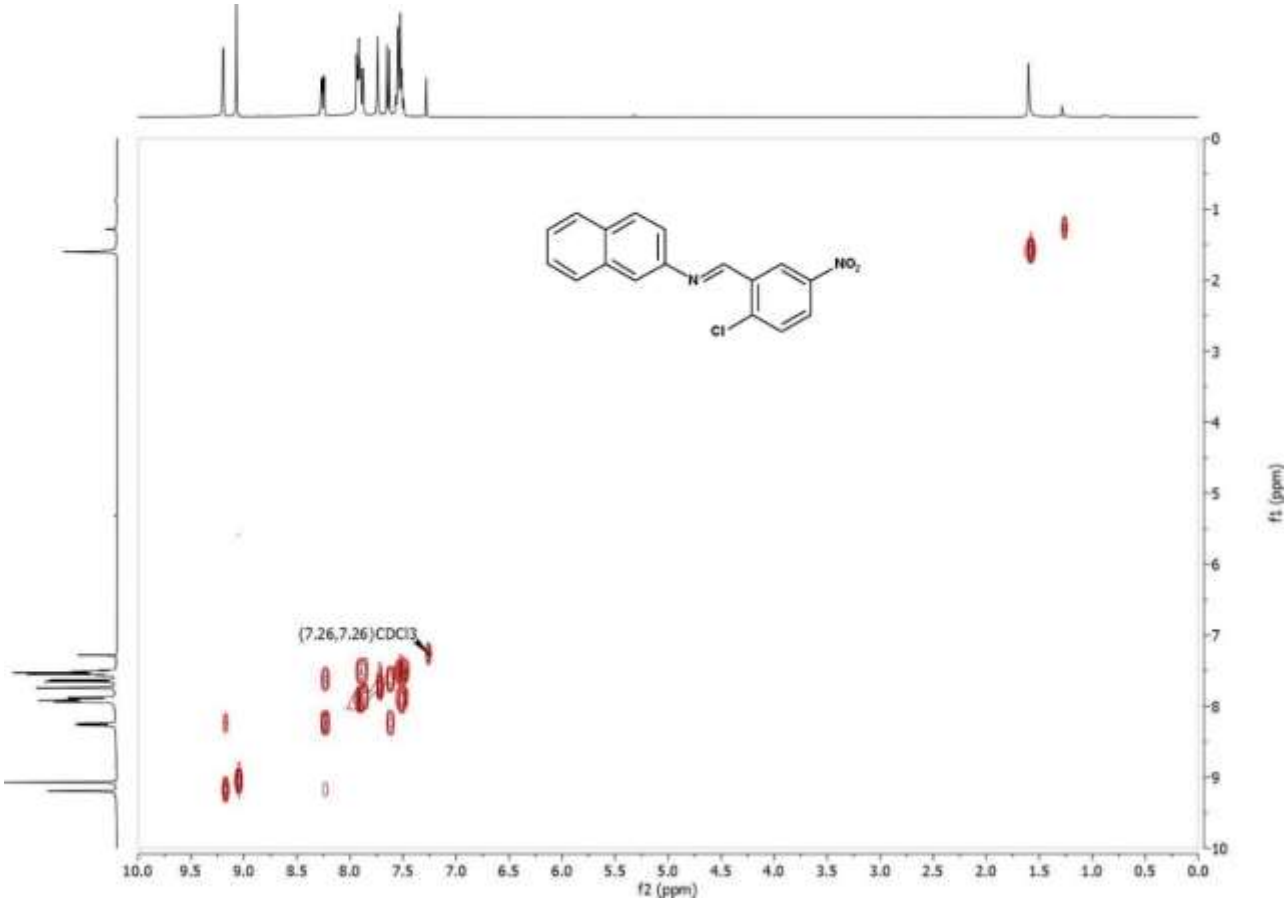

Figure C.52 COSY *spectrum of* ***5fd*** *in* $CDCl_3$.

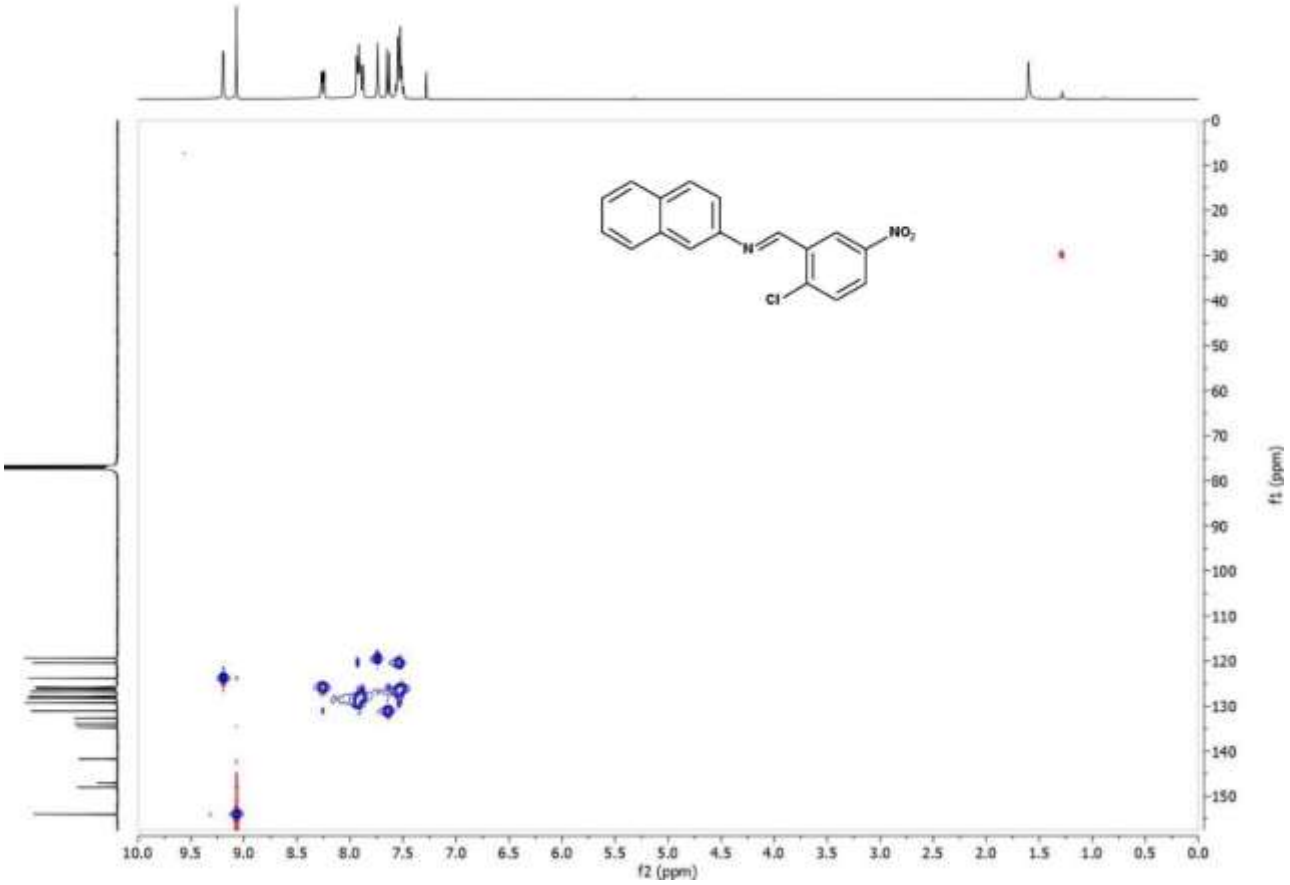

Figure C.53 HSQC spectrum of ***5fd*** in $CDCl_3$.

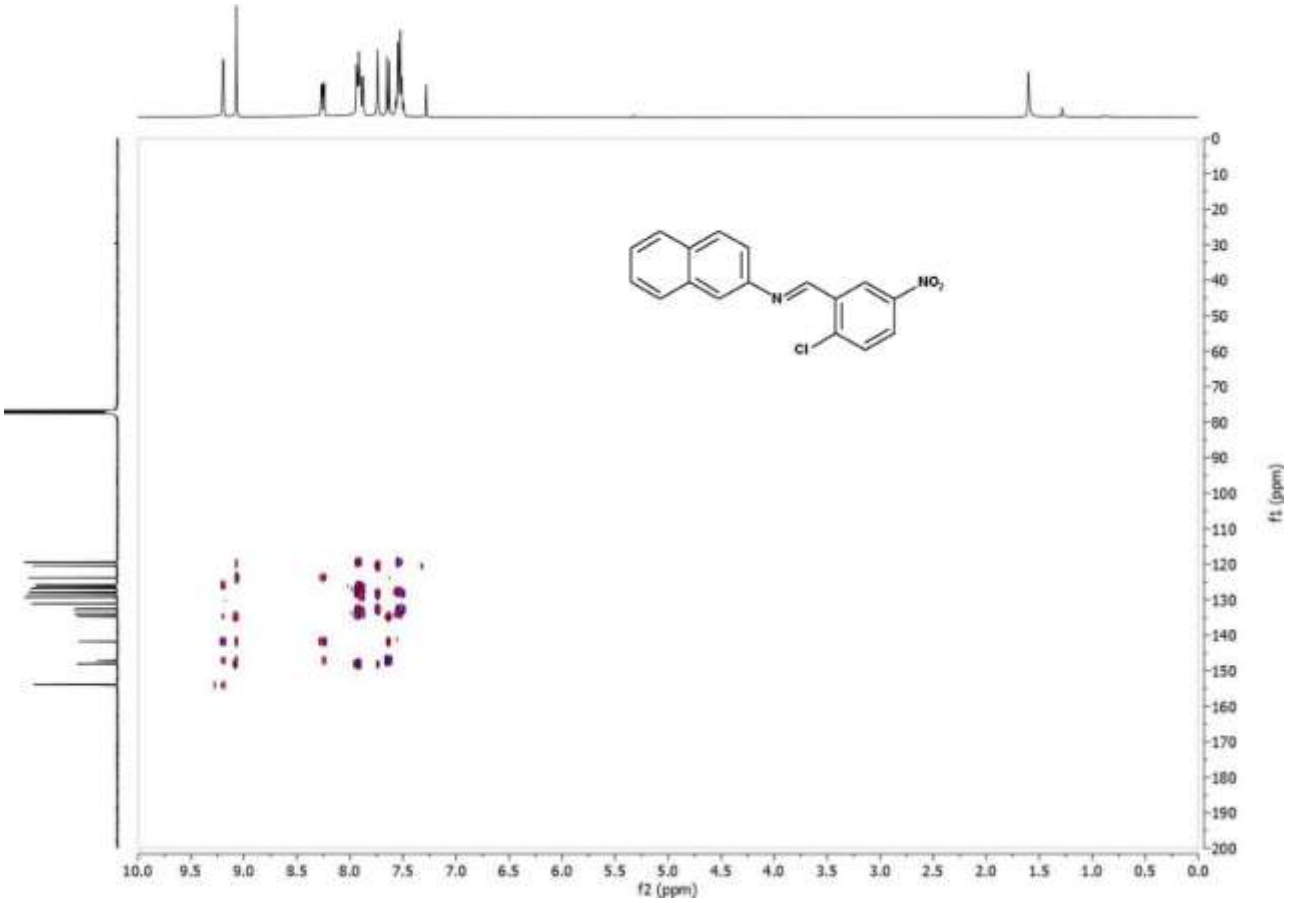

Figure C.54 HMBC spectrum of ***5fd*** in $CDCl_3$.

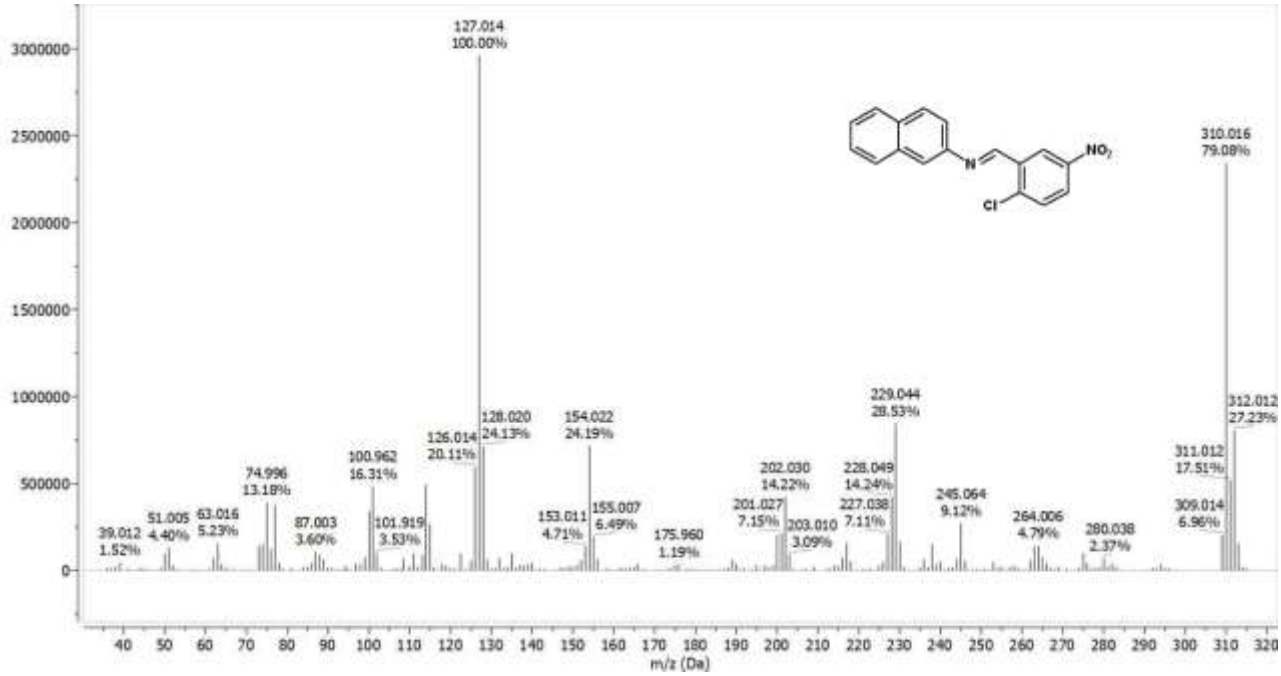

Figure C.55 GC-MS spectrum of imine **5fd**.

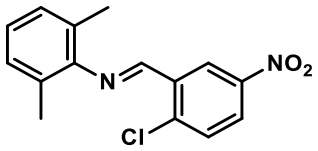

Chemical Formula: $C_{15}H_{13}ClN_2O_2$
Molecular Weight: 288,73100

5gd

^{1}H NMR (400 MHz, Chloroform-d) δ [ppm] = 9.14 (d, J = 2.8 Hz, 1H), 8.70 (s, 1H), 8.27 (dd, J = 8.7, 2.8 Hz, 1H), 7.64 (d, J = 8.8 Hz, 1H), 7.11 (d, J = 7.5 Hz, 2H), 7.05 – 6.98 (m, 1H), 2.18 (s, 6H).

^{13}C NMR (101 MHz, Chloroform-d) δ [ppm] = 157.78, 150.38, 147.24, 141.85, 134.67, 131.27, 128.43, 127.03, 126.24, 124.71, 123.53, 18.49.

GC/MS (EI): calc. for $C_{15}H_{13}ClN_2O_2$ $[M]^+$: 288.067; found: $[M]^+$ 288.023, $C_9H_{10}N$ 132.038, $C_{10}H_7$ 127.014, C_6H_5 77.011.

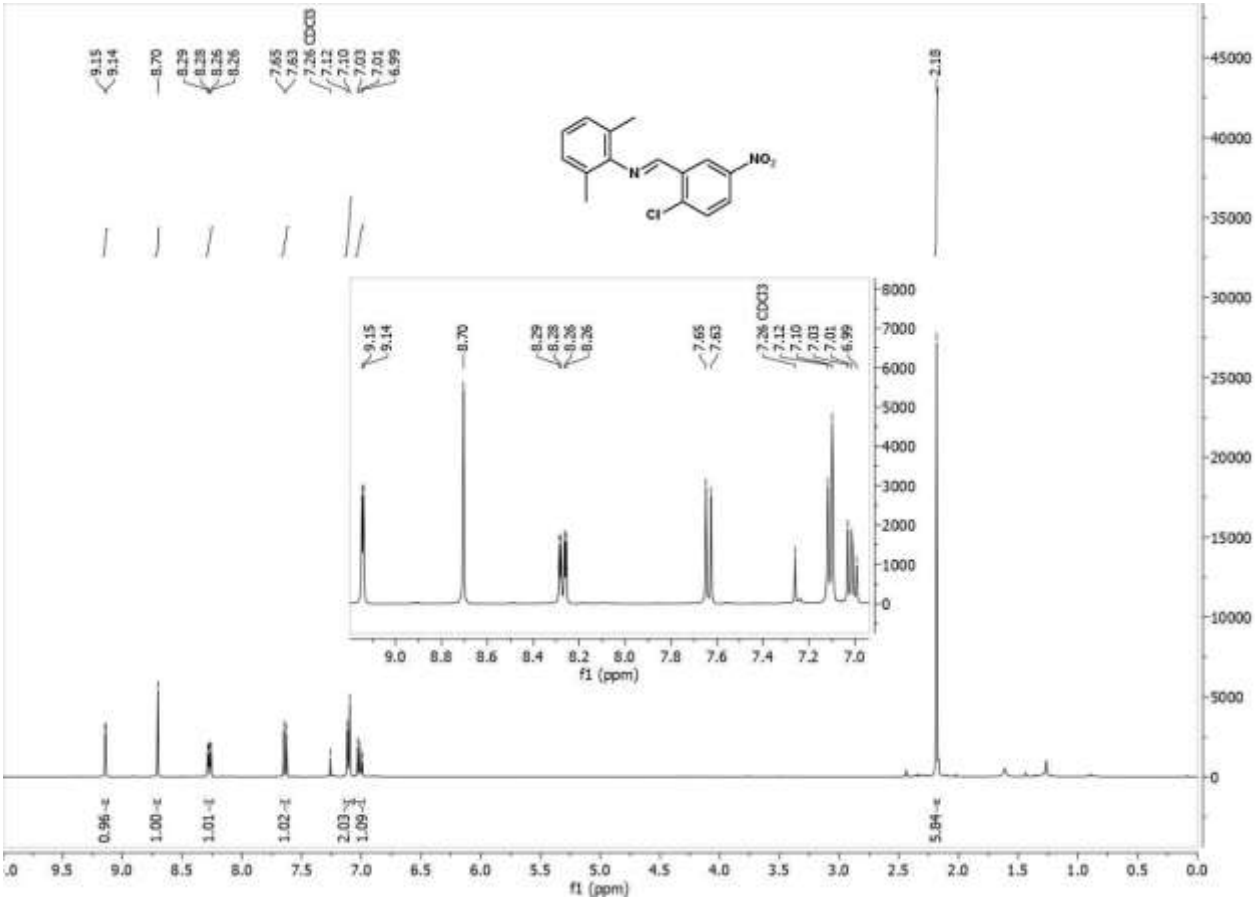

*Figure C.56 ^{1}H NMR spectrum of **5gd** in $CDCl_3$.*

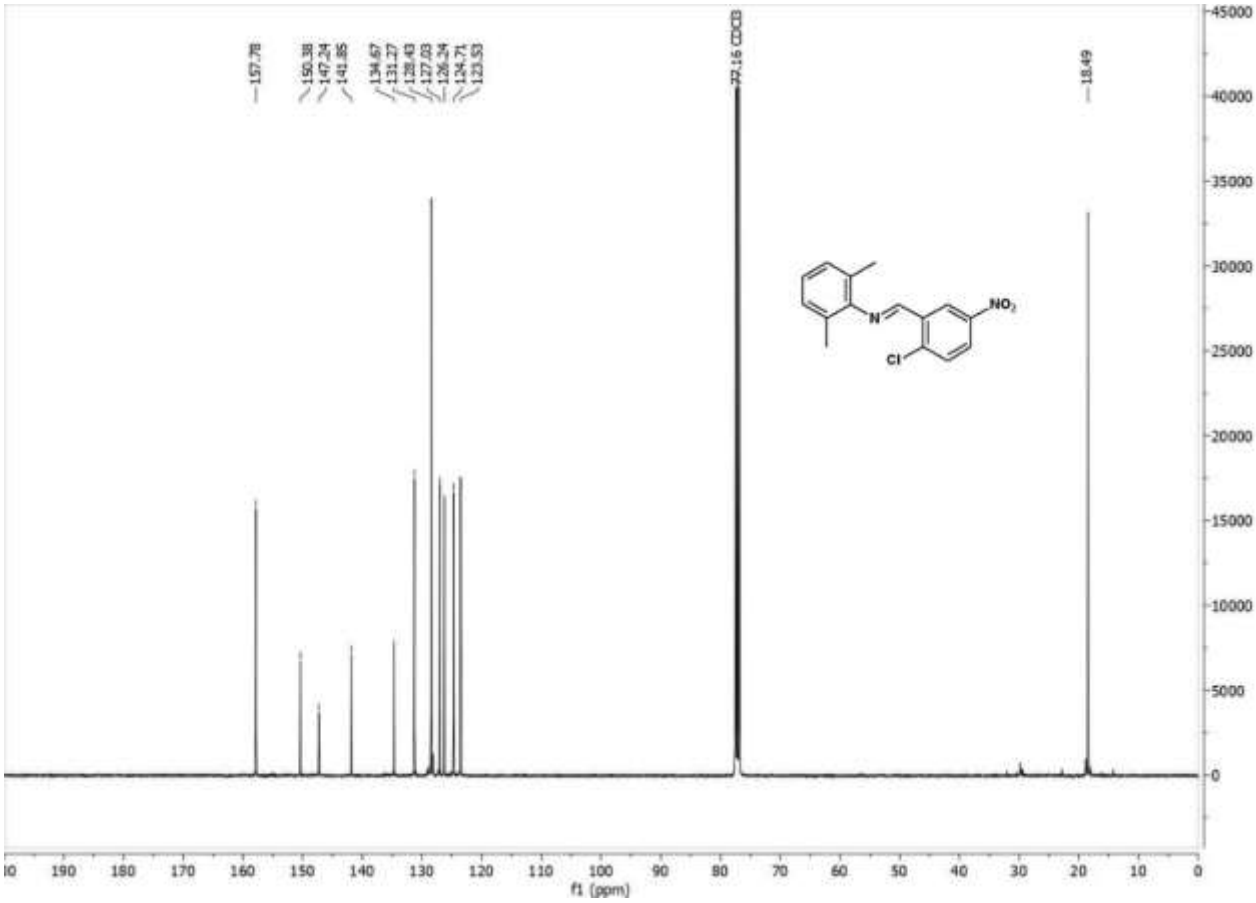

Figure C.57 $^{13}C(^{1}H)$ *NMR spectrum of* ***5gd*** *in* $CDCl_3$.

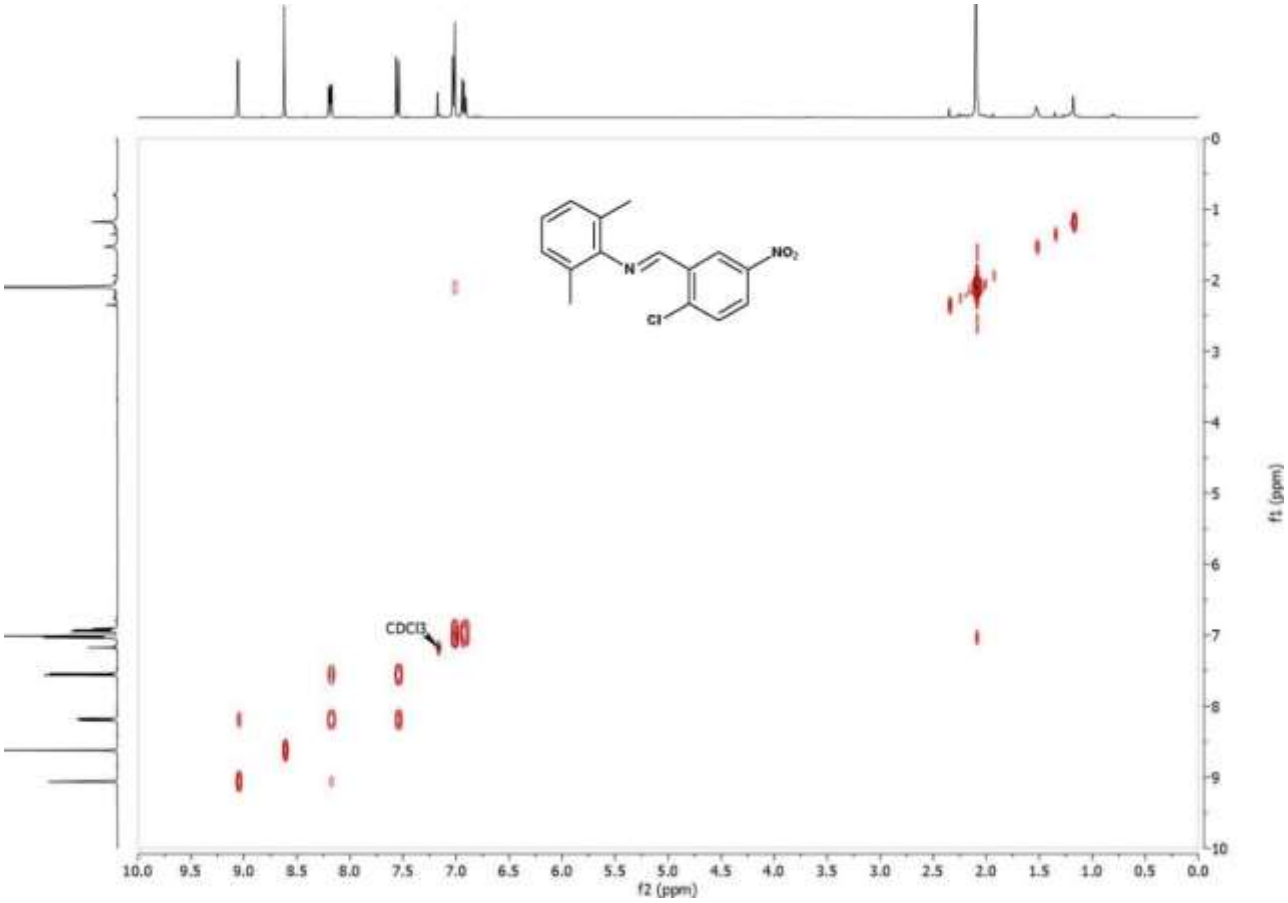

Figure C.58 COSY spectrum of ***5gd*** *in* $CDCl_3$.

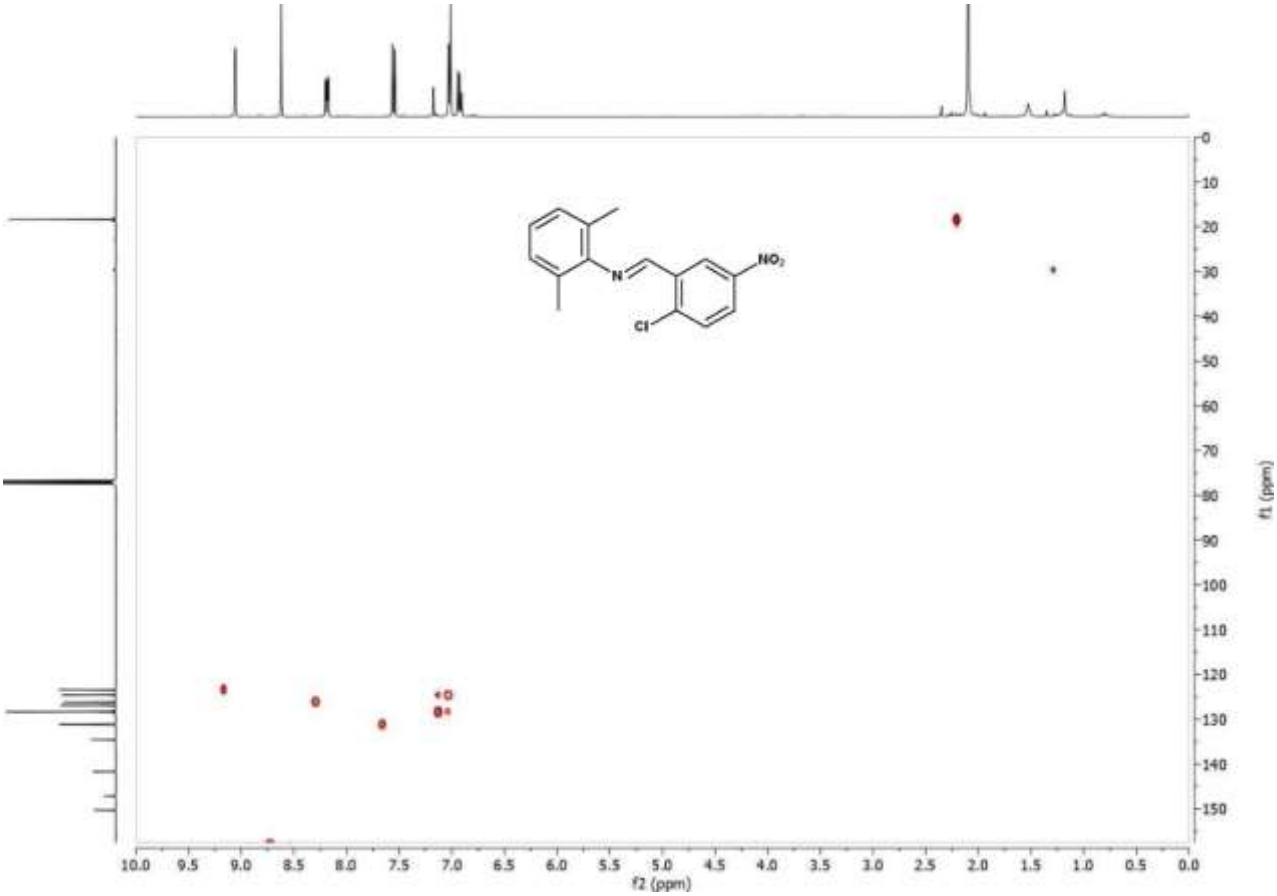

Figure C.59 HSQC spectrum of **5gd** in $CDCl_3$.

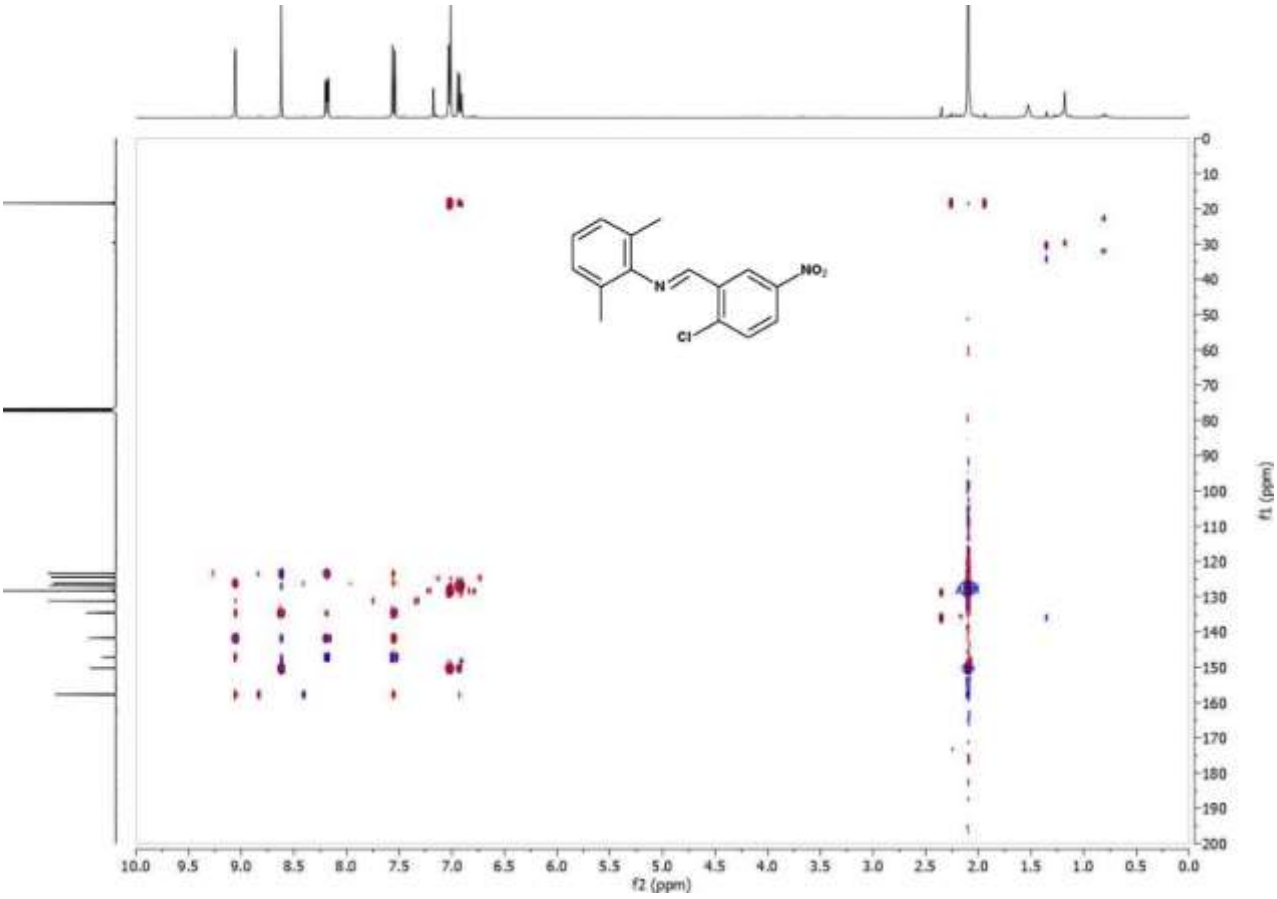

Figure C.60 HMBC spectrum of **5gd** in $CDCl_3$.

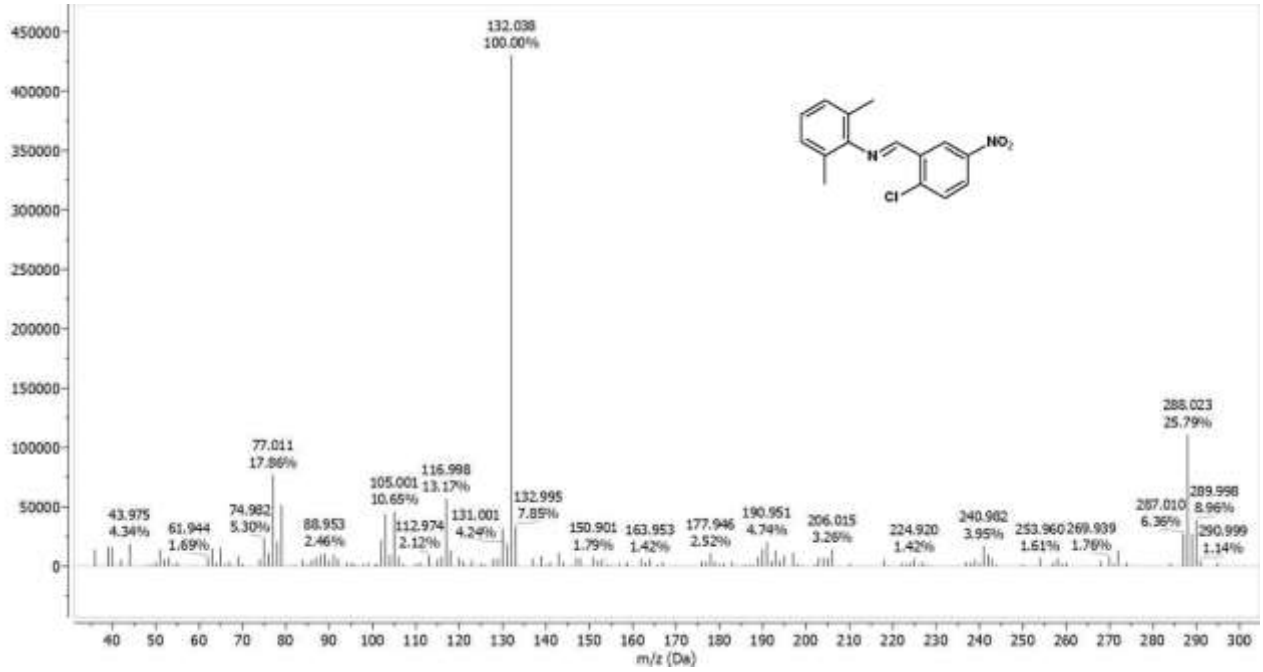

Figure C.61 *GC-MS spectrum of imine* ***5gd****.*

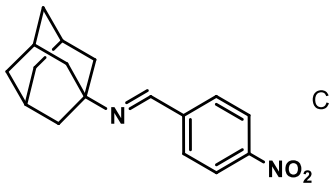

5ca

Chemical Formula: $C_{17}H_{20}N_2O_2$
Molecular Weight: 284,36

^{1}H NMR (400 MHz, Chloroform-d) δ [ppm] = 8.33 (s, 1H), 8.25 (d, J = 8.8 Hz, 2H), 7.91 (d, J = 8.7 Hz, 2H), 2.19 (s, 3H), 1.82 (d, J = 2.9 Hz, 6H), 1.74 (q, J = 12.5 Hz, 6H).

^{13}C NMR (101 MHz, CDCl3) δ [ppm] = 152.84, 148.93, 143.01, 128.69, 123.91, 58.71, 43.15, 36.66, 29.66.

GC/MS (EI): calc. for $C_{17}H_{20}N_2O_2$ $[M]^+$: 284.152; found: $[M]^+$ 284.145, $C_{10}H_{15}$ 135.126.

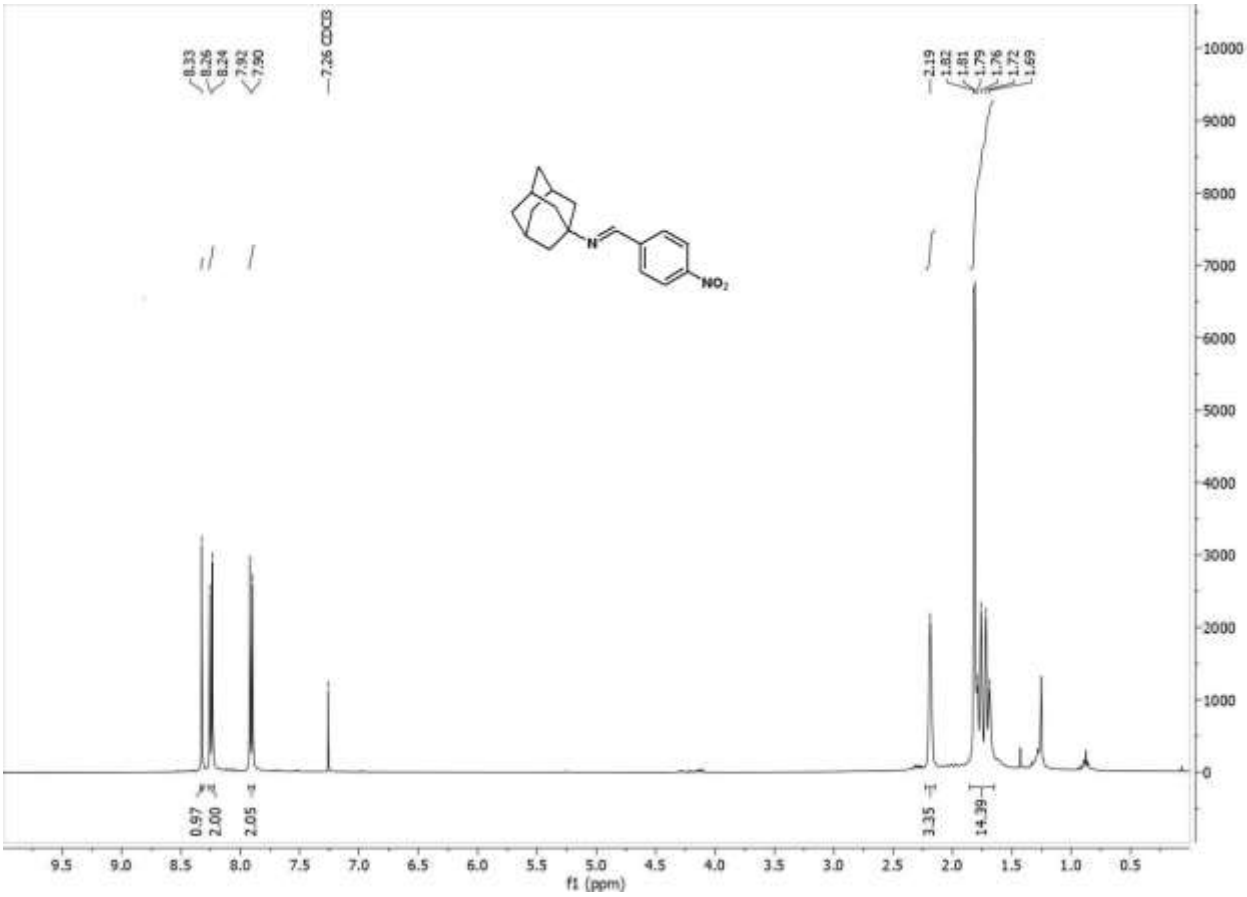

*Figure C.62 ^{1}H NMR spectrum of **5ca** in CDCl$_3$.*

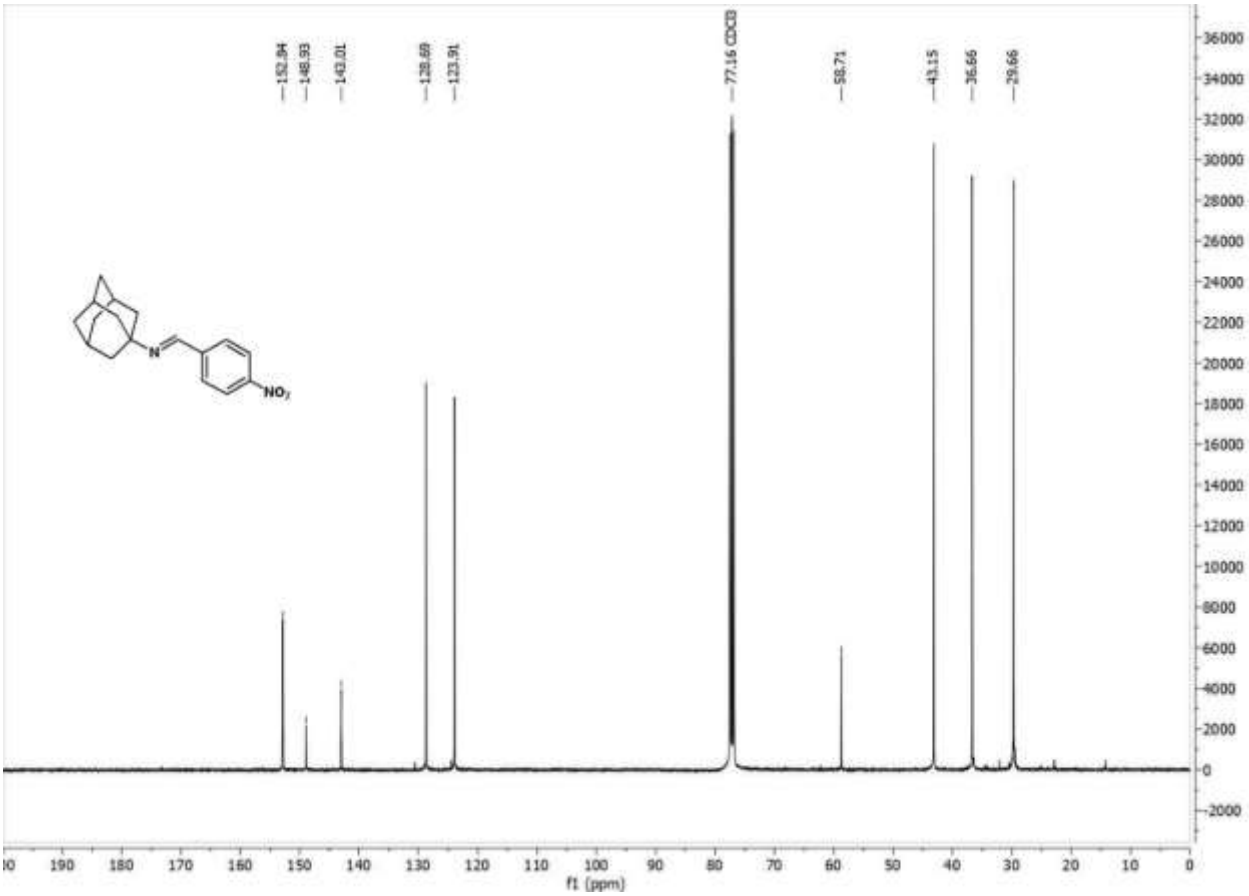

Figure C.63 $^{13}C(^{1}H)$ *NMR spectrum of* ***5ca*** *in* $CDCl_3$.

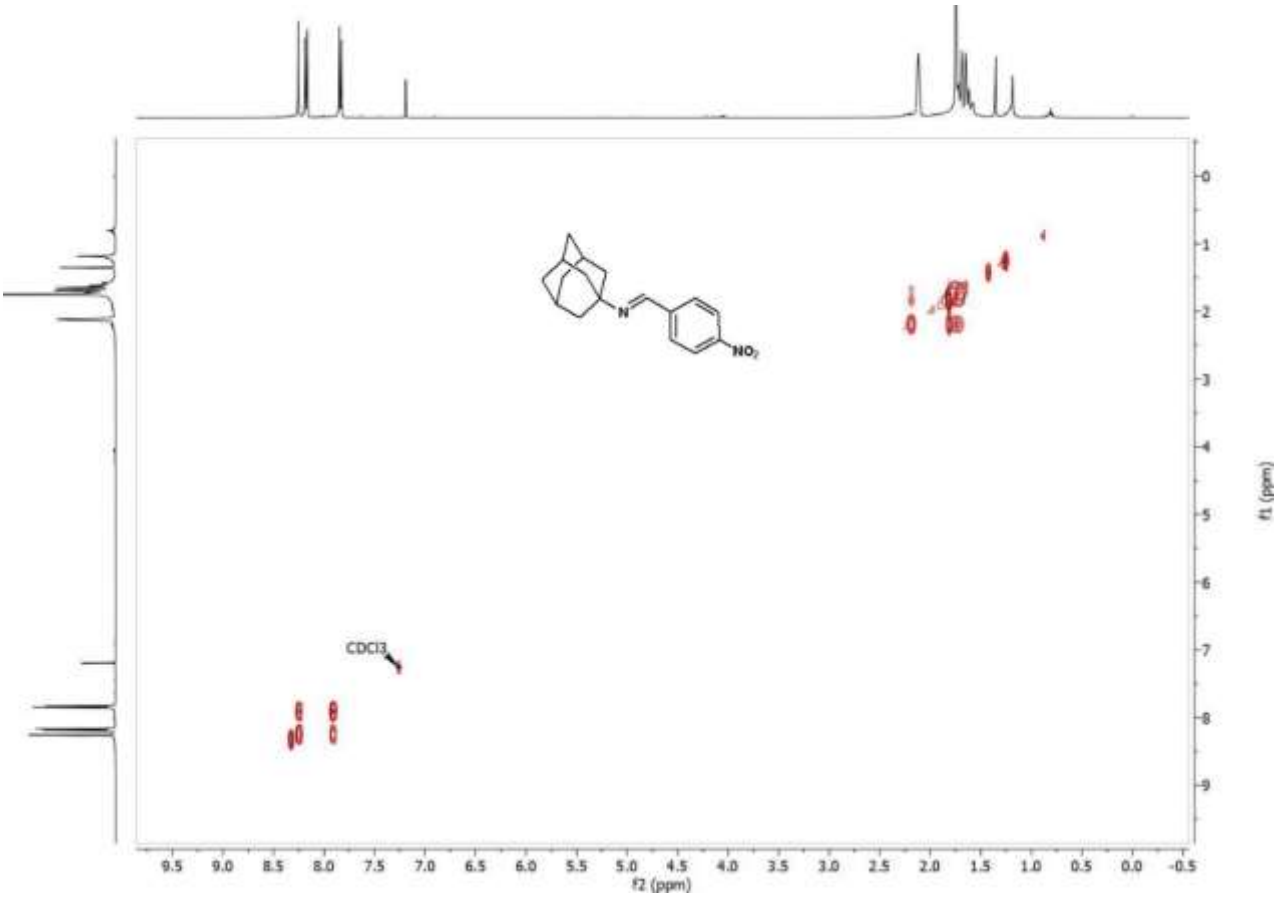

Figure C.63 COSY spectrum of ***5ca*** *in* $CDCl_3$.

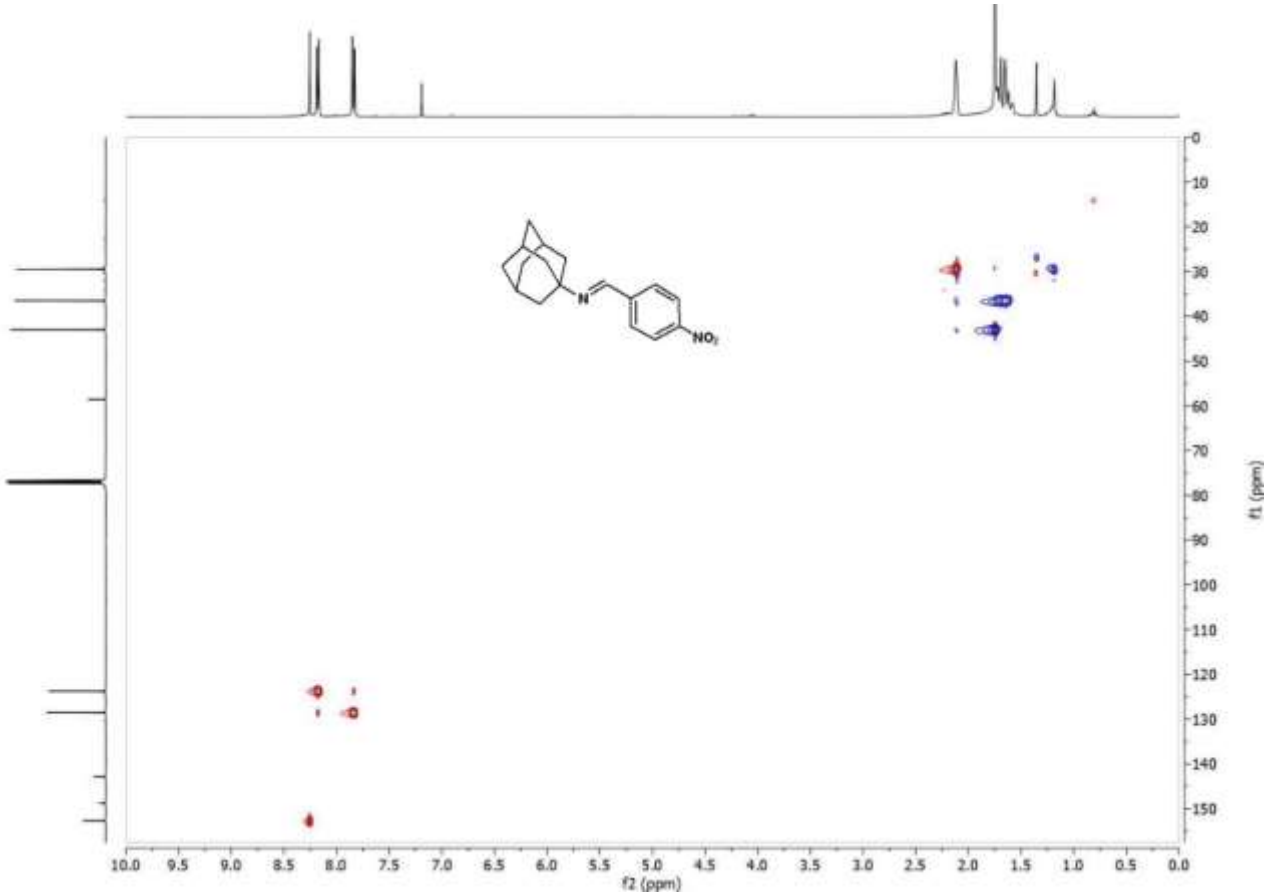

Figure C.64 HSQC spectrum of **5ca** in $CDCl_3$.

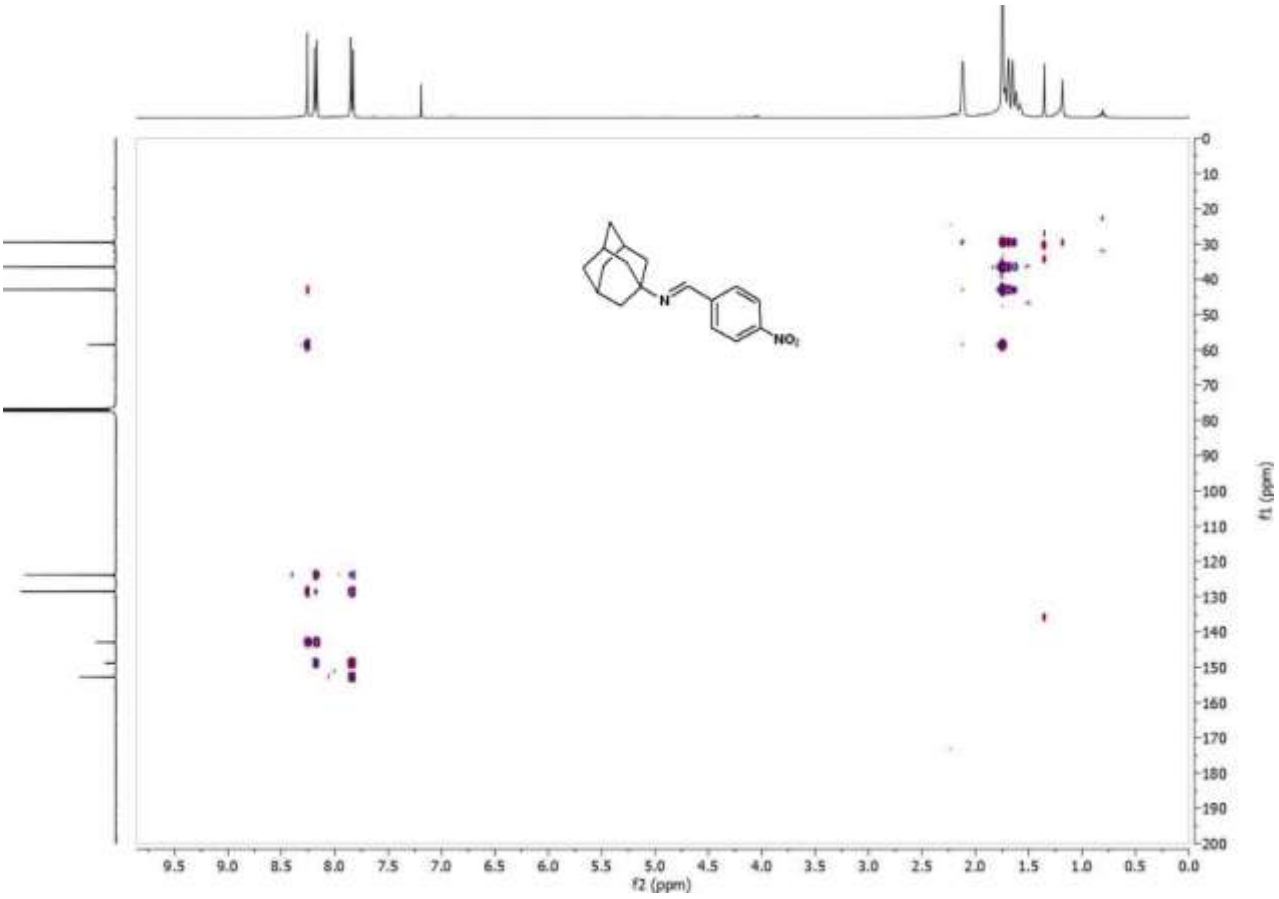

Figure C.65 HMBC spectrum of **5ca** in $CDCl_3$.

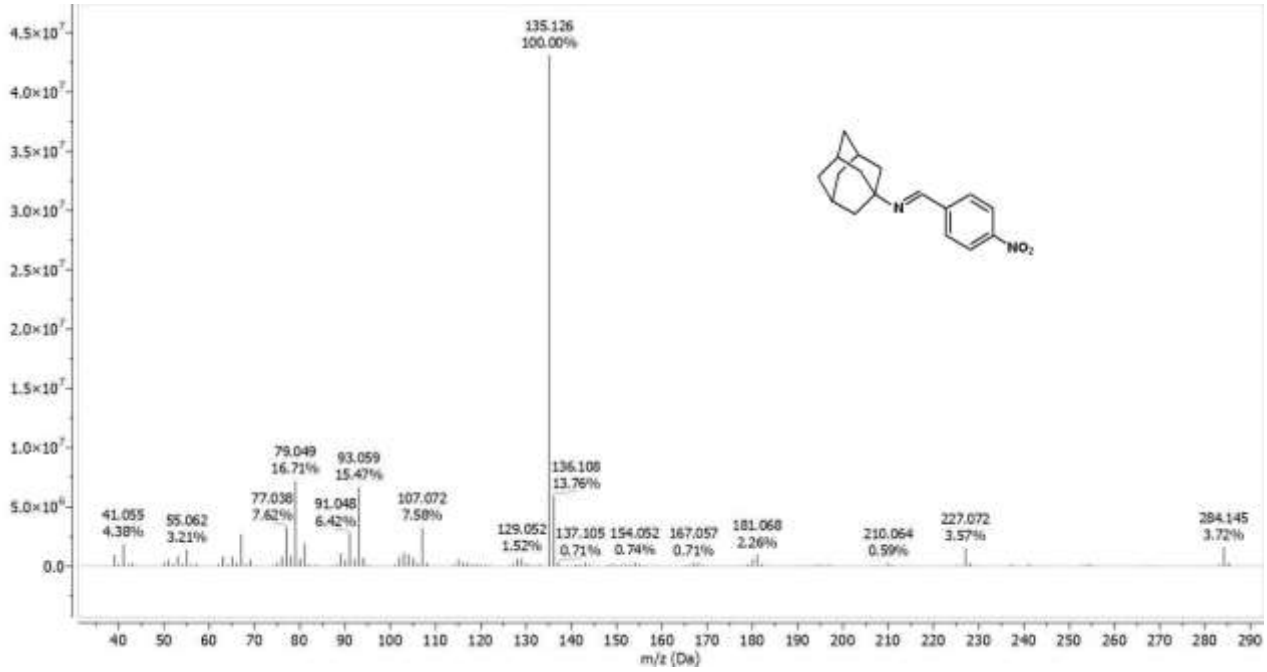

Figure C.66 GC-MS spectrum of imine **5ca**.

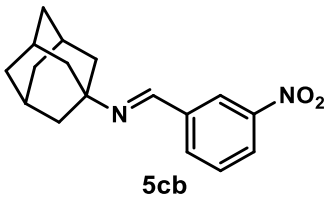

5cb

Chemical Formula: $C_{17}H_{20}N_2O_2$
Molecular Weight: 284,36

^{1}H NMR (400 MHz, Chloroform-d) δ [ppm] = 8.58 (t, J = 2.0 Hz, 1H), 8.32 (s, 1H), 8.23 (ddd, J = 8.2, 2.4, 1.1 Hz, 1H), 8.09 (dt, J = 7.7, 1.4 Hz, 1H), 7.57 (t, J = 7.9 Hz, 1H), 2.18 (s, 3H), 1.82 (d, J = 2.9 Hz, 6H), 1.72 (q, 14 Hz ,6H).

^{13}C NMR (101 MHz, Chloroform-d) δ [ppm] = 152.54, 148.75, 139.23, 133.55, 129.57, 124.68, 122.89, 58.40, 43.17, 36.66, 29.66.

GC/MS (EI): calc. for $C_{17}H_{20}N_2O_2$ $[M]^+$: 284.152; found: $[M]^+$ 284.131, $C_{10}H_{15}$ 135.128.

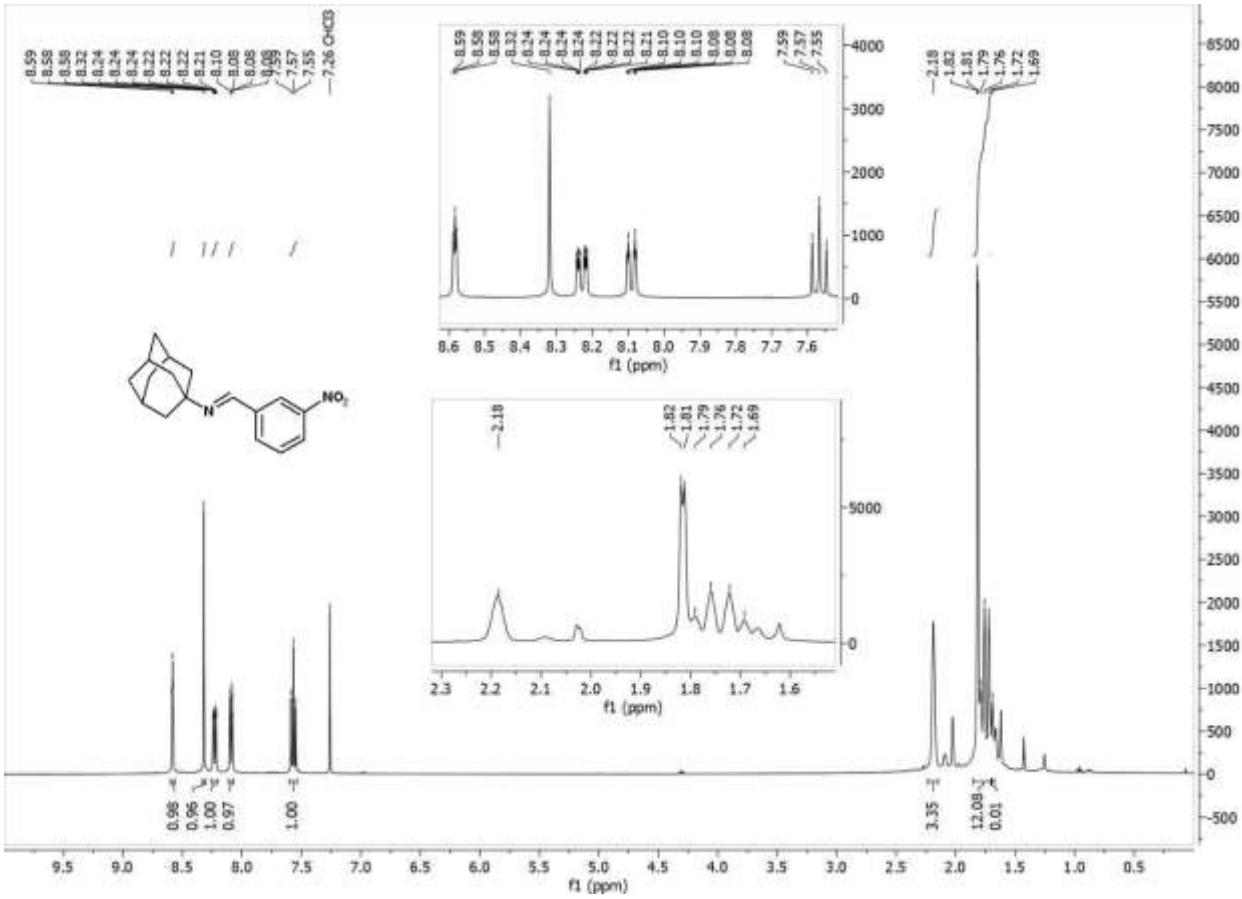

*Figure C.67 ^{1}H NMR spectrum of **5cb** in $CDCl_3$.*

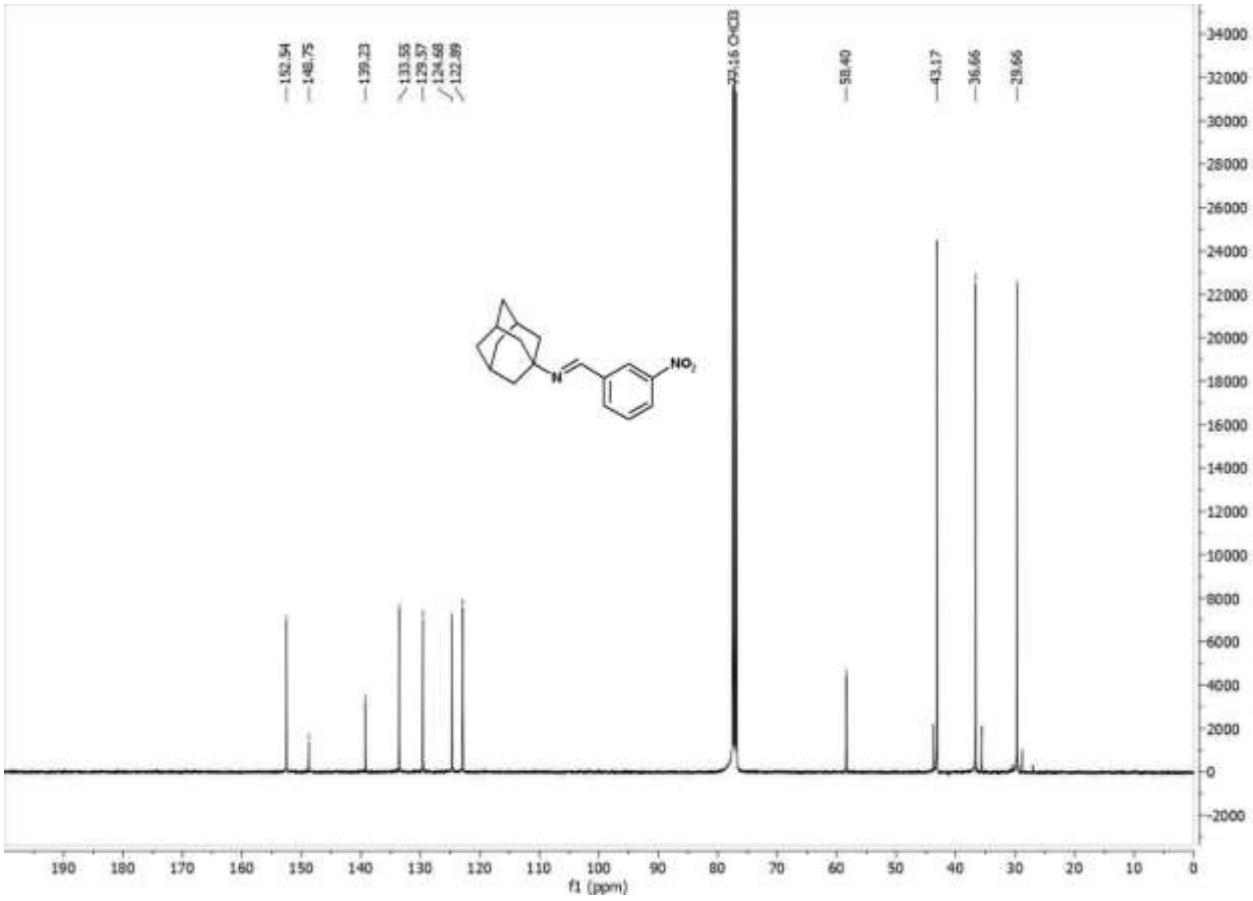

Figure C.68 $^{13}C(^{1}H)$ *NMR spectrum of* ***5cb*** *in* $CDCl_3$.

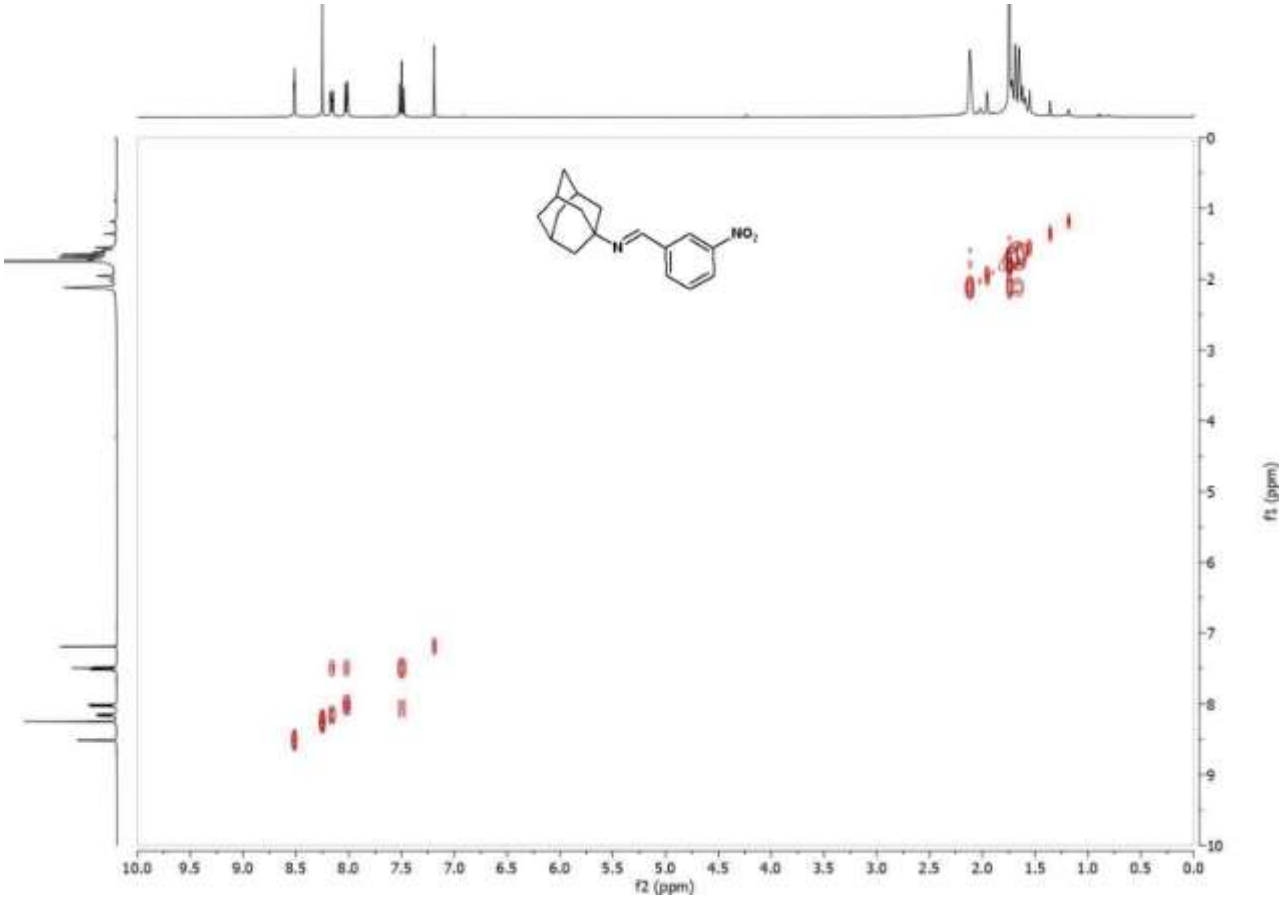

Figure C.69 COSY spectrum of ***5cb*** *in* $CDCl_3$.

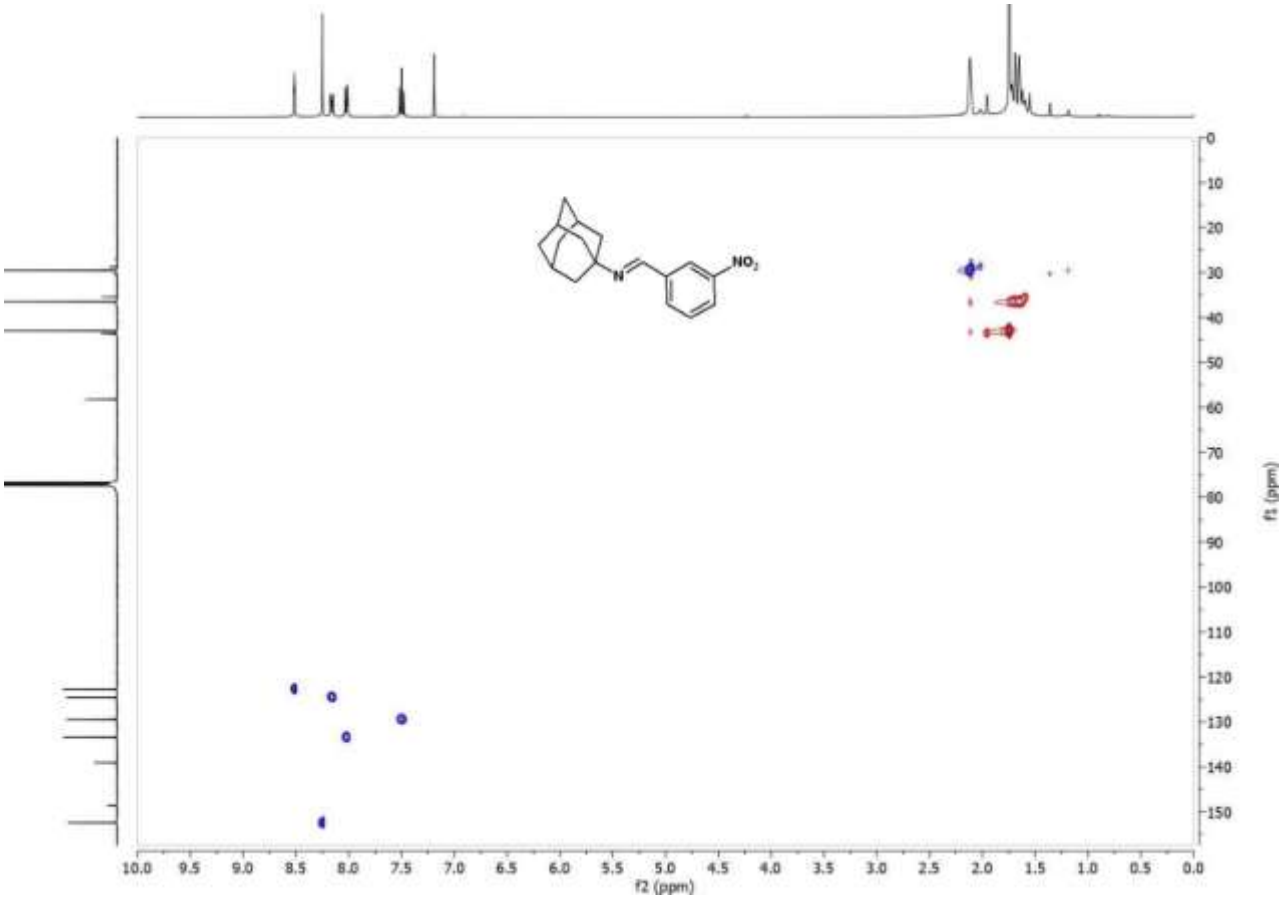

Figure C.70 HSQC spectrum of **5cb** in $CDCl_3$.

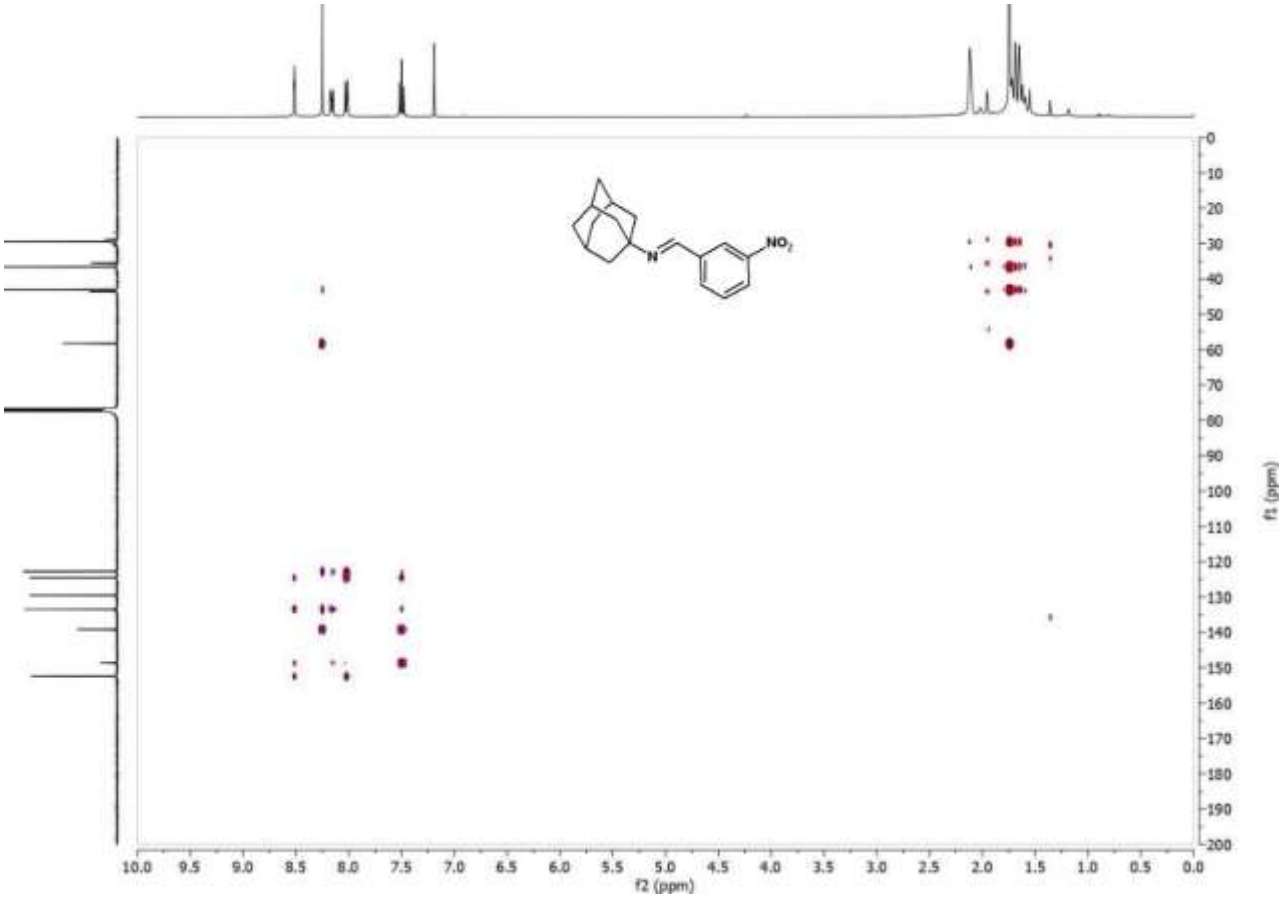

Figure C.71 HMBC spectrum of **5cb** in $CDCl_3$.

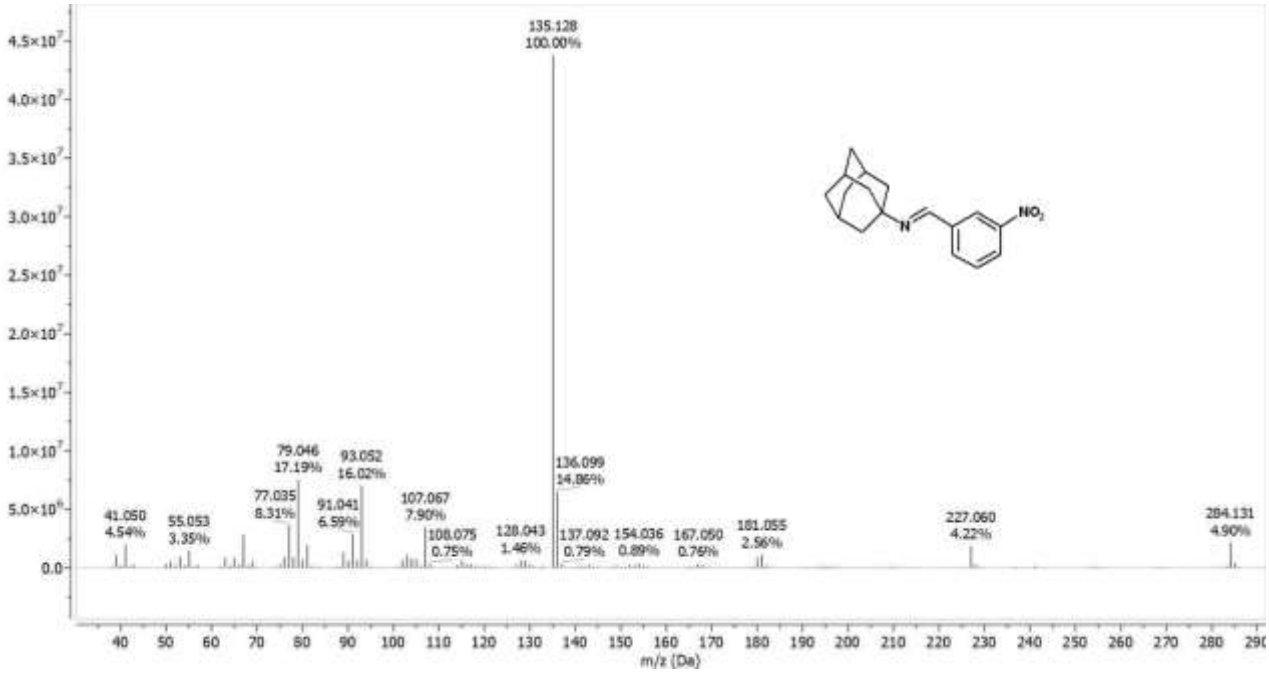

Figure C.72 *GC-MS spectrum of imine 5cb.*

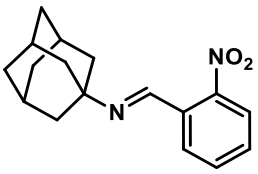

5cc

Chemical Formula: $C_{17}H_{20}N_2O_2$
Molecular Weight: 284,36

^{1}H NMR (400 MHz, Chloroform-d) δ [ppm] = 8.66 (s, 1H), 8.01 (d, J = 7.2 Hz, 2H), 7.65 (t, J = 7.6 Hz, 2H), 7.52 (t, J = 7.7 Hz, 1H), 2.18 (s, 3H), 1.83 (d, J = 2.9 Hz, 6H), 1.74 (q, J = 11.8 Hz, 6H).

^{13}C NMR (101 MHz, Chloroform-d) δ [ppm] = 151.90, 148.95, 133.66, 132.81, 130.24, 129.77, 124.34, 58.79, 43.04, 36.63, 29.66.

GC/MS (EI): calc. for $C_{17}H_{20}N_2O_2$ $[M]^+$: 284.152; found: $[M]^+$ 284.106 (very low intensity), $C_{10}H_{15}$ 135.105.

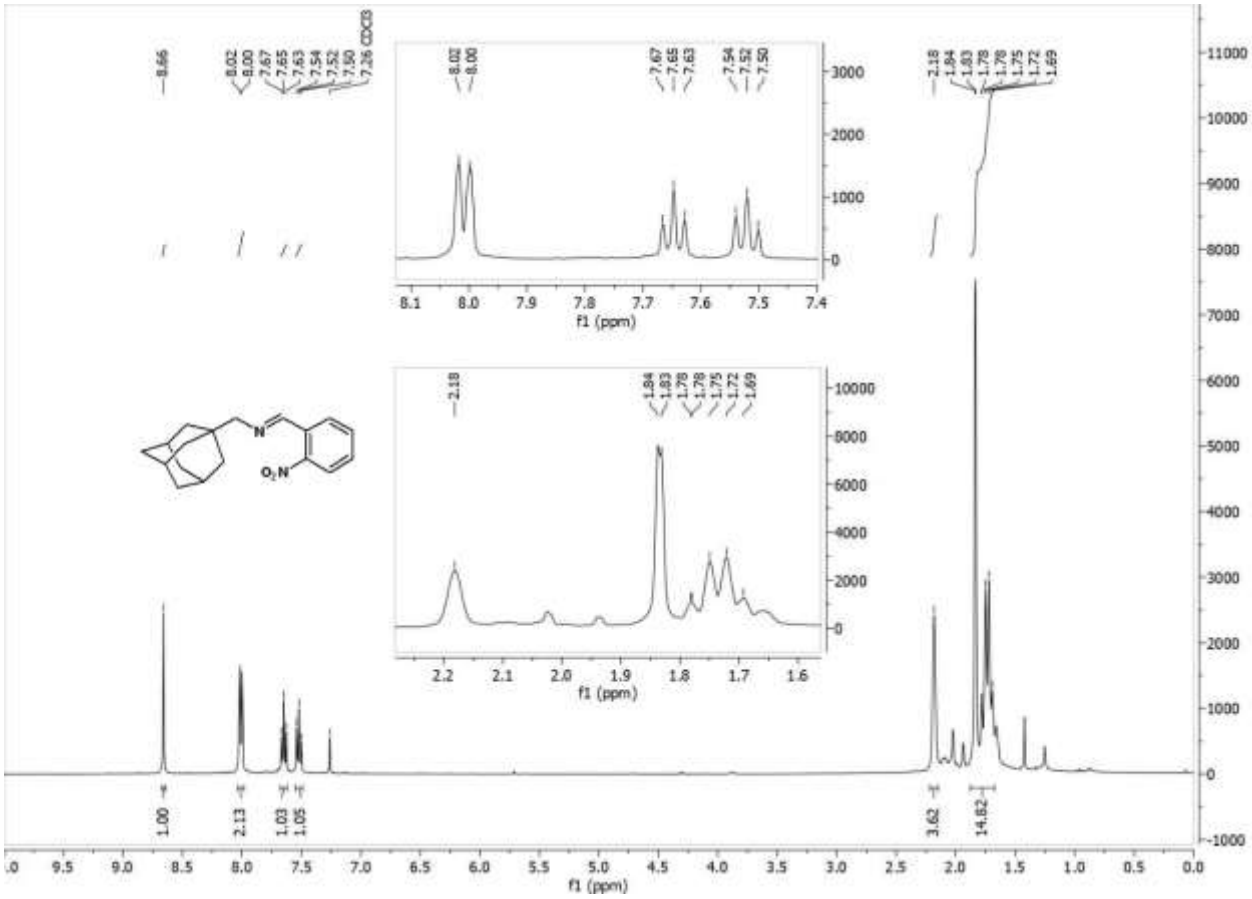

*Figure C.73 ^{1}H NMR spectrum of **5cc** in $CDCl_3$.*

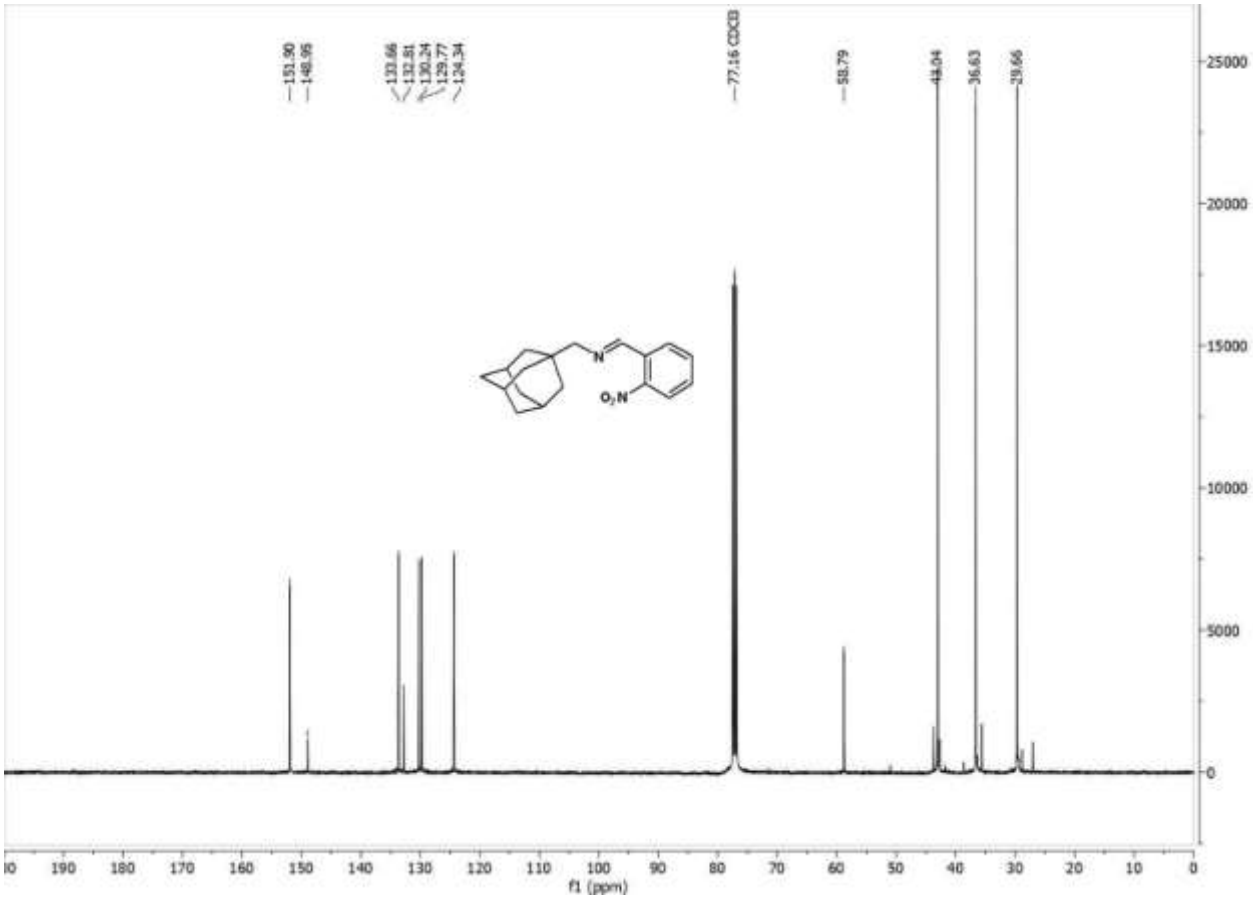

Figure C.74 $^{13}C(^{1}H)$ *NMR spectrum of* ***5cc*** *in* $CDCl_3$.

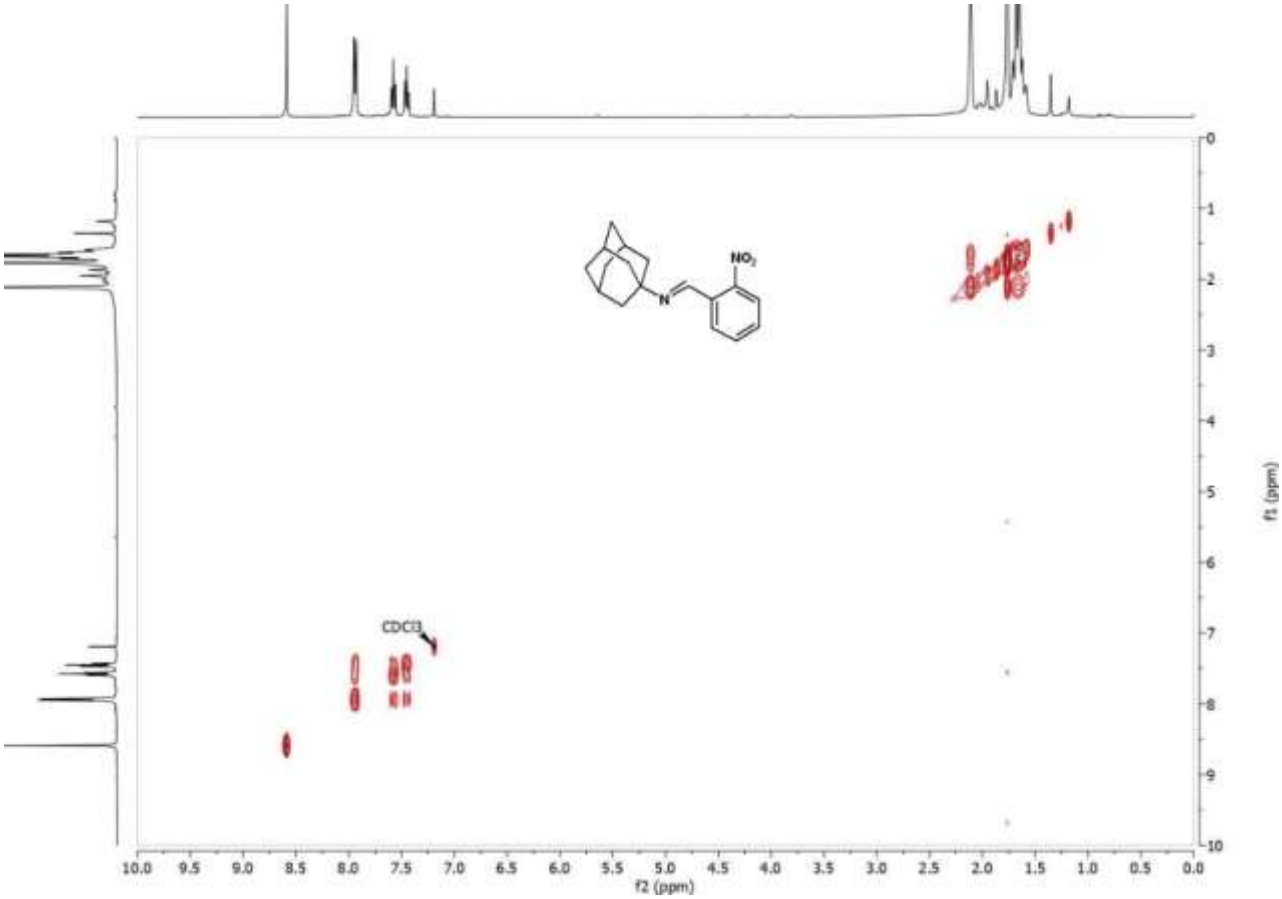

Figure C.75 COSY spectrum of ***5cc*** *in* $CDCl_3$.

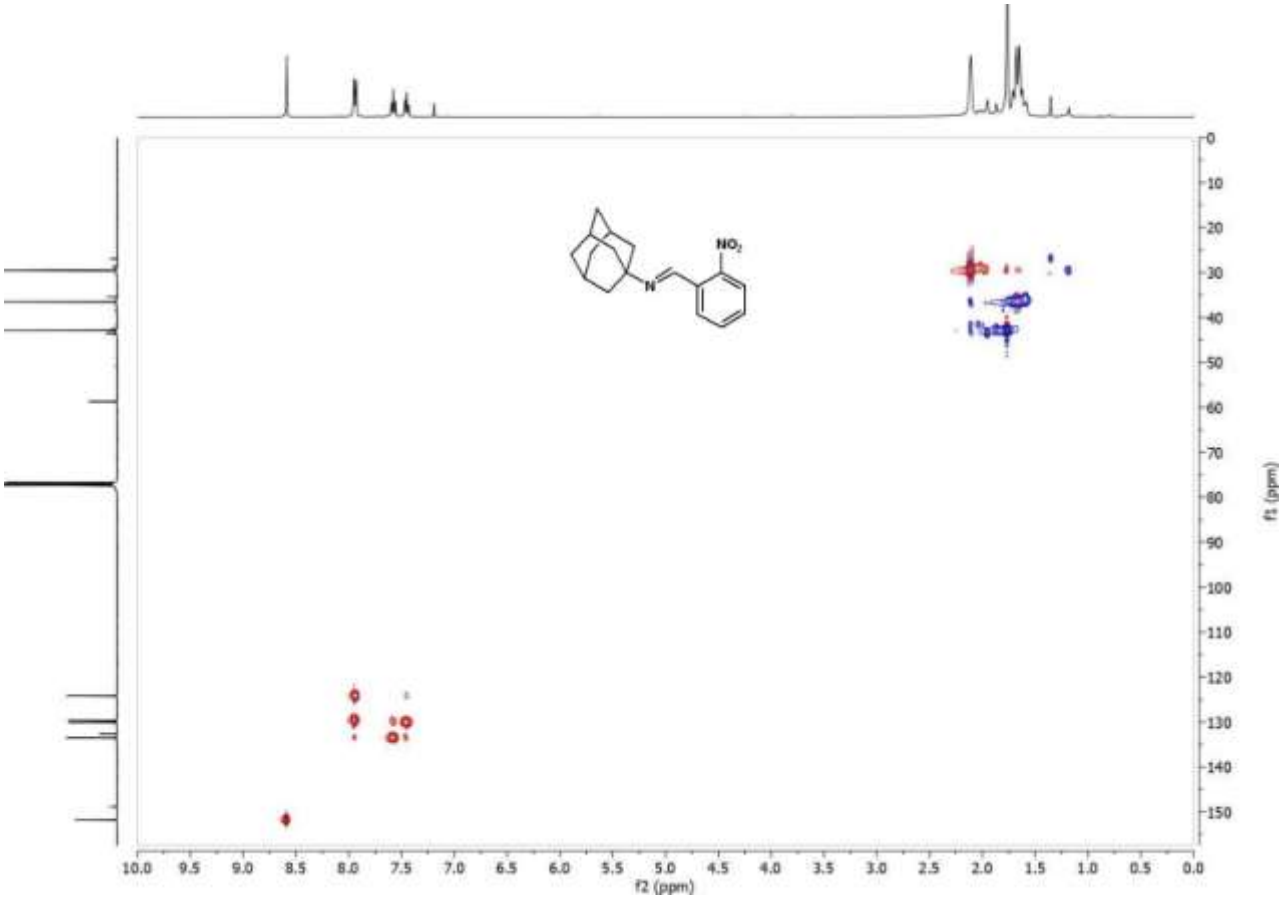

Figure C.76 HSQC spectrum of **5cc** in $CDCl_3$.

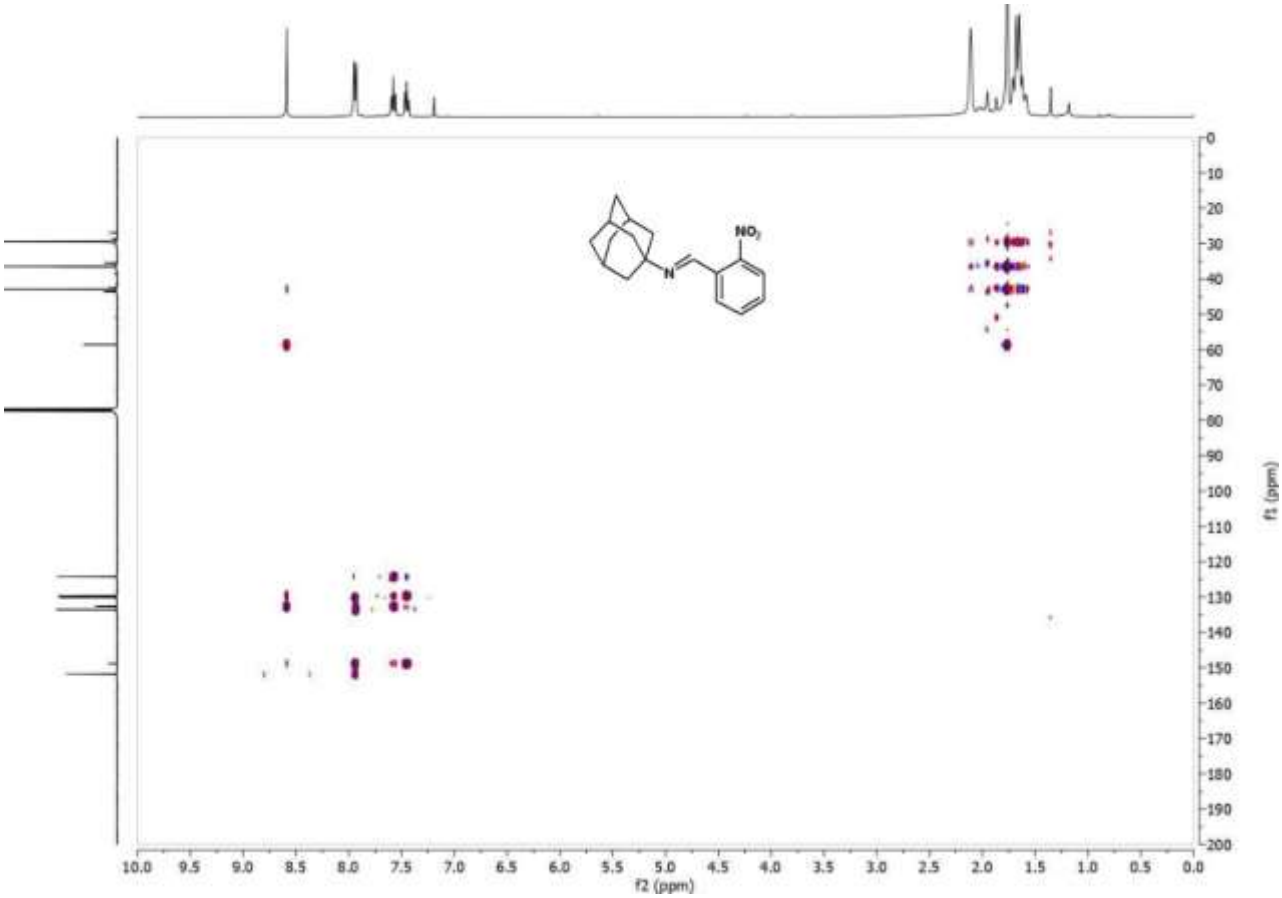

Figure C.78 HMBC spectrum of **5cc** in $CDCl_3$.

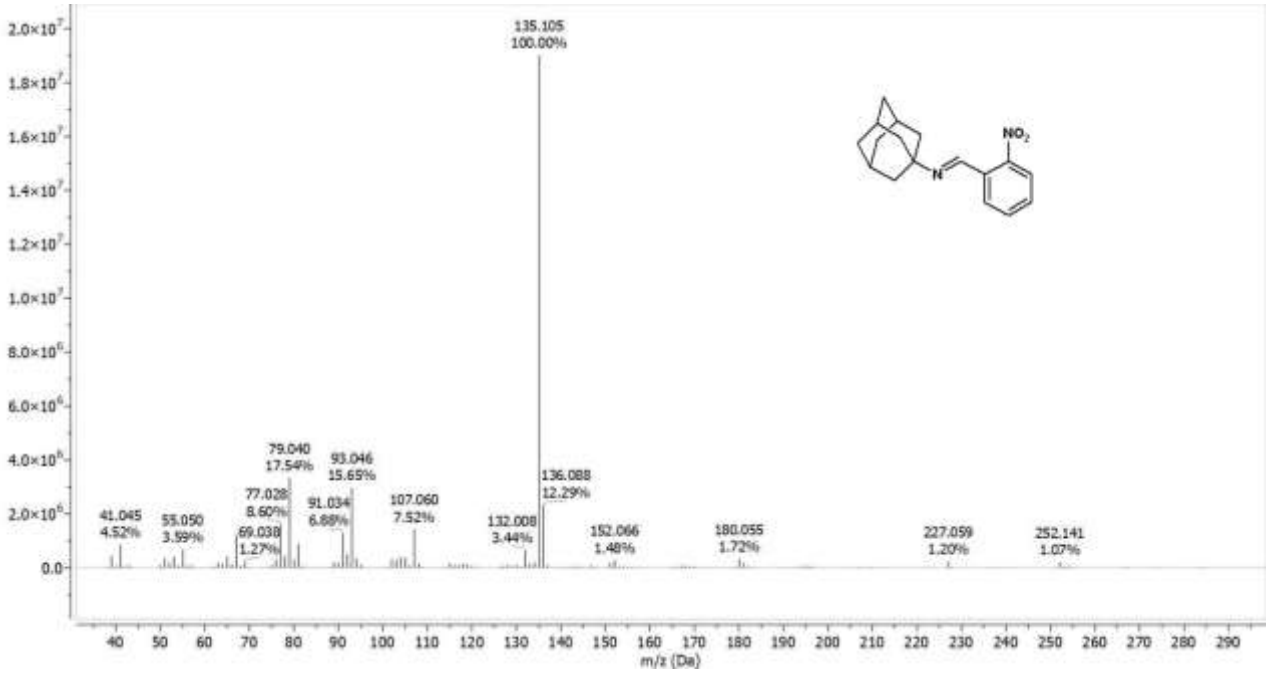

Figure C.79 GC-MS spectrum of imine **5cc**.

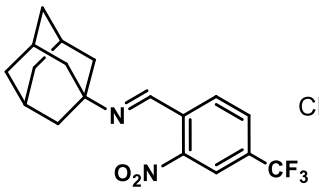

Chemical Formula: $C_{18}H_{19}F_3N_2O_2$
Molecular Weight: 352,36

5ce

^{1}H NMR (400 MHz, Chloroform-d) δ [ppm] = 8.67 (s, 1H), 8.27 (s, 1H), 8.21 (d, J = 8.1 Hz, 1H), 7.89 (d, J = 8.2 Hz, 1H), 2.20 (s, 3H), 1.83 (d, J = 2.9 Hz, 6H), 1.75 (q, J = 12.3 Hz, 6H).

^{13}C NMR (101 MHz, Chloroform-d) δ [ppm] = 150.57, 148.83, 135.73, 132.59 (q, J = 34.2 Hz), 130.92, 129.96 (q, J = 3.5 Hz), 122.9 (q, J = 273 Hz), 121.82 (q, J = 3.9 Hz), 59.45, 42.97, 36.57, 29.61.

^{19}F NMR (376 MHz, Chloroform-d) δ [ppm] = -62.98.

GC/MS (EI): calc. for $C_{18}H_{19}F_3N_2O_2$ $[M]^+$: 352.140; found: $[M]^+$ 352.124 (very low intensity), $C_{10}H_{15}$ 135.105.

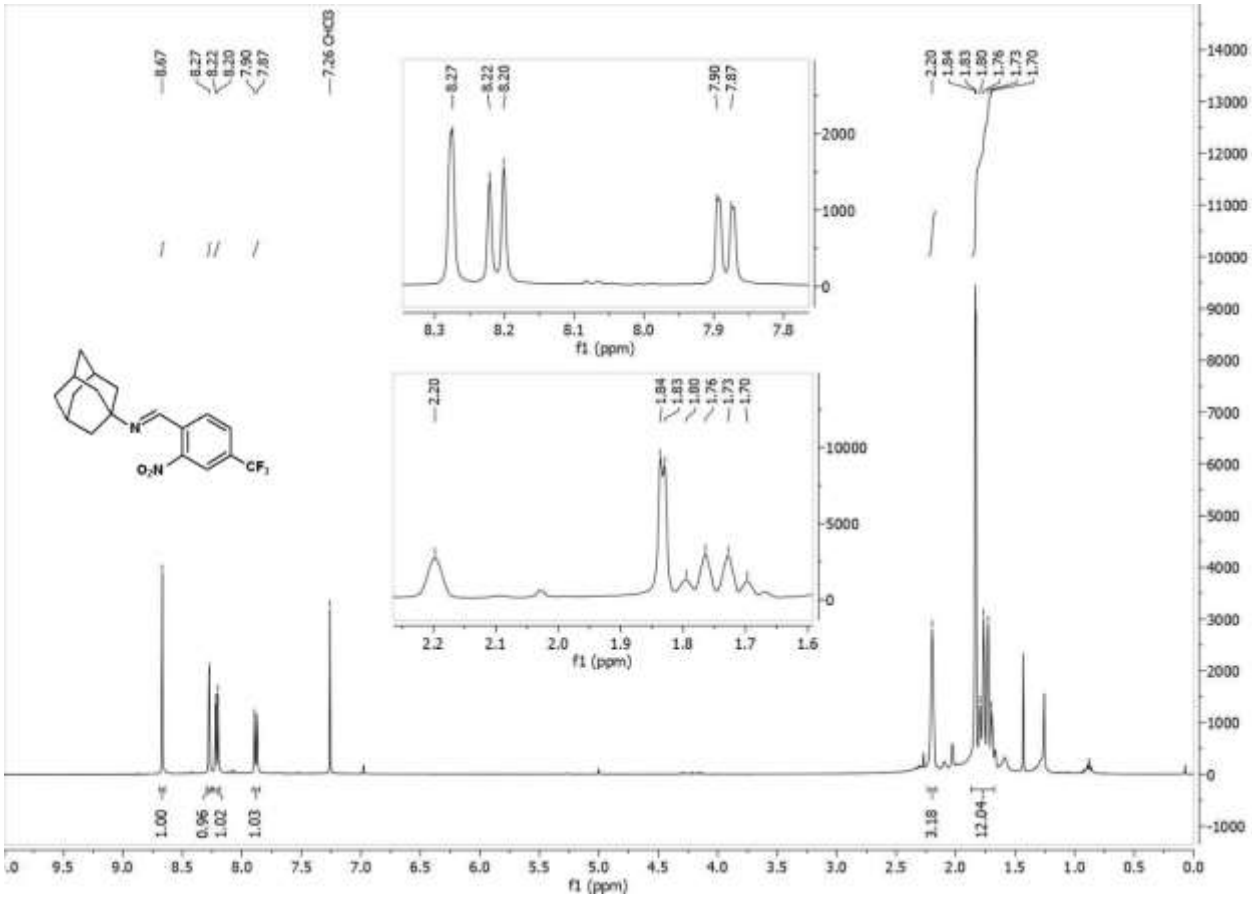

*Figure C.80 ^{1}H NMR spectrum of **5ce** in $CDCl_3$.*

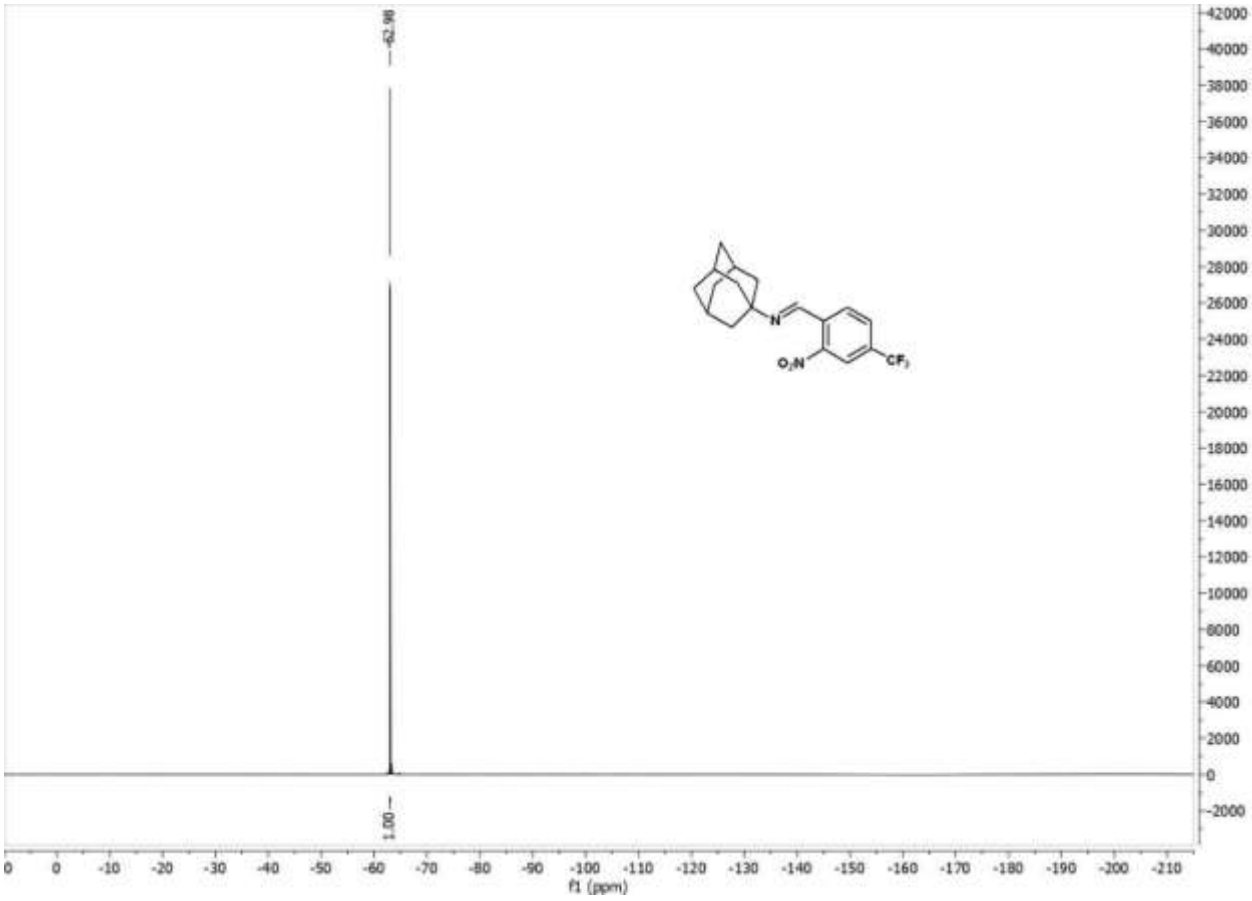

Figure C.81 *^{19}F NMR spectrum of 5ce in $CDCl_3$.*

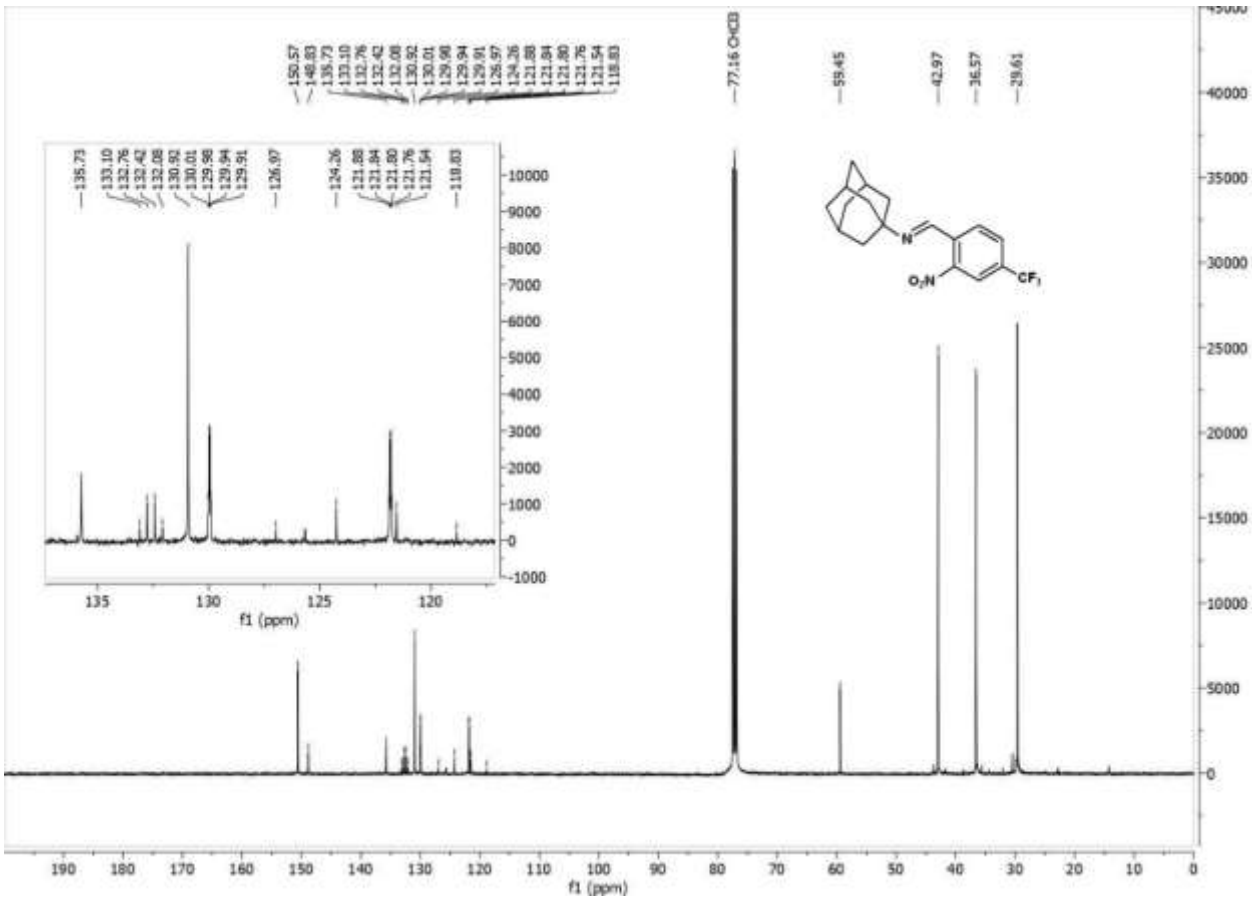

Figure C.82 *$^{13}C(^{1}H)$ NMR spectrum of **5ce** in $CDCl_3$.*

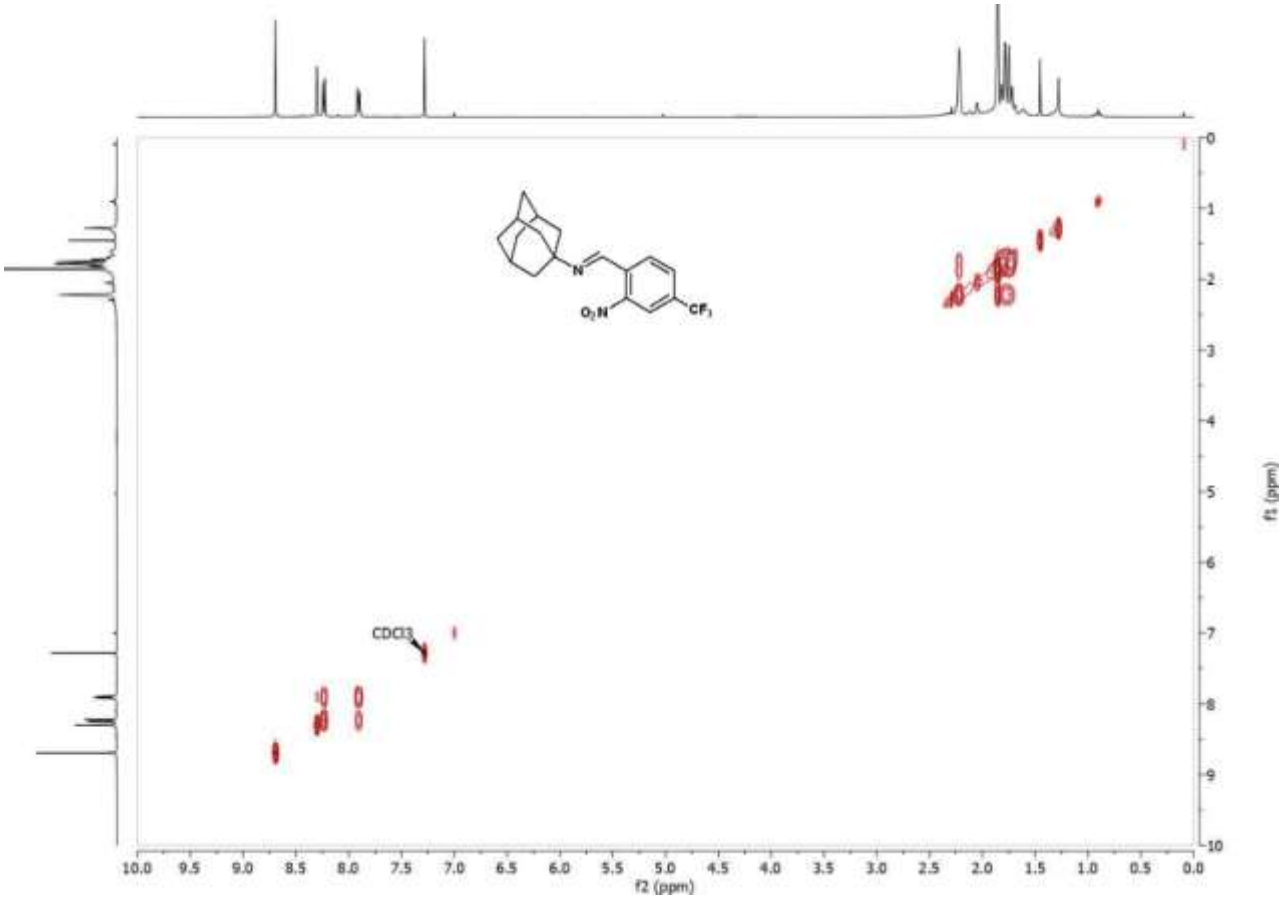

Figure C.83 COSY spectrum of **5ce** in $CDCl_3$.

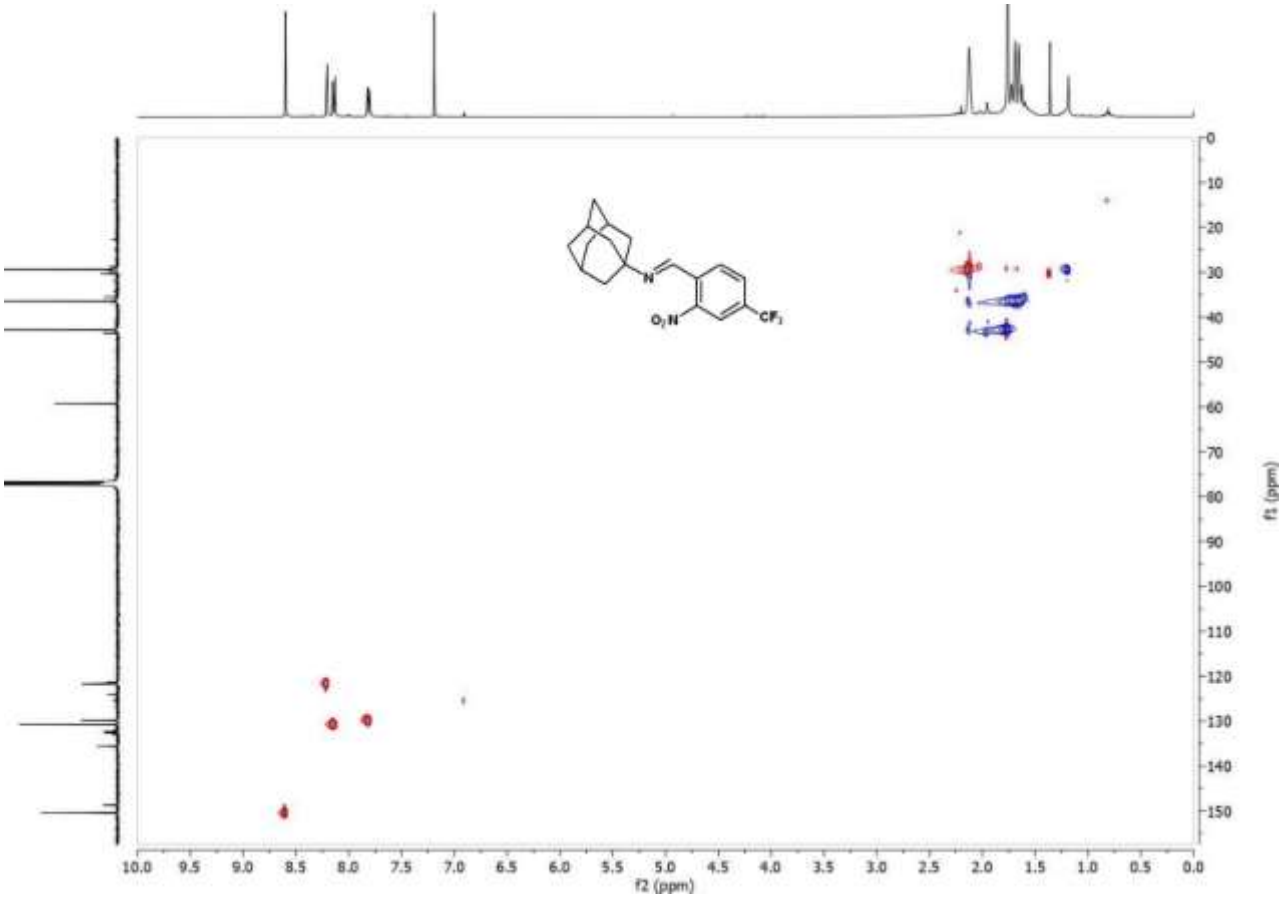

Figure C.84 HSQC spectrum of **5ce** in $CDCl_3$.

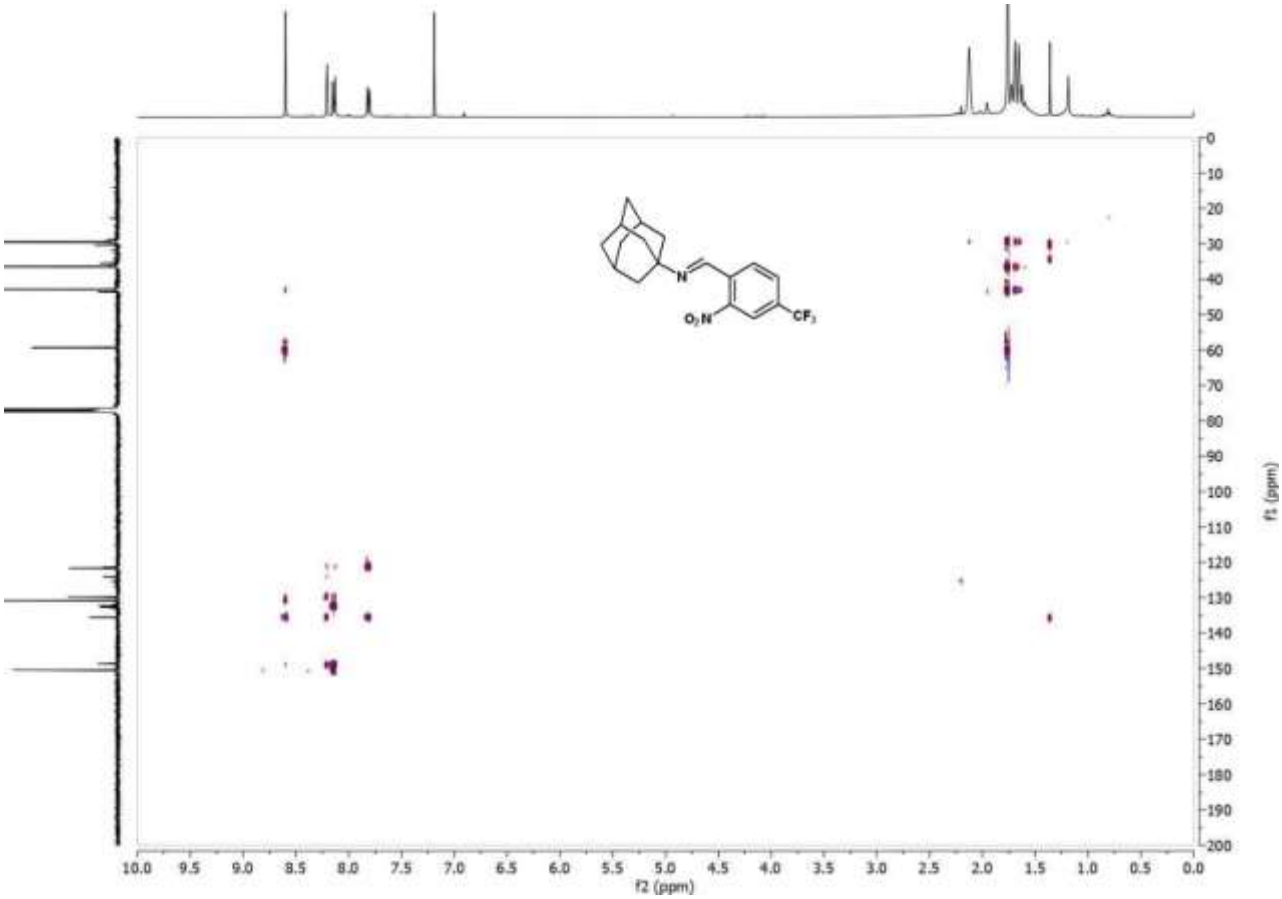

Figure C.85 HMBC spectrum of **5ce** in $CDCl_3$.

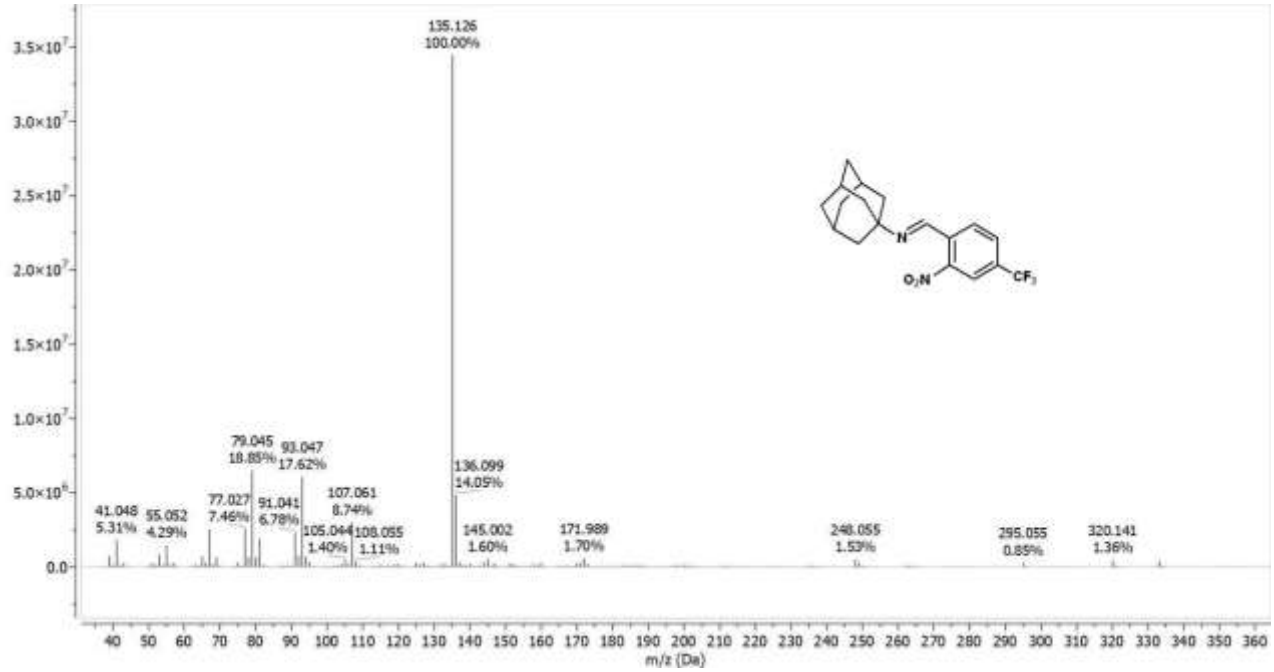

Figure C.86 GC-MS spectrum of imine **5ce**.

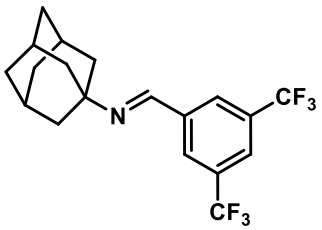

Chemical Formula: $C_{19}H_{19}F_6N$
Molecular Weight: 375,36

5cf

^{1}H NMR (400 MHz, Chloroform-d) δ [ppm] = 8.32 (s, 1H), 8.21 (s, 2H), 7.88 (s, 1H), 2.19 (s, 3H), 1.82 (d, J = 3.0 Hz, 6H), 1.75 (q, J = 15.5 Hz, 6H).

^{13}C NMR (101 MHz, Chloroform-d) δ [ppm] = 152.00, 139.45, 132.06 (q, J = 33.5 Hz), 128.05 - 127.85 (m), 123.52 (p, J = 3.7 Hz), 123.4 (q, J = 272 Hz), 58.61, 43.13, 36.65, 29.65.

^{19}F NMR (376 MHz, Chloroform-d) δ [ppm] = -62.90.

GC/MS (EI): calc. for $C_{19}H_{19}F_6N$ $[M]^+$: 375.142; found: $[M]^+$ 375.141, $C_{10}H_{15}$ 135.165.

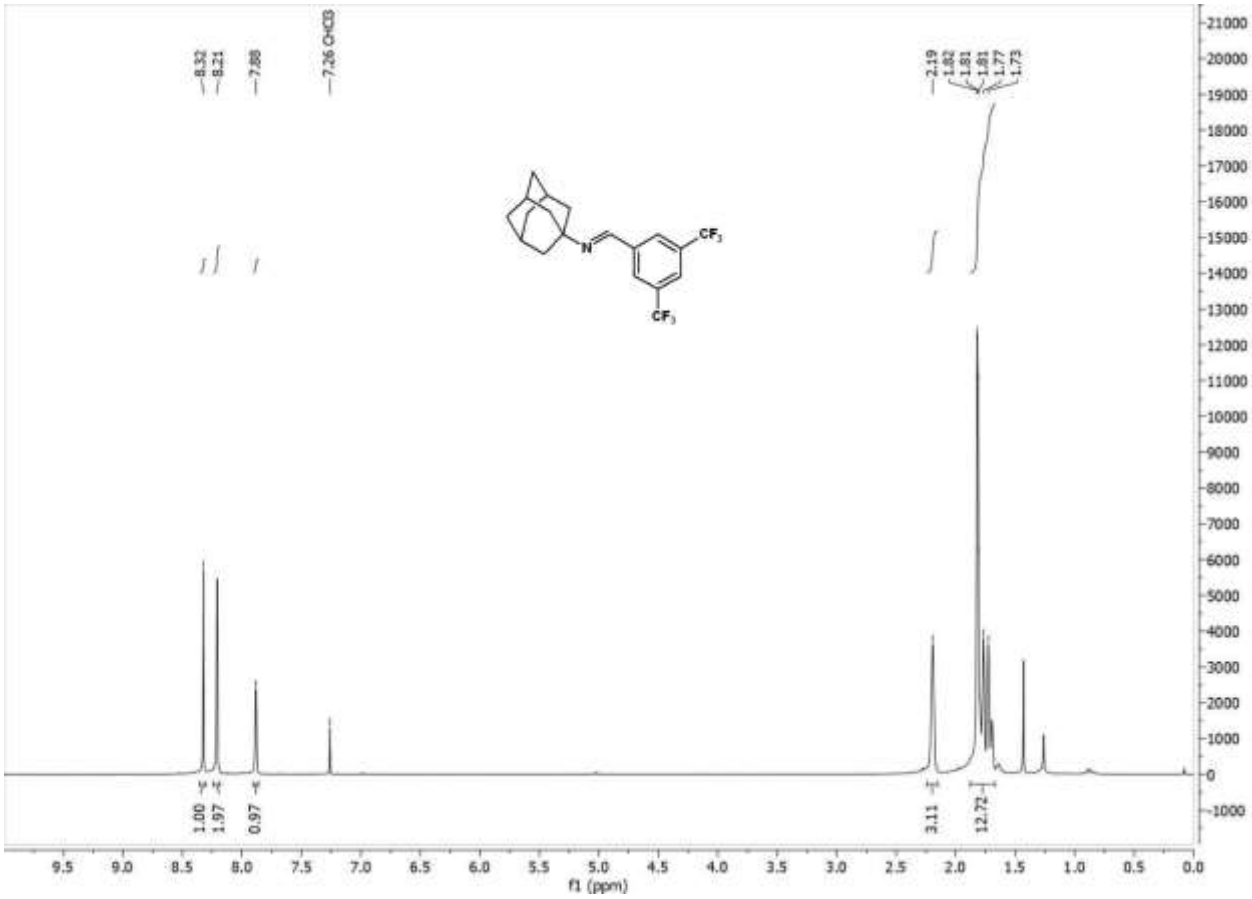

*Figure C.87 ^{1}H NMR spectrum of **5cf** in $CDCl_3$.*

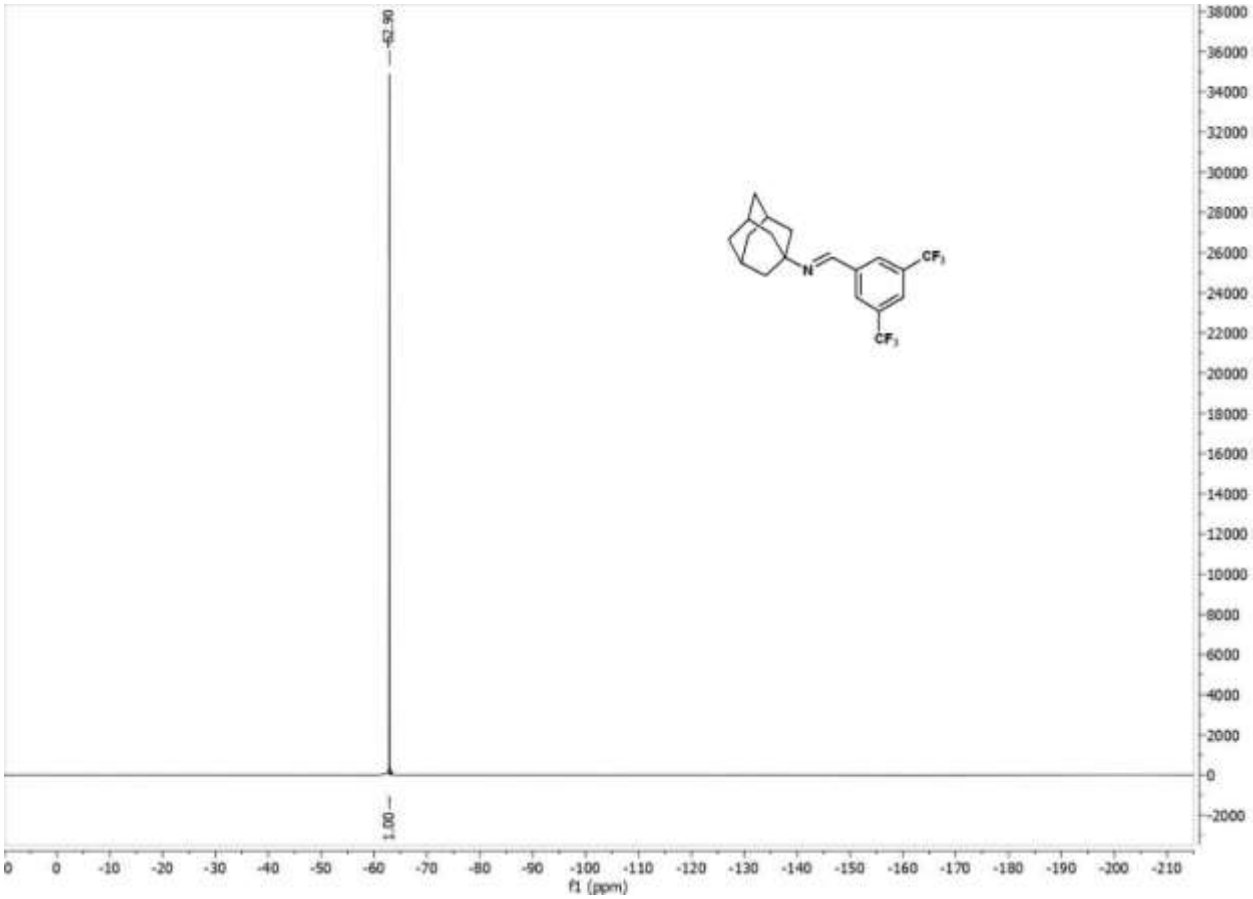

Figure C.88 ^{19}F *NMR spectrum of* ***5cf*** *in* $CDCl_3$.

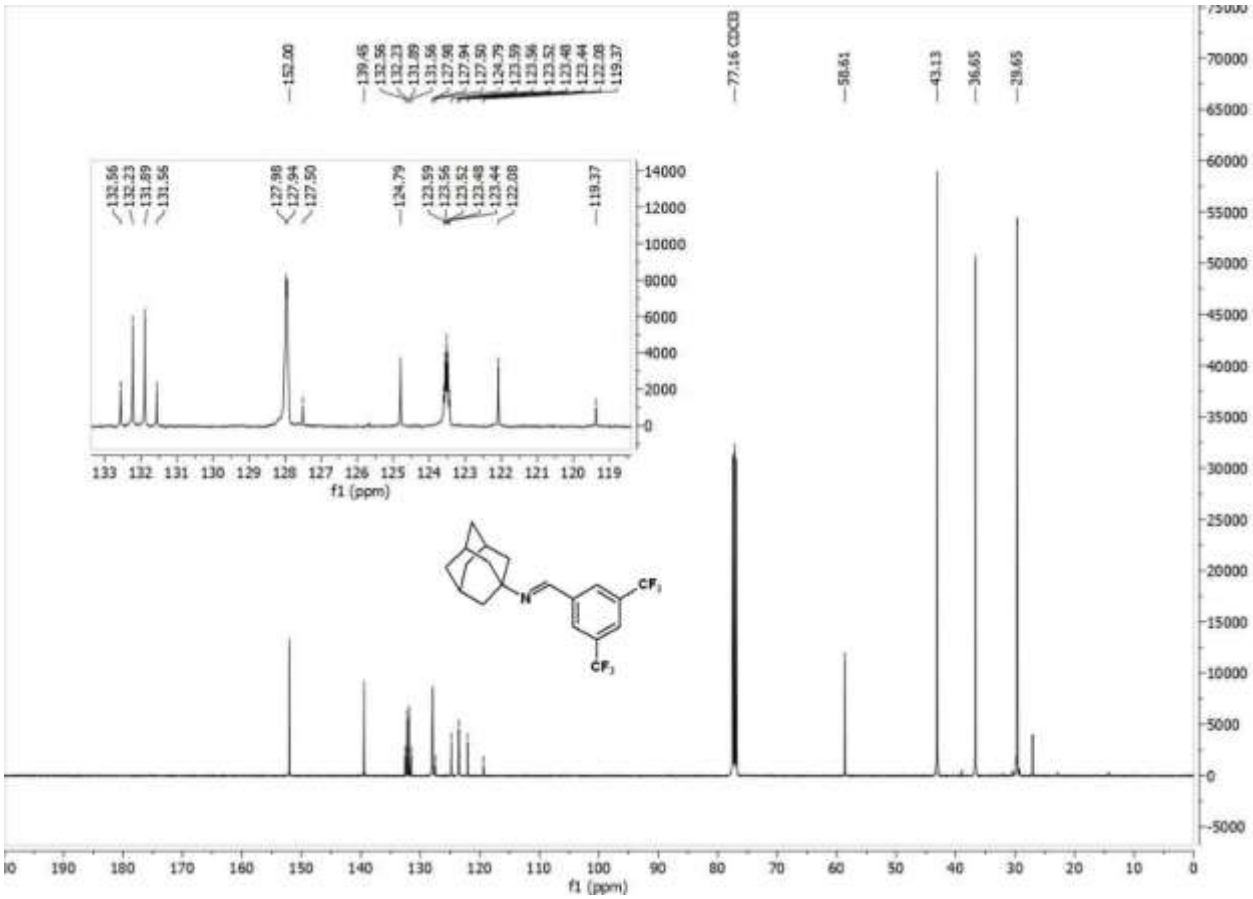

Figure C.89 $^{13}C(^{1}H)$ *NMR spectrum of* ***5cf*** *in* $CDCl_3$.

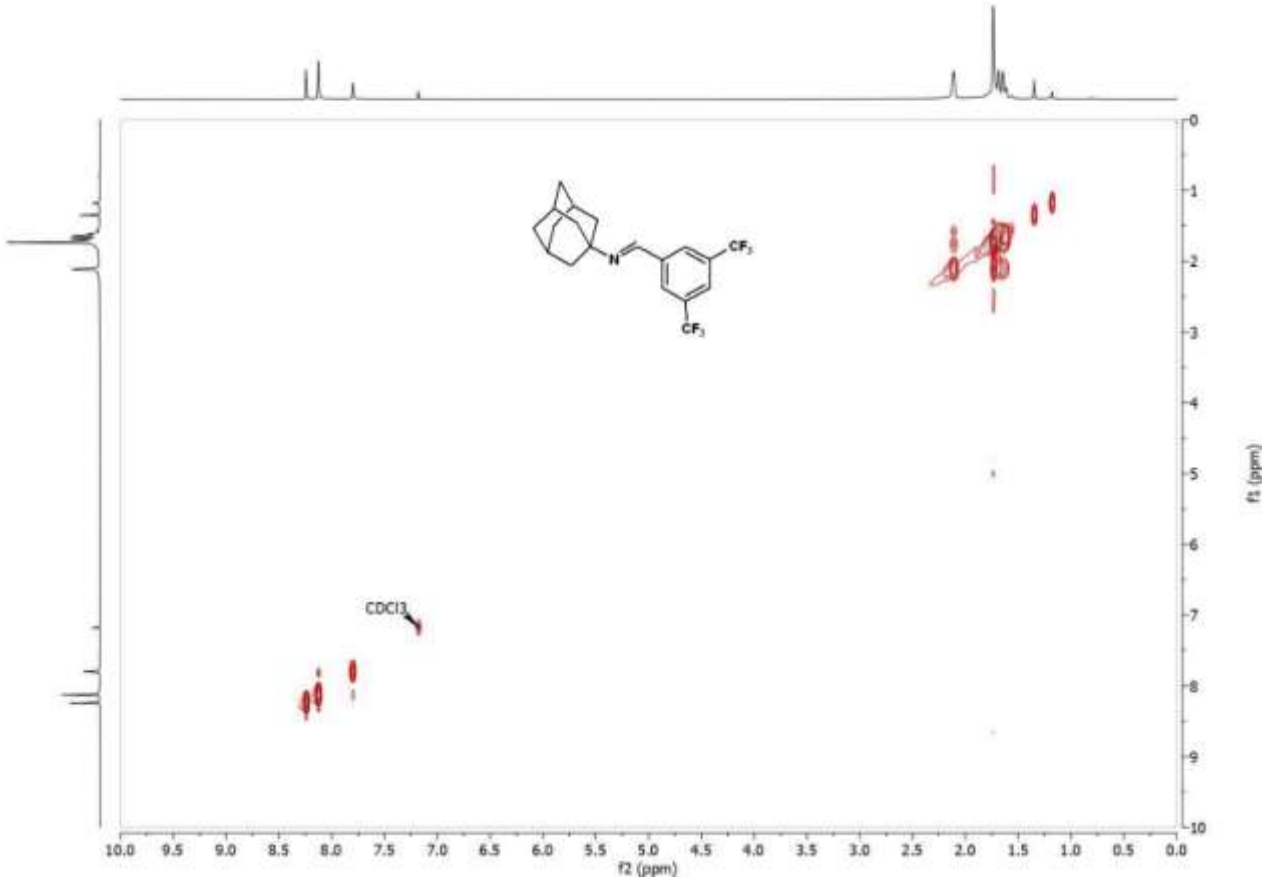

Figure C.90 COSY spectrum of **5cf** in $CDCl_3$.

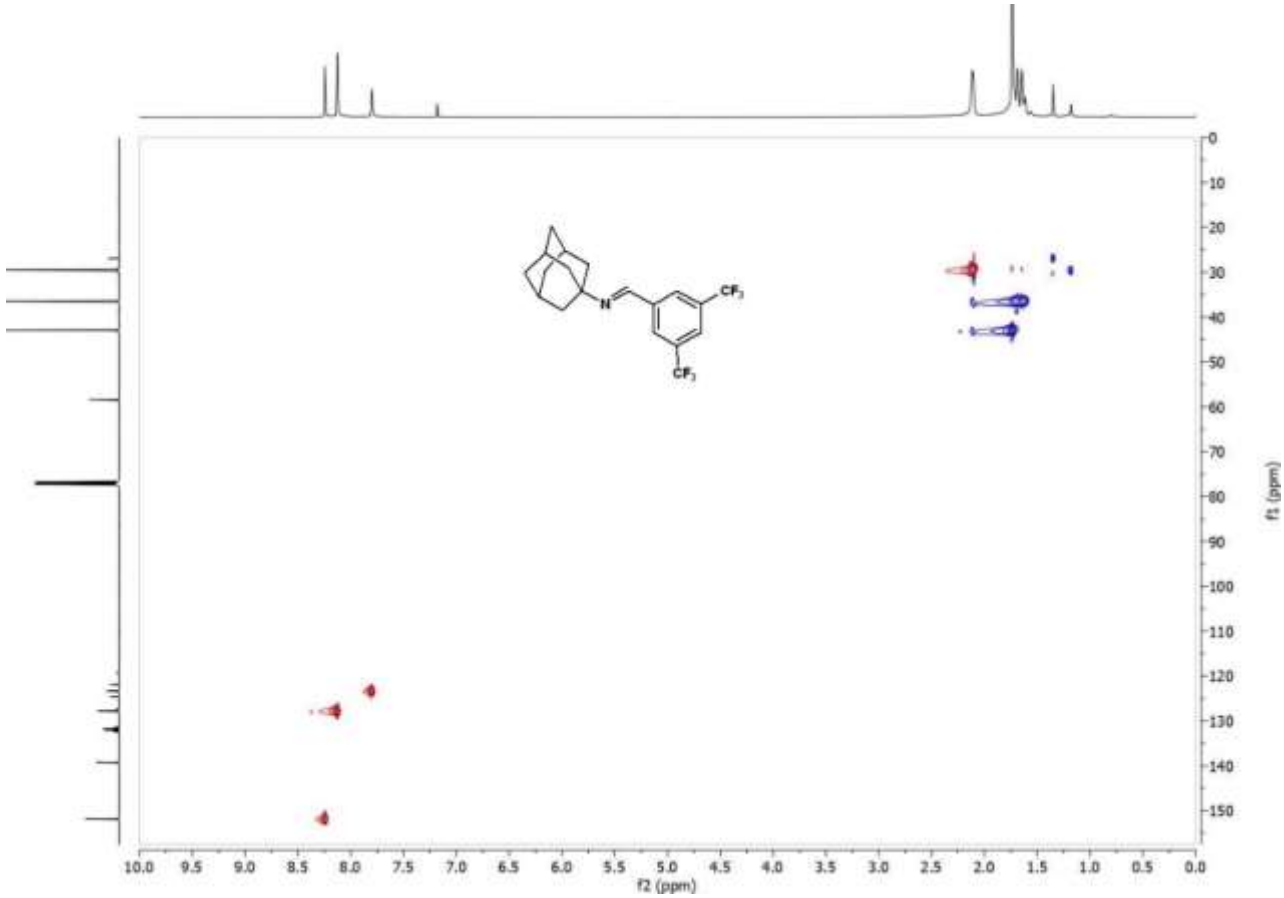

Figure C.91 HSQC spectrum of **5cf** in $CDCl_3$.

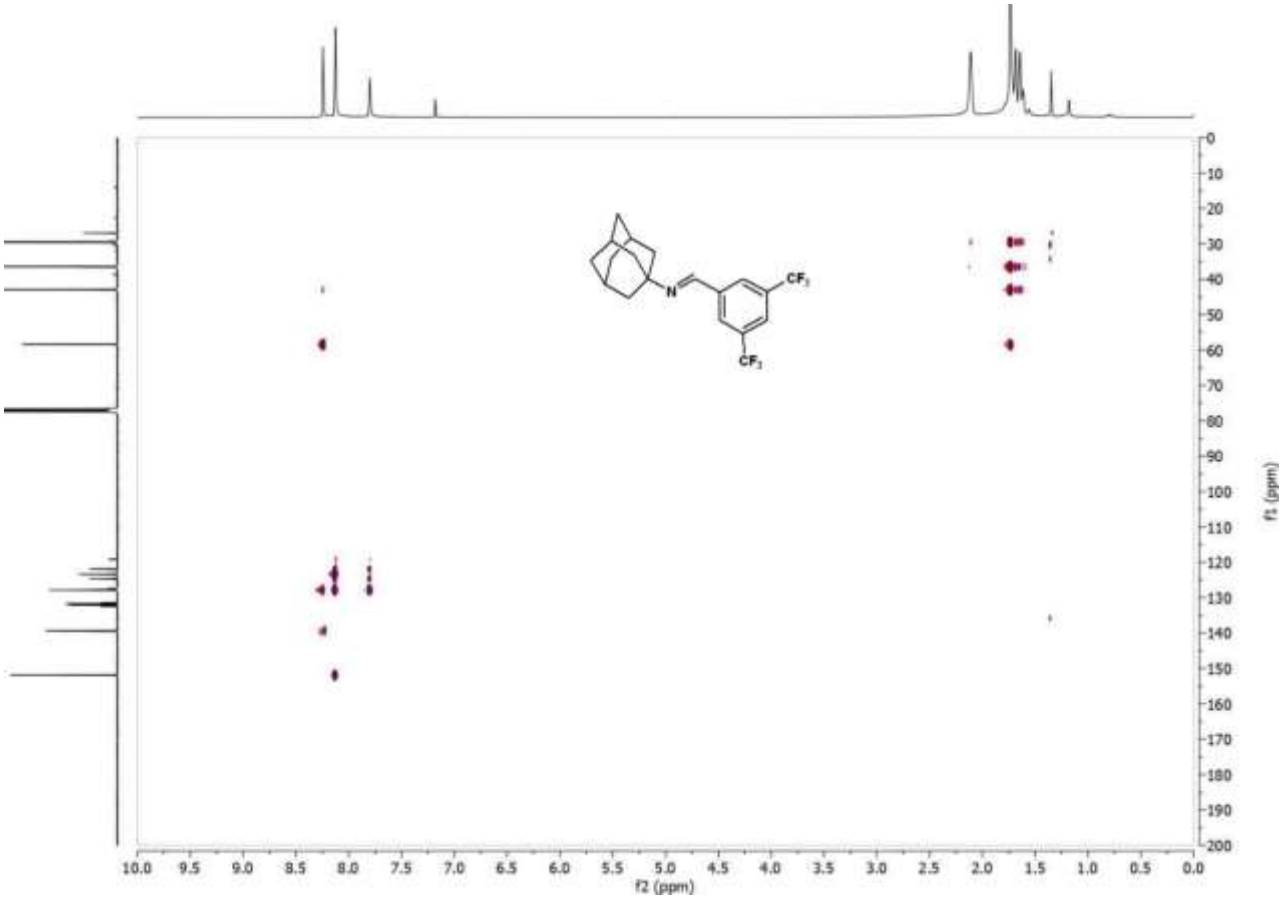

Figure C.92 HMBC spectrum of **5cf** in $CDCl_3$.

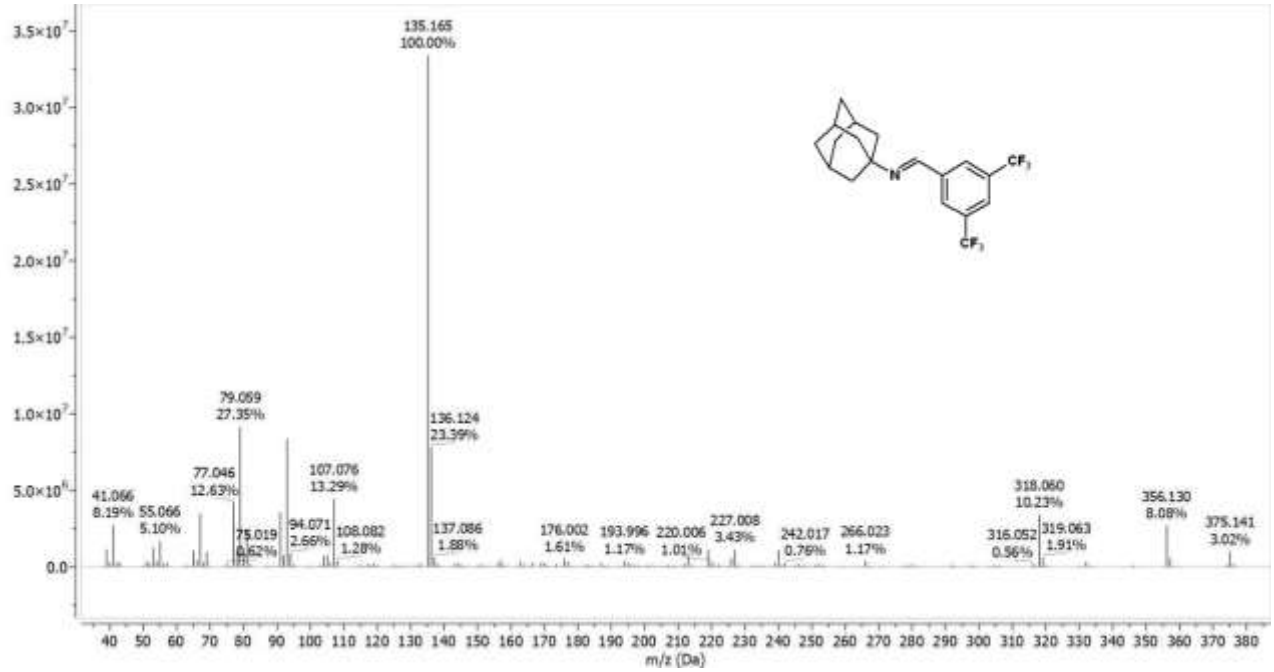

Figure C.93 GC-MS spectrum of imine **5cf**.

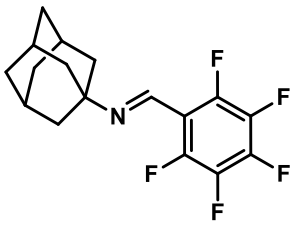

Chemical Formula: $C_{17}H_{16}F_5N$
Molecular Weight: 329,31

5cg

^{1}H NMR (400 MHz, Chloroform-d) δ [ppm] = 8.28 (s, 1H), 2.19 (s, 3H), 1.81 (d, J = 2.9 Hz, 6H), 1.72 (q, 6H).

^{13}C NMR (101 MHz, Chloroform-d) δ [ppm] = 147.19 – 144.11 (m), 143.90 (q, J = 2.6 Hz), 143.08 – 140.05 (m), 139.31 – 135.97 (m), 112.50 (td, J = 12.0, 3.7 Hz), 60.03, 42.71, 36.42, 29.45.

^{19}F NMR (376 MHz, Chloroform-d) δ [ppm] = -141.02 – -146.20 (m), -152.68 (tt, J = 20.7, 2.5 Hz), -162.25 – -162.43 (m).

GC/MS (EI): calc. for $C_{17}H_{16}F_5N$ $[M]^+$: 329.120; found: $[M]^+$ 329.100, $C_{10}H_{15}$ 135.106.

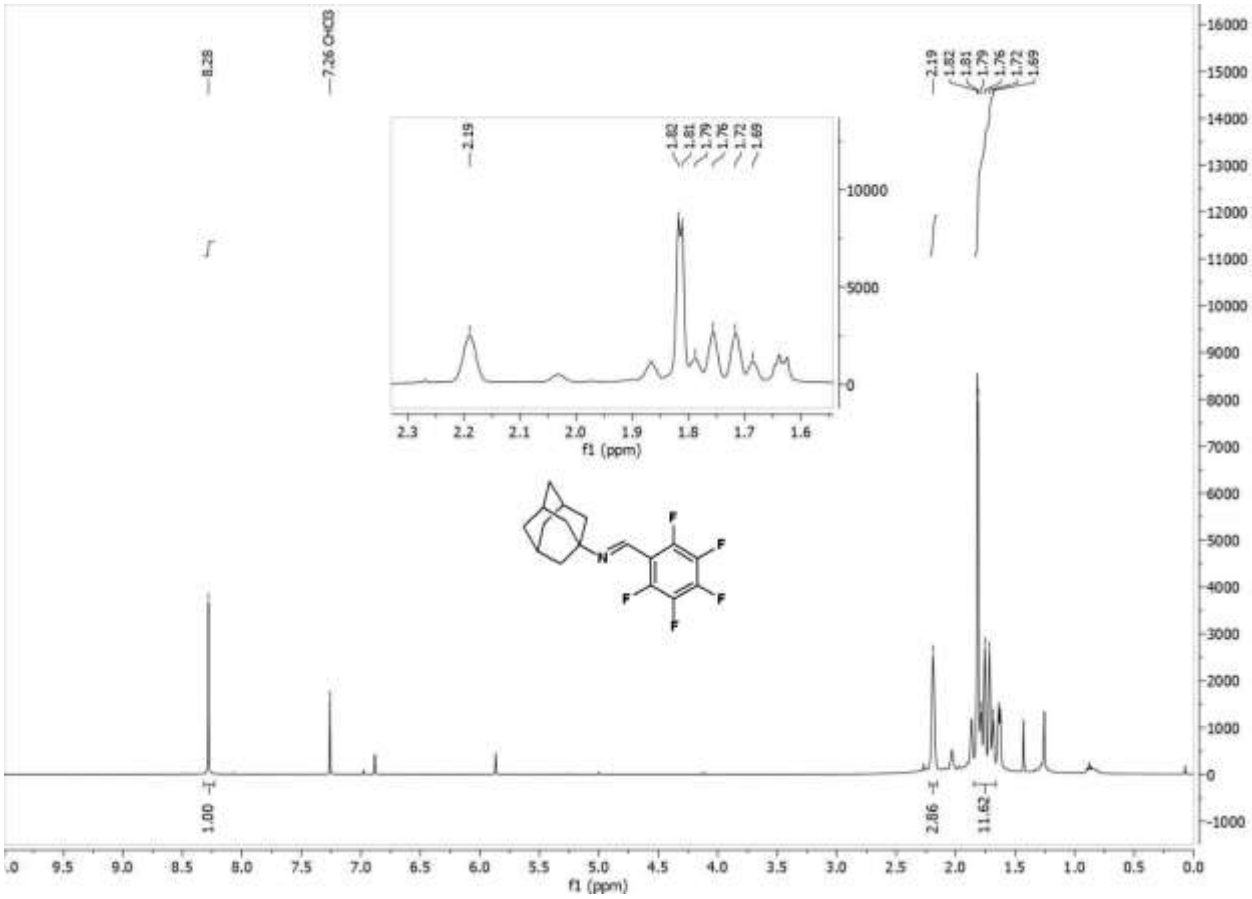

*Figure C.94 ^{1}H NMR spectrum of **5cg** in $CDCl_3$.*

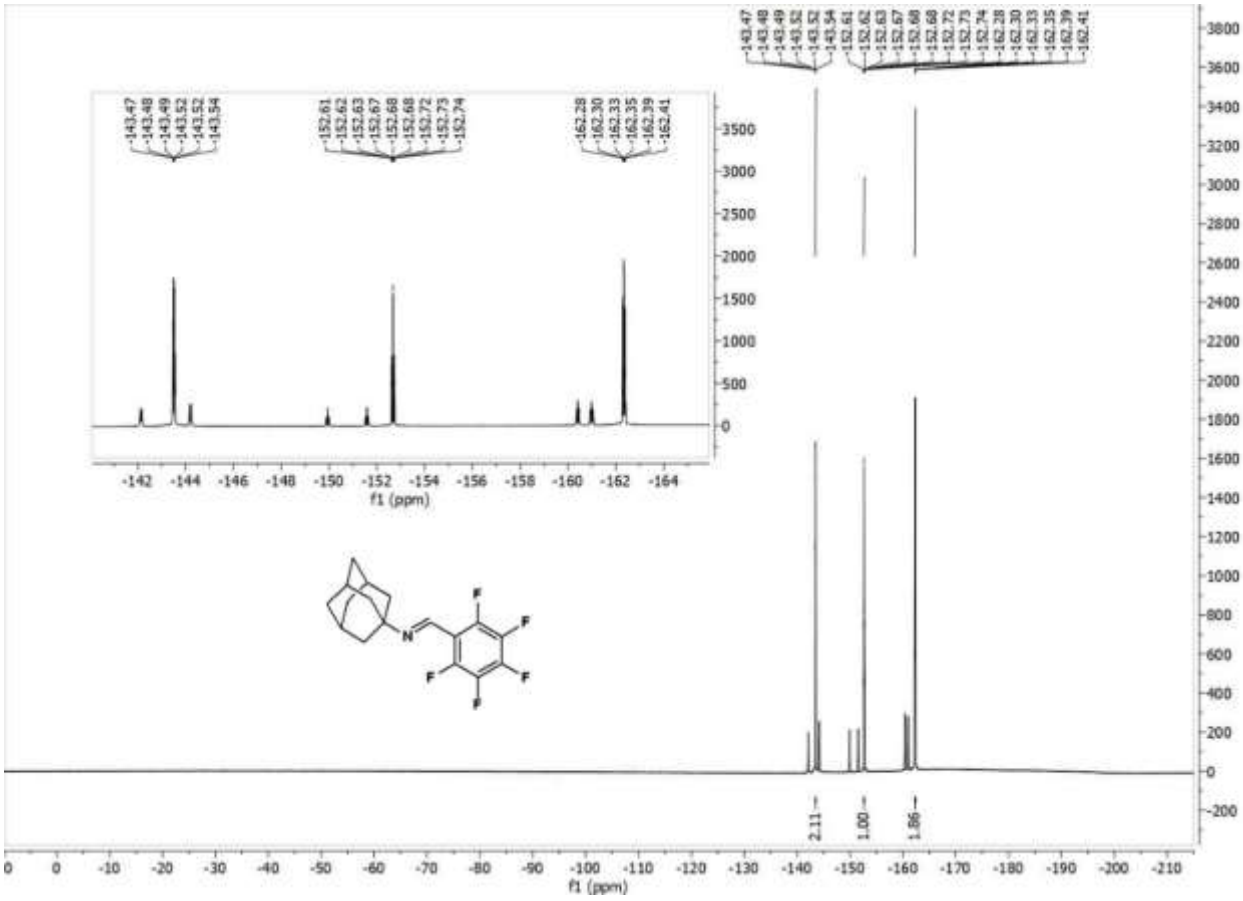

Figure C.95 ^{19}F *NMR spectrum of* ***5cg*** *in* $CDCl_3$.

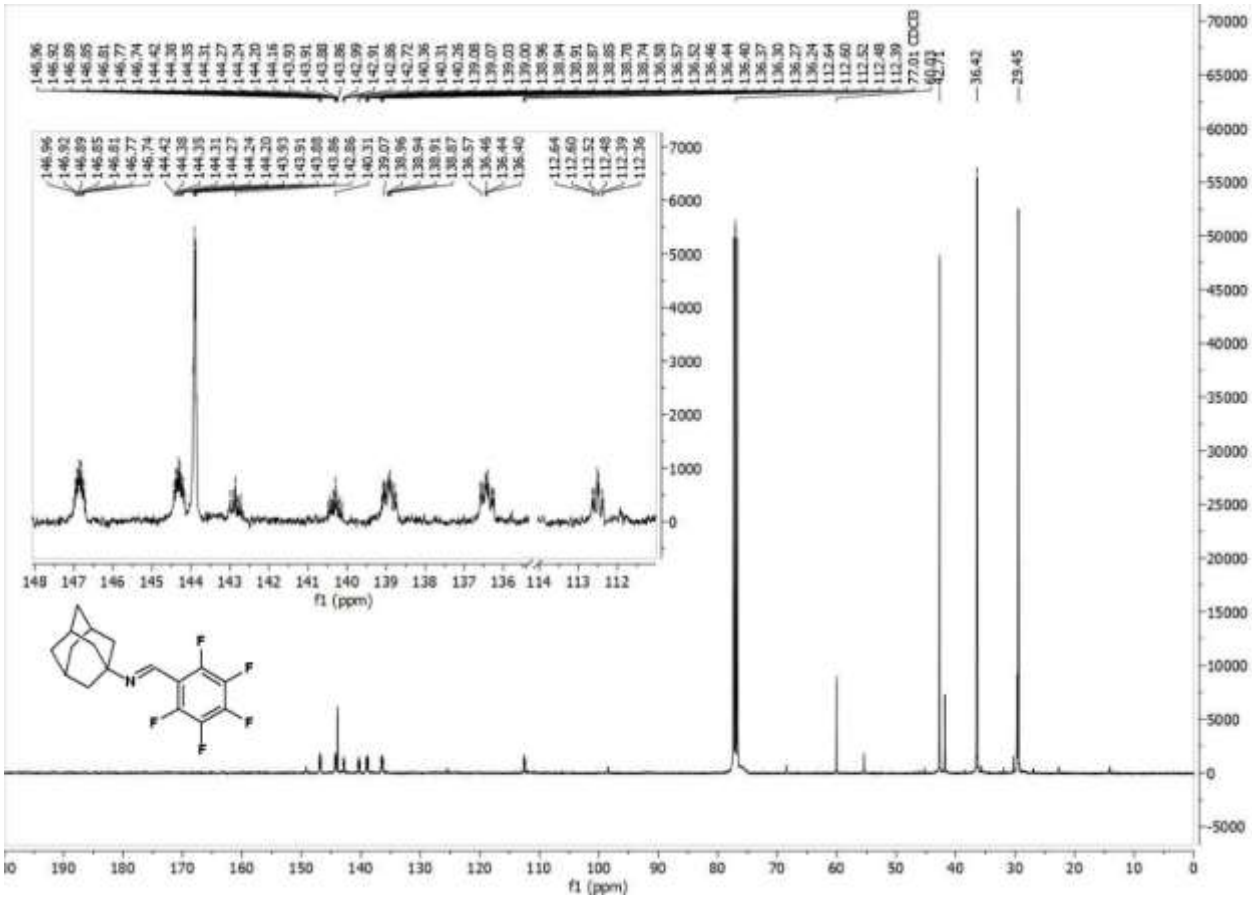

Figure C.96 $^{13}C(^{1}H)$ *NMR spectrum of* ***5cg*** *in* $CDCl_3$.

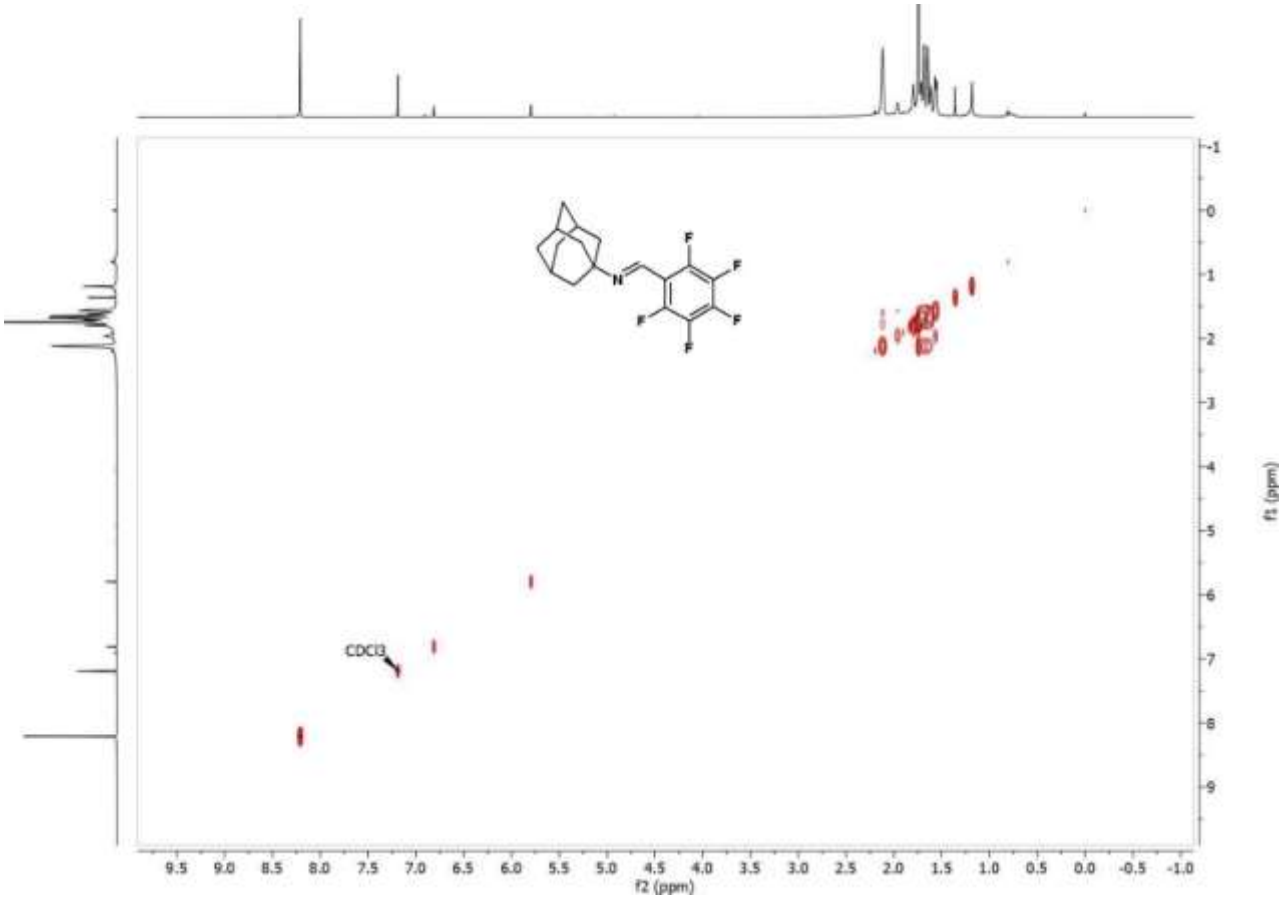

Figure C.97 COSY spectrum of **5cg** in $CDCl_3$.

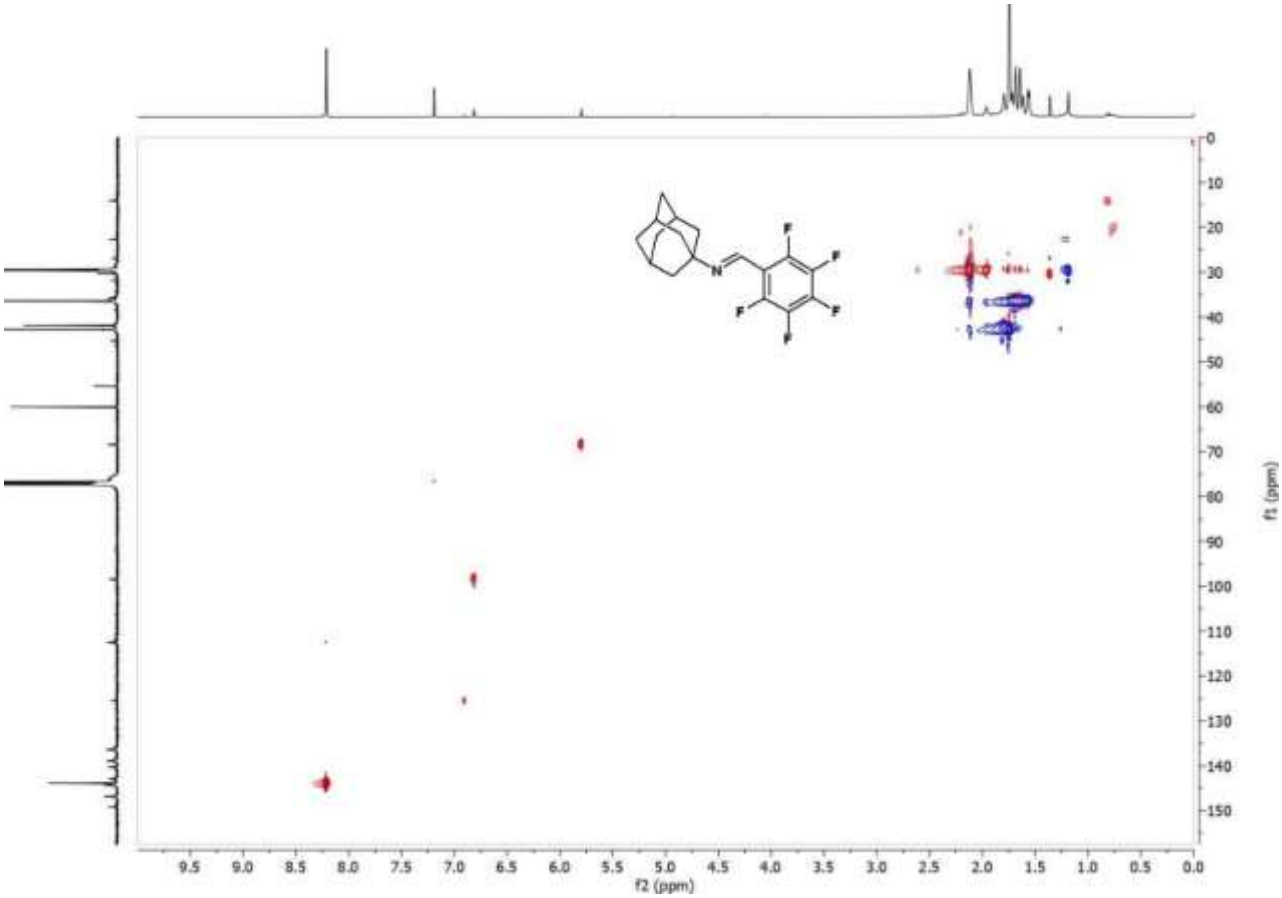

Figure C.98 HSQC spectrum of **5cg** in $CDCl_3$.

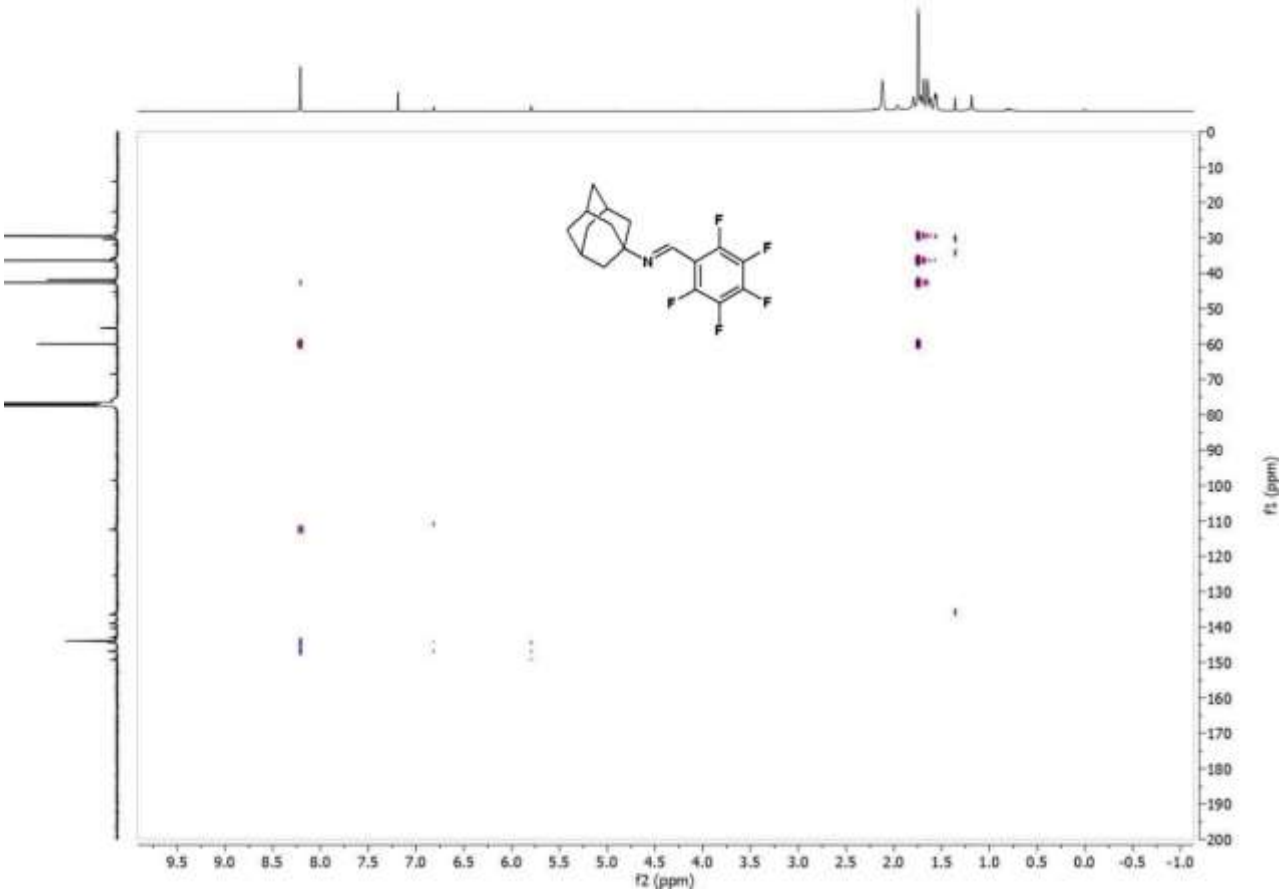

Figure C.99 HMBC spectrum of **5cg** in $CDCl_3$.

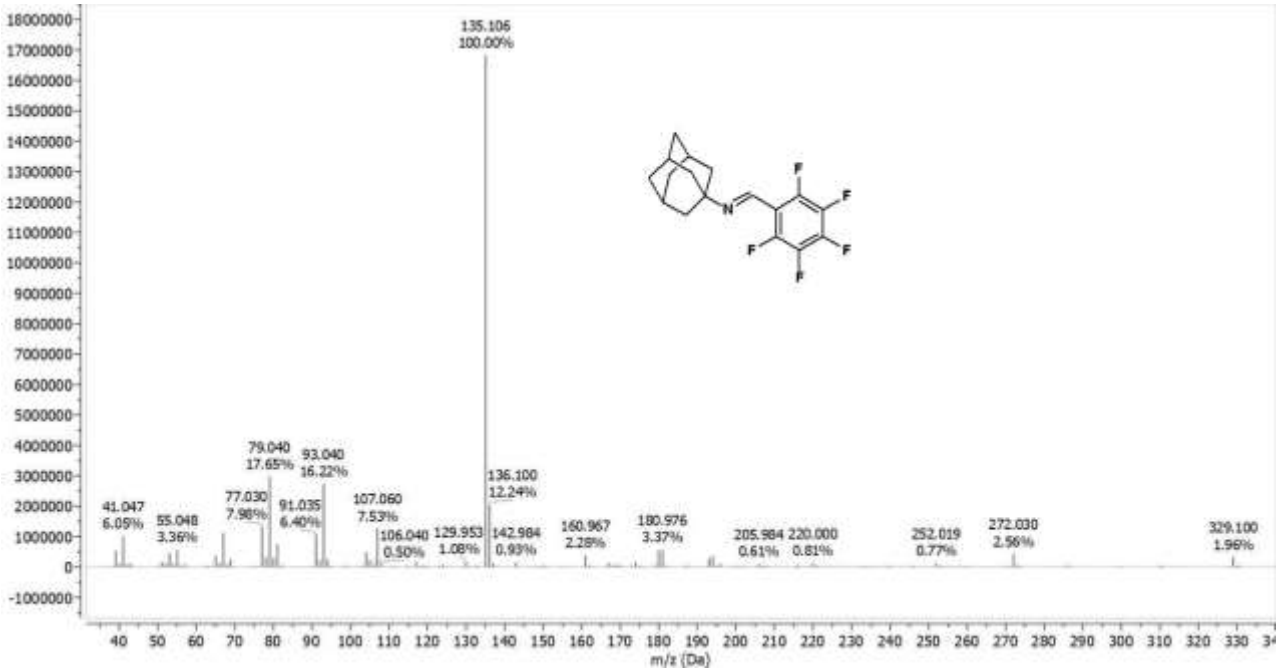

Figure C.100 GC-MS spectrum of imine **5cg**.

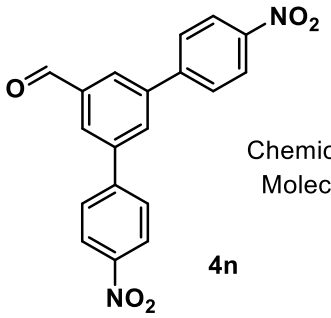

Chemical Formula: $C_{19}H_{12}N_2O_5$
Molecular Weight: 348,31400

4n

^{1}H NMR (400 MHz, Chloroform-d) δ [ppm] = 10.21 (s, 1H), 8.39 (d, J = 8.3 Hz, 4H), 8.20 (s, 2H), 8.09 (s, 1H), 7.85 (d, J = 8.3 Hz, 4H).

^{1}H NMR (400 MHz, DMSO-d6) δ [ppm] = 10.22 (s, 1H), 8.53 – 8.48 (m, 1H), 8.43 – 8.38 (m, 2H), 8.38 (d, J = 8.5 Hz, 4H), 8.22 (d, J = 8.6 Hz, 4H).

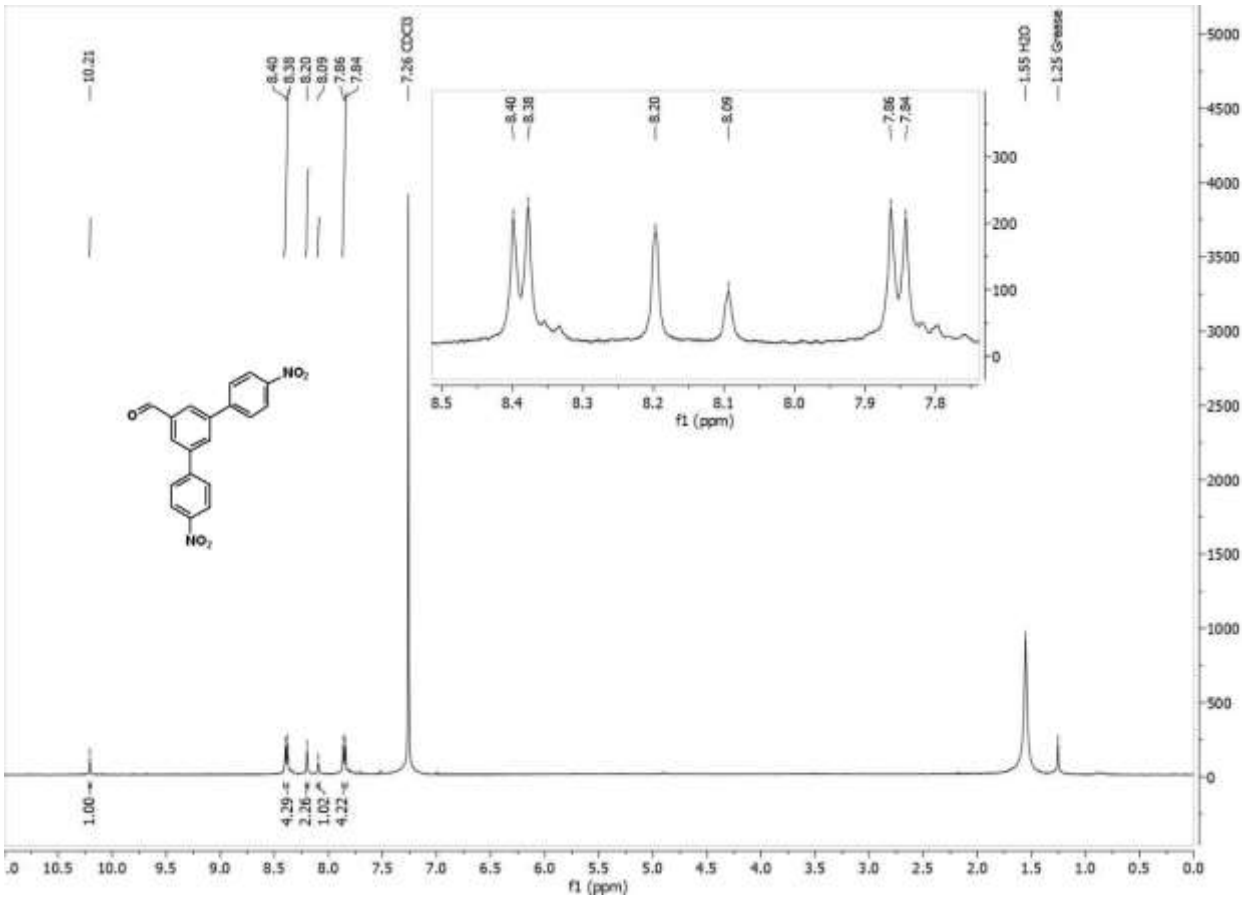

*Figure C.101 ^{1}H NMR spectrum of **4n** in $CDCl_3$.*

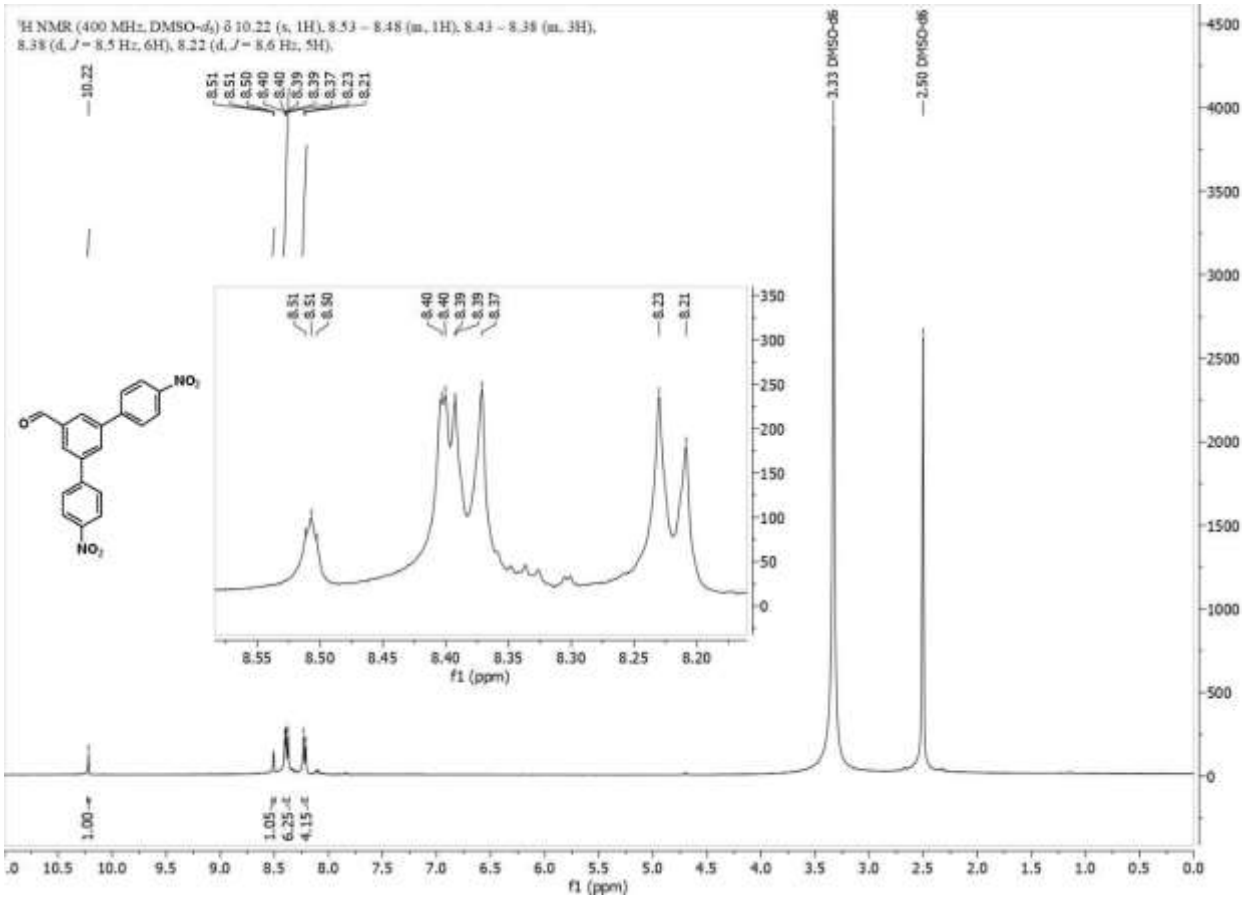

b

Figure C.102 ^{1}*H NMR spectrum of* ***4n*** *in DMSO-d*$_6$.

2. *C*- and *O*-substituted derivatives of *trans*-1,3-diphenylprop-2-en-1-ol

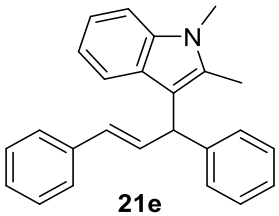

21e

Chemical Formula: $C_{25}H_{23}N$
Molecular Weight: 337,47

^{1}H NMR (400 MHz, Chloroform-*d*) δ = 7.34 – 7.25 (m, 5H), 7.23 – 7.16 (m, 5H), 7.14 – 7.08 (m, 2H), 7.08 – 7.03 (m, 1H), 6.93 – 6.87 (m, 1H), 6.77 (dd, *J* = 15.8, 7.3 Hz, 1H), 6.35 (d, *J* = 15.8 Hz, 1H), 5.10 (d, *J* = 7.3 Hz, 1H), 3.58 (s, 3H), 2.30 (s, 3H).

^{13}C NMR (101 MHz, Chloroform-*d*) δ = 143.80, 137.73, 136.95, 133.57, 132.52, 130.61, 128.59, 128.38, 128.34, 127.17, 127.09, 126.40, 126.16, 120.59, 119.54, 118.97, 112.31, 108.77, 45.49, 29.66, 10.91.

GC/MS (EI): calc. for $C_{25}H_{23}N$ $[M]^+$: 337.183; found: 337.166, $C_{24}H_{20}N$ 322.139, $C_{19}H_{18}N$ 260.115, C_7H_7 91.036, C_6H_5 77.032.

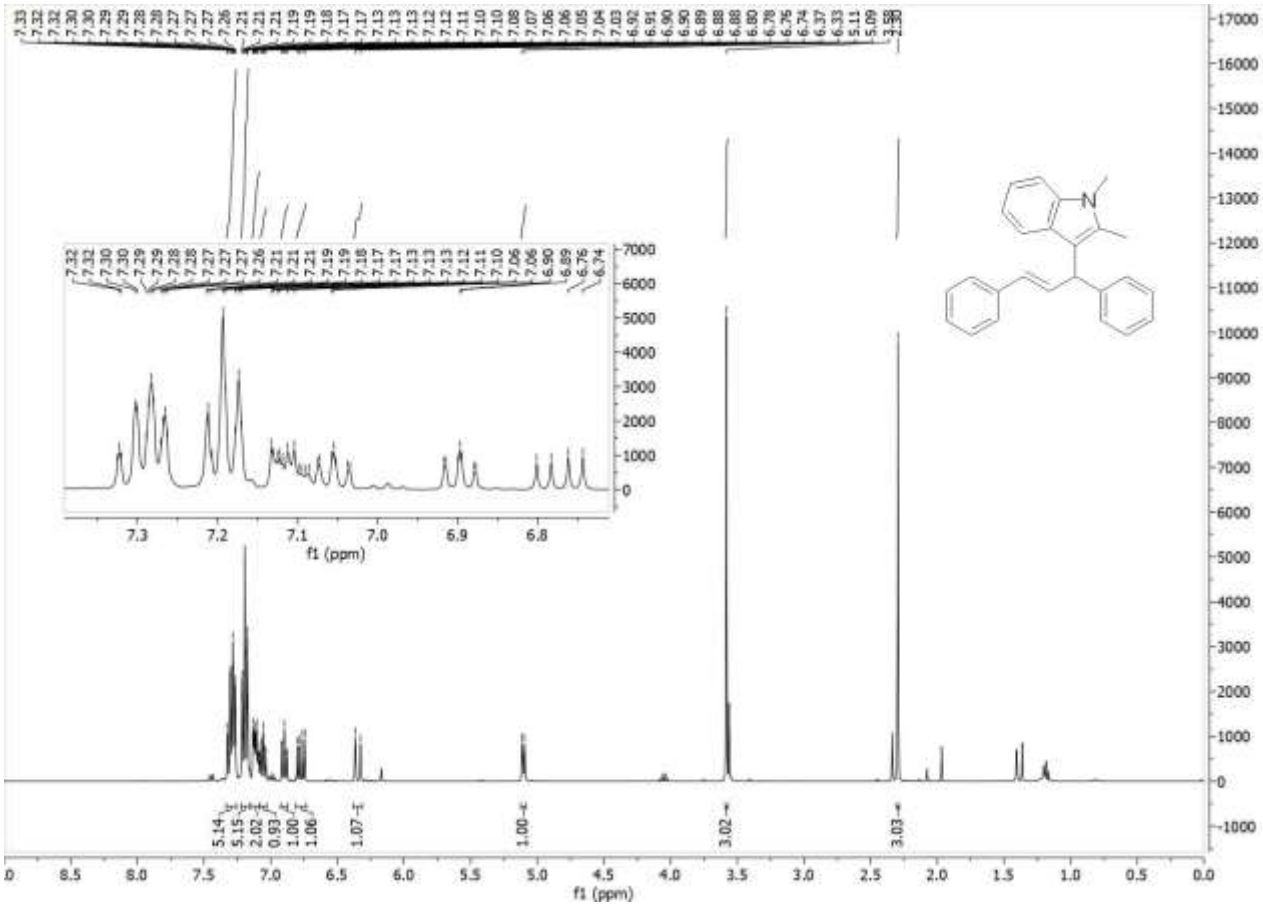

*Figure C.103 ^{1}H NMR spectrum of **21e** in $CDCl_3$.*

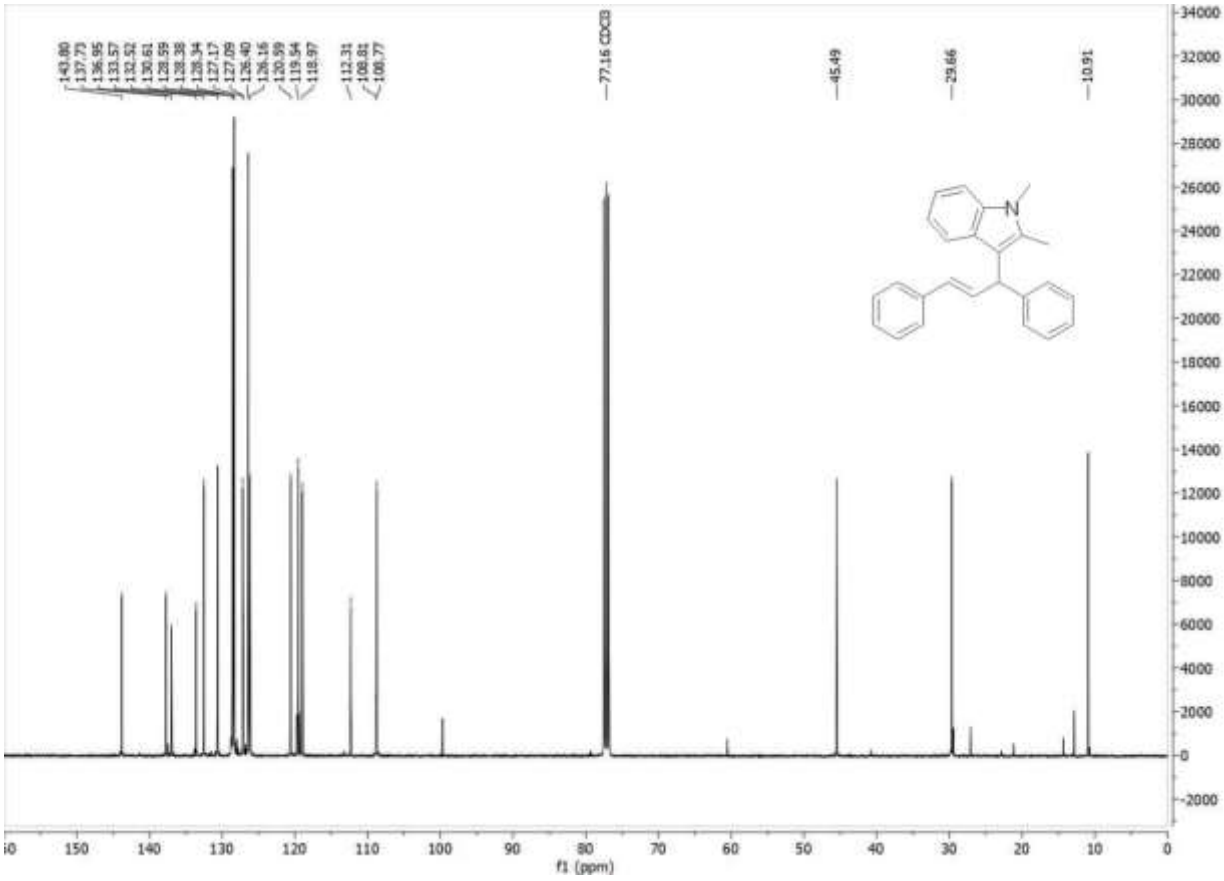

Figure C.104 $^{13}C(^{1}H)$ *NMR spectrum of* ***21e*** *in* $CDCl_3$.

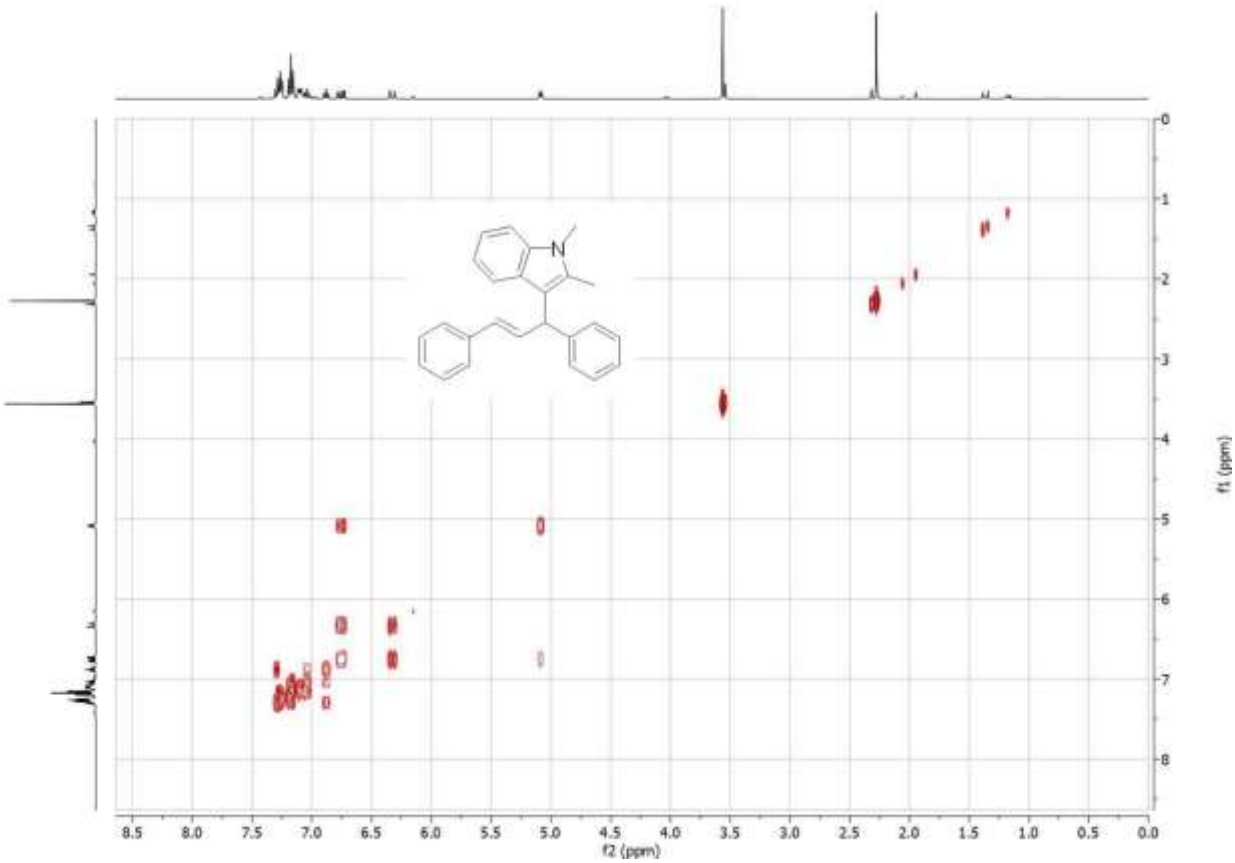

Figure C.105 COSY spectrum of ***21e*** *in* $CDCl_3$.

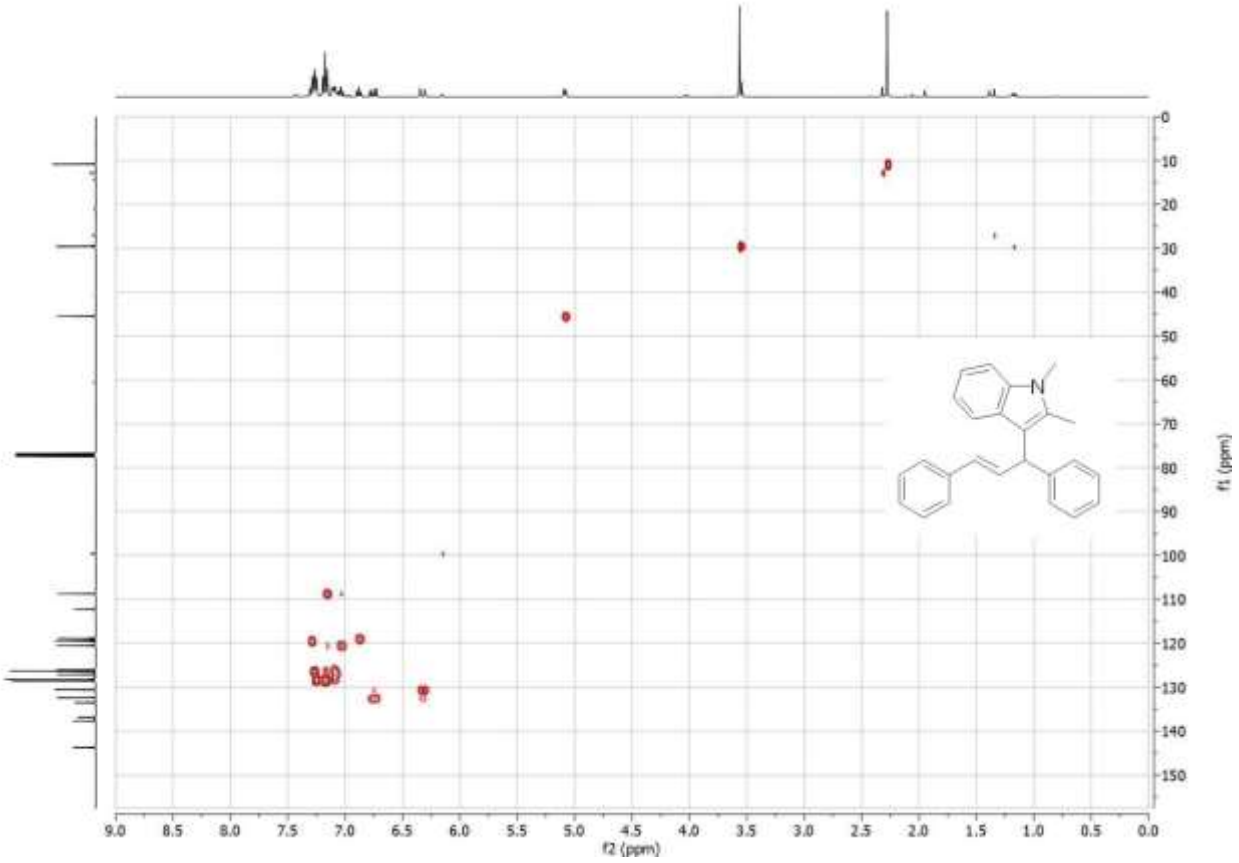

Figure C.106 HSQC spectrum of ***21e*** in $CDCl_3$.

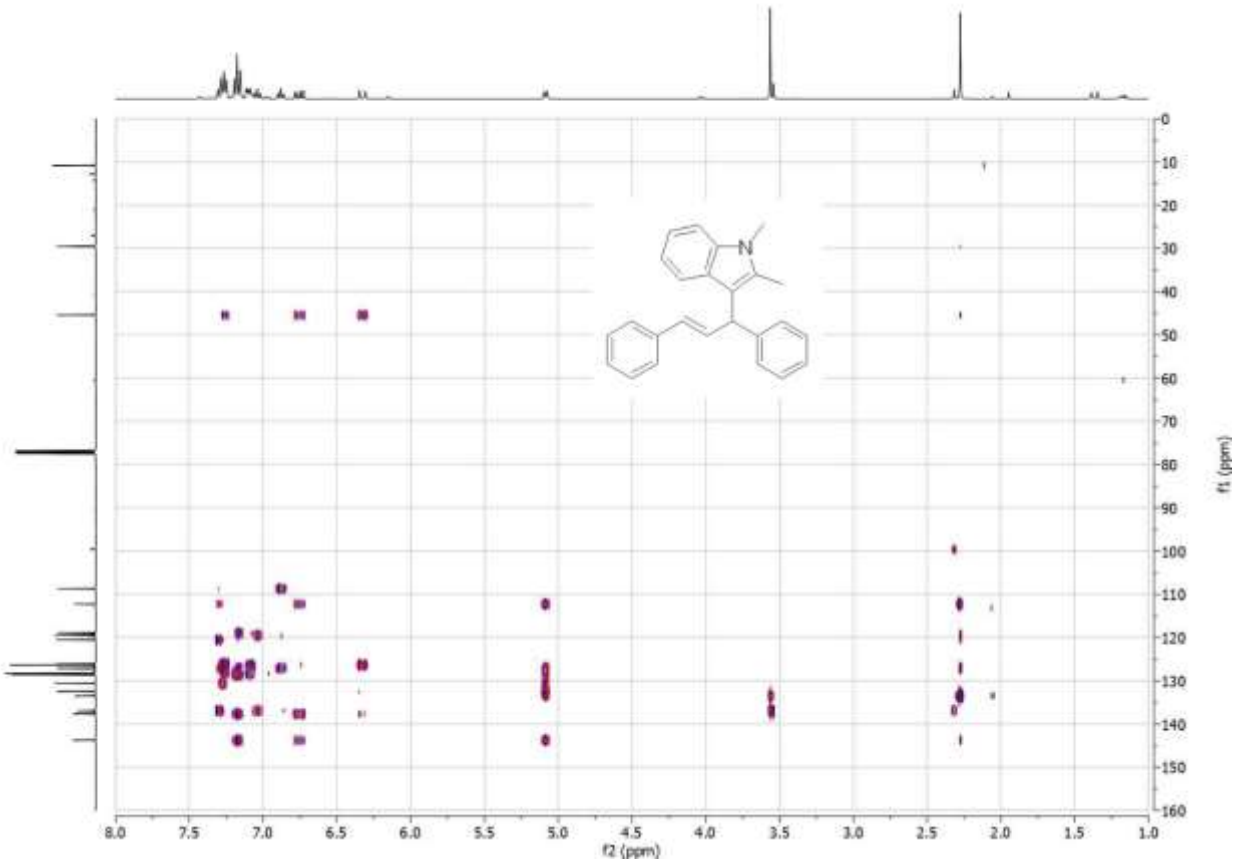

Figure C.107 HMBC spectrum of ***21e*** in $CDCl_3$.

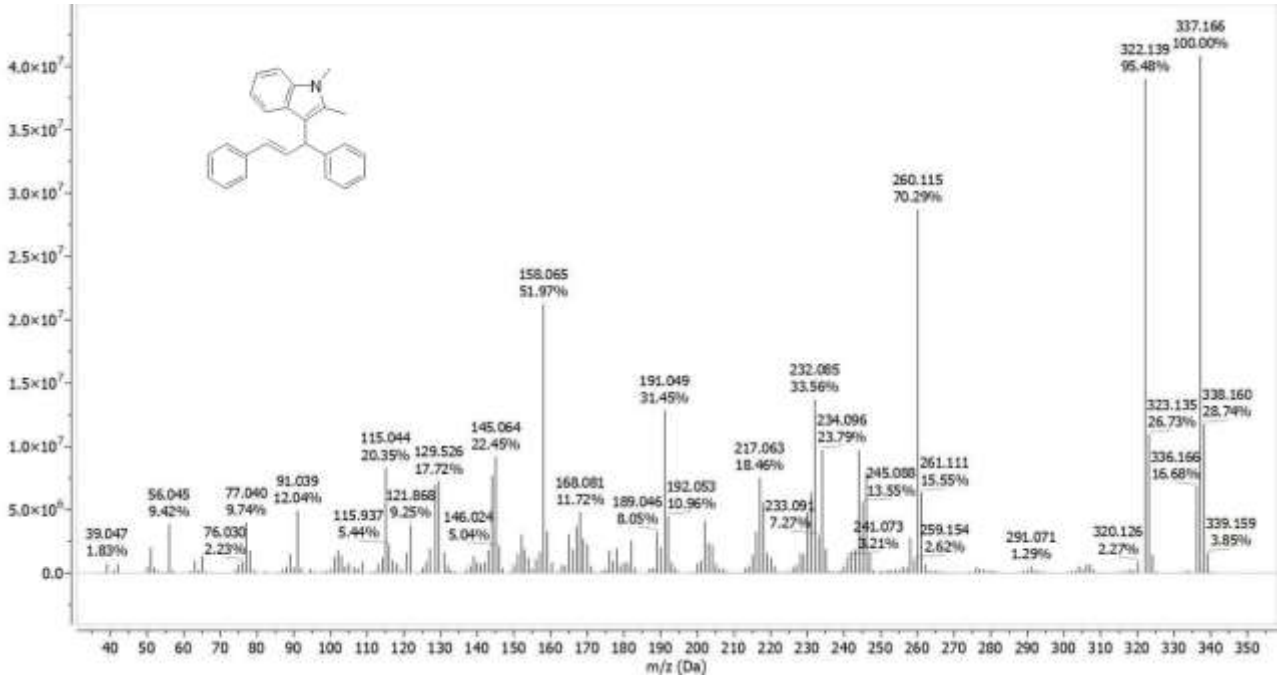

Figure C.108 GC-MS spectrum of ***21e***.

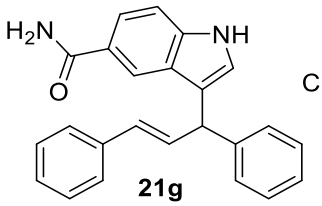

21g

Chemical Formula: $C_{24}H_{20}N_2O$
Molecular Weight: 352,44

^{1}H NMR (400 MHz, Chloroform-*d*) δ [ppm] = 8.29 (s, 1H), 7.87 (s, 1H), 7.68 (dd, *J* = 8.5, 1.8 Hz, 1H), 7.42 – 7.16 (m, 13H), 7.00 (d, *J* = 2.4 Hz, 1H), 6.71 (dd, *J* = 15.8, 7.3 Hz, 1H), 6.42 (d, *J* = 15.8 Hz, 1H), 5.15 (d, *J* = 7.2 Hz, 1H).

^{13}C NMR (101 MHz, Chloroform-*d*) δ [ppm] = 170.54, 143.08, 138.83, 137.42, 132.25, 131.05, 128.70, 128.68, 128.62, 127.46, 126.77, 126.63, 126.47, 124.91, 124.30, 121.90, 120.05, 119.90, 111.33, 46.02.

GC-MS: unavailable due to the low volatility of the compound.

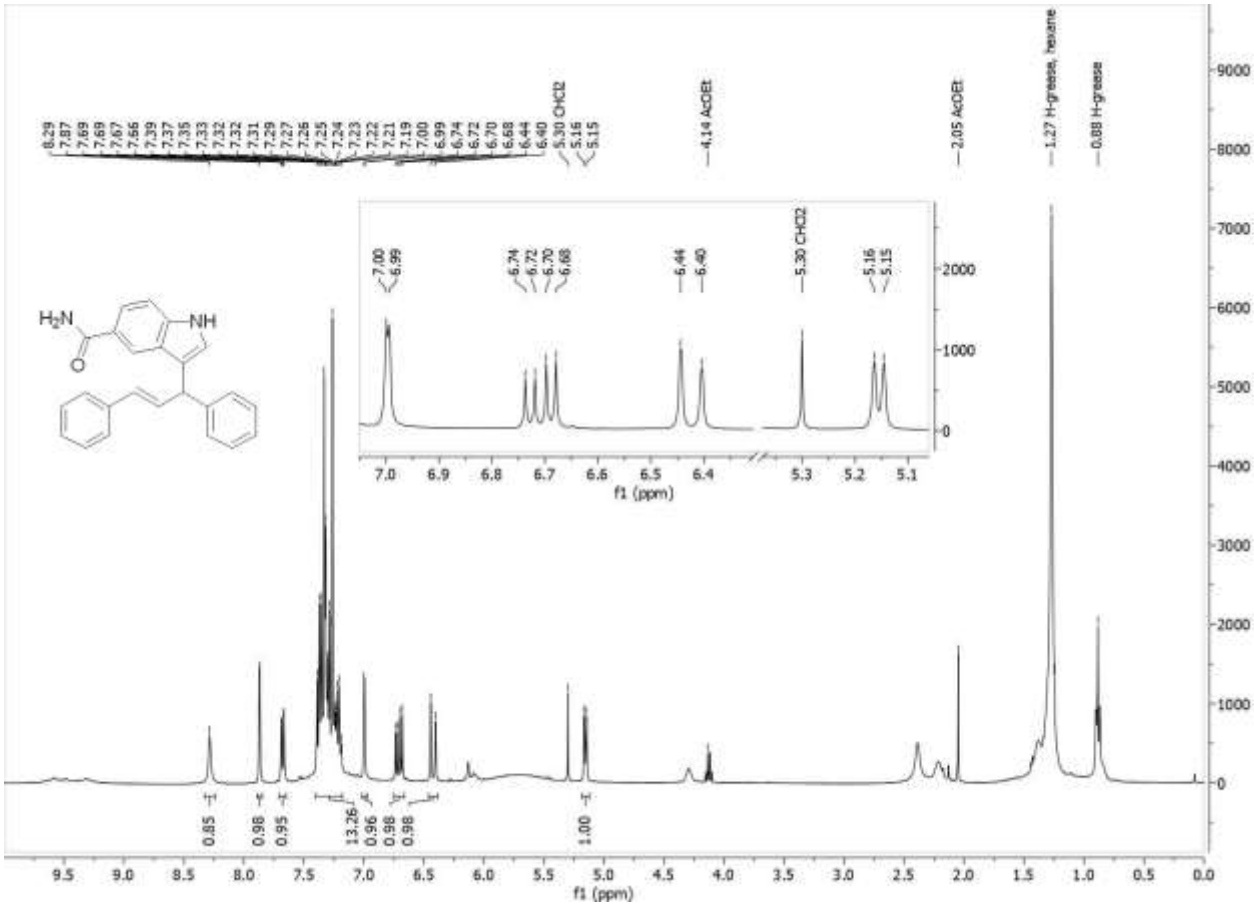

*Figure C.109 ^{1}H NMR spectrum of **21g** in $CDCl_3$.*

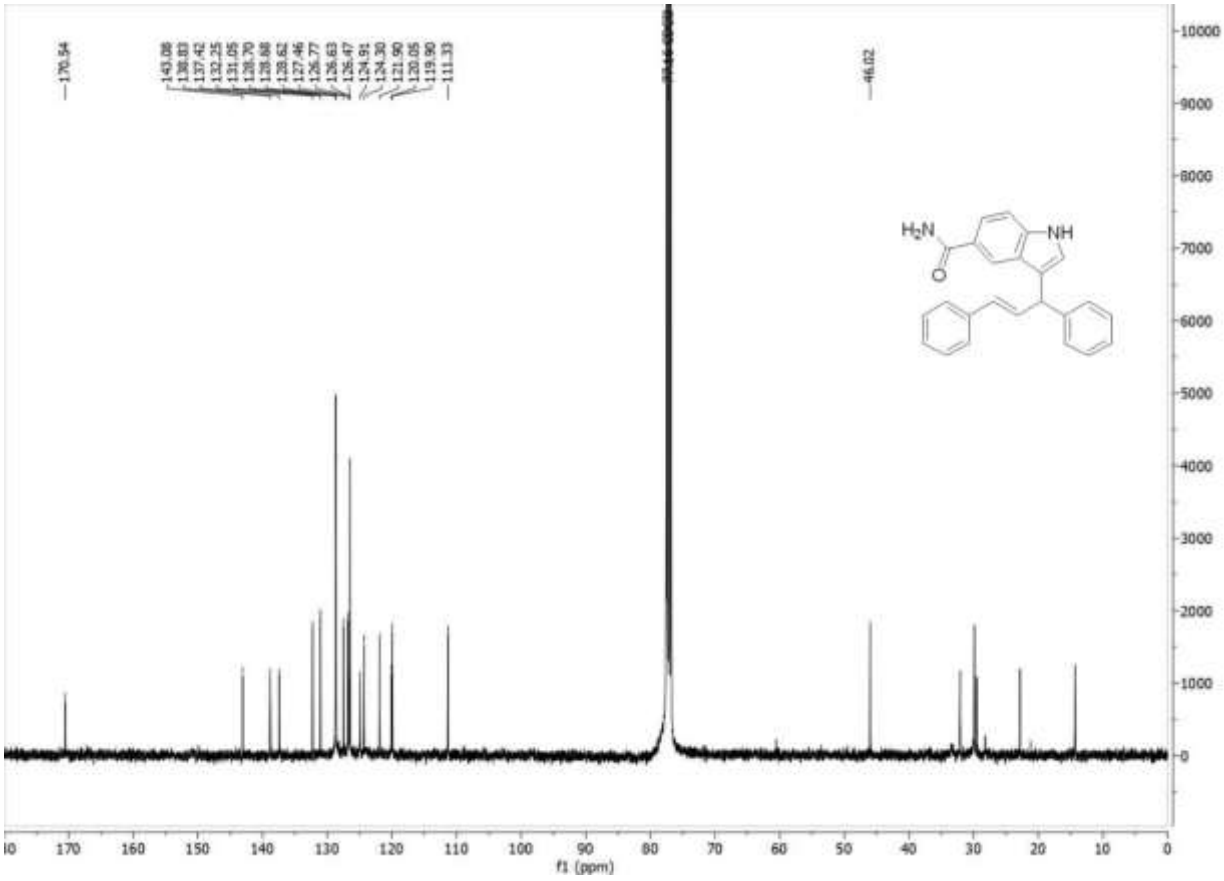

Figure C.110 $^{13}C(^{1}H)$ *NMR spectrum of* ***21g*** *in* $CDCl_3$.

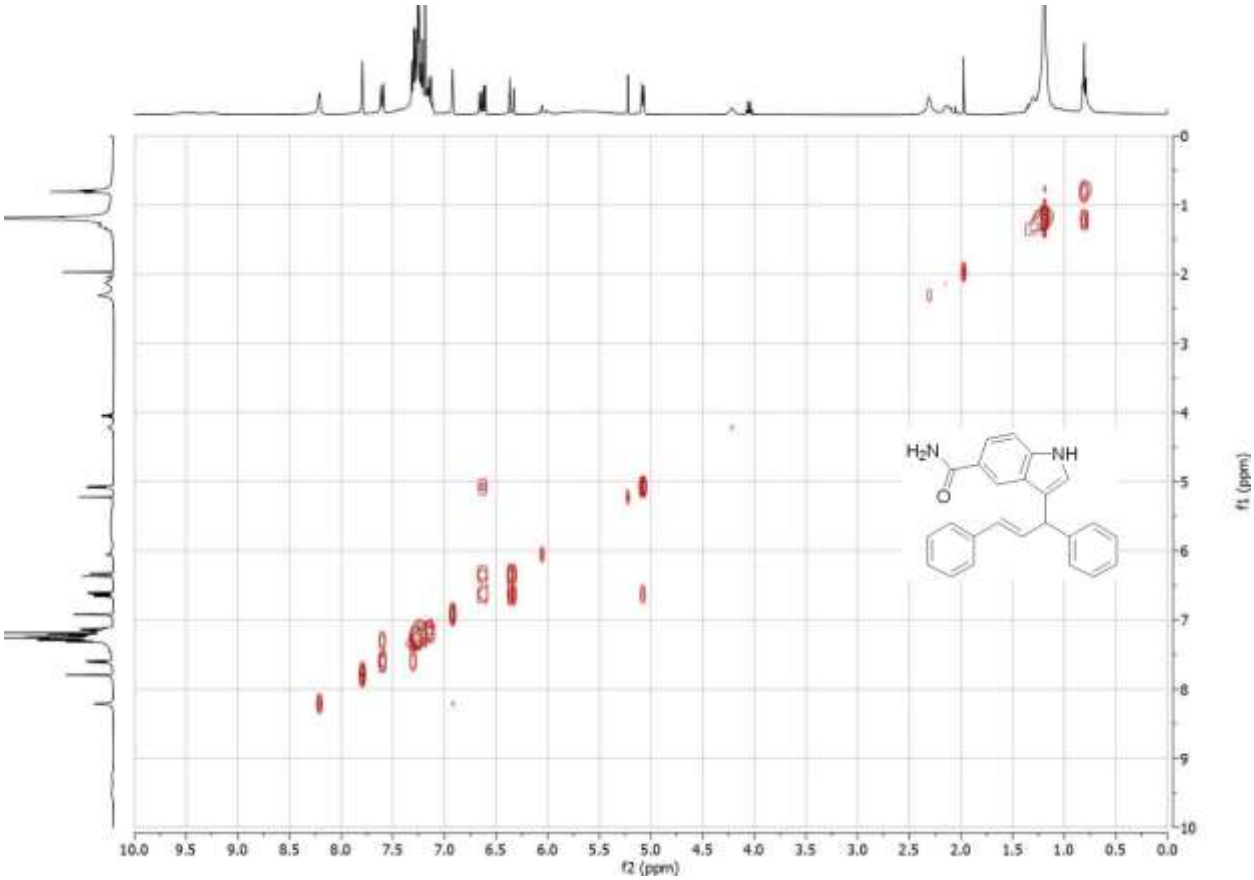

Figure C.111 COSY spectrum of ***21g*** *in* $CDCl_3$.

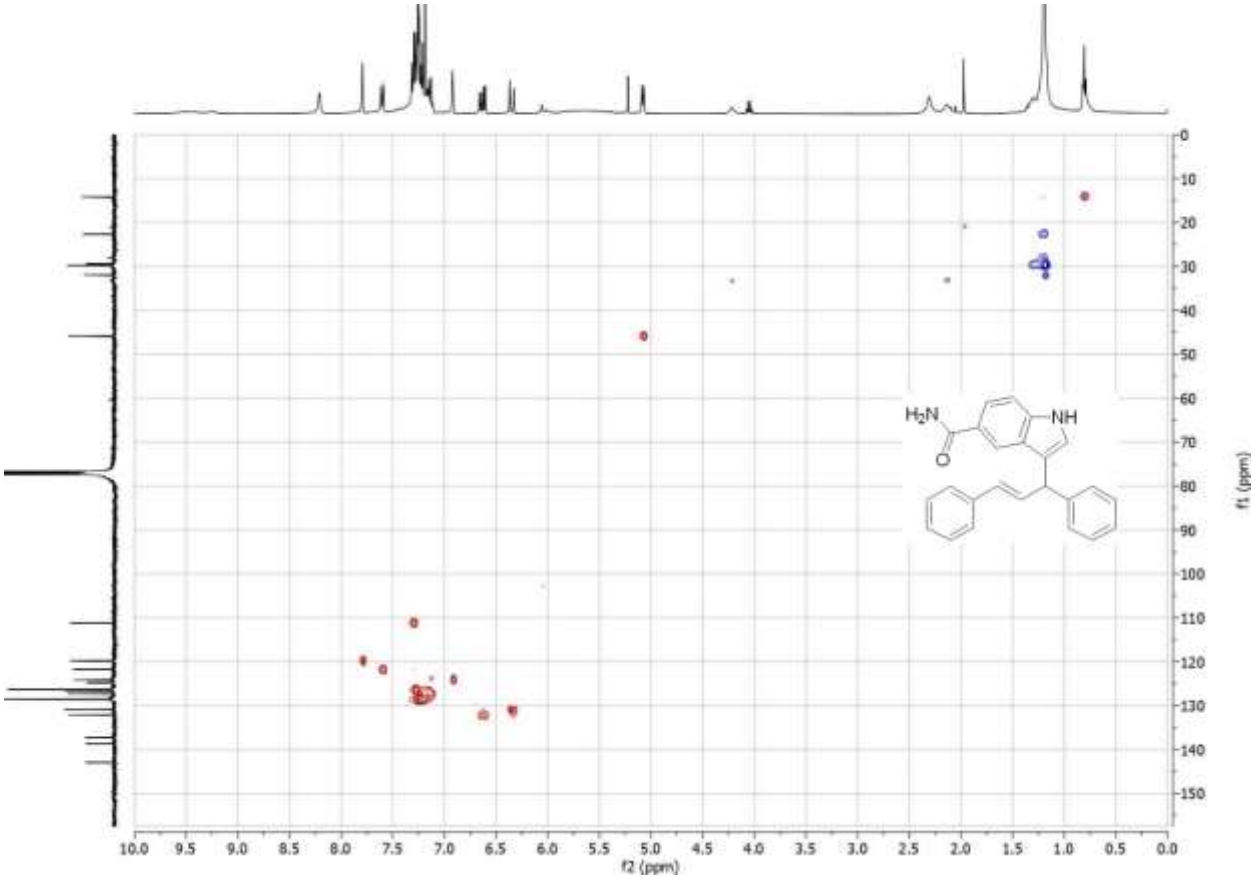

Figure C.112 HSQC spectrum of ***21g*** in $CDCl_3$.

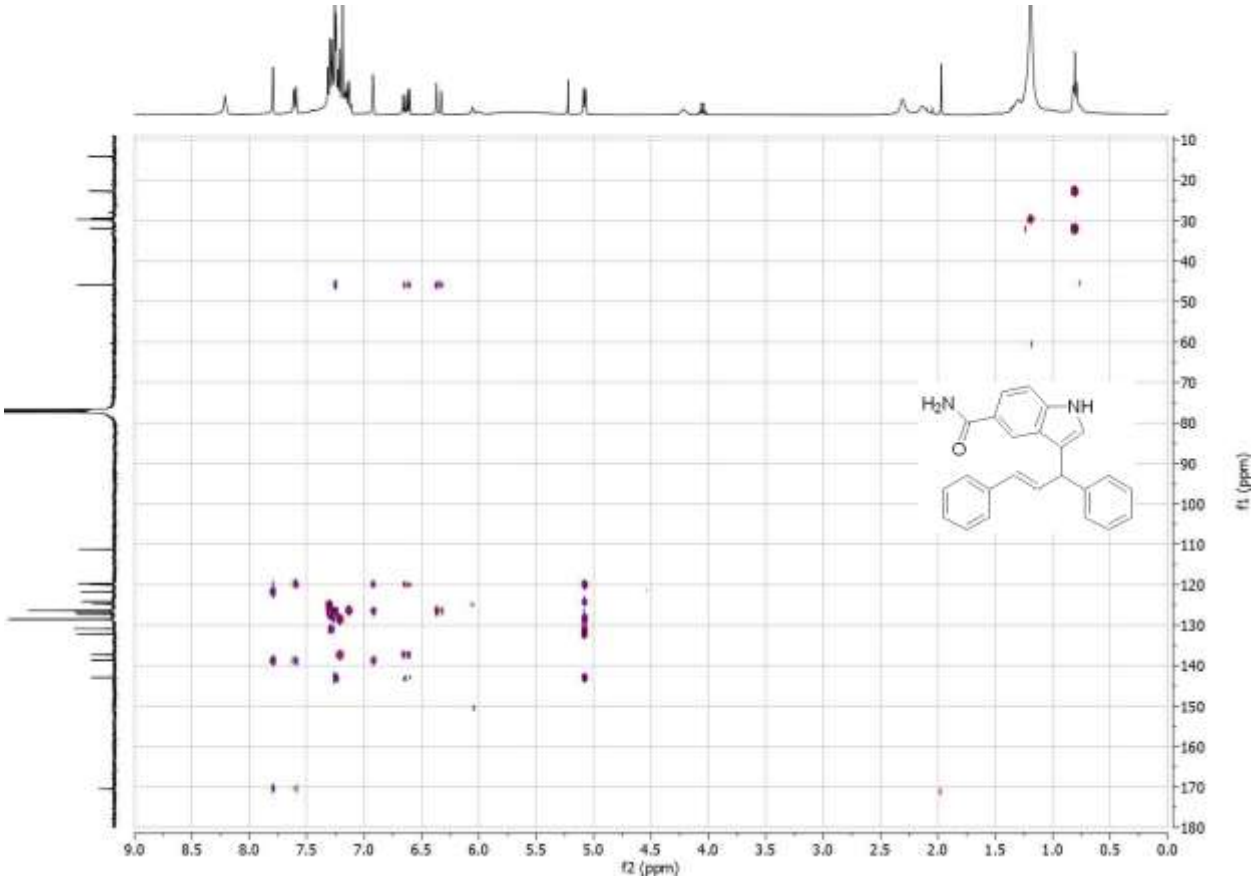

Figure C.113 HMBC spectrum of ***21g*** in $CDCl_3$.

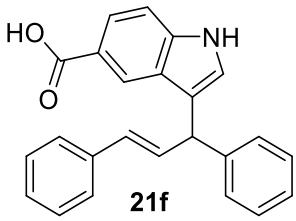

21f

Chemical Formula: $C_{24}H_{19}NO_2$
Molecular Weight: 353,42

^{1}H NMR (400 MHz, Methanol-d_4) δ [ppm] = 8.18 (d, *J* = 1.6 Hz, 1H), 7.82 (dd, *J* = 8.6, 1.7 Hz, 1H), 7.44 – 7.27 (m, 10H), 7.27 – 7.18 (m, 2H), 7.11 (s, 1H), 6.81 (dd, *J* = 15.8, 7.5 Hz, 1H), 6.46 (d, *J* = 15.8 Hz, 1H), 5.18 (d, *J* = 7.4 Hz, 1H).

^{13}C NMR (101 MHz, Methanol-d_4) δ [ppm] = 171.54, 145.00, 141.26, 138.94, 133.77, 131.74, 129.54, 129.47, 129.45, 128.17, 127.68, 127.42, 127.28, 125.54, 124.06, 123.78, 121.97, 120.47, 111.96, 47.44.

GC-MS: unavailable due to the low volatility of the compound.

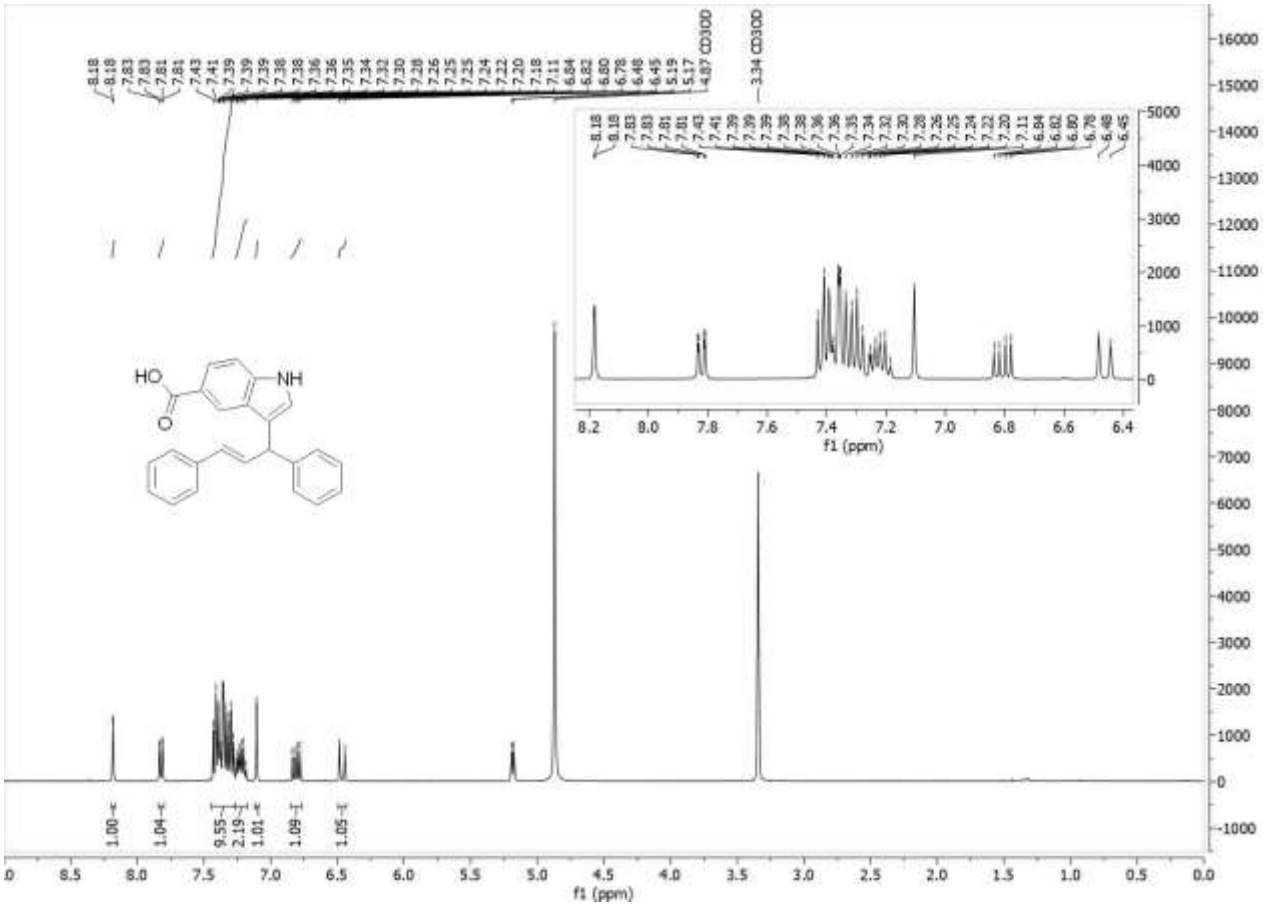

*Figure C.114 ^{1}H NMR spectrum of **21f** in methanol-d$_4$.*

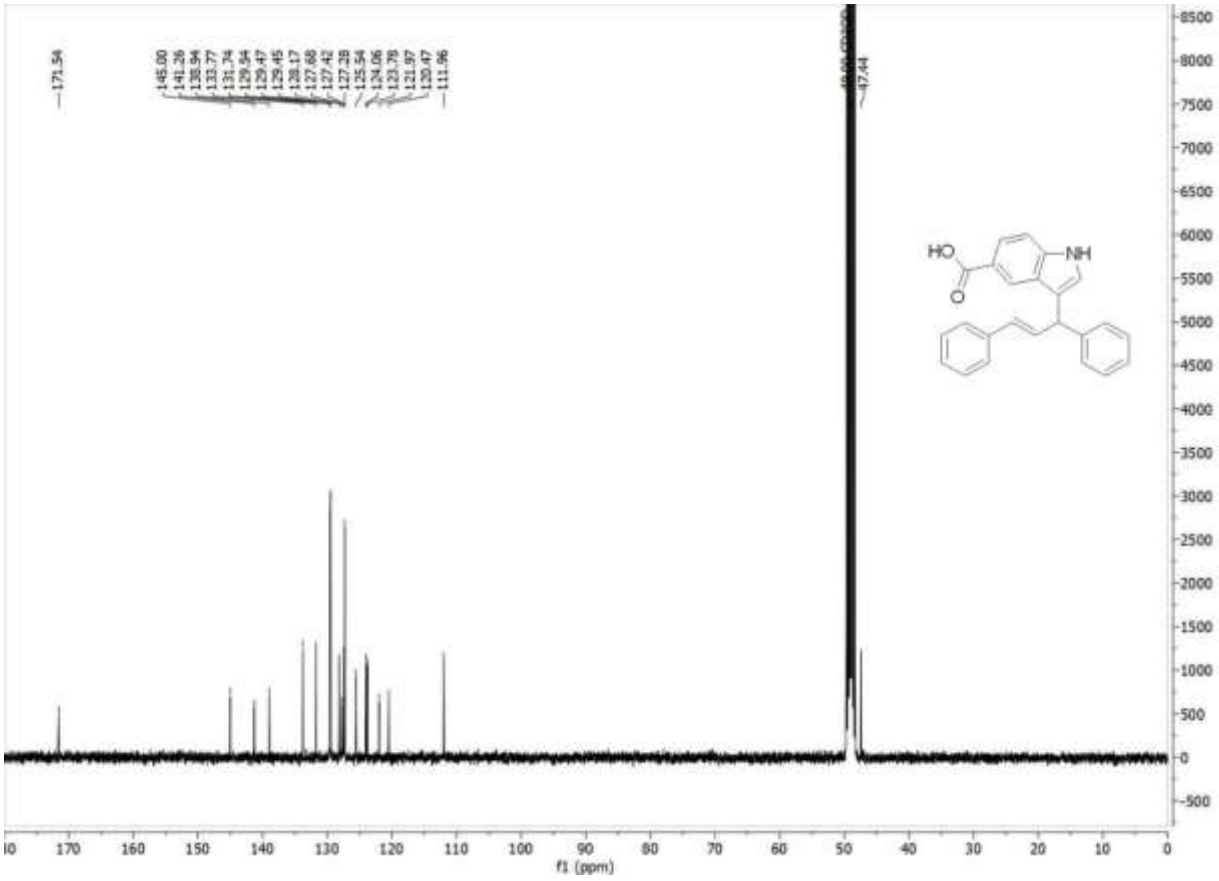

Figure C.115 $^{13}C(^{1}H)$ *NMR spectrum of* ***21f*** *in methanol-d₄.*

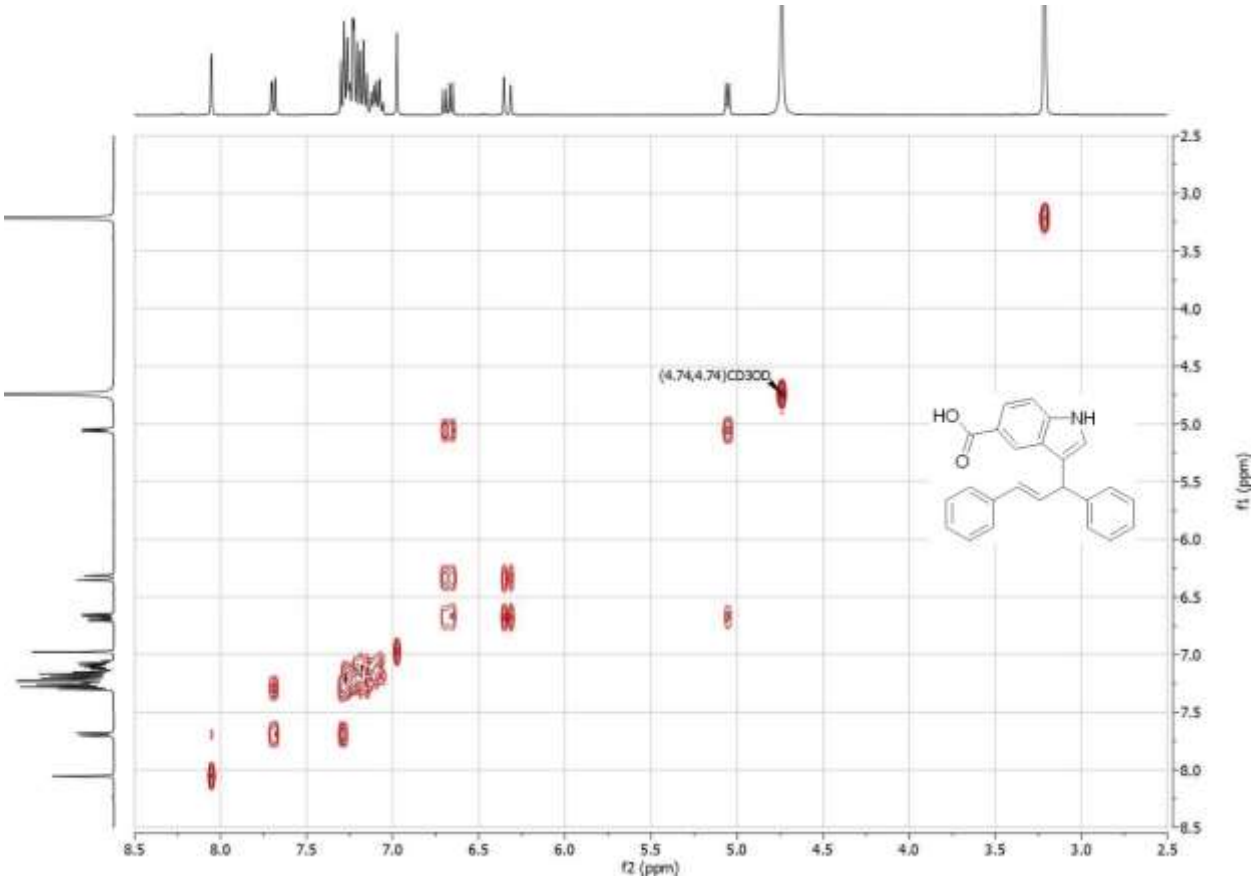

Figure C.116 COSY spectrum of ***21f*** *in methanol-d₄.*

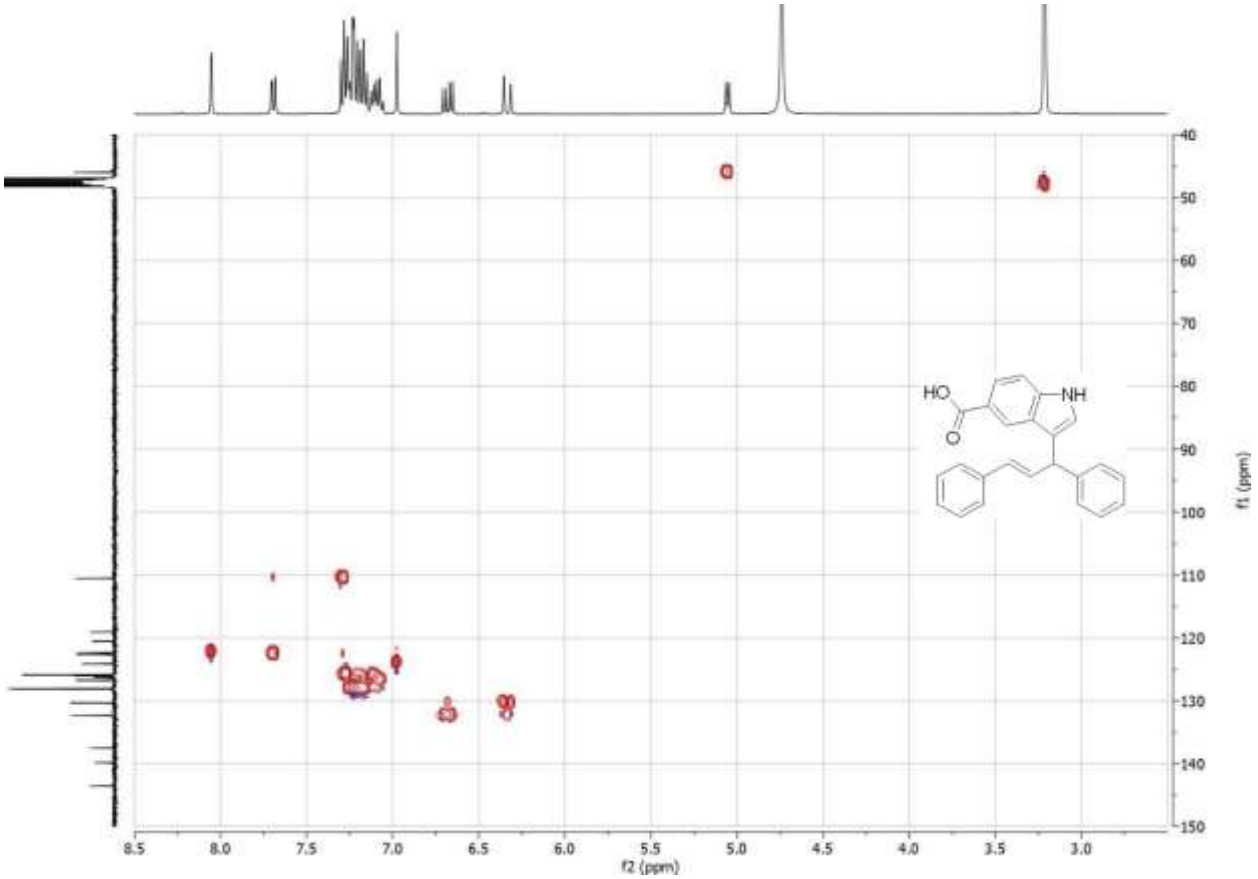

Figure C.117 HSQC spectrum of ***21f*** in methanol-d_4.

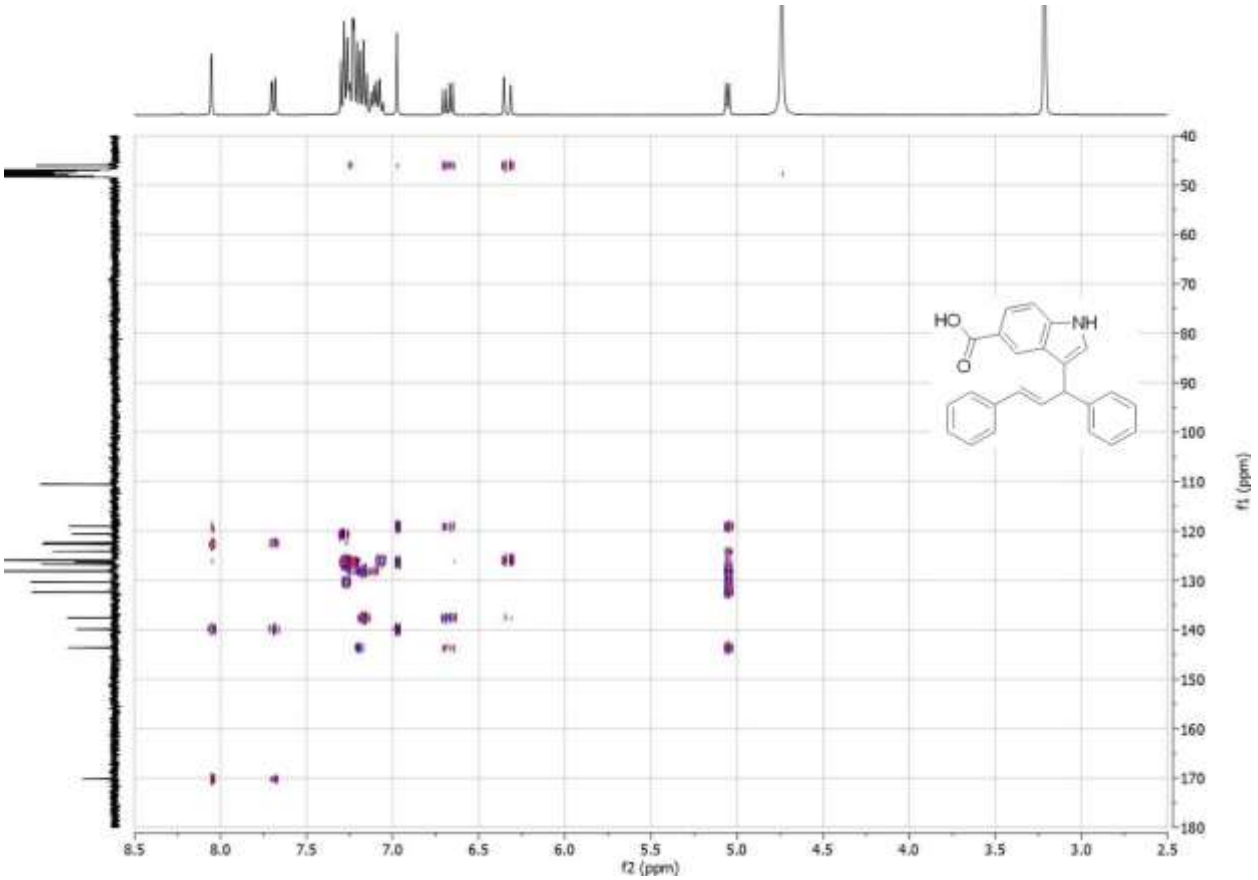

Figure C.118 HMBC spectrum of ***21f*** in methanol-d_4.

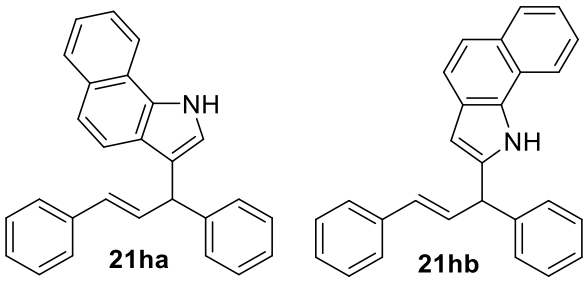

Chemical Formula: $C_{27}H_{21}N$
Molecular Weight: 359,4720

1.54 : 1

^{1}H NMR (400 MHz, Chloroform-*d*) δ [ppm] = 8.61 (s), 8.59 (s), 7.95 – 7.82 (m), 7.73 (d, *J* = 8.6 Hz), 7.67 (d, *J* = 8.5 Hz), 7.54 – 7.14 (m), 6.87 (d, *J* = 2.6 Hz), 6.77 (dd, *J* = 15.9, 7.4 Hz), 6.71 (d, *J* = 8.3 Hz), 6.69 – 6.67 (m), 5.19 (d, *J* = 7.2 Hz), 5.08 (d, *J* = 7.5 Hz).

^{13}C NMR (101 MHz, $CDCl_3$) δ [ppm] = 143.61, 141.70, 138.38, 137.60, 136.97, 132.75, 132.02, 131.34, 130.74, 130.57, 130.51, 130.29, 128.97, 128.95, 128.93, 128.72, 128.66, 128.64, 128.61, 128.57, 127.76, 127.30, 126.58, 126.53, 126.46, 125.50, 125.43, 124.44, 124.05, 123.93, 123.90, 123.73, 122.76, 122.39, 121.86, 121.59, 120.92, 120.78, 120.75, 120.66, 120.38, 119.90, 119.49, 104.28, 103.35, 48.63, 46.31.

GC/MS (EI): calc. for $C_{27}H_{21}N$ $[M]^+$: 359.167; found: 359.162, $C_{21}H_{16}N$ 282.108, $C_{19}H_{14}N$ 256.113, C_7H_7 91.036, C_6H_5 77.034.

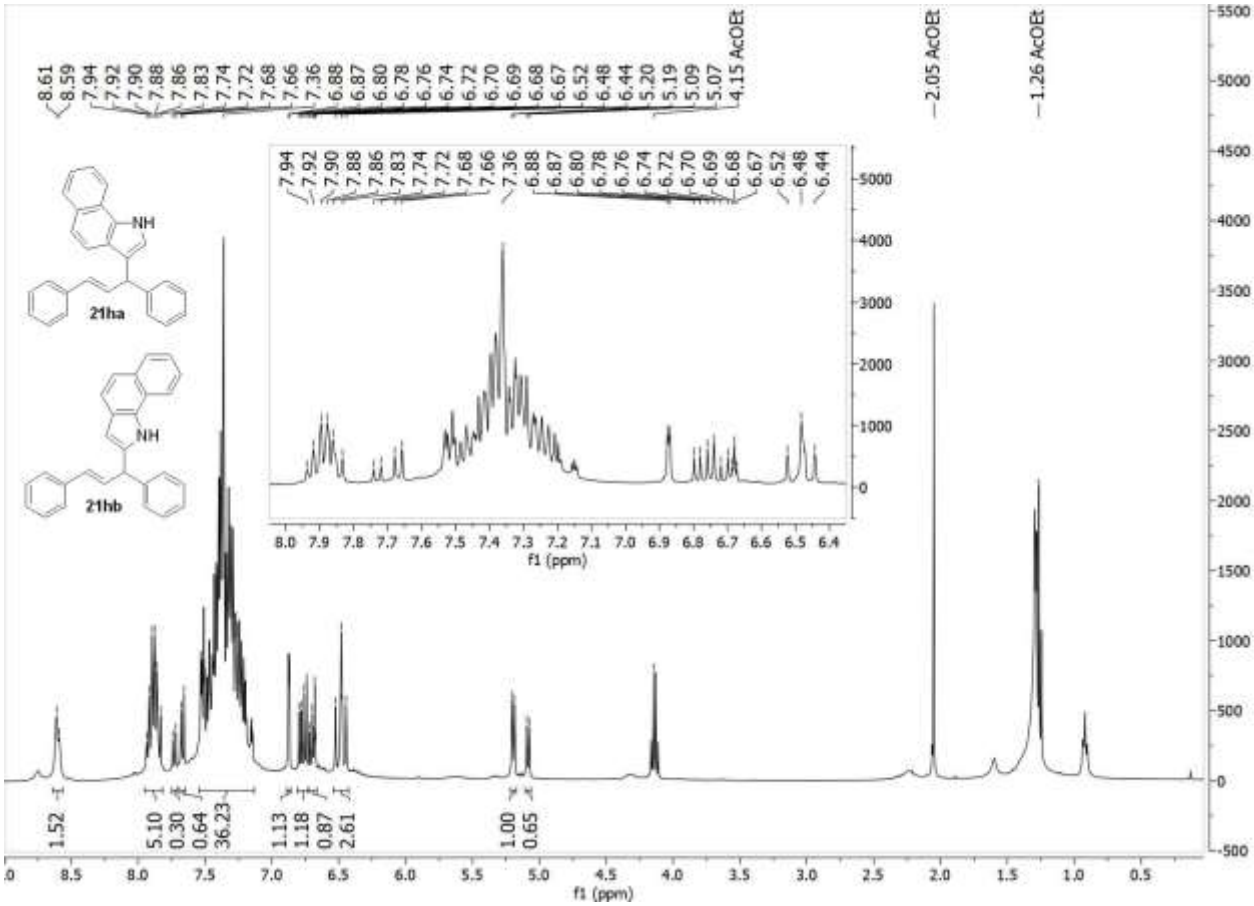

*Figure C.119 ^{1}H NMR spectrum of a 1.54:1 mixture of **21ha** and **21hb** in $CDCl_3$.*

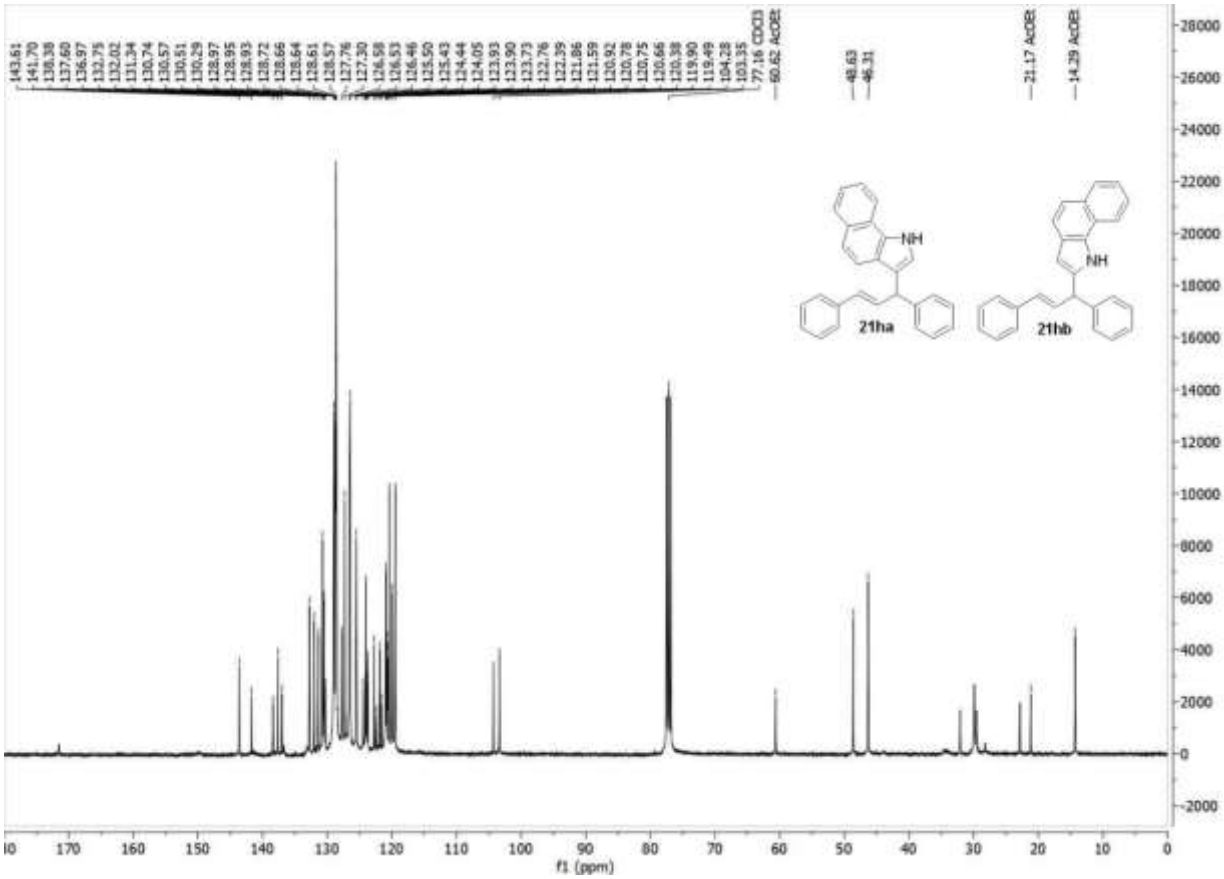

Figure C.120 $^{13}C(^{1}H)$ *NMR spectrum of a 1.54:1 mixture of 21ha and 21hb in* $CDCl_3$.

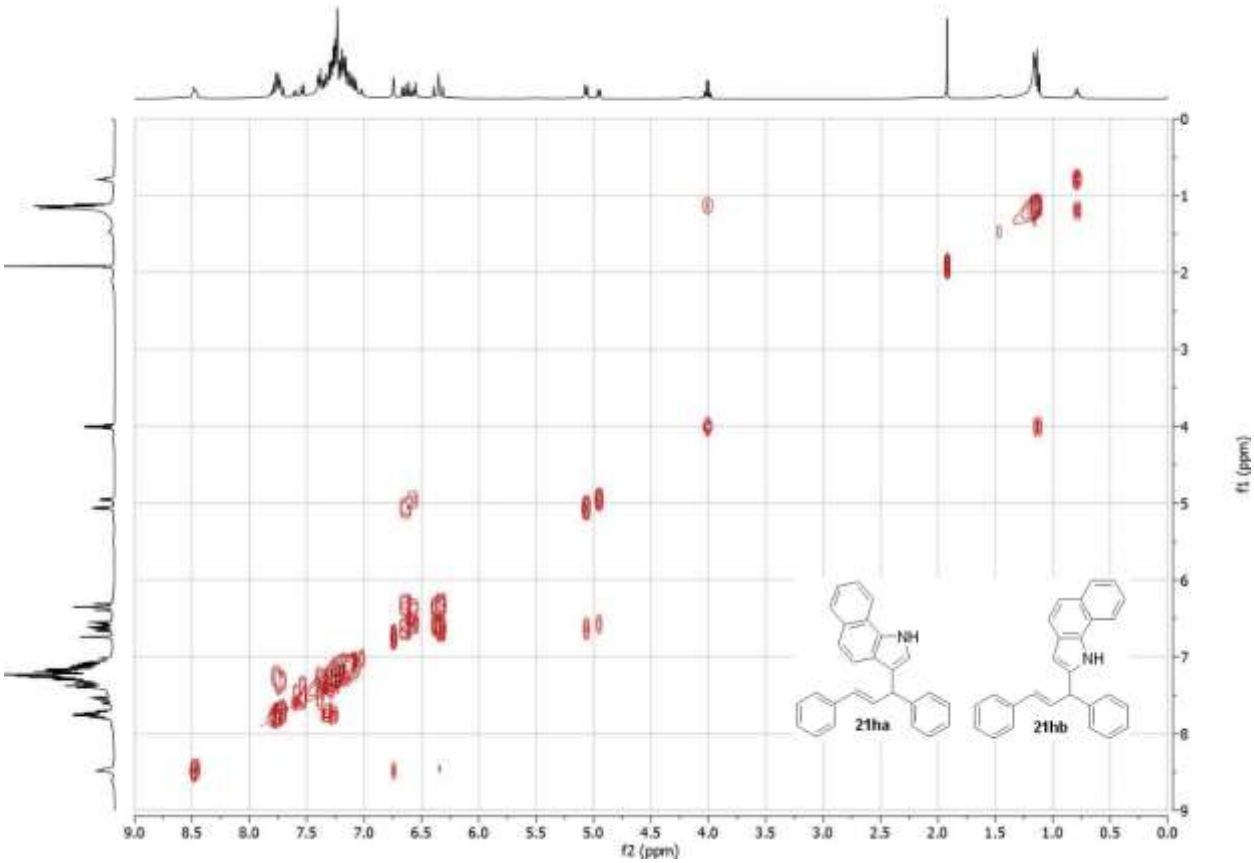

Figure C.121 COSY spectrum of a 1.54:1 mixture of ***21ha*** *and* ***21hb*** *in* $CDCl_3$.

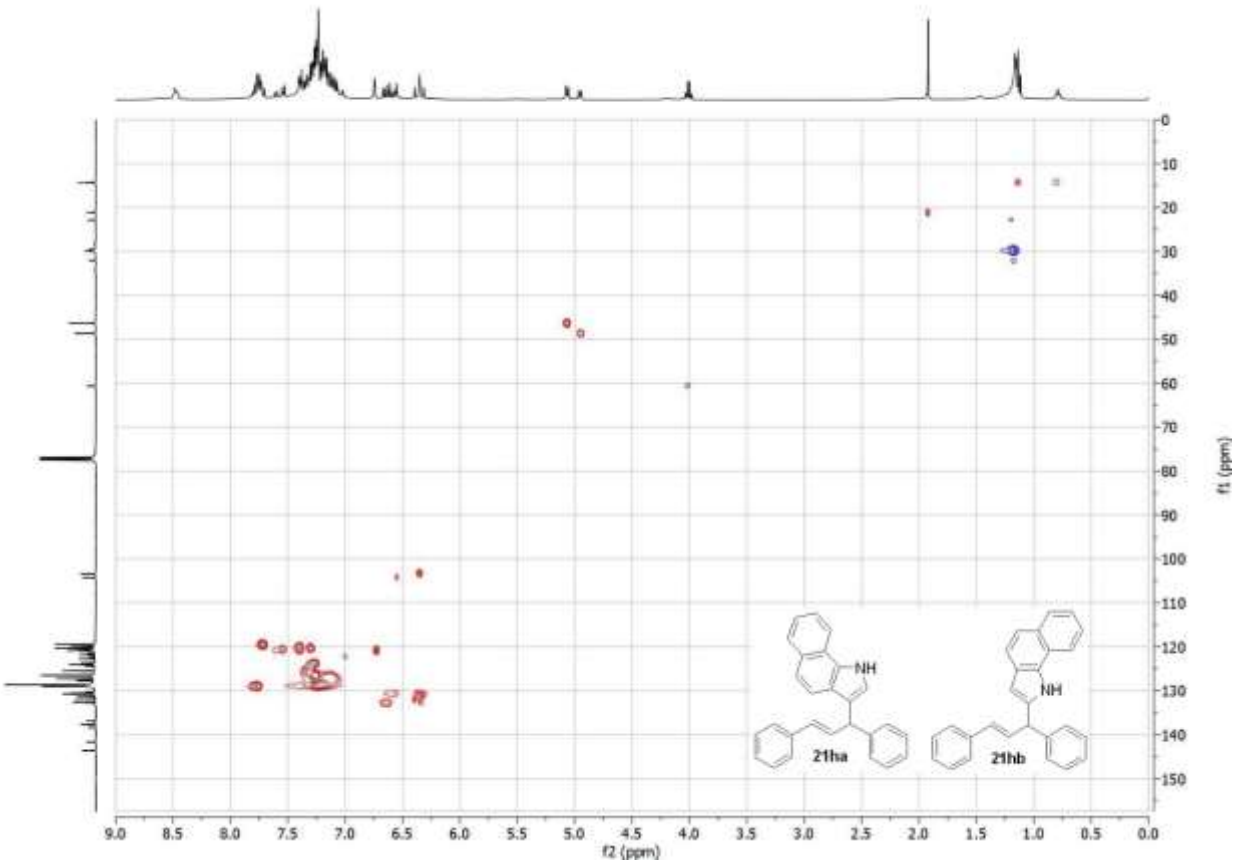

Figure C.122 *HSQC spectrum of a 1.54:1 mixture of* ***21ha*** *and* ***21hb*** *in* $CDCl_3$.

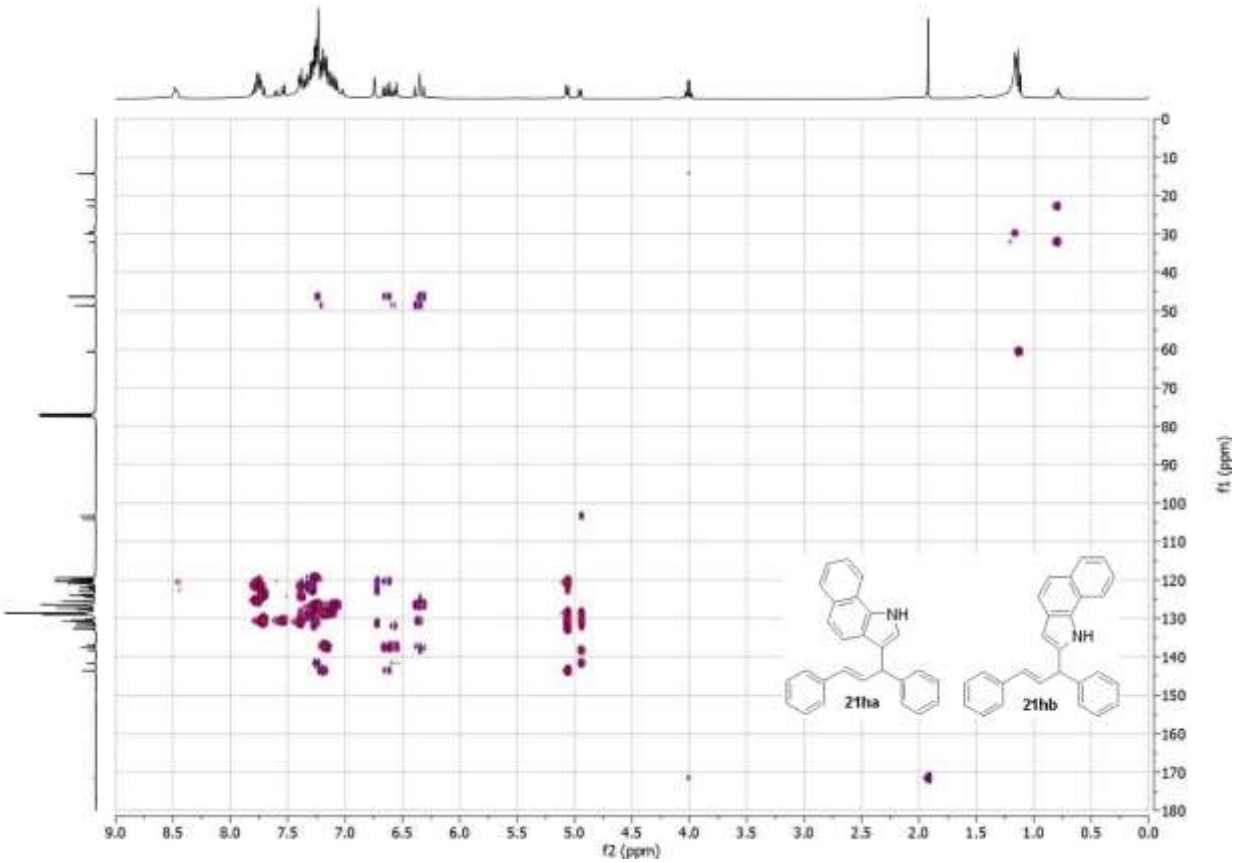

Figure C.123 *HMBC spectrum of a 1.54:1 mixture of 21ha and 21hb in* $CDCl_3$.

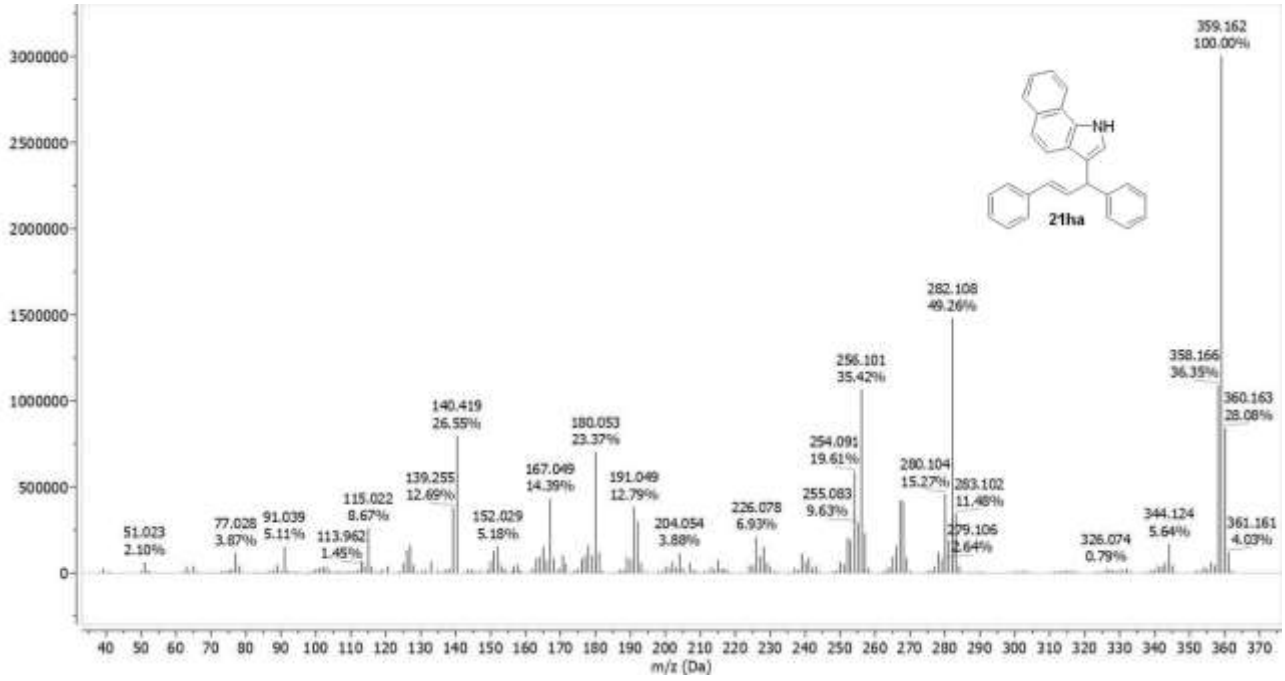

Figure C.124 *GC-MS spectrum of* ***21ha****.*

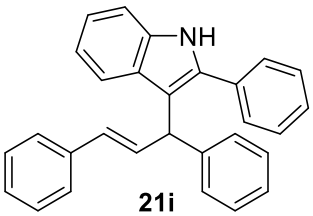

21i

Chemical Formula: $C_{29}H_{23}N$
Molecular Weight: 385,51

^{1}H NMR (400 MHz, Chloroform-*d*) δ [ppm] = 8.08 (s, 1H), 7.56 – 7.52 (m, 2H), 7.48 – 7.32 (m, 9H), 7.30 – 7.14 (m, 7H), 7.01 (m, 1H), 6.90 (dd, *J* = 15.8, 7.3 Hz, 1H), 6.42 (dd, *J* = 15.9, 1.4 Hz, 1H), 5.30 (d, *J* = 7.3 Hz, 1H).

^{13}C NMR (101 MHz, $CDCl_3$) δ [ppm] = 143.63, 137.65, 136.40, 135.73, 133.12, 132.41, 131.22, 128.95, 128.75, 128.58, 128.44, 128.40, 128.18, 128.06, 127.24, 126.45, 126.25, 122.25, 121.35, 119.84, 114.00, 111.07, 60.56, 45.28, 21.18, 14.33.

GC/MS (EI): calc. for $C_{29}H_{23}N$ $[M]^+$: 385.183; found: 385.187, $C_{23}H_{18}N$ 308.122, $C_{22}H_{16}N$ 294.118, $C_{15}H_{12}N$ 206, C_7H_7 91.036, C_6H_5 77.034.

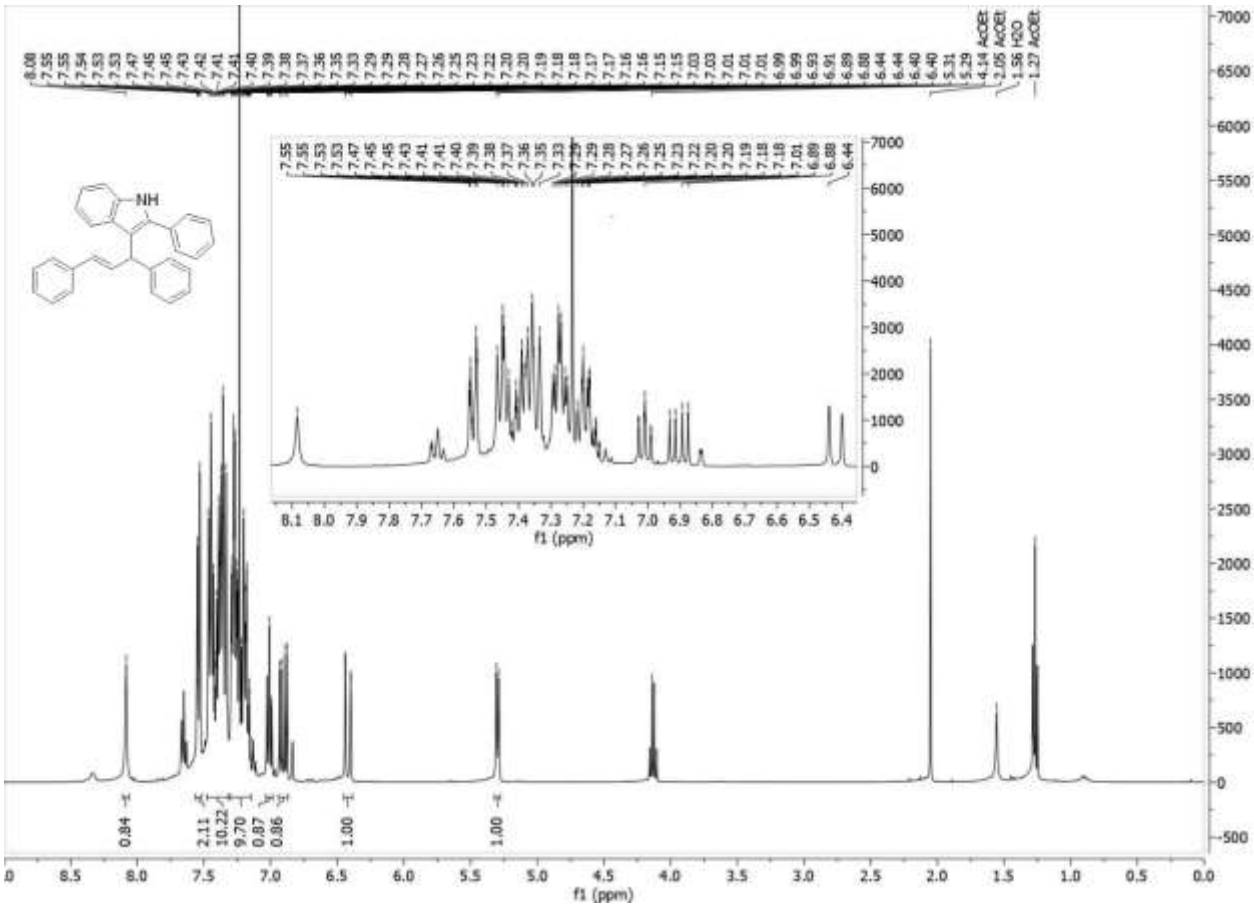

*Figure C.125 ^{1}H NMR spectrum of **21i** in $CDCl_3$.*

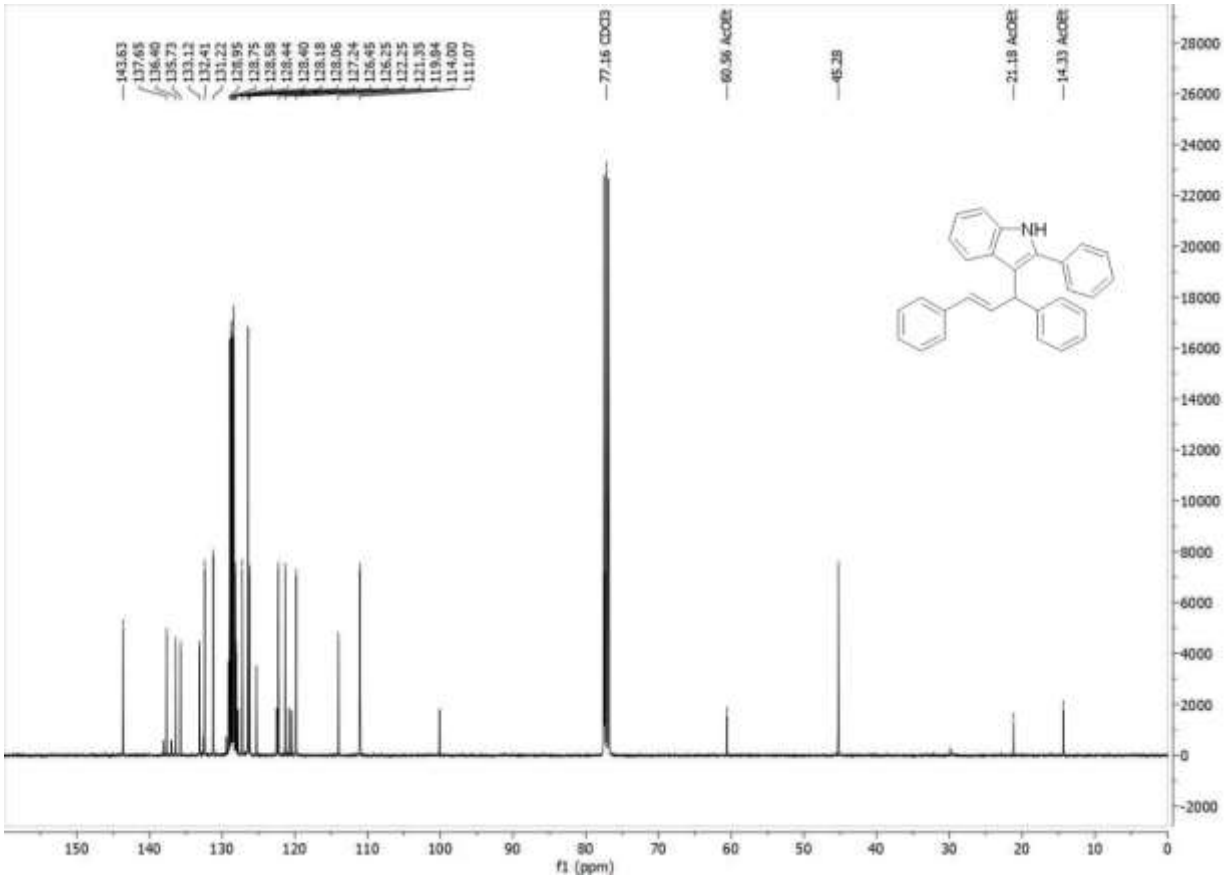

Figure C.126 $^{13}C(^{1}H)$ *NMR spectrum of* ***21i*** *in* $CDCl_3$.

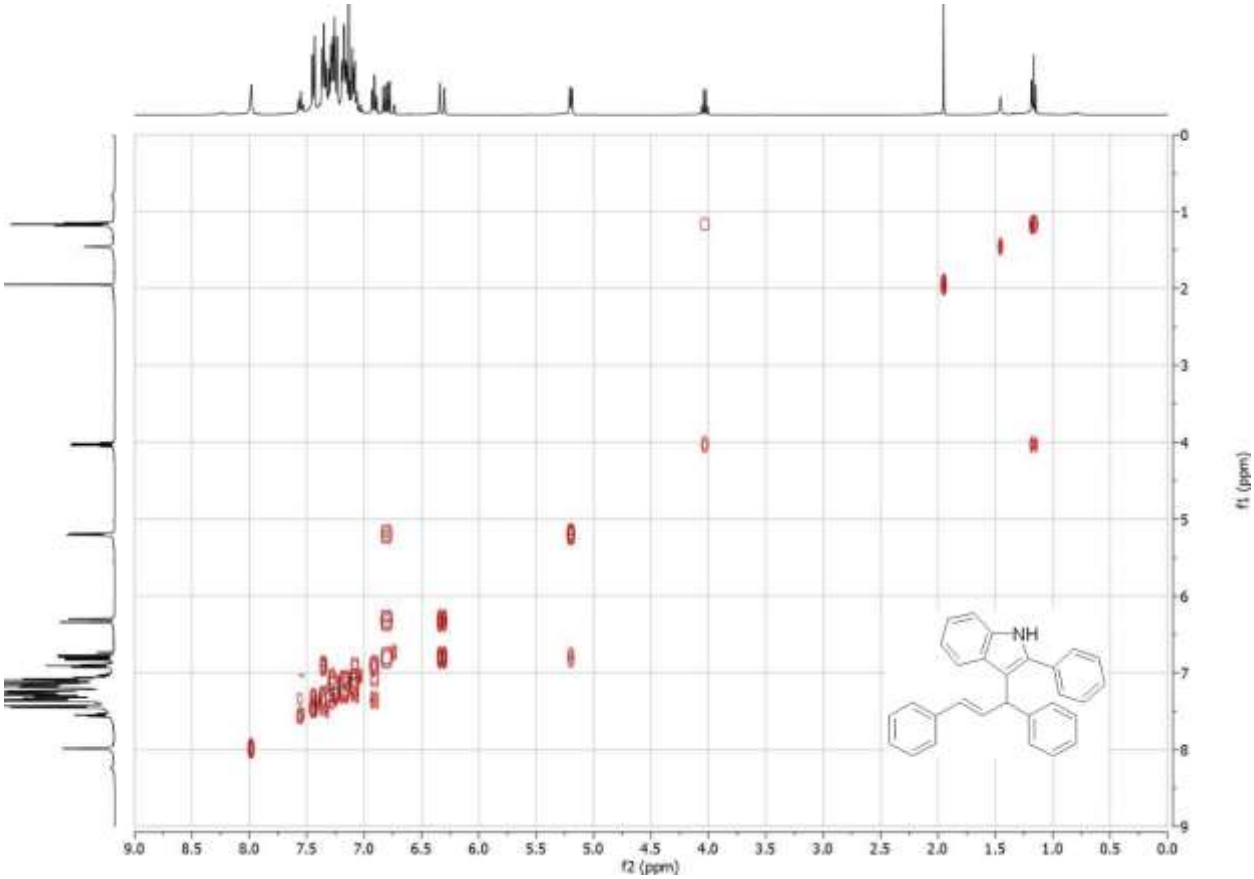

Figure C.127 COSY spectrum of ***21i*** *in* $CDCl_3$.

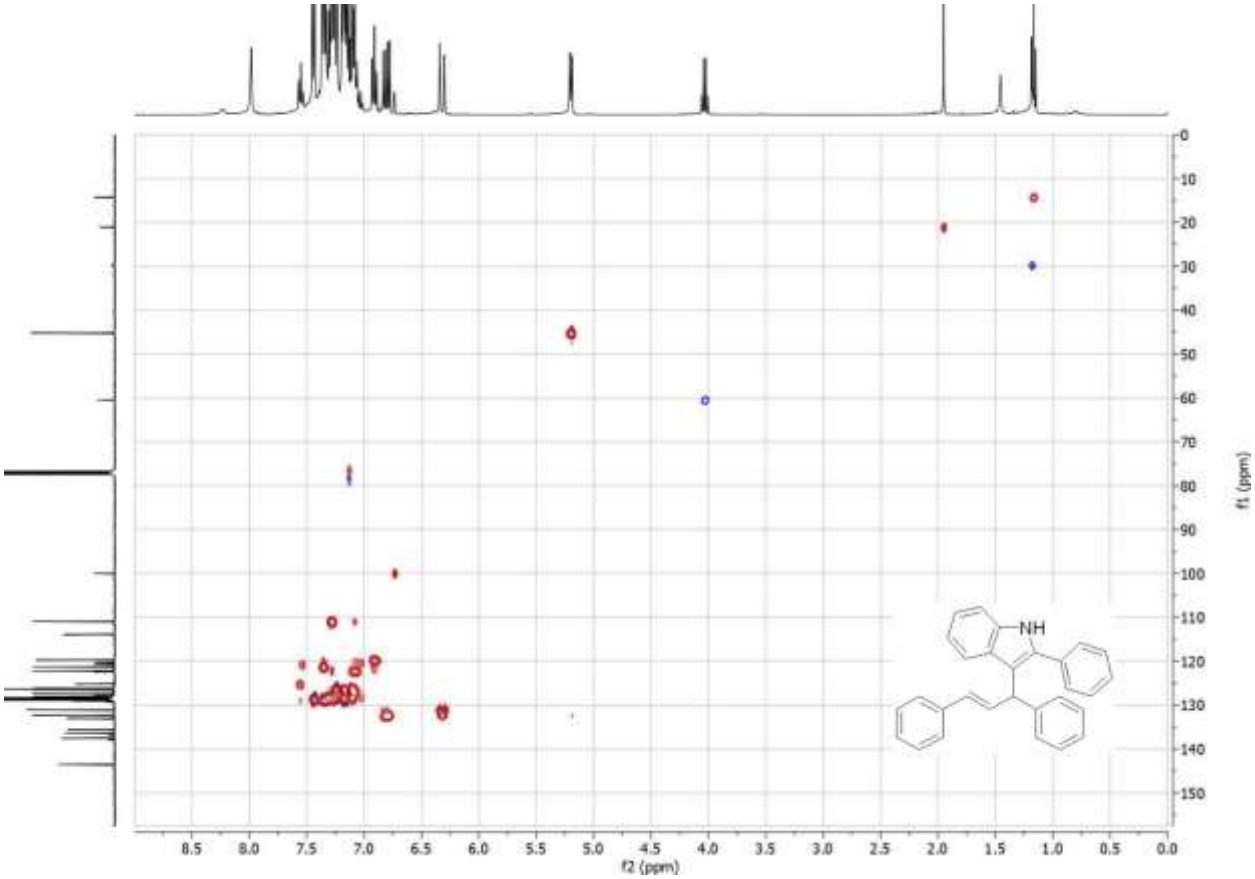

Figure C.128 HSQC spectrum of ***21i*** in $CDCl_3$.

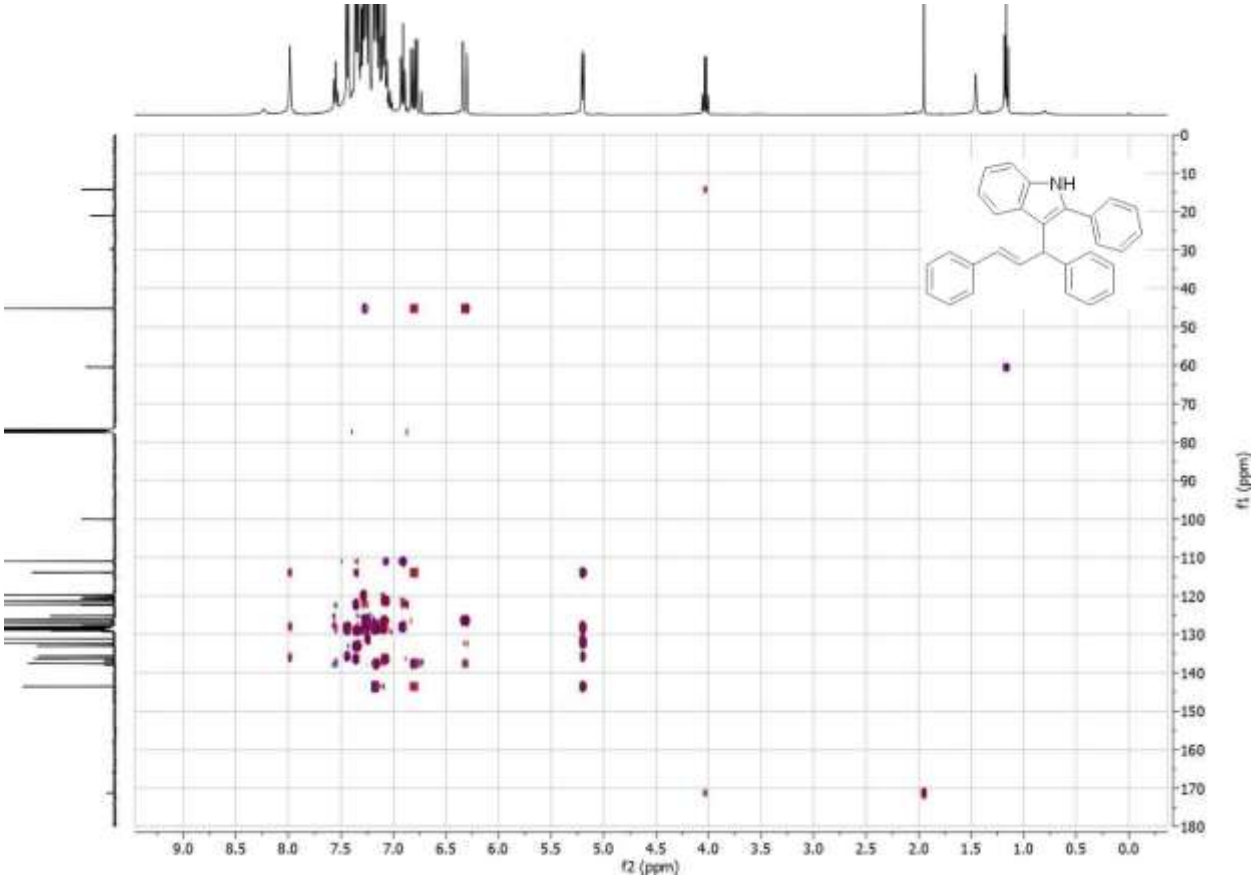

Figure C.129 HMBC spectrum of ***21i*** in $CDCl_3$.

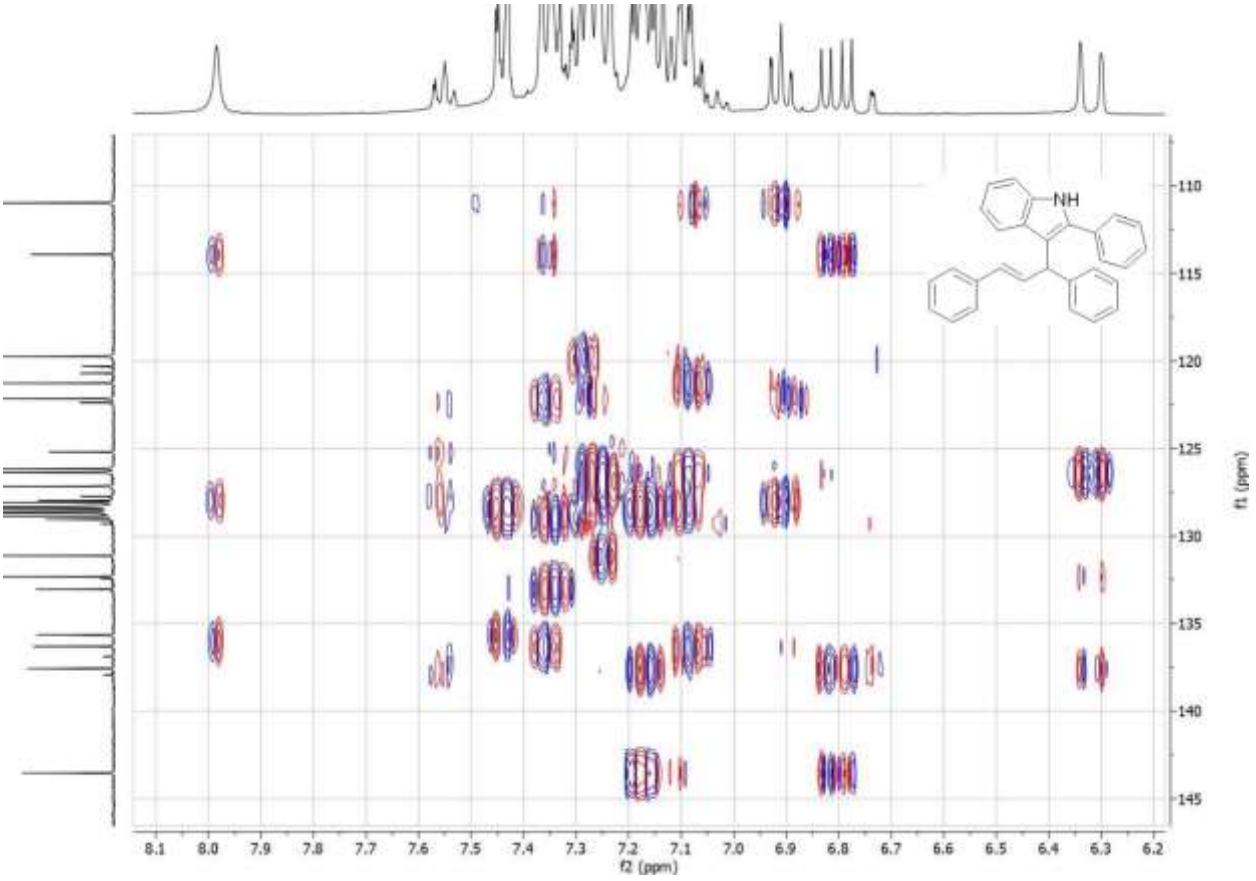

Figure C.130 Detail of the HMBC spectrum of **21i** in $CDCl_3$.

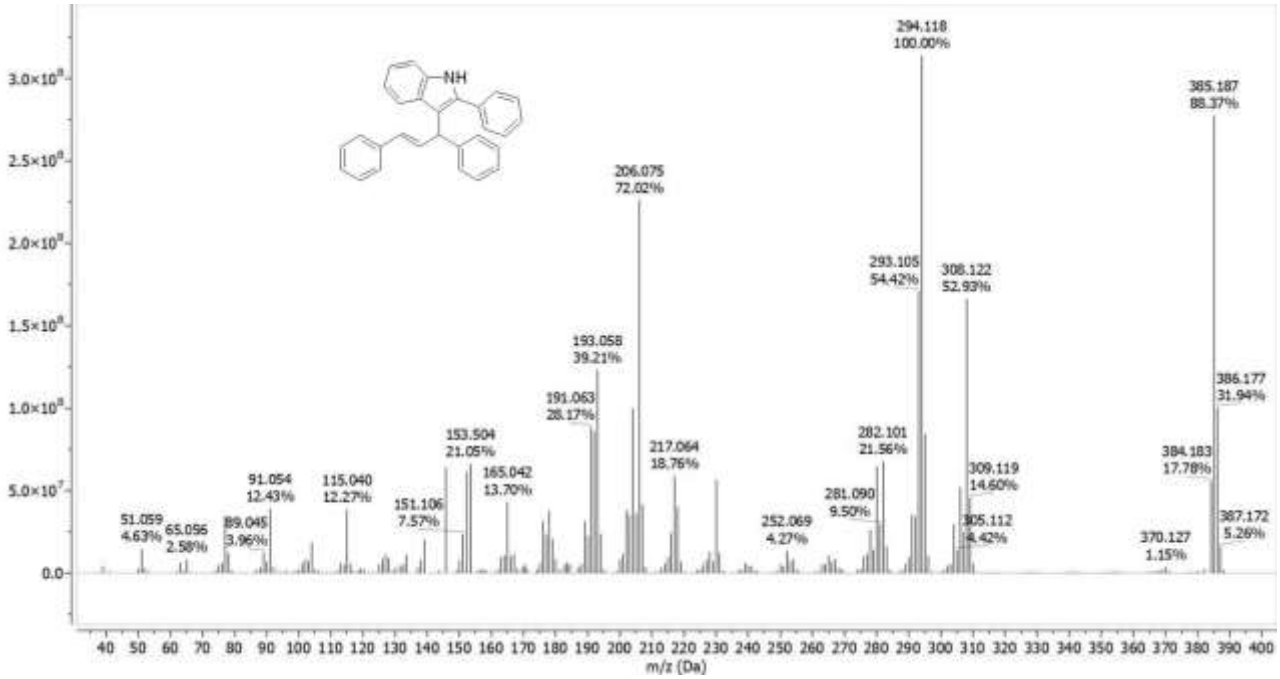

Figure C.131 GC-MS spectrum of **21i**.

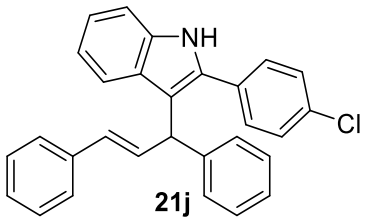

21j

Chemical Formula: $C_{29}H_{22}ClN$
Molecular Weight: 419,95

^{1}H NMR (400 MHz, Chloroform-*d*) δ [ppm] = 8.08 (s, 1H), 7.48 – 7.36 (m, 7H), 7.36 – 7.31 (m, 3H), 7.30 – 7.24 (m, 4H), 7.24 – 7.16 (m, 3H), 7.01 (t, *J* = 7.5 Hz, 1H), 6.87 (dd, *J* = 15.9, 7.3 Hz, 1H), 6.39 (d, *J* = 15.9 Hz, 1H), 5.22 (d, *J* = 7.2 Hz, 1H). Contaminated with 2-(4-chlorophenyl)indole **20j**, ^{1}H- and ^{13}C NMR spectra available at [1]. contamination confirmed also by GC-MS (calculated for $C_{29}H_{22}ClN$: 227.050 [M^+]; found: 227.016).

^{13}C NMR (101 MHz, $CDCl_3$) δ [ppm] = 143.63, 137.65, 136.40, 135.73, 133.12, 132.41, 131.22, 128.95, 128.75, 128.58, 128.44, 128.40, 128.18, 128.06, 127.24, 126.45, 125.30, 122.25, 121.35, 119.84, 114.00, 111.07, 45.28.

GC/MS (EI): calc. for $C_{29}H_{22}ClN$ [M]$^+$: 419.144; found: 419.121, $C_{23}H_{17}ClN$ 342.061, $C_{15}H_{10}ClN$ 240.022, C_7H_7 91.036, C_6H_5 77.034.

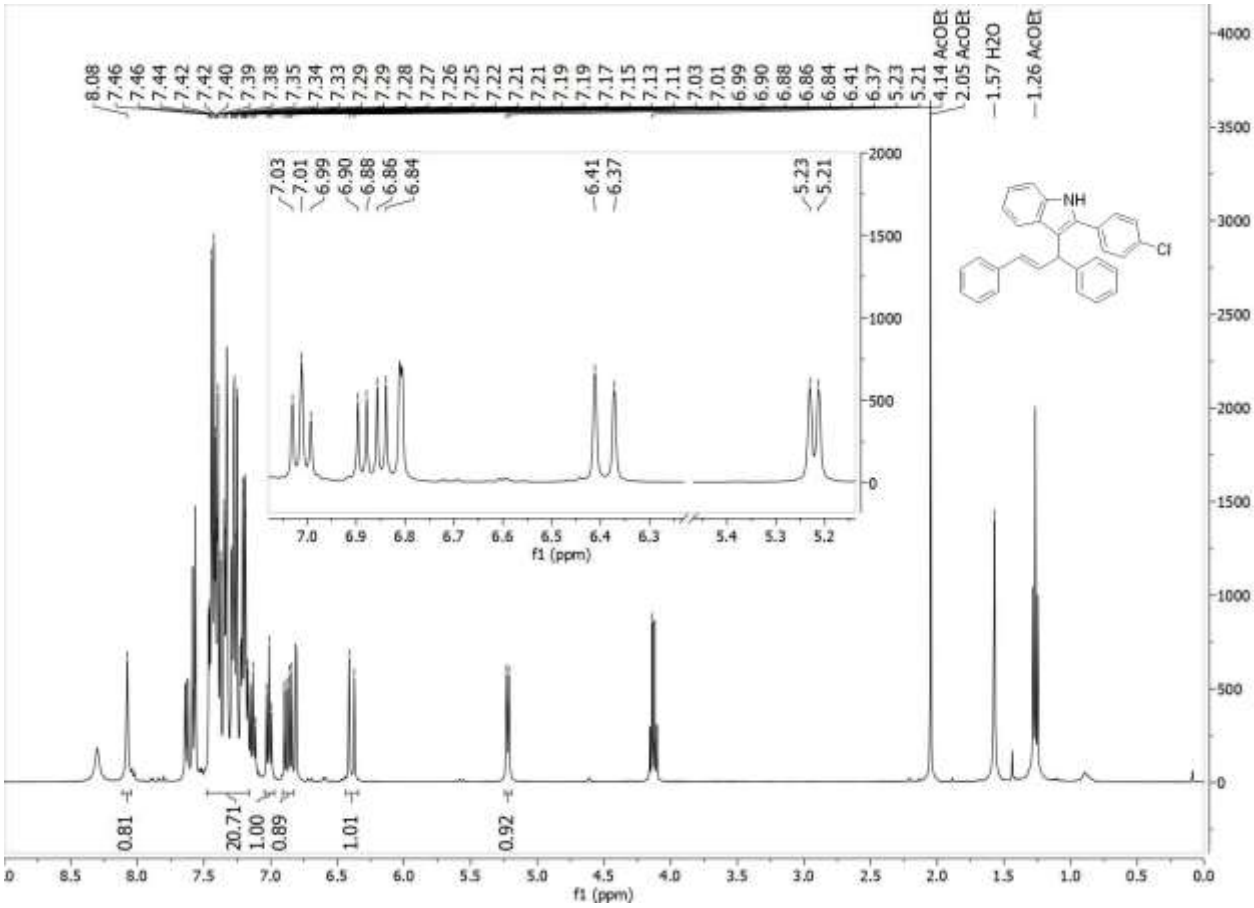

*Figure C.132 ^{1}H NMR spectrum of **21j** in $CDCl_3$.*

[1] Peña-López, M.; Neumann, H.; Beller, M. Ruthenium-Catalyzed Synthesis of Indoles from Anilines and Epoxides. *Chemistry – A European Journal* **2014**, *20* (7), 1818–1824. https://doi.org/10.1002/chem.201304432.

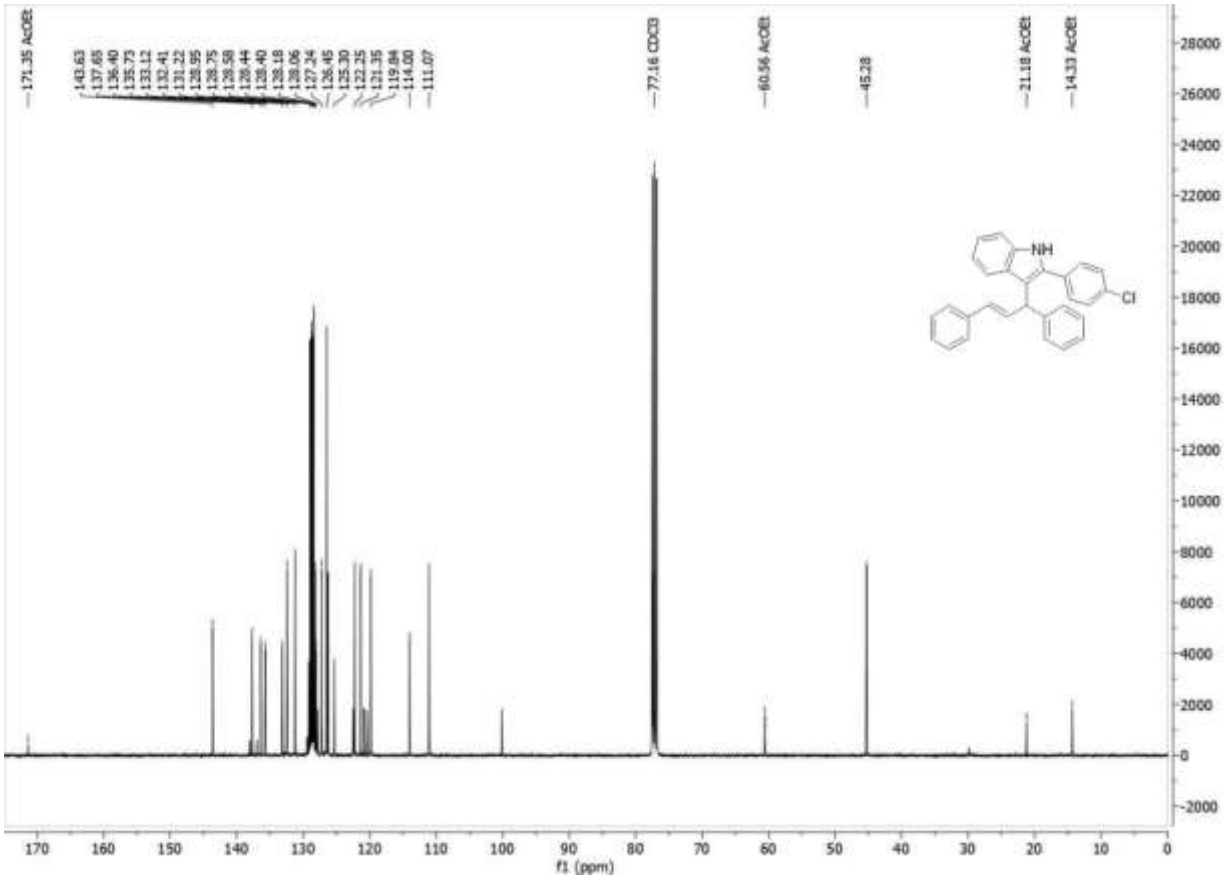

Figure C.133 $^{13}C(^{1}H)$ *NMR spectrum of* ***21j*** *in* $CDCl_3$.

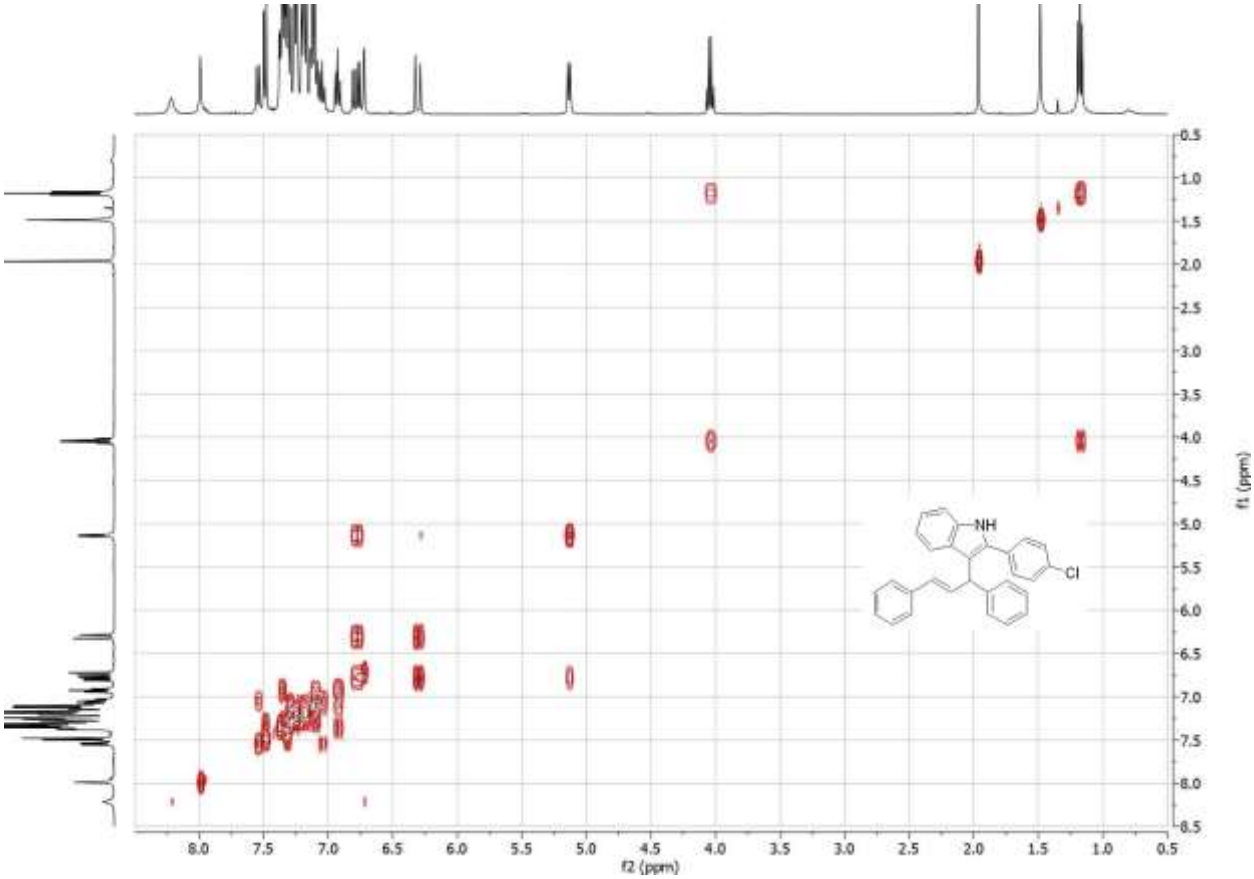

Figure C.134 COSY spectrum of ***21j*** *in* $CDCl_3$.

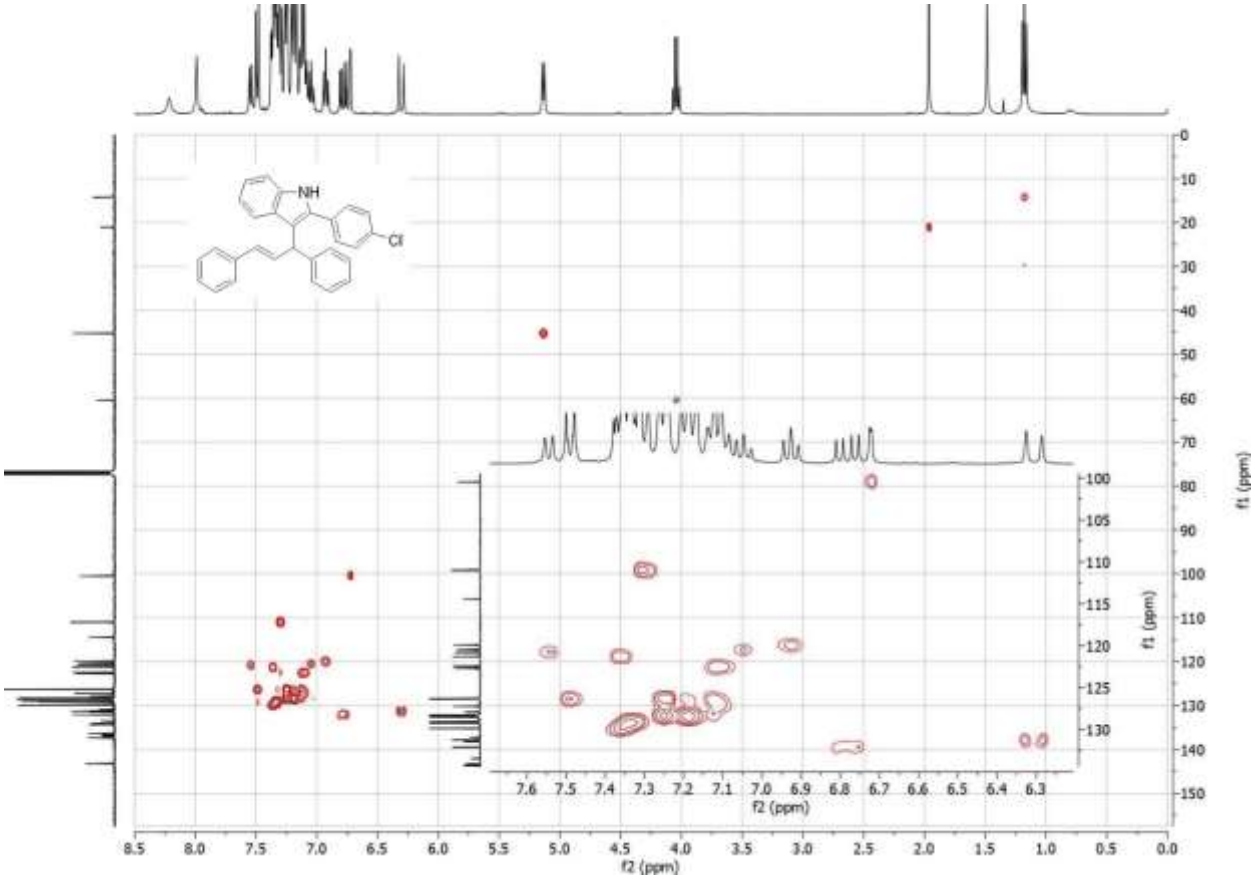

Figure C.135 HSQC spectrum of ***21j*** in $CDCl_3$.

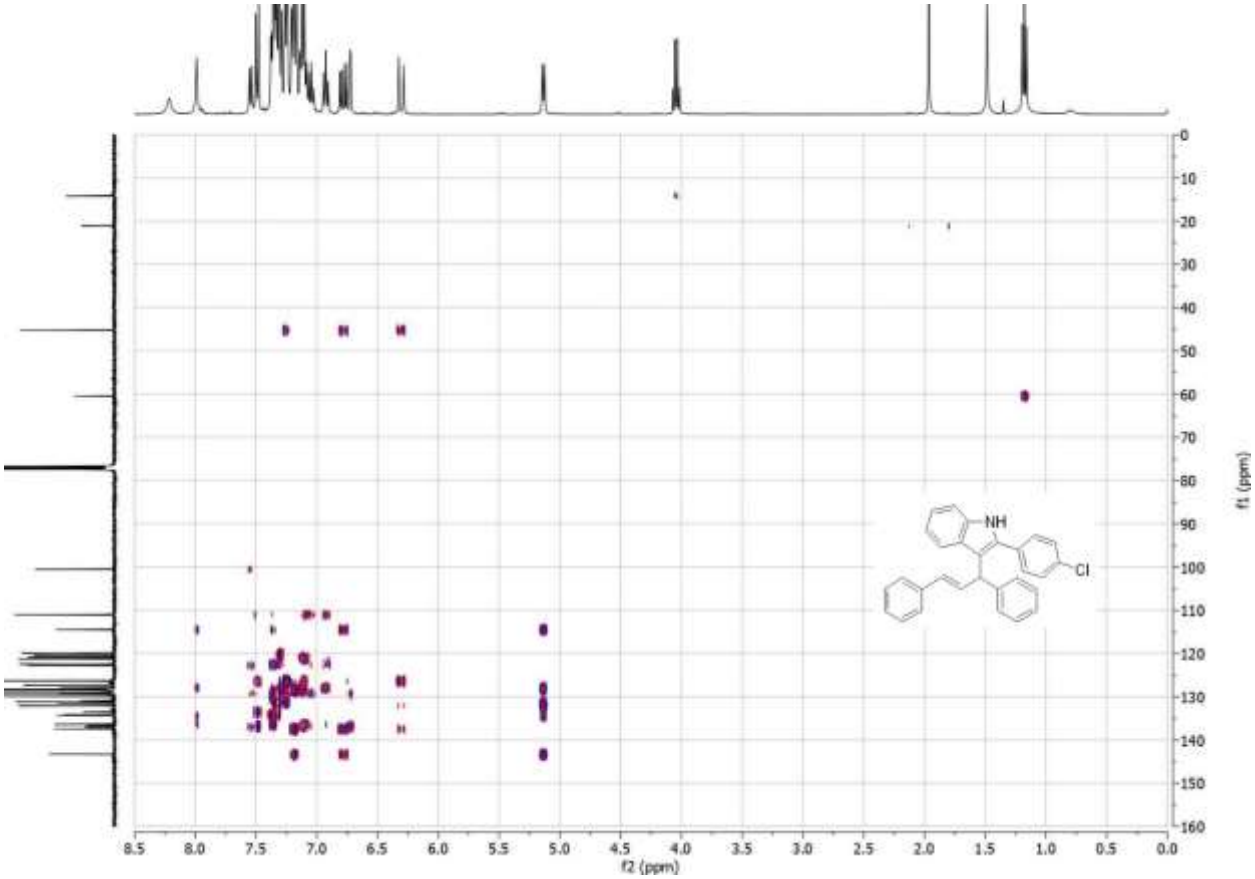

Figure C.136 HMBC spectrum of ***21j*** in $CDCl_3$.

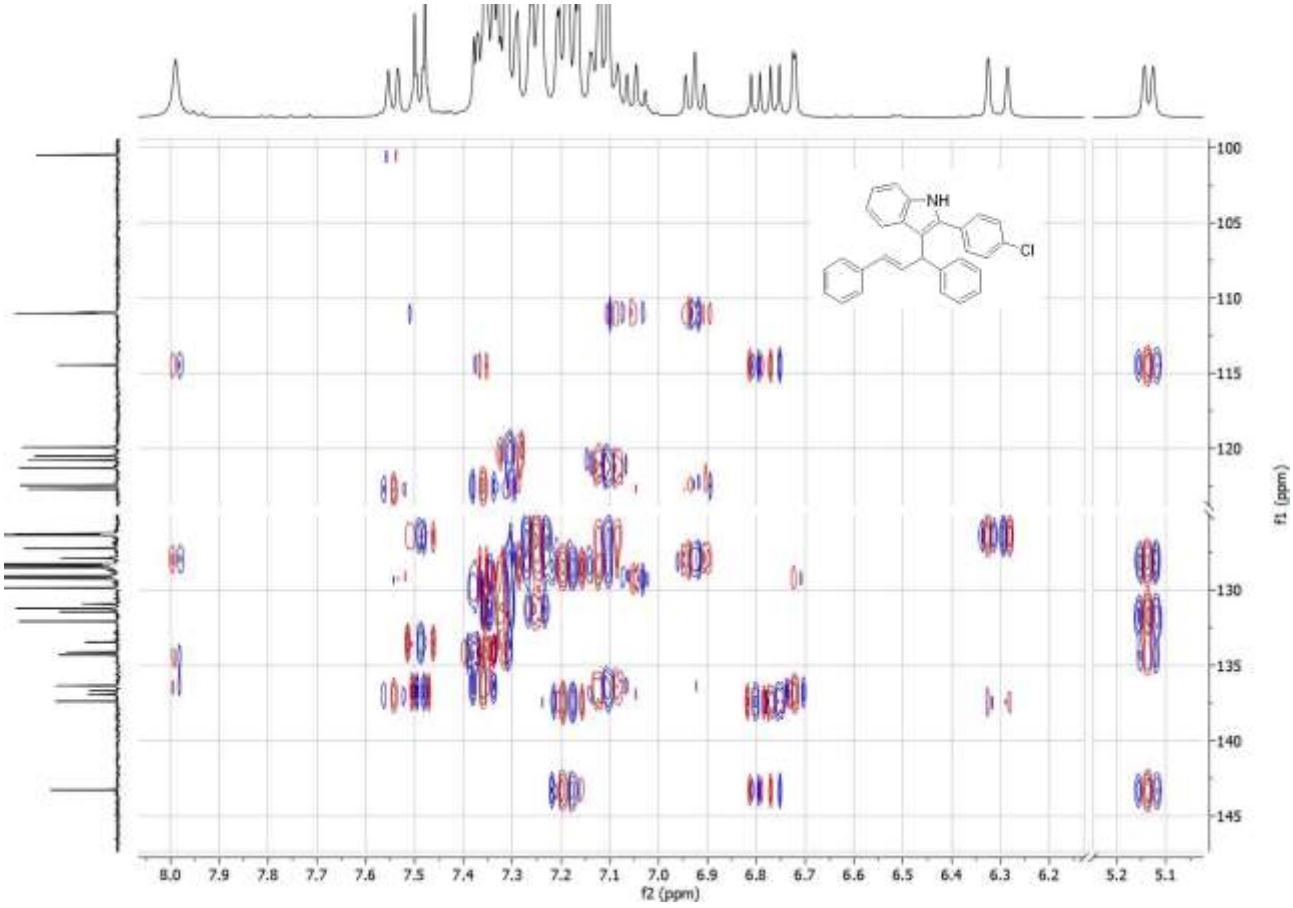

Figure C.137 Detail of the HMBC spectrum of **21j** in $CDCl_3$.

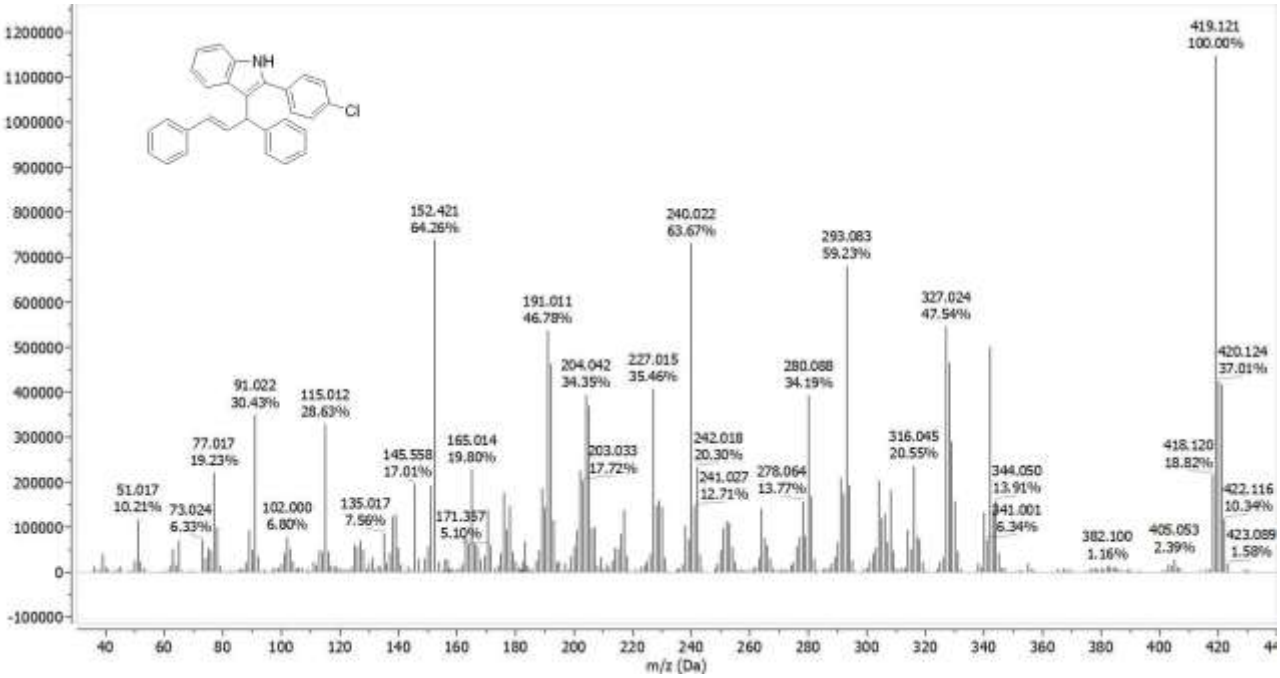

Figure C.138 GC-MS spectrum of **21j**.

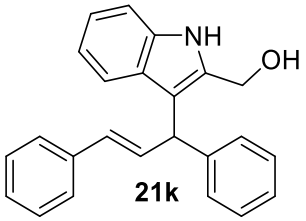

21k

Chemical Formula: $C_{24}H_{21}NO$
Molecular Weight: 339,44

^{1}H NMR (400 MHz, Chloroform-*d*) δ [ppm] = 8.37 (s, 1H), 7.46 (d, *J* = 8.0 Hz, 1H), 7.38 – 7.12 (m, 12H), 7.03 (t, *J* = 7.5 Hz, 1H), 6.82 (dd, *J* = 15.8, 7.2 Hz, 1H), 6.41 (d, *J* = 15.8 Hz, 1H), 5.21 (d, *J* = 7.1 Hz, 1H), 4.69 (s, 2H), 1.94 (s, 1H).

^{13}C NMR (101 MHz, Chloroform-*d*) δ [ppm] = 143.48, 137.36, 135.72, 133.90, 132.05, 131.10, 128.67, 128.55, 128.31, 127.69, 127.42, 126.52, 126.41, 122.23, 120.23, 119.69, 114.00, 111.17, 57.15, 44.94.

GC/MS (EI): calc. for $C_{23}H_{22}O_2$ $[M]^+$: 330.162; found: 319.109 corresponding to a decomposition product formed in the GC column (see Figure Sx), $C_{18}H_{11}N$ 241.060, C_6H_5 77.034.

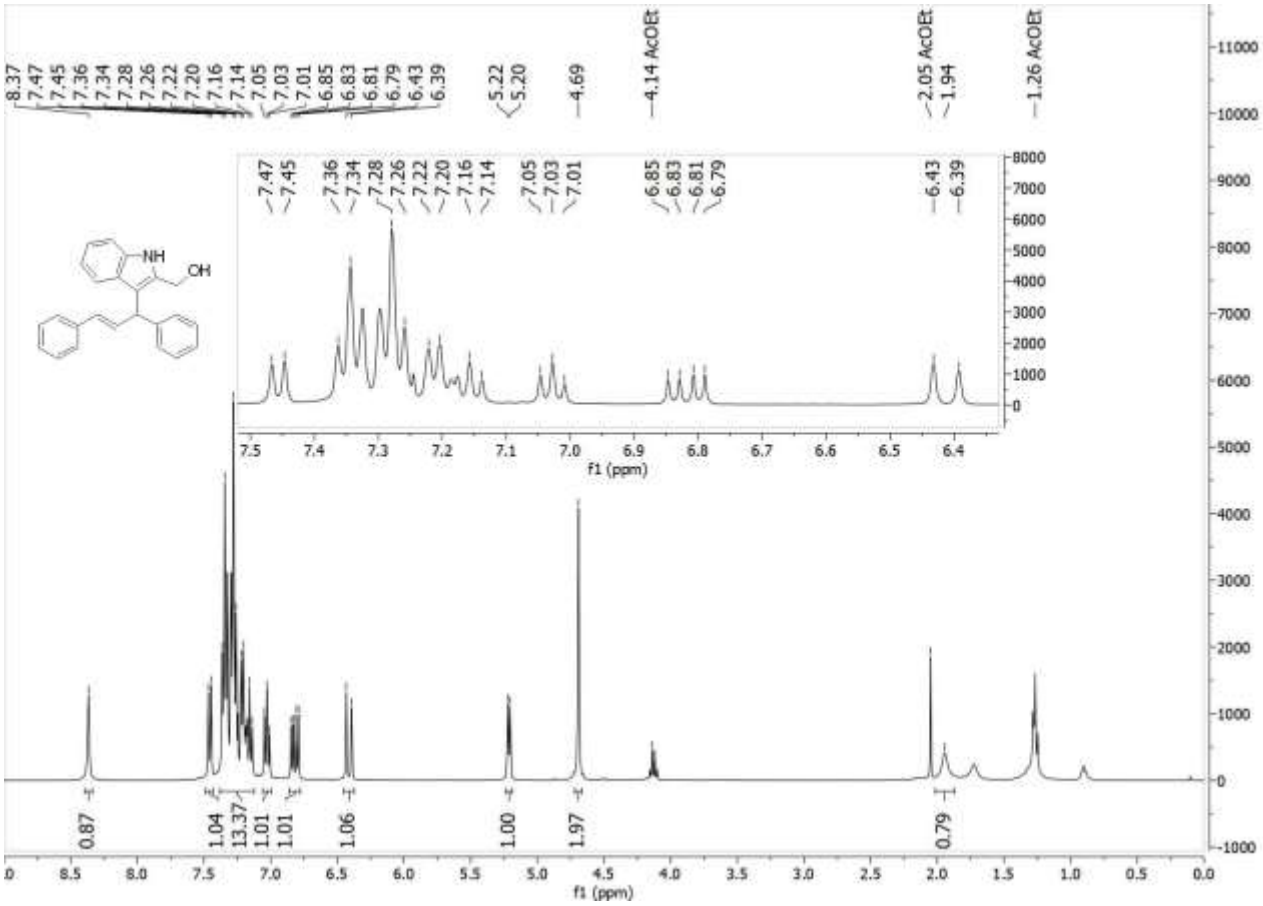

*Figure C.139 ^{1}H NMR spectrum of **21k** in $CDCl_3$.*

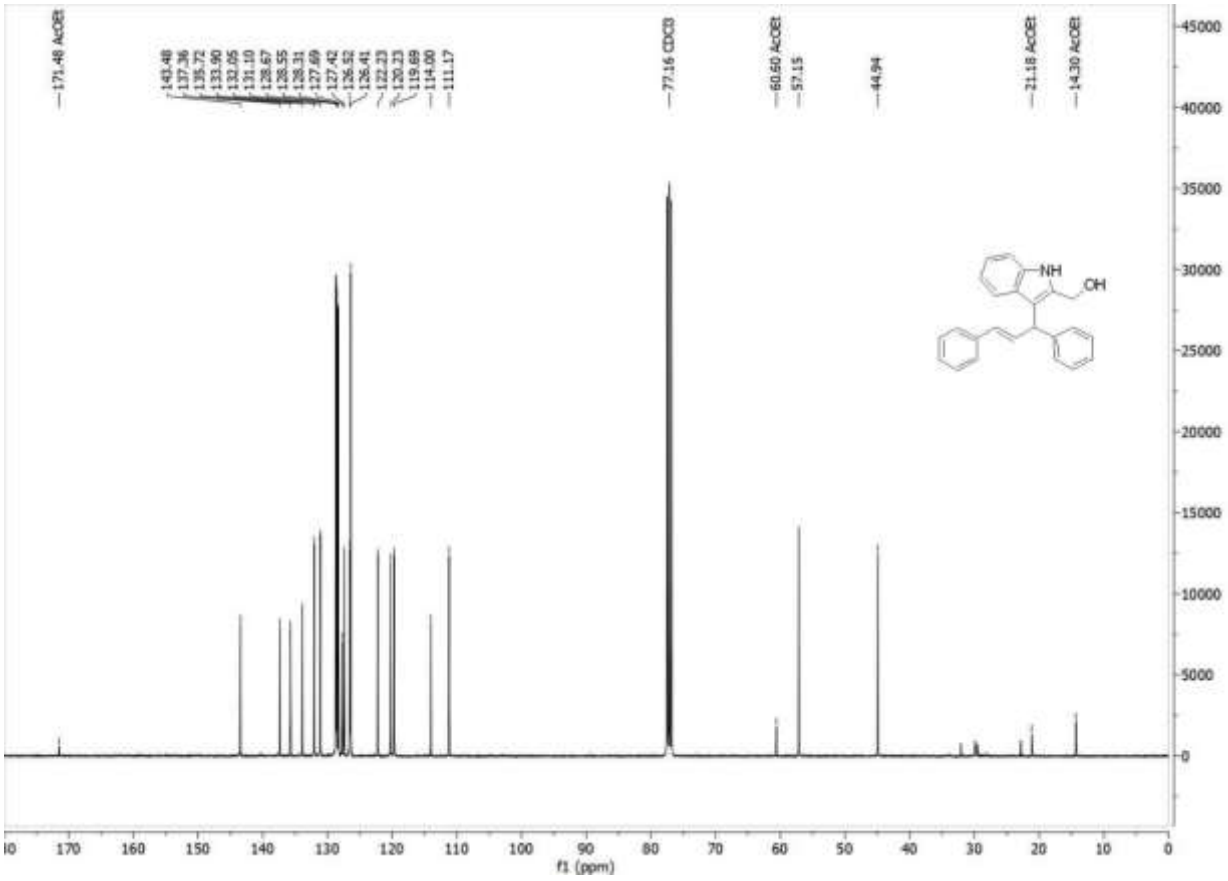

Figure C.140 $^{13}C(^{1}H)$ *NMR spectrum of* ***21k*** *in* $CDCl_3$.

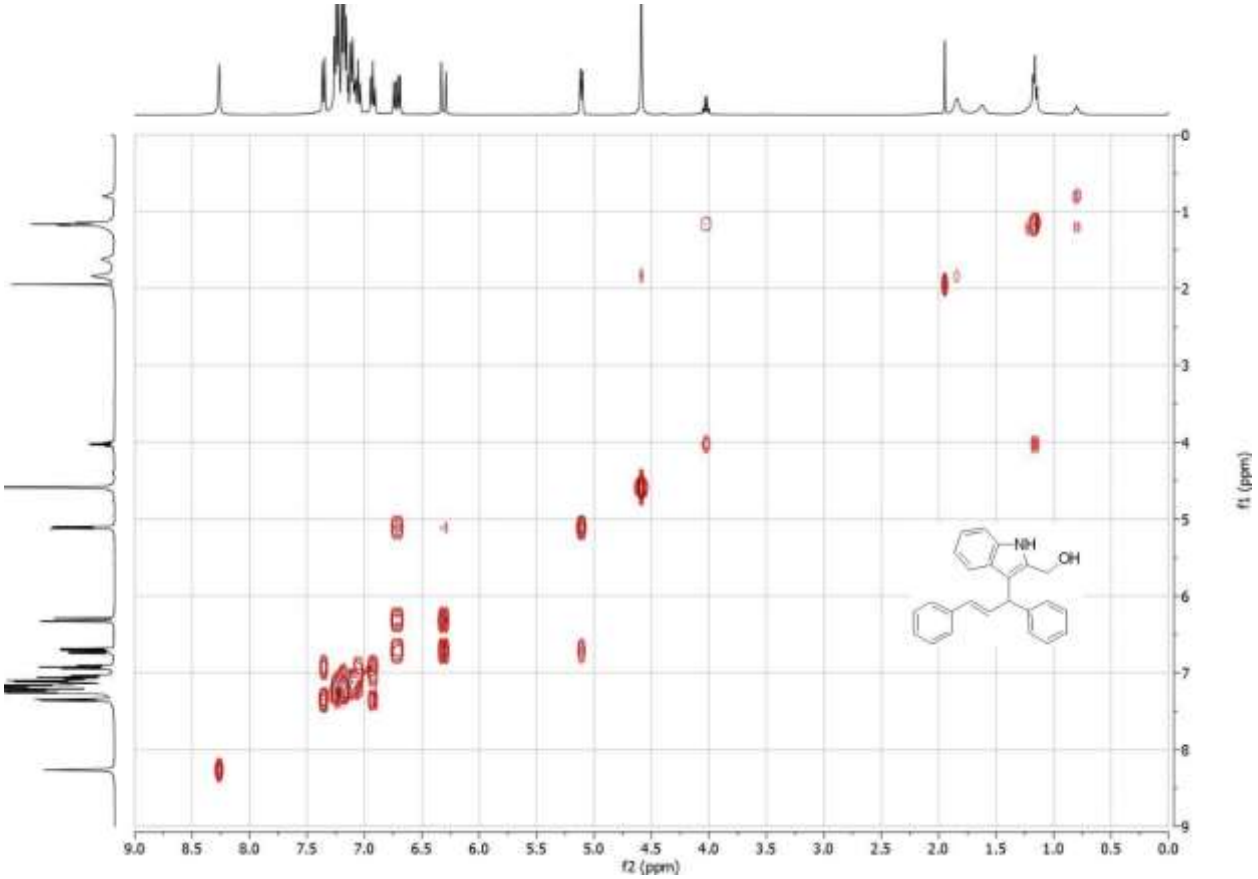

Figure C.141 COSY spectrum of ***21k*** *in* $CDCl_3$.

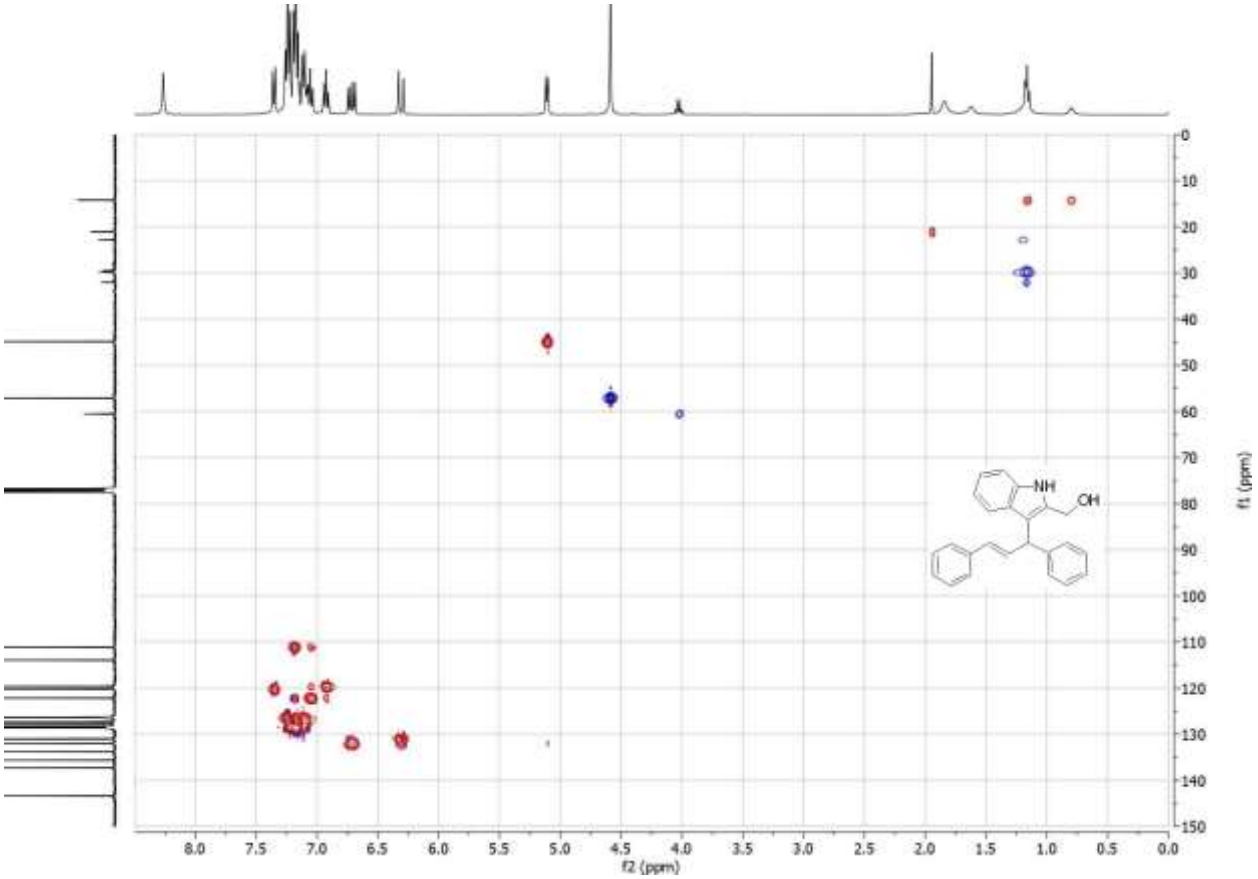

Figure C.142 HSQC spectrum of **21k** in $CDCl_3$.

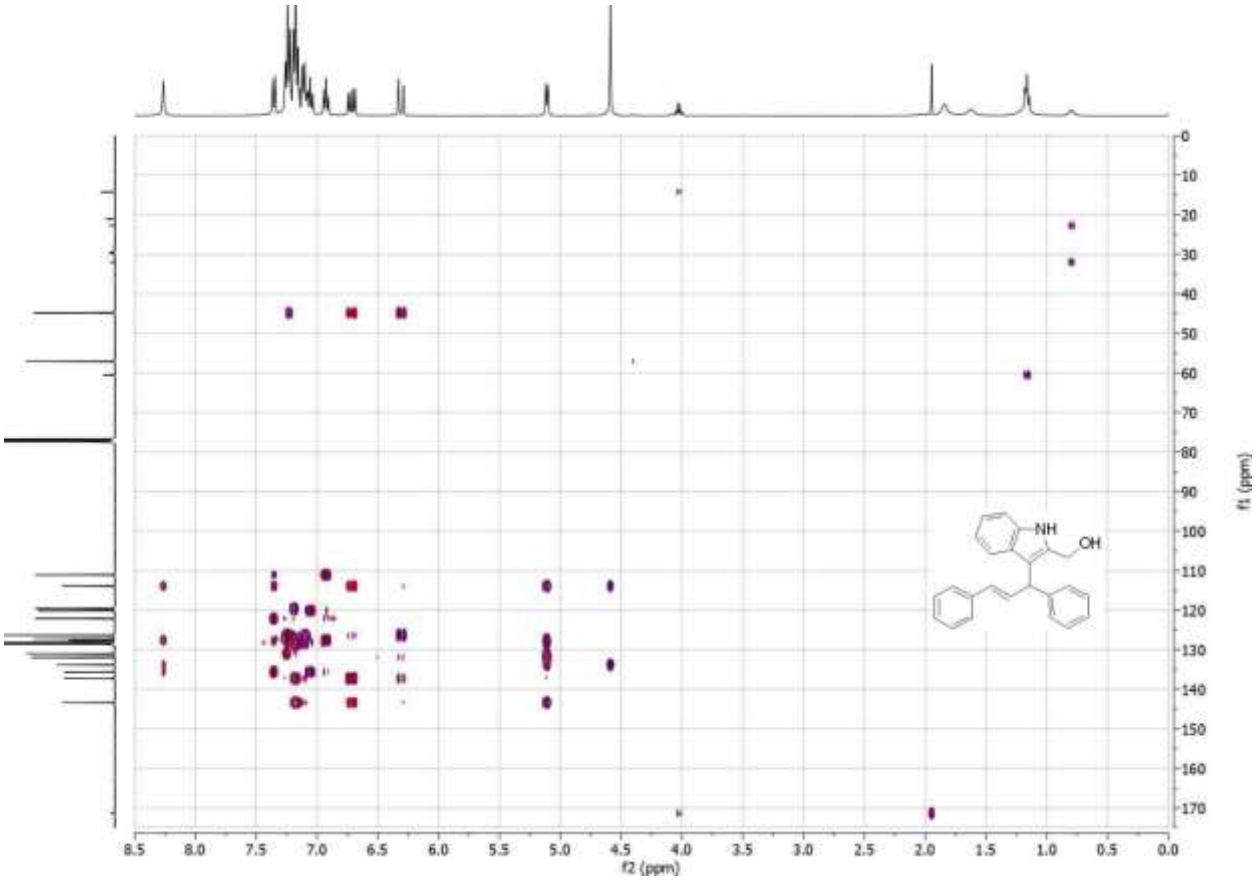

Figure C.143 HMBC spectrum of **21k** in $CDCl_3$.

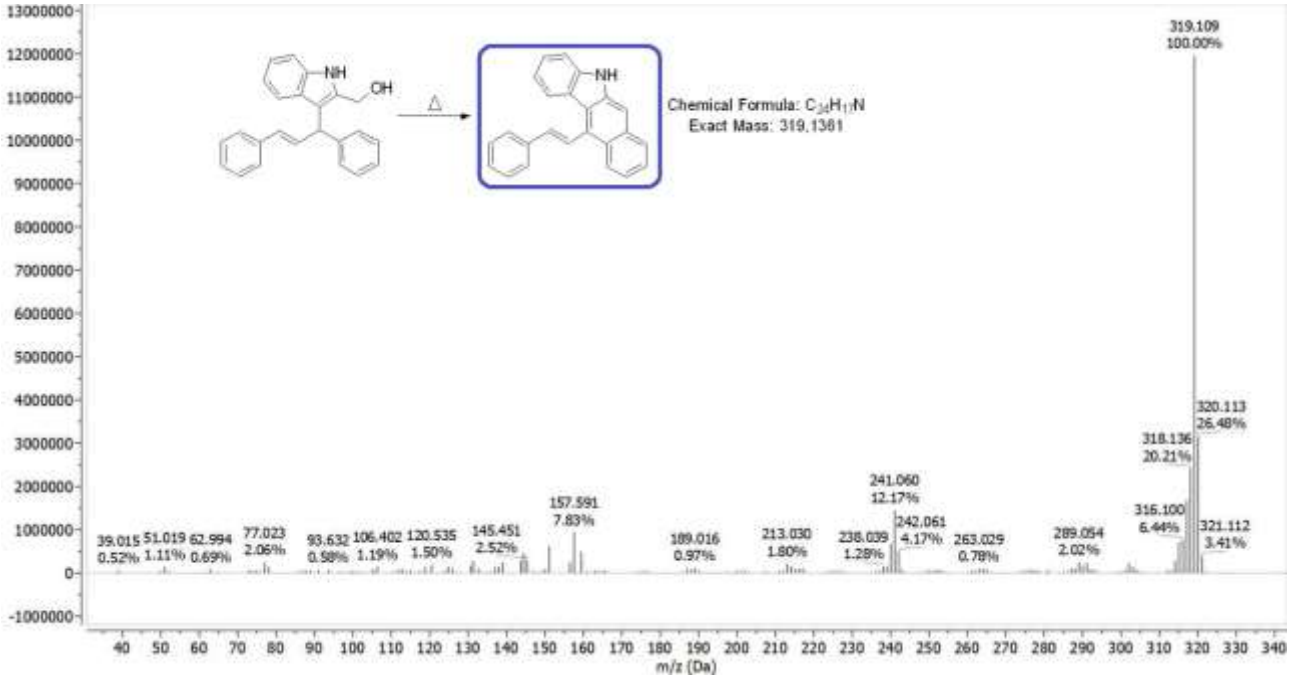

Figure C.144 GC-MS spectrum of the polycyclic thermal decomposition product of ***21k***.

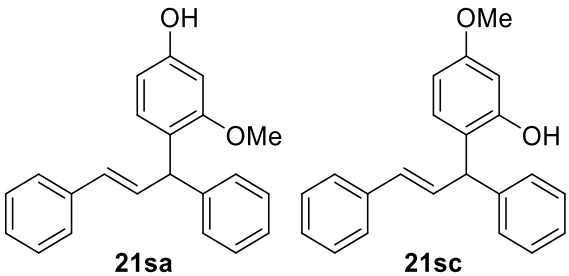

Chemical Formula: $C_{22}H_{20}O_2$
Molecular Weight: 316,400

21sa : **21sc**
2.63 : 1

The purification of **21sb** and **21sd** was not successful and thus their spectra are not available.

^{1}H NMR (400 MHz, Chloroform-*d*) δ [ppm] = 7.40 – 7.18 (m), 7.02 (d, *J* = 8.4 Hz), 7.01 (d, *J* = 8.2 Hz), 6.68 (dd, *J* = 15.9, 7.1), 6.66 (dd, *J* = 15.9, 7.1 Hz), 6.54 – 6.46 (m), 6.46 – 6.39 (m), 6.41 – 6.34 (m), 6.26 (dd, *J* = 15.8, 1.5 Hz), 5.22 (d, *J* = 6.9 Hz), 5.04 (d, *J* = 7.0 Hz), 4.90 (s), 4.78 (s), 3.78 (s), 3.74 (s).

^{13}C NMR (101 MHz, Chloroform-*d*) δ [ppm] = 159.82, 158.21, 155.46, 154.55, 143.83, 142.29, 137.74, 137.16, 132.90, 131.87, 131.51, 130.96, 130.48, 130.28, 130.11, 128.88, 128.74, 128.73, 128.72, 128.68, 128.59, 128.31, 127.61, 127.21, 126.98, 126.52, 126.39, 126.18, 124.49, 121.76, 107.90, 106.89, 106.59, 106.50, 102.67, 101.67, 99.38, 55.72, 48.19, 46.50.

GC/MS (EI): calc. for $C_{22}H_{20}O_2$ $[M]^+$: 316.146; found: 316.133, $C_{16}H_{15}O_2$ 239.077, $C_{15}H_{12}$ 192.078, C_7H_7 91.053, C_6H_5 77.049.

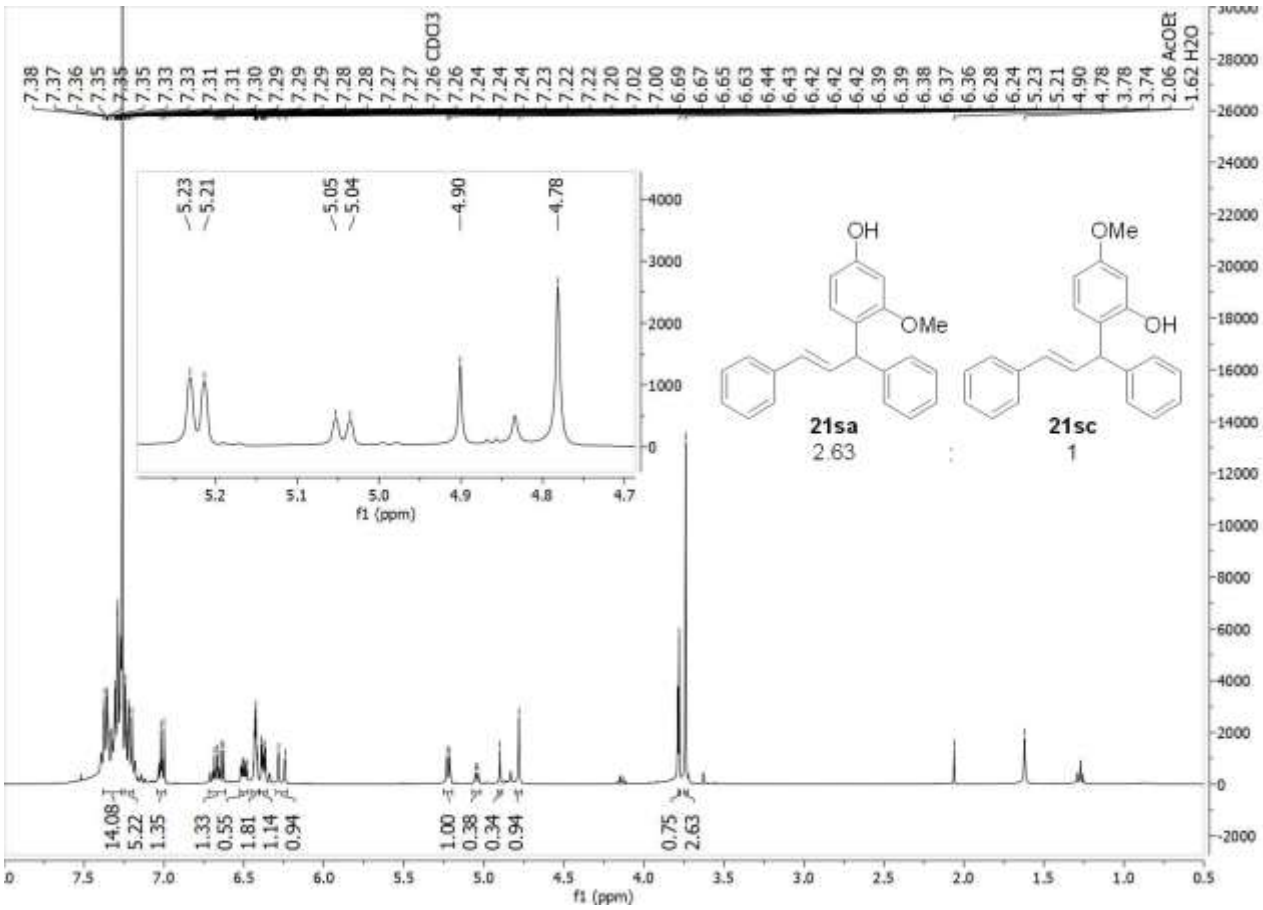

*Figure C.145 ^{1}H NMR spectrum of a 2.63:1 mixture of **21sa** and **21sc** in $CDCl_3$.*

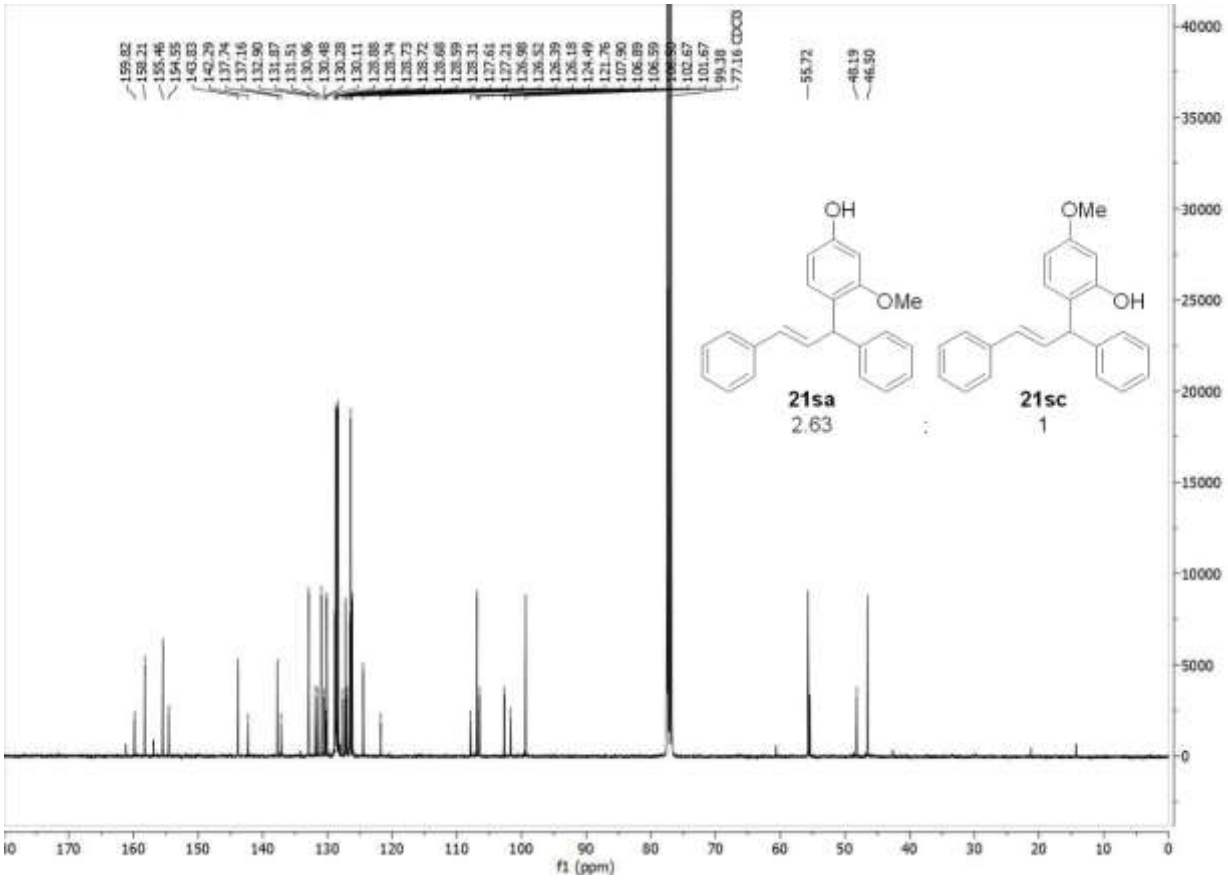

Figure C.146 $^{13}C(^{1}H)$ *NMR spectrum of a 2.63:1 mixture of* ***21sa*** *and* ***21sc*** *in* $CDCl_3$.

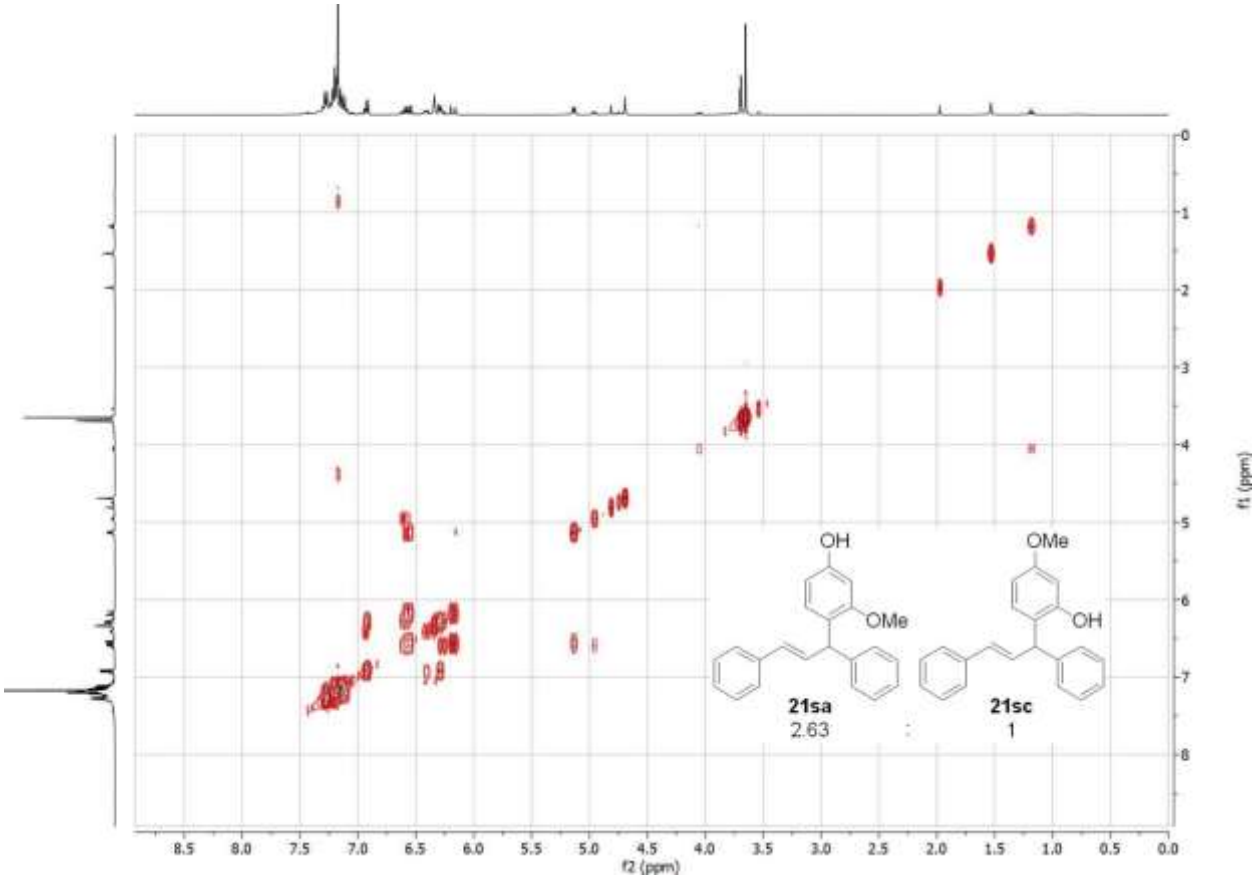

Figure C.147 COSY spectrum of a 2.63:1 mixture of ***21sa*** *and* ***21sc*** *in* $CDCl_3$.

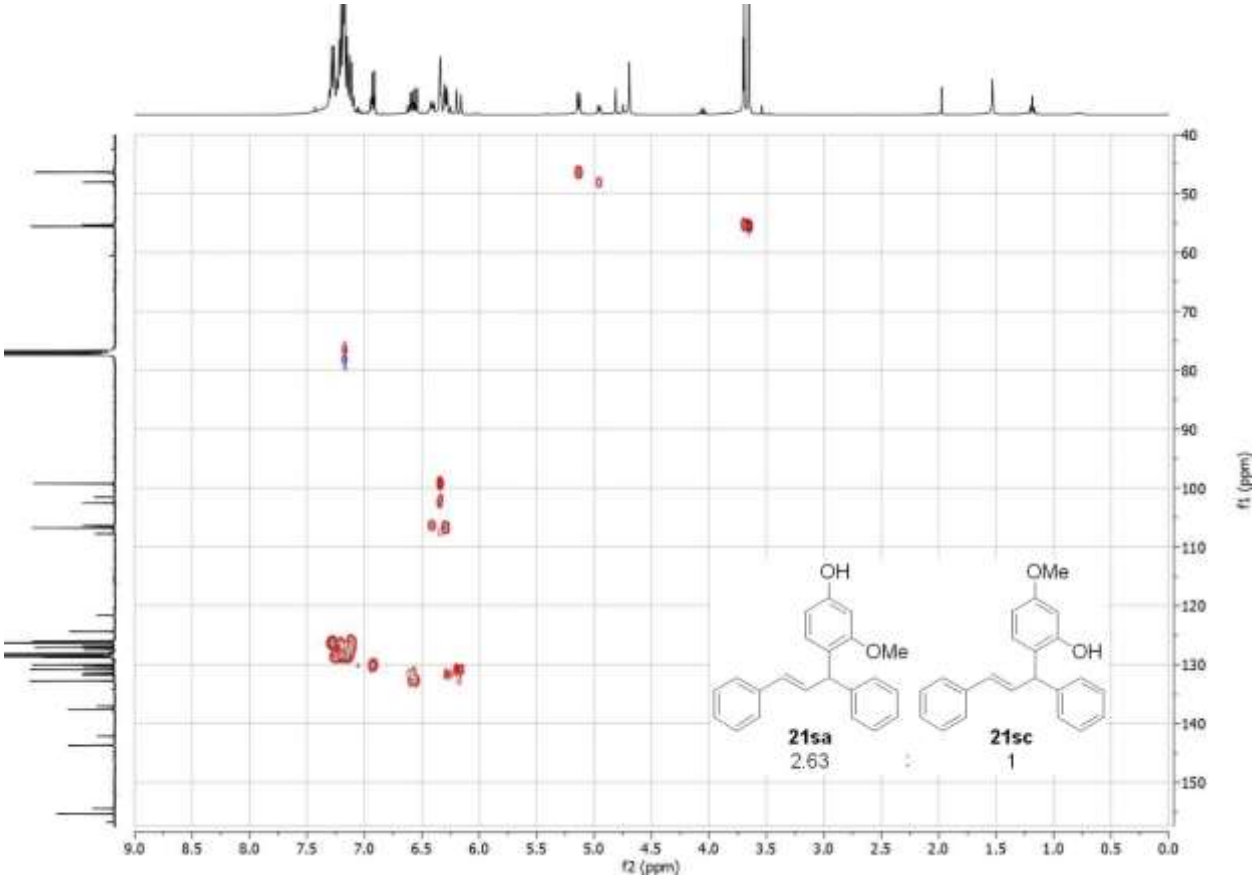

Figure C.148 HSQC spectrum of a 2.63:1 mixture of ***21sa*** and ***21sc*** in $CDCl_3$.

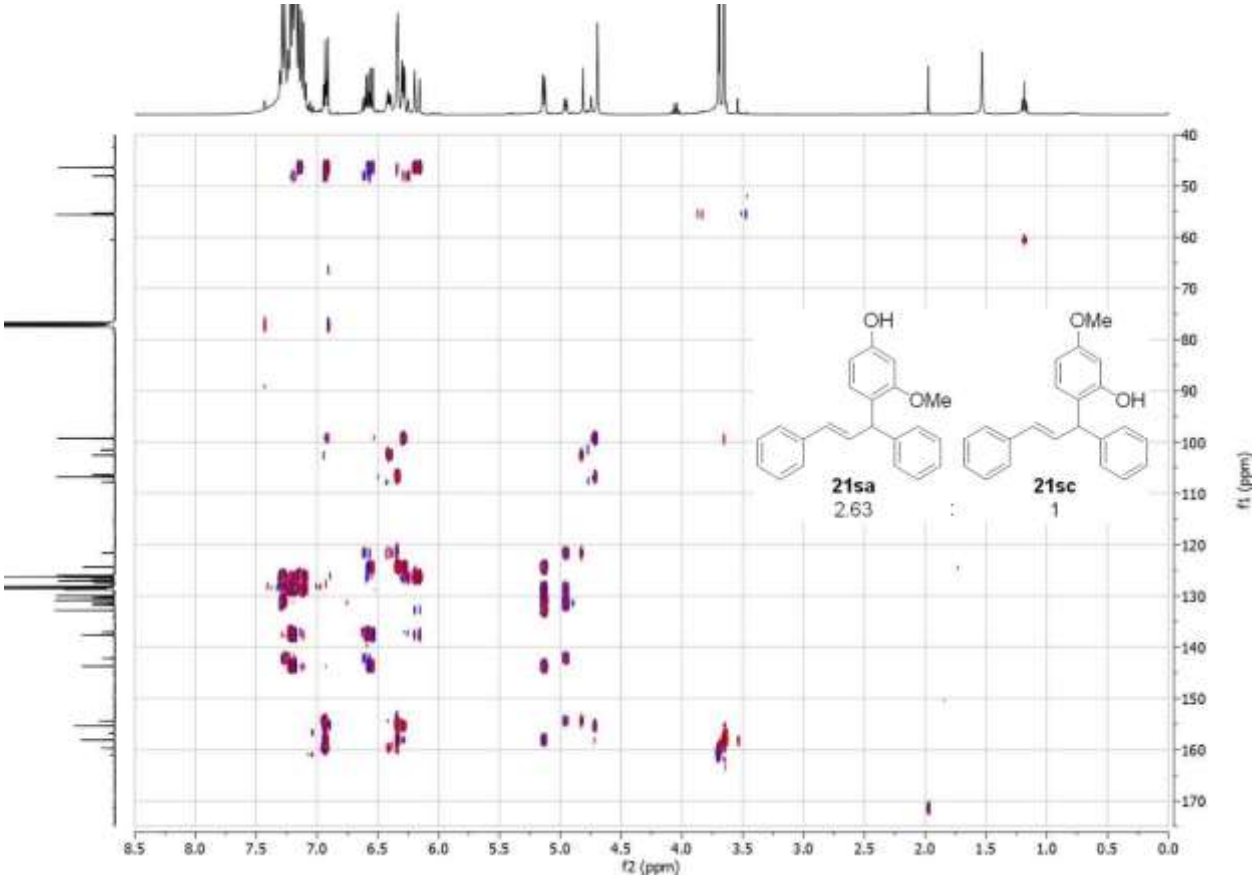

Figure C.149 HMBC spectrum of a 2.63:1 mixture of ***21sa*** and ***21sc*** in $CDCl_3$.

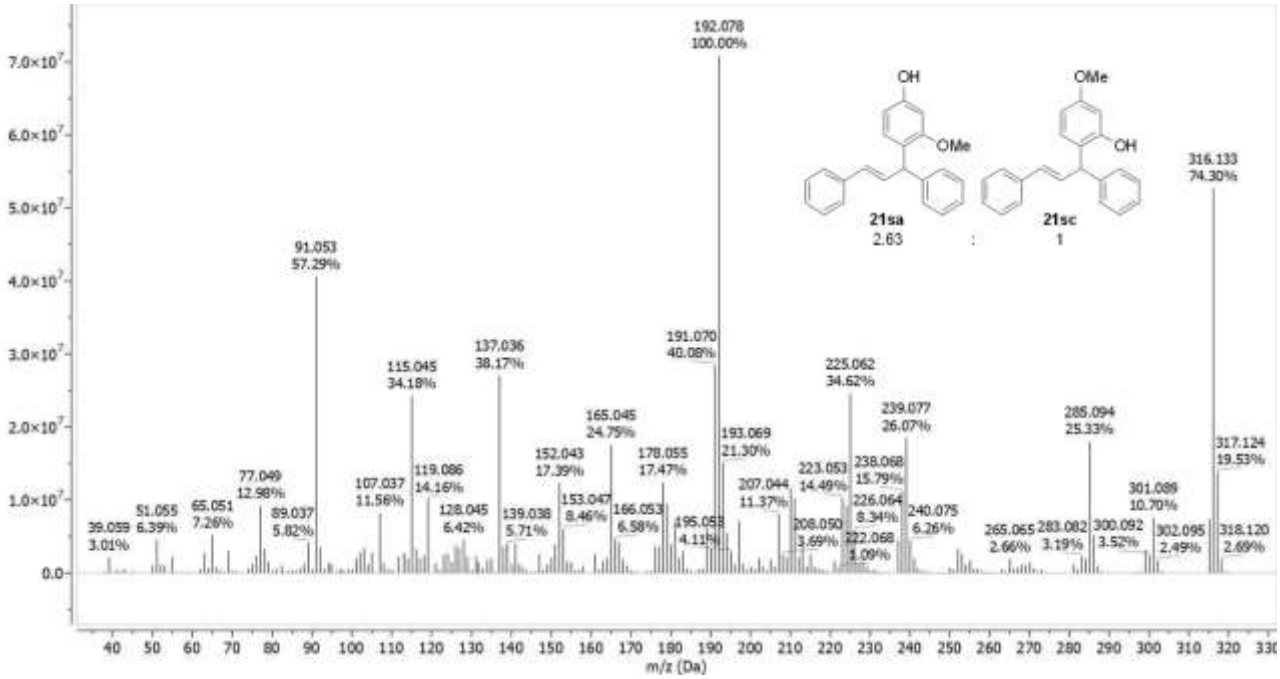

Figure C.150 *GC-MS spectrum of* ***21s****.*

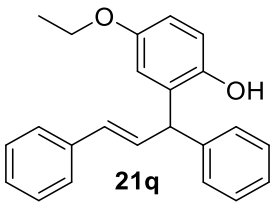

21q

Chemical Formula: $C_{23}H_{22}O_2$
Molecular Weight: 330,4270

^{1}H NMR (400 MHz, Chloroform-*d*) δ [ppm] = 7.42 – 7.19 (m, 10H), 6.78 – 6.63 (m, 4H), 6.36 (d, *J* = 16.0 Hz, 1H), 5.09 (d, *J* = 7.2 Hz, 1H), 4.46 (s, 1H), 3.94 (q, *J* = 7.0 Hz, 2H), 1.36 (t, *J* = 7.0 Hz, 3H).

^{13}C NMR (101 MHz, Chloroform-*d*) δ [ppm] = 153.40, 147.44, 142.00, 137.18, 132.08, 131.16, 130.90, 128.88, 128.77, 128.68, 127.62, 127.01, 126.55, 117.19, 116.69, 113.16, 64.07, 48.77, 15.05.

GC/MS (EI): calc. for $C_{23}H_{22}O_2$ $[M]^+$: 330.162; found: 330.130, $C_{15}H_{13}O_2$ 225.060, $C_9H_{12}O_2$ 152.021, C_7H_7 91.036, C_6H_5 77.034.

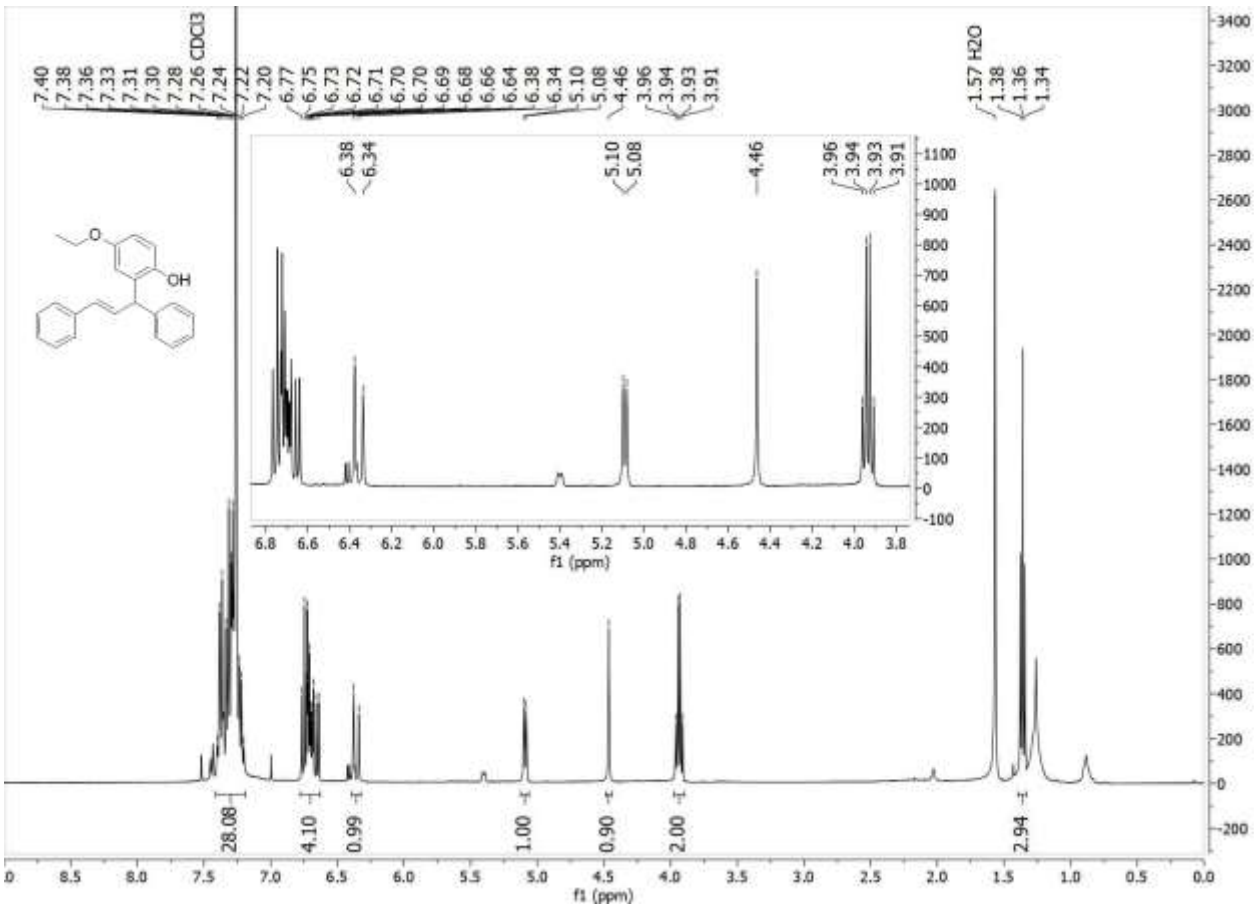

*Figure C.151 ^{1}H NMR spectrum of **21q** in $CDCl_3$.*

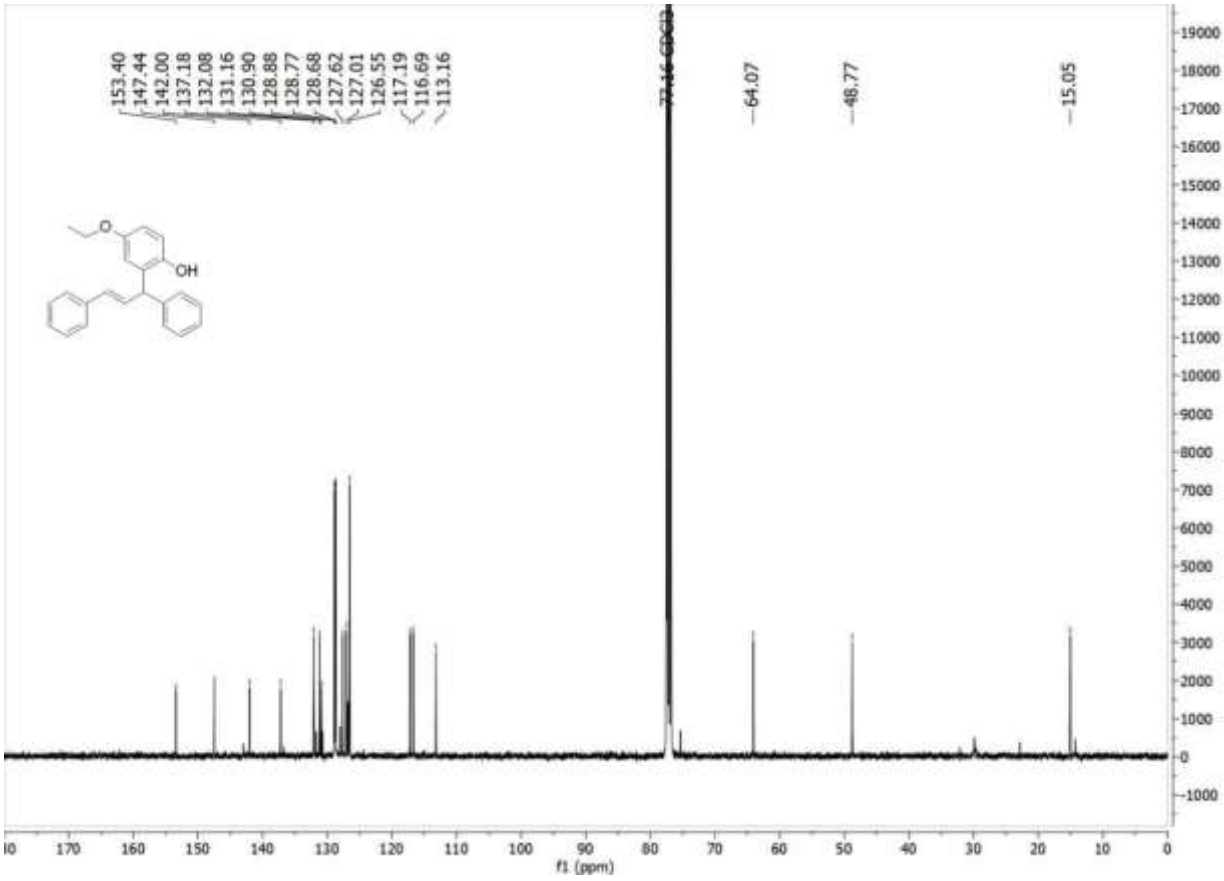

Figure C.152 $^{13}C(^{1}H)$ *NMR spectrum of* ***21q*** *in* $CDCl_3$.

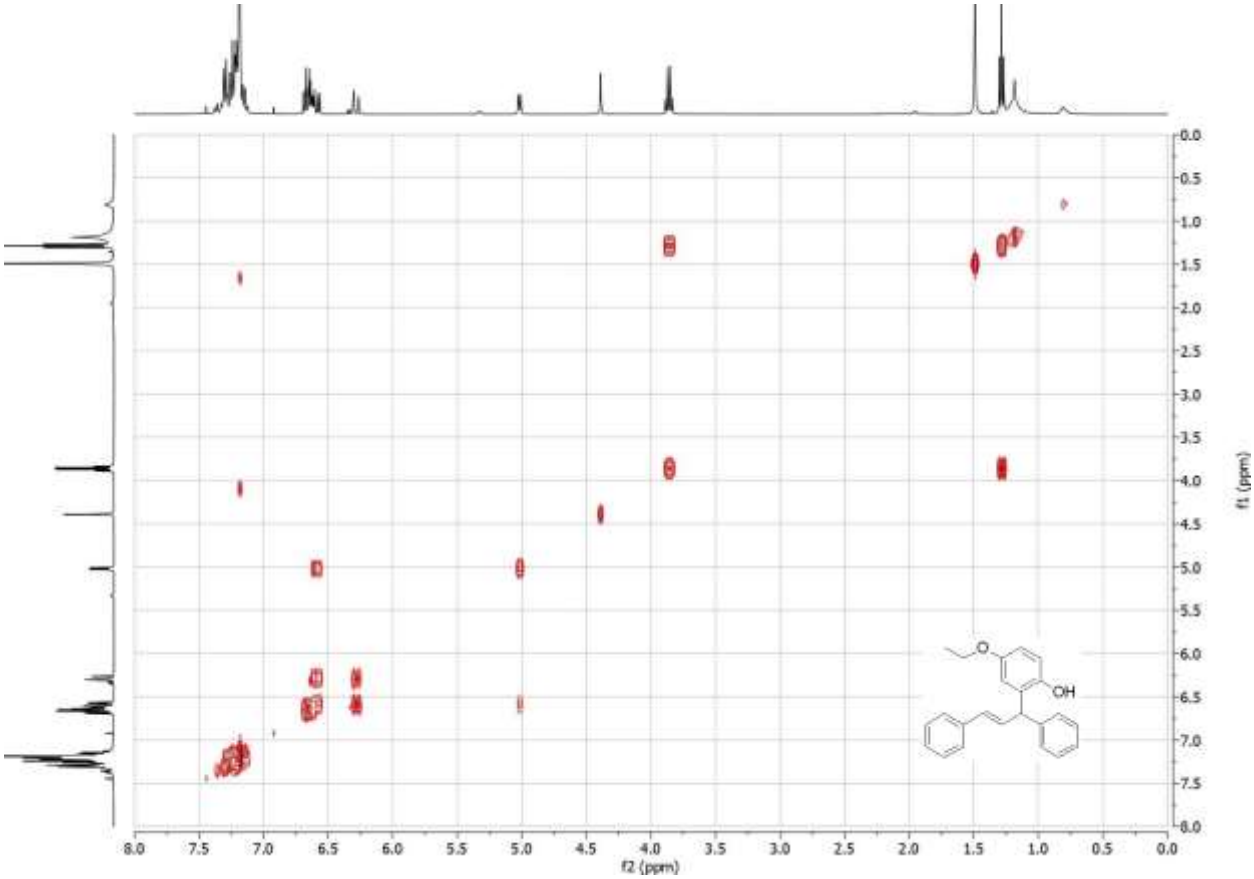

Figure C.153 COSY spectrum of ***21q*** *in* $CDCl_3$.

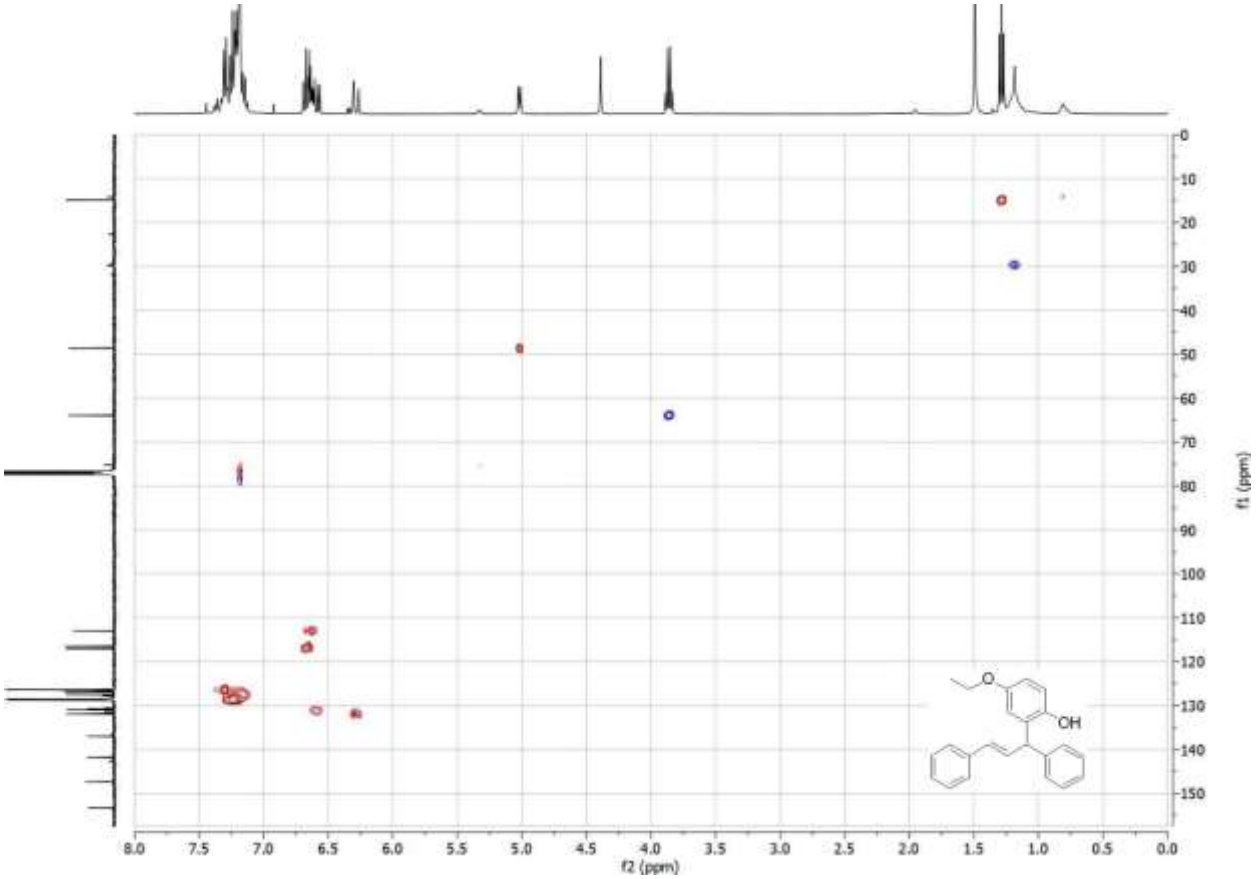

Figure C.154 HSQC spectrum of ***21q*** in $CDCl_3$.

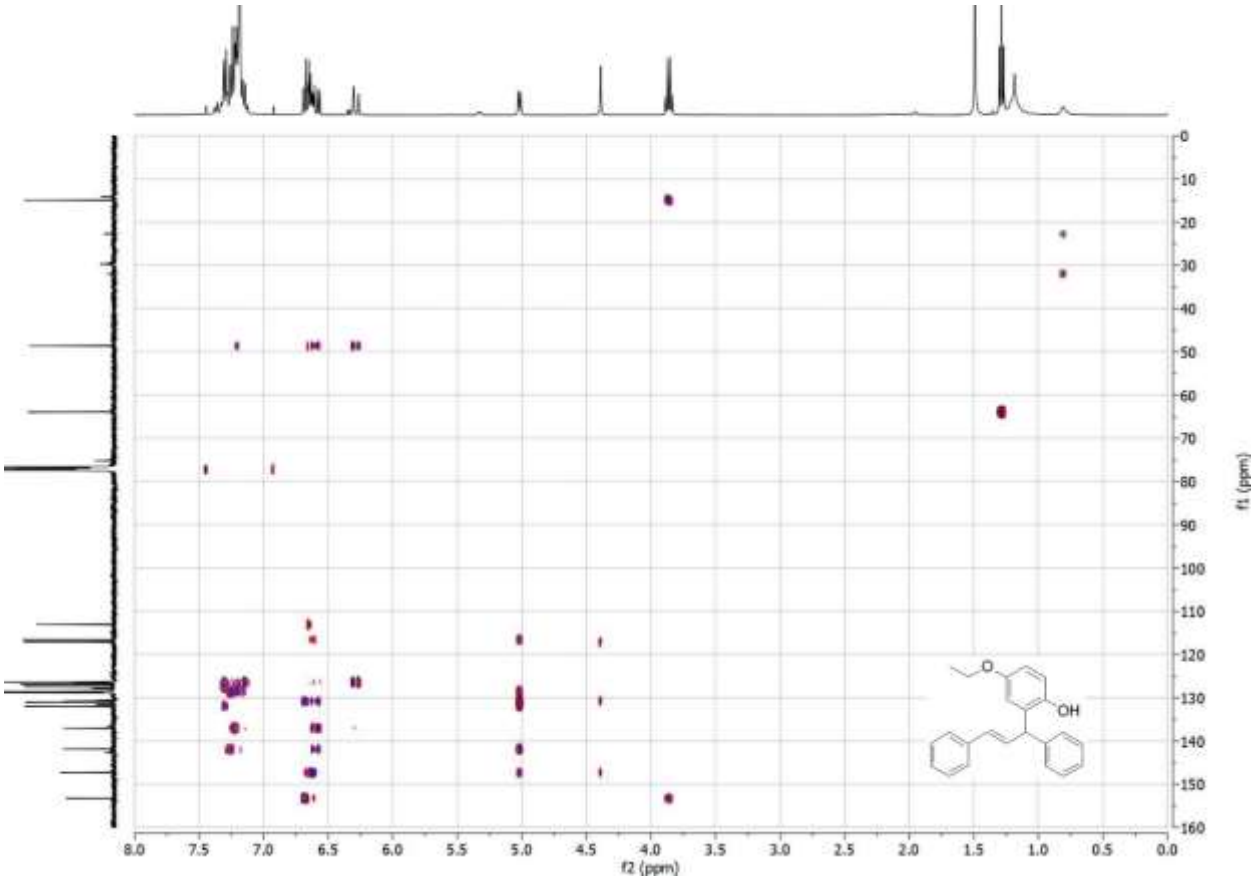

Figure C.155 HMBC spectrum of ***21q*** in $CDCl_3$.

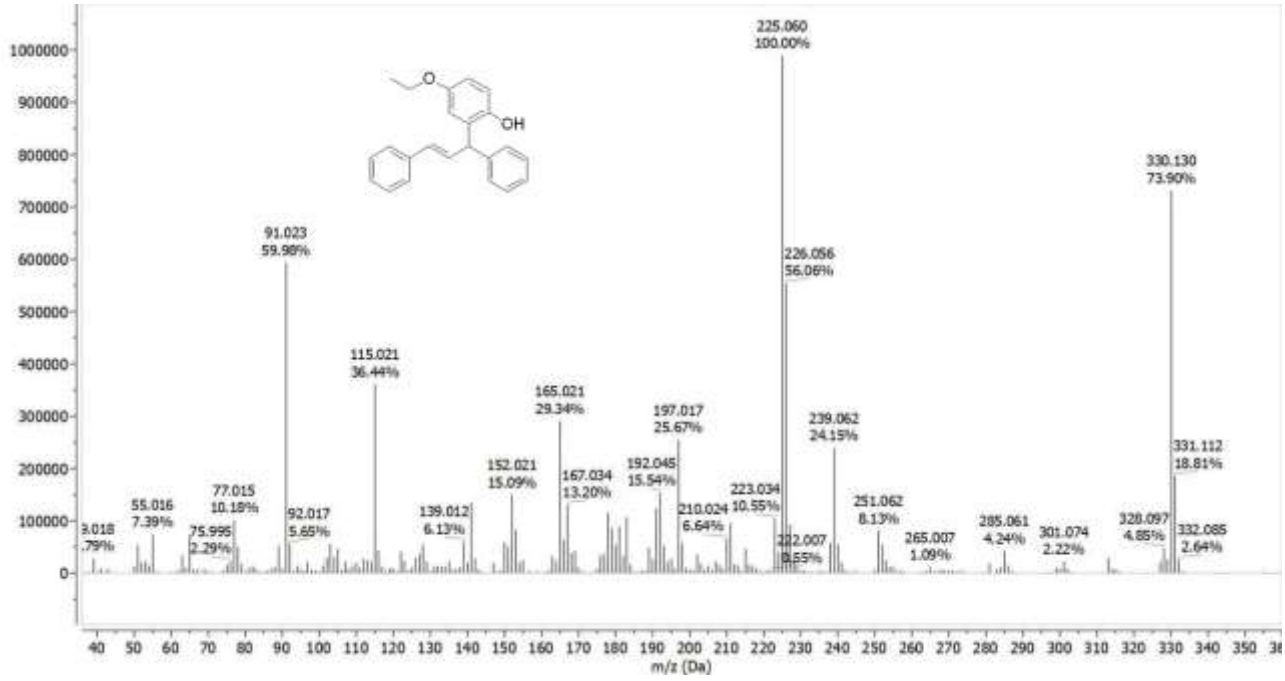

Figure C.156 GC-MS spectrum of ***21q***.

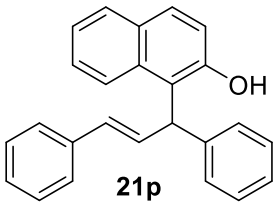

21p

Chemical Formula: $C_{25}H_{20}O$
Molecular Weight: 336,43

^{1}H NMR (400 MHz, Chloroform-*d*) δ = 7.99 (d, *J* = 8.6 Hz, 1H), 7.80 (d, *J* = 8.0 Hz, 1H), 7.74 (d, *J* = 8.8 Hz, 1H), 7.48 – 7.40 (m, 1H), 7.40 – 7.20 (m, 11H), 7.10 (d, *J* = 8.9 Hz, 1H), 6.96 (dd, *J* = 16.0, 6.8 Hz, 1H), 6.51 (dd, *J* = 16.0, 0.9 Hz, 1H), 5.88 (d, *J* = 6.8 Hz, 1H), 5.54 (s, 1H).

^{13}C NMR (101 MHz, Chloroform-*d*) δ = 152.46, 141.71, 136.90, 133.34, 133.15, 130.17, 129.90, 129.55, 129.09, 128.97, 128.70, 128.18, 127.80, 127.10, 126.87, 126.60, 123.37, 123.12, 119.73, 119.39, 45.42.

GC/MS (EI): calc. for $C_{25}H_{20}O$ $[M]^+$: 336.151; found: 336.145, $C_{18}H_{13}O$ 245.082, $C_{15}H_{13}$ 193.074, C_7H_7 91.036, C_6H_5 77.034.

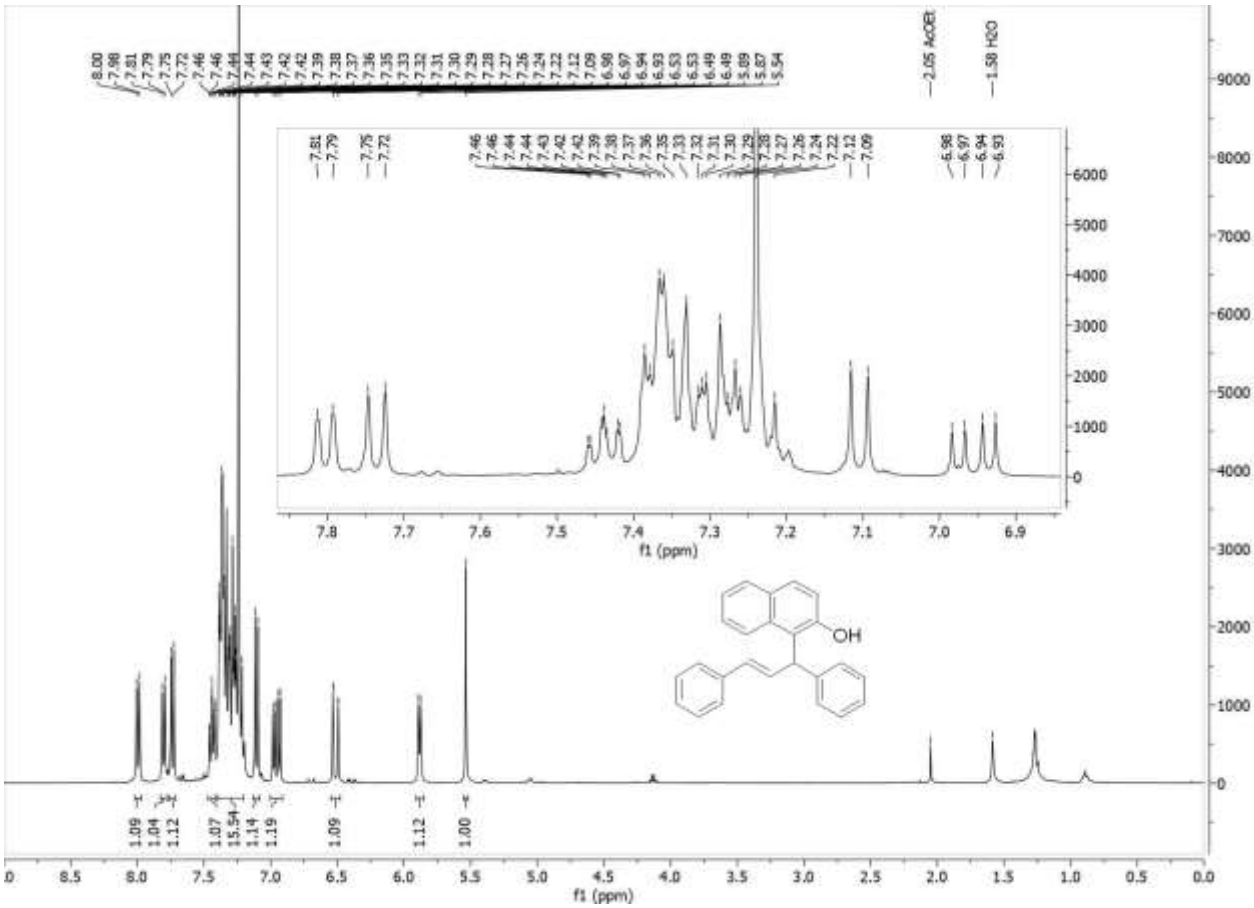

*Figure C.157 ^{1}H NMR spectrum of **21p** in $CDCl_3$.*

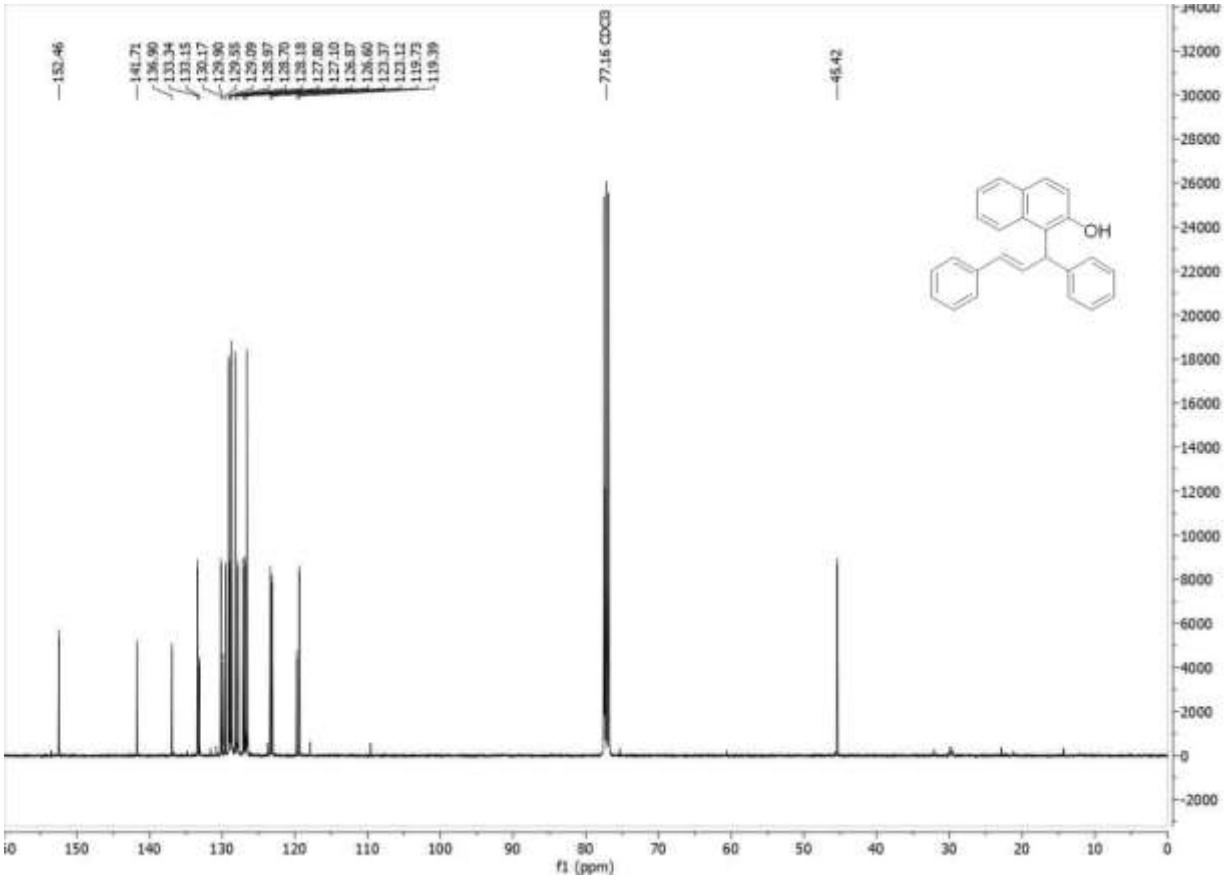

Figure C.158 $^{13}C(^{1}H)$ *NMR spectrum of* ***21p*** *in* $CDCl_3$.

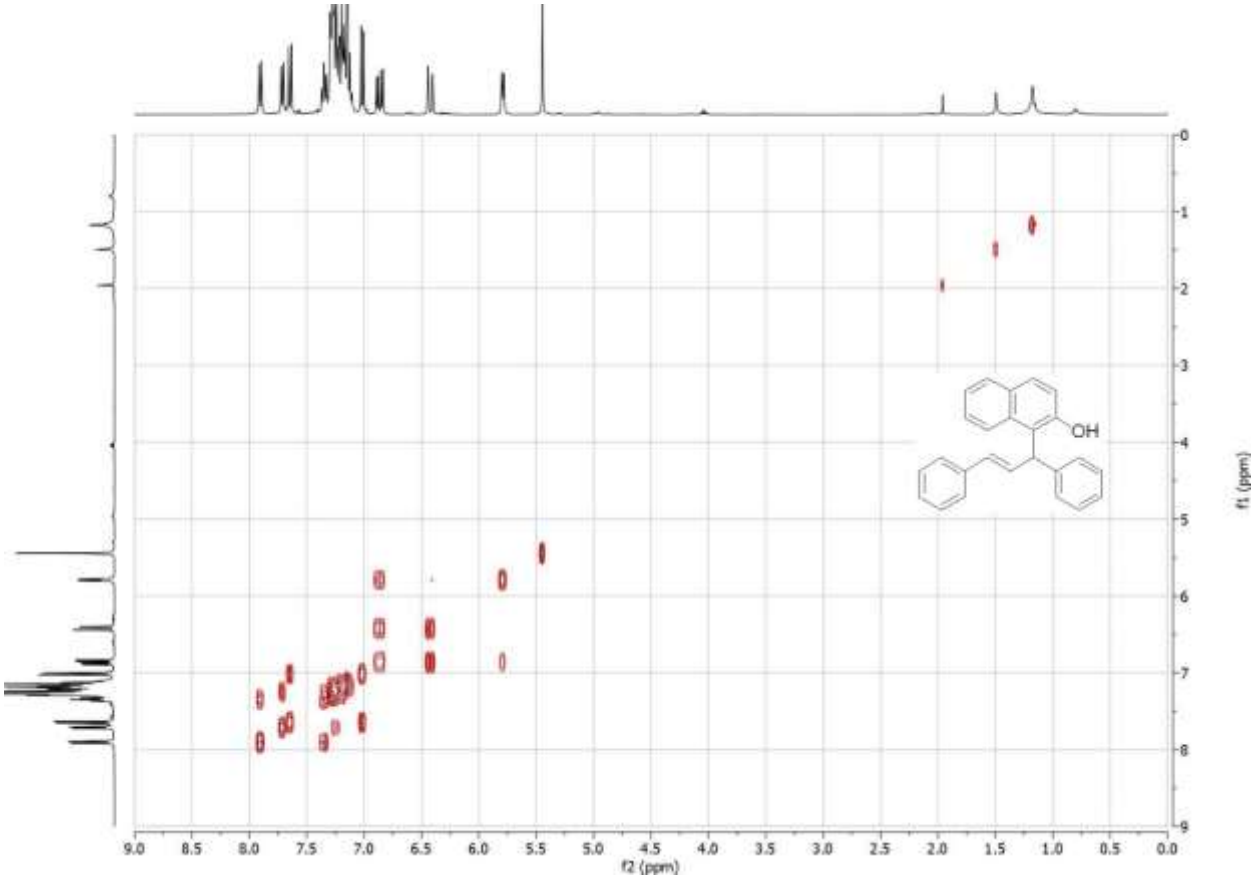

Figure C.159 COSY spectrum of ***21p*** *in* $CDCl_3$.

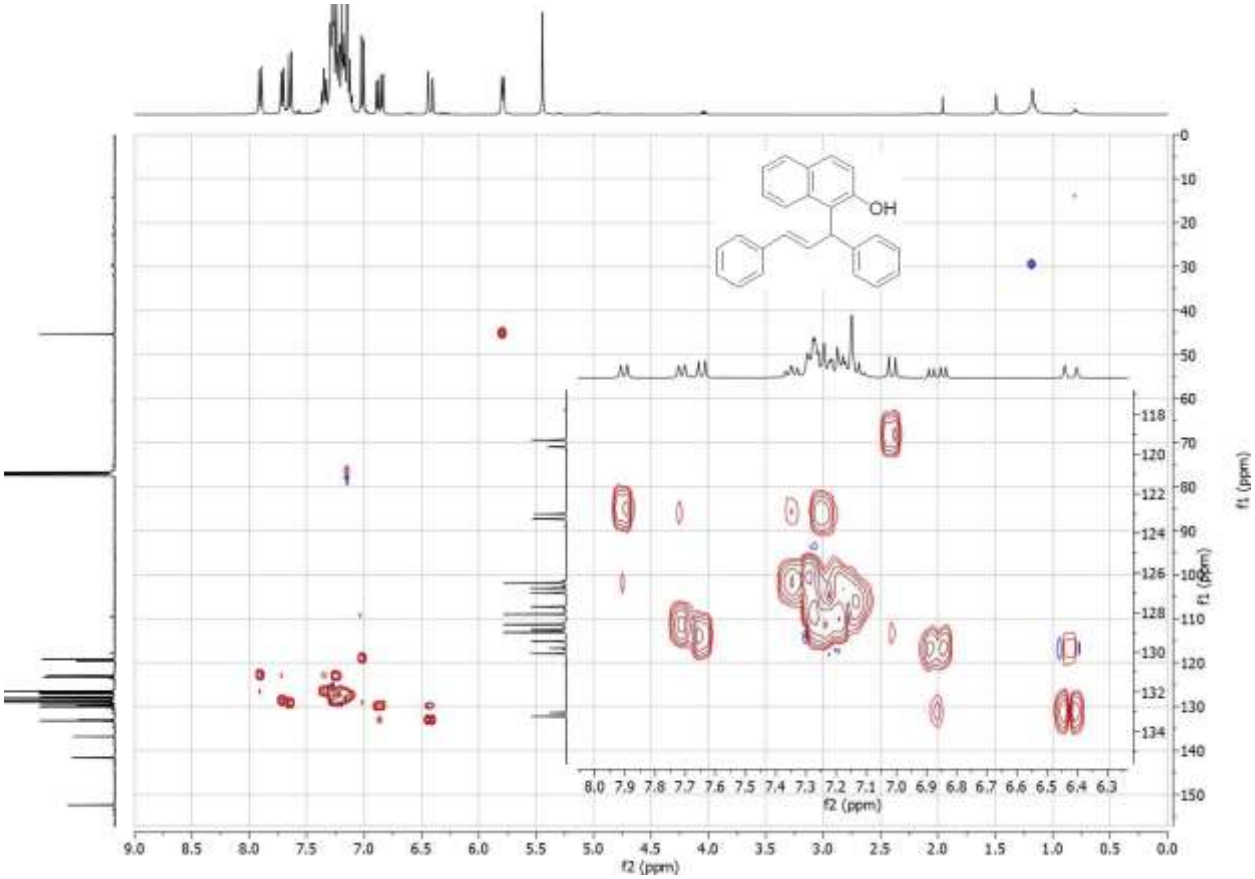

Figure C.160 HSQC spectrum of **21p** in $CDCl_3$.

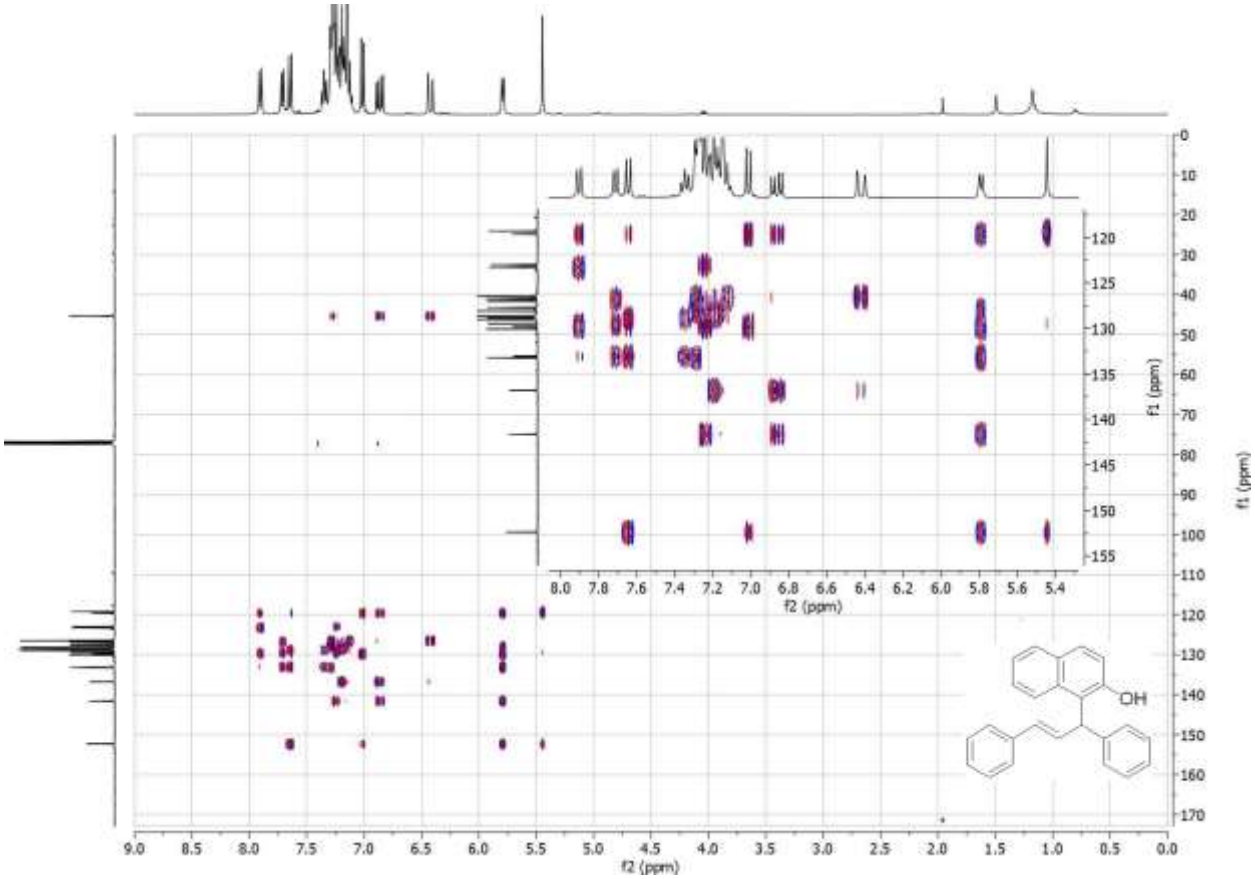

Figure C.161 HMBC spectrum of **21p** in $CDCl_3$.

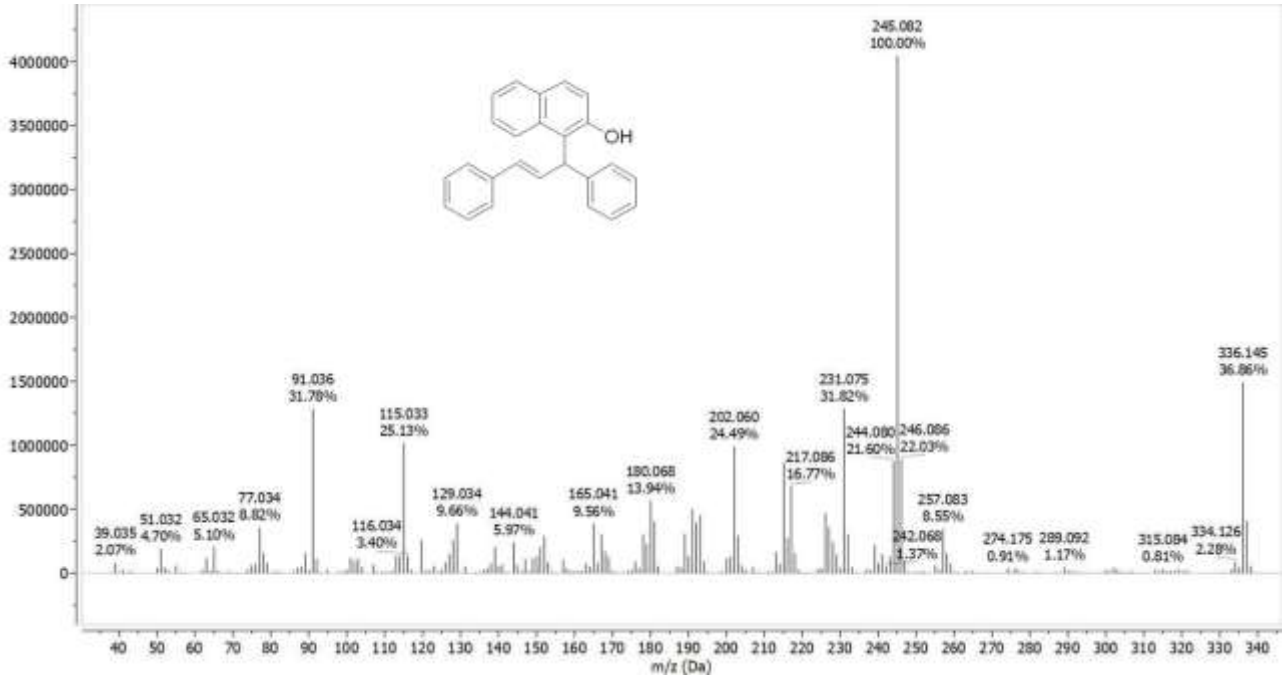

Figure C.162 *GC-MS spectrum of* ***21p****.*

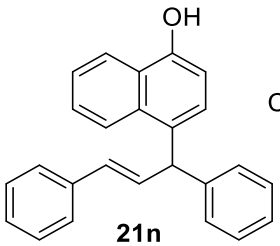

Chemical Formula: $C_{25}H_{20}O$
Molecular Weight: 336,43

21n

^{1}H NMR (400 MHz, Chloroform-*d*) δ [ppm] = 8.16 – 8.10 (m, 1H), 7.81 – 7.75 (m, 1H), 7.49 – 7.18 (m, 19H), 6.76 (dd, *J* = 15.9, 7.0 Hz, 1H), 6.42 (d, *J* = 16.0 Hz, 1H), 5.43 (s, 1H), 5.22 (d, *J* = 6.9 Hz, 1H).

^{13}C NMR (101 MHz, Chloroform-*d*) δ [ppm] = 149.07, 141.68, 136.90, 133.89, 132.60, 130.77, 129.14, 128.81, 128.74, 127.84, 127.72, 127.58, 127.33, 126.61, 126.20, 125.56, 125.32, 122.45, 121.64, 120.72, 49.50.

GC/MS (EI): calc. for $C_{25}H_{20}O$ $[M]^+$: 336.151; found: 336.140, $C_{18}H_{13}O$ 245.082, $C_{17}H_{11}O$ 231.080, $C_{17}H_{11}$ 215.084, C_7H_7 91.033, C_6H_5 77.032.

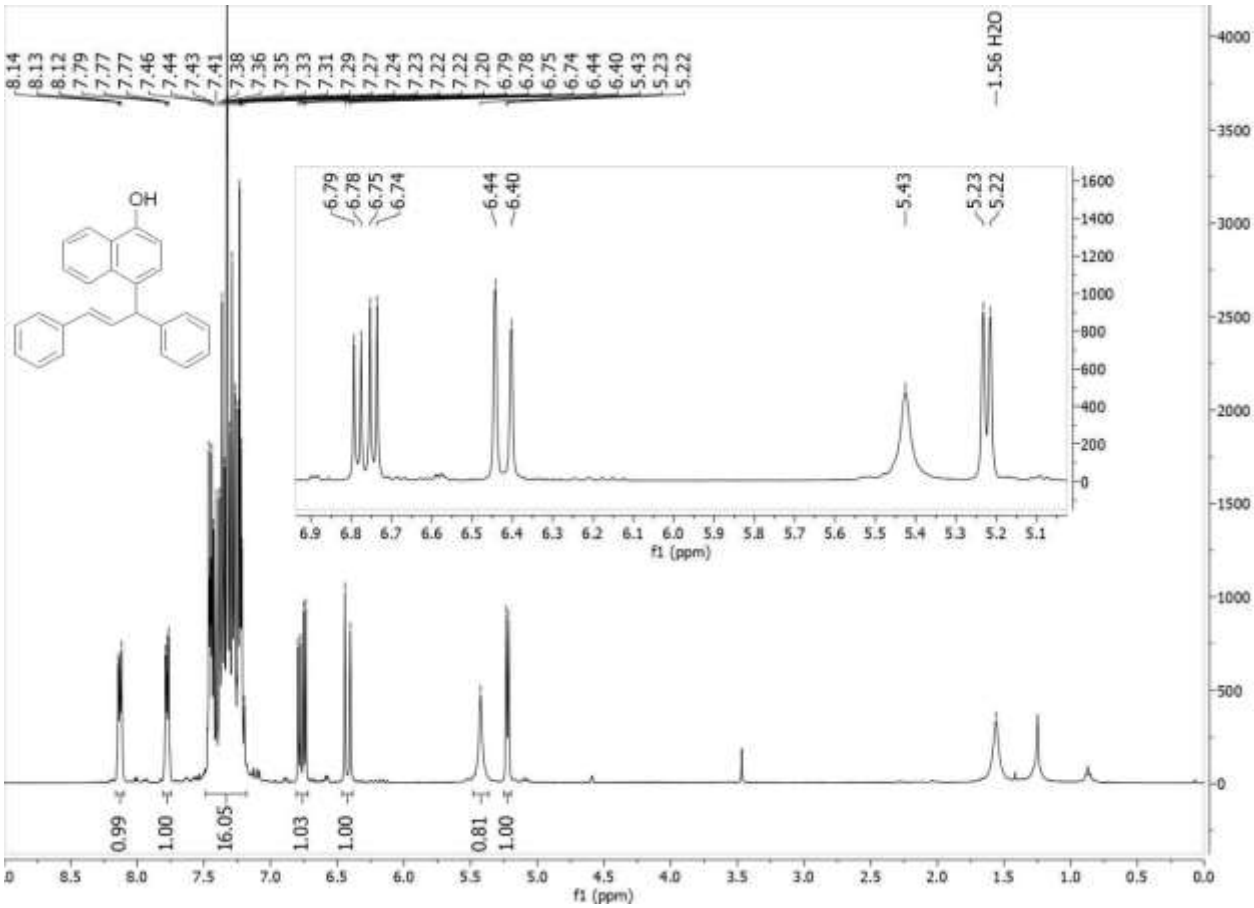

*Figure C.163 ^{1}H NMR spectrum of **21n** in $CDCl_3$.*

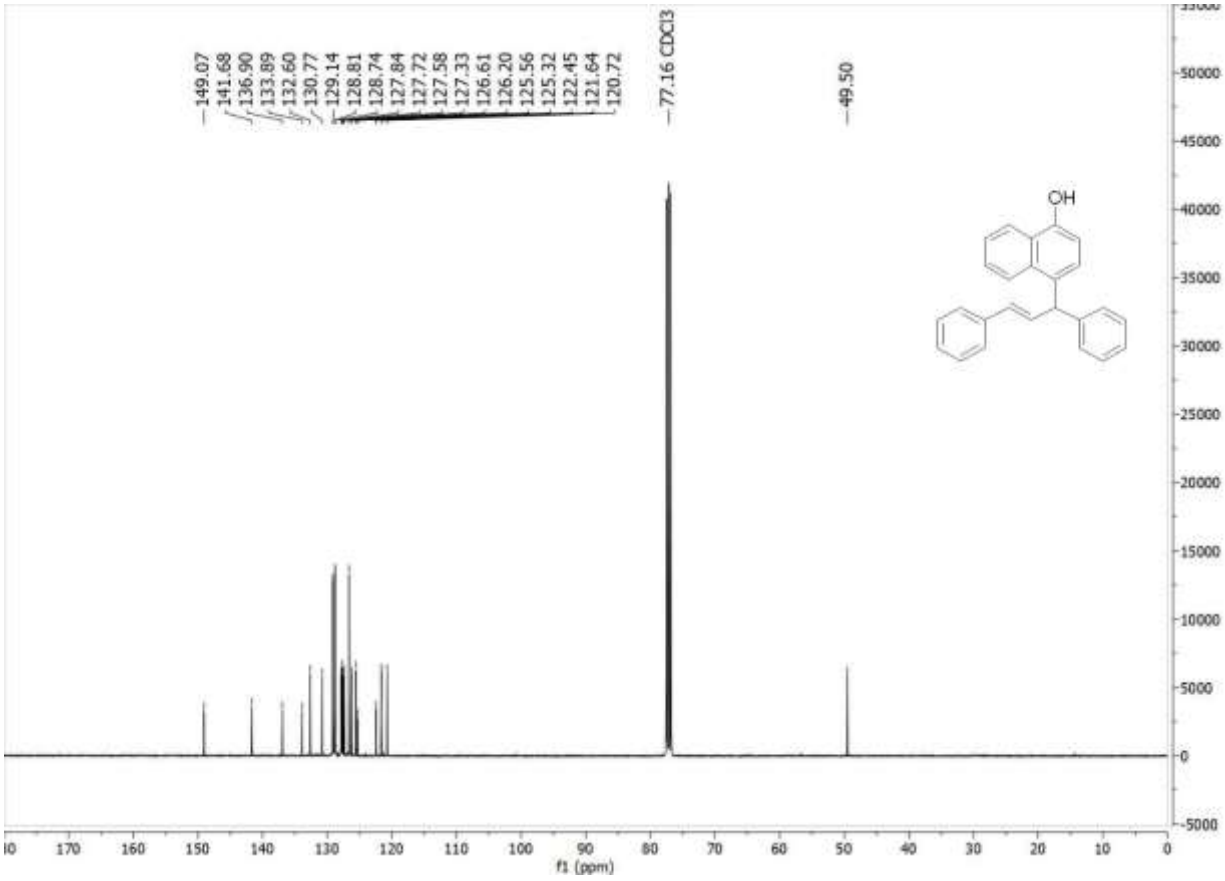

Figure C.164 $^{13}C(^{1}H)$ *NMR spectrum of* ***21n*** *in* $CDCl_3$.

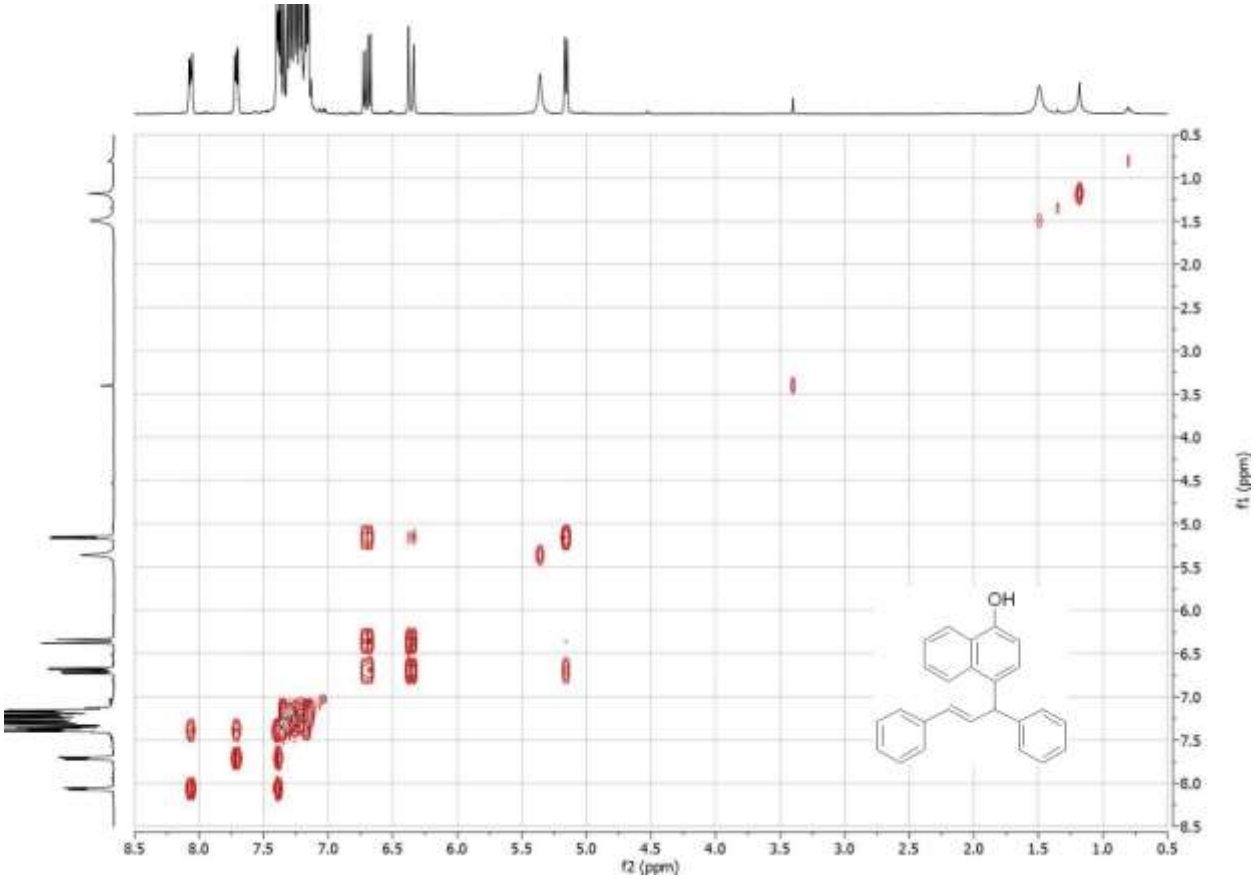

Figure C.165 COSY spectrum of ***21n*** *in* $CDCl_3$.

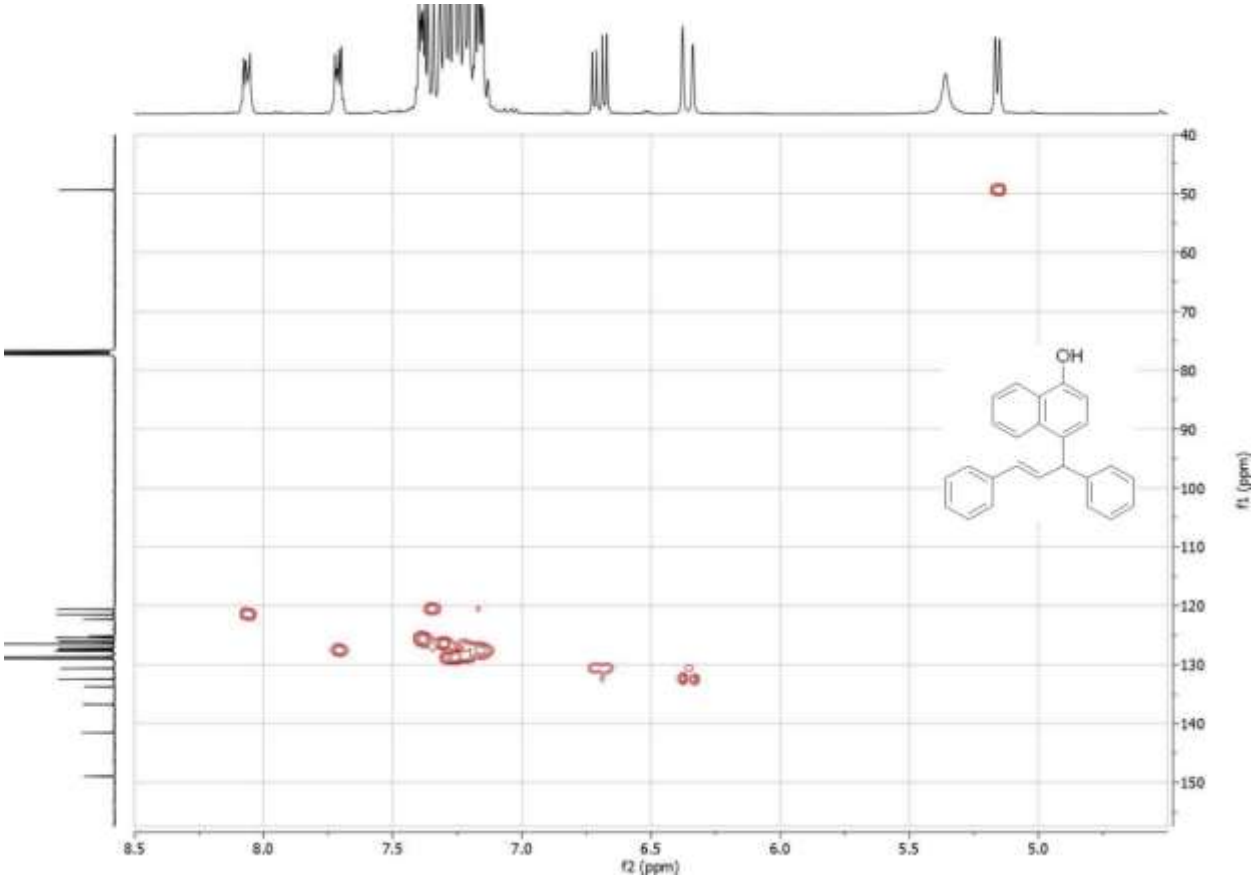

Figure C.166 HSQC spectrum of ***21n*** in $CDCl_3$.

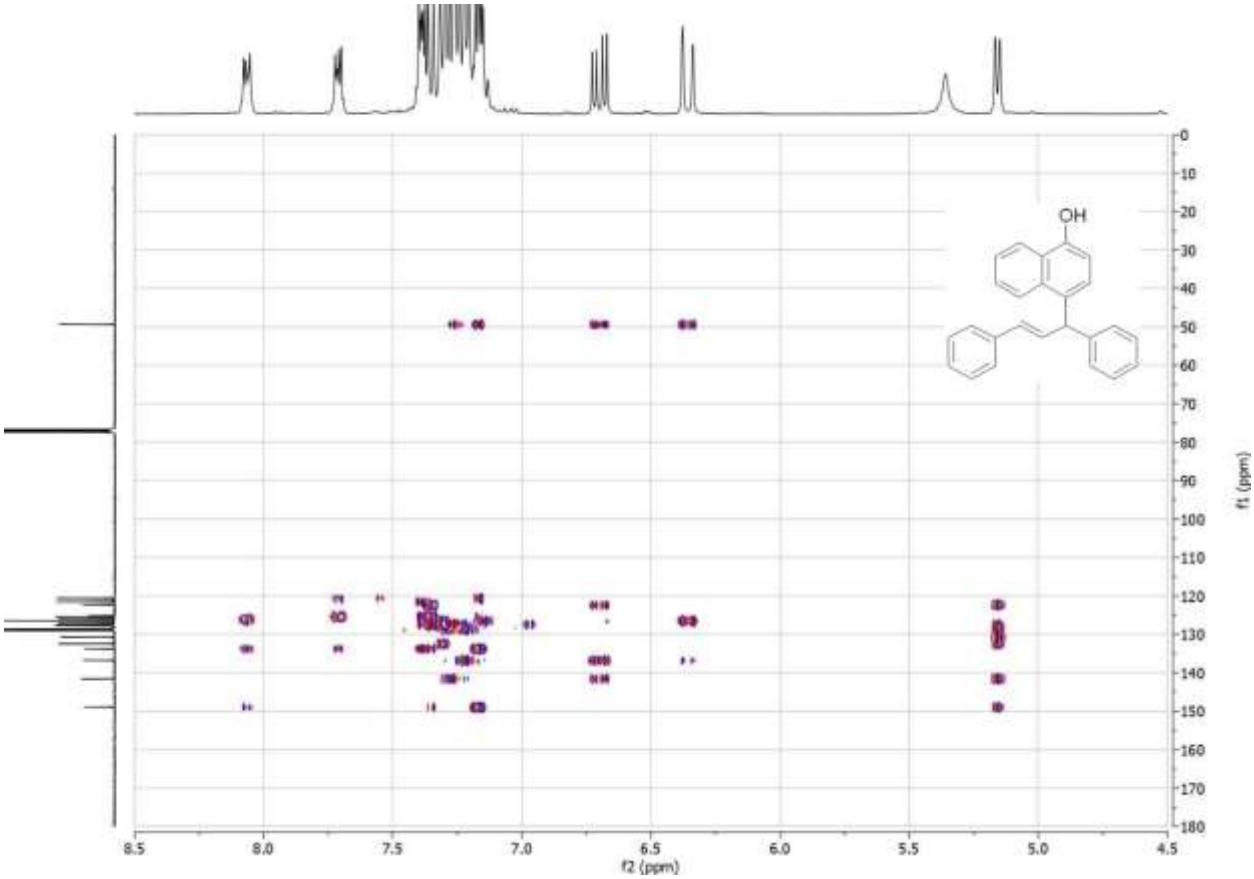

Figure C.167 HMBC spectrum of ***21n*** in $CDCl_3$.

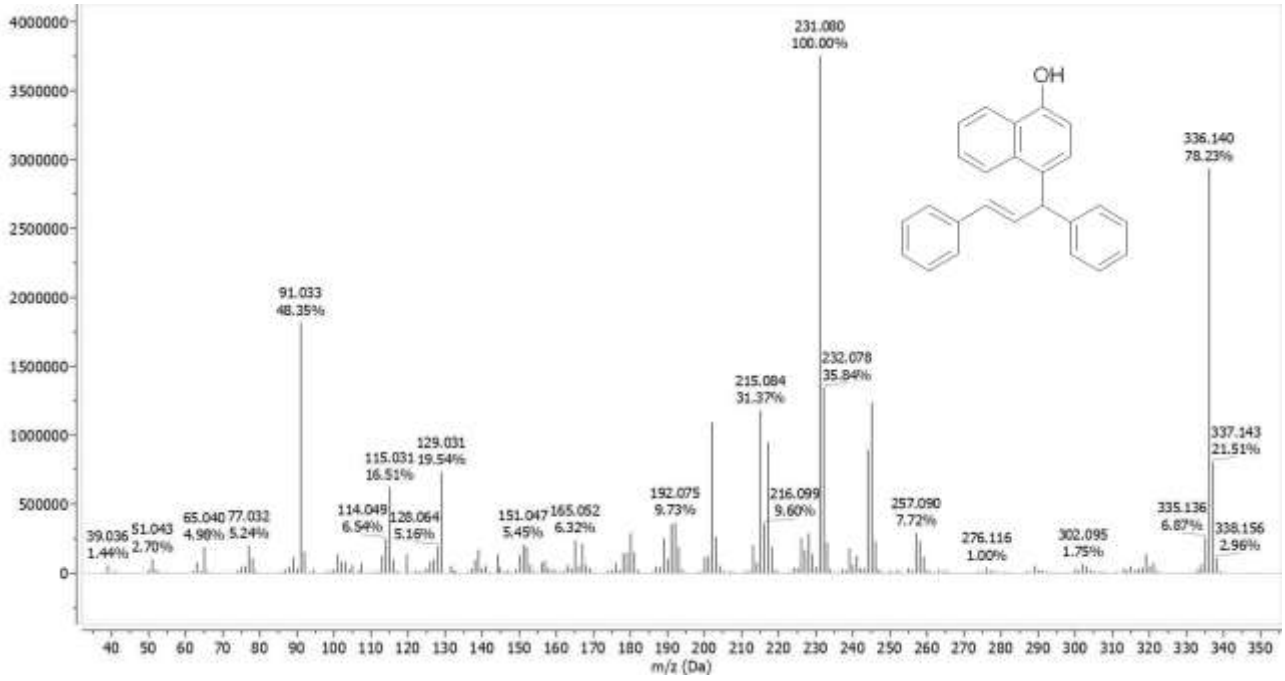

Figure C.168 GC-MS spectrum of ***21n***.

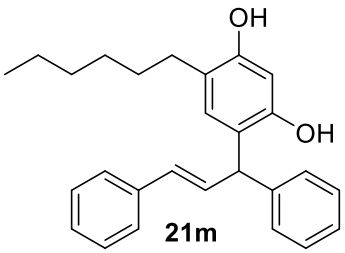

Chemical Formula: $C_{27}H_{30}O_2$
Molecular Weight: 386,54

^{1}H NMR (400 MHz, Chloroform-*d*) δ = 7.38 – 7.17 (m, 10H), 6.81 (s, 1H), 6.65 (dd, *J* = 15.9, 7.1 Hz, 1H), 6.33 (d, *J* = 16.0 Hz, 1H), 6.27 (s, 1H), 4.99 (d, *J* = 6.9 Hz, 1H), 4.75 (s, 1H), 4.68 (s, 1H), 2.50 – 2.43 (m, 2H), 1.57 – 1.46 (m, 2H) 1.35 – 1.20 (m, 6H), 0.89 – 0.80 (m, 3H).

^{13}C NMR (101 MHz, Chloroform-*d*) δ = 153.12, 152.41, 142.43, 137.24, 131.78, 131.71, 131.18, 128.84, 128.68, 127.57, 126.91, 126.54, 121.53, 121.01, 104.05, 48.33, 31.83, 30.15, 29.52, 29.23, 22.79, 14.22.

GC/MS (EI): calc. for $C_{27}H_{30}O_2$ $[M]^+$: 386.225; found: 386.200, $C_{21}H_{17}O_2$ 301.097, $C_{15}H_{12}$ 192.058, C_7H_7 91.036, C_6H_5 77.032.

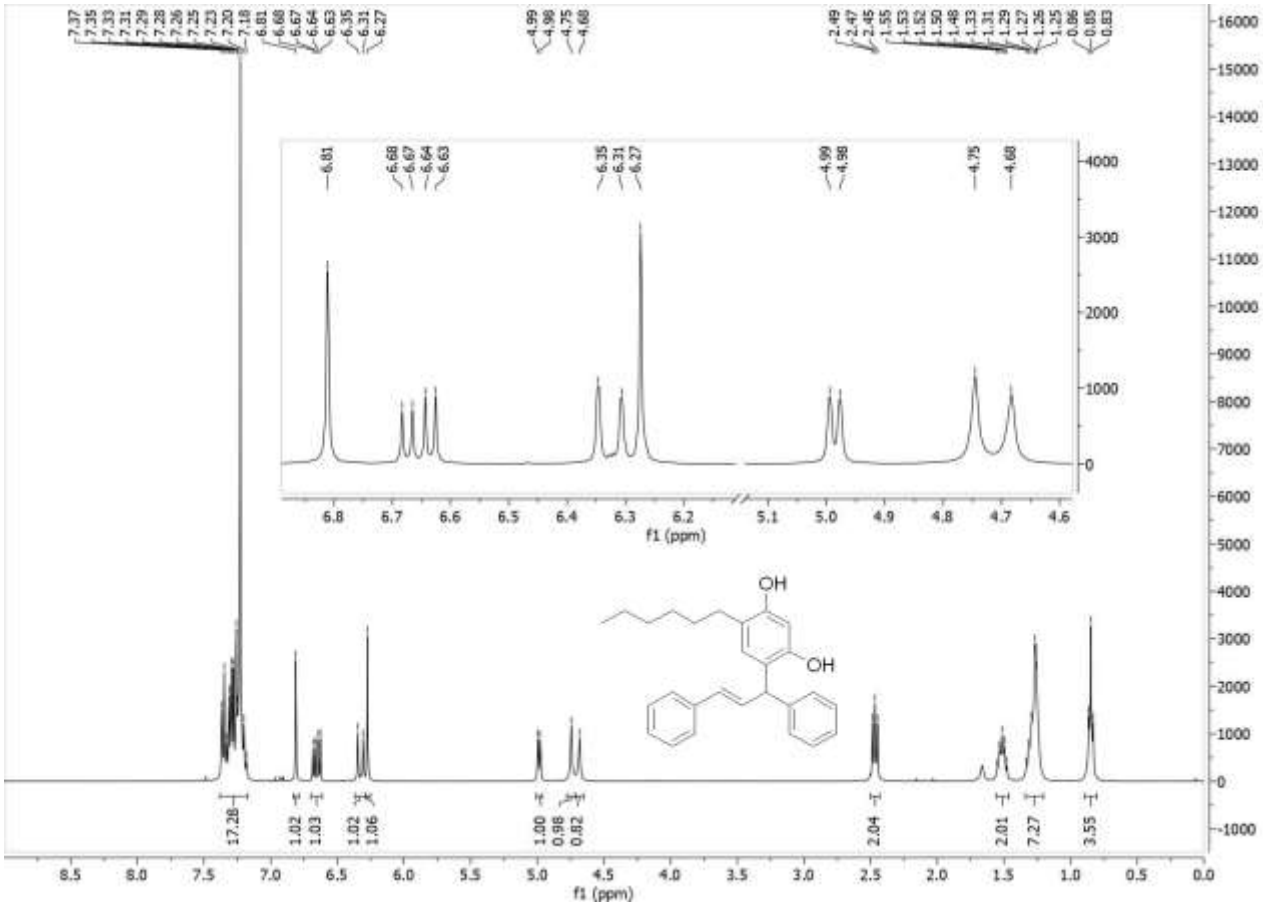

*Figure C.169 ^{1}H NMR spectrum of **21m** in $CDCl_3$.*

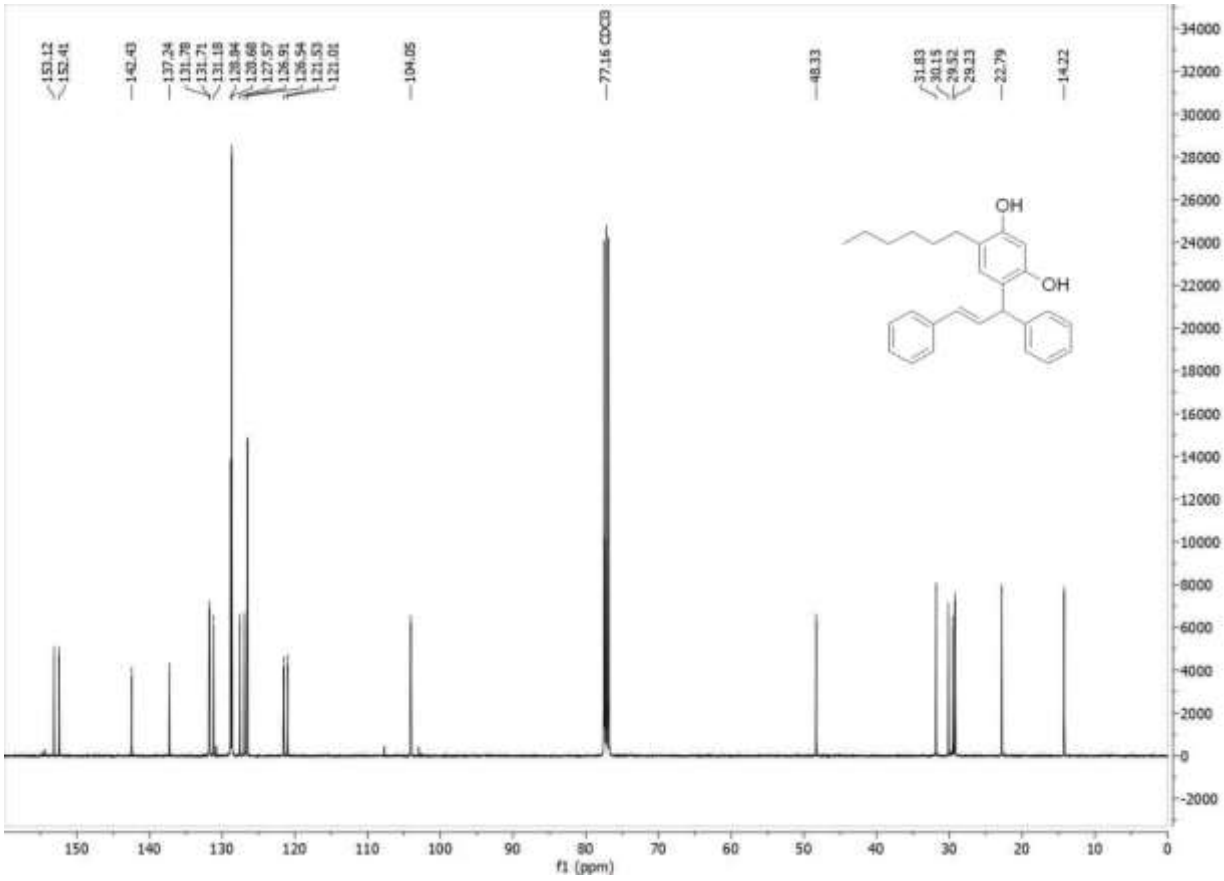

Figure C.170 $^{13}C(^{1}H)$ *NMR spectrum of* ***21m*** *in* $CDCl_3$.

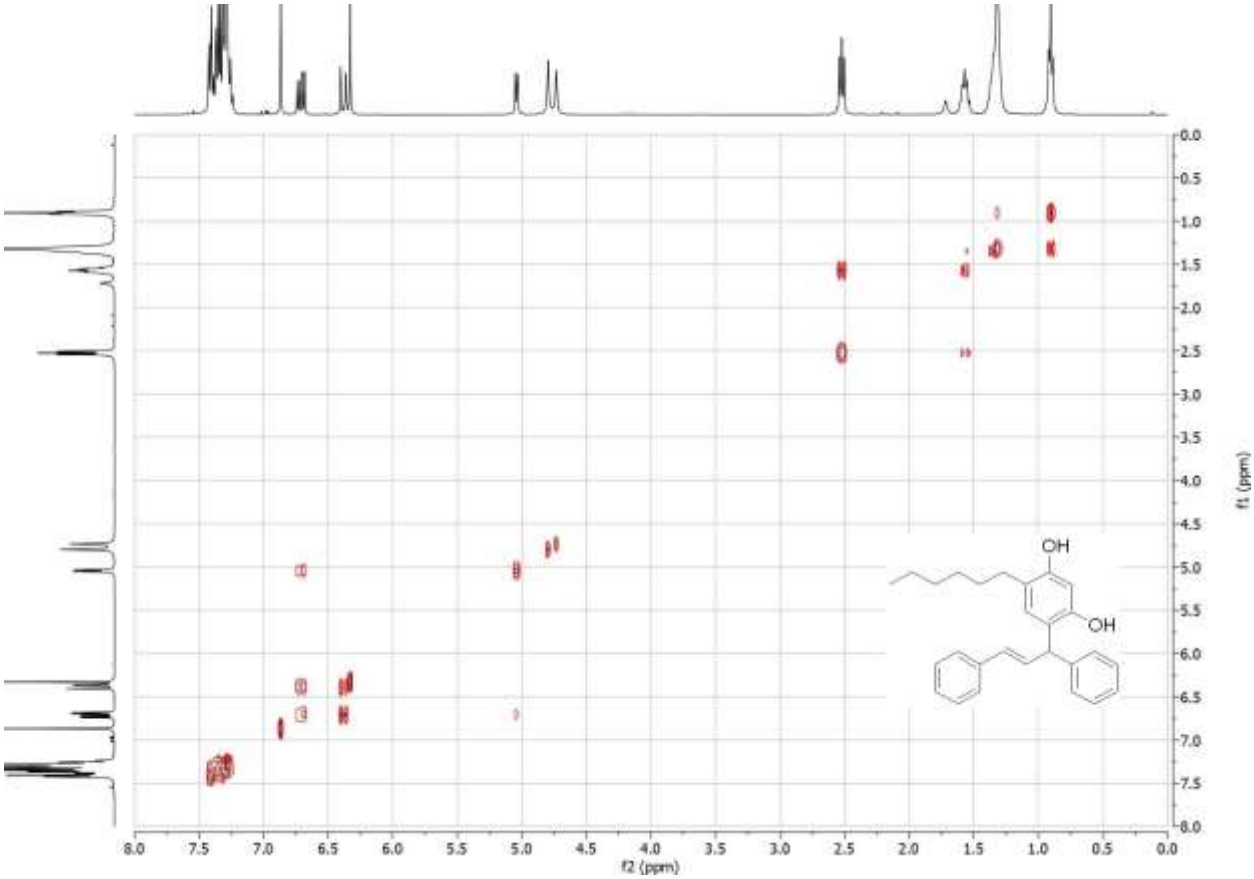

Figure C.171 COSY spectrum of ***21m*** *in* $CDCl_3$.

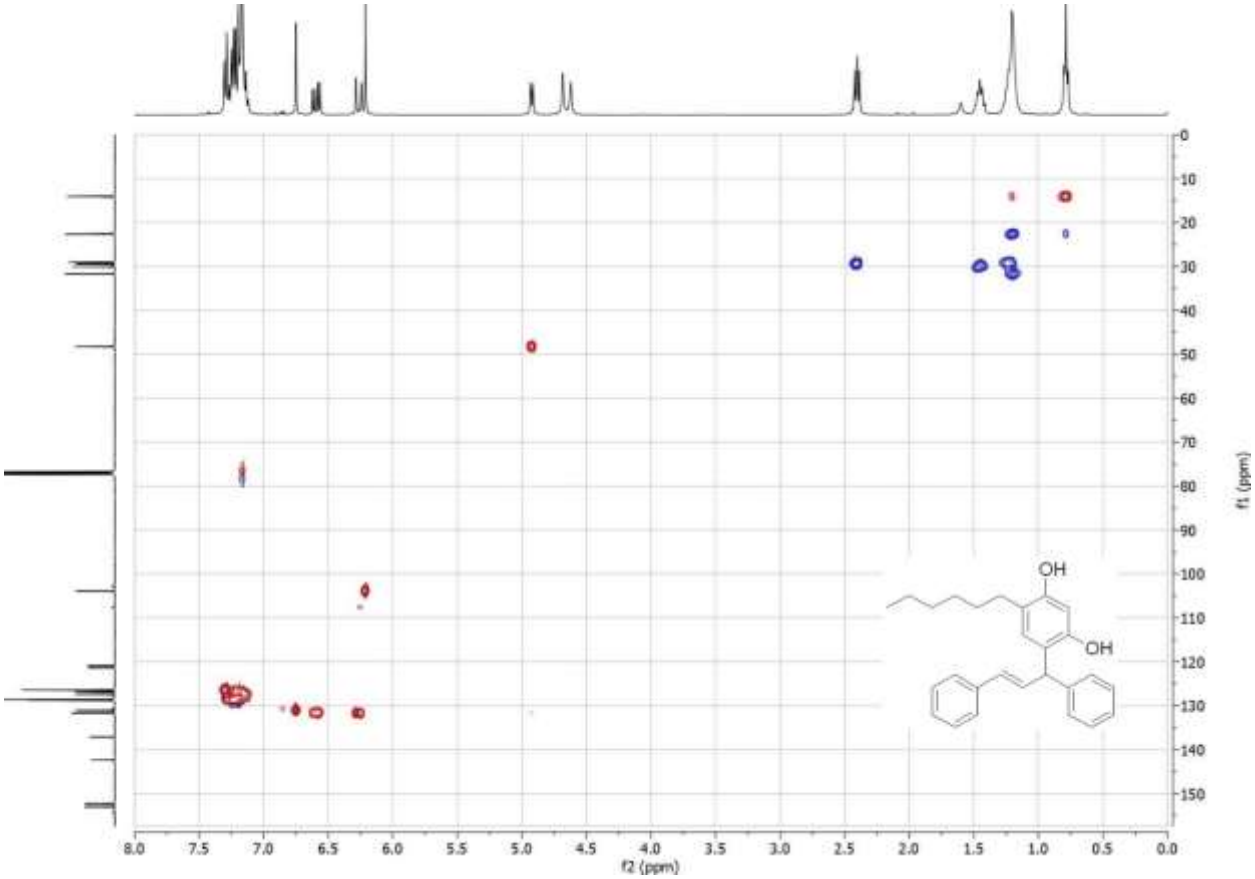

Figure C.172 HSQC spectrum of **21m** in $CDCl_3$.

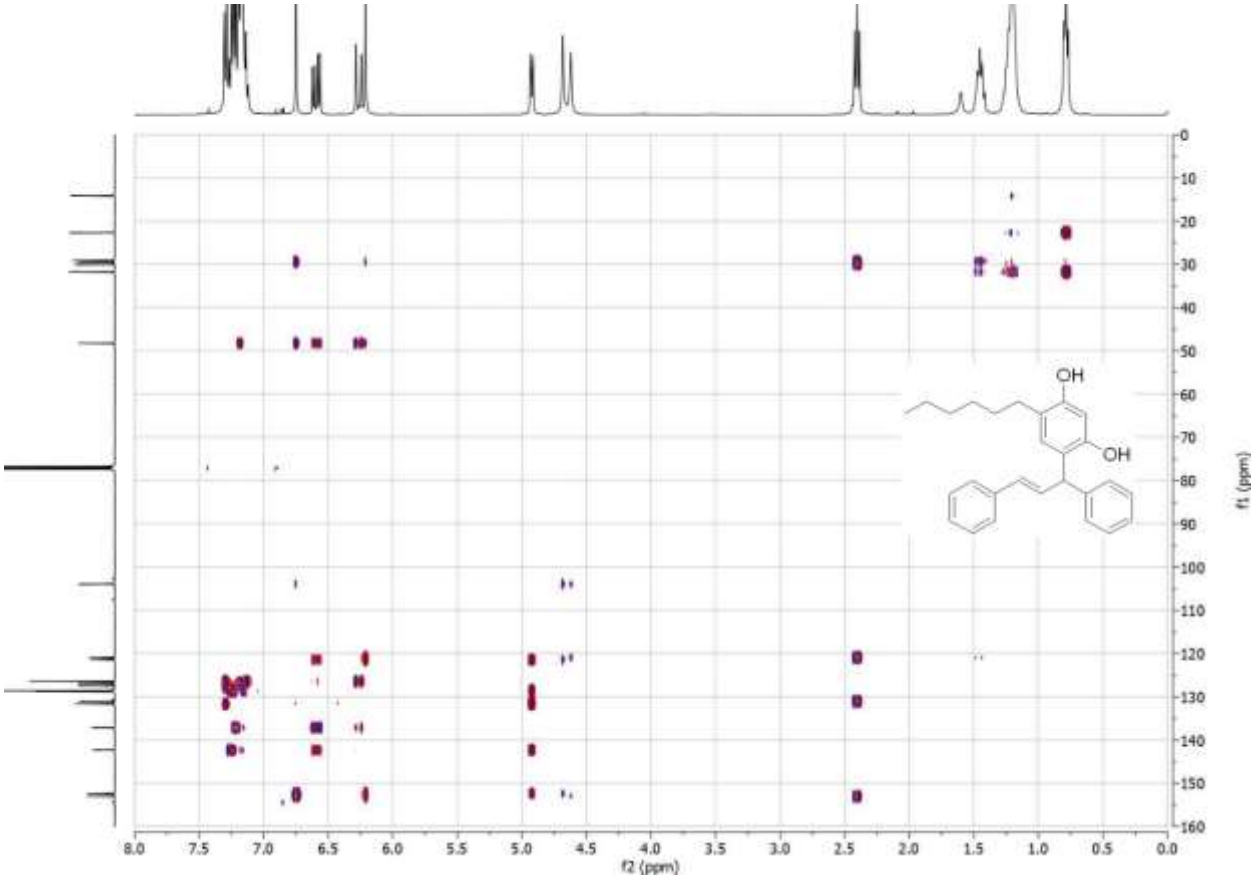

Figure C.173 HMBC spectrum of **21m** in $CDCl_3$.

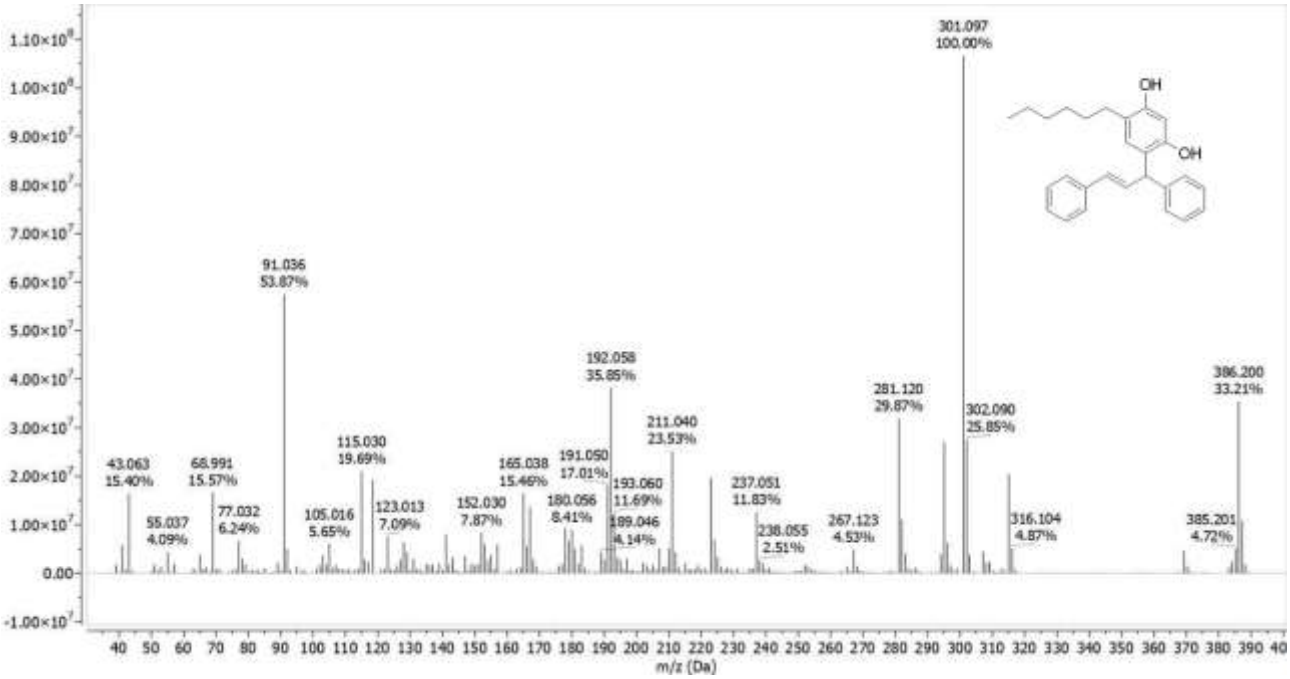

Figure C.174 GC-MS spectrum of ***21m***.

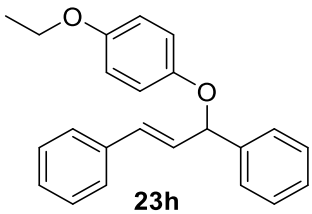

23h

Chemical Formula: $C_{23}H_{22}O_2$
Molecular Weight: 330,4270

^{1}H NMR (400 MHz, Chloroform-*d*) δ [ppm] = 7.50 – 7.19 (m, 10H), 6.94 – 6.88 (m, 2H), 6.81 – 6.74 (m, 2H), 6.66 (d, *J* = 15.7 Hz, 1H), 6.44 (dd, *J* = 15.9, 6.4 Hz, 1H), 5.69 (d, *J* = 6.4 Hz, 1H), 3.95 (q, *J* = 7.0 Hz, 2H), 1.37 (t, *J* = 7.0 Hz, 3H).

^{13}C NMR (101 MHz, Chloroform-*d*) δ [ppm] = 153.60, 152.13, 140.76, 136.59, 131.60, 129.73, 128.79, 128.67, 127.98, 127.96, 126.86, 126.80, 117.76, 115.38, 82.01, 64.03, 15.07.

GC/MS (EI): calc. for $C_{23}H_{22}O_2$ $[M]^+$: 330.162; found: 330.151, $C_{15}H_{13}O_2$ 225.110, $C_{13}H_9O_2$ 197.066, C_7H_7 91.056, C_6H_5 77.052.

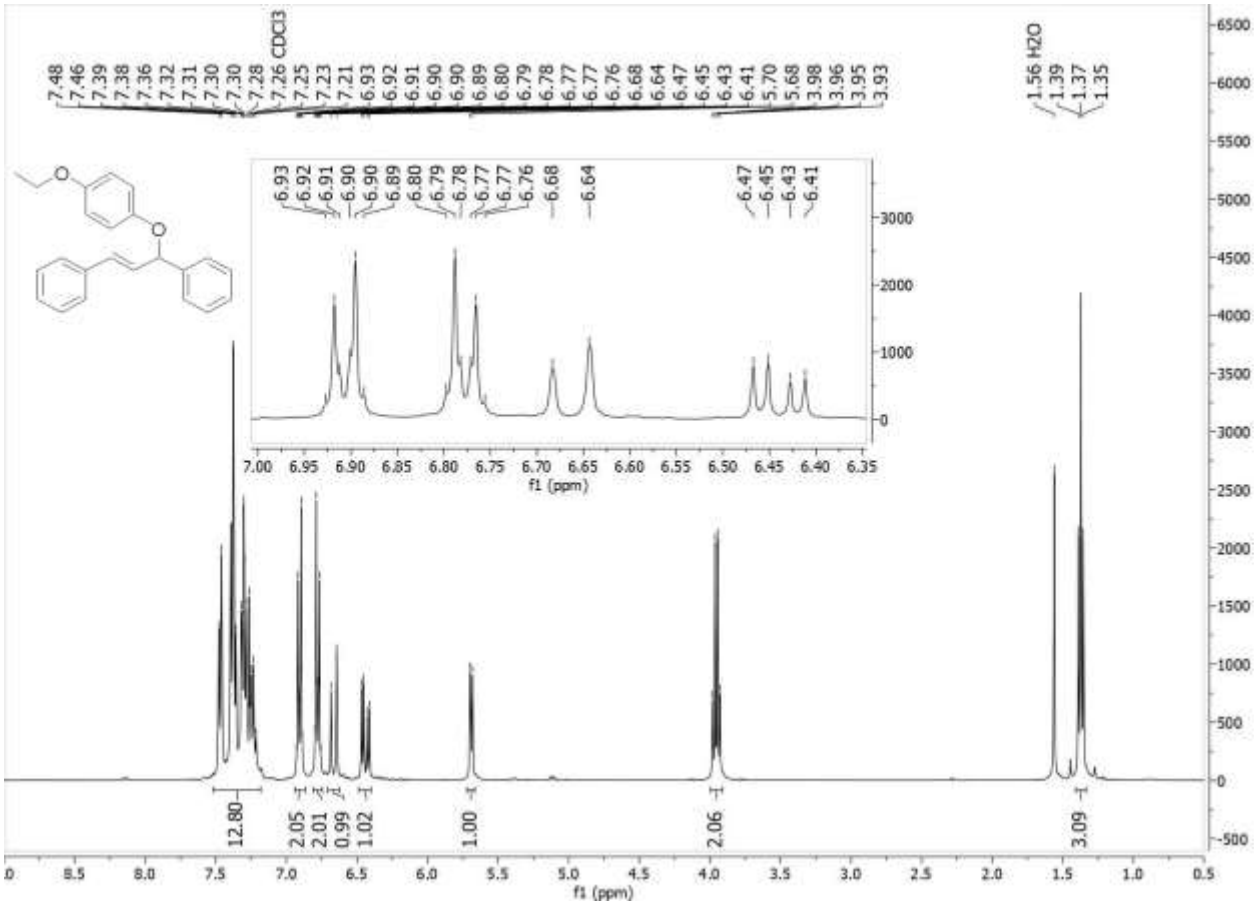

*Figure C.175 ^{1}H NMR spectrum of **23h** in $CDCl_3$.*

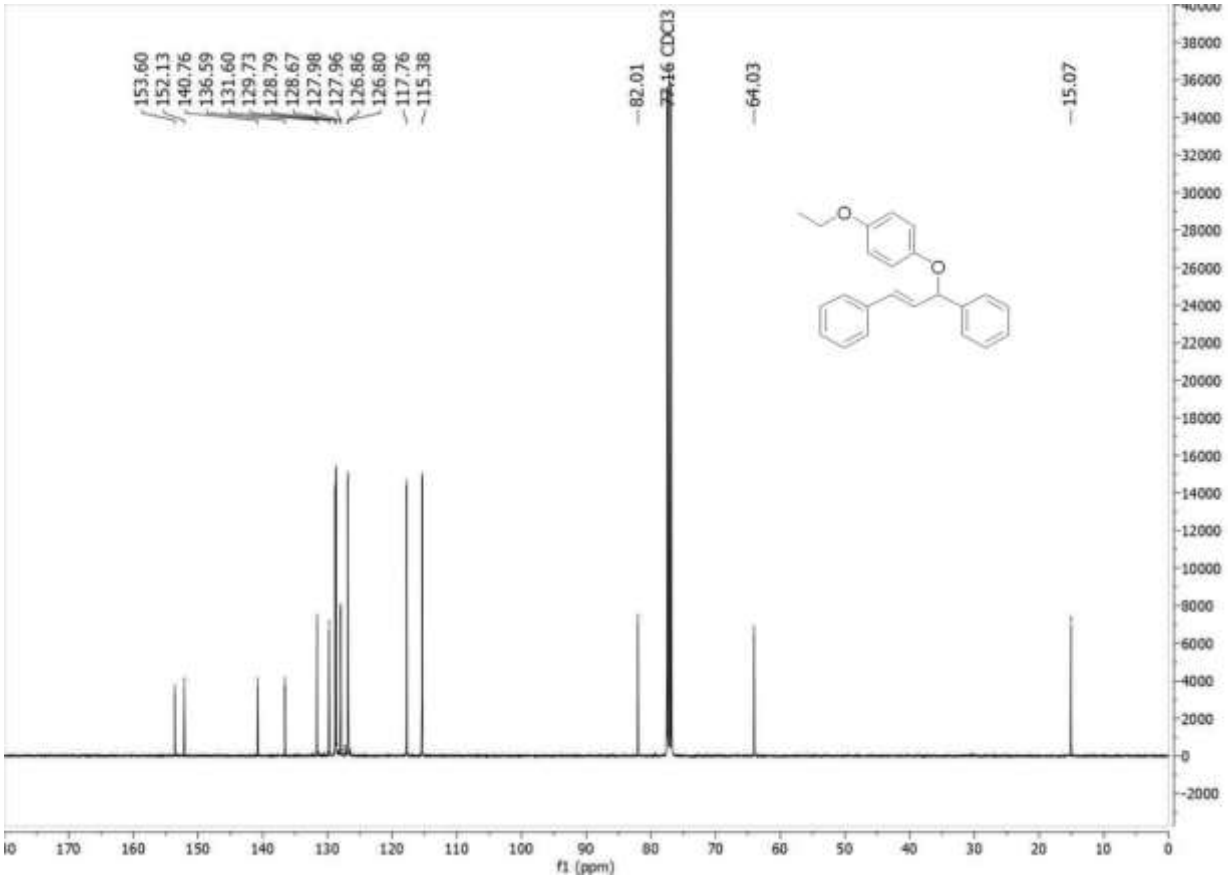

Figure C.176 $^{13}C(^{1}H)$ *NMR spectrum of* ***23h*** *in* $CDCl_3$.

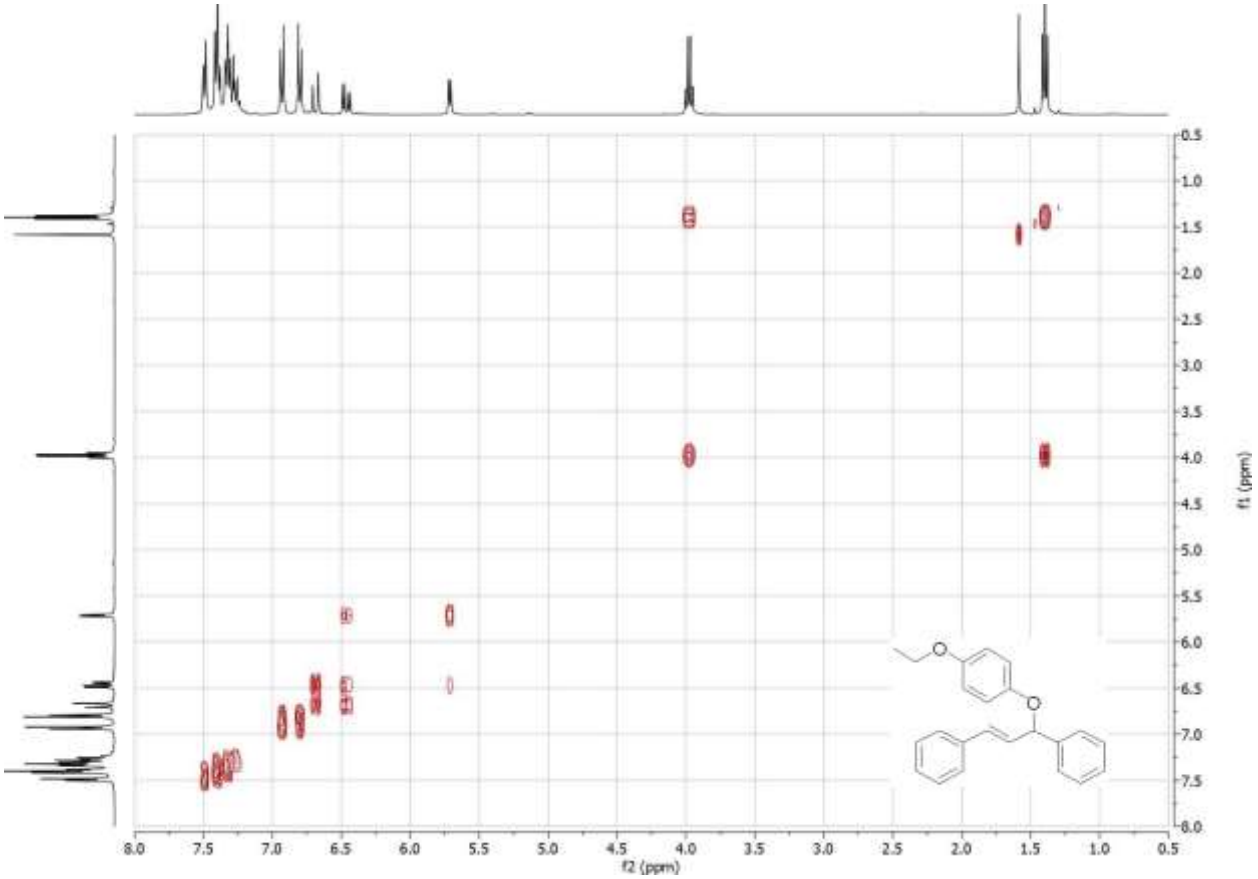

Figure C.177 COSY spectrum of ***23h*** *in* $CDCl_3$.

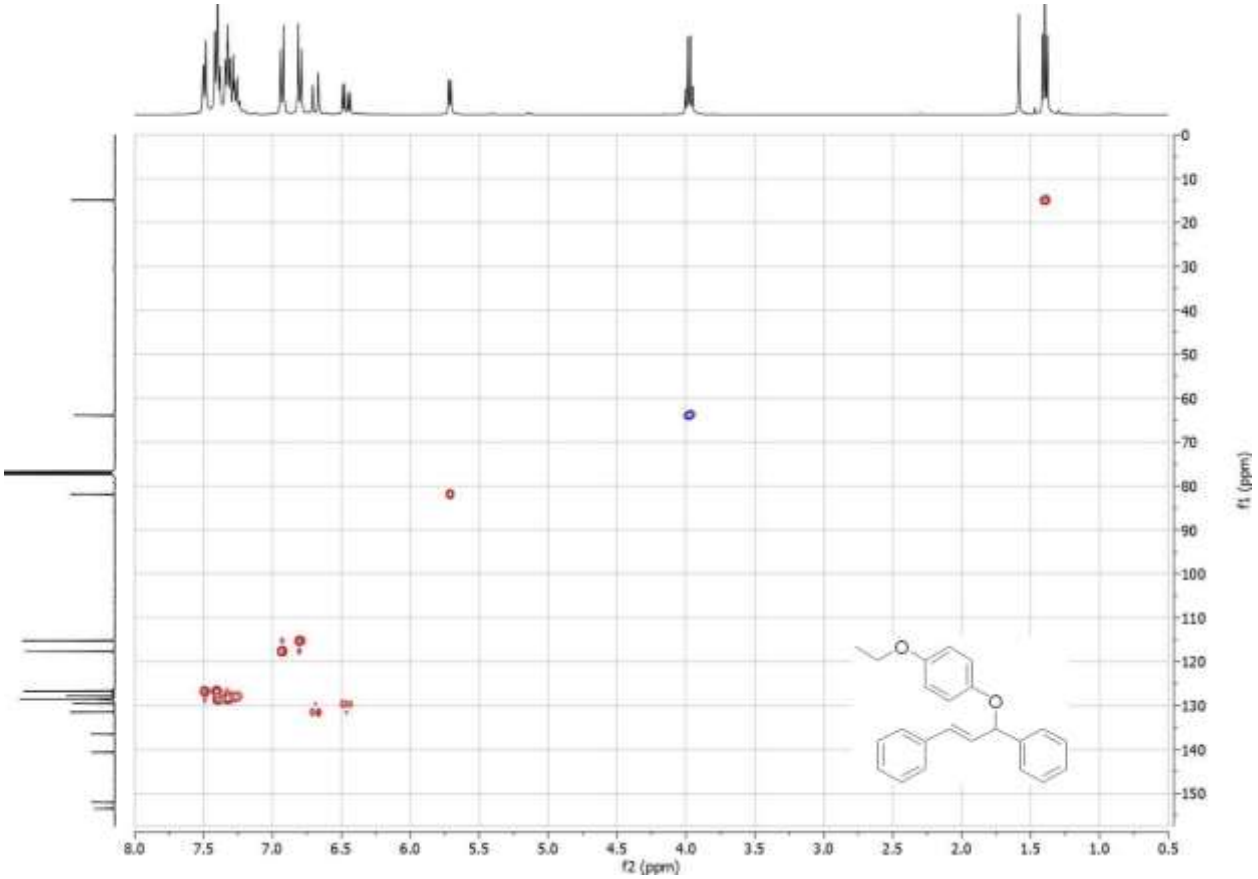

Figure C.178 HSQC spectrum of **23h** in $CDCl_3$.

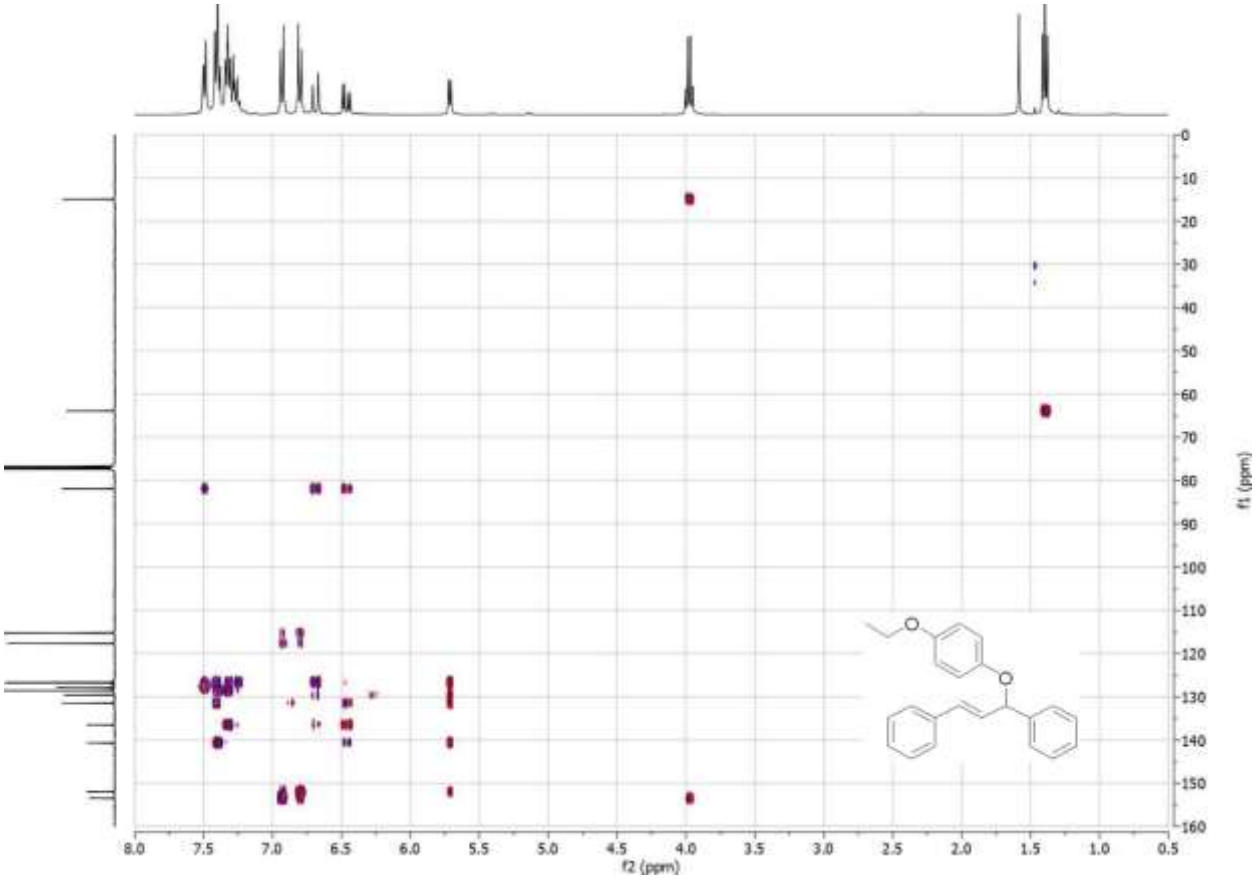

Figure C.179 HMBC spectrum of **23h** in $CDCl_3$.

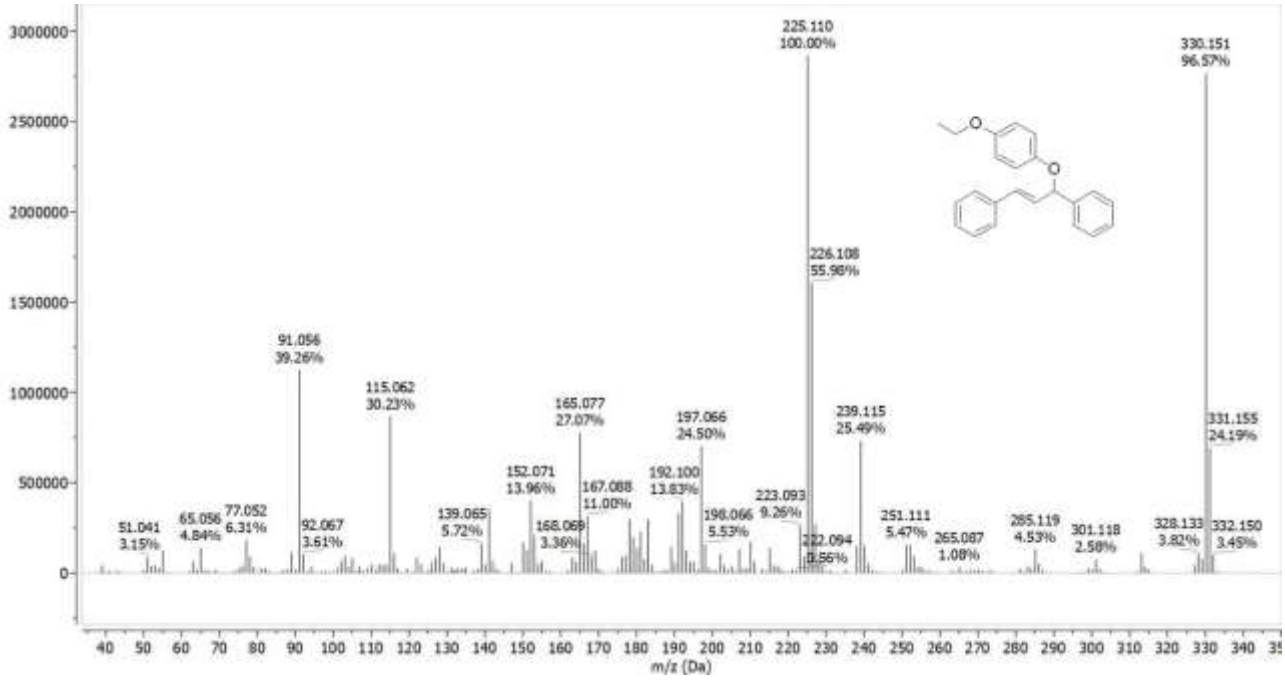

Figure C.180 GC-MS spectrum of **23h**.

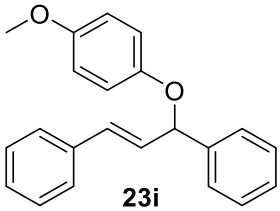

23i

Chemical Formula: $C_{22}H_{20}O_2$
Molecular Weight: 316,4000

^{1}H NMR (400 MHz, Chloroform-*d*) δ [ppm] = 7.50 – 7.19 (m, 10H), 6.95 – 6.88 (m, 2H), 6.81 – 6.74 (m, 2H), 6.66 (d, *J* = 15.9 Hz, 1H), 6.44 (dd, *J* = 16.0, 6.4 Hz, 1H), 5.69 (d, *J* = 6.3 Hz, 1H), 3.74 (s, 3H).

^{13}C NMR (101 MHz, Chloroform-*d*) δ [ppm] = 154.26, 152.20, 140.73, 136.58, 131.63, 129.69, 128.81, 128.68, 127.99, 127.98, 126.86, 126.81, 117.78, 114.67, 82.02, 55.78.

GC/MS (EI): calc. for $C_{22}H_{20}O_2$ $[M]^+$: 316.146; found: 316.141, $C_{14}H_{11}O_2$ 211.094 $C_{15}H_{12}$ 192.098, C_7H_7 91.059, C_6H_5 77.063.

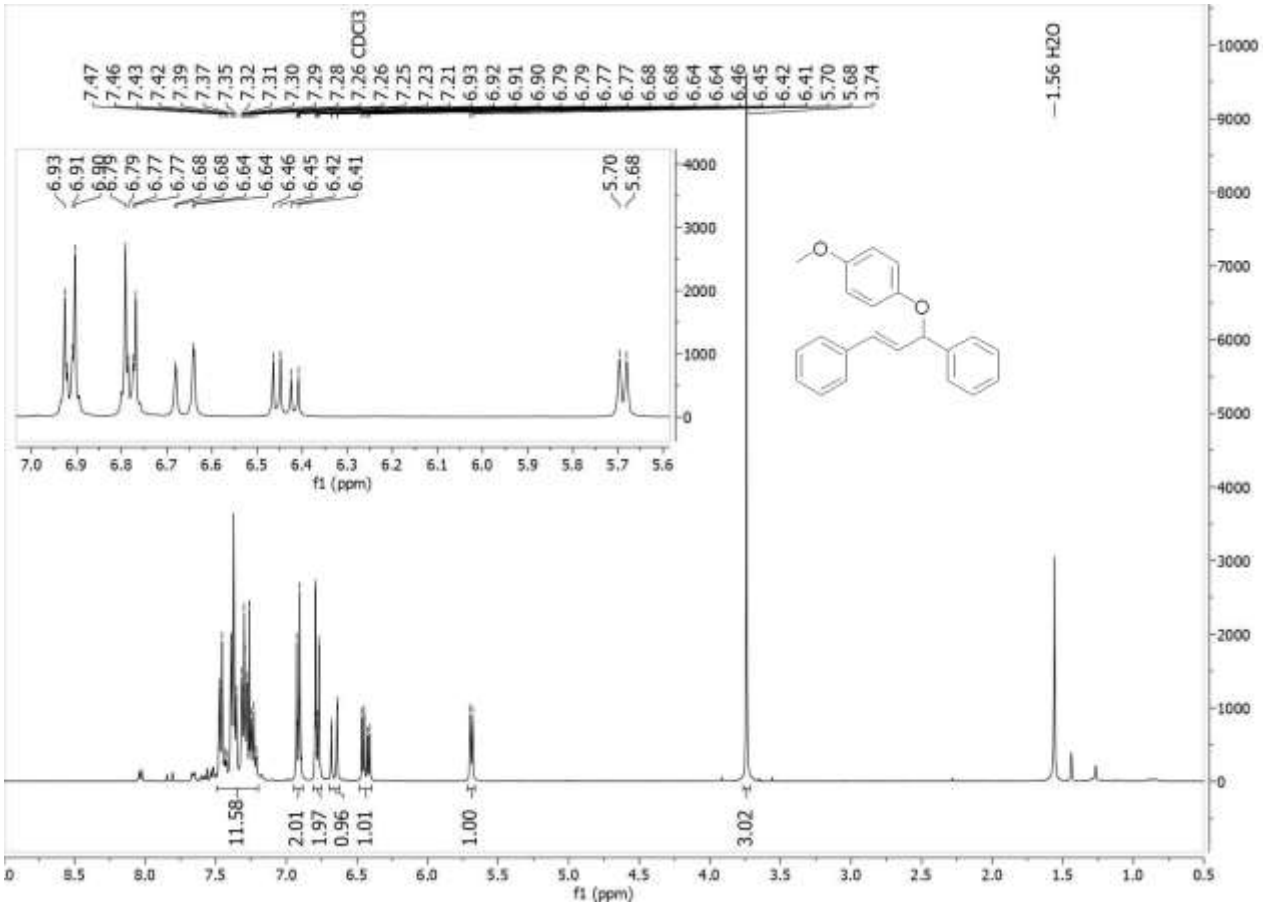

*Figure C.181 ^{1}H NMR spectrum of **23i** in $CDCl_3$.*

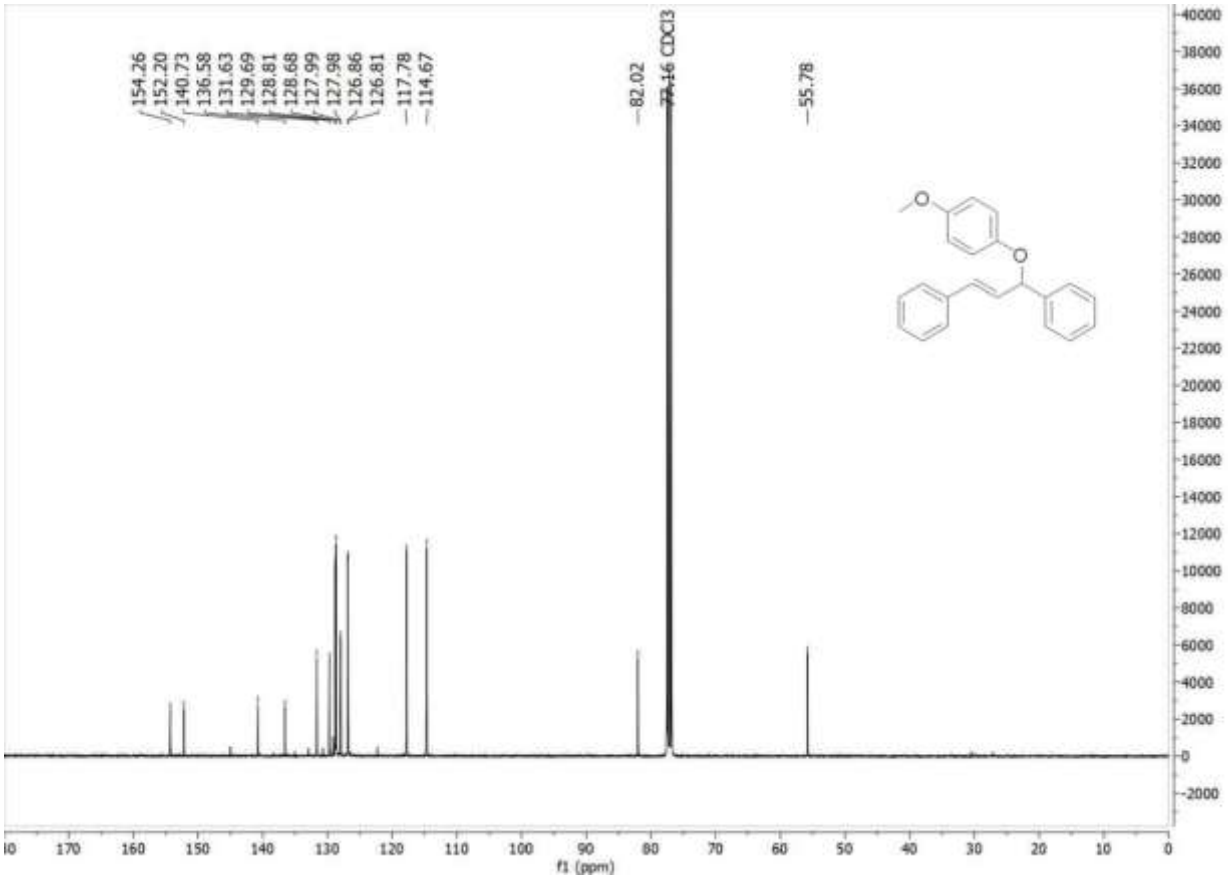

Figure C.182 $^{13}C(^{1}H)$ *NMR spectrum of* ***23i*** *in* $CDCl_3$.

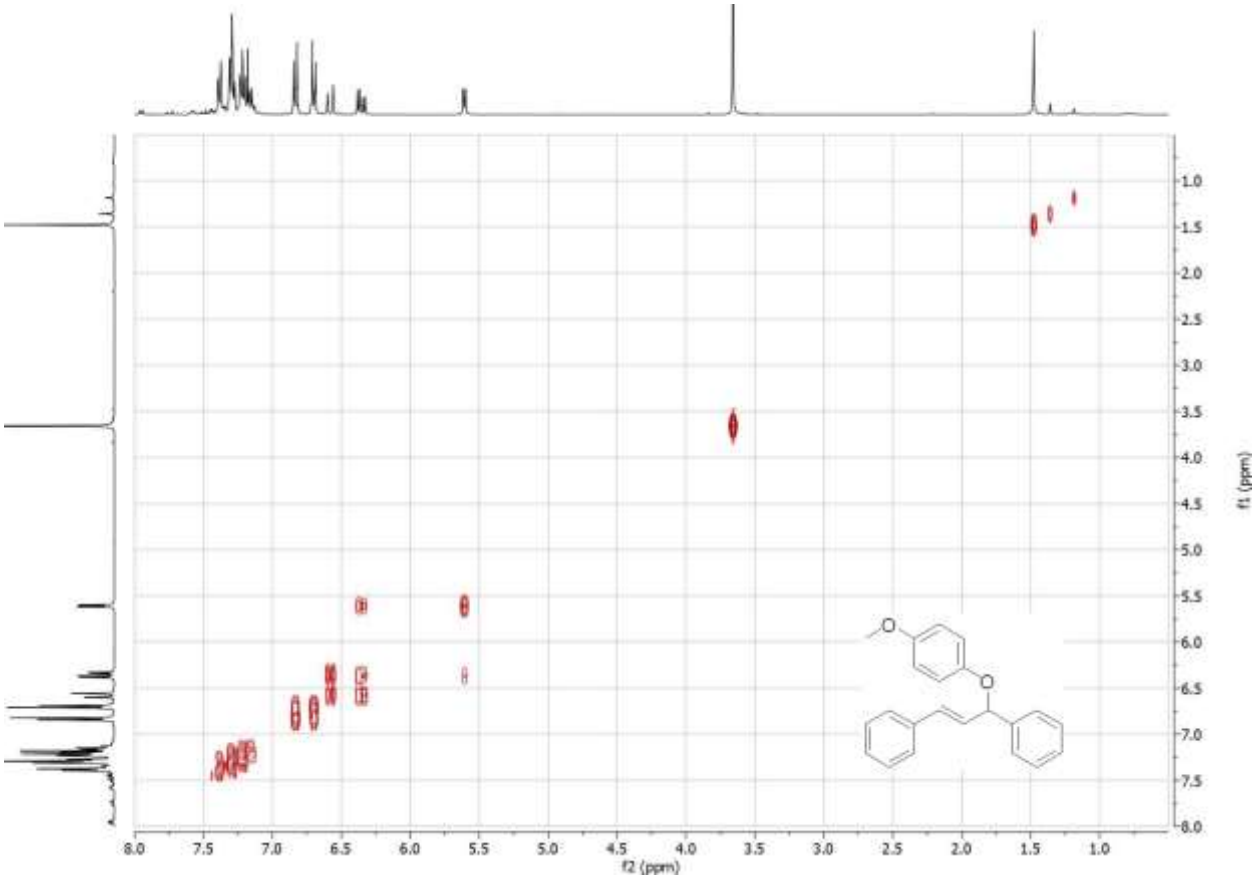

Figure C.183 COSY spectrum of ***23i*** *in* $CDCl_3$.

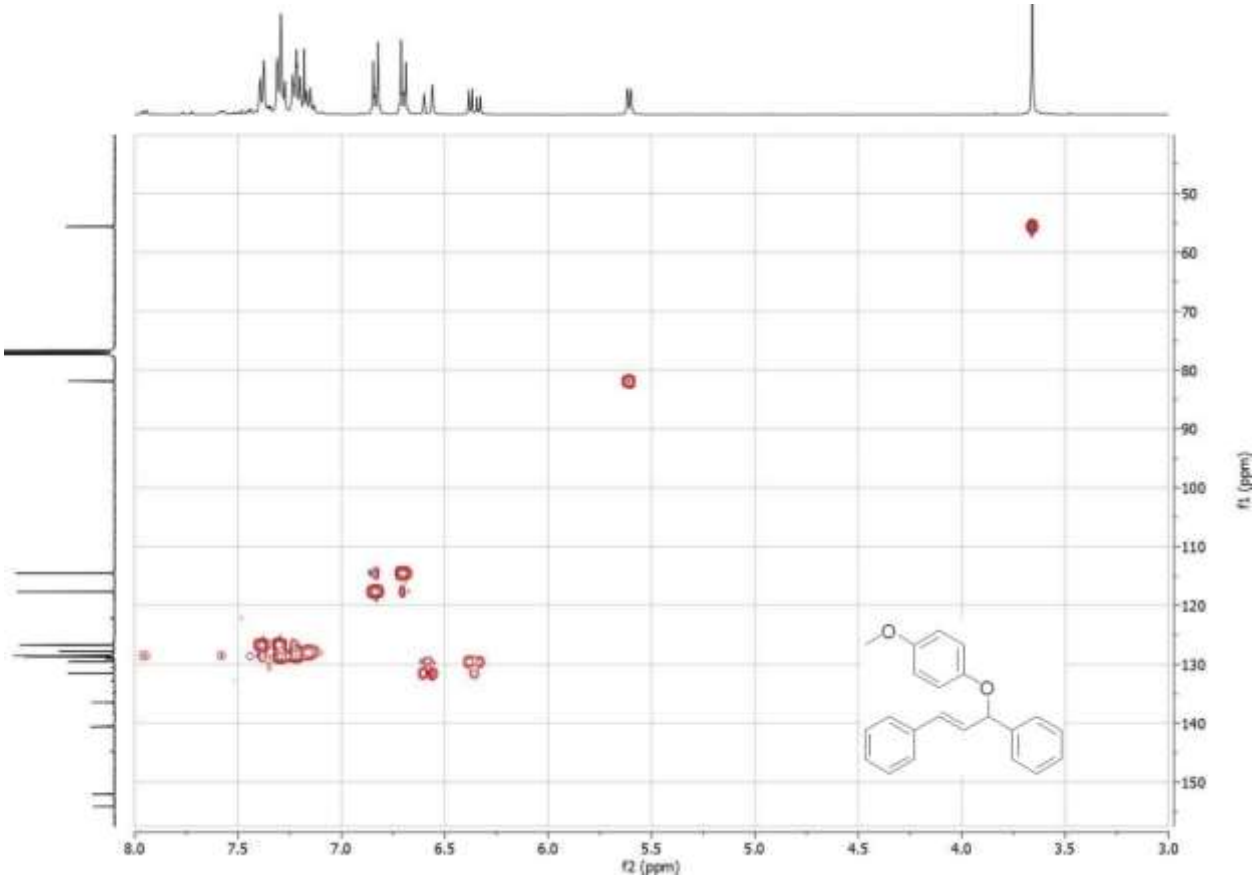

Figure C.184 HSQC spectrum of **23i** in $CDCl_3$.

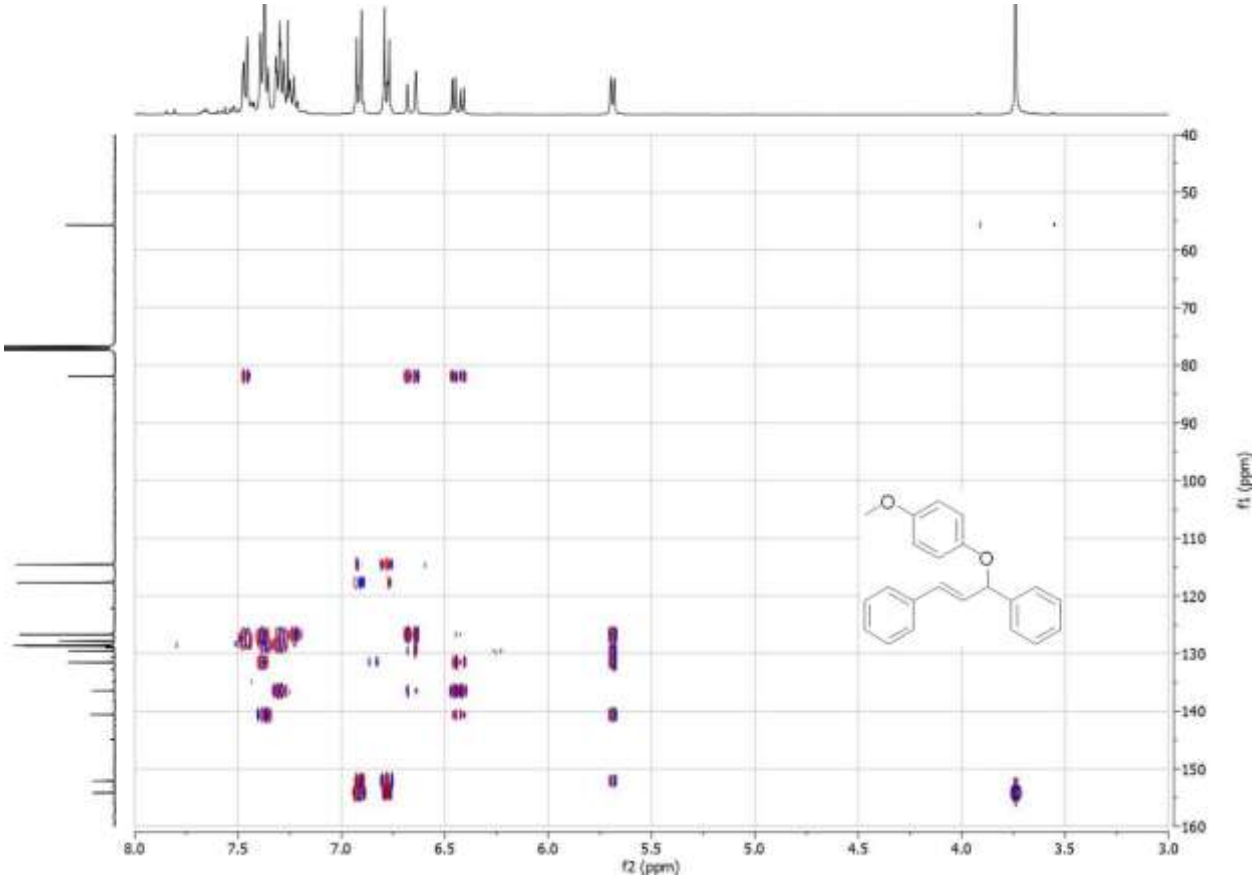

Figure C.185 HMBC spectrum of **23i** in $CDCl_3$.

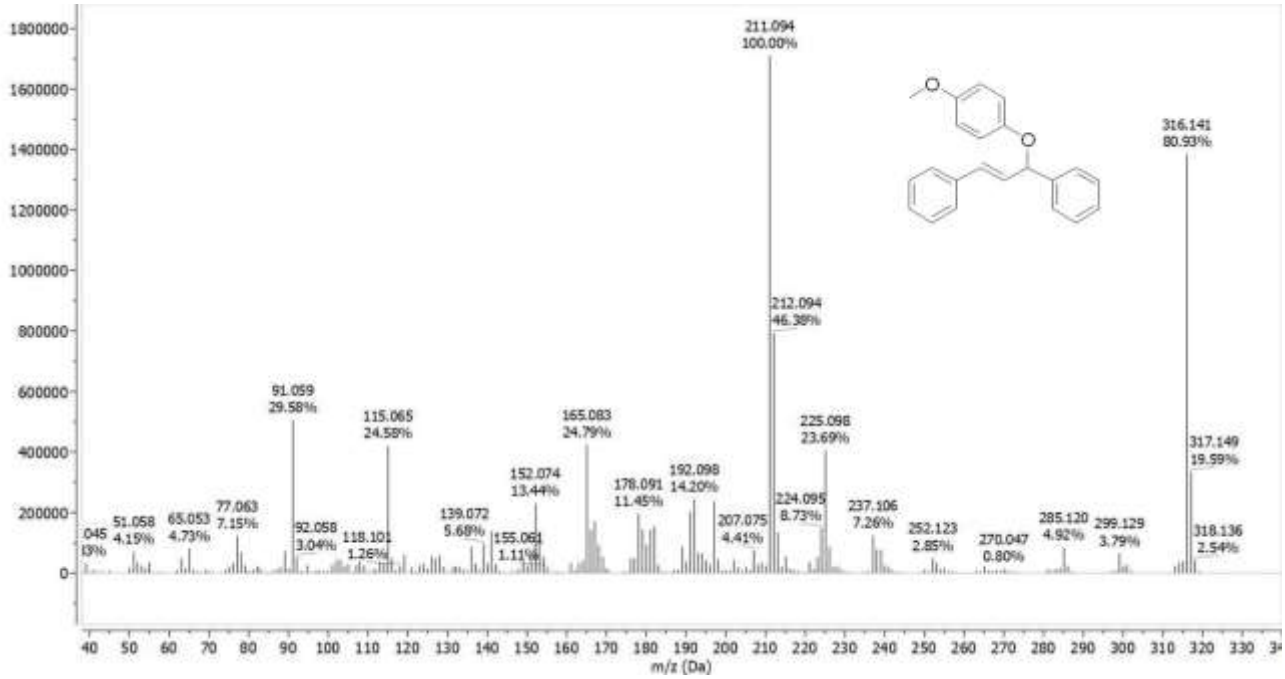

Figure C.186 GC-MS spectrum of ***23i***.

References

[1] Lehn, J.-M. Supramolecular Chemistry—Scope and Perspectives Molecules, Supermolecules, and Molecular Devices (Nobel Lecture). *Angew. Chem. Int. Ed. Engl*. **1988**, *27* (1), 89–112. https://doi.org/10.1002/anie.198800891.

[2] Pedersen, C. J. The Discovery of Crown Ethers (Noble Lecture). *Angew. Chem. Int. Ed. Engl.* **1988**, *27* (8), 1021–1027. https://doi.org/10.1002/anie.198810211.

[3] van Leeuwen, P. W. N. M. *Supramolecular Catalysis*, 1st ed.; Wiley, **2008**. https://doi.org/10.1002/9783527621781.

[4] Steed, J. W.; Atwood, J. L. *Supramolecular Chemistry*, 2nd ed.; Wiley: Chichester, UK, **2009**. https://doi.org/10.1002%2F9780470740880.

[5] Mecozzi, S.; Rebek, J., Jr. The 55 % Solution: A Formula for Molecular Recognition in the Liquid State. *Chemistry – A European Journal* **1998**, *4* (6), 1016–1022. https://doi.org/10.1002/(SICI)1521-3765(19980615)4:6<1016::AID-CHEM1016>3.0.CO;2-B

[6] Liu, Y.; Zhao, W.; Chen, C.-H.; Flood, A. H. Chloride Capture Using a C–H Hydrogen-Bonding Cage. *Science* **2019**, *365* (6449), 159–161. https://doi.org/10.1126/science.aaw5145.

[7] Chen, J.; Rebek, J. Selectivity in an Encapsulated Cycloaddition Reaction. *Org. Lett.* **2002**, *4* (3), 327–329. https://doi.org/10.1021/ol0168115.

[8] Stahl, I.; von Kiedrowski, G. "Kinetic NMR Titration": Including Chemical Shift Information in the Kinetic Analysis of Supramolecular Reaction Systems Such as Organic Replicators. *J. Am. Chem. Soc.* **2006**, *128* (43), 14014–14015. https://doi.org/10.1021/ja065894n.

[9] Borsato, G.; Scarso, A. Chapter 7 - Catalysis Within the Self-Assembled Resorcin[4]Arene Hexamer. In *Organic Nanoreactors*; Sadjadi, S., Ed.; Academic Press: Boston, 2016; pp 203–234. https://doi.org/10.1016/B978-0-12-801713-5.00007-0.

[10] Fischer, E. Einfluss Der Configuration Auf Die Wirkung Der Enzyme. *Berichte der deutschen chemischen Gesellschaft* **1894**, *27* (3), 2985–2993. https://doi.org/10.1002/cber.18940270364.

[11] Koshland, D. E. Application of a Theory of Enzyme Specificity to Protein Synthesis*. *Proceedings of the National Academy of Sciences* **1958**, *44* (2), 98–104. https://doi.org/10.1073/pnas.44.2.98.

[12] Koshland, D. E.; Neet, K. E. The Catalytic and Regulatory Properties of Enzymes. *Annual Review of Biochemistry* **1968**, *37* (1), 359–411. https://doi.org/10.1146/annurev.bi.37.070168.002043.

[13] "Enzyme substrate binding and catalysis." by Thomas Shafee CC BY 4.0

[14] Raynal, M.; Ballester, P.; Vidal-Ferran, A.; Leeuwen, P. W. N. M. van. Supramolecular Catalysis. Part 2: Artificial Enzyme Mimics. *Chemical Society Reviews* **2014**, *43* (5), 1734–1787. https://doi.org/10.1039/C3CS60037H.

[15] Houk, K. N.; Leach, A. G.; Kim, S. P.; Zhang, X. Binding Affinities of Host–Guest, Protein–Ligand, and Protein–Transition-State Complexes. *Angewandte Chemie International Edition* **2003**, *42* (40), 4872–4897. https://doi.org/10.1002/anie.200200565.

[16] Kang, J.; Rebek, J. Acceleration of a Diels–Alder Reaction by a Self-Assembled Molecular Capsule. *Nature* **1997**, *385* (6611), 50–52. https://doi.org/10.1038/385050a0.

[17] Kaphan, D. M.; Toste, F. D.; Bergman, R. G.; Raymond, K. N. Enabling New Modes of Reactivity via Constrictive Binding in a Supramolecular-Assembly-Catalyzed Aza-Prins Cyclization. *J. Am. Chem. Soc.* **2015**, *137* (29), 9202–9205. https://doi.org/10.1021/jacs.5b01261.

[18] Yoshizawa, M.; Klosterman, J. K.; Fujita, M. Functional Molecular Flasks: New Properties and Reactions within Discrete, Self-Assembled Hosts. *Angewandte Chemie International Edition* **2009**, *48* (19), 3418–3438. https://doi.org/10.1002/anie.200805340.

[19] Fujita, M.; Oguro, D.; Miyazawa, M.; Oka, H.; Yamaguchi, K.; Ogura, K. Self-Assembly of Ten Molecules into Nanometre-Sized Organic Host Frameworks. *Nature* **1995**, *378* (6556), 469–471. https://doi.org/10.1038/378469a0.

[20] Conn, M. M.; Rebek, J. Self-Assembling Capsules. *Chem. Rev.* **1997**, *97* (5), 1647–1668. https://doi.org/10.1021/cr9603800.

[21] Elidrisi, I.; Negin, S.; Bhatt, P. V.; Govender, T.; Kruger, H. G.; Gokel, G. W.; Maguire, G. E. M. Pore Formation in Phospholipid Bilayers by Amphiphilic Cavitands. *Org. Biomol. Chem.* **2011**, *9* (12), 4498–4506. https://doi.org/10.1039/C0OB01236J.

[22] Antesberger, J.; Cave, G. W. V.; Ferrarelli, M. C.; Heaven, M. W.; Raston, C. L.; Atwood, J. L. Solvent-Free, Direct Synthesis of Supramolecular Nano-Capsules. *Chem. Commun.* **2005**, No. 7, 892–894. https://doi.org/10.1039/B412251H.

[23] MacGillivray, L. R.; Atwood, J. L. A Chiral Spherical Molecular Assembly Held Together by 60 Hydrogen Bonds. *Nature* **1997**, *389* (6650), 469–472. https://doi.org/10.1038/38985.

[24] Avram, L.; Cohen, Y. Spontaneous Formation of Hexameric Resorcinarene Capsule in Chloroform Solution as Detected by Diffusion NMR. *J. Am. Chem. Soc.* **2002**, *124* (51), 15148–15149. https://doi.org/10.1021/ja0272686.

[25] a) Structures on the left: original images.

b) Resorcin[4]arene hexameric capsule 3D structure on the right: [26]

c) Snub cube: "Snubhexahedroncw.jpg" by en.wiki user Cyp CC-BY-SA 3.0

[26] Yamanaka, M.; Shivanyuk, A.; Rebek, J. Kinetics and Thermodynamics of Hexameric Capsule Formation. *J. Am. Chem. Soc.* **2004**, *126* (9), 2939–2943. https://doi.org/10.1021/ja037035u.

[27] Cavarzan, A.; Scarso, A.; Sgarbossa, P.; Strukul, G.; Reek, J. N. H. Supramolecular Control on Chemo- and Regioselectivity via Encapsulation of (NHC)-Au Catalyst within a Hexameric Self-Assembled Host. *J. Am. Chem. Soc.* **2011**, *133* (9), 2848–2851. https://doi.org/10.1021/ja111106x.

[28] Giust, S.; Sorella, G. L.; Sperni, L.; Strukul, G.; Scarso, A. Substrate Selective Amide Coupling Driven by Encapsulation of a Coupling Agent within a Self-Assembled Hexameric Capsule. *Chem. Commun.* **2015**, *51* (9), 1658–1661. https://doi.org/10.1039/C4CC08833F.

[29] Bianchini, G.; Sorella, G. L.; Canever, N.; Scarso, A.; Strukul, G. Efficient Isonitrile Hydration through Encapsulation within a Hexameric Self-Assembled Capsule and Selective Inhibition by a Photo-Controllable Competitive Guest. *Chem. Commun.* **2013**, *49* (46), 5322–5324. https://doi.org/10.1039/C3CC42233J.

[30] La Sorella, G.; Sperni, L.; Strukul, G.; Scarso, A. Supramolecular Encapsulation of Neutral Diazoacetate Esters and Catalyzed 1,3-Dipolar Cycloaddition Reaction by a Self-Assembled Hexameric Capsule. *ChemCatChem* **2015**, *7* (2), 291–296. https://doi.org/10.1002/cctc.201402631.

[31] Giust, S.; La Sorella, G.; Sperni, L.; Fabris, F.; Strukul, G.; Scarso, A. Supramolecular Catalysis in the Synthesis of Substituted 1 H-Tetrazoles from Isonitriles by a Self-Assembled Hexameric Capsule. *Asian Journal of Organic Chemistry* **2015**, *4* (3), 217–220. https://doi.org/10.1002/ajoc.201402229.

[32] Santamaría, J.; Martín, T.; Hilmersson, G.; Craig, S. L.; Rebek, J. Guest Exchange in an Encapsulation Complex: A Supramolecular Substitution Reaction. *Proceedings of the National Academy of Sciences* **1999**, *96* (15), 8344–8347. https://doi.org/10.1073/pnas.96.15.8344.

[33] Gaeta, C.; Talotta, C.; De Rosa, M.; La Manna, P.; Soriente, A.; Neri, P. The Hexameric Resorcinarene Capsule at Work: Supramolecular Catalysis in Confined Spaces. *Chemistry – A European Journal* **2019**, *25* (19), 4899–4913. https://doi.org/10.1002/chem.201805206.

[34] Zhang, Q.; Catti, L.; Tiefenbacher, K. Catalysis inside the Hexameric Resorcinarene Capsule. *Acc. Chem. Res.* **2018**, *51* (9), 2107–2114. https://doi.org/10.1021/acs.accounts.8b00320.

[35] Zhang, Q.; Rinkel, J.; Goldfuss, B.; Dickschat, J. S.; Tiefenbacher, K. Sesquiterpene Cyclizations Catalysed inside the Resorcinarene Capsule and Application in the Short Synthesis of Isolongifolene and Isolongifolenone. *Nat Catal* **2018**, *1* (8), 609–615. https://doi.org/10.1038/s41929-018-0115-4.

[36] Gaeta, C.; La Manna, P.; De Rosa, M.; Soriente, A.; Talotta, C.; Neri, P. Supramolecular Catalysis with Self-Assembled Capsules and Cages: What Happens in Confined Spaces. *ChemCatChem* **2021**, *13* (7), 1638–1658. https://doi.org/10.1002/cctc.202001570.

[37] Nenajdenko, V. *Isocyanide Chemistry: Applications in Synthesis and Material Science*; John Wiley & Sons, 2012.

[38] Ramozzi, R.; Chéron, N.; Braïda, B.; C. Hiberty, P.; Fleurat-Lessard, P. A Valence Bond View of Isocyanides' Electronic Structure. *New Journal of Chemistry* **2012**, *36* (5), 1137–1140. https://doi.org/10.1039/C2NJ40050B.

[39] Dömling, A.; Ugi, I. Multicomponent Reactions with Isocyanides. *Angewandte Chemie International Edition* **2000**, *39* (18), 3168–3210. https://doi.org/10.1002/1521-3773(20000915)39:18<3168::AID-ANIE3168>3.0.CO;2-U.

[40] Müller, E.; Zeeh, B. Lewis Acid-Catalyzed Reaction of Carbonyl Compounds with Tertbutyl Isonitrile. *Liebigs Ann. Chem* **1966**, *696*, 72–80.

[41] Kabbe, H.-J. Synthesis of Substituted Oxetane-2,3-Diimines from Isocyanides. *Angewandte Chemie International Edition in English* **1968**, *7* (5), 389–389. https://doi.org/10.1002/anie.196803891.

[42] Saegusa, T.; Taka-Ishi, N.; Fujii, H. Reaction of Carbonyl Compound with Isocyanide. *Tetrahedron* **1968**, *24* (10), 3795–3798.
[43] Cohen, A. D.; Showalter, B. M.; Toscano, J. P. Time-Resolved IR Detection and Study of an Iminooxirane Intermediate. *Org. Lett.* **2004**, *6* (3), 401–403. https://doi.org/10.1021/ol036327x.
[44] Lengyel, I.; Sheehan, J. C. α-Lactams (Aziridinones). *Angewandte Chemie International Edition in English* **1968**, *7* (1), 25–36. https://doi.org/10.1002/anie.196800251.
[45] Lorenzetto, T.; Fabris, F.; Scarso, A. A Resorcin[4]Arene Hexameric Capsule as a Supramolecular Catalyst in Elimination and Isomerization Reactions. *Beilstein J. Org. Chem.* **2022**, *18* (1), 337–349. https://doi.org/10.3762/bjoc.18.38.
[46] Catti, L.; Pöthig, A.; Tiefenbacher, K. Host-Catalyzed Cyclodehydration–Rearrangement Cascade Reaction of Unsaturated Tertiary Alcohols. *Advanced Synthesis & Catalysis* **2017**, *359* (8), 1331–1338. https://doi.org/10.1002/adsc.201601363.
[47] (a) Fujii, S.; Kimoto, H.; Nishida, M.; Cohen, L. A. Synthesis of 1-(Pentalfluorophenyl)-β-Carboline. *Journal of Fluorine Chemistry* **1990**, *46* (3), 479–489. https://doi.org/10.1016/S0022-1139(00)82931-0. **See also:** (b) Palumbo Piccionello, A.; Pace, A.; Pibiri, I.; Buscemi, S.; Vivona, N. Synthesis of Fluorinated Indazoles through ANRORC-like Rearrangement of 1,2,4-Oxadiazoles with Hydrazine. *Tetrahedron* **2006**, *62* (37), 8792–8797. https://doi.org/10.1016/j.tet.2006.06.100. (c) Palumbo, F. S.; Stefano, M. D.; Piccionello, A. P.; Fiorica, C.; Pitarresi, G.; Pibiri, I.; Buscemi, S.; Giammona, G. Perfluorocarbon Functionalized Hyaluronic Acid Derivatives as Oxygenating Systems for Cell Culture. *RSC Adv.* **2014**, *4* (44), 22894–22901. https://doi.org/10.1039/C4RA01502A
[48] Rosa, M. D.; Gambaro, S.; Soriente, A.; Sala, P. D.; Iuliano, V.; Talotta, C.; Gaeta, C.; Rescifina, A.; Neri, P. Carbocation Catalysis in Confined Space: Activation of Trityl Chloride inside the Hexameric Resorcinarene Capsule. *Chem. Sci.* **2022**, *13* (29), 8618–8625. https://doi.org/10.1039/D2SC02901D.
[49] a) Ripin, D. H.; Evans D. A. pKa's of Inorganic and Oxo-Acids. https://organicchemistrydata.org/hansreich/resources/pka/#pka_water_compilation_evans, accessed 31st August 2022. b) Guthrie, J. P. Hydrolysis of Esters of Oxy Acids: PKa Values for Strong Acids; Brønsted Relationship for Attack of Water at Methyl; Free Energies of Hydrolysis of Esters of Oxy Acids; and a Linear Relationship between Free Energy of Hydrolysis and PKa Holding over a Range of 20 PK Units. *Can. J. Chem.* **1978**, *56* (17), 2342–2354. https://doi.org/10.1139/v78-385.
[50] Rehan, M.; Nallagonda, R.; Das, B. G.; Meena, T.; Ghorai, P. Synthesis of Functionalized Benzo[b]Furans via Oxidative Cyclization of o-Cinnamyl Phenols. *J. Org. Chem.* **2017**, *82* (7), 3411–3424. https://doi.org/10.1021/acs.joc.6b02752.
[51] Li, S.; Zhang, J.; Li, H.; Feng, L.; Jiao, P. Preparation and Application of Amino Phosphine Ligands Bearing Spiro[Indane-1,2'-Pyrrolidine] Backbone. *J. Org. Chem.* **2019**, *84* (15), 9460–9473. https://doi.org/10.1021/acs.joc.9b00875.
[52] Lam, F. L.; Au-Yeung, T. T.-L.; Kwong, F. Y.; Zhou, Z.; Wong, K. Y.; Chan, A. S. C. Palladium–(S,PR)-FerroNPS-Catalyzed Asymmetric Allylic Etherification: Electronic Effect of Nonconjugated Substituents on Benzylic Alcohols on Enantioselectivity. *Angewandte Chemie International Edition* **2008**, *47* (7), 1280–1283. https://doi.org/10.1002/anie.200703955.
[53] a) Bianchini, G.; Scarso, A.; Sorella, G. L.; Strukul, G. Switching the Activity of a Photoredox Catalyst through Reversible Encapsulation and Release. *Chem. Commun.* **2012**, *48* (99), 12082–12084. https://doi.org/10.1039/C2CC37374B.
b) Sokolova, D.; Piccini, G.; Tiefenbacher, K. Enantioselective Tail-to-Head Terpene Cyclizations by Optically Active Hexameric Resorcin[4]Arene Capsule Derivatives. *Angewandte Chemie International Edition* **2022**, *61* (25), e202203384. https://doi.org/10.1002/anie.202203384.
[54] Ibert, Q.; Cauwel, M.; Glachet, T.; Tite, T.; Le Nahenec-Martel, P.; Lohier, J.-F.; Renard, P.-Y.; Franck, X.; Reboul, V.; Sabot, C. One-Pot Synthesis of Diazirines and 15N2-Diazirines from Ketones, Aldehydes and Derivatives: Development and Mechanistic Insight. *Advanced Synthesis & Catalysis* **2021**, *363* (18), 4390–4398. https://doi.org/10.1002/adsc.202100679.
[55] Huang, H.; Yu, C.; Li, X.; Zhang, Y.; Zhang, Y.; Chen, X.; Mariano, P. S.; Xie, H.; Wang, W. Synthesis of Aldehydes by Organocatalytic Formylation Reactions of Boronic Acids with Glyoxylic Acid. *Angewandte Chemie International Edition* **2017**, *56* (28), 8201–8205. https://doi.org/10.1002/anie.201703127.
[56] Wei, J.; Zhao, L.; He, C.; Zheng, S.; Reek, J. N. H.; Duan, C. Metal–Organic Capsules with NADH Mimics as Switchable Selectivity Regulators for Photocatalytic Transfer Hydrogenation. *J. Am. Chem. Soc.* **2019**, *141* (32), 12707–12716. https://doi.org/10.1021/jacs.9b05351.

[57] McGonigal, P. R.; de León, C.; Wang, Y.; Homs, A.; Solorio-Alvarado, C. R.; Echavarren, A. M. Gold for the Generation and Control of Fluxional Barbaralyl Cations. *Angewandte Chemie International Edition* **2012**, *51* (52), 13093–13096. https://doi.org/10.1002/anie.201207682.

[58] Stanek, F.; Stodulski, M. Organocatalytic α-Allylation of α-Branched Aldehydes by Synergistic Catalysis of Brønsted Acids and Amines. *European Journal of Organic Chemistry* **2016**, *2016* (28), 4768–4772. https://doi.org/10.1002/ejoc.201600725.

[59] Riveiros, R.; Tato, R.; Pérez Sestelo, J.; Sarandeses, L. A. Rhodium-Catalyzed Allylic Substitution Reactions with Indium(III) Organometallics. *European Journal of Organic Chemistry* **2012**, *2012* (15), 3018–3023. https://doi.org/10.1002/ejoc.201200104.

[60] Shen, R.; Yang, J.; Zhu, S.; Chen, C.; Wu, L. Gold(I)-Catalyzed Decarboxylation of Propargyl Carbonates: Reactivity Reversal of the Gold Catalyst from π-Lewis Acidity to σ-Lewis Acidity. *Advanced Synthesis & Catalysis* **2015**, *357* (6), 1259–1269. https://doi.org/10.1002/adsc.201401094.

[61] Paul, D.; Chatterjee, P. N. Exploring the Labile Nature of 2,4,6-Trimethoxyphenyl Moiety in Allylic Systems under Acidic Conditions: Exploring the Labile Nature of 2,4,6-Trimethoxyphenyl Moiety in Allylic Systems under Acidic Conditions. *Eur. J. Org. Chem.* **2020**, *2020* (30), 4705–4712. https://doi.org/10.1002/ejoc.202000631.

[62] Fan, G.-P.; Liu, Z.; Wang, G.-W. Efficient ZnBr2-Catalyzed Reactions of Allylic Alcohols with Indoles, Sulfamides and Anilines under High-Speed Vibration Milling Conditions. *Green Chem.* **2013**, *15* (6), 1659. https://doi.org/10.1039/c3gc40262b.

[63] Liu, Z.; Wang, D.; Wu, Y.; Chen, Y. Mild and Efficient Allylation of Indoles and Amides Using Amberlyst-15 as a Recyclable Heterogeneous Catalyst. *Synthetic Communications* **2012**, *42* (12), 1813–1823. https://doi.org/10.1080/00397911.2010.545162.

[64] Fan, G.-P.; Liu, Z.; Wang, G.-W. Efficient ZnBr2-Catalyzed Reactions of Allylic Alcohols with Indoles, Sulfamides and Anilines under High-Speed Vibration Milling Conditions. *Green Chem.* **2013**, *15* (6), 1659. https://doi.org/10.1039/c3gc40262b.

[65] Cullen, A.; Muller, A. J.; Williams, D. B. G. Protecting Group-Free Use of Alcohols as Carbon Electrophiles in Atom Efficient Aluminium Triflate-Catalysed Dehydrative Nucleophilic Displacement Reactions. *RSC Adv.* **2017**, *7* (67), 42168–42171. https://doi.org/10.1039/C7RA08784E.

[66] Shukla, P.; Choudhary, M.; Nayak, S. Microwave-Accelerated Alkylation of Arenes/Heteroarenes with Benzylic Alcohols Using Antimony(III) Chloride as Catalyst: Synthesis of O-Heterocycles. *Synlett* **2011**, *2011* (11), 1585–1591. https://doi.org/10.1055/s-0030-1260795.

[67] Šebesta, R.; Bilčík, F. Imidazolium-Tagged Ferrocenyl Diphosphanes in Allylic Substitution with Heteroatom Nucleophiles. *Tetrahedron: Asymmetry* **2009**, *20* (16), 1892–1896. https://doi.org/10.1016/j.tetasy.2009.07.039.

Ringraziamenti

Vi sono diverse persone che hanno preso parte, in vari modi, alla mia formazione, e credo sia giusto che tale merito sia loro riconosciuto.

In primis, voglio esprimere la mia gratitudine nei confronti del gruppo di ricerca SHOT dell'Università Ca' Foscari, il prof. Alessandro Scarso, il prof. Fabrizio Fabris, il dott. Giuseppe Borsato e il dott. Tommaso Lorenzetto, che mi hanno pazientemente istruito durante la mia attività di tirocinio e le cui professionalità e dedizione mi sono state d'ispirazione.

Un ringraziamento speciale va a Gianmarco, grande amico e inseparabile compagno di laboratorio per tutti i cinque anni di università, con cui ho costruito un rapporto che mi ha migliorato come professionista e come persona. Esprimo un ringraziamento anche a Giovanni, collega e amico con cui il confronto mi è stato prezioso.

Ringrazio i miei amici Anna, Lucrezia, Maria, Massimiliano, Matteo, Thomas e Walter, a fianco dei quali sono cresciuto, che mi hanno accompagnato in tutte le fasi della mia vita e su cui so di poter sempre contare.

Devo molta gratitudine a Elisabetta, con cui ho imparato a condividere le mie giornate e che è stata un inestimabile sostegno in molti momenti difficili.

Ringrazio mio fratello Davide e mia sorella Gaia, miei complici e compagni di ogni giorno, persone brillanti e sensibili che si meritano di avere sempre il vento in poppa.

Infine, dedico un grazie di cuore ai miei genitori Daniela e Marco, che con la loro infinita pazienza e amore sono stati la mia terraferma, il mio porto sicuro, e che rispondendo ad ogni mia domanda fin dall'infanzia hanno alimentato la mia inguaribile curiosità, dirigendola verso la dimensione della scienza.